Topics in Stereochemistry, Volume 15

Editors
Ernest L. Eliel
Samuel H. Wilen
Norman L. Allinger

JOHN WILEY & SONS

TOPICS IN STEREOCHEMISTRY

VOLUME 15

ADVISORY BOARD

TOPICS IN

STEREOCHEMISTRY

EDITORS

ERNEST L. ELIEL
Professor of Chemistry
University of North Carolina
Chapel Hill, North Carolina

SAMUEL H. WILEN
Professor of Chemistry
City College, City University of New York
New York, New York

NORMAN L. ALLINGER
Professor of Chemistry
University of Georgia
Athens, Georgia

VOLUME 15

AN INTERSCIENCE ® PUBLICATION
JOHN WILEY & SONS
New York • Chichester • Brisbane • Toronto • Singapore

An Interscience ® Publication

Library of Congress Catalog Number: 67-13943
ISBN 0-471-88564-9

Printed in the United States of America

10 9 8 7 6 5 4 3 2 1

To the memory of

SAN-ICHIRO MIZUSHIMA

INTRODUCTION TO THE SERIES

It is patently impossible for any individual to read enough of the journal literature so as to be aware of all significant developments that may impinge on his or her work, particularly in an area such as stereochemistry, which knows no topical boundaries. Stereochemical investigations may have relevance to an understanding of a wide range of phenomena and findings irrespective of their provenance. Because stereochemistry is important in many areas of chemistry, comprehensive reviews of high quality play a special role in educating and alerting the chemical community to new stereochemical developments.

The above considerations were reason enough for initiating a series such as this. In addition to updating information found in such standard monographs as *Stereochemistry of Carbon Compounds* (Eliel, McGraw-Hill, 1962) and *Conformational Analysis* (Eliel, Allinger, Angyal, and Morrison, Interscience, 1965; reprinted by American Chemical Society, 1981) as well as others published more recently, the series is intended also to deal in greater detail with some of the topics summarized in such texts. It is for this reason that we have selected the title *Topics in Stereochemistry* for this series.

The series is intended for the advanced student, the teacher, and the active researcher. A background of the basic knowledge in the field of stereochemistry is assumed. Each chapter is written by an expert in the field and, hopefully, covers its subject in depth. We have tried to choose topics of fundamental importance aimed primarily at an audience of inorganic and organic chemists but involved frequently with basic principles of physical chemistry and molecular physics, and dealing also with certain stereochemical aspects of biochemistry.

It is our intention to produce future volumes at intervals of one to two years. The editors will welcome suggestions as to suitable topics.

We are fortunate in having been able to secure the help of an international board of editorial advisors who have been of great assistance by suggesting topics and authors for several chapters and by helping us avoid, in so far as possible, duplication of topics appearing in other, related monograph series. We are grateful to the editorial advisors for this assistance, but the editors and authors alone must assume the responsibility for any shortcomings of *Topics in Stereochemistry*.

E. L. ELIEL
S. H. WILEN
N. L. ALLINGER

PREFACE

Volume 15, as did many of the previous volumes, contains four chapters. The first one, by Frank-Gerrit Klärner, deals with "walk rearrangements" (also called "circumambulatory rearrangements") in [n.1.0] bicyclic compounds, both neutral and ionic. These are rearrangements in which a divalent group, for example CR_2, NR, O, S, which forms part of a three-membered ring, undergoes a migration along the surface of a cyclic π-system. The scope of these rearrangements, which themselves are manifestations of the Woodward-Hoffmann rules, is greatly enlarged because numerous cyclopentadienoid and heterocyclopentadienoid systems may be photochemically converted, by electrocyclization, to [2.1.0] bicyclopentene systems, which may then undergo walk rearrangements and subsequently be thermally reopened to rearranged cyclopentadienoids. Alternate mechanisms are possible, and a number of these rearrangements are discussed in detail.

The second chapter, by Robert J. P. Corriu, Christian Guérin, and Joël J. E. Moreau, constitutes a monumental review of stereochemistry at silicon. This subject was last discussed comprehensively in a pioneering book by L. H. Sommer in 1965, with a brief 1973 update. In the present chapter the authors bring the literature up to date, discussing silicon stereochemistry in all of its aspects, especially with a view to reaction mechanism, in which area they have made a number of original contributions. This chapter will no doubt become required (and welcome) reading for anyone involved in any way with silicon stereochemistry.

The third chapter, by Masao Nakazaki, is concerned with the synthesis and stereochemistry of chiral organic molecules with high symmetry. It was recognized many years ago that the presence of symmetry axes in a molecule is no bar to chirality and the term dissymmetry has, in fact, been coined to imply that chiral molecules need not be asymmetric. In 1974, in the van't Hoff-Le Bel Commemorative Issue of *Tetrahedron*, M. Farina and C. Morandi collected what was then a fairly comprehensive list of chiral molecules of $\mathbf{C}_n$ ($n > 2$), $\mathbf{D}_n$, and higher symmetry. Nakazaki who, himself, has synthesized a sizeable number of molecules of this type, now brings the subject up to date with an extensive list of new and often quite intriguing molecules of $\mathbf{C}_3$, $\mathbf{D}_2$, $\mathbf{D}_3$ and higher symmetry. Much ingenuity has gone into the synthesis of such molecules.

The fourth and final chapter, by Heinz G. Floss, Ming-Daw Tsai, and Ronald W. Woodard leads into the realm of biochemistry, dealing with the stereochemistry of biological reactions at proprochiral centers. Prochiral centers are centers

of the type AX_2YZ, where A is generally a tetrahedral central atom such as carbon or tetracoordinate phosphorus; their stereochemistry is generally probed by replacing the prochiral center by a chiral one AXX'YZ, where X and X' are different isotopes of the same atomic number. For example, in Westheimer and Vennesland's classical work, the prochiral methylene center in CH_3CH_2OH has been investigated stereochemically by replacing it with a chiral center as in CH_3CHDOH. Proprochiral centers AX_3Z bear the same relation to prochiral centers $AX_2X'Z$ as prochiral centers bear to chiral ones. Probing their stereochemistry is quite an intricate task and requires double isotopic substitution of the type AXX'X''Z to create a true chiral center. Examples are $CHDTCO_2H$, first synthesized chirally and analyzed by Arigoni and by Cornforth, and $[ROP^{16}O^{17}O^{18}O]^{2-}$, synthesized and stereochemically diagnosed by Jeremy Knowles, John Gerlt, and Gordon Lowe. The present chapter deals with the detection of these proprochiral groups (or their isotopically labeled chiral analogs) and with their use in the probing of the stereochemistry of enzymatic reactions.

We must report, with sadness, the death of San-ichiro Mizushima on August 3, 1983. Professor Mizushima had been one of our editorial advisors since the inception of *Topics in Stereochemistry* in 1967. As professor at the University of Tokyo he undertook, in the 1930s, pioneering research concerned with the conformation of 1,2-dihaloethanes, using both dipole moment measurement and the then-novel technique of Raman spectroscopy as experimental tools. His studies culminated in the realization that these compounds, while crystallizing in the more stable anti conformation, were, in the liquid state, mixtures of gauche and anti-conformational isomers. This work is among the earliest leading to an understanding of the conformational behavior of acyclic molecules.

Mizushima had a deep understanding of the West as well as the East and, throughout his life, acted as a bridge between the two cultures. We shall miss his friendship and his advice.

ERNEST L. ELIEL
SAMUEL H. WILEN
NORMAN L. ALLINGER

Chapel Hill, North Carolina
New York, New York
Athens, Georgia
September 1983

CONTENTS

TOPICS IN STEREOCHEMISTRY

VOLUME 15

Walk Rearrangements in [*n*.1.0] Bicyclic Compounds

FRANK-GERRIT KLÄRNER

Abteilung für Chemie
Ruhr-Universität Bochum
Federal Republic of Germany

I. INTRODUCTION

[*n*.1.0] Bicycles of type 1 are homologous to annulenes of type 2. The question of homoaromaticity of these systems has been the subject of repeated theoretical and experimental investigations (1). The homoaromatic or homoantiaromatic character depends on the extent of interaction between the orbitals of the three-membered ring and the π-orbitals of the unsaturated bridge.

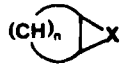

1

2

The walk rearrangement in an [*n*.1.0] bicycle has been defined as a reaction in which the divalent group X (e.g., CR_2, NR, O, S) that is part of a three-membered ring undergoes a migration along the surface of a cyclic π-system (2).

The term "walk rearrangement" used in this review is one of many that have been introduced into the literature to describe this type of reaction. Other illustrative descriptions include terms like "bones rearrangement," "merry-go-round," "ring runner," "circumambulation," and the more general "degenerate rearrangement."

Under the topic "circumambulatory rearrangements" R. F. Childs (3) has recently reviewed migrations of mono-, di-, tri- and tetravalent groups around the periphery of a ring. Walk rearrangements of [*n*.1.0] bicycles are included as one topic of this more general review.

The study of walk rearrangements has been important for developing and testing theoretical concepts in organic chemistry. Within the scope of the theory of sigmatropic reactions, Woodward and Hoffmann (4) have pointed out detailed stereochemical and topological consequences of orbital-symmetry controlled processes. In this chapter, mechanistic and theoretical aspects are examined in connection with individual examples of walking systems. In order to be able to compare the properties of closely related systems, the [*n*.1.0] bicycles are divided in two classes of compounds: neutral compounds with *n* even ($n = 2, 4, 6, \ldots$), and ionic compounds with *n* odd ($n = 1, 3, 5, \ldots$). Radical systems that do not fit into either of these two classes are discussed in the context of corresponding [*n*.1.0] bicycles having the same skeleton.

II. WALK REARRANGEMENTS IN NEUTRAL [*n*.1.0] BICYCLIC COMPOUNDS

A. Bicyclo[2.1.0]pent-2-ene

In a large number of five-membered heterocycles, a photochemical isomerization is observed leading to a redistribution of the ring atoms (5). In the explanation of this unusual reaction, two general types of mechanism may be discerned.

1. Electrocyclization followed by a walk of ring atom 5 in the intermediate heterobicyclo[2.1.0]pent-2-ene [path (a) in Figure 1].
2. A sequence of 1,3 shifts involving heterovinylcyclopropenes as intermediates [path (b) in Fig. 1].

Additional scrambling of the ring atoms can be achieved by further rearrangement, following path (a) as well as path (b).

Table 1 contains several examples of phototranspositions of five-membered heterocycles. Here the distinction between paths (a) and (b) is largely based on a comparison of the substitution pattern of starting material and product. In some cases intermediate heterovinylcyclopropenes and heterobicyclopentenes, respectively, were actually trapped or isolated. For example, in the interconversion of

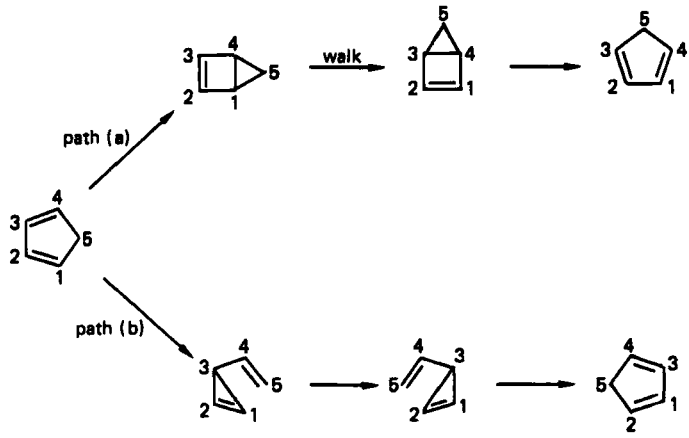

Figure 1. Possible pathways in the phototransposition of five-membered rings.

Table 1
Phototranspositions in Five-Membered Heterocycles

Entry	Reactants	Products	Reaction Path	Ref.
1	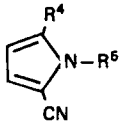 R^4 = H, H, CH_3 R^5 = H, CH_3, H	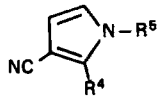	(a)	(6)
2	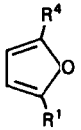 R^1 = CH_3, CH_3, t–C_4H_9 R^4 = H, CH_3, t–C_4H_9	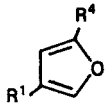	(b)	(7)
3	 R = CH_3, $CH_2C_6H_5$, t–C_4H_9, C_6H_5, CN		(a), (b)	(7c) (7d) (8)

Table 1 (*Continued*)

Entry	Reactants	Products	Reaction Path	Ref.
4	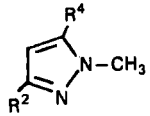 $R^2 = CH_3$, CN $R^4 = CH_3$, H, D, CH_3	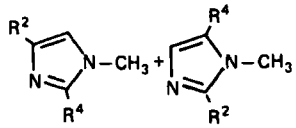	(a), (b)	(9)
5	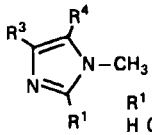 R^1 R^3 R^4 H CH_3 H H CH_3 CH_3 D CH_3 H	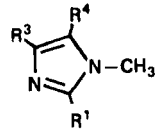	(a)	(9)
6	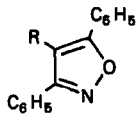 R = H, C_6H_5	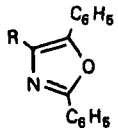	(b)	(10)
7	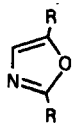 R = C_6H_5	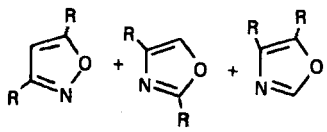	(a), (b)	(11)
8	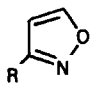 R = C_6H_5	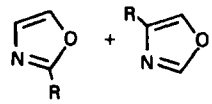	(a), (b)	(12)
9	 R^2 = H, CH_3, H R^3 = H, H, CH_3	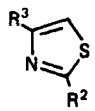	(b)	(13)
10	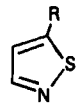 R = CH_3	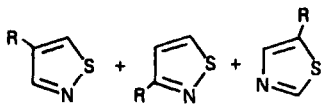	(a), (b)	(13)
11	 R = C_6H_5	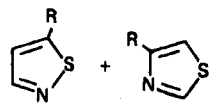	(a)	(14)

Table 1 (*Continued*)

Entry	Reactants	Products	Reaction Path	Ref.
12	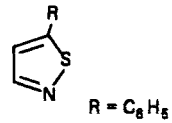 R = C_6H_5	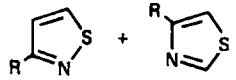	(a)	(14)
13	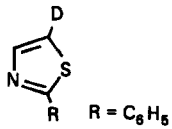 R = C_6H_5	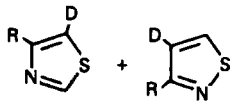	(a)	(14)
14	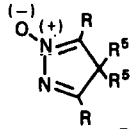 R = C_6H_5, CH_3 R^5 = CH_3, C_2H_5	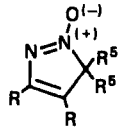	(a)	(15)

2,5- into 2,4-di-*t*-butylfuran (Table 1, entry 2) or in the isoxazole → oxazole isomerization (Table 1, entry 6), the corresponding cyclopropenylketone **3** (7d) and azirinylketone **4** (10), respectively, were characterized as intermediates.

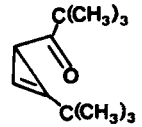

3

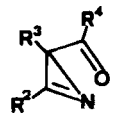

4

On irradiation of 4,4-diethyl-3,5-dimethyl-4H-pyrazole-1-oxide (**5**) at -78°C (15), the valence-tautomeric heterobicyclopentene **6** was detected as the primary photoproduct. At temperatures above -20°C, **6** undergoes thermal isomerization to **5** and **8**. Product **8** is obviously formed by walk rearrangement **6** → **7** followed by a fast electrocyclic ring opening **7** → **8**.

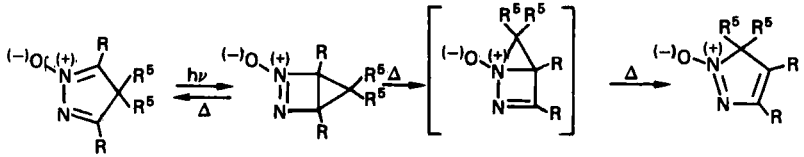

5 **6** **7** **8**

Trapping experiments and low-temperature photolysis studies indicate that a thermally induced walk rearrangement of the as yet undetected intermediate **9** is responsible for the phototransposition of several substituted pyrroles (Table 1, entry 1) (6b).

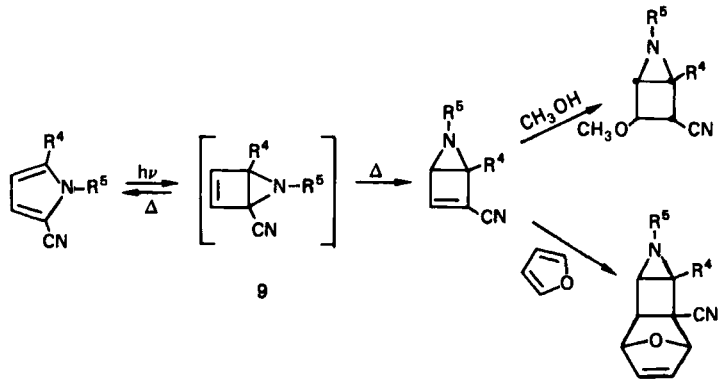

9

For some of the systems shown in Table 1 the results can only be explained by the assumption that pathways (a) and (b) are competing. The photoisomerization of thiophenes has been studied in great detail. Probably the most extensively studied substrate is 2-phenylthiophene which, upon irradiation, isomerizes to 3-phenylthiophene (Table 1; 3 ref. 8a,b). Deuterium and carbon-14 labeling experiments showed that a rather complex reaction had taken place. The intermediate formation of "valene" thiophenes and zwitterionic species has been proposed to rationalize the rearrangement patterns. Clear examples of a sulfur walk are provided by the rearrangements of the thiophene derivatives **10** and **13**. The photolysis of **10** gives the remarkably stable Dewar thiophene **11** (16). By dynamic ^{19}F NMR spectroscopy, **11** as well as its S-oxide **12** were shown to undergo a degenerate rearrangement in which the sulfur atom migrates around the four-membered ring (17). The surprisingly low activation barrier of the automerization in **11** and **12** has been explained in terms of so-called pseudopericyclic processes, in which the electrons of the lone pair on sulfur are involved. This assumption, however, has been put in question by quantum mechanical calculations (18).

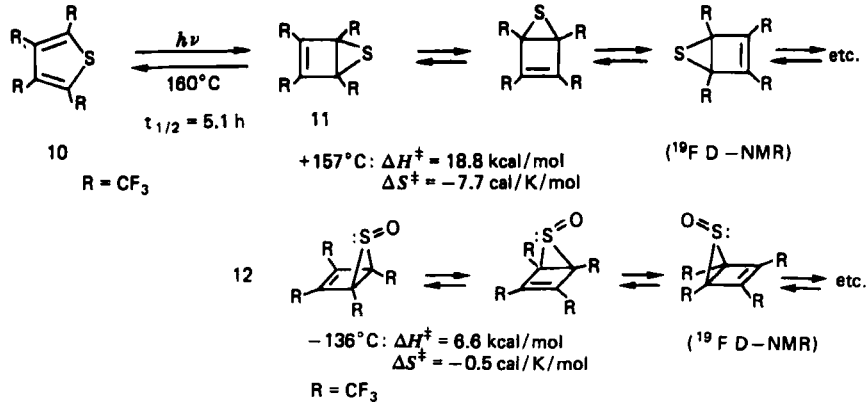

10
R = CF_3

$t_{1/2}$ = 5.1 h

11

+157°C: $\Delta H^{\ddagger}$ = 18.8 kcal/mol
$\Delta S^{\ddagger}$ = −7.7 cal/K/mol

(^{19}F D−NMR)

12

−136°C: $\Delta H^{\ddagger}$ = 6.6 kcal/mol
$\Delta S^{\ddagger}$ = −0.5 cal/K/mol

(^{19}F D−NMR)

R = CF_3

It is interesting that the systems related to **11**–pertrifluoromethyl Dewar pyrrole (19) and pertrifluoromethyl Dewar furan (20)–do not appear to undergo comparable walk rearrangements. Upon heating, these compounds isomerize to the corresponding substituted pyrrole and cyclopropenyltrifluoromethylketone, respectively.

Direct evidence of a thermally induced sulfur walk was also obtained in Dewar thiophene **14**, which rearranges to **15** with a half-life of 2 min at -35°C (8e).

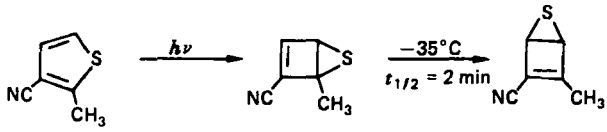

13 14 15

After the first preparation of the parent bicyclo[2.1.0]pent-2-ene in 1966 (21), most of the interest in the carbocyclic systems has been focused on the electrocyclic ring opening, which leads to chemically activated 1,3-cyclopentadienes (22). The irradiation of the cyclopentadiene [1,5-$^{13}C_2$]-**16** produces a redistribution of carbon-13 labels to the nonvicinal positions (C-2 and C-5) (23). A reasonable explanation for this result is a photoinduced walk rearrangement of the intermediate bicyclopentenes [1,5-$^{13}C_2$]-**17** → [2,5-$^{13}C_2$]-**17**. However, when labeled bicyclopentene [1,5-$^{13}C_2$]-**17** is heated, the thermal walk rearrangement cannot compete with the electrocyclic ring opening, which occurs slowly at room temperature already (22d).

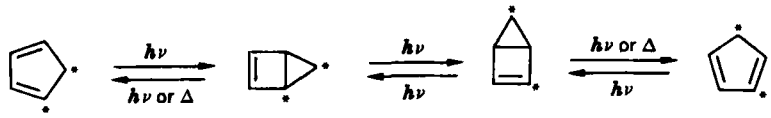

[1,5-$^{13}C_2$]-16 [1,5-$^{13}C_2$]-17 [2,5-$^{13}C_2$]-17 [2,5-$^{13}C_2$]-16

The phototransposition of 2,3,4-tri-*t*-butylcyclopenta-2,4-dienone provides an interesting example of another photoinduced walk rearrangement, probably of a bicyclo[2.1.0]pentenone derivative. Irradiation of this cyclopentadienone in an argon matrix at 10 K gave the isomeric 2,3,5-tri-*t*-butylcyclopentadienone and 1,2,3-tri-*t*-butylcyclobutadiene. From a detailed investigation at various temperatures and wavelengths, the mechanism depicted in Figure 2 was proposed for the interconversion of these two cyclopentadienones. Two of the postulated intermediates–one bicyclopentenone derivative and the cyclobutadiene-carbon monoxide complex–have been characterized by their spectral and chemical properties.

In some bicyclopentene systems substituted at C-5 by an ester or nitrile group, the thermally induced walk rearrangement competing with the electro-

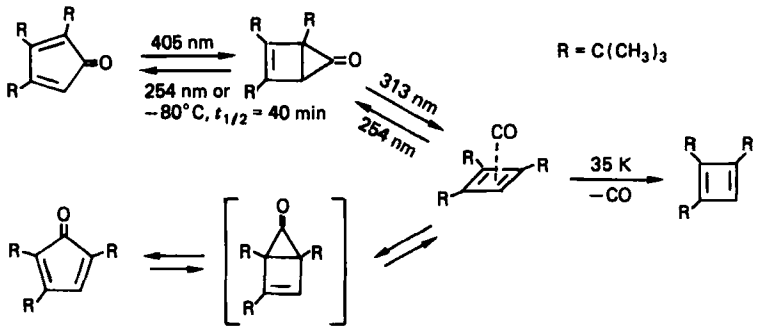

Figure 2. Photoinduced rearrangements and fragmentation of 2,3,5-tri-*t*-butylcyclopentadienone (24).

cyclic ring opening has been observed (25). For experimental verification the 1,5-dimethylbicyclopentene derivatives **19a**, **19b**, and **23a** were prepared by photolysis of the cyclopentadienes **18** and **22** at -50°C. At 0°C, each bicyclopentene derivative underwent a highly stereospecific walk rearrangement produc-

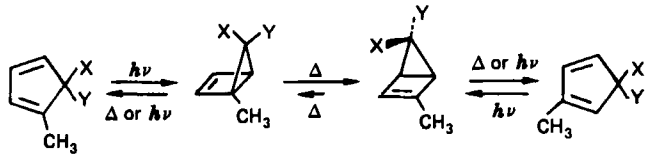

X	Y				
CH_3	CO_2CH_3	18	19a	20a	21
CO_2CH_3	CH_3	18	19b	20b	21
CH_3	CN	22	23a	24a	25
CN	CH_3	22	23b	24b	25

Table 2
Rate Constants and Gibbs Activation Energies of Walk Rearrangements and Electrocyclic Ring Openings in Ester-Substituted and Nitrile-Substituted Dimethylbicyclopentene Derivatives (25)

Reaction	Temp. (°C)	k X 10^6 (sec^{-1})	$\Delta G^{\ddagger}$ (kcal/mol)
19a → 20a	0.0	24.2	21.7
19a → 18	0.0	1.8	23.1
19b → 20b	0.0	0.08	24.8
19b → 18	0.0	2.5	22.9
23a → 24a	0.0	17.4	21.9
23a → 22	0.0	0.18	24.3
20a → 21	50.2	67.7	25.2
20b → 21	50.2	140	24.7
24a → 25	50.0	37.6	25.4
24b → 25	50.6	5.28	26.8

ing the corresponding 2,5-dimethylbicyclopentene **20a**, **20b**, or **24a** and the cyclopentadiene **18** and **22** respectively. Rate constants and Gibbs activation energies of the competing processes are listed in Table 2.

The 2,5-dimethyl derivatives **20a**, **20b** and **24a**, **24b** are more stable than the corresponding 1,5-dimethylbicyclopentenes. Their ring opening to the cyclopentadienes takes place only at temperatures of about 50°C (Tables 2 and 3). The formation of 2- as well as 1-methylcyclopentadienes (**21**, **25** as well as **18**, **22**) indicates the walk rearrangements **19a** ⇌ **20a** and **23a,b** ⇌ **24a,b** to be reversible (thus **20a** gives 8% **18**; **24a** gives 19% **22**; **24b** gives 12% **22**).

In no case is an exo-endo isomerization at C-5 observed. This finding rules out a migration of C-5 with retention ("suprafacial retention," *sr*) in the bicyclopentene systems, a process calculated by semiempirical molecular orbital (MO) methods to be the favored one (28). The observed stereochemistry corresponds to an inversion at C-5 ("suprafacial inversion," *si*) and is in accord with the stereochemical requirements for an orbital symmetry controlled process.

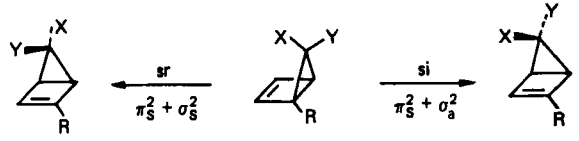

Table 3
Activation Parameters of Some
Bicyclopentene → Cyclopentadiene Isomerizations

Reaction	Temp (°C)	$\Delta G^{\ddagger a}$	$\Delta H^{\ddagger a}$	$\Delta S^{\ddagger b}$	Ref.
 17 16	50.0	24.9	26.3	+4.3	(26)
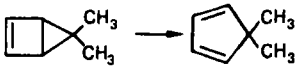	50.9	23.8	23.5	−0.8	27
 26a 27	50.5	24.5	25.1	+2.0	(25)
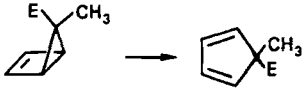 26b 27	50.5	24.3	25.6	+3.8	(25)
E = CO_2CH_3					

[a] kcal/mol
[b] cal/K/mol

Comparing the different thermal behaviors of the parent bicyclopentene [1,5-$^{13}C_2$]-**17** labeled with carbon-13 and the ester- and nitrile-substituted systems, it is tempting to attribute the substituent effect to a conjugative interaction between the π-acceptor and cyclopropane ring (29) with the result of weakening the adjacent cyclopropane bond and strengthening the distal one. The ester or nitrile function at C-5 effects a weakening of the adjacent bond, increasing the rate of the walk rearrangement. However, the rate of the electrocyclic ring opening, the breaking of the distal cyclopropane bond, is relatively insensitive to the C-5 substituent. For that reason the substituent seems to stabilize the transition state of the walk rearrangement (e.g. the radical center at C-5 in the case of a diradical process).

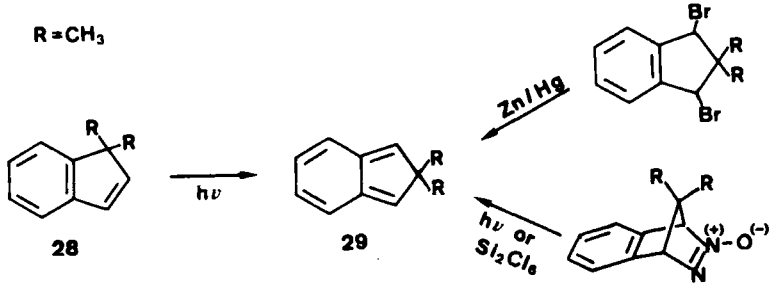

It has been suggested that walk rearrangements are responsible for the photoisomerization of benzanelated heterocycles and carbocycles (30). A remarkable example is the indene-isoindene rearrangement (31). Irradiation of 1,1-dimethylindene **28** produces the relatively stable 2,2-dimethylisoindene **29**, an *o*-chinodimethane derivative which was also synthesized by independent routes (32).

For the indene → isoindene rearrangement, two pathways, path (a) and path (b), have been considered (Figure 3). Path (a) consists of a photoinduced cyclization **30** → **31** followed by a thermal walk rearrangement **31** → **32**. A study with optically active 1,2-dimethylindene **30** ($R^1 = R^2 = CH_3$) indicates that the walk rearrangement must be highly stereoselective, proceeding with inversion at the migrating carbon.

A direct transformation of **30** to **32** has been postulated to be involved in path (b), a process called "conjugated" di-π-methane rearrangement, for which there is no exact analogy. In both pathways the observed products **34** and **35** are formed by subsequent electrocyclic ring opening **32** → **33** and 1,5-hydrogen shift **33** → **34** + **35**. However, the additional observation (33) that acid intercepts an intermediate between the excited states of **30** and **32** seems to rule out path (b).

B. Bicyclo[4.1.0]hepta-2,4-diene (Norcaradiene)

1,3,5-Cycloheptatriene, reported for the first time in 1883 (34), has been the subject of numerous investigations. Most of the interest has been focused on the

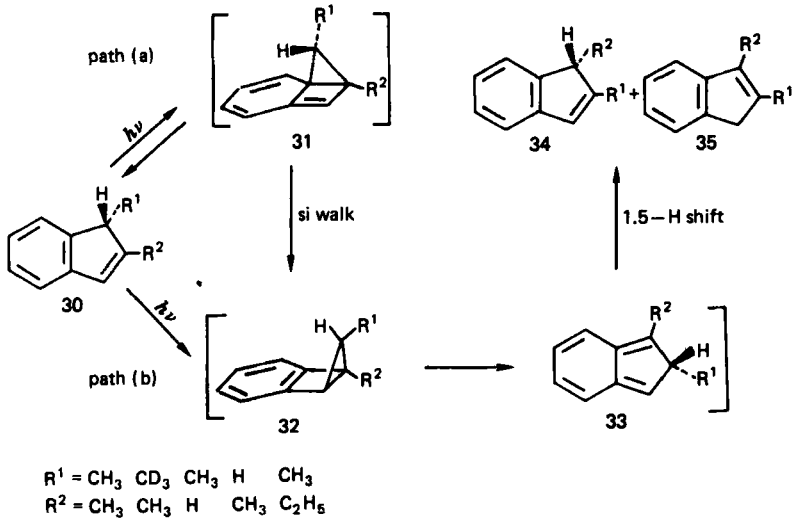

Figure 3. Possible pathways for the indene → isoindene rearrangement.

valence-tautomeric norcaradiene-cycloheptatriene equilibrium. In the parent system, the equilibrium concentration of norcaradiene appears to be very small (undectable with spectroscopic methods) (35). Nevertheless, many reactions of the compound are derived from the norcaradiene form.

Upon heating at 300°C, 3,7,7-trimethylcycloheptatriene **36c** rearranges to 2,7,7- and 1,7,7-trimethylcycloheptatriene **37c** and **38c** (36). The key reaction of this interconversion is a stepwise walk of C-7 in the norcaradiene form (**36a** ⇌ **37a** ⇌ **38a**), by way of consecutive [1,5] sigmatropic carbon shifts. The possibility of two subsequent [1,3] carbon shifts involving intermediate trimethyl-

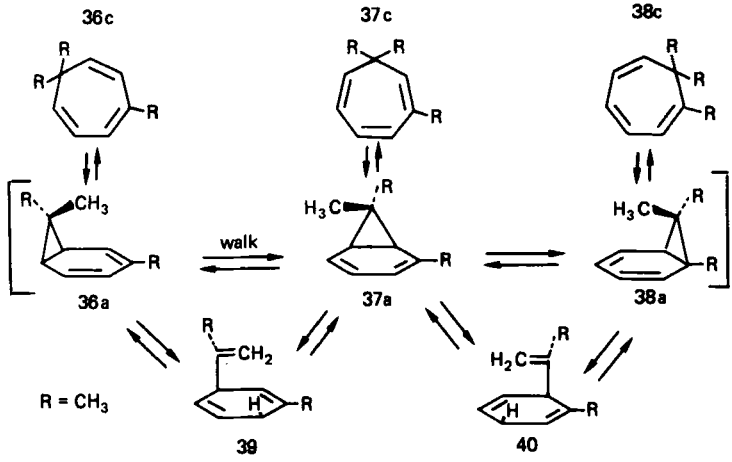

bicyclo[2.2.1]hepta-2,5-dienes, which would lead to the same result as a [1,5] shift, could be ruled out by an independent study of the thermal behavior of bornadiene (37). The additional products in the thermolysis of **36c**, the vinylcyclohexadienes **39** and **40**, are obviously formed by a reversible [1,5] homodienyl hydrogen shift of the norcaradiene forms. Evidently both reactions, [1,5] carbon and [1,5] hydrogen shift, are involved in the mutual interconversion of the trimethylcycloheptatrienes. Other potential reaction pathways were excluded by deuterium labeling experiments.

A clear example of the norcaradiene walk rearrangement is provided by the thermolysis of the norcaradiene **42** (38), which is interconverted with both isomers **41** and **43** even at 70°C, whereas the rearrangement of trimethylcycloheptatrienes **36c**, **37c**, and **38c** is negligible below 300°C. In terms of activation energy, this facilitation amounts to about 18 kcal/mol and is obviously due to two effects of the nitrile function: (i) Since the key intermediates proposed for this walk rearrangement are norcaradienes, the trimethyl compounds must perform an additional endothermic step for the cycloheptatriene → norcaradiene valence bond isomerization, which is not required of the dinitrile compounds (39). (ii) The nitrile groups decrease the dissociation energy of adjacent cyclopropane bonds by 7.2–8.9 kcal/mol per nitrile group (40), (41).

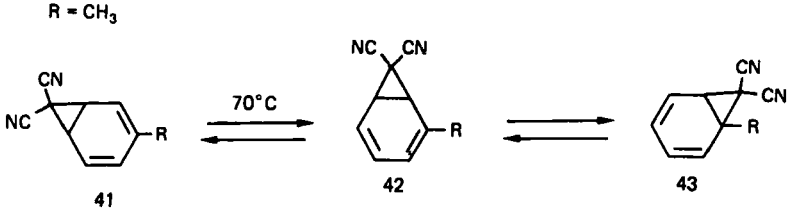

Walk rearrangements have been observed in many carbo- and heterocyclic norcaradiene ⇌ cycloheptatriene systems upon thermal as well as photochemical excitation. Table 4 contains selected examples. In this connection, the very different thermal stability of 11,11-dimethyl-1,6-methano[10]annulene and its radical anion is worth mentioning (59). The neutral hydrocarbon rearranges to 7,7-dimethyl-1,2-benzocycloheptatriene at temperatures between 150 and 190°C [Table 4, entry 3, X = $C(CH_3)_2$:log A = 13.4; E_A = 35.9 kcal/mol]. The corresponding rearrangement of the radical anion produced by reduction of the hydrocarbon with potassium occurs at -110°C already. The activation energy is lowered here by about 25 kcal/mol over that of the hydrocarbon. The norcaradiene walk has also gained some synthetic importance, for example, in the preparation of the unsaturated bicycle **44**, a precursor of heptalene (60).

The stereochemistry of the norcaradiene walk, studied for the thermal as well as photochemical process, has attracted special attention. The thermal rearrangement is discussed first.

Table 4

Thermally and Photochemically Induced Walk Rearrangements in Carbocyclic and Heterocyclic Norcardiene ⇌ Cycloheptatriene Systems

Entry	Reactants	Products	X	R^1	R^6	Ref.
	a. Thermal					
1	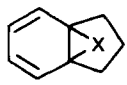	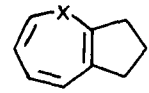	CH_2			(42)
			NCO_2CH_3			(43)
			O			(44)
2	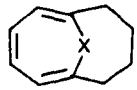	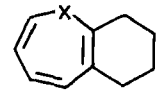	NCO_2CH_3			(43)
3	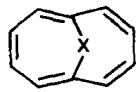	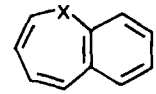	CH_2			(45)
			$C(CH_3)_2$			(46)
			O			(44a), (47)
4	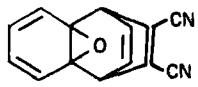	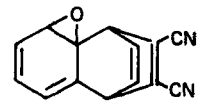				(47)
5	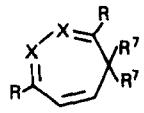	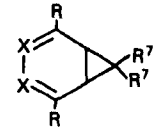	CH			(48)
	$R=C_6H_5$ $R^7=CH_3$		N			(2a)
6	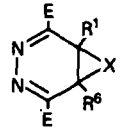	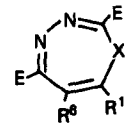	CH_2	H	H	
				C_6H_5	C_6H_5	(49)
			$C(CH_3)_2$	H	H	
				H	CH_3	
7	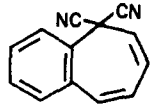	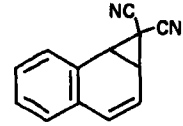				(50)
	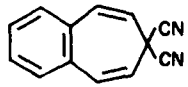					

Table 4 (*Continued*)

Entry	Reactants	Products	R	R^1	X	Ref.
8	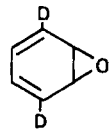 *b. Photochemical*	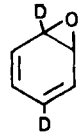				(2b)
9	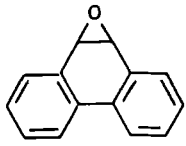	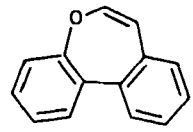				(2b), (51)
10	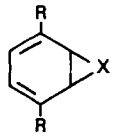 $R = C_6H_5$	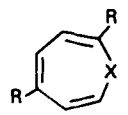			$CH(C_6H_5)$ $C(CH_3)_2$	(52) (48)
11	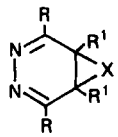	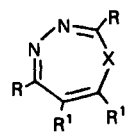	C_6H_5 C_6H_5 CH_3 Ar	H C_6H_5 C_6H_5 C_6H_5	$C(CH_3)_2$ CH_2 $CH(C_6H_5)$	(2a) (53)
12	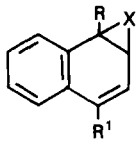 $E = CO_2CH_3$	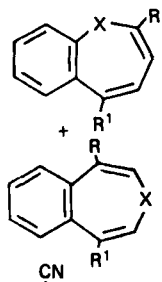	H H H H H H E E	H H H H $i-C_3H_7$ $t-C_4H_9$ H H	$C(CN)_2$ CH_2 CD_2 $CH(CH_2E)$ CH_2 CD_2	(50) (54) (55) (56) (57) (58)
13	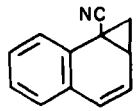	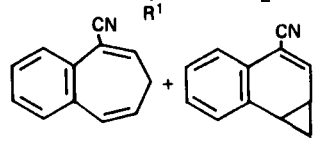				

There are three principal possibilities: (i) The suprafacial sigmatropic [1,5] carbon shift **45a** → **45b**′ is controlled by orbital symmetry (4) proceeding with retention at the migrating carbon C-7 (*sr* process). This requires the substituents X and Y to interchange places in **45a** with respect to the six-membered ring. (ii) The intermediate formation of the diradical **46** (61). In this case the potential

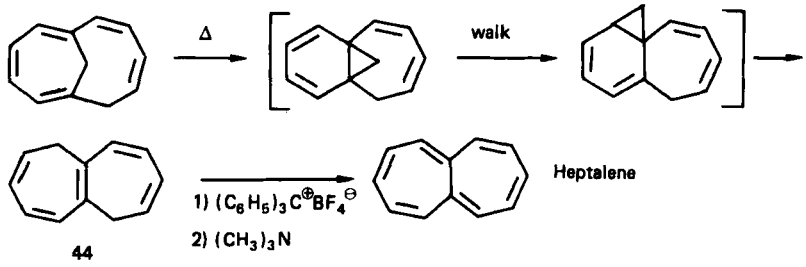

free rotation around the remaining single bond C-6–C-7 in **46** does not allow any "a priori" prediction of the stereochemical course. (iii) The migration of C-7 takes place with inversion **45a** → **45a'** (*si* process); this requires the least structural change and therefore is called the "least-motion" process (62). This process should pass through an antiaromatic transition state, which in some cases, however, is suggested to gain resonance stabilization over the diradical process by subjacent orbital interaction (63). A semiempirical MO calculation (MINDO/2) in fact favors the inversion process over the retention process by 1.4 kcal/mol (28).

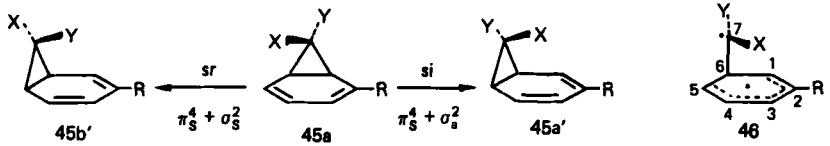

An experimental distinction among these three alternatives proved to be difficult, particularly as norcaradienes and cycloheptatrienes usually interconvert easily via valence bond isomerization (norcaradiene → cycloheptatriene: E_A = 6.5 kcal/mol log A = 11.8) (64) and cycloheptatriene ring inversion (1,3,5-cycloheptatriene: E_A = 6.3 kcal/mol) (Figure 4; ref. 65). Therefore it was necessary to resort to such devices as introducing chirality into the molecules by way of an additional stereochemical label.

Several experimental tests using the chiral norcaradiene ⇌ cycloheptatriene systems **47–51** (66–70) have been reported. Conflicting results have finally been

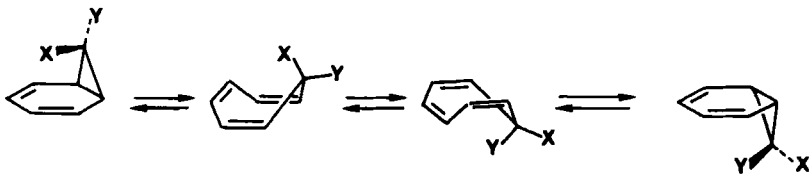

Figure 4. Exo-endo equilibration via facile norcaradiene-cycloheptatriene valence bond isomerization (64) and cycloheptatriene ring inversion (65).

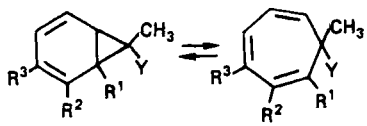

a: 7–endo–CH_3
b: 7–exo–CH_3

c

	Y	R^1	R^2	R^3	Ref.
47	CO_2CH_3	H	CH_3	H	(66)
48	CN	H	CH_3	H	(66)
49–1–*d*	CH_2OCH_3	D	H	CO_2CH_3	(67)
50–2–*d*	CH_2OCH_3	H	D	CH_3	(68, 70)
51	CH_2OCH_3	H	CH_3	H	(69)

reconciled in a very recent study (68, 70). In all cases 7,7-disubstituted systems are used to prevent [1,5] hydrogen shifts in the cycloheptatriene form from intruding into the stereochemical analysis (71).

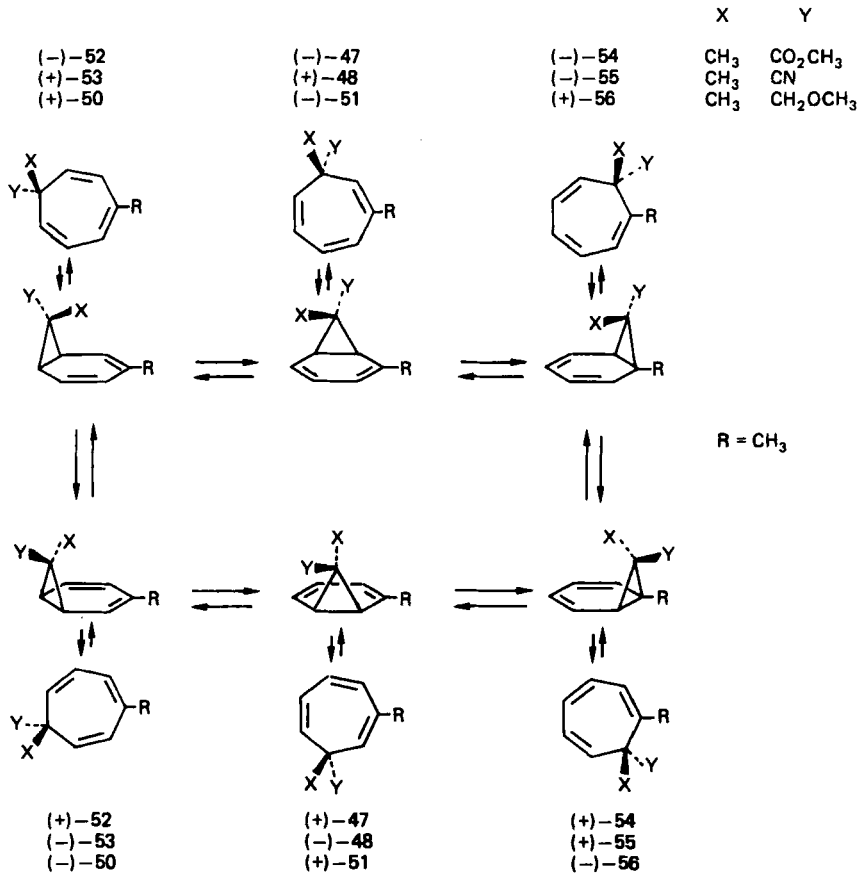

Figure 5. Walk rearrangement of chiral tropilidenes proceeding with inversion in each step (*si* process) (66, 70). The term tropilidene is used as a general designation for a cycloheptatriene-norcaradiene valency tautomeric pair. Since only relative configurations of tropilidenes have been assigned, each configuration depicted in this and the following figures may actually correspond to the opposite sign of optical rotation.

The same stereochemical course has been found for optically active ester (-)-**47** and nitrile (+)-**48** (Figure 5; ref. 66). In both systems the thermal interconversion leading to (-)-**52** and (-)-**54** or (+)-**53** and (-)-**55**, respectively, at 180°C is highly stereoselective (⩾99 and ⩾92% respectively), proceeding with inversion at the migrating carbon. The stereochemical assignment is based on kinetic analysis of the rates of interconversion and racemization of the optically active esters as well as on the correlation of the relative configurations of (-)-**47** and (-)-**52** (Figure 6). As expected for the mechanistic scheme in Figure 5, optical purities of products and recovered reactants determined by NMR using a chiral shift reagent are in accord with the assignment of substantial rate constants for the enantiomerizations (-)-**52** → (+)-**52** and (-)-**54** → (+)-**54** as well as of a zero value to the rate constant for direct enantiomerization (-)-**47** → (+)-**47**. In the case of the esters, a homodienyl hydrogen shift competing with walk rearrangement to a minor extent gives 1,4-cyclohexadienes, for example, optically active **57** starting from (-)-**47** (Figure 6). The hydrogen shift is reversible not only to the starting material (-)-**47** but also to the rearranged tropilidene (-)-**52**. The stereochemical course of the hydrogen shift from (-)-**47** to (-)-**52** via the cyclohexadiene **57** is unambiguously fixed and corresponds to a walk rearrangement with inversion at the migrating carbon. The interconversion of the optically active esters into the corresponding optically active nitriles provides information on the stereochemical course of the walk rearrangement of the latter systems.

Upon heating optically active **49**-1-*d* at 230°C (67) deuterium scrambling isomerization **49**-1-*d* → **49**-5-*d* and racemization (+)-**49** → (-)-**49** were observed to take place at approximately the same rate. A reasonable explanation of this result is a degenerate walk rearrangement with inversion at C-7.

The previous results discussed here were put in question by a stereochemical study for the optically active ether (+)-**50**-2-*d* (68). In this case a one-center

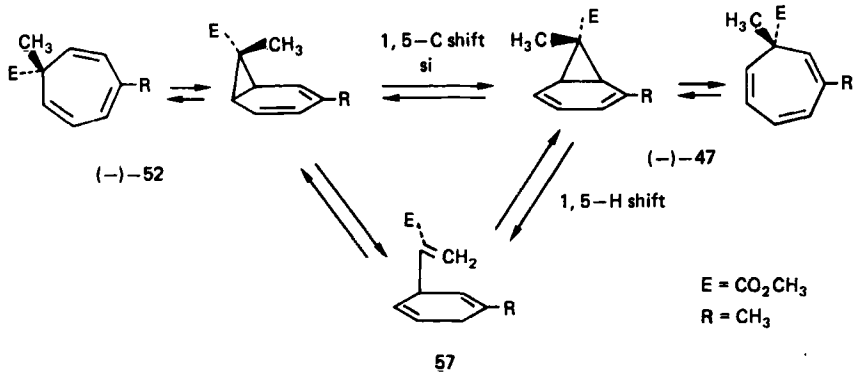

Figure 6. Assignment of the relative configurations of chiral tropilidenes (-)-**47** and (-)-**52** via the 1,5-homodienyl hydrogen shift of chiral dihydrobenzene **57** (66).

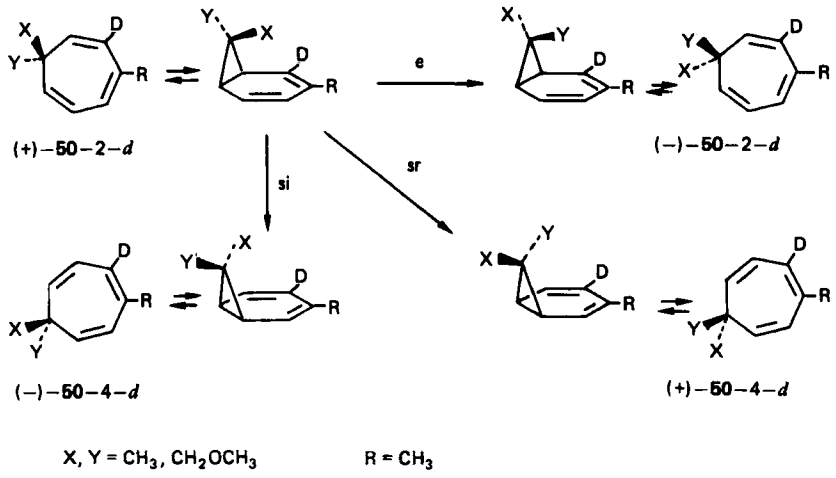

Figure 7. Possible processes for deuterium scrambling and racemization in (+)-**50**-2-*d* (68, 70).

epimerization (*e*) and a walk rearrangement with retention (*sr*) were claimed to be the dominating processes (Figure 7).

The reasons for the conflicting results—inversion and no one-center epimerization in **47** or **48** vs. the dominating one-center epimerization and retention in **50**—are not immediately evident. One obvious difference in these systems is the substituent at the migrating carbon (CO_2CH_3 and CN vs. CH_2OCH_3). A study of optically active ether (-)-**51**, however, demonstrates that this structural difference does not affect the stereochemistry of the migration (69). The walk rearrangement of (-)-**51** to (+)-**50** and (+)-**56** follows the same stereochemical route as that of the corresponding ester- and nitrile-substituted systems occurring predominantly (⩾95%) with inversion (Figure 5). The observation that (-)-**51** of undiminished optical purity is recovered from partial pyrolysis to (+)-**50** and (+)-**56** excludes the one-center epimerization in this system. Very recently the rearrangement of optically active (+)-**50**-2-*d* was carefully reexamined (70). The thermolysis mixture turned out to contain a small amount of (-)-**51**-1-*d*, the product of the nondegenerate walk rearrangement of (+)-**50**-2-*d* undetected in the first analysis (68). The updated kinetic result ($k_{si}:k_{sr}:k_e$ = 2.96:0.08:0.10) demonstrates that, in this system as well, the walk rearrangement proceeds almost exclusively with inversion at the migrating carbon. The assignment of the relative configurations of chiral tropilidenes (-)-**50** and (-)-**51** according to Figure 8 (72) provides an independent confirmation of the stereochemical course of this rearrangement.

The observed stereochemistry of the norcaradiene walk rearrangement excludes orbital symmetry control (4) as well as a conformationally equilibrated diradical intermediate of type **46** (61). The stereoselective course of the walk re-

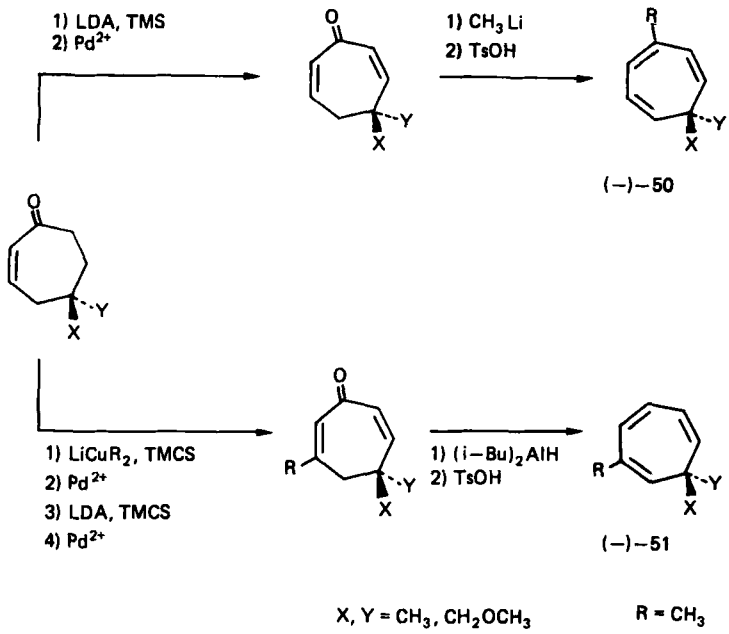

Figure 8. Assignment of the relative configurations of chiral tropilidenes (−)-**50** and (−)-**51** (72).

arrangement, however, does not differ basically from that of other processes that, it has been suggested, pass through trimethylene or tetramethylene diradicals. Some of these processes are also highly stereoselective (73). Stereoselectivity can be explained by competition between ring closure and conformational equilibration reactions in the diradical intermediate. The activation barriers of cyclization reactions in 1,3- and 1,4-diradicals seem to be small, contrary to previous thermochemical estimates (61)* and in accord with quantum mechanical calculations (74). In diradical **46**, where the parting atoms C-1 and C-7 have left the region of bonding interaction, only a slight rotation around the single bond between C-6 and C-7 is necessary to form a new bond between C-7 and C-5. This process leads to the observed inversion.

As an alternative explanation one must consider that in the diradical intermediate **46**, rotation around the tertiary radical site may be much slower than ring closure to form the inversion product.† Finally, as mentioned above, the 1,5 car-

*Thermochemical estimates using updated values of bond dissociation energies result in only small activation barriers for the cyclization of diradicals (75).

†In the case of the stereomutation of 1-methycyclopropane-1,2-dicarbonitrile, however, the rotational barrier around the tertiary carbon (substituted by CH_3 and CN) was found to be increased only slightly (by a factor of 1.37) over the rotation around the secondary carbon (substituted by H and CN) (40).

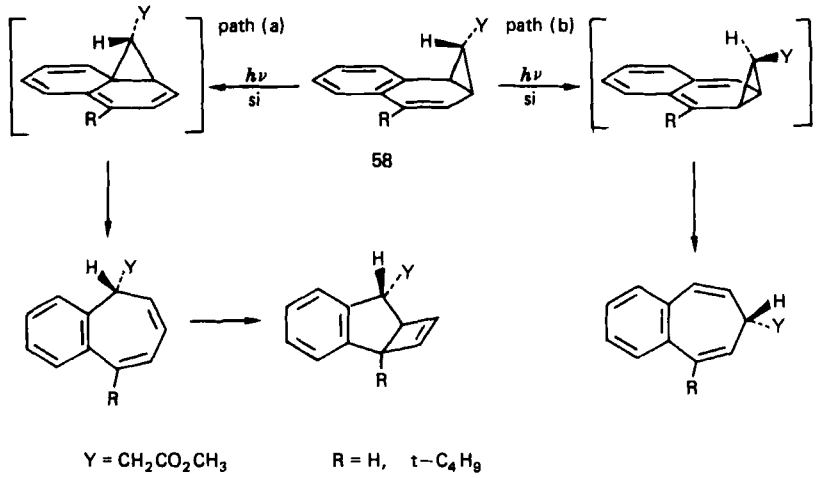

Figure 9. Stereochemical course of the photoinduced walk rearrangement. In the case of **58** (Y=$CH_2CO_2CH_3$, R=H), only path (a) was observed (55-57).

bon shift with inversion may be favored by subjacent orbital effects (28, 63). A distinction among these mechanistic possibilities has so far not been effected.

The stereochemistry of the photoinduced walk rearrangement was studied, using optically active benzonorcaradiene derivatives of type **58** (Figure 9; refs. 55, 57). On direct irradiation, the walk rearrangement of **58** occurs according to an assignment of absolute configurations of reactants and products with inversion at the migrating carbon atom. This result has been interpreted in terms of an orbital symmetry controlled process.

The stereochemical course of the photoinduced walk rearrangement sensitized by benzophenone was examined for the optically active ester (-)-**47** and nitrile (+)-**48** (76). Similarly, as in the corresponding thermal rearrangement (Figure 5), the inversion process is preferred in both systems (stereoselectivity for **47**: ⩾92%, for **48**: ⩾76%). In nitrile **48** an additional racemization made of the starting material due to a one-center epimerization at C-7 competes with the rearrangement. Stereoselective diradical processes of the triplet states were proposed to explain these results.

C. Bicyclo[6.1.0]nona-2,4,6-triene

cis-Bicyclo[6.1.0]nona-2,4,6-triene and its derivatives show rather complex thermal and photochemical behavior, which is not discussed here in all details (77). The parent compound **59** (X = Y = H) undergoes an irreversible isomerization to *cis*- and *trans*-8,9-dihydroindene **60** and **61** at 90°C (78). Trapping experiments and independent syntheses of the valence bond isomers **62**, **63**, and **64**

provided evidence that equilibration reactions **59** ⇌ **62** ⇌ **63** (79) and **59** ⇌ **64** (80) precede the irreversible isomerization **59** → **60** + **61**. Several substituted derivatives of **59** undergo epimerization at C-9, or a rearrangement to bicyclo[4.2.1] nonatrienes of type **65**,* or both.

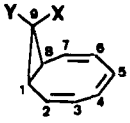

59

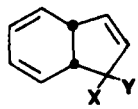

60

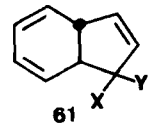

61

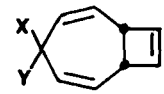

62

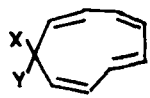

63

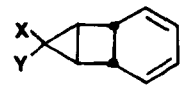

64

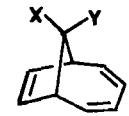

65

The thermolysis of [2,7-$(C_6H_5)_2$]-**59** (79b) and **59**-1,2,7,8,9,9-d_6 (88) does not provide any evidence for a walk rearrangement competing with dihydroindene formation. Both compounds rearrange to dihydroindene derivatives having the substitution pattern expected for the exclusive cleavage of the cyclopropane bond between C-1 and C-8. A walk rearrangement, however, was discovered for the diastereomeric systems **66a** and **66b** (89). Upon heating at about 100°C a migration of carbon atom C-9 around the periphery of the eight-membered ring occurs in each system with high stereospecificity. In no case is an exo-endo epimerization observed. The stereochemical integrity of C-9 remained preserved up to a temperature of about 180°C where the typical reactions of the bicyclo-[6.1.0] nonatriene system† occur.

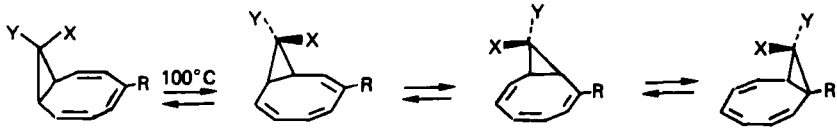

66a: X = CH_3; Y = CN
66b: X = CN, Y = CH_3

R = CH_3

*Epimerization at C-9: **59**-9-CO_2CH_3 (81), **59**-9-CN (82), **59**, 9-F, 9-OCH_3 (83) and **59**-9-*d* (84); rearrangement: 9-Phenyl-9-phospha-**59** (85), **59**-9,9-$(CN)_2$ (86), **59**-9-F, **59**-9-$N(CH_3)_2$ (83), and spiro **59**-1,9-cyclopenta-2,4-diene (87).

†Namely, isomerization to dihydroindene derivatives and bicyclo[4.2.1]nonatriene derivatives and epimerization at C-9. These processes were studied for **59a** (X = CN, Y = CH_3) and **59b** (X = CH_3, Y = CN) (89, 90).

The observed stereochemistry of the walk rearrangement corresponds to an inversion at the migrating carbon atom C-9 and fits the stereochemical requirements for an orbital symmetry controlled process (4). The different thermal behavior of **66a**, **66b** on the one hand and [2,7-$(C_6H_5)_2$]-**59**, **59**-1,2,7,8,9,9-d_6 on the other hand can be attributed to the stabilizing effect of the nitrile group* on the transition state of the walk rearrangement similar to the case observed in the bicyclo[2.1.0] pentene system.

D. Conclusions

The comparison of the walk rearrangements in the vinylogous systems bicyclo[2.1.0] pentene, norcaradiene, and bicyclo[6.1.0]nonatriene is particularly instructive in the context of the borderline between concerted and nonconcerted processes. Each rearrangement turns out to occur with inversion at the migrating carbon atom. In the case of bicyclopentene and bicyclononatriene, the stereochemical course is in accord with the predictions of orbital symmetry (4), but this is not so for the norcaradiene. Obviously stereochemistry is no reliable criterion for the distinction between a concerted and nonconcerted process in these cases.

The walk rearrangements shown in Figure 10 are initiated by cleavage of a cyclopropane bond similarly substituted in each case.†

The Gibbs activation energy of the bicyclopentene rearrangement, however, turns out to be considerably smaller than that of the other rearrangements. This may be attributed to a favorable resonance stabilization of an aromatic transition state. An alternative or additional explanation comes from an anomalously high ground state enthalpy of the bicyclopentene system.

As shown in Table 5, the heat of hydrogenation of the olefinic double bond in the parent bicyclo[2.1.0] pentene and its 5,5-dimethyl derivative is higher by about 10 kcal/mol than that of other cyclobutene systems (27).

This additional energy content is attributed to an antiaromatic destabilization of the bicyclopentene ground state. The homoantiaromatic character of bicyclopentene has been postulated on the basis of quantum mechanical calculations (94) and has recently also been derived from the photoelectron spectrum (95).

In the transition state of the bicyclopentene rearrangement the destabilization of the ground state vanishes and thereby the activation energy is lowered. The observed alternation of the Gibbs activation energies in Figure 10 might, in-

*In the case of the bicyclo[6.1.0]nonatriene system, substituents at C-9 also have an influence on the rate of the cleavage of the central cyclopropane bond between C-1 and C-8 (91).
†The additional methyl group at C-1 in the bicyclopentene systems should facilitate the opening of the bond between C-1 and C-5 by about 2 kcal/mol (40). The homolytic cleavage of a cyclopropane bond is expected to have a smaller activation barrier in norcaradiene than in bicyclopentene (by about 5.3 kcal/mol) due to the different stabilization of the radical site at C-1, pentadienyl resonance vs. allyl resonance (92). The nonplanar geometry of the cyclooctatriene ring does not permit any prediction for the bicyclo[6.1.0]nonatriene system.

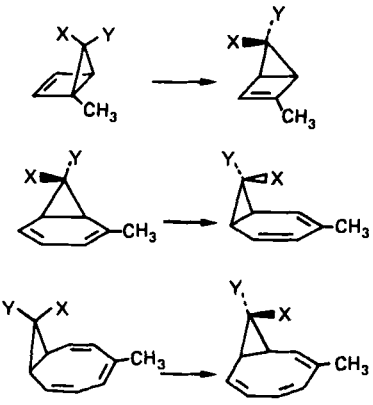

X	Y	Temp. [°C]	$\Delta G^{\ddagger}$	Ref.
CH_3	CO_2CH_3	0.0	21.7	(25)
CH_3	CN	0.0	21.9	
CH_3	CO_2CH_3	180.0	37.1	(66)
CH_3	CN	180.5	35.3	
CN	CH_3	102.5	28.8	(89)
CH_3	CH_3	102.5	29.0	

Figure 10. Comparison of the stereochemical course and the Gibbs activation enthalpies of the walk rearrangements in bicyclo[2.1.0]pentene, bicyclo[4.1.0]heptadiene, and bicyclo-[6.1.0]nonatriene. $\Delta G^{\ddagger}$ values are in kcal/mol.

deed, be based entirely on ground state effects (96). In the case of norcaradiene, conjugative interaction between the cyclopropane ring and the unsaturated π-system has been calculated to stabilize the ground state by resonance (94). This effect should increase the activation barrier of the norcaradiene walk rearrangement. In order to obtain conclusive information on the mechanism of these walk

Table 5
Heats of Hydrogenation at 25°C (in Cyclohexane) (27)

Reaction	ΔH (kcal/mol)
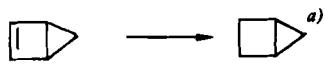	42.5
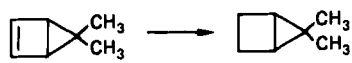	42.0
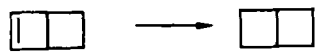	32.6
	32.7
	31.1

[a] In heptane.
[b] Calculated from the heats of formation (93).

rearrangements, it will be necessary to determine the ground state effect of the norcaradiene system experimentally.

III. WALK REARRANGEMENTS IN IONIC [n.1.0] BICYCLIC COMPOUNDS

A. Bicyclo[1.1.0]butyl Cation

Since the first preparation of cyclobutenyl cations in 1964 (97), the importance of 1,3 overlap in connection with the question of the homoaromatic nature of these cations has attracted considerable attention (98). In the case of the pentamethyl-substituted cation 67-1,3-$(CD_3)_2$ labeled by trideuteriomethyl

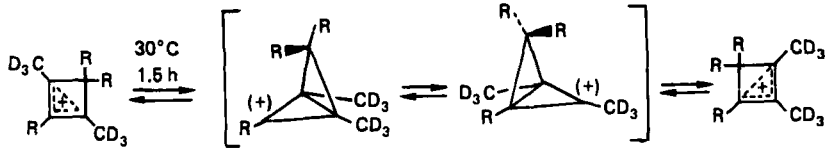

67-1,3-$(CD_3)_2$ 67-1,2-$(CD_3)_2$

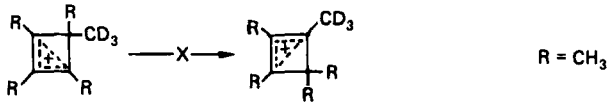

67-5-CD_3 67-1-CD_3

groups at C-1 and C-3, a degenerate rearrangement was discovered (99). A scrambling of the labeled groups between positions 1, 2, and 3 but not 4 was observed. This result can best be explained in terms of a walk rearrangement in the intermediate bicyclo[1.1.0]butyl cation. No experimental evidence of the stereochemical course is so far available. According to quantum-mechanical calculations (100), the inversion process is favored by more than 30 kcal/mol over the retention pathway predicted by orbital symmetry to be the favored one. The preference for inversion was explained by a strong interaction between the vacant orbital of the migrating center and the occupied antisymmetric Walsh type orbital of the cyclopropene ring. This interaction could provide an outstanding example of subjacent orbital symmetry control. Because the low activation barrier for the interconversion of exo and endo substituents via a planar cyclobutenyl cation, an experimental test of the stereochemical course would probably be difficult, requiring optically active cations.

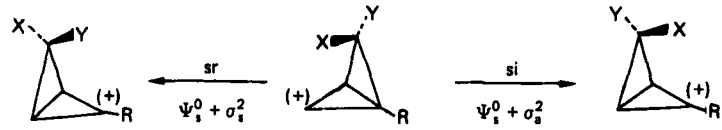

B. Bicyclo[3.1.0]hexenyl Cation

Walk rearrangements of zwitterionic bicyclo[3.1.0]hexenyl intermediates have been suggested to explain the course of photoinduced "dienone rearrangements of Type A" (Figure 11; ref. 101). Trapping experiments and independent generation via nonphotochemical routes have confirmed the intermediacy of zwitterions in several examples (102-108). Obviously, photochemical excitation is only required for the ring closure of the cyclohexadienones to the bicyclohexenyl zwitterions, which then undergo a thermally induced walk rearrangement to the observed bicyclohexenone products. Chemically activated cyclohexadienone derivatives show the same reactivity as those obtained by photochemical excitation (105).

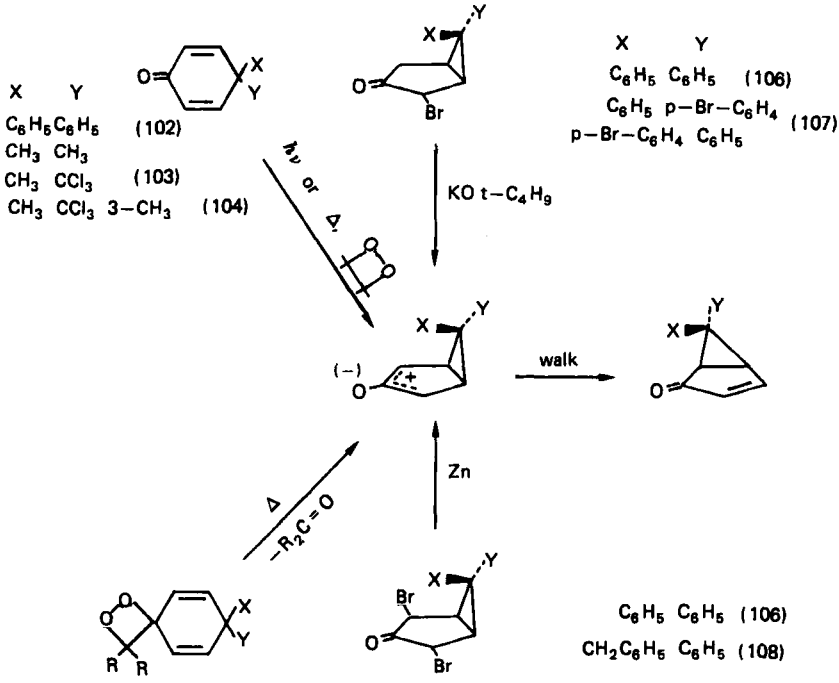

Figure 11. Reaction course of the "Type A dienone rearrangement."

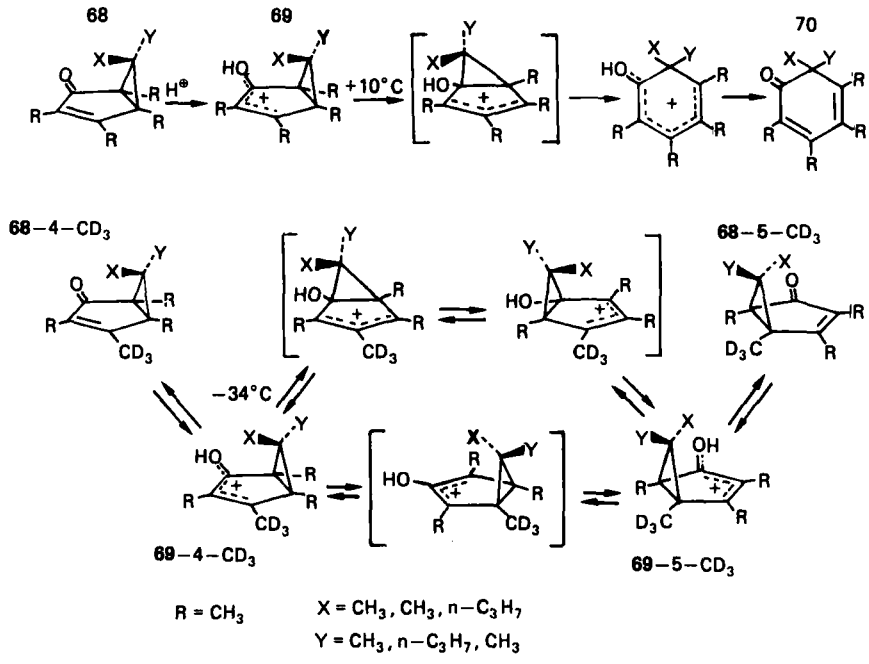

Figure 12. Walk rearrangements involved in the acid-catalyzed bicyclo[3.1.0]hexenone → cyclohexadienone isomerization (109).

A walk rearrangement of hydroxybicyclohexenyl cation **69** is involved in the acid catalyzed isomerization of bicyclohexanone **68** to cyclohexadienone **70**. The reversible nature of this walk rearrangement has been demonstrated by the equilibration **69**-4-CD_3 ⇌ **69**-5-CD_3, which precedes the ring opening to the protonated cyclohexadienone derivative (Figure 12) (109).

The highly specific nature of the bicyclohexenyl walk rearrangement became evident with the heptamethylbicyclohexenyl cation **72** (110). Bicyclic cation **72** produced by photocyclization of **71** undergoes a degenerate rearrangement, which was detected in its NMR spectrum by a temperature-dependent averaging of the resonances of the methyl groups on the five-membered ring. No averaging of the signals of the C-6 methyl groups was observed. The retained stereochemical identity of these methyl groups requires the walk rearrangement to occur with inversion at the migrating center (*si*). The retention process (*sr*), however, would be expected to produce an interchange and hence magnetic equivalence of the C-6 methyl groups. From the half-width of the NMR signals of the C-6 methyl groups at 9°C, where the rearrangement is rapid on the NMR time scale, the energy difference between the inversion and the retention process was extrapolated to be in excess of 4.6 kcal/mol.

Similarly, as in the neutral systems bicyclo[2.1.0]pent-2-ene and bicyclo[6,1.0]nona-2,4,6-triene, in the bicyclo[3.1.0]hexenyl cation the reversible

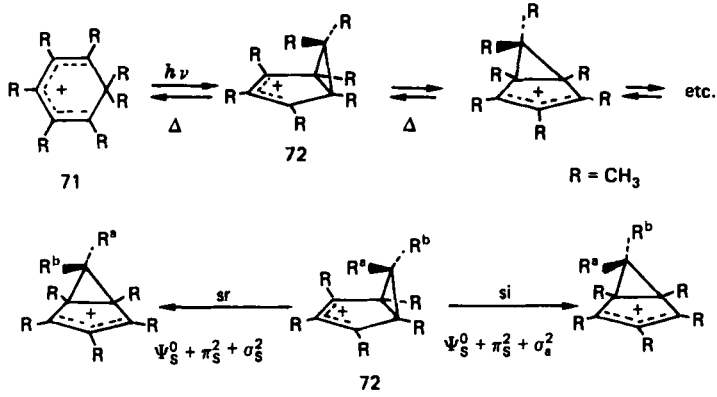

walk rearrangement competes with the irreversible electrocyclic ring opening leading to the cyclohexadienyl cation. Thus the dynamic NMR method can only be applied when the walk rearrangement proceeds much faster than ring opening. Only the hepta- and hexamethyl cations **72** and **73** fulfill this requirement (110, 111). Experimental evidence of walk rearrangements in the other systems shown in Table 6 was obtained by the use of specifically labeled starting materials (110).

The walk rearrangement in the parent bicyclo[3.1.0]hexenyl cation was examined by using deuterium labels at C-2 and C-6 (113).

The walk rearrangement in all bicyclo[3.1.0]hexenyl cations hitherto studied occurs stereospecifically with inversion at the migrating carbon. This is also true for the examples mentioned in Figures 11 and 12. The observed inversion fits the stereochemical requirements of a sigmatropic [1,4] carbon shift controlled by orbital symmetry (4). According to ab initio SCF calculations (4-31G) the *si* process is favored over the *sr* process by 12 kcal/mol (114). The same stereochemical outcome would be expected if the rearrangement included the formation of the bicyclo[2.1.1]hexenyl cation as a transient intermediate. In the case of the hexamethyl-substituted cation **73** such a possibility could be ruled out by the finding that bicyclo[2.1.1]hexenyl cation **75** independently synthesized is stable under conditions where the walk rearrangement of **73** is rapid (110).

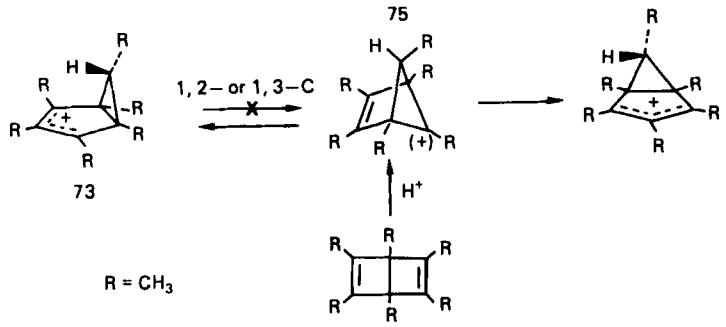

Table 6
Gibbs Activation Enthalpies of the Competing Process
in Bicyclo[3.1.0]hexenyl Cations

Compound	Walk Rearrangement $\Delta G^{\ddagger}$ (kcal/mol)	Electrocyclic Ring Opening $\Delta G^{\ddagger}$ (kcal/mol)	Ref.
R = CH_3 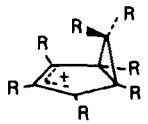 72	10.1 (−86.6°C)	19.8 (−9°C)	(110)
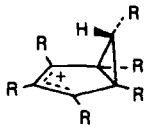 73	12.0 (−36.5°C)	21.6 (+20°C)	(110, 111)
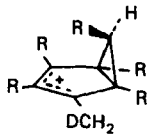 DCH_2	17.5 (−38°C)	17.4 (−35°C)	(110)
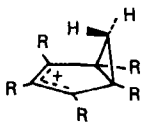	not observed > 13	17.6 (−35°C)	(112)
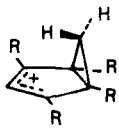	not observed > 18.6	17.1 (−31°C)	(112)
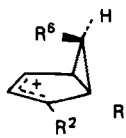	15±1 (−90°C)	19.8 (−20°C)	(113)

	R^2	R^6
74−2−*d*	D	H
74−6−*d*	H	D

The data of Table 6 show that substituents at C-6 stabilizing a positive charge decrease the activation barrier of the walk rearrangement. Therefore, considerable positive charge at C-6 must be developed during the reaction and the transition state must have the nature of a cyclopentadienylmethyl cation. The importance of C-6 substituents on the rate of the walk rearrangement has also been substantiated by MO calculations (114). Suitably substituted cyclopentadienylmethyl cations might possibly be more stable than the corresponding bicyclo[3.1.0]hexenyl cations. In such cases the bicyclo[3.1.0]hexenyl cation would be expected to be the transition state (or intermediate) for migration of C-6. Indeed, a rapid circumambulation of the acyl group has been observed for Lewis acid complexes of 5-acylpentamethylcyclopentadienes (115). The dependence of reaction rate on substituent R^1 shows that in the transition state the positive charge is substantially removed from the acyl group. It has been suggested that the migration occurs via the zwitterionic bicyclo[3.1.0]hexenyl system rather than via a "simple" [1,5] shift of the acyl group.

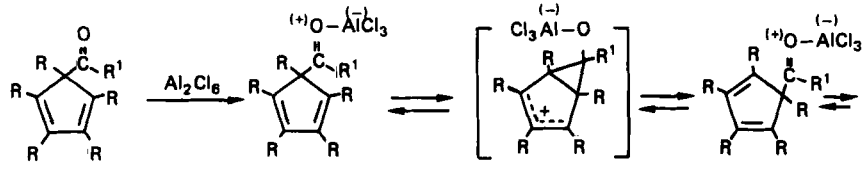

$R = CH_3$	R^1: *p*-CF_3—C_6H_4	C_6H_5	*p*-CH_3O—C_6H_4	CH_3	OC_2H_5
$\Delta G^{\ddagger}$ (kcal/mol)	5.0	8.0	11.2	10.9	≥ 18.2

Oxygen and nitrogen walk rearrangements might be involved in the photoreactions of pyrylium cation (116), 4-pyrones (117), and pyridinium cations (118), respectively. Walk rearrangements of bicyclo[3.1.0]hexenyl systems are not restricted to cations and related zwitterions. A similar rearrangement was detected in the case of a bicyclohexenyl radical labeled by deuterium at C-3 (119). Radical **76**-3-*d* generated in an adamantane matrix at -196°C was found to be stable up to -60°C at which temperature it isomerized to a mixture of the deuterated cyclohexadienyl radicals **77**-1-, -2-, or -3-*d* ($\Delta G^{\ddagger}$ = 16.4 kcal/mol). The statistical distribution of deuterium among carbon atoms C-1, 2, and 3 in **77** indicates a rapid walk rearrangement to occur below -60°C having a smaller activation energy than the ring opening.

In bicyclohexenyl radicals additionally substituted at C-6, an endo → exo-isomerization was found to proceed with a rate comparable to the walk rearrangement (120). If one starts with endo-**78**-3-*d* (R = CH_2OH), the reaction product consist of a mixture of exo-**78**-2- and -3-*d*. Both reactions, walk rearrangement and endo → exo isomerization, have been assumed to involve an intermediate cyclopentadienylmethyl radical of type **79**. In view of MO considera-

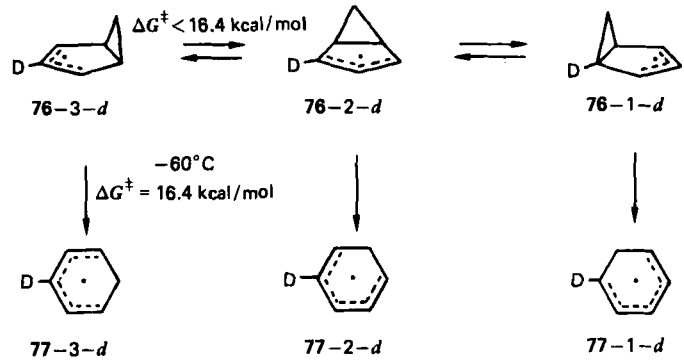

tions in the radical system, the energy difference between a concerted sigmatropic [1,4] carbon shift and an intermediate of type **79** is expected to be negligibly small (119).

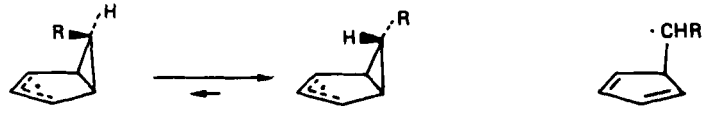

R = CH_2OH, CN, COOH

C. Bicyclo[5.1.0]octadienyl Cation

The homotropylium cation, easily available to protonation of cyclooctatetraene (121), has attracted considerable attention, particularly due to its nonclassical homoaromatic structure (1). Two pathways can be discerned for the mutual interconversion of endo- into exo-**80**-8-*d* (122): (i) a conformational ring inversion passing through a planar classical cyclooctatrienyl cation, (ii) a walk rearrangement of the bicyclo[5.1.0]octadienyl cation formed as an intermediate, proceeding with retention at the migrating carbon atom C-8 (*sr* process) as postulated for an orbital symmetry controlled process (4).

The possibility of a walk rearrangement was ruled out by thermolysis of **80**-4-*d* (122, 123). No deuterium scrambling could be observed even when **80**-4-*d* was heated almost to complete destruction of the cation (75 min at 65°C in FSO_3H). By exclusion, the conformational ring inversion is the most likely mechanism for the 8-endo/8-exo hydrogen interchange in the homotropylium cation. A similar result was also obtained for the 8-carbethoxy-2-deuteriohomotropylium cation. This finding places a lower limit of 26-27 kcal/mol on the Gibbs activation energy for the walk rearrangement in the parent homotropylium cation and its 8-carbethoxy derivative (122).

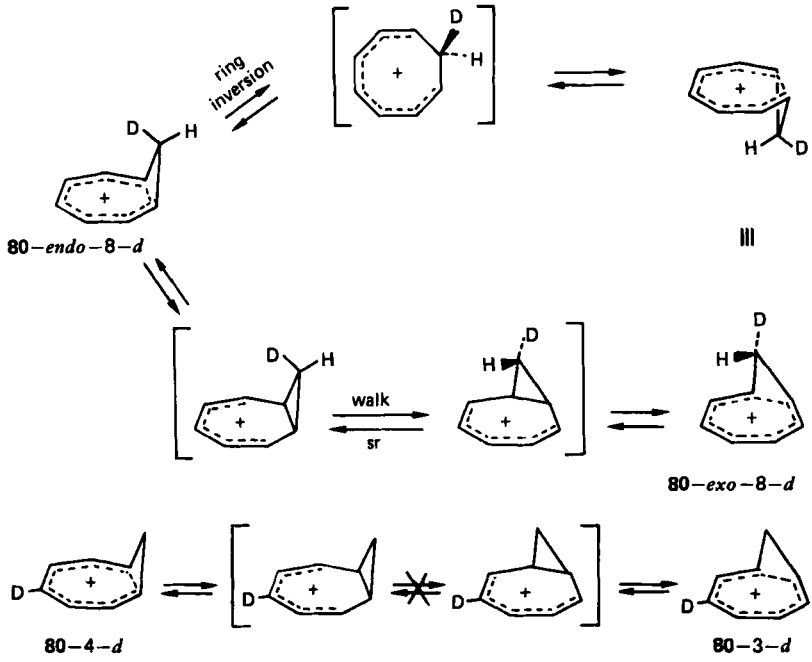

No walk rearrangement could be detected in the case of the exo-8-methyl-1-hydroxyhomotropylium cation. Upon heating at 37°C it isomerized only to protonated propiophenone (124b). A thermally induced walk rearrangement of a homotropylium cation was finally observed when carbon atom C-8 was substituted by two methyl groups (Figure 13; ref. 124). The parent 8,8-dimethylhomotropylium cation undergoes a facile isomerization to the isopropyltropylium cation even at -50°C, which prevents the detection of the degenerate walk rearrangement by using the dynamic NMR method. A slow walk rearrangement of this system at -75°C was uncovered by labeling one ring carbon with an additional methyl group (125).

In the effort to prepare 1,5-methano[10]annulene, elimination of HI from iodotetraene **83** was found to give the rearranged pentaene **84** (126). A reasonable explanation for its formation is a walk rearrangement of the intermediate 1,7-bridged bicyclo[5.1.0]octadienyl cation. In this case the walk may be favored by the steric effect of the three-atom linkage, which probably constrains the homotropylium cation to the closest bicyclo[5.1.0]octadienyl form.

Photochemically induced walk rearrangements were observed for several 2-hydroxyhomotropylium cations. On irradiation, these cations isomerize to the corresponding 1-hydroxy ions (124b, 127). The stereochemical course, though not known for the thermal walk rearrangement, was clarified for the photochemical reaction by using the diastereomeric cations exo- and endo-**85** (124b, 127).

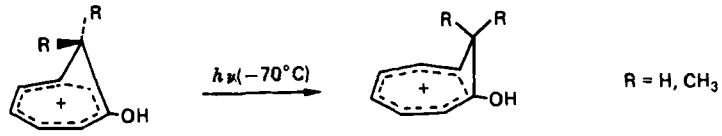

As shown in Figure 14, interconversion of each diastereomeric cation occurs with inversion at the migrating carbon. The stereochemical analysis of the rearrangement of endo-**85** proved to be difficult, because the starting material contained a small amount of exo-**85** and the product, endo-**86**, underwent a slow isomerization to exo-**86** even at -70°C under the conditions of photolysis. The low conformational stability of endo-**85** might be due to the conjugative interaction of the hydroxy group in the planar cyclooctatrienyl cation. The inversion

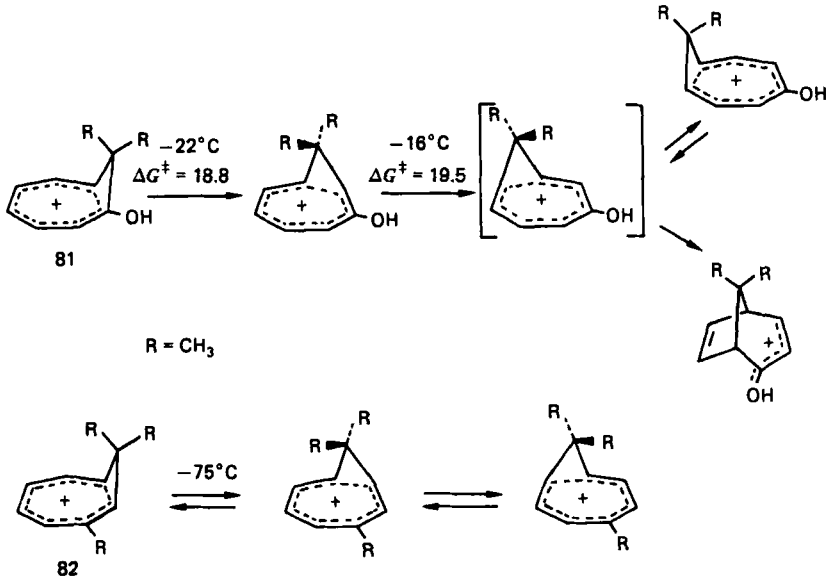

Figure 13. Walk rearrangements in a substituted 8,8-dimethylhomotropylium cations. $\Delta G^{\ddagger}$ values are in kcal/mol (124, 125).

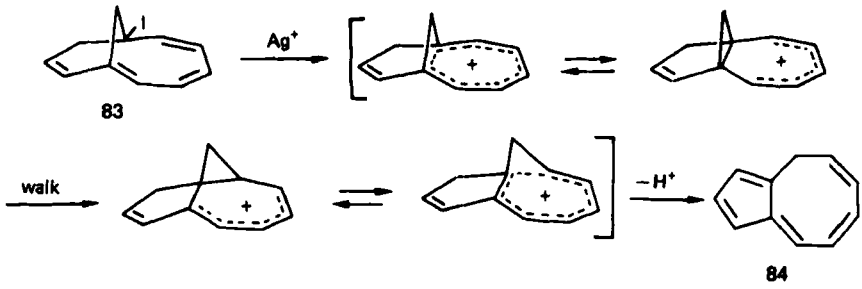

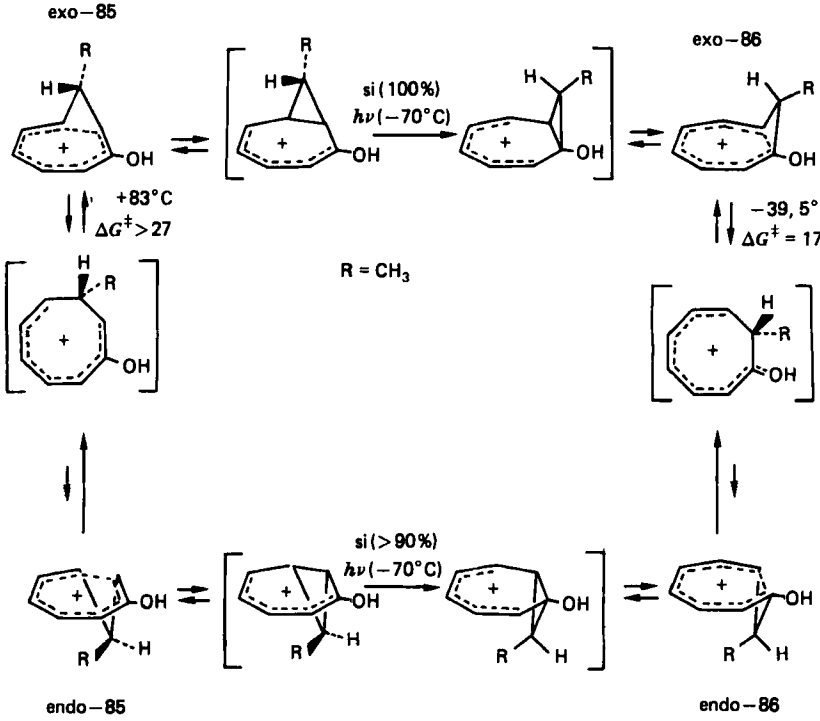

Figure 14. Stereochemistry of the photochemically induced walk rearrangement in homotropylium cations. Gibbs activation energy of the thermal endo → exo isomerization is in kcal/mol (124B, 127).

observed on photochemical excitation is as expected for an orbital symmetry controlled process (4).

D. Conclusions

The comparison of thermal walk rearrangements in the vinylogous bicyclo[3.1.0]hexenyl and bicyclo[5.1.0]octadienyl cations shows that, in both cases, the activation barrier is lowered by methyl substituents at the migrating carbon atom. In both transition states the positive charge seems to be largely localized there.

The influence of methyl substituents on the rates of the rearrangement predicted by ab initio MO calculations agrees with the experimental observations (114). Surprisingly, the calculations suggest the experimentally hitherto unknown stereochemical course of the thermal homotropylium walk to depend on the substitution pattern at C-8. As postulated by orbital symmetry considerations, the walk rearrangement in the parent homotropylium cation is predicted

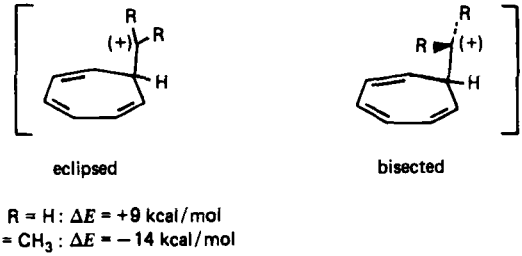

Figure 15. Calculated differences in energy (ΔE) between the bisected transition state, "Woodward-Hoffmann forbidden," and the eclipsed transition state, "Woodward-Hoffmann allowed" (114).

to occur with retention at the migrating carbon C-8, passing through an eclipsed transition state. In the case of the 8,8-dimethyl derivative, the calculations favor the inversion process passing through a bisected transition state (Figure 15).

Two effects have to be considered for understanding the substantially different Gibbs activation energies of the walk rearrangements in the deuterated parent compounds bicyclo[3.1.0]hexenyl cation ($\Delta G^{\ddagger}$ = 15 kcal/mol) (113) and homotropylium cation ($\Delta G^{\ddagger} > 27$ kcal/mol) (122). The situation here is very similar to that of the neutral compounds, bicyclo[2.1.0]pent-2-ene and norcaradiene, discussed above. The different height of the activation barrier could be the result of either ground state or transition state effects. At present a conclusive distinction between these effects is impossible. So far no experimental data are available for the ground state enthalpies of bicyclo[3.1.0]hexenyl and homotropylium cations. MO calculations, however, suggest that the homotropylium cation is substantially stabilized by resonance while the bicyclo[3.1.0]hexenyl cation is not stabilized or even destabilized by the conjugative interaction between the cyclopropane ring and the π-system (94).

Based on ab initio SCF calculations (114), the difference in the activation energies required for the two walk rearrangements might result entirely from these ground state differences between the bicyclo-[3.1.0]hexenyl and homotropylium cations.

Comparable walk rearrangements of bicyclo[3.1.0]hexenyl or bicyclo-[5.1.0]octadienyl anions do not appear to have been reported. Bicyclo[3.1.0]-hexenyl anions were found to undergo a very facile disrotatory electrocyclic ring opening to the corresponding cyclohexadienyl anions (Meisenheimer complexes) (128). The more stable bicyclo[5.1.0]octadienyl anion (129) exhibits a temperature independent NMR spectrum over the range of -80° to -20°C indicating that any degenerate walk rearrangement is slow on the NMR time scale. As shown in Fig. 16, thermolysis leads to the methylenecycloheptadienyl anion (129a) and photolysis to the cyclooctatrienyl anion, which is not stable in the case of the parent anion (129b) but is stable in the case of the 8,8-dimethyl de-

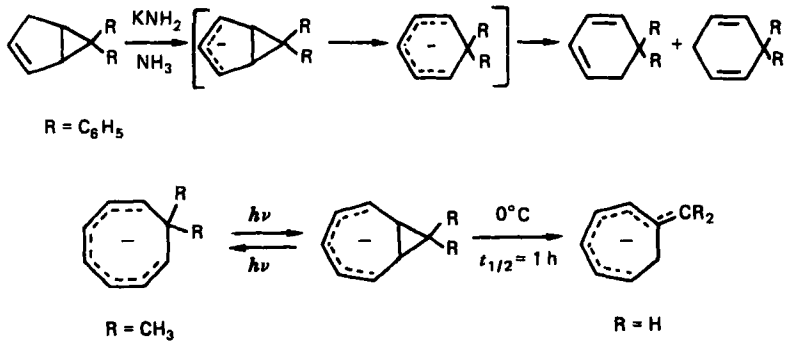

Figure 16. Isomerization reactions of bicyclo[3.1.0]hexenyl and bicyclo[5.1.0]octadienyl anions (128, 129).

rivative (129c). In the absence of any ring labels it is not clear whether walk rearrangements can compete with the other processes here.

In the transition states of walk rearrangements in bicyclo[3.1.0]hexenyl and bicyclo[5.1.0]octadienyl anions, a considerable amount of negative charge should be developed at the migrating center. Therefore, substituents stabilizing a negative charge (e.g., ester or nitrile groups) might well favor walk rearrangements over other processes. Experimental tests for the hitherto hypothetical walk rearrangements in anions are, however, yet to come.

ACKNOWLEDGMENTS

I thank Professor Dr. Wolfgang Roth for many helpful comments, my coworkers Dr. Friedhelm Adamsky, Mrs. Barbara Dogan (Brassel), Mr. Michael Wette, and Dr. Salih Yaslak, who have done most of the experimental work related to our contributions to this field, and Mrs. Margot Bock for skillfully typing the manuscript. In addition, I am grateful to the Deutsche Forschungsgemeinschaft and Fonds der Chemischen Industrie for financial support.

REFERENCES

1. Reviews: Winstein, S. *Q. Rev. Chem. Soc.* **1969**, *23*, 141. Warner, P. M. In "Topics in Nonbenzoid Aromatic Chemistry," Vol. 2; Nozoe, T., Ed. Breslow, R.; Hafner, K.; Ito, S.; Murata, I.; Hirokawa, Tokio; Paquette, L. A., *Angew. Chem.* **1978**, *90*, 114; *Angew. Chem. Int. Ed. Engl.* **1978**, *17*, 106.
2. (a) Zimmerman, H. E.; Eberbach, W. *J. Am. Chem. Soc.* **1973**, *95*, 3970. (b) Jerina, D. M.; Witkop, B.; McIntosh, C. L.; Chapman, O. L. *ibid.* **1974**, *96*, 5578.
3. Childs, R. F. *Tetrahedron* **1982**, *38*, 567.

4. Woodward, R. B.; Hoffmann, R. *Angew Chem.* **1969**, *81*, 797; *Angew. Chem. Int. Ed. Engl.* **1969**, *8*, 781.
5. Reviews: Lablache-Combier, A. In "Photochemistry of Heterocyclic Compounds," Buchardt, O., Ed.; Wiley: New York, 1976; p. 122. Padwa, A. In "Rearrangements in Ground and Excited States," Vol. 3; de Mayo, P., Ed.; Academic Press: New York, 1980, p. 501.
6. (a) Hiraoka, H. *Chem. Comm.* **1970**, *1306*; *ibid.* **1971**, 1610. (b) Barltrop, J.; Day, A. C.; Moxon, P. D.; Ward, R. R. *J. Chem. Soc., Chem. Comm.* **1975**, 786. (c) Barltrop, J. A.; Day, A. C.; Ward, R. W. *ibid.* **1978**, 131.
7. (a) Srinivasan, R. *J. Am. Chem. Soc.* **1967**, *89*, 1758, 4812; *Pure Appl. Chem.* **1968**, *16*, 65. (b) Hiraoka, H. *J. Phys. Chem.* **1970**, *74*, 574. (c) Couture, A.; Lablache-Combier, A. *Chem. Comm.* **1971**, 891. Couture, A.; Delevallee, A.; Lablache-Combier, A.; Parkanyl, C. *Tetrahedron* **1975**, *31*, 785. (d) van Tamelen, E. E.; Whitesides, T. H. *J. Am. Chem. Soc.* **1968**, *90*, 3894; *ibid.* **1971**, *93*, 6129.
8. (a) Review: Wynberg, H. *Acc. Chem. Res.* **1971**, *4*, 65. (b) Wynberg, H.; van Driel, H. *J. Am. Chem. Soc.* **1965**, *87*, 3998. Wynberg, H.; Kellogg, R. M.; van Driel, H.; Beekhuis, G. E. *ibid.* **1966**, *88*, 5047. Wynberg, H.; Beekhuis, G. E.; van Driel, H.; Kellogg, R. M. *ibid.* **1967**, *89*, 3498. Wynberg, H.; van Driel, H.; Kellogg, R. M.; Buter, J. *ibid.* **1967**, *89*, 3487. Kellogg, R. M.; Wynberg, H. *Tetrahedron Lett.* **1968**, 5895. Wynberg, H.; Kellogg, R. M.; van Driel, H.; Beekhuis, G. E. *J. Am. Chem. Soc.* **1967**, *89*, 3501. (c) Couture, A.; Lablache-Combier, A. *Tetrahedron* **1971**, *27*, 1059. (d) Kellogg, R. M. *Tetrahedron Lett.* **1972**, 1429. (e) Barltrop, J. A.; Day, A. C.; Irving, E. *J. Chem. Soc., Chem. Comm.* **1979**, 881, 966.
9. (a) Beak, P.; Miesel, J. L.; Messer, W. R. *Tetrahedron Lett.* **1967**, 5315. Beak, P.; Messer, W. *Tetrahedron* **1969**, *25*, 3287. (b) Barltrop, J. A.; Day, A. C.; Mack, A. G.; Shahrisa, A.; Wakamatsu, S. *J. Chem. Soc., Chem. Comm.* **1981**, 604.
10. (a) Ullmann, E. F.; Singh, B. *J. Am. Chem. Soc.* **1966**, *88*, 1844; *ibid.* **1967**, *89*, 6911. (b) Kurtz, D. W.; Shechter, H. *Chem. Comm.* **1966**, 689.
11. Kojima, M.; Maeda, M. *Tetrahedron Lett.* **1969**, 2379.
12. Maeda, M.; Kojima, M. *J. Chem. Soc., Chem. Comm.* **1973**, 539.
13. Catteau, J. P.; Lablache-Combier, A.; Pollet, A. *Chem. Comm.* **1969**, 1018. Lablache-Combier, A.; Pollet, A. *Tetrahedron* **1972**, *28*, 3141.
14. Vernin, G.; Poite, J.-C.; Metzger, J.; Aune, J. P.; Dou, H. J. M. *Bull. Soc. Chim. Fr.* **1971**, 1103. Vernin, G.; Jauffred, R.; Ricard, C.; Dou, H. J. M.; Metzger, J. *J. Chem. Soc., Perkin II* **1972**, 1145. Vernin, G.; Riou, C.; Dou, H. J. M.; Bouscasse, L.; Metzger, J.; Loridan, G. *Bull. Soc. Chim. Fr.* **1973**, 1743. Riou, C.; Poite, J.-C.; Vernin, G.; Metzger, J. *Tetrahedron* **1974**, 30, 879. Riou, C.; Vernin, G.; Dou, H. J. M.; Metzger, J. *Bull. Soc. Chim. Fr.* **1972**, 2673. Vernin, G.; Poite, J.-C.; Dou, H. J. M.; Metzger, J. *ibid.* **1972**, 3157. Kojima, M.; Maeda, M. *Chem. Comm.* **1970**, 386. Maeda, M.; Kojima, M. *Tetrahedron Lett.* **1973**, 3523. Ohashi, M.; Iio, A.; Yonezawa, T. *Chem. Comm.* **1970**, 1148.
15. Williams, W. M.; Dolbier, W. R., Jr. *J. Am. Chem. Soc.* **1972**, *94*, 3955.
16. Wiebe, H. A.; Braslavsky, S.; Heicklen, J. *Can. J. Chem.* **1972**, *50*, 2721. Kobayashi, Y.; Kumadaki, I.; Ohsawa, A.; Sekine, Y. *Tetrahedron Lett.* **1975**, 1639.
17. Ross, J. A.; Seiders, R. P.; Lemal, D. M. *J. Am. Chem. Soc.* **1976**, *98*, 4325. Bushweller, C. H.; Ross, J. A.; Lemal, D. M. *ibid.* **1977**, *99*, 629.
18. Synder, J. P.; Halgren, T. A. *J. Am. Chem. Soc.* **1980**, *102*, 2861. Minkin, V. I.; Minyaev, R. M. *J. Org. Chem. USSR* **1979**, *15*, 1401.
19. Kobayashi, Y.; Ando, A.; Kawada, K.; Kumadaki, I. *J. Org. Chem.* **1980**, *45*, 2966.
20. Wirth, D.; Lemal, D. M. *J. Am. Chem. Soc.* **1982**, *104*, 847.

21. Brauman, J. I.; Ellis, L. E.; van Tamelen, E. E. *J. Am. Chem. Soc.* **1966**, *88*, 846. van Tamelen, E. E.; Brauman, J. I.; Ellis, L. E. *ibid.* **1971**, *93*, 6145. Andrist, A. H.; Baldwin, J. E.; Pinschmidt, R. K., Jr. *Org. Synth.* **1976**, *55*, 15.
22. (a) Baldwin, J. E.; Pinschmidt, R. K., Jr.; Andrist, A. H. *J. Am. Chem. Soc.* **1970**, *92*, 5249, Baldwin, J. E.; Andrist, A. H. *Chem. Comm.* **1970**, 1561. Baldwin, J. E.; Andrews, G. D. *J. Am. Chem. Soc.* **1972**, *94*, 1775. (b) McLean, S.; Findlay, D. M.; Dmitrienko, G. I. *ibid.* **1972**, *94*, 1380. (c) Flowers, M. C.; Frey, H. M. *ibid.* **1972**, *94*, 8636. Brauman, J. I.; Farneth, W. E.; D'Amore, M. B. *ibid.* **1973**, *95*, 5043. Andrews, G. D.; Davalt, M.; Baldwin, J. E. *ibid.* **1973**, *95*, 5044. Farneth, W. E.; D'Amore, M. B.; Brauman, J. I. *ibid.* **1976**, *98*, 5546. (d) Andrews, G. D.; Baldwin, J. E. *ibid.* **1977**, *99*, 4853.
23. Andrews, G. D.; Baldwin, J. E. *J. Am. Chem. Soc.* **1977**, *99*, 4851.
24. Maier, G.; Schäfer, U.; Sauer, W.; Hartan, H.; Matusch, R.; Oth, J. F. M. *Tetrahedron Lett.* **1978**, 1837.
25. Klärner, F.-G.; Adamsky, F. *Angew. Chem.* **1979**, *91*, 738; *Angew. Chem. Int. Ed. Engl.* **1979**, *18*, 674; *Chem. Ber.* **1983**, *116*, 299.
26. Brauman, J. I., Golden, D. M. *J. Am. Chem. Soc.* **1968**, *90*, 1920; *Trans. Faraday Soc.* **1969**, *65*, 464.
27. Roth, W. R.; Klärner, F.-G.; Lennartz, H.-W. *Chem. Ber.* **1980**, *113*, 1818.
28. Schoeller, W. W. *J. Am. Chem. Soc.* **1975**, *97*, 1978.
29. Hoffmann, R. *Tetrahedron Lett.* **1970**, 2907. Günther, H., *Tetrahedron Lett.* **1970**, 5173; Hoffmann, R.; Stohrer, W.-D. *J. Am. Chem. Soc.* **1971**, *93*, 6941. Hoffmann, R.; Fujimoto, H.; Swenson, J. R.; Wan, C. C. *ibid.* **1973**, *95*, 7644.
30. An example studied intensively is the isomerization of indazole to benzimidazole: Tiefenthaler, H.; Dörscheln, W.; Göth, H.; Schmid, H. *Helv. Chim. Acta* **1967**, *50*, 2244. Dubois, J. R.; Labhart, H. *Chimia* **1969**, *23*, 109. Heinzelmann, W.; Märky, M.; Gilgen, P. *Helv Chim. Acta* **1976**, *59*, 1512, 1528.
31. Palensky, F. J.; Morrison, H. A. *J. Am. Chem. Soc.* **1977**, *99*, 3507. Padwa, A.; Loza, R.; Getman, D. *Tetrahedron Lett.* **1977**, 2847; Giacherio, D.; Morrison, H. *J. Am. Chem. Soc.* **1978**, *100*, 7109. Morrison, H.; Giacherio, D.; Palensky, F. J. *J. Org. Chem.* **1982**, *47*, 1051.
32. Dolbier, W. R., Jr.; Matsui, K.; Michl, J.; Horak, D. V. *J. Am. Chem. Soc.* **1977**, *99*, 3876. Dolbier, W. R., Jr.; Matsui, K.; Dewey, H. J.; Horak, D. V.; Michl, J. *ibid.* **1979**, *101*, 2136. Dolbier, W. R., Jr.; Matsui, K.; McCullagh, L.; Anapolle, K. E. *J. Org. Chem.* **1979**, *44*, 2842. Dolbier, W. R., Jr.; Anapolle, K. E.; McCullagh, L.; Matsui, K.; Riemann, J. M.; Rolison, D. *ibid.* **1979**, *44*, 2845.
33. Morrison, H.; Giacherio, D. *J. Org. Chem.* **1982**, *47*, 1058.
34. Ladenburg, A. *Liebigs Ann. Chem.* **1883**, *217*, 74.
35. Warner, P. M.; Lu, S. L. *J. Am. Chem. Soc.* **1980**, *102*, 331 and references cited therein.
36. Berson, J. A.; Willcott, M. R., III. *J. Am. Chem. Soc.* **1965**, *87*, 2751–52; *ibid.* **1966**, *88*, 2494. Berson, J. A. *Acc. Chem. Res.* **1968**, *1*, 152.
37. Willcott, M. R., III; Boriack, C. J. *J. Am. Chem. Soc.* **1968**, *90*, 3287; *ibid.* **1971**, *93*, 2354.
38. Berson, J. A.; Grubb, P. W.; Clark, R. A.; Hartter, D. R.; Willcott, M. R., III. *J. Am. Chem. Soc.* **1967**, *89*, 4076.
39. Ciganek, E. *J. Am. Chem. Soc.* **1965**, *87*, 652; *ibid.* **1967**, *89*, 1454; *ibid.* **1971**, *93*, 2207. Reich, H. J.; Ciganek, E.; Roberts, J. D. *ibid.* **1970**, *92*, 5166.
40. Doering, W. v. E.; Horowitz, G.; Sachdev, K. *Tetrahedron* **1977**, *33*, 273.
41. Baldwin, J. E. In "Pericyclic Reactions," Vol. 2, Academic Press: New York, 1977,

p. 286. Baldwin has suggested an unusual norcaradiene → cycloheptatriene isomerization of type (A) as an alternative mechanism for the walk rearrangement. In the rate-determining step of this mechanism, the bond C_5–C_6 must be cleaved also. The substantial effect of substituents at C_7 (36, 38), however, is not in accord with this proposal.

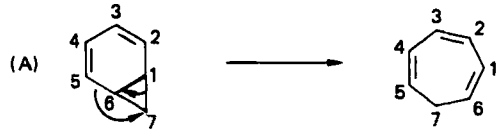

42. Vogel, E.; Wiedermann, W.; Roth, H.-D.; Eimer, J.; Günther, H. *Justus Liebigs Ann. Chem.* **1972**, *759*, 1.
43. Paquette, L. A.; Kuhla, D. E.; Barrett, J. H.; Haluska, R. J. *J. Org. Chem.* **1969**, *34*, 2866. Paquette, L. A. *Angew. Chem.* **1971**, *83*, 11; *Angew. Chem. Int. Ed. Engl.* **1971**, *10*, 11.
44. (a) Vogel, E.; Günther, H. *Angew. Chem.* **1967**, *79*, 429; *Angew. Chem. Int. Ed. Engl.* **1967**, *6*, 385. (b) Bruice, P. Y.; Kasperek, G. J.; Bruice, T. C.; Yagi, H.; Jerina, D. M. *J. Am. Chem. Soc.* **1973**, *95*, 1673.
45. Vogel, E.; Roth, H.-D. *Angew. Chem.* **1964**, *76*, 145; *Angew Chem. Int. Ed. Engl.* **1964**, *3*, 228. Vogel, E. "Aromaticity," *Chem. Soc. (London)*, Spec. Publ. **1967**, *21*, 113; *Pure Appl. Chem.* **1969**, *20*, 237.
46. Vogel, E.; deCleur, E.; Jabs, G., cited by Gerson, F.; Huber, W.; Müllen, K. *Angew. Chem.* **1978**, *90*, 216; Angew. Chem. *Int. Ed. Engl.* **1978**, *17*, 208.
47. Klärner, F.-G.; Vogel, E. *Angew. Chem.* **1973**, *85*, 864; *Angew. Chem. Int. Ed. Engl.* **1973**, *12*, 840.
48. Paquette, L. A.; Leichter, L. M. *J. Am. Chem. Soc.* **1970**, *92*, 1765; *ibid.* **1971**, *93*, 5128.
49. Fühlhuber, H. D.; Sauer, J. *Tetrahedron Lett.* **1977**, 4393.
50. Ciganek, E. *J. Am. Chem. Soc.* **1967**, *89*, 1458.
51. Brightwell, N. E.; Griffin, G. W. *J. Chem. Soc., Chem. Comm.* **1973**, 37.
52. Toda, T.; Nitta, M.; Mukai, T. *Tetrahedron Lett.* **1969**, 4401.
53. Kolbinger, H.; Reissenweber, G.; Sauer, J. *Tetrahedron Lett.* **1976**, 4321. Reissenweber, G.; Sauer, J. *ibid.* **1977**, 4389.
54. Gruber, G. W.; Pomerantz, M. *J. Am. Chem. Soc.* **1969**, *91*, 4004.
55. Kato, M.; Kawamura, M.; Okamoto, Y.; Miwa, T. *Tetrahedron Lett.* **1972**, 1171. Kato, M.; Funakura, M.; Tsuji, M.; Miwa, T. *J. Chem. Soc., Chem. Comm.* **1976**, 63.
56. Kato, M.; Tsuji, M.; Miwa, T. *Bull. Chem. Soc. Jpn.* **1978**, *51*, 1450.
57. Kato, M.; Takatoku, K.; Ito, S.; Funakura, M.; Miwa, T. *Bull. Chem. Soc. Jpn.* **1980**, *53*, 3648; Kato, M.; Kobayashi, H.; Yamamoto, H.; Seto, K.; Ito, S.; Miwa, T. *ibid.* **1982**, *55*, 3523. Very recently M. Kato *et al.* studied the stereochemistry of the photochemically induced benzonorcaradiene walk rearrangement under sensitized conditions. The stereochemical outcome depends on steric effects of the substituents used for the analysis.
58. Madigan, M. D.; Swenton, J. S. *J. Am. Chem. Soc.* **1971**, *93*, 6316. Swenton, J. S.; Burdett, K. A.; Madigan, D. M.; Johnson, T.; Rosso, P. D. *ibid.* **1975**, *97*, 3428.
59. Gerson, F.; Huber, W.; Müllen, K. *Angew. Chem.* **1978**, *90*, 216; *Angew. Chem. Int. Ed. Engl.* **1978**, *17*, 208.
60. Vogel, E.; Königshofen, H.; Wassen, J.; Müllen, K.; Oth, J. F. M. *Angew. Chem.* **1974**, *86*, 777; *Angew. Chem. Int. Ed. Engl.* **1974**, *13*, 732. Alternative syntheses of

heptalene were reported by the following: Dauben, H. J., Jr.; Bertelli, D. J. *J. Am. Chem. Soc.* **1961**, *83*, 4659. Vogel, E.; Kerimis, D.; Allison, N. T.; Zellerhoff, R.; Wassen, J. *Angew. Chem.* **1979**, *91*, 579; *Angew. Chem. Int. Ed. Engl.* **1979**, 18, 545. Paquette, L. A.; Browne, A. R.; Chamot, E. *Angew. Chem.* **1979**, *91*, 581; *Angew. Chem. Int. Ed. Engl.* **1979**, *18*, 546.

61. According to a thermochemical estimate, diradical **46** (X = Y = H) is expected to have an activation barrier of 9.3 kcal/mol for the ring closure to norcaradiene and of as much as 24 kcal/mol for the closure to norbornadiene. O'Neal, H. E.; Benson, S. W. *Int. J. Chem. Kinet.* **1970**, *II*, 423.
62. Hine, J. *J. Org. Chem.* **1966**, *31*, 1236. Altmann, J. A.; Tee, O. S.; Yates, K. *J. Am. Chem. Soc.* **1976**, *98*, 7132, and references cited therein. Berson, J. A. "Rearrangements in Ground and Excited States," Vol. 1; de Mayo, P., Ed. Academic Press: New York, 1980, p. 376. Berson gives a critical comment on the "principle of least motion."
63. Berson, J. A.; Salem, L. *J. Am. Chem. Soc.* **1972**, *94*, 8917. Berson, J. A. *Acc. Chem. Res.* **1972**, *5*, 406. Epiotis, N. D.; Yates, R. L.; Bernadi, F. *J. Am. Chem. Soc.* **1975**, *97*, 4198. de Dobbelaere, J. R.; van Dijk, J. M. F.; de Haan, J. W.; Buck, H. M. *ibid.* **1977**, *99*, 392. Bouma, W. J.; Vincent, M. A.; Radom, L. *Int. J. Quant. Chem.* **1978**, *14*, 767.
64. Rubin, M. B. *J. Am. Chem. Soc.* **1981**, *103*, 7791, and references cited therein. Both diastereomeric norcaradiene forms could be observed for the equilibration of several substituted 7-methyl-(norcaradiene ⇌ cycloheptatriene)-7-carbonitriles. Klärner, F.-G. *Tetrahedron Lett.* **1974**, *19*. Klärner, F.-G.; Yaslak, S.; Wette, M. *Chem. Ber.* **1977**, *110*, 107. Klärner, F.-G.; Schmidt, E. K. G.; Abdel Rahman, M. A. *Angew. Chem.* **1982**, *94*, 136; *Angew. Chem. Int. Ed. Engl.* **1982**, *21*, 138. Klärner, F.-G., Schmidt, E. K. G.; Abdel Rahman, M. A.; Kollmar, H. *Angew. Chem.* **1982**, *94*, 137; *Angew. Chem. Int. Ed. Engl.* **1982**, *21*, 139.
65. Anet, F. A. L. *J. Am. Chem. Soc.* **1964**, *86*, 458. Jensen, F. R.; Smith, L. A. *ibid.* **1964**, *86*, 956.
66. Klärner, F.-G. *Angew. Chem.* **1974**, *86*, 270; *Angew. Chem. Int. Ed. Engl.* **1974**, *13*, 268. Klärner, F.-G.; Yaslak, S.; Wette, M. *Chem. Ber.* **1979**, *112*, 1168.
67. Berson, J. A.; Hansen, R. T., unpublished results. Hansen, R. T. Ph.D. Thesis, Yale University, New Haven, 1976; *Chem. Abstr.* **1977**, *87*, 101, 708 p; *Diss. Abstr. Int. B.* **1977**, *37*, 6130.
68. Baldwin, J. E.; Broline, B. M. *J. Am. Chem. Soc.* **1978**, *100*, 4599.
69. Klärner, F.-G.; Brassel, B. *J. Am. Chem. Soc.* **1980**, *102*, 2469.
70. Baldwin, J. E.; Broline, B. M. *J. Am. Chem. Soc.* **1982**, *104*, 2857.
71. Review: Spangler, C. W. *Chem. Rev.* **1976**, *76*, 187. ter Borg, A. P.; Kloosterziel, H.; Van Meurs, N. *Proc. Chem. Soc.* **1962**, 359; *idem*, *Rec. Trav. Chim. Pays-Bas* **1963**, *82*, 717. ter Borg, A. P.; Kloosterziel, H. *ibid.* **1963**, *82*, 741. Büchi, G.; Burgess, E. M. *J. Am. Chem. Soc.* **1962**, *84*, 3104. Weth, E.; Dreiding, A. S. *Proc. Chem. Soc.* **1964**, 59.
72. Baldwin, J. E.; Broline, B. M. *J. Org. Chem.* **1982**, *47*, 1385.
73. For example, methylencyclopropane rearrangement: Gajewski, J. J. *J. Am. Chem. Soc.* **1968**, *90*, 7178. Doering, W. v. E.; Roth, H. D. *Tetrahedron* **1970**, *26*, 2825. Doering, W. v. E.; Birladeanu, L. *ibid.* **1973**, *29*, 499. Gilbert, J. C.; Higley, D. P. *Tetrahedron Lett.* **1973**, 2075. Decomposition of Δ^1-pyrazolines: Clarke, T. C.; Wendling, L. A.; Bergman, R. G. *J. Am. Chem. Soc.* **1977**, *99*, 2740, and references cited therein. [2 + 2] Cycloaddition: Wheland, R.; Bartlett, P. D. *ibid.* **1973**, *95*, 4003, and references cited therein.
74. Horsley, J. A.; Jean, Y.; Moser, C.; Salem, L.; Stevens, R. M.; Wright, J. S. *J. Am.*

Chem. Soc. **1972**, *94*, 279. Other calculations for the trimethylene diradical: Hoffmann, R. *ibid.* **1968**, *90*, 1475. Hay, P. J.; Hunt, W. J.; Goddard, W. A., III. *ibid.* **1972**, *94*, 638. Kollmar, H. *ibid.* **1973**, *95*, 966. Bodor, N.; Dewar, M. J. S.; Wasson, J. S. *ibid.* **1972**, *94*, 9095. Siu, A. K. Q.; St. John, W. M., III; Hayes, E. F. *ibid.* **1970**, *92*, 7249.

75. Doering, W. v. E. *Proc. Natl. Acad. Sci. U.S.A.* **1981**, *78*, 5279.
76. Klärner, F.-G.; Yaslak, S. *Chem. Ber.* **1979**, *112*, 2286.
77. Review: Staley, S. W. *Intra-Sci. Chem. Rep.* **1971**, *5*, 149. Gajewski, J. J. "Hydrocarbon Thermal Isomerizations"; Academic Press: New York, 1981, pp. 296-307.
78. Vogel, E. *Angew. Chem.* **1961**, *73*, 548. Vogel, E., *ibid.* **1962**, *74*, 829. Vogel, E.; Wiedemann, W.; Kiefer, H.; Harrison, W. F. *Tetrahedron Lett.* **1963**, 673.
79. (a) Anastassiou, A. G.; Griffith, R. C. *J. Am. Chem. Soc.* **1971**, *93*, 3083. (b) Paquette, L. A.; Epstein, M. J. *ibid.* **1971**, *93*, 5936; **1973**, *95*, 6767. These authors prepared [2,6-$(C_6H_5)_2$]-**62** (X = Y = H) and studied its thermal isomerization to [2,7-$(C_6H_5)_2$]-**59**. (c) Boche, G.; Weber, H.; Benz, J. *Angew. Chem.* **1974**, *86*, 238; *Angew. Chem. Int. Ed. Engl.* **1974**, *13*, 207. Baldwin, J. E.; Bryan, D. B. *J. Am. Chem. Soc.* **1974**, *96*, 319.
80. Okamura, W. H.; Osborn, T. W. *ibid.* **1970**, *92*, 1061. Baxter, C. S.; Garratt, P. J. *ibid.* **1970**, *92*, 1062. Barborak, J. C.; Su, T.-M.; Schleyer, P. v. R.; Boche, G.; Schneider, G. *ibid.* **1971**, *93*, 279. Scholes, G.; Graham, C. R.; Brookhart, M. *ibid.* **1974**, *96*, 5665.
81. Sohn, M. B.; Jones, Jr., M.; Fairless, B. *ibid.* **1972**, *94*, 4774.
82. Anastassiou, A. G.; Griffith, R. C. *Tetrahedron Lett.* **1973**, 3067.
83. Brown, J. M.; Ogilvy, M. M. *J. Am. Chem. Soc.* **1974**, *96*, 292.
84. Lewis, C. P.; Brookhart, M. *ibid.* **1975**, *97*, 651.
85. Katz, T. J.; Nicholson, C. R.; Reilly, C. A. *ibid.* **1966**, *88*, 3832.
86. Ciganek, E. *ibid.* **1966**, *88*, 1979. Anastassiou, A. G.; Cellura, R. P.; Ciganek, E. *Tetrahedron Lett.* **1970**, 5267.
87. Schönleber, D. *Chem. Ber.* **1969**, *102*, 1789.
88. Baldwin, J. E.; Andrist, A. H.; Pinschmidt, R. K., Jr. *J. Am. Chem. Soc.* **1972**, *94*, 5845.
89. Klärner, F.-G. *Angew. Chem.* **1972**, *84*, 892. *Angew. Chem. Int. Ed. Engl.* **1972**, *11*, 832. Klärner, F.-G.; Wette, M. *Chem. Ber.* **1978**, *111*, 282.
90. Klärner, F.-G. *Tetrahedron Lett.* **1971**, 3611.
91. Boche, G.; Schneider, G. *Tetrahedron Lett.* **1974**, 2449.
92. Frey, H. M.; Krantz, A. *J. Chem. Soc.*, A **1969**, 1159.
93. Benson, S. W.; Cruickshank, F. R.; Golden, D. M.; Haugen, G. R.; O'Neal, H. E.; Rodgers, A. S.; Shaw, R.; Walsh, R. *Chem. Rev.* **1969**, *69*, 279.
94. Jorgensen, W. L. *J. Am. Chem. Soc.* **1976**, *98*, 6784, and references cited therein.
95. Andrews, G. D.; Baldwin, J. E.; Gilbert, K. E. *J. Org. Chem.* **1980**, *45*, 1523.
96. Hehre, W. J. *J. Am. Chem. Soc.* **1974**, *96*, 5207.
97. Katz, T. J.; Gold, E. H. *ibid.* **1964**, *86*, 1600.
98. Olah, G. A.; Staral, J. S.; Spear, R. J.; Liang, G. *ibid.* **1975**, *97*, 5489, and references cited therein.
99. Koptyug, V. A.; Shleider, I. A.; Isaev, I. S. *J. Org. Chem. USSR* **1971**, *7*, 864. Shleider, I. A.; Isaev, I. S.; Koptyug, V. A. *ibid.* **1972**, *8*, 1357.
100. Devaquet, A. J. P.; Hehre, W. J. *J. Am. Chem. Soc.* **1974**, *96*, 3644. Hehre, W. J.; Devaquet, A. J. P. *ibid.* **1976**, *98*, 4370.
101. Reviews: Schaffner, K.; Demuth, M. "Rearrangements in Ground and Excited

States," Vol. 3; de Mayo, P., Ed.; Academic Press: New York, 1980, p. 281. Schuster, D. I. *Acc. Chem. Res.* **1978**, *11*, 65.

102. Zimmerman, H. E.; Schuster, D. I. *J. Am. Chem. Soc.* **1961**, *83*, 4486; *ibid.* **1962**, *84*, 4527. Zimmerman, H. E.; Cowley, B. R.; Tseng, C.-Y.; Wilson, J. W. *ibid.* **1964**, *86*, 947. Zimmerman, H. E.; Swenton, J. S. *ibid.* **1967**, *89*, 906. Zimmerman, H. E. *Pure Appl. Chem.* **1964**, *9*, 493.
103. Schuster, D. I.; Patel, D. J. *J. Am. Chem. Soc.* **1968**, *90*, 5154. Schuster, D. I.; Liu, K.-C. *ibid.* **1971**, *93*, 6711. Samuel, C. J. *J. Chem. Soc., Chem. Comm.* **1979**, 275; *J. Chem. Soc., Perkin II* **1981**, 736.
104. Schuster, D. I.; Prabhu, K. V.; Smith, K. J. *Tetrahedron* **1980**, *36*, 3495.
105. Zimmerman, H. E.; Keck, G. E. *J. Am. Chem. Soc.* **1975**, *97*, 3527. Zimmerman, H. E.; Keck, G. E.; Pflederer, J. L. *ibid.* **1976**, *98*, 5574.
106. Zimmerman, H. E.; Doepp, D.; Huyffer, P. S. *ibid.* **1966**, *88*, 5352.
107. Zimmerman, H. E.; Crumrine, D. S. *ibid.* **1968**, *90*, 5612. Zimmerman, H. E.; Crumrine, D. S.; Doepp, D.; Huyffer, P. S. *ibid.* **1969**, *91*, 434. Zimmerman, H. E.; Pasteris, R. J. *J. Org. Chem.* **1980**, *45*, 4864; *ibid.* **1980**, *45*, 4876.
108. Brennan, T. M.; Hill, R. K. *J. Am. Chem. Soc.* **1968**, *90*, 5614.
109. Swatton, D. W.; Hart, H. *ibid.* **1967**, *89*, 5075. Hart, H.; Rodgers, T. R.; Griffiths, J. *ibid.* **1969**, *91*, 754. Childs, R. F.; Winstein, S. *ibid.* **1974**, *96*, 6409.
110. Childs, R. F.; Winstein, S. *J. Am. Chem. Soc.* **1968**, *90*, 7146; *ibid.* **1974**, *96*, 6409. Isaev, I. S.; Mamatyuk, V. I.; Kuzubova; L. I.; Gordymova, T. A.; Koptyug, V. A. *J. Org. Chem. USSR* **1970**, *6*, 2493.
111. Koptyug, V. A.; Kuzubova, L. I.; Isaev, I. S.; Mamatyuk, V. I. *Chem. Comm.* **1969**, 389; *J. Org. Chem. USSR* **1970**, *6*, 1854.
112. Childs, R. F.; Sakai, M.; Winstein, S. *J. Am. Chem. Soc.* **1968**, *90*, 7144. Childs, R. F.; Parrington, B. *Chem. Comm.* **1970**, 1540. Childs, R. F.; Sakai, M.; Parrington, B. D.; Winstein, S. *J. Am. Chem. Soc.* **1974**, *96*, 6403.
113. Berson, J. A.; Hasty, N. M. Jr. *ibid.* **1971**, *93*, 1549. Vogel, P.; Saunders, M.; Hasty, N. M. Jr.; Berson, J. A. *ibid.* **1971**, *93*, 1551.
114. Hehre, W. J. *ibid.* **1972**, *94*, 8908; *ibid.* **1974**, *96*, 5207.
115. Zeya, M.; Childs, R. F. *ibid.* **1971**, *94*, 289. Childs, R. F.; Zeya, M. *ibid.* **1974**, *96*, 6418.
116. Barltrop, J. A.; Baxter, A. W.; Day, A. C.; Irving, E. *J. Chem. Soc., Chem. Comm.* **1980**, 606, and references cited therein.
117. Barltrop, J. A.; Day, A. C.; Samuel, C. J. *J. Am. Chem. Soc.* **1979**, *101*, 7521, and references cited therein.
118. Kaplan, L.; Pavlik, J. W.; Wilzbach, K. E. *ibid.* **1972**, *94*, 3283.
119. Sustmann, R.; Lübbe, F. *ibid.* **1976**, *98*, 6037. *Chem. Ber.* **1979**, *112*, 42.
120. Lübbe, F., Sustmann, R. *ibid.* **1979**, *112*, 57.
121. Rosenberg, J. L. V., Jr.; Mahler, J. E.; Pettit, R. *J. Am. Chem. Soc.* **1962**, *84*, 2842. Winstein, S.; Kaesz, H. D.; Kreiter, C. G.; Friedrich, E. C. *ibid.* **1965**, *87*, 3267. Warner, P.; Harris, D. L.; Bradley, C. H.; Winstein, S. *Tetrahedron Lett.* **1970**, 4013.
122. Berson, J. A.; Jenkins, J. A. *J. Am. Chem. Soc.* **1972**, *94*, 8907.
123. Other examples of exclusive conformational ring inversion in labeled homotropylium cations were reported by Brookhart, M. S.; Atwater, M. A. M. *Tetrahedron Lett.* **1972**, 4399. Paquette, L. A.; Jacobsson, U.; Ley, S. V. *J. Am. Chem. Soc.* **1976**, *98*, 152.
124. (a) Childs, R. F.; Rogerson, C. V. *ibid.* **1978**, *100*, 649. (b) *ibid.* **1980**, *102*, 4159.
125. Childs, R. F., unpublished results cited in ref. 3, p. 601.

126. Scott, L. T.; Brunsvold, W. R. *J. Am. Chem. Soc.* **1978**, *100*, 6535.
127. Childs, R. F.; Rogerson, C. V. *ibid.* **1976**, *98*, 6391.
128. Atkinson, D. J.; Perkins, M. J.; Ward, P. *Chem. Comm.* **1969**, 1390, Kloosterziel, H.; van Drunen, J. A. A. *Rec. Trav. Chim. Pay-Bas* **1970**, *89*, 368. Staley, S. W.; Erdman, J. P. *J. Am. Chem. Soc.* **1970**, *92*, 3832.
129. (a) Kloosterziel, H.; Zwanenburg, E. *Rec. Trav. Chim. Pay-Bas* **1969**, *88*, 1373. (b) Kloosterziel, H.; Gorter-La Roy, G. M. *J. Chem. Soc., Chem. Comm.* **1972**, *352*; (c) Staley, S. W.; Pearl, N. J. *J. Am. Chem. Soc.* **1973**, *95*, 2731.

Stereochemistry at Silicon

ROBERT J. P. CORRIU, CHRISTIAN GUÉRIN, AND JOËL J. E. MOREAU

Laboratoire des Organométalliques
Equipe de Recherche Associée au CNRS
Université des Sciences et Techniques du Languedoc
Montpellier Cédex 34060, France

I. INTRODUCTION

The elucidation of reaction mechanisms in organic chemistry has involved both kinetic and stereochemical studies. Similarly, the stereochemistry of silicon (1, 2) has played a determining role in understanding the reaction mechanism in organosilicon compounds.

Unlike carbon compounds, optically active organosilanes are not natural species. Therefore, it is not surprising that studies of stereochemistry at silicon are relatively recent. Nonetheless, the need for optically active silicon compounds was early understood by Kipping and coworkers (3) and also by Eaborn and Pitt (4), who resolved tetrasubstituted organosilanes. Stereochemical studies at silicon began in 1959 with the resolution of a functional trisubstituted silane by Sommer and Frye (5). Other groups have contributed to the many studies performed in the field of organosilicon stereochemistry and mechanisms since the original publication of Sommer.

The organic chemistry of silicon is very different from that of carbon. Among the features dominating silicon chemistry are: the ability to expand its coordina-

tion number, its lack of tendency to form silicenium ion [although evidence for unimolecular solvolysis reaction has recently been presented (6)], and its general inability to form stable derivatives with multiple bonds [although a solid Si=C (7) and a solid Si=Si (8) derivative have recently been isolated, and the ways to generate such intermediates as silabenzene (9) are now known].

Concerning stereochemistry, reactions at silicon usually proceed with high stereoselectivity, with either retention or inversion of configuration, and only rarely with racemization. Moreover, asymmetric silyl radicals and silyl anions show significant optical stability.

This chapter aims to review stereochemistry at silicon and its mechanistic implications, to which considerable work has been devoted since the first reviews by Sommer (1, 2). The following aspects are discussed:

1. General features of chirality at silicon and the routes to optically active compounds. It is now timely to cover this area, since various methods of wide applicability, including asymmetric synthesis, have become available.
2. The mechanism and stereochemistry of nucleophilic substitution at silicon. We have already devoted two reviews to this topic (10, 11) but it seems appropriate here to discuss some new stereochemical aspects and to focus on the most recent developments regarding the mechanisms of displacement.
3. The mechanism and stereochemistry of reactions with transition metals. In connection with the mechanism of hydrosilylation reactions, it is of interest to discuss the stereochemistry of silyl-transition metal complexes (12) and the stereochemical aspects of the reactions of silicon hydrides with transition metals.
4. The expansion of coordination at silicon. Pentacoordinated species seem to be quite intimately involved in many processes taking place at silicon. Expansion of coordination is the fundamental step not only in the nucleophilic induced racemization reviewed some years ago (13), but also in nucleophilic substitution activated by nucleophiles.* A part of this review is devoted to the stereochemical and mechanistic aspects of nucleophilic activation. Furthermore, in connection with a possible isomerization of trigonal bipyramidal silicon by Berry pseudorotation, the dynamic stereochemistry of pentacoordinated silicon compounds is discussed.

Along the way in this chapter, a few results obtained with related germanium and tin compounds are mentioned, although some aspects of their stereochemistry have been recently reviewed (14). On the other hand, some topics are not

*$SN_{NA}Si$ = Nucleophilic substitution at silicon activated by (other) nucleophiles.

covered in this chapter. The stereochemistry of molecular rearrangements of organosilicon compounds has been discussed in a recent review by Brook and Bassindale (15). The steroechemistry of silacycloalkanes has also been covered elsewhere (16), and only a few recent results are mentioned in this chapter.

II. OPTICALLY ACTIVE ORGANOSILICON COMPOUNDS

Numerous tetrahedral optically active organosilicon compounds have now been obtained, and various resolution procedures have been successfully employed. They include resolution through separation of diastereomers as well as kinetic resolution and asymmetric synthesis. Moreover, the stereospecificity of substitution reaction at silicon makes possible the synthesis of various optically active compounds starting from resolved organosilicon compounds.

Before reviewing the different routes to optically active silanes and discussing some relevant points, namely, the determination of enantiomeric purity and configuration, we shall give a brief overview of the stereochemical stability of chiral silicon species.

A. Configurational Stability of Chiral Organosilicon Species

Since the stereochemical behavior of chiral silicon species differs from that of corresponding carbon species, it seems of interest to summarize briefly the current status of the field, making comparison also with related germanium and tin compounds.

1. Tetracovalent Compounds

Tetracoordinated organosilicon compounds exhibit high configurational stability. By comparison, germanium and to a much larger extent tin compounds are less optically stable.

Chiral tetraalkylsilanes R_4Si, and trialkylsilanes R_3SiH have high optical stability. However, whereas optically active tetraalkylgermanes or stannanes are stable, a lower optical stability is observed for hydrogermanes R_3GeH and stannanes R_3SnH. Chiral hydrogermanes are configurationally stable but racemize slowly upon heating. Hydrostannanes are less stable and racemize at room temperature (14). This is related to the formation of pyramidal radical species that slowly invert their configuration (cf. Sect. II-A-2).

Functional silicon compounds R_3SiX are also optically stable. Racemization is observed only in the presence of nucleophilic agents. Kinetic studies of the nucleophilically assisted racemizations of halogenosilanes, germanes, and stannanes have revealed that they involve two molecules of nucleophile in the rate-

determining step (13). Such a process is controlled by the entropy of activation and takes place without substitution of X in R_3SiX. Whereas silicon compounds are optically stable enough in nucleophilic solvents to allow stereospecific substitution reactions, this is not the case for tin compounds in which the racemization at tin is sufficiently rapid to be observed on the NMR time scale (14).

The optical stability of halides decreases in the order Si > Ge >> Sn. It follows the ability of the central atom to expand its coordination. A detailed study of the racemization has been reported and the subject reviewed a few years ago (13; cf. also Sect. V).

2. *Chiral Silyl Radicals*

Interestingly, the pyramidal silyl radical exhibits significant configurational stability. Inversion of the pyramidal species is slow enough to allow reactions in which the configuration at silicon is retained.

Reactions of optically active organosilanes that involve intermediate silyl radicals were shown to proceed with predominant retention of configuration at silicon.

The photolysis of an optically active acetyl silane **1** (eq. [1]) implies the formation of an asymmetric radical **2** which retained its configuration upon trapping by carbon tetrachloride (17). The chlorosilane **3** was then reduced to the hydrosilane **4** with inversion of configuration.

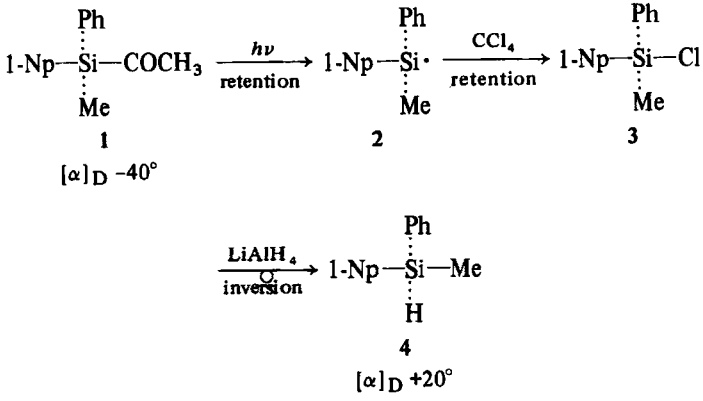

[1]

Since the reduction step is stereospecific, it may be deduced from the (known) enantiomeric purity of **1** and **4** that formation and trapping of the silyl radical occurs with 65% retention.

Similarly, the generation of silyl radical from optically active hydrosilane **4** in

the presence of dibenzoyl peroxide followed by chlorine abstraction from CCl_4 demonstrates the optical stability of the asymmetric silyl radical (18) (eq. [2]).

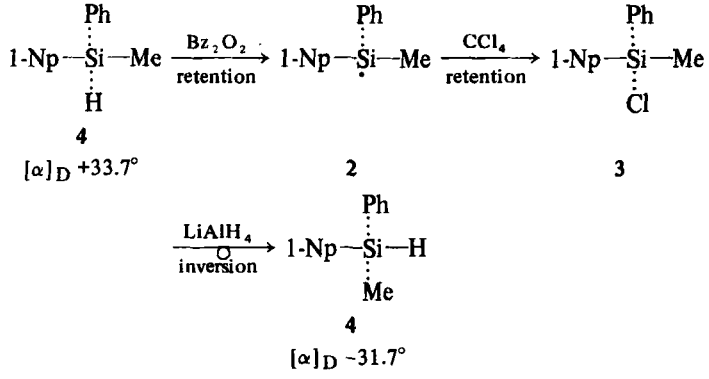

[2]

These experiments offer good chemical evidence in support of the pyramidal structure of the silyl radical and its relatively slow rate of inversion. However a marked destabilization was observed for the chiral disilanyl radical **6** (eq. [3]) (19).

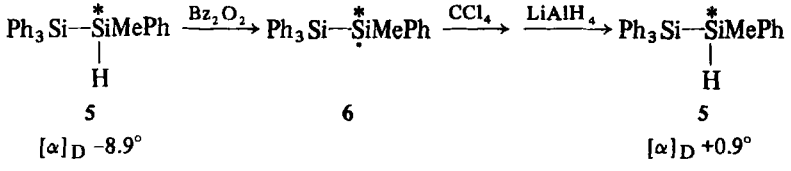

[3]

The low stereoselectivity here is consistent with ESR data which had indicated a more planar structure for the pentamethyldisilanyl radical $Me_3Si\dot{S}iMe_2$ (20).

Evidence for optically active germyl radicals has also been reported. The optically active hydrogermane **7** reacted with CCl_4 at 80°C in the presence of dibenzoyl peroxide to yield the chlorogermane **8** with substantial retention of configuration (eq. [4]) (21).

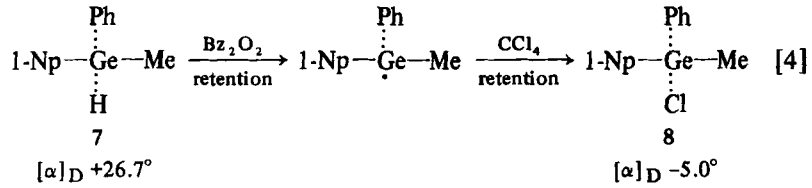

[4]

Predominant retention of configuration was also found in the thermal radical hydrogermylation reaction shown in (eq. [5]) (22, 23).

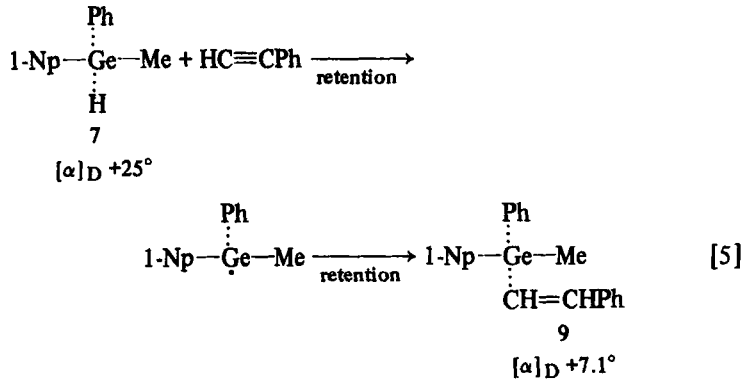

In a recent report, Sakurai (24) showed that the asymmetric germyl radical is of limited configurational stability.

No observation of a chiral tin radical has been recorded because tin compounds are of low configurational stability. Inversion of the trivalent tin radical is responsible for the slow racemization of optically active hydrostannanes at room temperature in the presence of AIBN (eq. [6]) (14).

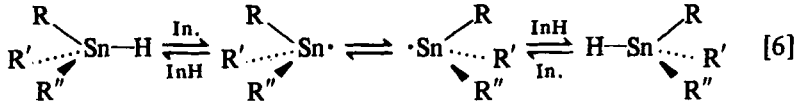

3. *Chiral Silyl Anions*

An important contribution to the chemistry of silylmetallic compounds has been made by Gilman and coworkers (25).

The formation of an asymmetric silyllithium reagent by lithium cleavage of the silicon-silicon bond of an optically active disilane **10** (eq. [7]) has been reported (26). Hydrolysis of the silyllithium reagent **11** yielded an optically active silicon hydride. This result demonstrates that silyllithium has considerably enhanced optical stability relative to acyclic alkyllithium compounds.

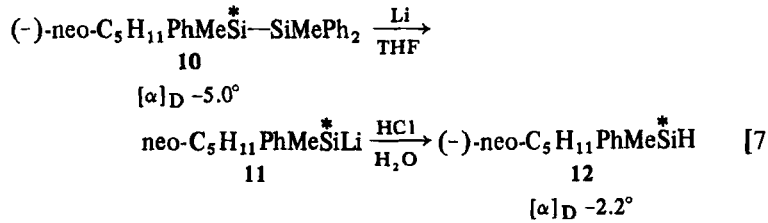

The intermediate formation of chiral silyllithium and silyl Grignard reagents has also been observed in the reaction of methyllithium (eq. [8]) and methylmagnesium bromide (eq. [9])

$$\underset{\textbf{13}}{1\text{-NpPhMe}\overset{*}{\text{Si}}\text{—Co(CO)}_4} \xrightarrow{\text{MeLi}} 1\text{-NpPhMe}\overset{*}{\text{Si}}\text{Li} \xrightarrow{\text{H}_2\text{O}} \underset{\textbf{4}}{1\text{-NpPhMe}\overset{*}{\text{Si}}\text{H}} \quad [8]$$

70% retention

$$\underset{\textbf{13}}{1\text{-NpPhMe}\overset{*}{\text{Si}}\text{—Co(CO)}_4} \xrightarrow{\text{MeMgBr}} 1\text{-NpPhMe}\overset{*}{\text{Si}}\text{MgBr} \xrightarrow{\text{H}_2\text{O}} \underset{\textbf{4}}{1\text{-NpPhMe}\overset{*}{\text{Si}}\text{H}}$$

55% retention

$$\text{CH}_2\text{=CH—CH}_2\text{Br} \rightarrow 1\text{-NpPhMe}\overset{*}{\text{Si}}\text{CH}_2\text{—CH=CH}_2$$

$$\underset{\textbf{14}}{}$$

59% retention [9]

with an optically active silyl-cobalt carbonyl complex **13** (27, 28).

However, hydrolysis, or condensation with allyl bromide, of these anions led to products of low optical purity. Since the cleavage reaction of the Si-Co bond (eq. [9]) may not be stereospecific, it is difficult to know whether some racemization of the silyl anion occurs.

The formation of an optically active silyl-mercurial derivative **15** has also been reported (29) (eq. [10]).

$$\underset{\substack{\textbf{4}\\ [\alpha]_D\ +34.0^\circ}}{1\text{-NpPhMe}\overset{*}{\text{Si}}\text{H}} \xrightarrow{(t\text{-Bu})_2\text{Hg}} \underset{\substack{\textbf{15}\\ [\alpha]_D\ -19.2^\circ}}{(1\text{-NpPhMe}\overset{*}{\text{Si}})_2\text{Hg}} \xrightarrow{\text{LiAlH}_4} \underset{\substack{\textbf{4}\\ [\alpha]_D\ +2.8^\circ}}{1\text{-NpPhMe}\overset{*}{\text{Si}}\text{H}} \quad [10]$$

Compound **15** was isolated in apparently low optical purity and underwent thermal racemization.

The preceding experiments provide chemical evidence for significant configurational stability of silyl anions. An NMR study of diisopropylphenylsilyllithium showed that the isopropyl methyl groups are anisochronous up to 185°C, indicating that the barrier to inversion at silicon in the silyl anion is greater than 24 kcal/mol. (30).

The analogous asymmetric germyl anion appears to be even more optically stable. Solutions of optically active germyllithium **17** are easily prepared by treatment of a chiral hydrogermane with *n*-butyllithium (eq. [11]).

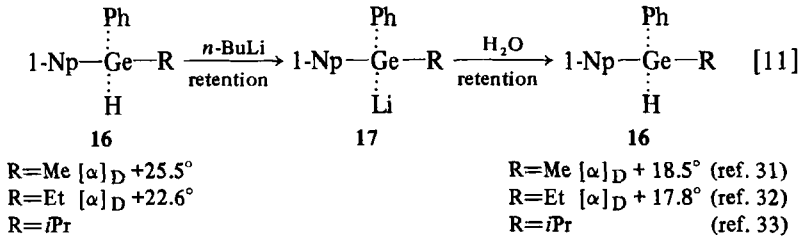

[11]

Since the original preparation of optically active germyllithium by Brook and Peddle (31), these reagents have been found to undergo various stereospecific reactions. Carbonation and reaction with carbonyl compounds (eq. [12]) lead to retention of configuration at germanium (31).

$$1\text{-NpPhMe}\overset{*}{\text{Ge}}\text{CO}_2\text{H} \xleftarrow[\text{retention}]{CO_2} 1\text{-NpPhMe}\overset{*}{\text{Ge}}\text{Li} \xrightarrow[\text{retention}]{Ph_2CO} 1\text{-NpPhMe}\overset{*}{\text{Ge}}\text{C(OH)Ph}_2 \qquad [12]$$

Alkylation reactions with alkyl chlorides or bromides also occured with predominant retention of configuration (34) (eq. [13]).

$$1\text{-NpPhEt}\overset{*}{\text{Ge}}\text{Li} \xrightarrow[\text{retention}]{RX} 1\text{-NpPhEt}\overset{*}{\text{Ge}}\text{—R} \qquad [13]$$

R = alkyl, allyl
X = Cl, Br

By contrast, alkyl iodides reacted with overall inversion at germanium, due to a halogen-metal exchange reaction (34) (eq. [14])

$$1\text{-NpPhEt}\overset{*}{\text{Ge}}\text{Li} \xrightarrow[\text{retention}]{RI} 1\text{-NpPhEt}\overset{*}{\text{Ge}}\text{I} + \text{RLi} \xrightarrow[\text{inversion}]{} 1\text{-NpPhEt}\overset{*}{\text{Ge}}\text{R} \qquad [14]$$

The synthesis of digermanes was similarly achieved using stereospecific reactions of germyllithium (33). The optically active anion **17** reacted with a menthoxygermane of the same, **18** (or opposite, **19**) relative configuration, leading to the meso, **20** (or optically active, **21**) digermane (Scheme 1).

The asymmetric germyl anion also permitted preparation of chiral germyl-transition-metal complexes (35, 36) by substitution of a halogen from a metal halide (eq. [15]).

$$1\text{-NpPhMe}\overset{*}{\text{Ge}}\text{Li} + (\eta\text{-C}_5\text{H}_5)\text{PPh}_3\text{NiCl} \xrightarrow[\text{retention}]{} 1\text{-NpPhMe}\overset{*}{\text{Ge}}\text{—Ni(PPh}_3)(\eta\text{-C}_5\text{H}_5) \qquad [15]$$

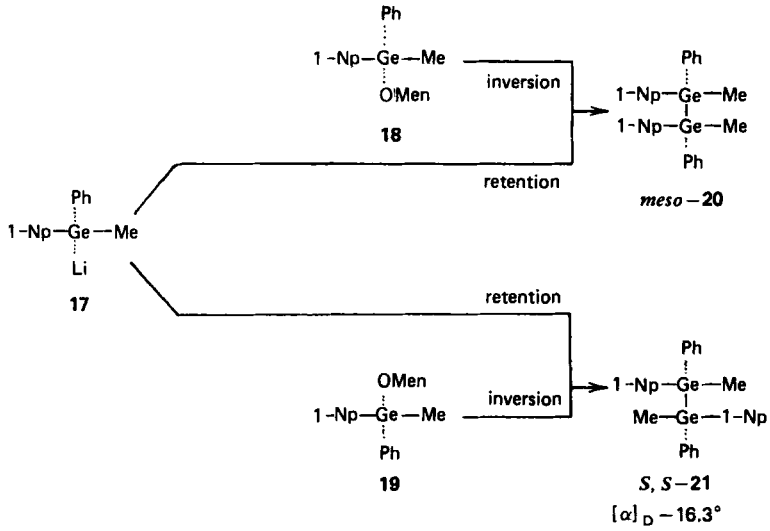

Scheme 1. Stereospecific synthesis of digermanes from a chiral germyl anion.

However, halogen-metal exchange was also observed in some cases (eq. [16]).

$$Ph_3GeLi + L_nMX \longrightarrow Ph_6Ge_2 + (L_nM)_2 \qquad [16]$$

$L_nM = (CO)_5Mn, (\eta\text{-}C_5H_5)(CO)_2Fe$

$X = Cl, Br, I$

Reaction of the chiral anion with metal carbonyls provided a general route to optically active germyl-metal carbonyl anions (eq. [17]).

$$1\text{-NpPhMe}\overset{*}{\text{Ge}}\text{Li} + M(CO)_n \xrightarrow{Et_4NCl} [(1\text{-NpPhMe}\overset{*}{\text{Ge}})(CO)_{n-1}M]^- Et_4N^+ \qquad [17]$$

$M(CO)_n = Cr(CO)_6, Mo(CO)_6, W(CO)_6, Fe(CO)_5, Mn(\eta\text{-}C_5H_5)(CO)_3$

Such a chiral ligand also allowed resolution of chiral molybdenum and tungsten complexes (37) (eq. [18]).

$$[(\eta\text{-}C_5H_5)(CO)_2(NO)M] \xrightarrow{R_3\overset{*}{\text{Ge}}Li} [(\eta\text{-}C_5H_5)(CO)(NO)\overset{*}{M}\text{—}\overset{*}{\text{Ge}}R_3]^- \xrightarrow{CH_3I} [(\eta\text{-}C_5H_5)(CO)(NO)(CH_3)\overset{*}{M}\text{—}\overset{*}{\text{Ge}}R_3] \qquad [18]$$

$R_3 = 1\text{-NpPhMe}, M = Mo, W$

Evidence for the formation of an optically active germyl Grignard reagent has also been obtained (eq. [19]) (38).

$$\underset{\substack{7\\ [\alpha]_D\ +25.1^\circ}}{1\text{-NpPhMe}\overset{*}{\text{Ge}}\text{H}} \xrightarrow[\text{retention}]{\text{PhCH}_2\text{MgCl}} \underset{22}{[1\text{-NpPhMe}\overset{*}{\text{Ge}}\text{MgCl}]} \xrightarrow[\substack{(PPh_3)_2NiCl_2\\ \text{retention}}]{1\text{-NpPhMe}\overset{*}{\text{Ge}}\text{H}}$$

$$\underset{\substack{23\\ [\alpha]_D\ -17.8^\circ}}{[1\text{-NpPhMeGe}-]_2} \qquad [19]$$

The obtention of the chiral digermane **23** implies overall retention of configuration. Retention in both steps was proposed since it appears the most probable steric course in the formation of the germyl Grignard reagent **22** and since retention was demonstrated in the nickel-catalyzed condensation of Grignard reagents with hydrogermanes.

The asymmetric germyl anions appear to have a higher configurational stability than their silyl analogs. This may be due to the tendency of silyl anions to react by electron-transfer processes (as illustrated in eq. [20])

$$Ph_3SiK + Ph_2C{=}O \longrightarrow Ph_6Si_2 + PhCH(OH)CH(OH)Ph \qquad [20]$$

whereas germyl anions react as nucleophiles (39).

4. Penta- and Hexacoordinate Compounds

Compounds of the group IV elements below carbon exhibit a marked tendency to expand their coordination, leading to five- or six-coordinate species.

No optically active five-coordinated silicon compounds have been obtained. However a chiral hexacoordinate silicon trisacetylacetonate cation (**23**) has been resolved by Dhar, Doron, and Kirschner (40) through the separation of diastereomeric dibenzoyl-*d*-tartrate salts (eq. [21]).

$$\underset{\substack{24\\ (\pm)}}{(\pm)\text{-}[Si(acac)_3]Cl \cdot HCl} + \textit{d}\text{-}(-)\text{-}Na_2C_{18}H_{12}O_8 \xrightarrow[\text{crystallization}]{}$$

$$\underset{\substack{25\\ [\alpha]_D\ -773^\circ}}{(-)\text{-}[Si(acac)_3]\,\textit{d}\text{-}(-)\text{-}HC_{18}H_{13}O_2} \xrightarrow{\text{resin-Cl}} \underset{\substack{24\\ (-)\\ [\alpha]_D\ -965^\circ}}{(-)\text{-}[Si(acac)_3]Cl \cdot HCl} \qquad [21]$$

The cationic complexes **24** and **25** were of low optical stability and racemization was observed after 6 hr. However, recent dynamic NMR studies have permitted the observation of chiral pentacoordinated species without resolution. The compounds are configurationally stable on the NMR time scale. The racemization of such species opens up the problem of permutational isomerization, which will be discussed in detail in Sect. V-C.

At this point, it is of interest that, whereas trisubstituted tin halides R_3SnX are of low optical stability, Van Koten and Noltes (41) have found increased configurational stability at the chiral tin center as a result of intramolecular coordination. Thus the five-coordinate tin compound **26**, which is in equilibrium with its four-coordinate form **27** (eq. [22]),

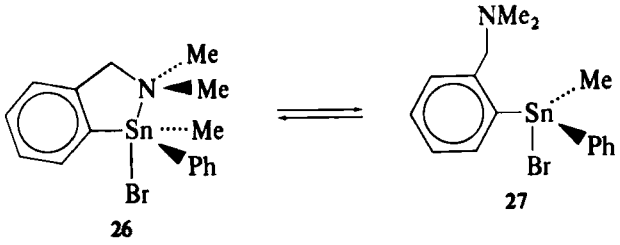

26 **27** [22]

exhibited no rapid inversion at tin on the NMR time scale up to 123°C. Hence the racemization process has an activation energy barrier much in excess of 24 kcal/mol. This finding, in turn, led to the preparation of the first tin halide with a chiral pentacoordinate tin atom in a given configuration (eq. [23]) (41).

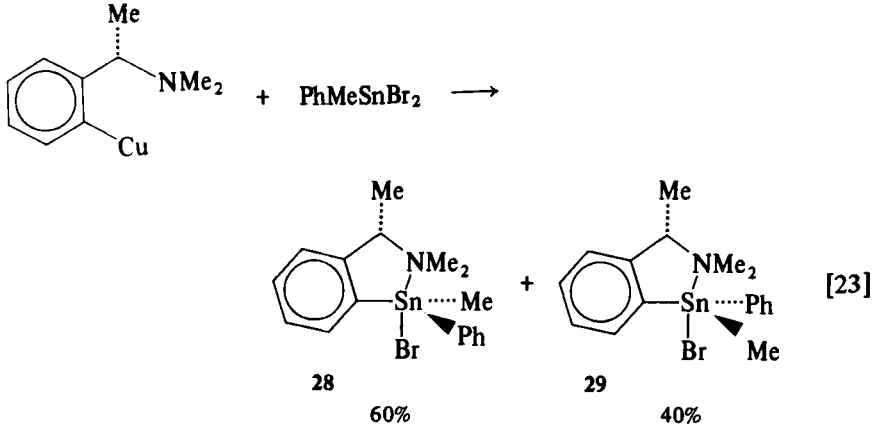

28 60% **29** 40% [23]

Fractional crystallization led to isolation of diastereomer **29**; its structure was determined by X-ray diffraction (42). It was shown to isomerize slowly in solution and upon heating. The slow epimerization, which involves inversion of con-

figuration at the tin atom, was attributed to the formation of a hexacoordinate intermediate arising by association of two diastereomers.

B. Resolution via Diastereomer Formation

The classical procedure of resolution through diastereomer formation and separation, widely applied in organic chemistry (43), was first applied to silicon compounds by Sommer. (-)-Menthol proved to be a convenient resolving agent for organosilicon compounds. Using this method, acyclic and cyclic organosilanes have been resolved, as detailed in the sequel.

1. Acyclic Organosilicon Compounds

a. **Monofunctional Compounds.** Sommer's original resolution involving separation of (±)-1-naphthylphenylmethyl-(-)-menthoxysilane (44) is illustrated in Scheme 2.

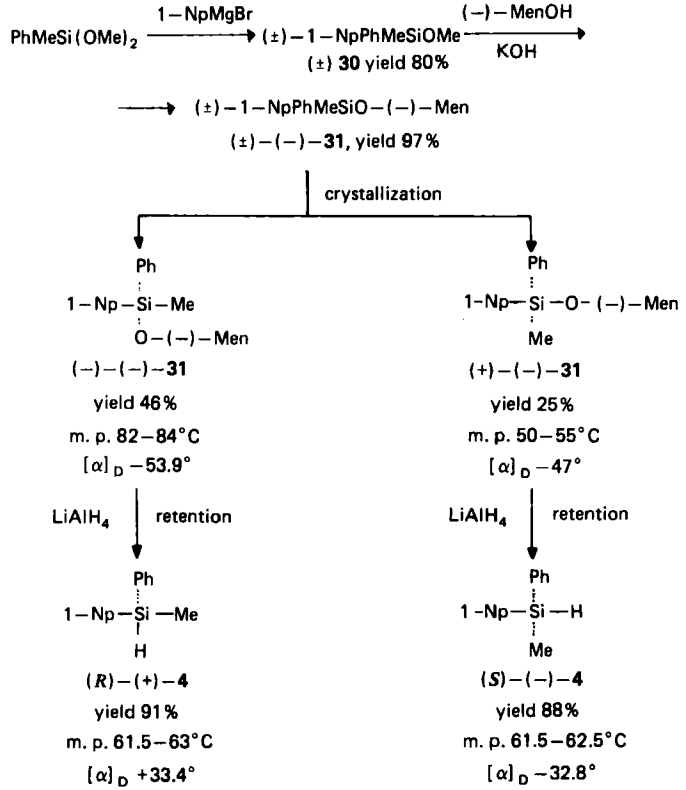

Scheme 2. Resolution of 1-Naphthylphenylmethylsilane (44).

Treatment of racemic methoxysilane **30** with (-)-menthol afforded a mixture of diastereomeric menthoxysilanes **31**. Fractional crystallization from pentane gave the less soluble diastereomer ($[\alpha]_D$ -53.9°) in 46% yield. Lithium aluminum hydride reduction led to (+)-1-naphthylphenylmethylsilane (**4**, $[\alpha]_D$ +33.4°). The more soluble diastereomer similarly gave rise to (-)-1-NpPhMeSiH ($[\alpha]_D$ -32.8°). The absolute configuration of (+)-1-NpPhMeSiH was shown to be *R* by X-ray diffraction studies (45).

Similar reaction sequences were used to resolve 1-naphthylphenylvinyl- and -ethyl-silane **32** and **33** (46, 48). The Fredga method was used to establish the relative configuration of these compounds and to correlate them with the known absolute configuration of Sommer's compounds (49). Figure 1 shows the configuration of the compounds obtained by reduction of the less soluble (-)-menthoxy diastereomer.

Other optically active organosilicon compounds containing Si-Si (50) or Si-Ge (51) linkages were also obtained according to Scheme 3. The absolute configurations of compounds **35** ($[\alpha]_D$ -55°) and **37** ($[\alpha]_D$ +7.3°) were proposed to be *R* at silicon on the basis of chemical correlations (51).

b. Difunctional Compounds. The diversity of optically active organosilicon compounds was greatly enhanced by the resolution of difunctional organosilanes. As described in Scheme 4, the separation of diastereomeric (±)-1-NpPh(MeO)SiO-(-)-Men **38** has been achieved (52). The absolute configuration of the less soluble diastereomer (m.p. 102°C, $[\alpha]_D$ -58.4°) was shown to be *S* at the silicon atom according to X-ray diffraction studies (53). This new compound proved to be of synthetic interest since it allowed regiospecific and stereospecific substitution of one alkoxy group by organometallic reagents. The synthesis of other 1-naphthylphenylalkylmenthoxysilanes has been reported (52).

The theoretical and synthetic interest of difunctional organosilicon compounds prompted the resolution of several other compounds, shown in Figure 2. The configuration and properties in each case refer to the less soluble diastereomer. Chemical correlations were used to establish the relative configuration

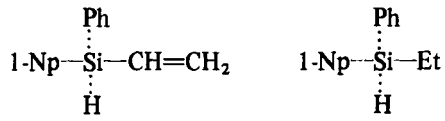

(*R*)-(+)-**32**
$[\alpha]_D$ +17.6°

(*R*)-(+)-**33**
m.p. 45-46°C
$[\alpha]_D$ +24.6°

Figure 1. Absolute configuration of (+)-1-naphthylphenylvinyl- and -ethyl-silane.

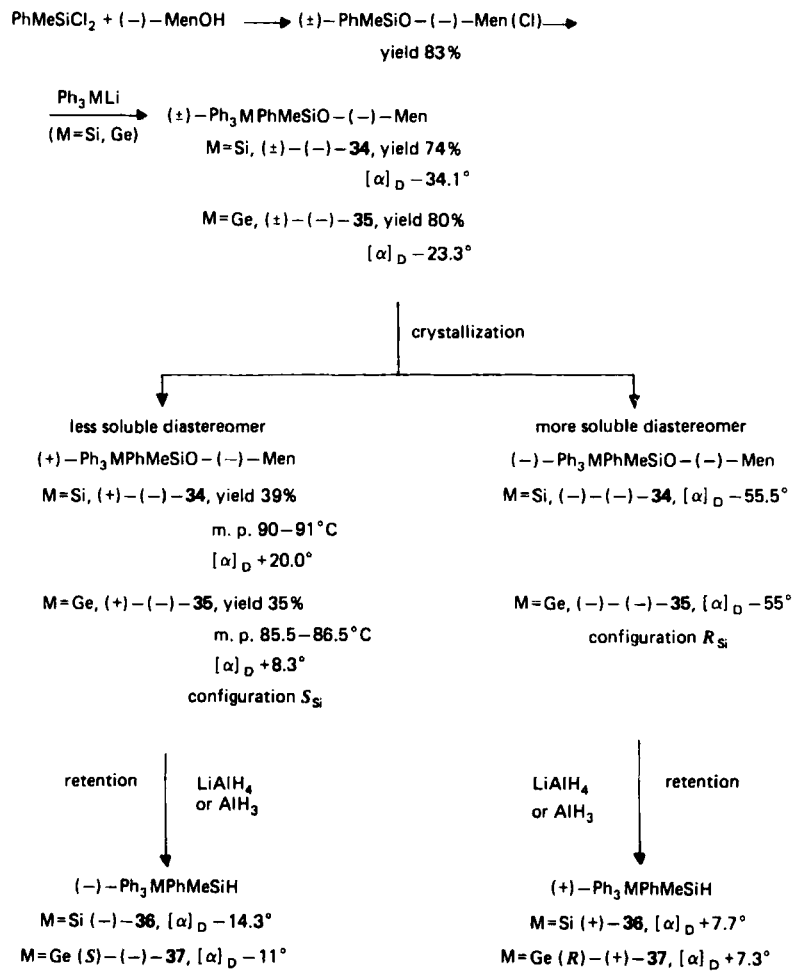

Scheme 3. Resolution of chiral compounds containing Si-Si and Si-Ge linkages.

of these compounds and correlate them to the known absolute configuration of methoxymenthoxysilane **38**. An extension of the Fredga method was also proposed for the determination of the relative configurations around silicon in these diastereomeric compounds (58).

Difunctional organosilicon compounds **39-43** allowed an easy access to various enantiomerically pure new derivatives by stereospecific substitution reactions of one functional group (59, 60).

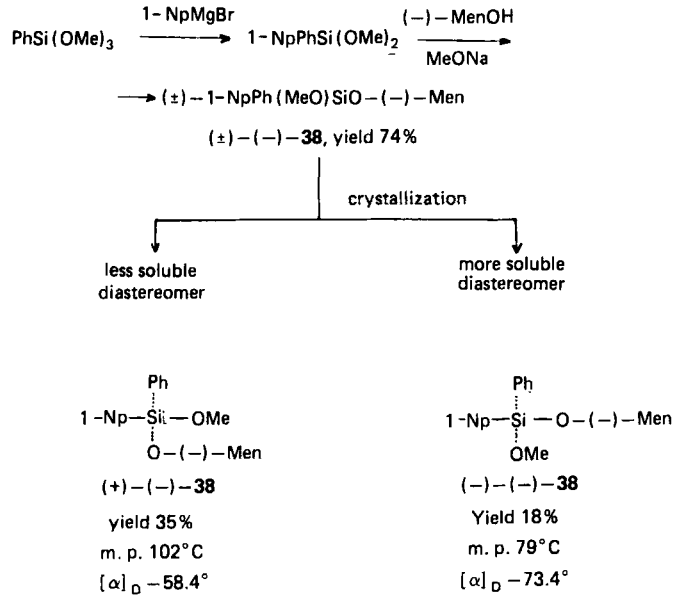

Scheme 4. Resolution of 1-Naphthylphenylmethoxymenthoxysilane (52).

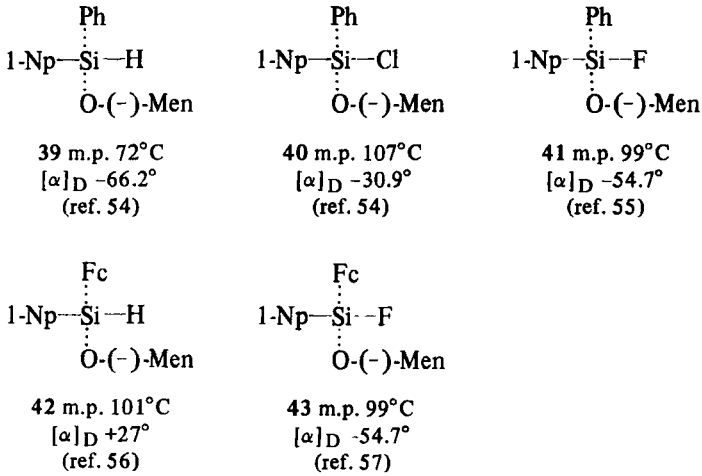

F_c = ferrocenyl

Figure 2. Absolute configurations of difunctional (−)-menthoxysilanes.

2. *Cyclic Organosilicon Compounds*

Interest in the influence of the structure of organosilanes on reactivity stimulated the synthesis of optically active silacycloalkanes. The preparation of three of them has been achieved through the separation of menthoxysilane diastereomers.

The synthesis and resolution of 2-(1-naphthyl)-2-sila-1,2,3,4-tetrahydronaphthalene **45** (61) is shown in Scheme 5. Its configuration was determined by chemical correlation with respect to the established absolute configuration of *S*-(-)-2-fluoro-2-(1-naphthyl)-2-sila-1,3,4-trihydronaphthalene. (62)

Another six-membered ring system, resolved by Citron (63), is presented in Scheme 6. Pyrolysis of a racemic mixture of Sommer's compound **4** afforded a 7-silabenz[d,e]anthracene **46**, which again was resolved through separation of the menthoxy diastereomers **47**. The absolute configuration at silicon is not known.

A five-membered ring system, 1-silaacenaphthene **48**, has also been resolved by Roark and Sommer (64), as shown in Scheme 7.

C. Kinetic Resolution

The preparation of new asymmetric organosilicon compounds using the principles of asymmetric synthesis so widely employed in organic chemistry (65) has also been envisaged. Kinetic resolution, as depicted in Scheme 8, is of general

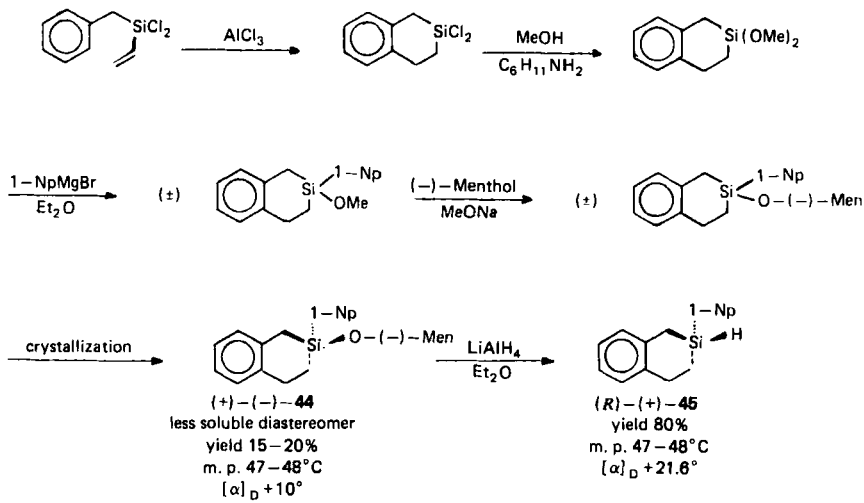

Scheme 5. Synthesis and resolution of 2-(1-Naphthyl)-2-sila-1,2,3,4-tetrahydronaphthalene (61).

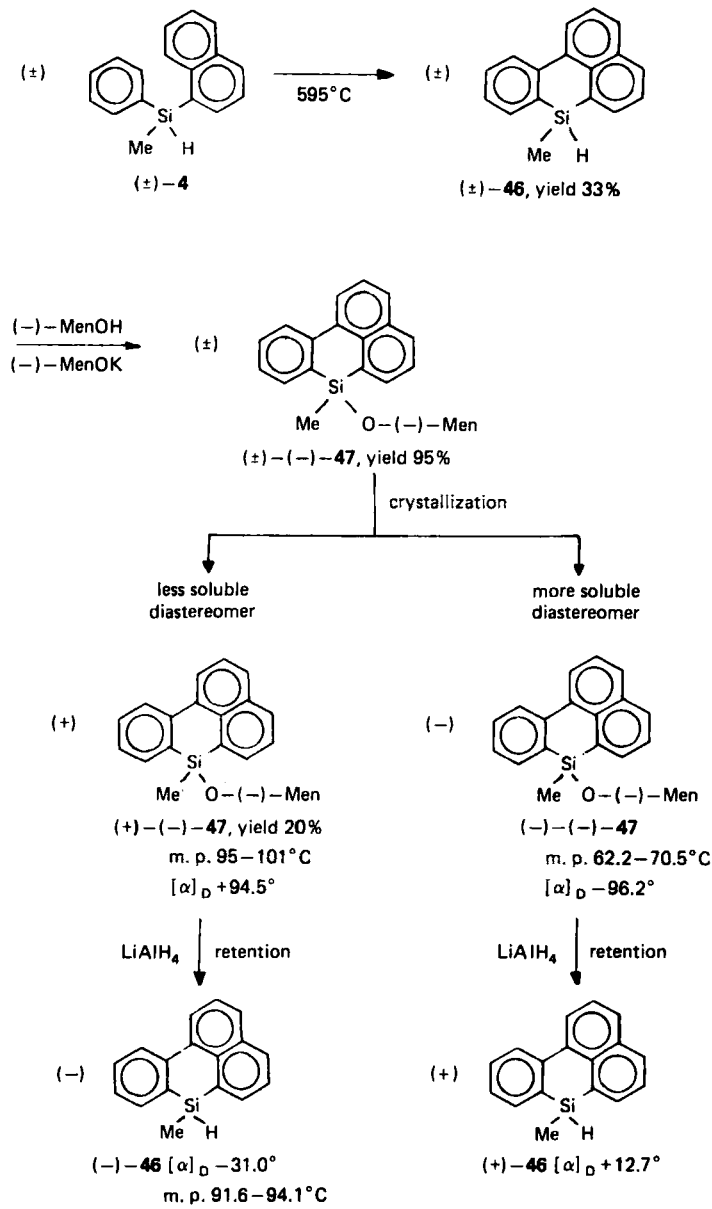

Scheme 6. Synthesis and resolution of 7-methyl-7-sila-benz[*d*,*e*]anthracene (63).

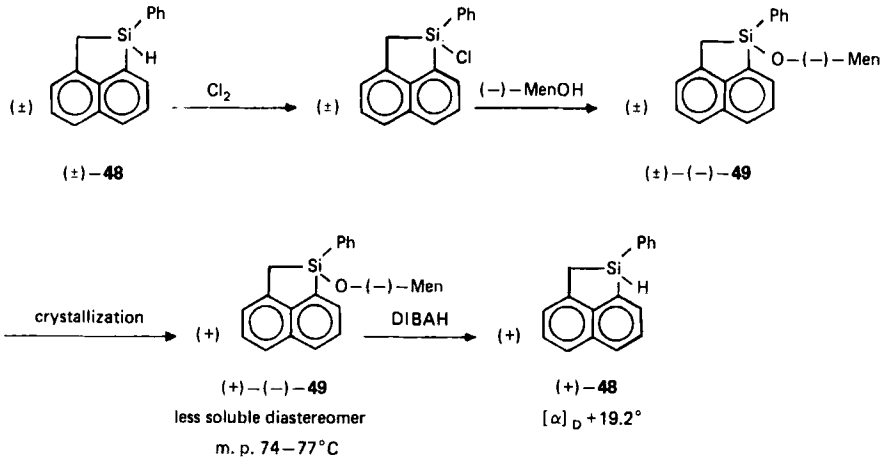

Scheme 7.

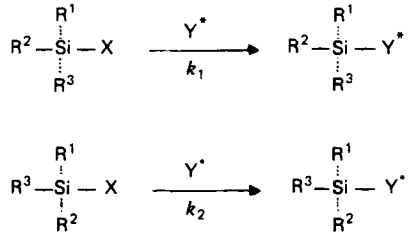

Scheme 8. Kinetic resolution of tetrahedral functional silanes.

potential interest in organosilicon chemistry. The rates of substitution of the functional group X of the two enantiomeric $R^1R^2R^3SiX$ compounds by a chiral reagent Y* will, in general, be different. If the reaction is stopped before completion, unequal amounts of the diastereomeric substituted silanes $R^1R^2R^3SiY^*$ should thus be obtained. The remaining unreacted starting material will also exhibit optical activity.

1. Partial Reduction of Racemic Methoxysilanes

Kinetic resolution was first observed in the partial reduction of racemic methoxysilanes by chiral reducing complexes of lithium aluminum hydride (66) (eq. [24].)

$$(\pm)\text{-}R^1R^2R^3SiOMe \xrightarrow[\text{chiral alkaloid or alcohol}]{LiAlH_4} R^1R^2R^3\overset{*}{S}iH \qquad [24]$$

Incomplete reduction (30 to 60% conversion) led to optically active hydrosilane and unreacted methoxysilane. Whereas the use of alcohols as chiral complexing agents gave products of low enantiomeric excess, the use of alkaloids led to higher optical purity. Some selected examples are given in Table 1. Using (+)-cinchonine, phenylethylmethylsilane was obtained in 41% enantiomeric excess. However, the generally much lower purity seen in other instances (Table 1) plus the necessity of stopping reduction short of completion limit the synthetic utility of this method.

2. *Menthanolysis of 1-Naphthylphenylchlorosilane*

Kinetic resolution with total chemical transformation of the organosilane starting material can nevertheless be envisaged if the latter rapidly racemizes during the course of the reaction. This has been observed for menthanolysis of 1-naphthylphenylchlorosilane **50** (54), as illustrated in Scheme 9.

The chlorosilane **50** undergoes rapid racemization, which is faster than alcoholysis. The menthoxysilane diastereomers **39** are obtained quantitatively in a ratio 1:2 close to that of the rate constants $k_1 : k_2$. Fractional crystallization of the mixture of diastereomeric menthoxysilanes **39** allowed isolation of the less soluble diastereomer (-)-(-)-**39** ($[\alpha]_D$ -66.2°, m.p. 72°C) in almost 70% recovery.

D. Asymmetric Synthesis

Although asymmetric synthesis in carbon chemistry has been widely studied, examples of asymmetric induction at heteroatoms are limited (65). In organic

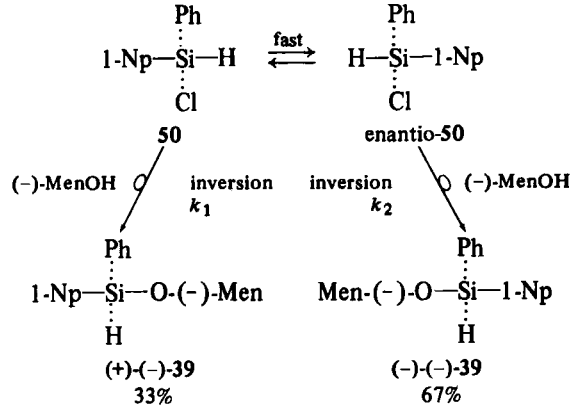

Scheme 9. Kinetic resolution of 1-Naphthylphenylchlorosilanes (54).

Table 1
Partial Reduction of Racemic Methoxysilane by Alkaloids/$LiAlH_4$ (66)

$R^1R^2R^3SiOMe$	Alkaloid	% Reduction	Unreacted $R^1R^2R^3SiOMe$ $[\alpha]_D$ (°)	Unreacted $R^1R^2R^3SiOMe$ Optical Purity (%)	$R^1R^2R^3SiH$ $[\alpha]_D$ (°)	$R^1R^2R^3SiH$ Optical Purity (%)
1-NpPhMeSiOMe	(−)-Quinine	35	−0.24	1.4	+1.52	4.3
	(+)-Quinidine	33	−0.93	5.5	+1.96	5.5
	(+)-Cinchonine	43	−0.40	2.4	+1.24	3.5
	(+)-ψ-Ephedrine	27	−0.86	5.1	+4.53	12.8
PhEtMeSiOMe	(−)-Cinchonidine	51	+0.59		−0.18	7.1
	(+)-Quinidine	54	−1.35		+0.44	14.4
	(+)-Cinchonine	56	−3.89		+0.5	41.2
$PhCH_2PhMeSiOMe$	(−)-Quinine	47	−0.28		+1.77	
	(−)-Cinchonidine	48	−0.86		+3.64	
	(+)-Cinchonine	42	+1.86		−7.80	
	(+)-ψ-Ephedrine	20	+0.46		−5.69	
MesitylPhMeSiOMe	(−)-Quinine	27	+2.52		−4.02	
	(+)-Quinidine	34	−1.01		+1.77	
Ph*i*-PrMeSiOMe	(+)-Quinidine	58	−4.61		+0.30	

chemistry, trigonal carbon constitutes the most important category of prochiral moiety which allows asymmetric induction. In silicon chemistry, the absence of stable compounds with trigonal silicon leads to much more limited possibilities.

1. Asymmetric Synthesis at Trigonal Silicon

Asymmetric induction at the silicon atom of transient prochiral silaethylenes has been observed recently (67). As shown in Scheme 10, prochiral silaethylenes were generated by photolysis of substituted silacyclobutanes. Trapping the short-lived silaethylenes with a chiral alcohol resulted in the formation of unequal amounts of diastereomeric alkoxysilanes. The diastereomer ratio was determined by NMR.

Only the bulky (-)-isoborneol gave appreciable enantiomeric excess. This very interesting example appears of limited synthetic utility. However, it clearly demonstrates the prochiral nature of transient trigonal silicon atoms.

2. Asymmetric Synthesis at Tetragonal Silicon

Starting with a tetrahedral silicon, the only possible structure for a prochiral compound is that of a disubstituted organosilane (Scheme 11).

The rates of substitution of the enantiotopic groups X of the prochiral compound $R^1R^2SiX_2$ by a chiral group Y* are, in principle, different. Unequal amounts of the two diastereomers **51** and **52** of opposite configuration around the silicon atom are thus formed in a ratio $k_1 : k_2$.

According to Scheme 11, asymmetric synthesis at silicon will be observed if (i) substitution by Y* is selective in the sense of leading to monosubstitution products, and (ii) substitution by Y* is stereoselective. We have also suggested that higher optical yields will be obtained for substitutions occurring with inversion rather than retention of configuration (68).

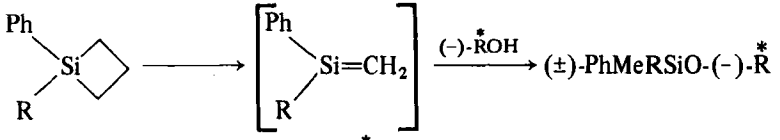

	(-)-ROH	e.e. (%)
R = Et	(-)-Borneol	0
	(-)-Menthol	0
	(-)-Isoborneol	24
R = *t*-Bu	(-)-Borneol	0
	(-)-Menthol	6
	(-)-Isoborneol	30

Scheme 10. Asymmetric synthesis at trigonal silicon (67).

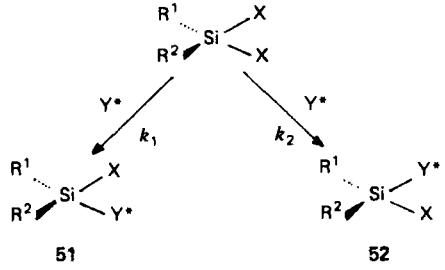

51 52

Scheme 11. Asymmetric synthesis at tetragonal silicon.

a. **Prochiral bis-(Acetamido) Silanes.** The first example of an asymmetric synthesis at silicon was reported by Klebe and Finkbeiner (69) and is illustrated in (eq. [25]). The reaction of bis(*N*-methylacetamido)phenylmethylsilane **53**

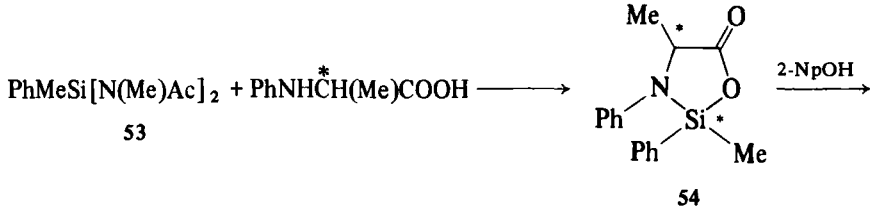

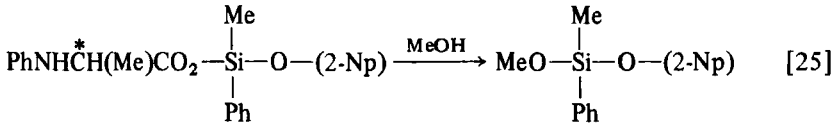

[25]

with optically active amino acids led to unequal amounts of the two diastereomeric 2-silaoxazolidones **54**. These were shown to undergo a second-order asymmetric transformation: crystallization was accompanied by a rearrangement of the less abundant into the predominant diastereomer. A cleavage reaction of silaoxazolidone **54** with 1-naphthol and methanol yielded the optically active dialkoxysilane **55** ($[\alpha]_D$ +21.9°).

b. **Prochiral Dihydrosilanes.** We have reported (68, 73, 78) the interesting potentialities of prochiral dihydrosilanes for asymmetric synthesis at silicon. Dihydrosilanes were shown to react selectively with alcohols and ketones in the presence of rhodium complexes to yield, quantitatively, difunctional hydro-

alkoxysilanes (70, 71). In this case direct substitution at the silicon atom does not occur and intervention of the catalyst must be considered. Presumably, the first step is oxidative addition of the organosilane to the rhodium complex (eq. [26]), forming an intermediate with pentacoordinate rhodium. Such pentacoordinated rhodium complexes have been isolated and are dissociated in solution (72). Prochiral silanes will lead to the formation of two enantiomeric complexes **56** and **57**, which, as a result of dissociation, will exist in equilibrium in solution. Scheme 12 is a kinetic scheme suitable for asymmetric synthesis analogous to that indicated for menthanolysis of 1-naphthylphenylchlorosilane (Scheme 9; see Sect. II-C-2).

$$R_2SiH + (PPh_3)_3RhCl \rightleftharpoons (R_3Si)(PPh_3)_2Rh(H)Cl + PPh_3 \qquad [26]$$

The existence of a very fast equilibrium between complexes **56** and **57** is supported by the instantaneous exchange of protium and deuterium between Et_3SiH and Ph_3SiD catalyzed by $(PPh_3)_3RhCl$ (73), (eq. [27]).

$$Et_3SiH + Ph_3SiD \underset{C_6H_6,\ 20°C}{\overset{(PPh_3)_3RhCl}{\rightleftharpoons}} Et_3SiD + Ph_3SiH \qquad [27]$$

These catalytic reactions of dihydrosilanes make possible the use of asymmetric catalysts to produce chiral silicon compounds. Introduction of a chiral ligand L* on the rhodium complex will not change the validity of the kinetic Scheme 12. However, in this case complexes **56** and **57** will be diastereomeric and their equilibrium concentrations will be different. The ratio of the substituted silanes will be close to $k_1 \cdot [\mathbf{56}] : k_2 \cdot [\mathbf{57}]$.

Asymmetric Alcoholysis of Dihydrosilanes. Optically active difunctional silanes have been obtained by asymmetric alcoholysis of prochiral dihydrosilanes catalyzed by rhodium complexes (73) (eq. [28]).

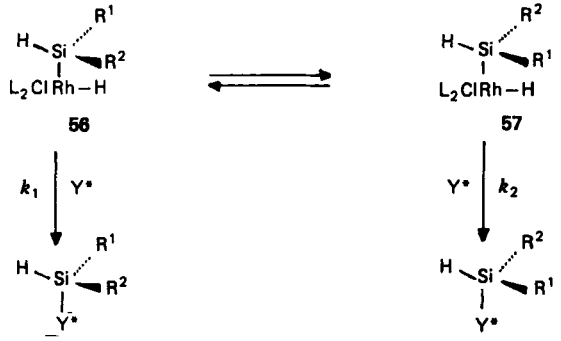

Scheme 12. Rhodium catalyzed reactions of prochiral dihydrosilanes.

$$R^1R^2SiH_2 + ROH \xrightarrow{\text{"}L_2RhCl\text{"}} R^1R^2\overset{*}{S}iH(OR) + H_2 \xrightarrow[\text{retention}]{R^3MgX} R^1R^2R^3\overset{*}{S}iH \qquad [28]$$

Chirality can be introduced by use of an asymmetric alcohol and/or an asymmetric catalyst. The optical yield and predominant configuration around silicon were determined by conversion of the diastereomeric alkoxysilanes to a trisubstituted silane of known configuration and maximum specific rotation. Reaction of Grignard reagents to this end is both quantitative and stereospecific.

The results are summarized in Table 2. Optical yields up to 54% have been observed with various dihydrosilanes. 1-NpPhSiH$_2$ gave the highest enantiomeric excess. It is noteworthy that in the reactions with a chiral alcohol, regardless of what asymmetric catalyst is used, the optical yields are similar to those obtained with $(PPh_3)_3RhCl$. This indicates but a weak interaction between alcohol and catalyst during the reaction course. To account for this observation, a mechanism involving nucleophilic attack of the alcohol at the coordinated silicon has been suggested (77) (cf. Sect. IV-A-2).

Asymmetric Hydrosilylation with Dihydrosilanes. Chiral alkoxysilanes have also been obtained in the rhodium catalyzed hydrosilylation of carbonyl compounds (68, 78, 79) (eq. [29]).

$$R^1R^2SiH_2 + R^4R^5C{=}O \xrightarrow{\text{"}L_2^*RhCl\text{"}} R^1R^2(H)\overset{*}{S}i\overset{*}{O}CHR^4R^5 \xrightarrow{R^3MgX} R^1R^2R^3\overset{*}{S}iH + R^4R^5\overset{*}{C}HOH \qquad [29]$$

When prochiral silane and ketone are used, hydrosilylation, in the presence of a chiral catalyst, results in asymmetric induction at both the silicon and carbon centers. Treatment of the diastereomeric alkoxysilane by a Grignard reagent leads to recovery of an organosilane and an alcohol of different optical purity. Results obtained in the asymmetric hydrosilylation of ketones and aldehydes by prochiral silanes in the presence of an asymmetric catalyst are summarized in Tables 3 and 4.

Optically active silanes were obtained from symmetrical ketone, RCOR, in up to 46% enantiomeric excess, the catalyst being the only source of chirality. Asymmetric induction was also observed at the prochiral carbon of constitutionally unsymmetrical ketones, RCOR′: The optical yield at the carbon atom is different from that at silicon. This is well understood on the basis of kinetic Scheme 13. The diastereomeric complexes **56** and **57** interconvert rapidly in solution. Each complex reacts with different rates at the two faces (α and β) of the ketone. The optical purity at the silicon center depends on the relative rates of

Table 2
Asymmetric Alcoholysis of Prochiral Dihydrosilanes (73)

Dihydrosilane $R^1R^2SiH_2$	Alcohol	Catalyst Ligand[a]	e.e.[b] %	Configuration $R^1R^2R^3SiH$
1-NpPhSiH$_2$	(−)-Menthol	PPh_3	48	*R*
	(−)-Cholesterol	PPh_3	3	*R*
	(+)-Cinchonine	PPh_3	13	*S*
	(−)-Borneol	PPh_3	6	*S*
	(−)-Ephedrine	PPh_3	54	*R*
	(+)-Ephedrine	PPh_3	54	*S*
	(±)-PhMeCHOH	PPh_3	20[c]	–
	(±)-Ph*t*-BuCHOH	PPh_3	14[c]	–
	(±)-Mesityl *i*-PrCHOH	PPh_3	50[c]	–
	(−)-Menthol	C_8H_{14}	38	*R*
	(−)-Ephedrine	C_8H_{14}	50	*R*
1-NpEtSiH$_2$	(−)-Menthol	PPh_3	21	*S*
1-NpPhCH$_2$SiH$_2$	(−)-Menthol	PPh_3	20	*S*
Ph*i*-BuSiH$_2$	(−)-Menthol	PPh_3	16	*S*
PhMeSiH$_2$	(−)-Menthol	PPh_3	2	*S*
1-NpPhSiH$_2$	MeOH	(+)-DIOP	3	*R*
	i-PrOH	(+)-DIOP	8	*R*
	t-BuOH	(−)-DIOP	7	*S*
	cyclo-$C_6H_{11}OH$	(+)-DIOP	17	*R*
	cyclo-$C_6H_{11}OH$	NMDPP	2	*S*
	Ph_2CHOH	(−)-DIOP	18	*S*
	Ph_2CHOH	(+)-DIOP	19	*R*
	Thymol	(−)-DIOP	9	*S*
1-NpPhSiH$_2$	(−)-Menthol	(−)-DIOP	31	*R*
	(−)-Menthol	(+)-DIOP	49	*R*
	(−)-Menthol	NMDPP	22	*R*
	(−)-Menthol	MDPP	44	*R*
	(−)-Ephedrine	(−)-DIOP	42	*R*
	(−)-Ephedrine	(+)-DIOP	46	*R*
	(+)-Ephedrine	(−)-DIOP	44	*S*
	(+)-Ephedrine	(+)-DIOP	40	*S*
	(−)-Ephedrine	NMDPP	53	*R*
	(−)-Ephedrine	MDPP	52	*R*
	(+)-Ephedrine	NMDPP	54	*S*
	(+)-Ephedrine	MDPP	54	*S*

[a]Catalyst: $L_2RhCl(S)$, (S = solvent); Ligands: C_8H_{14} = cyclooctene, DIOP = 2,3-0-isopropylidene-2,3-dihydroxy-1,4-bis(diphenylphosphino)butane (74); NMDPP = neomenthyldiphenylphosphine; MDPP = menthyldiphenylphosphine (75).

[b]Enantiomeric excess, determined after conversion of the alkoxysilanes to a trisubstituted silane.

[c]Determined using the Horeau method (76).

Table 3
Asymmetric Hydrosilylation of Symmetric Ketones and Aldehydes by Prochiral Dihydrosilanes (68, 79, 80)

Dihydrosilane $R^1R^2SiH_2$	Carbonyl Compound	Catalyst Ligand[a]	e.e.[b] %	Configuration $R^1R^2R^3SiH$	Ref.
1-NpPhSiH$_2$	Me_2CO	(+)-DIOP	30	*R*	68
	Et_2CO	(+)-DIOP	46	*R*	68
		(−)-DIOP	44	*S*	68
		(*R*)-BMPP[c]	7.2	*S*	79
	nPr_2CO	(+)-DIOP	39	*R*	68
	iBu_2CO	(+)-DIOP	36	*R*	68
	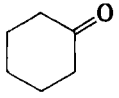	(+)-DIOP	32	*R*	68
		(R)-BMPP[c]	3.1	*S*	80
	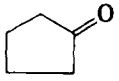	(+)-DIOP	35	*R*	68
	Ph_2CO	(+)-DIOP	31	*R*	68
		(−)-DIOP	46	*S*	80
		(*R*)-BMPP[c]	27.7	*S*	79
	EtCHO	(+)-DIOP	14	*R*	68
	n-PrCHO	(+)-DIOP	16	*R*	68
	i-BuCHO	(+)-DIOP	4	*R*	68
	n-$C_6H_{13}CHO$	(+)-DIOP	13	*R*	68
	PhCHO	(+)-DIOP	7	*R*	68
1-NpMeSiH$_2$	Me_2CO	(*R*)-BMPP[c]	7.4	*R*	79
	Et_2CO	(+)-DIOP	12	*S*	68
		(*R*)-BMPP[c]	8.6	*R*	79
	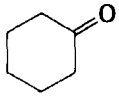	(*R*)-BMPP[c]	7.2	*R*	80
	Ph_2CO	(+)-DIOP	7	*S*	68
		(−)-DIOP[c]	18.8	*R*	80
		(*R*)-BMPP[c]	19.7	*R*	79
1-NpEtSiH$_2$	Et_2CO	(+)-DIOP	21	*S*	68
	Ph_2CO	(+)-DIOP	33	*S*	68

[a] See footnote *a*, Table 2. (*R*)-BMPP ≈ (*R*)-Benzylmethylphenylphosphine.
[b] Enantiomeric excess, determined after conversion of the alkoxysilane to a trisubstituted silane.
[c] Catalyst: $[L_2RhH_2(S_2)]^+ ClO_4^-$. Elsewhere catalyst is $L_2RhCl(S)$.

Table 4
Asymmetric Hydrosilylation of Prochiral Ketones by Prochiral Dihydrosilanes (68)

Dihydrosilane $R^1R^2SiH_2$	Ketone R^3R^4CO	Catalyst Ligand[a]	$R^1R^2R^3SiH$ e.e.[b] %	$R^1R^2R^3SiH$ Config.	R^4R^5CHOM e.e. %	R^4R^5CHOM Config.
1-NpPhSiH$_2$	PhMeCO	(−)-DIOP	32	*S*	55	*R*
	PhEtCO	(+)-DIOP	30	*R*	56	*S*
	EtMeCO	(−)-DIOP	40	*S*	42	*R*
	EtMeCO	(+)-DIOP	39	*R*		
	t-BuMeCO	(+)-DIOP	35	*R*		

[a]See Footnote *a*, Table 2.
[b]Enantiomeric excess.

reaction of the complexes **56** and **57**: $(k_1^{\alpha} + k_1^{\beta})$ [**56**] : $(k_2^{\alpha} + k_2^{\beta})$ [**57**]. The optical purity at the carbon atom is different, since it depends on the attack on the faces (α) and (β); k_1^{α} [**56**] + k_2^{α} [**57**] : k_1^{β} [**56**] + k_2^{β} [**57**]. Thus 1-NpPhSiH$_2$ functions as an interesting reducing agent for the asymmetrically catalyzed reduction of ketones to alcohols (68, 80, 81).

The hydrosilylation of chiral (−)-menthone and (+)-camphor has also been investigated. Results are presented in Tables 5 and 6.

Reaction of (−)-menthone or (+)-camphor resulted in the formation of four diastereomeric alkoxysilanes, depending on the configuration, *R* or *S*, at the silicon atom and mode of attack at one face or the other of the ketone. The hydrosilylation of (−)-menthone gave two menthoxy- and two neomenthoxysilanes, that of (+)-camphor the bornyloxy- and isobornyloxysilanes. The relative pro-

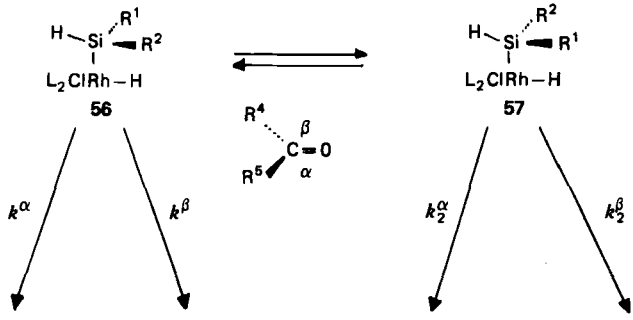

Scheme 13.

Table 5
Asymmetric Hydrosilylation of (-)-Menthone by Prochiral Dihydrosilanes (78)

Dihydrosilane $R^1R^2SiH_2$	Catalyst Ligand[a]	Alkoxysilanes Neomenthoxy %	Alkoxysilanes Menthoxy %	e.e.[b] at Carbon %	$R^1R^2R^3SiH$[a] e.e. %	$R^1R^2R^3SiH$[a] Config.
1-NpPhSiH$_2$	PPh_3	73	27	46	67	*R*
	C_8H_{14}	66	34	32	23	*S*
	(+)-DIOP	86	14	72	82	*R*
	(-)-DIOP	68	32	36	46	*R*
	MDPP	58	42	16	4	*S*
	NMDPP	69	31	38	16	*S*
1-NpEtSiH$_2$	PPh_3	73	27	46	51	*R*
	(+)-DIOP	73	27	46	4	*R*
	(-)-DIOP	56	44	12	13	*R*
PhMeSiH$_2$	PPh_3	73	27	46	0	–
	(+)-DIOP	73	27	46	21	*S*
	(-)-DIOP	56	44	12	9	*R*

[a]See footnotes of Table 2.
[b]Enantiomeric excess.

portions of the two groups of diastereomers reflect the stereoselectivity of attack on the carbonyl group.

With both ketones, the less stable diastereomers (neomenthoxy and isobornyloxy), corresponding to the attachment of the hydrogen atom to the less hindered face of the carbonyl compound, were preferentially formed. The stereoselectivity varied from 12 to 80%.

Table 6
Asymmetric Hydrosilylation of (+)-Camphor by 1-NpPhSiH$_2$ (78)

Dihydrosilane $R^1R^2SiH_2$	Catalyst Ligand[a]	Alkoxysilanes Isobornyloxy %	Alkoxysilanes Bornyloxy %	e.e.[b] at Carbon %	$R^1R^2R^3SiH$[a] e.e. %	$R^1R^2R^3SiH$[a] Config.
1-NpPhSiH$_2$	PPh_3	88	12	76	62	*S*
	C_8H_{14}	77	23	54	9	*R*
	(+)-DIOP	68	32	36	20	*S*
	(-)-DIOP	90	10	80	31	*S*
	NMDPP	83	17	66	7	*S*
	MDPP	71	29	42	13	*S*

[a]See footnotes of Table 2.
[b]Enantiomeric excess.

Optical purities at silicon of up to 82% were obtained. The nature of the catalyst ligands exerts a determining influence on the optical yield and configuration, even with an achiral catalyst. The combination of chiral ketone with a chiral catalyst may raise or decrease the optical yield. As previously, enantiomeric excess at carbon is different from that at silicon and also varies greatly according to reactants and catalysts.

The strong dependence of the stereochemical course of the reaction on substrates and catalyst ligands points to the importance of an intermediate rhodium complex in which both ketone and silane are coordinated to the rhodium. Moreover, enantiomeric excess at silicon has been shown to be largely influenced by which face of the chiral ketone is attacked. This strongly supports π-coordination of the carbonyl group to the rhodium. The predominant configurations obtained have been tentatively explained on the basis of steric interactions in a hexacoordinated rhodium complex (82).

From a synthetic point of view, asymmetric synthesis at silicon in dihydrosilanes has proved to be useful. It provided the basis for a one-pot synthesis of Sommer's compound, R-(+)- or S-(-)-1-NpPhMeSiH, in 96% e.e. with a 51% chemical yield starting from 1-NpPhSiH$_2$ (83). The synthesis of a new optically active oxasilacycloalkane has also been realized in this way (84). Moreover, the stereochemistry of a cleavage reaction of a silicon-carbon bond has been determined using asymmetric synthesis (85). The configurations of the pertinent compounds could not be correlated in any other way.

c. **Prochiral Dialkoxysilanes.** Asymmetric synthesis at silicon has also been achieved using optically active prochiral dialkoxysilanes (86) (eq. [30])

$$R^1R^2Si(\overset{*}{O}R)_2 \xrightarrow{EtLi} R^1R^2Et\overset{*}{S}i\overset{*}{O}R \qquad [30]$$

Reaction with ethyllithium at low temperature led to unequal amounts of diastereomeric monoalkoxysilanes. Their ratio, which reflects the enantiomeric excess at silicon, was measured by NMR. Results are given in Table 7.

An interesting feature of these reactions is that they permit the synthesis of simple chiral silicon compounds in up to 69% optical purity using readily available reagents. Moreover the method appears to be of wide applicability.

E. Stereospecific Synthesis of Chiral Organosilicon Compounds

Substitution reactions at silicon have been shown to proceed with high stereoselectivity. Either inversion or retention of configuration at silicon is commonly observed (see Sect. III.) A large number of chiral silicon compounds have thus been prepared by stereospecific substitution of resolved organosilanes. Most of them are mentioned along the way in this review; however, at this point we shall

Table 7
Reactions of Chiral Prochiral Dialkoxysilanes with Ethyllithium (86)

Dialkoxysilane $R^1R^2Si(OR)_2$	Reaction Temperature °C	e.e.[a] %
1-NpMeSi[O-(-)-Men]$_2$	-30	15
	-70	28
PhMeSi[O-(-)-Men)]$_2$	-30	14
	-70	49
(*p*F-Ph)MeSi(O-(-)-Men)$_2$	-70	51
(*p*MeOPh)MeSi(O-(-)-Men)$_2$	-70	50
(*m*MeOPh)MeSi(O-(-)-Men)$_2$	-70	40
(*o*MeOPh)MeSi(O-(-)-Men)$_2$	-70	60
VinylMeSi(O-(-)-Men)$_2$	-70	69
AllylMeSi(O-(-)-Men)$_2$	-70	30
PhMeSi(O-(-)-Bornyl)$_2$	-10	50
PhMeSi(O-(+)-neomenthyl)$_2$	-70	36
(*o*MeO-Ph)PhSi(O-(-)-Men)$_2$	-70	50

[a]Enantiomeric excess.

detail compounds which have a novel structural environment around silicon and which have led to important findings in the study of substitution reactions at silicon.

1. Optically Active Alkylphenylmethylsilanes

As a result of stereospecific cleavage of the silicon-naphthyl bond, new optically active acyclic organosilanes have been obtained according to Scheme 14 (87).

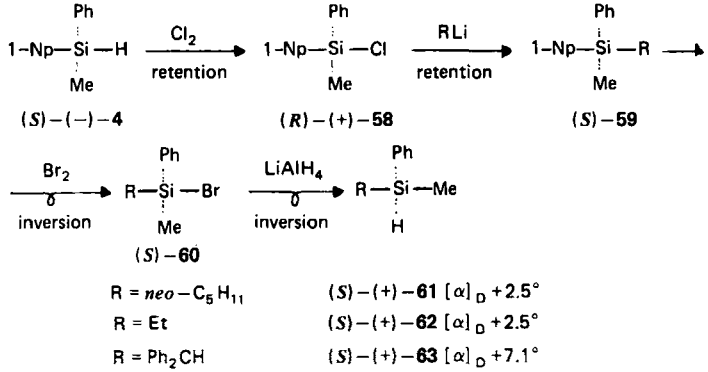

Scheme 14. Synthesis of optically active alkylphenylmethylsilanes.

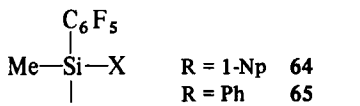

Figure 3. Preparation of perfluorophenyl derivatives.

Starting with enantiomerically pure (*S*)-(-)-1-NpPhMeSiH **4**, successive chlorination, condensation with alkyllithium, bromine cleavage of the silicon naphthyl bond, and reduction with lithium aluminum hydride afforded the new (*S*)-(+)-alkylphenylmethylsilanes **61–63**. Their configurations were established using chemical correlations, cleavage of silicon-aryl bonds having been shown independently to cause inversion at the silicon atom (88).

The preparation of the perfluorophenyl derivatives **64–65** (Figure 3) has also been reported (89).

2. *Optically Active Silacycloalkanes*

a. Oxa- and Thiasilacyclopentanes. Optically active oxasilacyclopentane **68** has been obtained according to Scheme 15 (90). The γ-hydroxysilane **67** was ob-

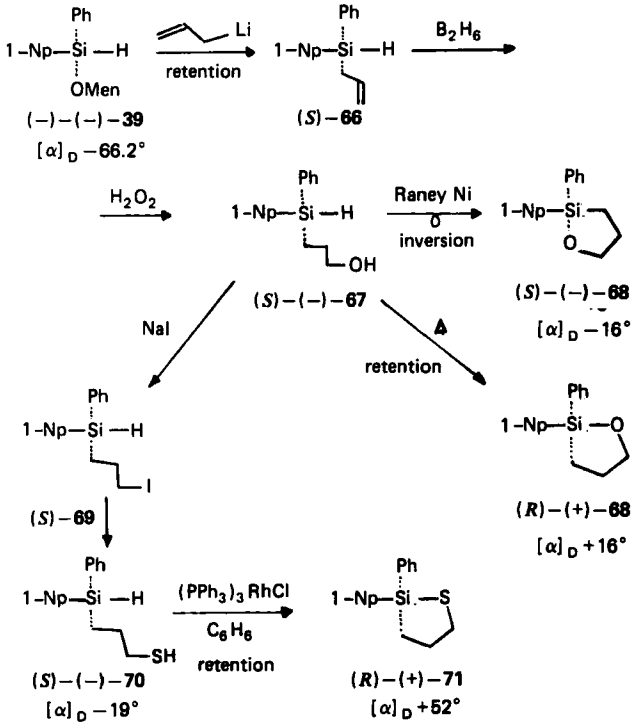

Scheme 15. Synthesis of optically active oxa- and thiasilacyclopentanes **68** and **71**.

tained with retention of configuration from $S_{(Si)}$-1-NpPhHSiO-(-)-Men (**39**). Catalytic or thermal dehydrogenative cyclization led to (*S*) or (*R*)-oxasilacyclopentane **68** with inversion or retention at the silicon atom, respectively.

Similarly, (*R*)-(+)-thiasilacyclopentane **71** has been isolated (91). The γ-hydroxysilane **67** was converted to the thiol **70**, which was cyclized with retention of configuration at silicon.

b. Oxasilacyclohexane. An optically active oxasilacyclohexane **76** has been synthesized by an analogous method (84), as shown in Scheme 16. The optically active compound was obtained using asymmetric synthesis at silicon. Reaction of (-)-ephedrine with 1-NpPhSiH$_2$ gave **72** as the predominant diastereomer. Treatment with the homoallyl Grignard reagent led to the homoallylsilane **74** with retention of configuration. The δ-hydroxysilane **75** was isolated after hydroboration of **74** and cyclized by means of Raney nickel with inversion, yielding the *R*-(-)-oxasilacyclohexane **75**. According to previous results in related asymmetric syntheses (83), the optical purity of the final product **75** is probably about 50%.

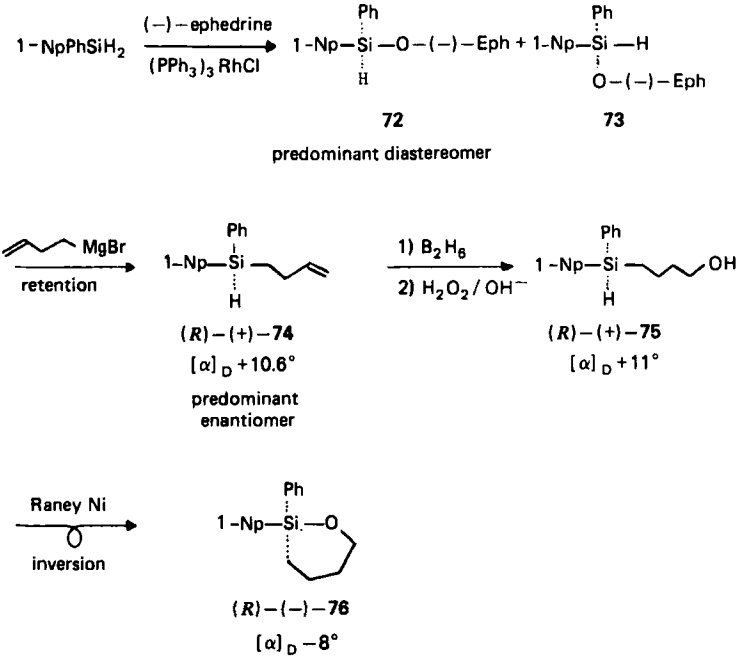

Scheme 16. Synthesis of optically active oxasilacyclohexane **76**.

F. Determination of Enantiomeric Purity and of Configuration

The assignment of configuration and the measurement of enantiomeric purity is a necessary step in any stereochemical study. Both the physical and chemical techniques used have been described in detail in the case of carbon compounds (92, 93). In this section we give a brief overview of their application to organosilicon stereochemistry.

1. Determination of Enantiomeric Purity

The methods for the determination of enantiomeric purity have been the subject of reviews (92-95). If the maximum rotation of an optically active compound is known, measurement of the specific rotation of a given sample indicates its optical purity, provided the sample is chemically pure. The maximum specific rotation of most chiral organosilanes (in given solvents) is now known since their enantiomeric purity has been determined independently.

When a crystalline enantiomer is obtained, although the observation of unchanged melting point and specific rotation upon further crystallization, is, in principle, not a reliable criterion of its being enantiomerically pure, nonetheless, this criterion has often led to correct estimates of enantiomeric purity of optically active organosilicon compounds.

The determination of the enantiomeric purity of many organosilanes has been achieved by the method of differential scanning calorimetry devised by Jacques, Fouquey, and colleagues (93, 94); this method is of wide applicability and high precision.

Enantiomeric purity is also accessible by chemical correlations. Taking advantage of the various stereospecific substitutions that occur at silicon, one can correlate an enantiomer of unknown absolute rotation with a known one. Such chemical correlations are similar to those used to establish relative configuration (cf. Sect. II-F-3).

2. Absolute Configuration

The only direct method that gives rise to the absolute configuration is X-ray diffraction employing Bijvoet's method. However, the relative configurations of many organosilanes have been correlated to each other using physical and chemical methods (cf. Sect. II-F-3). Therefore the X-ray determination of a key chiral compound leads to the absolute configuration of many related molecules, just as has been the case for chiral carbon compounds.

In organosilicon chemistry the molecular structure and absolute configuration of only a few chiral silanes have been determined by the Bijvoet method. These

include organic silicon compounds as well as inorganic transition metal-silicon compounds, which are mentioned in Sects. II and IV.

3. Relative Configuration

The correlation of the configuration of one compound to that of another (relative configuration) has been achieved in several ways. We give selected examples of each method.

a. Physical Correlations. Several physical methods of correlating configurations have been applied to chiral silicon compounds; we mention here the quasi-racemate (phase diagram) method, X-ray diffraction, and chiroptic (ORD-CD) methods.

Melting-Point Phase Diagrams. The principle of this method, extensively used in carbon stereochemistry by Fredga (96), has been described in detail (92, 93). It is based on the construction of melting point phase diagrams of mixtures of two enantiomerically pure compounds of similar structural environment around the chiral center. Its application to chiral silicon compounds gave reliable results since both enantiomers of the compound to be correlated were available. Thus, if the phase diagram of two compounds *A* and *B* shows that they form a solid solution, and that of *A* and the enantiomer of *B* exhibits a eutectic, then *A* and *B* are of the same configuration.

A good example has been reported (49); it led to the assignment of the relative configuration of various alkylphenylnaphthylsilanes.

Interestingly, the Fredga method has been extended to the correlation of configuration at silicon of diastereomeric menthoxysilanes differing only in their environment around silicon (58).

X-ray Diffraction. Instead of deducing solid solution formation from melting point behavior, it may be deduced from X-ray powder diagrams. Using this technique the relative configurations of (-)1-NpPhMeSiH, (-)1-NpPhMeSiF, and (+)1-NpPhMeSiCl were shown to be the same (44). Pure and mixed crystals have similar crystallographic constants and the intensities of diffracted X-rays from the mixed crystals appeared as the summation of those of the pure component crystals.

Optical Rotatory Dispersion and Circular Dichroism. The comparison of optical rotations, at several wavelengths, of silanes of similar environment around silicon often gives a useful indication of their relative configuration. However, optical comparison alone is not a method of unquestioned validity.

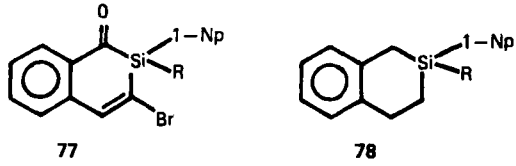

Figure 4.

The comparison of optical rotatory dispersion (ORD) or circular dichroism (CD) curves gives more reliable correlations. If the molecule contains an asymmetrically perturbed symmetric chromophore, the sign of the Cotton effect reflects the stereochemistry of the environment of the chromophore.

The naphthyl substituent appeared to be a suitable chromophore and pertinent ORD or CD curves led to the correlation of the configuration of alkylphenylnaphthylsilanes (49, 97). The results were consistent with those deduced from phase diagrams (49).

Another interesting example relates to the case of optically active silyl ketones **77** (98) (Figure 4). Their relative configurations, deduced from the sign of the Cotton effect in their ORD curves, are consistent with those of their parent silanes **78** (Figure 4) also assigned by ORD studies. Thus silylketones **77** of negative specific rotation have the same configuration as silanes **78** of positive specific rotation.

b. Chemical Correlations. The correlation of the configuration of two optically active organosilanes by a series of chemical reactions can now be achieved easily, since many reactions are stereospecific and their stereochemistry has been demonstrated.

In the study of dynamic stereochemistry, the main problem is to decide whether a substitution reaction occurs with retention or inversion. As an illustration of how this problem was solved, we discuss two examples.

The use of Walden cycles is illustrated in Scheme 17 for a series of stereospecific reactions of 1-NpPhMeSiH (44). The same relative configuration was established (cf. Sect. II-F-3a) for (-)-R_3SiH, (-)-R_3SiF, and (+)-R_3SiCl. It allows one to assign inversion, retention, and inversion of configuration respectively for reactions iii, iv, and v. This implies that reactions i and ii implicated in the Walden cycle occur with opposite stereochemistry. The same conclusion is reached for reactions vi and vii. Reactions i and vi, which involve the same reagent on similar alkoxysilanes certainly occur with the same stereochemistry. Moreover on the basis of the similarity of the reagents used in reactions v and vii, inversion can be assigned to reaction vii. Therefore the logical choice is retention for i and vi and inversion for ii and viii.

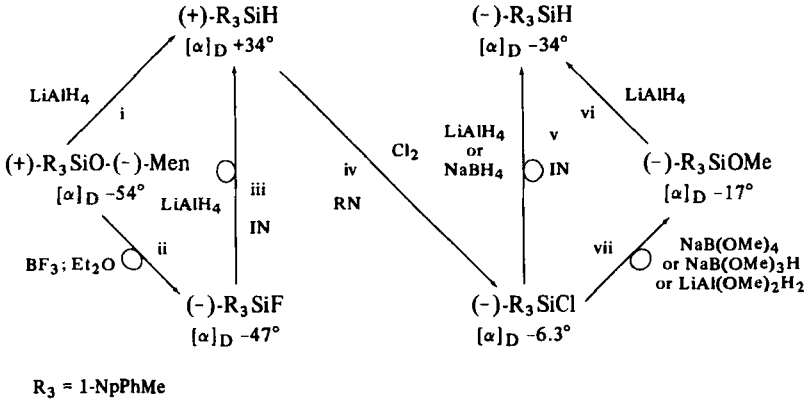

Scheme 17. Chemical correlations of optically active 1-NpPhMeSiX.

Chemical transformations in which the chiral silicon center is not implicated allow one to correlate the configuration of two different compounds. Step iii in Scheme 18 is a case in point (58). Since this step does not change the configuration at silicon and steps iv and v involve the same stereochemistry (retention), the propyl and allyl alkoxysilanes correspond in configuration and since steps i and ii involve displacement of different ligands, they must proceed with opposite stereochemistry. On the basis of other, related results, retention and inversion were assigned to steps i and ii respectively.

The knowledge of the stereochemistry of many reactions in turn makes possible a number of more complex stereochemical correlations. For instance, the stereochemistry of a ring opening reaction was determined by a series of known stereochemical pathways, including an asymmetric synthesis step, to obtain one of the necessary optically active intermediates (85). As shown in Scheme 19, the configuration of the ring-opened product **83** was correlated with that of com-

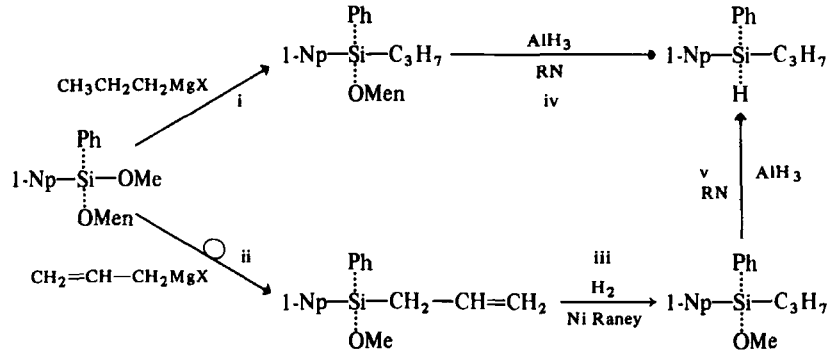

Scheme 18. Chemical correlations of optically active propyl- and allylalkoxysilanes.

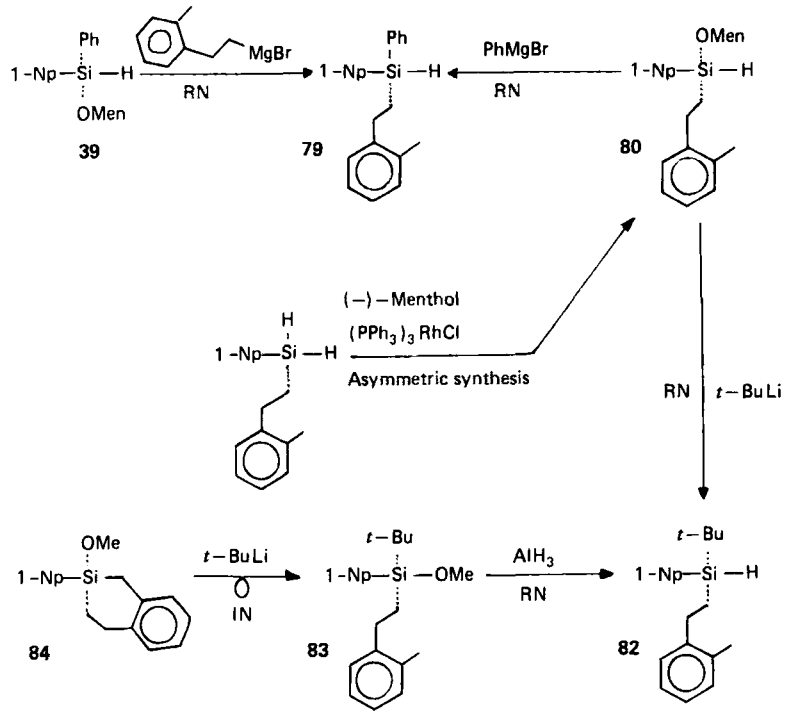

Scheme 19. Determination of the stereochemistry of ring opening in compound **84**.

pound **80** obtained by an asymmetric menthanolysis, whose configuration, in turn, was correlated to that of compound **39** of known absolute configuration. Since the absolute configuration of the cyclic compound **84** is known, inversion of configuration is established for the ring opening step.

III. STEREOCHEMISTRY OF NUCLEOPHILIC DISPLACEMENT AT SILICON AND ITS RATIONALIZATION

A. Introduction and General Considerations*

This section focuses on the main factors controlling the stereochemistry of substitution; a possible rationalization of the experimental data based on a frontier-orbital approximation is presented (99, 100). A more detailed analysis may be found in our two previous comprehensive reviews (10, 11).

*Predominant stereochemistry of 90% inversion (retention) indicates a reaction path involving 90% inversion (retention) and 10% retention (inversion), giving a product that is 80% enantiomerically pure from an enantiomerically pure starting material.

Before entering upon this problem, we examine briefly the three following questions:

1. Is the R_3Si^+ cation acting as an intermediate in displacement reactions at silicon?
2. Are the nucleophilic substitutions at silicon consistent with the occurrence of the rate-determining formation of a five-coordinate silicon intermediate?
3. Is substitution at silicon a nucleophilic or a one-electron transfer process?

1. Role of R_3Si^+ As a Reaction Intermediate

The role of carbonium ions R_3C^+ as reaction intermediates (S_N1 process) is well documented (101). In such unimolecular reactions, the carbon atom attached to the leaving group undergoes racemization.

Currently, R_3Si^+ siliconium ions are not believed to be intermediates in any reaction in solution (1, 2, 10, 11). The device, well known in carbon chemistry, of placing unsaturated groups next to the developing positive charge, does not change the mechanism in the silicon series (102); thus monofunctional triarylsilanes do not solvolyze by way of an Ar_3Si^+ cationic intermediate, and *p*-methoxy substituents retard substitution relative to unsubstituted phenyl (103). Moreover, nucleophilic substitutions at silicon are found to be very stereoselective, occurring with a high degree of either retention or inversion of configuration. Even vinyl- or ferrocenylsilanes, the structure of which might favor sp^2 cation formation due to the stabilization from the substituents, do not lead to racemic solvolysis products (Table 8) (104, 105).

Table 8
Stereochemistry of Solvolysis of Vinyl- and Ferrocenylsilanes

Silane[a]	Reagent	Product	Predominant Stereochemistry[b]	Ref.
1-NpPhViSi-Cl $[\alpha]_D = -5.7°$ (CCl_4)	CH_3-OH/pentane	R_3Si-OCH_3 $[\alpha]_D = -9.3°$	100% RN	104
	H_2O/Et_2O	R_3Si-OH $[\alpha]_D = -9.2°$	89% IN	104
	KOH/xylene	R_3Si-OK $[\alpha]_D = +24.9°$	98.5% IN	104
1-NpPhFcSi-Cl $[\alpha]_D = +33.8°$ (CCl_4)	CH_3OH/pentane	R_3Si-OCH_3 $[\alpha]_D = -14.8°$	IN	105

[a] Vi = Vinyl; Fc = ferrocenyl; 1-Np = 1-naphthyl.
[b] IN = inversion; RN = retention.

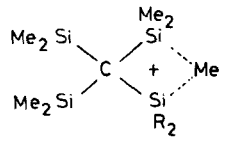

85

Figure 5.

Finally, it was established that, even in hydroxylic solvents, there is no S_N1-type reaction at silicon (13): the data are discussed in a later section (V-B). However, Eaborn and Mahmoud (6) have pointed out that lack of evidence for rate-determining ionizations of organosilicon halides and similar species might be in part attributable to their normally very high reactivity in bimolecular (S_N2) processes, i.e. it simply means that S_N1 processes have no chance to compete. The obvious way to suppress the bimolecular reaction is by steric hindrance. For instance, Eaborn and colleagues have studied the methanolysis of the compounds $TsiSiMe_2(OClO_3)$ [Tsi = $(Me_3Si)_3C$], $[(Me_3Si)_2(Ph_2MeSi)]CSiMe_2OClO_3$, TsiSiHPhX (X = I, Br, ONO_2), and TsiSiHMeI (6). The kinetic features of these reactions provide strong evidence for an S_N1 mechanism, and the authors suggest a rate-determining ionization of the Si-$OClO_3$ or Si-I bonds to give a methyl-bridged cation such as **85** (Figure 5).

2. *Role of a Five-Coordinate Intermediate in Nucleophilic Displacement*

a. Kinetic Probes. In order to determine the reaction energy profile (Scheme 20), the rates of reactions occurring either with retention or inversion at silicon were studied (106). Some results for reactions leading to retention are summarized in Table 9, and those for reactions giving inversion in Table 10.

Two types of behavior are observed: in one, rate constants for pairs of leaving groups are related by a factor of 1-50, in the other by a factor $>10^3$. The former are in the majority and apply to both retention and inversion modes, whereas the latter are only found for F and OMe in reactions giving inversion.

Table 9
Kinetic Data for Reactions Occurring with Retention

Organosilane	X = α	X = β	RM	Solvent	k_α/k_β
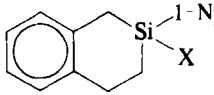	F	OMe	EtMgBr	Et_2O	1.5-2.5
	F	OMe	PhMgBr	Et_2O	2-3
	F	OMe		Et_2O	4-5
1-NpPhEtSi-X	OMe	H	*n*-BuLi	Et_2O	5-6
	H	D	*n*-BuLi	Et_2O	1
	F	OMe	*n*-BuLi	Et_2O	50

Table 10
Kinetic Data for Reactions Occurring with Inversion

Organosilane	X = α	X = β	RM	Solvent	k_α/k_β
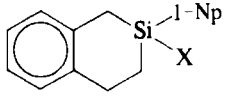	F	Cl	CH_3MgBr	Et_2O	1
	F	Cl	$PhCH_2MgBr$	Et_2O	1.6
	F	OMe	allylMgBr	Et_2O	$>10^5$
	F	OMe	$PhCH_2MgBr$	Et_2O	2×10^3–5×10^3

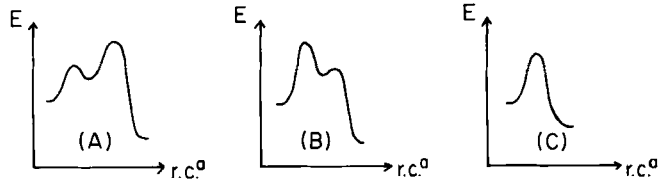

Scheme 20. Energy diagrams. (A) Rapid formation of an intermediate complex followed by slow cleavage of the Si–X bond to give products. (B) Formation of an intermediate in the rate-determining step followed by fast breakdown to the products. (C) Synchronous bond-forming and bond-breaking, involving a single transition state. [a]r.c. = reaction coordinate.

Factors near 1 show that the rate-determining step does not involve Si–X bond cleavage. Thus the energy profile (Scheme 20, diagram C) involving a single transition state can be excluded. The small kinetic influence of the leaving group agrees with the rate-determining formation of a pentacoordinate intermediate; the very small (negligible) deuterium isotope effect confirms this proposal (106).

b. Chemical Probes. Pentavalent silicon anions, including silicon anions with four carbon substituents, are postulated as intermediates in the reactions of organosilicon compounds with nucleophiles, but under normal circumstances have lifetimes too short for study (10, 11).

Of particular interest are the reactions reported by Sullivan, DePuy, and Damrauer (107). In the gas phase, pentavalent silicon anions, including silicon anions with five carbon substituents, have been generated by reaction of anions with substituted silanes. For example, direct addition of F^- or of the allyl anion occurs, leading to anions formulated as pentacoordinate species (Scheme 21).

These findings suggest that the formation of pentavalent silicon anions may take place even in the case of a silicon atom bearing carbon ligands.

3. Substitution at Silicon: Nucleophilic or One-Electron Transfer Process?

Coupling reactions of a nucleophilic reagent, Nu^-, with an organosilane, R_3Si–X, are usually represented by a one-stage nucleophilic mechanism (eq. [31]) (10, 11).

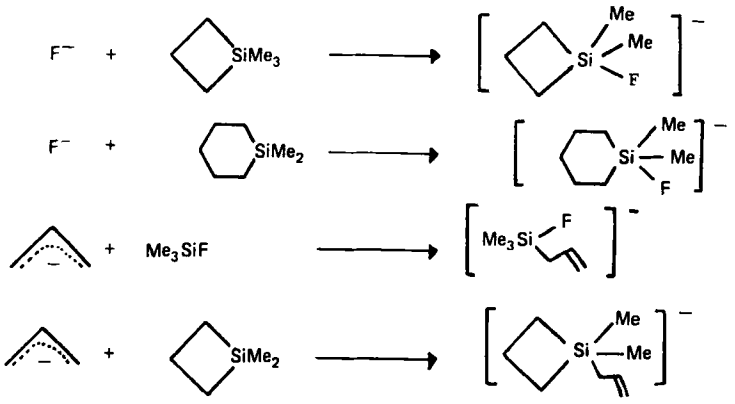

Scheme 21.

$$Nu^- + R_3Si{-}X \longrightarrow R_3Si{-}Nu + X^- \qquad [31]$$

A two-stage reaction pathway might, however, be invoked as an alternative, the first step being a single-electron transfer from the electron-rich nucleophile, Nu^-, to the electrophilic silicon atom (eq. [32]).

$$Nu^- + R_3Si{-}X \xrightarrow[\text{transfer}]{e^-} \overline{Nu^{\cdot} + R_3Si{-}X^{\cdot -}} \longrightarrow R_2Si{-}Nu + X^- \qquad [32]$$

The one-electron transfer process can be eliminated on the basis of the following chemical and electrochemical data:

1. The $CpFe(CO_2)^-$ anion reacts concurrently by S_N2 and free radical processes with alkyl halides (108) (Scheme 22, eq. [33]); the same ion is easily able to displace Cl from silicon, leading to the formation of an Fe-Si bond (Scheme 22, eq. [34]) (109). At the opposite extreme, Cp(DPPE)FeMgBr shows very low nucleophilicity and reacts with alkyl halides only by a radical process (Scheme 22, eq. [35]) (109). This same reagent was found completely unreactive toward halosilanes, which are known to be very reactive substrates in nucleophilic reactions (Scheme 22, eq. [36]) (109).
2. The low ability of a Si—X bond to react by a one-electron transfer process is also clearly indicated by the electrode potential data derived from the electrochemical reduction of silicon halides (Table 11) (110).

Although the electrochemical reduction of halosilanes exhibits a single irreversible wave (a fast dimerization of the presumed intermediate radical occurs at

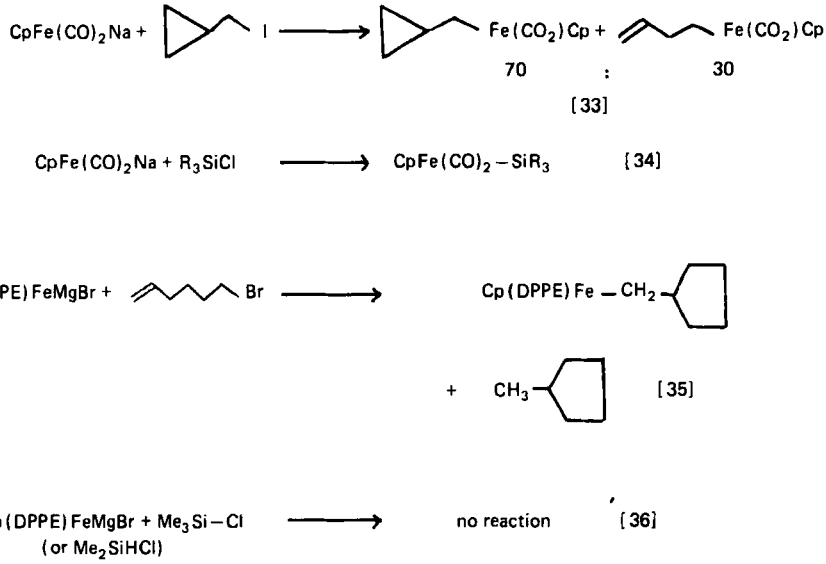

Scheme 22.

the electrode), the half-wave reduction potentials are much more negative than the $E_{1/2}$ values measured for organic halides. This indicates a more difficult addition of an extra electron to a Si-X as compared to a C-X bond.

Thus we may conclude that coupling reactions between organosilanes and nucleophiles occur only by a one-stage nucleophilic process.

Table 11
Half-Wave Reduction Potential of Some Organic Halides (111) and Halosilanes (110)

RX or R_3Si-X	Solution[a]	$-E$ (Volts)	Reference[a] Electrode
CH_3-Cl	DO	2.23	S.C.E.
CH_3-Br	DO	2.01	S.C.E.
CH_3-I	DO	1.63	S.C.E.
Ph_3Si-F	THF	2.60	S.C.E.
Ph_3Si-Cl	THF	2.40	S.C.E.
Ph_3Si-Br	THF	2.37	S.C.E.

[a]THF = tetrahydrofuran; DO = dioxane; S.C.E. = Saturated calomel electrode.

B. Factors Controlling the Stereochemistry and Geometry of Displacement

Displacement reactions proceed either with retention or inversion of configuration at silicon (1, 2, 10, 11). The change in stereochemistry is mainly a function of the nature of the leaving group and of the nucleophile. In borderline cases, other factors, such as the geometry of the organosilane, may also influence the stereochemical pathway.

1. Influence of the Leaving Group

a. Stereochemistry Governed by the Nature of the Leaving Group. Table 12 summarizes results for diverse nucleophiles. The following comments may be made:

1. The Si-H bond is displaced with retention of configuration. Inversion occurs only in reactions with Ph_2CHLi (112).

Table 12
Influence of the Leaving Group on Stereochemistry

$$1\text{-NpPh(R)Si-X} + Nu^- \longrightarrow 1\text{-NpPh(R)Si-Nu} + X^-$$

(R = Me, Et, *i*-Pr, Vi)

Nucleophile	Predominant Stereochemistry					Ref.
	X = H	OMe	F	SMe or SPh	Cl, Br	
R′Li (R′ = alkyl, aryl)	RN	RN	RN	RN	IN	(112–116)
Allyllithium	RN	RN	IN	IN	IN	(112–116)
$PhCH_2Li$	RN	IN	IN	IN	IN	(112–116)
Ph_2CHLi	IN	IN	IN	–	–	(112)
R′MgX (R′ = alkyl, aryl)	–	RN	IN	IN	IN	(114, 116, 117)
R′MgX (R′ = allyl, $PhCH_2$)	–	IN	IN	IN	IN	(112, 116, 117)
$LiAlH_4$	–	RN	IN	IN	IN	(44, 101, 115, 116, 118–120)
t-BuOK/*t*-BuOH R_3SiOK (xylene) or KOH (Xylene)	RN	RN	RN	–	IN	(101, 114, 118, 120–123)

2. Chloro- and bromosilanes undergo mainly inversion.
3. The Si-F and the Si-SR bonds show parallel behavior, leading either to inversion or retention according to the nature of the nucleophile.
4. The Si-OR bond is displaced mainly with retention by organolithiums, except for some charge-delocalized reagents such as $PhCH_2Li$ and Ph_2CHLi. Similar behavior is observed with Grignard reagents (114, 112, 117).

Bifunctional organosilanes, 1-NpRSi(Y)X (R = phenyl or ferrocenyl), are good models to study the relative ability of two leaving groups (X and Y) to be displaced. Typical reactions are shown in Table 13.

The (H) substituent appears to be the least effective leaving group with 1-NpPhSiH(OR) and 1-NpFcSi(H)F derivatives (125). Only displacement of F and OR occurs; so both of these are better leaving groups than (H). At the opposite extreme, the chlorine substituent is the best leaving group. With 1-NpPhSi(Cl)-OMen and 1-NpFcSi(F)Cl, displacement of Cl only occurs with inversion, whatever the nucleophile. Comparison of F and OR substituents is more complex (125). However, when the reaction takes place with inversion, only highly stereoselective displacement of the fluorine atom occurs.

Finally, we note that acyclic fluorosilanes show a general shift of the stereochemistry from retention to inversion of configuration, as indicated below:

$$R_1R_2Si(H)F > R_1R_2R_3Si{-}F > R_1R_2\underset{\displaystyle F}{\overset{\displaystyle |}{Si}}{-}OR$$

$$RN \longrightarrow IN$$

Table 13
Influence of the Leaving Group: Behavior of Some Bifunctional Organosilanes

Substrate	Nucleophile	Product	Predominant Stereochemistry	Ref.
1-NpFcSi(F)Cl[a]	RLi or RMgX	1-NpFcSi(F)R	IN	(60)
1-NpFcSi(H)F	RLi	1-NpFcSi(H)R	RN	(60)
	RMgX (R = Me, Et, allyl)	1-NpFcSi(H)R	IN	(60)
1-NpFcSi(F)OEt	RLi (R = Ph, allyl, PhC≡C)	1-NpFcSi(R)OEt	IN	(57, 124)
	allyl MgBr	1-NpFcSi(allyl)OEt	IN	(57, 124)

[a]Fc = ferrocenyl.

Table 14
A Comparison of the Stereochemical Behavior of
Acyclic Fluorosilanes (57, 113, 114, 126)

RM	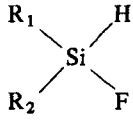	$R_1R_2R_3Si—F$	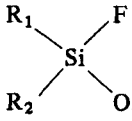
AllylLi, PhMgBr Ph—C≡C—MgBr	RN	IN	IN
ArylLi, Ph—C≡C—Li	RN	RN	IN

This stereochemical shift is illustrated by the following data (Table 14). The mutual influence of one of the two leaving groups on the other changes its lability and thereby the stereochemistry of its displacement by nucleophiles.

b. A Rationalization of the Dominant Influence of the Leaving Group. The above experimental facts show in the main, parallel chemical and stereochemical behavior for mono- and bifunctional silanes. The relative ease of displacement is:

$$Br, Cl > F, SR > OR > H$$

This empirical order parallels a general change of the stereochemistry of displacement from inversion to retention:

Ability to be cleaved	OTs, OCOR (127), Br, Cl, > F, SR > OR > H
Stereochemistry	IN ⟶ RN

Attempted rationalization of the stereochemical changes in terms of the pK_a of the conjugate acid of the leaving group (1, 2) or in terms of its electron polarizability according to Brewster [I > Br > Cl; SH ~ SR > Cl; OH ~ OR > H > F] (128) does not give a satisfactory picture of the stereochemical changes observed. Thus

1. The Si-SR and Si-F bonds, for example, show very similar stereochemical behavior leading either to retention or inversion (Table 12). Yet the

*Ease of pentacoordination at silicon and order of apicophilicity for groups bonded to a pentacoordinate silicon atom are discussed in detail in Sect. V-C.

-SR group (the corresponding conjugate acid, RSH, has a $pK_a > 10$) should be a poor leaving group and undergo displacement mainly with retention, whereas the fluoro substituent (HF, $pK_a \simeq 3.5 - 4$) should be a good leaving group and undergo inversion.

2. The highly polarizable Si-Cl and Si-SR bonds are always displaced with inversion. If Si-F is compared to Si-OR and Si-H bonds, Si-F is far less polarizable; nevertheless the Si-F bond is more easily cleaved by nucleophiles with inversion of configuration (Table 12), instead of retention, as would be expected. In fact, Si-F resembles Si-SR in stereochemical behavior, as already mentioned.

However, if polarizability is defined as the ability of a Si-X bond to be stretched under the influence of an attacking nucleophile, the relative tendency of Si-X bonds to undergo inversion and their order of polarizability run parallel. This dependence is well-illustrated by the following data:

1. The X-ray crystal structure analysis of the five-membered chloro-(*N*-chlorodimethylsilylacetamido)methyldimethylsilane **86** shows the chlorine atom in apical position trans to the oxygen (Figure 6) (129); the Si-Cl bond is considerably longer [2.348 Å instead of 2.01 Å (130) in tetravalent organosilanes]. A similar pronounced lengthening of the $Si\text{-}Cl_{ax}$ bonds (**87**: 2.27 Å, **88**: 2.21 Å, **89**: 2.15 Å) was recently observed in the case of the pentacoordinated complexes of silicon with the chelating ligand 1,2,3,4-tetrahydro-1,10-phenanthroline (Figure 6) (131).

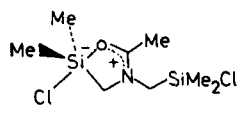

86

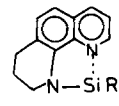

87 : $SiMe_2Cl$
88 : $SiMeCl_2$
89 : $SiCl_3$

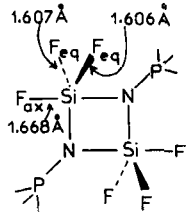

90

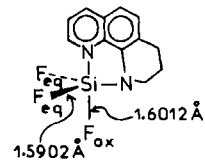

91

Figure 6.

In contrast, for the fluorine-containing complexes **90** (132) and **91** (131) (Figure 6), no significant differences are observed in the bond lengths between Si-F_{ax} and Si-F_{eq}. Thus, if Si-F is compared with Si-Cl and Si-Br, these observations suggest that the Si-F bond here is less able to be stretched under the influence of an incoming nucleophile; as a consequence, the stereochemistry is displaced toward retention (Table 12, entries 1 and 8).

2. The ^{1}H NMR spectra of *o*-$(Me_2NCH_2)C_6H_4SiX_2R$ and *o*-(Me_2NCH_2)-$C_6H_4SiXR_1R_2$ show the expansion of coordination at silicon by an intramolecular Si-N bond. The ease of pentacoordination may be ranked as follows (133):

$$H, OR < F, SR < OAc, Cl, Br^*$$

Moreover, the low-temperature ^{19}F NMR spectra of *o*-$(Me_2NCH_2)C_6H_4$-$SiMeF_2$ and *o*-$(Me_2NCH_2)_2C_6H_4SiF_3$ lead to the following orders of apicophilicity for groups bonded to a pentacoordinate silicon atom (134):

$$Cl > F, \quad F > OR, \quad \text{and} \quad F > H^*$$

It is noteworthy to find chlorine more apicophilic than fluorine, although the latter is more electronegative. This may explain the stereochemical behavior of 1-NpFcSi(Cl)F (60): only chlorine is displaced by carbon nucleophiles and inversion is the predominant stereochemistry.

The above data, together with previous reports (10, 11, 13), suggest a close relationship between the rate of racemization of halosilanes, the substitution of R_3Si-X with inversion of configuration, and the ease of pentacoordination at silicon atom:

Pentacoordination ability	H, OR < F, SR < OAc, Cl, Br
Predominant stereochemistry	RN ⟶ IN
Racemization ability	Si—Br > Si—Cl > Si—F

Thus, the above observations can be taken as good evidence that the ease of stretching of the Si-X bond is a significant factor in directing the stereochemistry of substitution towards inversion of configuration. Similar effects are found in nucleophilic displacement at phosphorus (135).

2. *Influence of the Nucleophile*

The stereochemistry at silicon is extremely sensitive to the electronic character of the nucleophile (Table 12). The percentage of RN or IN is quite sensitive

to small changes in the structure of the anion, the metal, or the solvent (Table 15). The data in Table 15 might be analyzed as follows:

1. The harder the organic anionic group (alkyl or *p*-methoxyphenoxide anions), the closer the stereochemistry is to pure retention; the softer the nucleophile (allyl, benzyl, or *p*-nitrophenoxide anions), the more the stereochemistry tends toward inversion (Tables 12 and 15).
2. Concerning the nature of the metal, the softer (harder) the cation M^+, the more covalent (ionic) the R-M bond of the organometallic and softer (harder) the organic anionic group R (139), the greater the extent of inversion (retention). Thus, the organolithiums, which are harder than the analogous Grignard reagents, react mainly with retention whereas the Grignard reagents react with inversion (Tables 12 and 15).
3. An increase of the solvating power of the solvent ($Et_2O < THF < DME$) modifies the electronic character of the nucleophile and hence the steric course of reaction. Thus a Grignard reagent is harder in THF or DME than in ether (Scheme 23); the more coordinating solvents polarize the carbon-metal bond and increase the hardness of the nucleophile, orienting the stereochemistry toward retention of configuration (117, 140).

We will now give a more detailed analysis of the available data, using the following cases:

1. Coupling reactions with phenoxides. Influence of electronic character and effect of ion-pair dissociation.
2. Coupling reactions with alkoxides. Influence of solvation.
3. Nucleophilic substitution at silicon by carbon nucleophiles.
4. Reduction reactions by alanes, $AlH_nY_{(3-n)}$.

a. Coupling Reactions with Phenoxides. ***Influence of Electronic Character.*** In these reactions, the electronic character of the negative charge on the phenoxide oxygen atom can be changed by varying the substituent Y in the para position. Pertinent data are given in Table 16.

With the same reaction center (oxygen atom), the stereochemistry depends greatly on the para substituent Y and on the extent of dissociation of the ion pair.

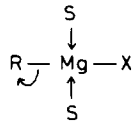

(S = a coordinating solvent)

Scheme 23.

Table 15
Influence of the Nucleophile on Stereochemistry

Organosilane	Nu	Solvent	Product (Stereochemistry)	Ref.
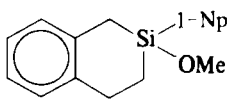	*n*-PrMgBr	Et_2O	R_3Si—*n*-Pr (RN)	(136)
		Et_2O	R_3Si  (IN)	(136)
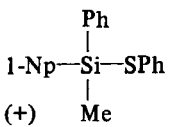	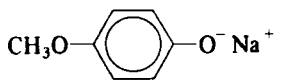	THF	R_3Si—O 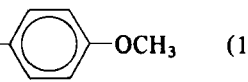 (RN)	(137)
	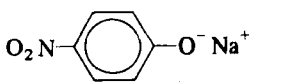	THF	R_3Si—O 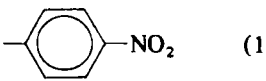 (IN)	(137)
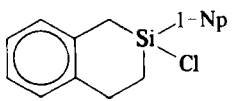	EtLi	Et_2O	R_3Si—Et (RN)	(138)
	EtMgBr	Et_2O	R_3Si—Et (IN)	(136)
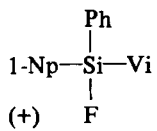	EtMgBr	Et_2O	R_3Si—Et (IN)	(117)
	EtMgBr	DMe	R_3Si—Et (RN)	(117)

Table 16
Stereochemistry of Reactions of R_3SiX with Phenoxides (Solvent = THF)

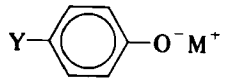
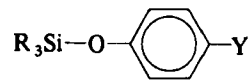

R_3Si—X	Y	M^+	$[\alpha]_D$	Stereochemistry
Ph 1-Np—Si—SPh (+) Me	MeO	Na^+	+6°	RN
	MeO	Na^+*	+9°	RN
	MeO	NR_4^+	+8°	RN
	H	Na^+	+2°	IN
	H	Na^+*	+5°	IN
	NO_2	Na^+	+3°	IN
	NO_2	Na^+*	+8°	IN
	NO_2	NR_4^+	+5°	IN
Ph 1-Np—Si—Me (+) F	MeO	Na^+	-4.5°	RN
	MeO	Na^+*	-6°	RN
	H	Na^+	+3°	RN
	H	Na^+*	-2.5°	IN
	NO_2	Na^+	+0.5°	RN
	NO_2	Na^+*	-4°	IN

*Reactions carried out with a cryptand specific for Na^+.

Influence of the Substituent on the Phenyl Group. An electron-releasing substituent (MeO group) that increases the negative charge on the nucleophilic center and thus its hardness favors retention as the stereochemical outcome. On the other hand, a significant decrease of selectivity in retention or even predominant inversion occurs with an electron-withdrawing substituent such as $-NO_2$. In this case there is greater delocalization of the negative charge over the aromatic system, resulting in a softer nucleophile.

Influence of the Dissociation of the ArO^-M^+ Ion Pair. The effect of a variable delocalization of the negative charge is increased when the reaction is carried out in a basic solvent (137) or with a cryptand specific for the Na^+ cation (Table 16). With *p*-methoxyphenoxide, dissociation of the ion pair leads to increase of the negative charge on the oxygen atom and the proportion of retention increases. On the other hand, with a softer anion, such as *p*-nitrophenoxide, complexing the Na^+ cation favors delocalization of the negative charge and thus favors inversion. The same observation is made when Na^+ is substituted by the bulky NR_4^+ cation: dissociation of the ion pair is increased and once again we see the above stereochemical shift toward greater retention with the -OMe group and toward greater inversion with $-NO_2$.

Table 17
Coupling Reactions with Alkoxides

$$R_3Si{-}X + n\text{-}Bu{-}OH/n\text{-}Bu{-}OLi \xrightarrow{\text{benzene}} R_3Si{-}O{-}(n\text{-}Bu)$$

Organosilane[a]	ROH/ROM mol. mol.	ROH/R_3Si—X mol. mol.	Predominant Stereochemistry
R_3Si—OMe	10	2.6	100% RN
	72	47	65% IN
	210	79	>81% IN
R_3Si—F	2	1.31	92% RN
	14.3	1.11	62% RN
	32	1.37	88% IN
R_3Si—SMe	0.7	1.15	70% RN
	3	1.13	61% IN
	39	1.22	85% IN

[a] R_3Si = 1-NpPhMeSi.

b. Coupling Reactions with Alkoxides: ***Influence of Solvation.*** Concerning the influence of solvation, pertinent data were reported by Sommer and Fujimoto (141) for nucleophilic substitution by alkoxides at Si-OMe, Si-F and Si-SMe bonds (Table 17).

The most important fact that emerges from the data in Table 17 is the stereochemical crossover from retention to inversion upon increasing the alcohol content of the medium. Whatever the nature of the leaving group (OMe, F, SMe), inversion becomes predominant; the same shift of the stereochemistry toward inversion is observed with *n*BuONa (47). The most striking data are observed with R_3Si-F and R_3Si-SMe; for nearly constant ROH/R_3Si-X proportions of 1 : 1 to 1 : 4, a change in the ROH/ROM proportion (from 1 to 40) is enough to invert the stereochemistry.

These observations suggest an explanation of the above data in terms of electronic factors. The RO^-M^+ species in benzene have a localized negative charge on the oxygen atom, that is, they act as hard anions and react with retention. On increasing the alcohol ratio, the charge is dispersed by strong hydrogen bonding interactions:

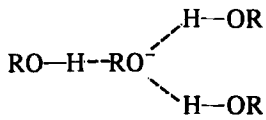

Such dispersal of the negative charge produces a softer species that reacts with predominant inversion.

c. **Substitution at Silicon by Carbon Nucleophiles.** In the case of carbon organometallics, it is readily possible to modify the electronic character of the nucleophile while preserving the same reacting atomic center. The stereochemical data are quite clear.

Influence of the Nature of R^-. Pertinent data reported in the literature are summarized in Table 18.

Aryl-, phenylethynyl- and alkylorganolithiums, that is, species with a well-localized negative charge, react mainly with retention. Inversion is observed only with the best leaving groups, Cl or Br (49, 112–116).

In contrast, allyl- or benzyllithiums in which the negative charge is delocalized over an sp^2 carbon system, always react with inversion, except with hydrogen, the poorest leaving group (Table 12). The Ph_2CH^- anion, in which the negative charge is particularly well delocalized, leads only to inversion, even with hydrogen as leaving group (112).

Quite significant also is the case of the p-$MeOC_6H_4CH_2^-$ anion. p-$MeOC_6H_4$-CH_2Li cleaves the Si-OMe bond with retention instead of inversion for C_6H_5-CH_2Li (112). The p-methoxybenzyl anion, in which the negative charge is more localized on the carbon reactive center because of the electron-donor methoxy

Table 18
Influence of the Nature of the Organic Anion

Substrate	Nucleophile	Predominant Stereochemistry	Ref.
R | 1-NpPhSi—F R = Et or Vi	Ph—C≡C—Li	100% RN	(49)
	MeLi	93% RN	(49)
	n-PrLi	97% RN	(49)
	n-BuLi	93% RN	(49)
	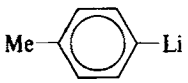	98% IN	(49)
	EtMgBr	65% IN	(117)
	$PhCH_2Li$	82% IN	(49)
	 (ether)	93% IN	(117)
	$PhCH_2MgCl$	91% IN	(117)
Vi | 1-NpPhSi—F	PhC≡CMgBr (THF)	76% RN	(117)
	n-BuMgBr (THF)	59% RN	(117)
	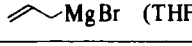 (THF)	62% IN	(117)

group, is a harder reagent than the benzyl anion. Consequently the stereochemistry is shifted toward retention.

Influence of the Metal. Concerning the nature of the metal, the softer (harder) the cation M^+, the more covalent (ionic) is the R-M bond of the organometallic and the softer (harder) is the anion R^- (44). Thus the organolithiums, RLi, will be harder reagents than the analogous Grignard reagents, RMgX. Organolithiums react mainly with retention whereas Grignard reagents react with inversion. Some pertinent data are summarized below (Table 19). As might be expected, that organolithium and organosodium compounds behave similarly to each other (113).

Influence of the Solvent and Complexing Agents (TMDA, Cryptands). In this section, we shall consider stereochemical and kinetic data which clearly demonstrate that the stereochemistry (and mechanism) for some leaving groups is extremely sensitive to solvent or complexing agents such as TMDA or cryptands. This is specially so in the case of borderline leaving groups, such as the

Table 19
Comparison of the Stereochemical Behaviors of RLi and RMgX

Substrate	Nucleophile	Predominant Stereochemistry	Ref.
1-NpPh(R)Si—F (R = Me, Et, *i*-Pr, Vi)	R′Li (R′ = Me, Et, *n*-Pr *n*-Bu)	RN	(49, 20)
	R′MgX (R′ = Me, *n*-Bu)	IN	(117)
1-NpFc(H)Si—F	RLi (R = Me, Et, CH=CH—CH_2)	RN	(60)
	RMgX (R = Me, Et, CH_2=CH—CH_2)	IN	(60)
1-NpPhMeSi—X (X = SMe or SPh)	RLi (R = Et, *n*-Bu, neo-C_5H_{11})	RN	(115, 116)
	RMgX (R = Et, *n*-Bu)	IN	(115, 116)
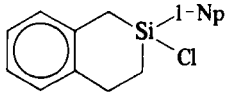	RLi (R = Me, Et, *n*-Pr, *n*-Bu)	RN	(138)
	RMgX (R = Me, Et, *n*-Pr, *n*-Bu)	IN	(136)

Table 20
Influence of the Solvent on Stereochemistry
for Grignard Reagents
(Substrate = 1-NpPhViSi—F) (117)

Nucleophile	Solvent	Predominant Stereochemistry
EtMgBr	Et_2O	⩾65% IN
	THF	66% IN
	DME	59% RN
n-BuMgBr	Et_2O	⩾67% IN
	THF	⩾59% RN
	DME	⩾71% RN
$(n\text{-Bu})_2Mg$	Et_2O	⩾69% IN
	THF	⩾75% RN
	DME	⩾74% RN

fluorine atom, which can be displaced either with retention or inversion. We may summarize the most striking data as follows: In the case of Grignard reagents, nucleophilic solvents such as DME or THF promote retention of configuration (or decrease the percentage of inversion) (see Table 20). Moreover, for all Grignard reagents used, whether there is retention or inversion or a transition from one to the other, a net rate increase is observed when the basicity of the solvent is increased ($Et_2O < THF < DME$) (see Table 21). The influence of complexing agents, such as TMDA or cryptand, is well-illustrated in coupling reactions between organosilanes and organolithiums. Some stereochemical data are given in Table 22 (143). Nonpolar solvents, such as benzene or *n*-heptane, in which alkyllithiums are more aggregated, increase the proportion of inversion. At the opposite extreme, complexing agents for the Li^+ cation, such as TMDA, or better, K_{Li^+} which generates free anions (144), promote retention of configuration. Moreover, the kinetic effect of the addition of a lithium cryptand is also very clear (143): a 10^3-10^4-fold rate acceleration is observed.

Clearly, these data are in opposition to a quasicyclic mechanism (S_Ni-Si, Scheme 24) (1, 2). In such a process, the electrophilic assistance of the counterion M^+ determines the apical attack of the nucleophile with the leaving group in an equatorial position, and thus governs the stereochemistry. The use of a

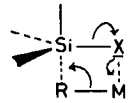

Scheme 24. S_Ni-Si mechanism.

Table 21

Stereochemistry and Rates of Reaction with Grignard Reagents in Various Solvents (142)

Substrate = 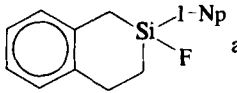 and 1-NpPhViSi—F

92 93

Substrate	Organometallic (Solvent)	Stereochemistry	Absolute Rate	$\frac{k_{THF}}{k_{Et_2O}}$	$\frac{k_{DME}}{k_{THF}}$	$\frac{k_{DME}}{k_{Et_2O}}$
92	*n*-PrMgBr (Et_2O)	RN	6×10^{-4}	75	24	1800
	n-PrMgBr (THF)	RN	4.5×10^{-2}			
	n-PrMgBr (DME)	RN	1.1			
92	*n*-BuMgBr (Et_2O)	RN	6×10^{-4}			1300
	n-BuMgBr (DME)	RN	0.8			
93	*n*-PrMgBr (Et_2O)	IN	1.7×10^{-4}	36	2.8	100
	n-PrMgBr (THF)	RN	6.2×10^{-3}			
	n-PrMgBr (DME)	RN	1.7×10^{-2}			
93	*n*-BuMgBr (Et_2O)	IN	5×10^{-5}			200–300
	n-BuMgBr (DME)	RN	1×10^{-2}			
93	$PhCH_2MgCl$ (Et_2O)	IN	5.4×10^{-4}	215	$\geqslant 50$	$\geqslant 10^4$
	$PhCH_2MgCl$ (THF)	IN	0.11			
	$PhCH_2MgCl$ (DME)	IN	$\geqslant 5$			

Table 22
Effect of Complexing Agents on the Stereochemical Behavior of Organolithiums

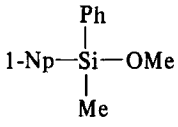

$[\alpha]_D = -16.5°$
94

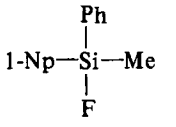

$[\alpha]_D = +47°$
95

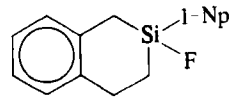

$[\alpha]_D = -34°$
92

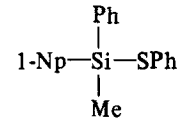

$[\alpha]_D = +27°$
96

Runs	Reagents	94	95	92	96
1	$EtLi/K_{Li^+}/Et_2O$[a]	98% RN[c]	95% RN	100% RN	
2	EtLi/TMDA/Et_2O[b]	96% RN	91% RN	99% RN	
3	$EtLi/Et_2O$	90% RN	90% RN	96% RN	
4	EtLi/benzene	76% RN	70% RN		
5	*n*-BuLi/K_{Li^+}/Et_2O	100% RN	98% RN		86% RN
6	*n*-BuLi/TMDA/Et_2O	90% RN	82% RN		
7	*n*-BuLi/Et_2O	86% RN	80% RN		65% RN
8	*n*-BuLi/heptane	68% RN			

[a] K_{Li^+} = Kryptofix 211, (tetraoxa-4,7,13,18- diaza-1,10- bicyclo-8,5,5-eicosane), specific for Li^+ cation.
[b] TMDA = tetramethylethylenediamine.
[c] Predominant stereochemistry; the $[\alpha]_D$ of optically pure R_3SiEt and R_3SiBu-*n* are known (1).

more basic solvent or a cryptand would lead to a shift of the stereochemistry to inversion and to a rate decrease.

In contrast, it is obvious that an increase of the solvating power of the solvent ($Et_2O < THF < DME$) modifies the electronic character of the nucleophile. A solvent which coordinates more strongly at the metal polarizes the carbon-metal bond and increases the hardness of the nucleophile, orienting the stereochemistry toward retention of configuration (Table 20). Similarly, a cryptand or TMDA favors the dissociation of the R^-Li^+ ion pair and increases the negative charge on the carbon reactive center; thus the hardness of R^- when it is an alkyl group (Table 22) is increased and the stereochemistry directed to retention.

d. Reductions. Table 23 gives stereochemical data for reductions of optically active silanes by alanes, $AlH_nY_{(3-n)}$ (145). Two interesting effects are to be discussed, substituent and solvent effects on the reactivity of alanes.

Effect of Substituents on the Stereochemistry of Reduction. Substitution of hydrogen atoms in AlH_3 by OR or SR groups leads to increased inversion

Table 23
Reduction Reactions of Optically Active Organosilanes by Alanes

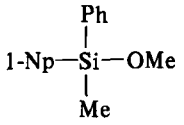

94

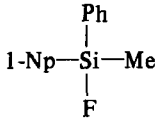

95

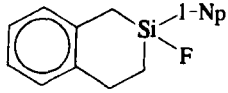

92

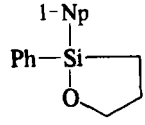

68

Reagent (Solvent)	Predominant Stereochemistry			
	94	95	92	68
Dibal (hexane)	100% RN (146)	98% RN (146)	100% RN	$[\alpha]_D = +19°$ RN
Dibal (Et_2O)	99% RN (146)	90% IN (146)	80% RN	$[\alpha]_D = +16°$ RN
Dibal (TMDA-hexane)	95% RN (146)	90% IN (146)	70% RN	$[\alpha]_D = +15°$ RN
Dibal (THF)				$[\alpha]_D = +10°$ RN
AlH_3 (Et_2O)	92% RN	96% IN	100% RN	$[\alpha]_D = +16°$ RN
AlH_3 (THF)	90% RN	100% IN	70% IN	$[\alpha]_D = +8°$ RN
$(t\text{-BuO})_2AlH(Et_2O)$	90% RN	100% IN	75% IN	
$(t\text{-BuO})_2AlH$(THF)	90% RN	100% IN	80% IN	$[\alpha]_D = -14°$ IN
$(EtS)_2AlH$ (THF)	85% RN	100% IN	85% IN	$[\alpha]_D = -16°$ IN
H_2AlI (THF)	55% RN		80% IN	$[\alpha]_D = -18°$ IN

when the resulting reagent attacks at silicon. In the case of H_2AlI, there is very high selectivity toward inversion of configuration. These observations are in good agreement with our hypothesis that a change of the Y group leads to a change in the electronic character of the Al-H bond.

Solvent Effects. The nature of solvent effects is also very clear. For AlH_3 $(t\text{-BuO})_2AlH$ and $(EtS)_2AlH$, an increase of the basicity of the solvent leads to increased inversion at silicon (Table 23). $i\text{-Bu}_2AlH$ is specially interesting in this respect. In hexane, it substitutes all Si-X bonds (X = Cl, SR, F, and OR) with retention (146). In contrast, the percentage of inversion at silicon increases with the basicity of the solvent (hexane $< Et_2O <$ THF) or the use of a complexing agent such as TMDA.

In addition, we must mention the striking change of stereochemistry with $LiAlH_4$ when a cryptand specific for Li^+ is added (Table 24) (143, 147). In the presence of the [2.1.1] cryptand, $LiAlH_4$ in Et_2O (naked AlH_4^- anions) gives inversion at silicon, whereas $LiAlH_4$ in the absence of the macrocyclic ether leads to predominant retention. Thus the more localized on the hydrogen atom the negative charge, the easier is the inversion at silicon. This fact is also well illustrated by the behavior of $(i\text{-Bu})_2AlH$ or AlH_3 in hexane as solvent. The Al-H bond is slightly polarized and these species behave as hard reagents. On the

Table 24
Stereochemistry of Reduction of Organosilanes by $LiAlH_4$: A Change of the Stereochemistry with Cryptand

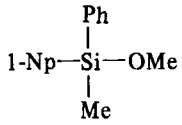

94

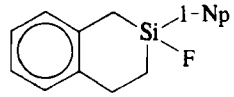

92

Reagent (Solvent)	Predominant Stereochemistry	
	94	92
$LiAlH_4(Et_2O)$	95% RN	Rac
$LiAlH_4/K_{Li^+}(Et_2O)$	75% RN	65% IN

other hand, when used in a basic solvent, the coordination of the solvent at the aluminum atom delocalizes the negative charge on hydrogen (Scheme 25). Consequently, under these conditions, $(i\text{-Bu})_2AlH$ and AlH_3 behave as soft species and the inversion ratio at silicon increases.

3. *Geometry of Attack of the Nucleophile*

The dominant influence of the nucleophile on the stereochemistry at silicon cannot be interpreted in terms of the stability of the intermediate on the basis of the apicophilicity rule as stated in phosphorus chemistry (148-153) (see Sect. V-C-1). Such an attempted interpretation fails to explain retention of configuration as the stereochemical outcome. No better explanation can be based on the quasicyclic mechanism proposed by Sommer et al. (1, 2). On the other hand, we have presented extensive data obtained with various nucleophiles which all show clearly that the stereochemistry at silicon is controlled by the electronic character of the nucleophile; the harder the nucleophile, the closer the stereochemistry is to pure retention, as summarized for organometallics in Scheme 26.

Scheme 25. Effect of the solvent in reactions with alanes.

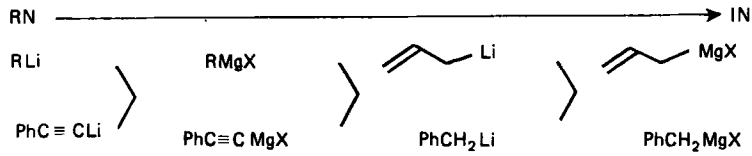

Scheme 26. Stereochemical behavior of organometallics.

In other words, this factor initially determines the geometry of attack of the nucleophile at silicon, which leads, in a first reaction step, to the formation of a pentacoordinate intermediate (106). We have proposed the following:

Concerning the reaction occurring with inversion, the stereochemistry requires a back-side attack of the nucleophile opposite the leaving group (intermediate **97**, Figure 7).

Concerning the reaction occurring with retention, a nucleophilic attack at 90° to the leaving group is required. For the same leaving group, the geometry of attack is determined only by the electronic character of the nucleophile. Two different mechanisms may be proposed. One is apical attack of the nucleophile, leading to an intermediate such as **98** with the electronegative leaving group in an equatorial position (Figure 8). However, some data are inconsistent with such a process:

1. Klanberg and Muetterties (154) have shown that the electronegative fluorine atoms always occupy the apical position of pentacoordinate anions such as $RSiF_4^-$ or $R_2SiF_3^-$. Thus we may assume that the most stable intermediate resulting from apical attack of the nucleophile is **97**. This latter explains only inversion at silicon.

2. Allyl and *n*-butyl anions in the substitution of an optically active fluorosilane, 1-NpPhMeSi-F, display opposite behavior. The former leads to inversion (91% IN) and the latter to retention (98% RN) (137) when the reactions with allyl and *n*-butyllithium are carried out in the presence of a cryptand specific for the lithium cation. The use of the cryptand makes it possible to study the differ-

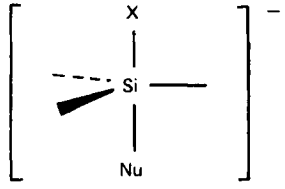

97

Figure 7.

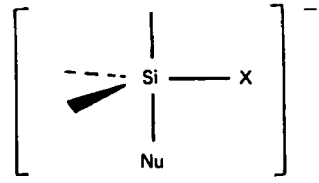

98

Figure 8.

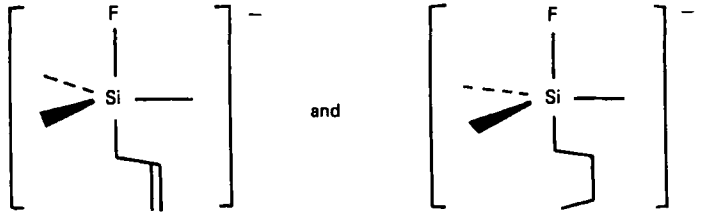

99 100

Figure 9.

ence in behavior of the anion species alone, since it avoids the possibility of electrophilic assistance by Li^+, which could affect the apicophilicity of the fluorine atom. However, apical attack of the entering nucleophile would lead to the intermediates **99** and **100** with the most electronegative group, F, in the apical position (Figure 9). Structures **99** and **100** can explain inversion only; they cannot lead to the substitution of the fluorine atom with retention.

The other mechanism that may be proposed is equatorial attack of the nucleophile, the leaving group being apical in a trigonal bipyramid-like intermediate **101** (Figure 10).

Equatorial attack is strongly supported by structural investigations on pentacoordinate silicon species by Perozzi and Martin (155). The siliconates **102** and **103** (Figure 11) are obtained by nucleophilic attack (Ph^- or 4-Me_2N-C_5H_4N) at a tetravalent silicon center. Their structures, established by NMR spectroscopy,

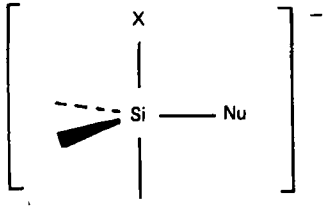

101

Figure 10.

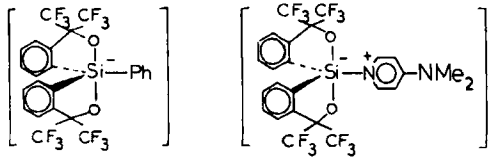

102 103

Figure 11.

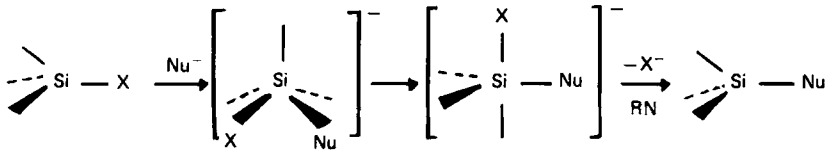

104 101

Scheme 27.

confirm clearly that the electronegative groups (oxygen atoms) are apical, the two five-membered rings apical-equatorial, and the entering group is in an equatorial position.

Hence, equatorial attack seems the most reasonable and simplest way to describe approach of the nucleophile at 90° to the leaving group, leading to the most stable pentacoordinate intermediate. However, it is also possible to postulate a square pyramidal structure such as **104** as a transition state that would change into intermediate **101** (Scheme 27). Such a structure was previously proposed in phosphorus chemistry by Hudson et al. to explain the alkaline hydrolysis of cyclic phosphonamidates.

C. Rationalization by a Frontier-Orbital Approximation

Anh and Minot have reported (99, 100) a rationalization of the stereochemistry at silicon by an extension of Salem's treatment of the Walden inversion (157). The frontier-orbital approximation is assumed, that is, the major interaction during the reaction occurs between the HOMO of the nucleophile and the LUMO of the substrate σ^*_{Si-X}; HOMO-LUMO overlap maps have been studied for H^- approaching SiH_3Cl and SiH_3F. The calculated structure of the σ^*_{Si-X} LUMO is shown below, with the big lobes of the hybrid AOs pointing toward each other (Scheme 28). Front-side attack, corresponding to an attack on the big lobe of silicon, leads to retention. When unfavorable out-of-phase overlap between the nucleophile and the orbitals of the leaving group predominates, nucleophilic attack occurs at the rear of the molecule, opposite X, leading to inversion. Therefore, retention and inversion may be considered to be the result of a fine balance

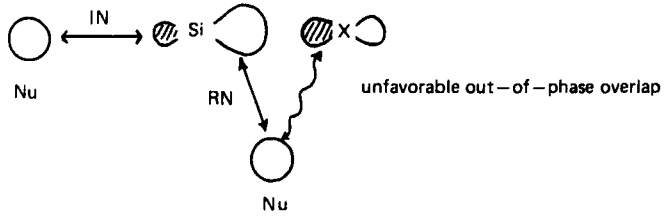

Scheme 28. Structure of the substrate LUMO, σ^*_{Si-X}.

between the in-phase and out-of-phase orbital overlap between the nucleophile and the LUMO of the substrate σ^*_{Si-X}. In other words, it is possible to increase the probability of retention of configuration by increasing the favorable interaction between the nucleophile and silicon, or by decreasing the unfavorable interaction between the nucleophile and the leaving group, or both.

Salem's frontier-orbital treatment for Walden inversion is consistent with the fact that retention of configuration is a commonly observed stereochemical outcome at silicon (Table 12), whereas there is still no proven example of an S_N2 reaction with retention at carbon (158). Because Si-X bonds are significantly longer than C-X bonds, the unfavorable interaction between X and the nucleophile for front-side RN attack is less for silicon than for carbon (Scheme 28). The valence orbitals also change from $2s$ and $2p$ for carbon to $3s$ and $3p$ for silicon and therefore become more diffuse and capable of overlap with the nucleophile at longer distances. Consequently, the probability of attack with retention is enhanced.

The shape of the σ^*_{Si-X} LUMO is quite sensitive to the leaving group X. Anh and Minot have shown that a group X of high electronegativity, for instance X = F in the case of H_2Si-F, increases the s character around silicon, leading to a more dissymetric hybrid atomic orbital at silicon with a bigger lobe between Si and X. Increasing the electronegativity of the leaving group will therefore favor retention of configuration. At the same time, the stereochemical outcome will be influenced by the length of the Si-X bond and by the size of the valence orbitals around X (Scheme 28).

The influence of the nucleophile is analyzed as follows. A hard reagent is usually a small one (159), with contracted valence orbitals. Its long-range, out-of-phase unfavorable overlap with the leaving group will be negligible, and front-side attack leading to retention is therefore possible. On the other hand, a soft nucleophile usually has diffuse valence orbitals (159). It has therefore a sizable out-of-phase overlap with the leaving group and stereochemistry is shifted towards inversion (rear-side attack).

The size of the reagent is not the only controlling factor since a change in the hardness of the nucleophile implies a modification of its valence orbitals and also of its HOMO energy level (Scheme 29) (160). When the level is high (i.e., in a hard nucleophile), frontier-orbital interaction is predominant. When the level is low (i.e., in a soft nucleophile), the relative importance of the nucleophile HOMO-substrate superjacent MO (161) interaction is increased. The structure of the latter is shown below (Scheme 30) for the Si-F bond. The big lobe of the Si hybrid orbital points to the rear in the superjacent MO, which therefore favors inversion of configuration.

Our purpose is now to show that the Anh-Minot approach gives a qualitatively rational explanation for most of the stereochemical data at silicon. To this end, we select only the most significant data; a more detailed discussion has pre-

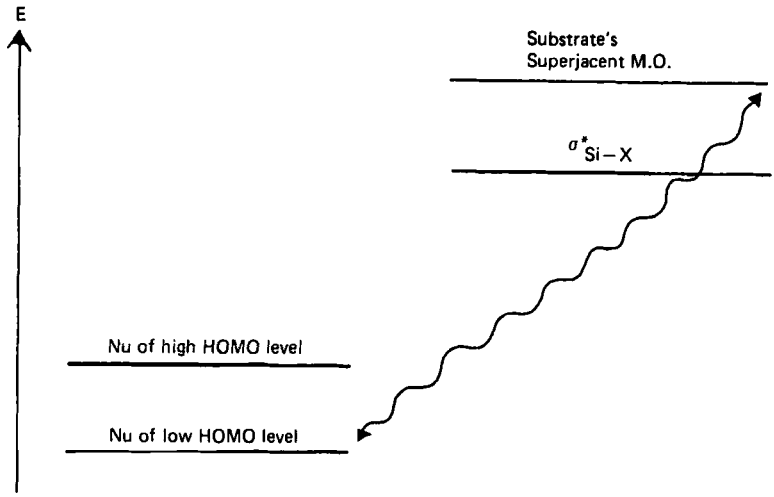

Scheme 29.

viously been given (11). We shall successively examine the following features: Stereochemical changes with the leaving group, stereochemical changes with the nucleophile, and stereochemical changes with angle strain at silicon.

1. Stereochemical Changes with the Leaving Group

a. Substitution of the Si-H Bond. Although the Si-H bond is quite short (130) and hydrogen has low electronegativity, retention of configuration is commonly observed with H as the leaving group (Table 12). The hydrogen 1*s* orbital is small and overlaps little with the orbitals of the nucleophile. Furthermore, hydrogen is the only leaving group with no lone pair; the H-Nu repulsion is therefore drastically reduced, and retention is favored (Scheme 28).

The stereochemical behavior of Ph_2CHLi, that is, cleavage of the Si-H bond with predominant inversion, can be explained as follows. We are faced with a very soft nucleophile of low HOMO level (Scheme 29). The substrate superjacent MO-nucleophile HOMO interaction prevails. The big lobe of the Si hybrid orbital points to the rear in the superjacent MO (Scheme 30), and inversion is therefore favored. However, this reaction is quite slow (112).

Scheme 30. Structure of the superjacent MO of SiH_3F.

b. Br, Cl, and F as Leaving Groups. Stereochemical studies on nucleophilic displacements of halosilanes suggest the following generalizations: (i) Fluorosilanes lead either to retention or inversion according to the nature of the nucleophile (Table 12). (ii) Bromo- and chlorosilanes react with inversion, whatever the nucleophile (Table 12). Retention is observed only for dibal in hexane (146).

The Anh-Minot model explains these observations as follows:

1. When chlorine or bromine are replaced by fluorine as the leaving group, the latter's electronegativity increases the *s* character at the silicon atom. The σ^*_{Si-X} MO shows a bigger lobe pointing between Si and X.
2. The valence orbitals of X become more contracted for the fluorine atom, and this decreases the unfavorable overlap between X and the nucleophile (Scheme 28).
3. At the same time, the Si-X bond shortens, increasing the unfavorable X-Nu overlap in an attack with retention (Scheme 28).

The two former factors favor a front-side attack leading to retention. Moreover, numerical calculations indicate that in this example, the Si-X bond shortening does not compensate for the two former effects. Therefore, retention is favored.

2. *Stereochemical Changes with the Nucleophile*

In the foregoing discussion (Sect. III-B-2), we stressed the dominant influence of the electronic character of the nucleophile on the stereochemistry at silicon. We propose the following concerning this effect.

a. Carbon Nucleophiles and Phenoxides. Alkyllithiums react mainly with retention. Inversion is only observed with the best Cl or Br leaving groups (Table 12). The cryptand effect results in an increase of the retention ratios (Table 22) (143). A parallel increase of the rate is observed. For instance, in the case of R_3Si-OMe, there is a 10^2-10^3 fold rate acceleration (143). Similar behavior is observed for the *p*-methoxyphenoxide anion (Table 16).

Alkyllithiums have a negative charge on carbon, which is in part transferred to the Li^+ cation. When the Li^+ cation is trapped, the ion pair is much less tight and the negative charge is contracted on the reactive carbon center. In the latter case, we may assume smaller valence orbitals on carbon (Scheme 31). The out-of-phase overlap with the leaving group is diminished, and therefore retention is favored. This is in agreement with the experimental data.

In the case of the *p*-methoxyphenoxide anion, Taft et al. have shown that the oxygen atom has a high degree of sp^3 character (162). We are faced with a nu-

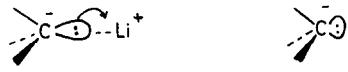

Scheme 31. Supposed shapes of the HOMO of alkyllithium and of naked alkyl anions.

Scheme 32. Supposed shapes of the HOMO of the *p*-methoxyphenoxide anion and of sodium *p*-methoxyphenoxide.

cleophile that is quite similar to hard alkyl anions from an electronic point of view, that is, a nucleophile with contracted valence orbitals around oxygen (Scheme 32). The unfavorable out-of-phase overlap with the leaving group is minimized (Scheme 28). Front-side attack, leading to retention is therefore the normal pathway (Table 16). When the Na^+ is trapped (naked anion), the negative charge is concentrated on the oxygen reactive center (Scheme 32). In the latter case, as the valence orbitals are smaller, the out-of-phase overlap with the leaving group is diminished and retention is favored (Scheme 28). This is in agreement with the experimental data. The extent of retention increases when the ion pair is separated (Table 16).

Allyllithium is a softer nucleophile than alkyllithiums, so it can lead to inversion of configuration (Table 12). When the Li^+ cation is complexed, the extent of inversion is always increased (Table 25) (137). The above data may be explained as follows. In the case of allyllithium, Clark, Jemmis, and Schleyer (163) have shown that the valence orbitals are centered toward Li^+ and have some sp^3 character. In contrast, the valence orbitals of the naked allyl anion have a pure p character, and thus are more diffuse (Scheme 33). In the latter case, the un-

Table 25
Stereochemical Behavior of Allyllithium (137)

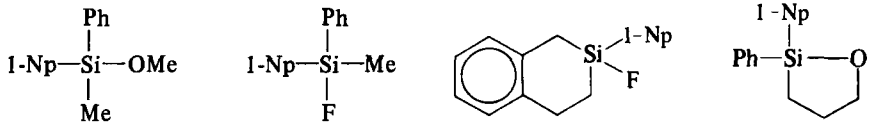

	94	95	92	68
	Predominant Stereochemistry			
Nucleophile				
Allyllithium/Et_2O	85% RN	71% IN	87% RN	$[\alpha]_D = -5°$ IN
Allyllithium/K_{Li^+}/Et_2O[a]	75% RN	90% IN	75% RN	$[\alpha]_D = +10°$ IN

[a] K_{Li^+} = a cryptand specific for Li^+.

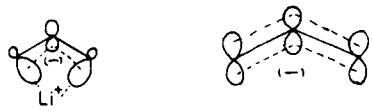

Scheme 33. Supposed shapes of the allyllithium HOMO and of the allyl anion HOMO.

favorable out-of-phase overlap with the leaving group is increased: the rear-side attack of the nucleophile is promoted, and therefore more inversion is observed when Li^+ is trapped.

In the case of the *p*-nitrophenoxide, we propose similar explanations. The oxygen atom of the *p*-nitrophenoxide anion has a high degree of sp^2 character (162). The *p* character of the nucleophile center, as we had assumed in the case of the allyl anion, implies a delocalization of the negative charge over the aromatic system (162). We thus deal with diffuse valence orbitals around oxygen, and thus the sizable overlap with the leaving group prevails. A rear-side attack leading to inversion is thereby favored (Scheme 28). Concerning the effect of the counter cation, the sodium *p*-nitrophenoxide is similar to the allyllithium case. The counter cation reduces the *p* character of the oxygen and prevents the delocalization of the negative charge over the aromatic system. The valence orbitals are centered toward Na^+, while for the naked anion they are more disposable, or, in other words, more diffuse (Scheme 34). Therefore in the latter case, the unfavorable out-of-phase overlap with the leaving group is increased; rear-side attack of the nucleophile and thereby inversion, is promoted (Table 16).

Compared with organolithiums, the stereochemistry shifts generally towards inversion of configuration with Grignard reagents (Table 12). The carbon–magnesium bond is moderately covalent, and as a consequence the electrons of the nucleophile are those of the C-Mg bond, which are localized in a MO between the two atoms. It is probable that this MO is more voluminous than the small valence orbitals around the nucleophilic carbon of an alkyl organolithium (Scheme 35). Thus the greater aptitude of Grignard reagents to give rise to inversion compared with organolithiums can be understood.

Similar arguments allow an explanation of the change of stereochemistry observed with Grignard reagents when solvent basicity is increased (Table 20). The addition of a basic solvent (THF, DME) implies a modification of the carbon–

Scheme 34. Supposed shapes of the HOMO of the *p*-nitrophenoxide anion and of sodium *p*-nitrophenoxide.

Scheme 35. Supposed shapes of the HOMO of alkyllithium and alkyl Grignard reagents.

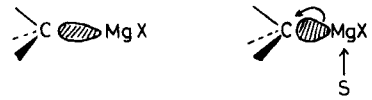

Scheme 36. Supposed shape of the RMgX HOMO (influence of a basic solvent).

magnesium MO, which becomes more concentrated on the carbon atom (Scheme 36). As a consequence the nucleophile is smaller in size and the stereochemistry is shifted to retention (Table 20).

b. Nucleophilic Displacements by Hydrides. In alanes, $AlH_{(3-n)}Y_n$(Y = OR, SR or I), the hydrogen atom has no unshared electron pairs, and therefore the electrons of the nucleophile are those of the Al-H bond. Moreover, since hydrogen has no lone pair, the unfavorable Nu leaving group repulsion is reduced.

In a noncoordinating solvent such as hexane (Table 23), the valence orbitals of the nucleophile are contracted. The unfavorable overlap with the leaving group is feeble and whatever its nature, retention is favored. In solvents such as THF or TMDA, i.e., those able to coordinate at Al, the structure of the nucleophile HOMO is modified by diffusion of the valence orbitals around H and an increase in the electron density (Scheme 37). Since the valence orbitals around H are more diffuse, the out-of-phase repulsion with the leaving group becomes dominant. Rear-side attack at silicon is favored and inversion is observed with the best leaving group (Br, Cl, F, SR) (146). In contrast, we get retention with OR groups.

The above discussion shows clearly that in the case of the alanes, the more the negative charge is displaced toward hydrogen, the more voluminous the valence orbitals are and the more inversion is favored. It seems interesting to introduce, at this point, the case of the naked AlH_4^- anion. In the latter, the negative charge is completely localized on the hydrogen atoms. Therefore, we may assume valence orbitals around this species to be diffuse (Scheme 38). This explains the general shift of stereochemistry to inversion when AlH_4^- anions are used (Table 24). In contrast, when using $LiAlH_4$ or $LiAlH_4$/LiBr, an increase of the RN ratio is observed (143, 147). Li^+ and AlH_4^- are tightly associated in aggregates of unknown structure. Our results and those of others (164) suggest aggregates in which the Li^+ cation prevents the delocalization of the negative charge. One possibility could be that shown in Scheme 39. Such assumptions are supported by the crystal structures of $LiAl(Et)_4$ (165) and $KAl(Me)_4$ (166). The

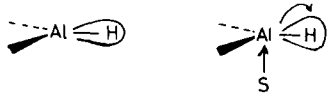

Scheme 37. Shape of the σ_{Al-H}.

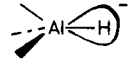

Scheme 38. Supposed AlH_4 valence orbitals.

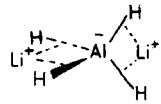

Scheme 39. Supposed structure for $LiAlH_4$.

structure of the latter compound consists of isolated K^+ and $Al(Me)_4^-$ ions: the bonding between the central atoms and ligands shows a highly polar character which causes a considerable weakening of the Al-C bond. This is a good model for the structure of naked AlH_4^-: the negative charge is highly delocalized around the H atoms. On the other hand, the structure of $LiAlEt_4$ consists of linear chains of alternating lithium and aluminum: there is some evidence of weak covalent interaction involving lithium. Such an interaction would explain the behavior of $LiAlH_4$/LiBr aggregates in preventing the delocalization of the negative charge to hydrogen atoms.

3. Stereochemical Changes with Angle Strain at Silicon

The stereochemical patterns reported for optically active 1-naphthylphenylmethylsilanes can be generally extended to other acyclic R_3Si^*-X systems. The examination of the stereochemical data for derivatives in which the substituents to silicon encompass significant variation in their steric and polar effects leads to the following comments: Concerning possible steric effects on the stereochemistry it seems clear from the experimental data that introduction of R groups of moderate to large steric requirements leaves the stereochemistry unchanged (1, 2, 10, 11). Concerning possible polar effects on the stereochemistry, comparison of the 1-NpPhMeSi-X and 1-NpC_6F_5MeSi-X systems is interesting. Although the pentafluorophenyl group is a powerful electron-withdrawing group relative to phenyl, these two systems do not differ to any significant extent (2, 89). A similar comparison can be made between the 1-NpPhEtSi-X and 1-NpPhViSi-X derivatives.

On the other hand, structures in which silicon is included in a ring, particularly a strained ring, have stereochemical behavior that is strongly influenced by the geometry of the substrate.

a. Stereochemical Behavior of Cyclic Strained Organosilanes. Both exocyclic leaving groups (attached to a silicon-containing ring) and endocyclic leaving groups (forming part of the sila-ring) will be considered.

Stereochemical Behavior of Exocyclic Leaving Groups. Important changes in stereochemistry, compared to acyclic silanes, were reported with the cyclic systems shown in Table 26. These stereochemical data lead to the following comments:

Table 26
Stereochemical Behavior of Exocyclic Leaving Groups

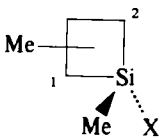

105

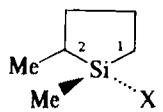

106

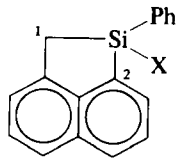

107

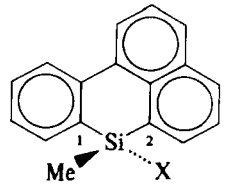

108

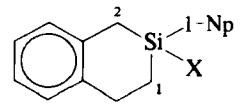

109

Substrate	Angle (C_1—Si—C_2)	$LiAlH_4$	RLi R = alkyl	RLi R = aryl	RMgX R = alkyl	RMgX R = aryl	Ref.
105 (Si—Cl)	<90° (167)	RN	–	–	RN	RN	(168, 169)
105 (Si—F)	<90°	RN	RN	–	RN	–	(168, 169)
105 (Si—OR)	<90°	RN	RN	–	RN	–	(168, 169)
107 (Si—Cl)	93.4°	RN	–	–	–	–	(64)
108 (Si—Cl)	≃90°	IN	–	–	–	–	(63)
108 (Si—F)	≃90°	RN	–	–	–	–	(63)
106 (Si—Cl)	92°-96° (172)	IN	–	IN	IN	–	(170)
106 (Si—F)	92°-96°	Rac.	–	–	–	–	(170)
106 (Si—H)	92°-96°	–	–	RN	–	–	(170)
109 (Si—Cl)	≃105° (173)	IN	RN	RN	IN	RN	(137, 138)
109 (Si—F)	≃105°	Rac.	RN	RN	RN	RN	(137, 138)
109 (Si—OR)	≃105°	Rac.	RN	RN	RN	RN	(137, 138)
109 (Si—H)	≃105°	–	RN	RN	–	–	(137, 138)
R_3Si—Cl	≃109° (45)	IN	IN	IN	IN	IN	(1, 2, 10, 11)
R_3Si—F	≃109°	IN	RN	–	IN	IN	(1, 2, 10, 11)
R_3Si—OMe	≃109°	RN	RN	RN	–	–	(1, 2, 10, 11)
R_3Si—H	≃109°	–	RN	RN	–	–	(1, 2, 10, 11)

1. Increased angle strain at silicon always leads to a significant change of the stereochemistry toward retention. This general trend is particularly evident with most angle-strained silacyclobutanes (Table 26). These latter react with predominant retention, whatever the nature of the nucleophile (168, 169). Even coupling reactions between **105** (Si-Cl) and $LiAlH_4$ or Grignard reagents occur with complete retention of configuration, whereas the same reactions carried out with 1-NpPhMeSi-Cl lead to complete inversion (1, 2).
2. A small amount of angle strain is enough to bring about such a stereochemical change. 1-Naphthyl-2-sila-2-tetrahydro-1,2,3,4-naphthalene, **109**, shows significant deviations from the norm compared with 1-NpPhMeSi-X (Table 27) (128). Compound **109** (Si-Cl) reacts with alkyllithiums, leading to complete retention instead of inversion with R_3Si-Cl; allyllithium or benzyllithium and alkyl Grignard reagents also cleave the Si-F bond of **109** with retention instead of the inversion as observed with 1-NpPhMeSi-F.
3. It is noteworthy that ring strain does not change the main factors that govern the stereochemistry, that is, the nature of the leaving group and the electronic character of the nucleophile. We observe only a general shift of the stereochemistry toward retention.

Stereochemical Behavior of Endocyclic Leaving Groups. Optically active cyclic systems, **68** and **71**, containing both a silicon atom and a leaving group, have been investigated (84, 90, 91). Stereochemical data are summarized in Tables 28 and 29 and compared with those observed with 1-NpPhMeSi-X (X = OMe, SMe, and SPh). Two points are noteworthy: (i) Cyclic compounds show behavior quite similar to that of their acyclic analogs. Again we find the dominant influence of the leaving group on the stereochemistry. The SR groups (Table 29) favor inversion of configuration, compared to analogous OR groups (Table 28) Concerning the influence of the nucleophile, charge-localized nucleophiles (alkyllithiums or alkyl Grignard reagents) and $LiAlH_4$ lead to the expected stereochemical outcome in the case of alkoxy leaving groups, that is, retention of configuration. Charge-delocalized nucleophiles react with inversion (Table 28). The same observations can be made with SR leaving groups (Table 29). (ii) In borderline cases, some differences are apparent. Nucleophiles, such as allyllithium, *p*-methoxybenzyllithium, and the $LiAlH_4$-4CuI reagent lead to inversion in the case of the five-membered ring oxasilacyclopentane **68** (Table 28), whereas retention is observed with the acyclic analog **94**.

b. Rationalization of the Effect of Angle Strain. The influence of angle strain on the stereochemistry of nucleophilic displacements is a general feature. When the phosphorus atom of phospholane oxides and phosphonium ions is in-

Table 27
Comparison of the Stereochemical Behavior of **109** and 1-NpPhMeSi—X, **110** (X = Cl, F, OMe, H)

	Si—Cl		Si—F		Si—OMe		Si—H	
	109	**110**	**109**	**110**	**109**	**110**	**109**	**110**
EtLi	63% RN	100% IN	96% RN	90% RN	94% RN	90% RN	100% RN	–
n-BuLi	82% RN	59% IN	98% RN	80% RN	96% RN	86% RN	100% RN	100% RN
CH_2=$CHCH_2$Li	86% RN	100% IN	95% RN	71% IN	97% RN	85% RN	85% RN	89% RN
$PhCH_2$Li	99% RN	100% IN	70% RN	85% IN	75% RN	79% IN	96% RN	90% RN

Table 28
Stereochemical Behavior of the Endocyclic OR Leaving Group: Comparison with 1-NpPhMeSi—OMe **94** (84, 90)

Nucleophile	Products	Predominant Stereochemistry	
		94	**68**[a]
EtLi	R_3Si—Et	95% RN	–
MeLi	R_3Si—Me	–	$[\alpha]_D = -8°$ RN
$LiAlH_4$	R_3Si—H	90% RN	$[\alpha]_D = +13°$ RN
$LiAlH_4$/4CuI/THF	R_3Si—H	55% RN	$[\alpha]_D = -18°$ IN
CH_2=CH—CH_2Li	R_3Si—CH_2CH=CH_2	85% RN	$[\alpha]_D = -5°$ IN
p-$CH_3OC_6H_4CH_2Li$	R_3Si—$CH_2C_6H_4$-(*p*-OCH_3)	90% RN	$[\alpha]_D = -4°$ IN
$C_6H_5CH_2Li$	R_3Si—CH_2Ph	79% IN	$[\alpha]_D = -3°$ IN
$C_6H_5CH_2MgBr$	R_3Si—CH_2Ph	75% IN	$[\alpha]_D = -3.7°$ IN

[a] **68** = 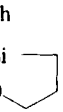

corporated into a four- or five-membered ring, the reduction or displacement reactions proceed, as a rule, with retention of configuration, in contrast to the analogous reactions in acyclic systems where inversion is the normal stereochemistry (148-153). Ring strain is invoked as the main factor in determining the stability of the intermediate. The analysis takes the following form. The diequatorial position is unfavorable for five-membered rings in a trigonal bipyramidal intermediate; the apical-equatorial position is the favored one. Consequently, the nucleophile, Nu^-, displaces the leaving group X with retention involving pseudorotation (Scheme 40).

Table 29
Stereochemical Behavior of an Endocyclic SR Leaving Group: Comparison with 1-NpPhMeSi—SMe, **111**, and 1-NpPhMeSi—SPh, **96** (91)

Nucleophile	Product	Predominant Stereochemistry		
		111	**96**	**71**[a]
Dibal/hexane	R_3Si—H	RN	RN	RN
$LiAlH_4$	R_2Si—H	IN	IN	IN
R′Li (R′ = alkyl)	R_3Si—R′	RN	RN	RN
R′MgX (R′ = Me, Et)	R_3Si—R′		IN	IN

[a] **71** = 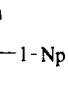

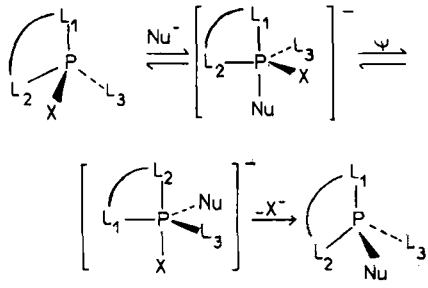

Scheme 40.

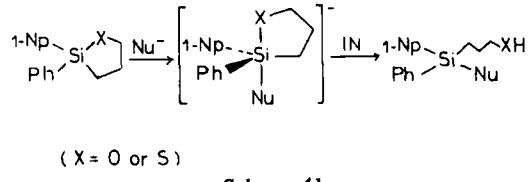

Scheme 41.

With organosilanes, we might invoke such a factor to explain the general shift towards retention for exocyclic leaving groups. In contrast, for an endocyclic leaving group, it would agree with a change to inversion (Scheme 41).

However, a more careful analysis shows that this explanation does not take into account all the experimental facts: (i) Ring strain favors retention of configuration as the stereochemical outcome (Table 26); however, this does not change the dominant influence of the leaving group and of the electronic character of the nucleophile. (ii) Experimental data for exocyclic leaving groups show a gradual change of the stereochemistry from inversion to retention when the angle strain at silicon is increased as indicated in the following scheme:

IN ⟶ RN

109°	105°	93–96°	90°
Acyclic silanes	**Six-membered rings**	**Silacyclopentanes**	**Silacyclobutanes**

This fact cannot be easily rationalized on the basis of geometric considerations as developed in the case of phosphorus compounds. In particular, the ring strain does not explain why the six-membered ring **109** ($\sphericalangle C_1\text{-Si-}C_2 \simeq 105°$) favors retention instead of inversion of configuration (Table 27). This angular value suggests that intermediates such as **112** and **113** are energetically similar, and both inversion and retention would be expected (Scheme 42).

The above data can be easily explained in terms of a change of the hybridization of the Si-R bond around the tetracoordinated silicon atom as proposed by

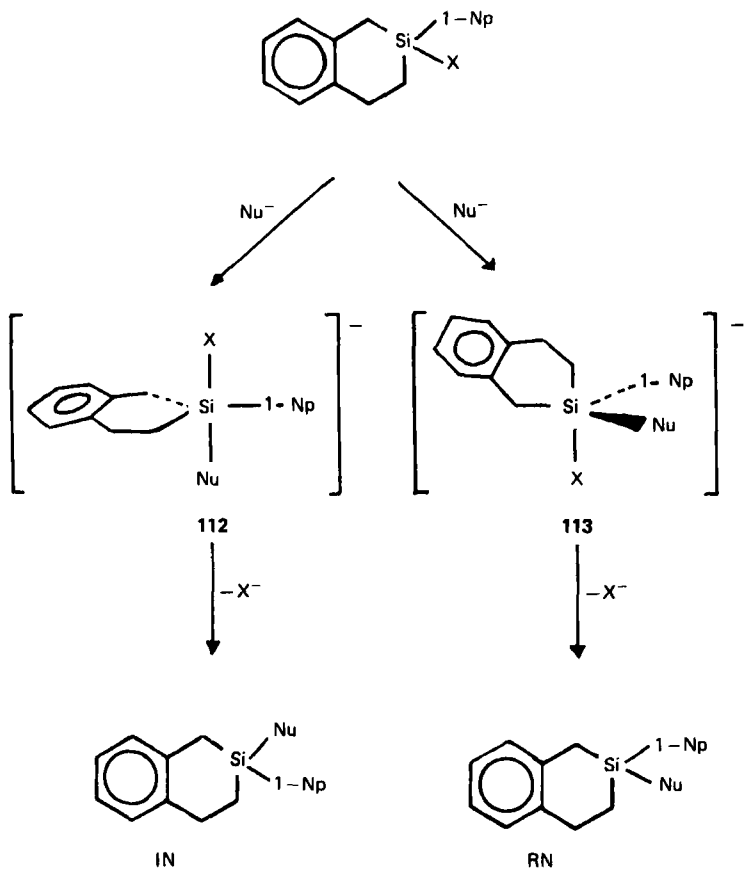

Scheme 42.

Anh and Minot (99, 100). When the C_1-Si-C_2 angle becomes smaller than the tetrahedral value, the two orbitals used for making Si-C_1 and Si-C_2 bonds have less *s* character, whereas the atomic orbital of the Si-X bond acquires more *s* character (Scheme 43). As shown by Anh and Minot (99), an increase of *s* character implies an easier front-side attack at silicon and, therefore, a greater proportion of retention. It follows that if the Si atom is included in a strained ring whereas X remains extracyclic, the percentage of retention will increase. In contrast, if Si and X are both in the ring, inversion of configuration will be favored.

Scheme 43.

The above conclusions explain the general effect of angle strain on stereochemistry and agree well with the following experimental facts:

1. Silacyclobutanes are highly strained ring compounds. This means that in the Si-X bond (X = leaving group), the hybrid atomic orbital has a large amount of *s* character and is quite dissymetric. It follows that the favorable overlap between Si and the incoming nucleophile is increased for a retention type attack (Scheme 28). Even coupling reactions between a chlorosilacyclobutane and $LiAlH_4$ or Grignard reagents occur with complete retention of configuration (Table 26).
2. When Si and OR are both in a five-membered ring, the σ^*_{Si-OR} MO has more *p* character, and front-side attack is less favorable (Scheme 28). However the experimental data indicate a shift of the stereochemistry only in borderline cases since the angular tension is not high (Table 28).
3. In the case of the six-membered ring 1-naphthyl-2-sila-2-tetrahydro-1,2,3,4-naphthalene (173), the small angular distortion at silicon implies a small increase of the *s* character in the Si-X bond. As a consequence, this change is enough to shift the stereochemistry toward retention only in borderline cases. For instance, alkyllithiums, which are rather hard nucleophiles with a negative charge concentrated on the reactive carbon center, cleave the Si-Cl bond with predominant retention (Tables 26 and 27); in contrast, Grignard reagents, which are softer reagents, cleave the same Si-Cl bond with inversion of configuration, that is, with the normal stereochemical outcome (Table 12).

Finally, similar hybridization arguments explain the order of reactivity of bicyclic systems. The results of the solvolysis studies show the relative reactivities to follow the same general trend as in nucleophilic substitutions (Scheme 44) (174). Because of the cage structure of the above bicyclic systems, only front-side attack at silicon is possible. Thus, an increase of the reactivity would be observed for the Si-X bonds that have a high degree of *s* character. Our analysis is as follows.

In the case of the silabicyclo[2.2.1]heptane ($\measuredangle C_1\text{-Si-}C_2 = 94.4°$; Figure 12) (175), a highly strained molecule, the large angular distortion at the silicon

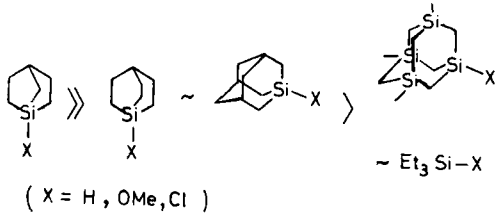

Scheme 44.

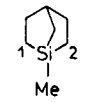

$\langle C_1-Si-C_2 = 94.4°$

$\langle C_1-Si-C_2 = 103.9°$

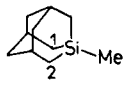

$\langle C_1-Si-C_2 = 103.2°$

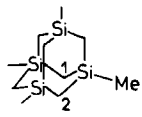

$\langle C_1-Si-C_2 = 109.5°$

Figure 12.

bridgehead leads to a significant increase of *s* character on silicon. Thus the σ^*_{Si-X} LUMO shows a big lobe on silicon directed toward the X leaving group. The rate of nucleophilic cleavage of the Si-X bond is increased because the overlap between the nucleophile and the reaction center is quite favorable.

In the silabicyclo[2.2.2]octane, the angular distortion at the silicon atom is not so large ($\measuredangle C_1$-Si-C_2 = 103.9°) (176). As a consequence, the silicon atom has less *s* character than in the above example, and the rate increase is smaller. Moreover, the 1-silaadamantyl system ($\measuredangle C_1$-Si-C_2 = 103.2°) (177) is only slightly less reactive than the 1-silabicyclo[2.2.2]octyl system (174).

The tetrasilaadamantyl system shows a silicon bridgehead which is a normal sp^3 hybridized atom [$\measuredangle C_1$-Si-C_2 = 109.5°, (1); Figure 12]. Its reactivity was not extensively studied but, at first sight, appears quite similar to that of acyclic compounds (174).

The hybridization arguments employed above may be compared with recent work of Shen Quang, Barton, and colleagues (178) relative to the structure of 1-methyl-1-silabicyclo[2.2.2]octatriene **114** (Figure 13). This molecule was found to exhibit a great deal of angular distortion at the silicon bridgehead ($\measuredangle C_1$-Si-C_2 = 98.8°). Relative to the normal sp^3 hybrid, there is a large shift

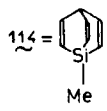

Figure 13.

toward *s* character in the Si-Me bond; from the observed valence angles, the authors concluded that the localized orbital on silicon has 60% *s* character. This bonding model is entirely consistent with our rationalizations.

IV. STEREOCHEMISTRY AND MECHANISM OF REACTIONS WITH TRANSITION METALS

The chemistry of organosilicon compounds has expanded with the use of transition metals. Both catalytic processes (179) and the chemistry of silicon transition metal compounds (180) have been developed. Catalytic reactions of organosilanes and more recently, reactions of silyl-transition metal complexes have already found interesting applications in organic synthesis (80, 181, 182).

Chiral organosilanes have been shown to undergo stereospecific catalytic reactions leading to the preparation of optically active silyl-transition metal complexes. We first discuss the stereochemistry and mechanism of transition metal catalyzed reactions of organosilicon compounds. Then the stereochemistry of chiral organosilyl-transition metal complexes are described. The chemistry of optically active silyl- and germyl-transition metals has been the subject of a recent review (12), and we concentrate here on mechanistic implications, especially in the field of homogeneous catalytic reactions.

A. Transition Metal Catalyzed Reactions of Chiral Organosilicon Compounds

In this section we mainly discuss the reactions of hydrosilanes, R_3SiH. Functional organosilanes, R_3SiX (X = OR, halogen . . .), undergo a large number of substitution reactions; Sect. III deals with nucleophilic substitutions. Hydrosilanes R_3SiH are less reactive toward nucleophilic reagents. However, the activation of the silicon-hydrogen bond by transition metal catalysts in both heterogeneous and homogeneous phases, leads to enhanced reactivity. It is noteworthy that the behavior of hydrosilanes and molecular dihydrogen toward transition metals is very similar, as first emphasized by Chalk and Harrod (183). Catalytic hydrosilylation is formally analogous to catalytic hydrogenation. Recently the hydroformylation reaction also has found its silicon analog (184).

1. Hydrosilylation Reactions

The term hydrosilylation is used to describe addition reactions of R_3SiH compounds to unsaturated reagents. The industrial importance of alkene hydrosilylation has led to a rapid development in this area. The synthetic scope of these reactions has been reviewed (179, 185, 187) so, again, we discuss here only the stereochemical and mechanistic aspects.

a. Hydrosilylation of Carbon-Carbon Multiple Bonds. The hydrosilylation of alkenes (eq. [37]) was first observed under free radical conditions (188).

$$R_3SiH + CH_2{=}CH{-}R \longrightarrow R_3SiCH_2CH_2R \qquad [37]$$

The use of transition metal catalysts permits the reaction to proceed smoothly. Many catalysts have been found efficient: not only homogeneous and heterogeneous platinum catalysts, but also complexes of iron, cobalt, nickel, rhodium, ruthenium, palladium, and iridium (186, 187). Among the large number of experiments that have been carried out, a few important aspects should be emphasized. The results may be summarized as follows:

1. Addition occurs readily with terminal olefins yielding almost exclusively linear adducts.
2. Hydrosilylation is often accompanied by olefin isomerization.
3. Internal olefins exhibit a marked tendency to produce terminal addition products (eq. [38]) (189).

$$CH_3{-}CH{=}CH{-}CH_2CH_3 \xrightarrow[H_2PtCl_6]{Cl_3SiH} Cl_3Si(CH_2)_4CH_3 \qquad [38]$$

Stereochemistry of Hydrosilane Addition to Alkynes: Platinum and Rhodium Catalysts. Hydrosilylation of hex-1-yne with trichlorosilane in the presence of hexachloroplatinic acid gave a mixture of two vinylsilanes (eq. [39]) (190).

$$C_4H_9C{\equiv}CH \xrightarrow[H_2PtCl_6]{Cl_3SiH} \underset{78\%}{\overset{C_4H_9}{\underset{H}{\overset{H}{\diagdown\!=\!\diagup}}}\!SiCl_3} + \underset{22\%}{\overset{C_4H_9}{\diagdown\!=\!CH_2}\;\;Cl_3Si} \qquad [39]$$

The stereochemistry of the 1-silyl isomer has been shown to be trans. It is produced by exclusive cis addition.

Another elegant demonstration of the cis addition processes using platinum on charcoal as catalyst has been reported by Brook and coworkers (191) and is described in Scheme 45. Cis addition to diphenylacetylene affords the silylstilbenes **117**. Their geometry was established by photochemical cyclization to the 9-silylphenanthrenes **118** as well as by comparison with the coupling product of chlorosilanes **116** and *cis*-stilbenyllithium.

More recently, using the very efficient homogeneous diplatinum catalyst $[Pt(SiR_3)(\mu H)(C_6H_{11})_3P]_2$, the hydrosilylation of but-1-yne and phenylacetylene was shown to afford *trans*-vinylsilanes **119** as the major products corresponding to cis Si-H addition (192) (eq. [40]). Products corresponding to nonterminal addition **(120)** were formed in minor amounts.

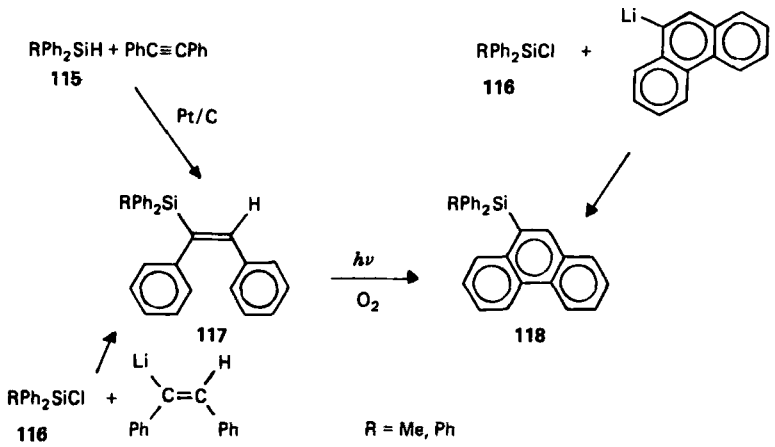

Scheme 45. Stereochemistry of the platinum-catalyzed hydrogenation of diphenylacetylene.

$$R_3SiH + R'C{\equiv}CH \xrightarrow[[Pt(SiR_3)(\mu H)(C_6H_{11})_3P]_2]{} \underset{\textbf{119}\ 100\text{–}68\%}{\overset{H}{\underset{R'}{\overset{SiR_3}{=}}}\overset{}{\underset{}{H}}} + \underset{\textbf{120}\ 0\text{–}32\%}{\overset{R_3Si}{\underset{R'}{\overset{H}{=}}}\overset{}{\underset{}{H}}} \qquad [40]$$

R′ = Me, Ph
R_3 = Me_2Ph, Et_3, Cl_3, Cl_2Me, $ClMe_2$, $(OEt)_3$

Cis addition is a characteristic feature of the hydrosilylation of acetylenic compounds in the presence of platinum catalysts. This is in marked contrast to the trans addition giving cis adduct on using free radical initiators (193). Free radical hydrogermylation (23) and hydrostannylation (194) also proceed with trans stereochemistry.

The rhodium catalyzed hydrosilylation (195-198) and hydrogermylation (23) reactions (eq. [41]) present the same particular features, which may be summarized as follows:

$$RC{\equiv}CH + R_3MH \xrightarrow{(PPh_3)_3RhCl} \underset{\textbf{121}\ \text{cis adduct}}{\overset{R}{\underset{H}{\overset{MR_3}{=}}}\overset{}{\underset{}{H}}} + \underset{\textbf{122}\ \text{trans adduct}}{\overset{H}{\underset{R}{\overset{MR_3}{=}}}\overset{}{\underset{}{H}}} \qquad [41]$$

M=Si, Ge

1. Addition gives two main products **121** and **122**, arising from cis addition and trans addition processes, respectively.
2. No cis-trans isomerization occurs in the presence of the rhodium catalyst, but a slow isomerization takes place when both rhodium complex and hydrogermane are present.
3. The cis-trans ratio depends on catalyst concentration. Lowering the catalyst concentration increases the percentage of cis adduct (trans addition process).
4. An increase in the silane (germane) concentration results in an increase of the percentage of cis adduct.
5. The formation of the cis adduct is also favored by raising the temperature.

The results shown in equation 42 illustrate these experimental observations (198).

$$Et_3SiH + n\text{-}C_4H_9C{\equiv}CH \xrightarrow{(PPh_3)_3RhCl} \underset{H}{\overset{Et_3Si}{\diagdown}}{=}\underset{C_4H_9}{\overset{H}{\diagup}} + \underset{H}{\overset{Et_3Si}{\diagdown}}{=}\underset{H}{\overset{C_4H_9}{\diagup}} \qquad [42]$$

Silane	Alkyne	Catalyst	Temperature (°C)	trans (%)	cis (%)
1	1	0.001	20	82	16
1	1	0.0001	20	36	59
1	1	0.0001	60	25	72
1	1	0.001	60	46	46
1	1	0.01	60	45	40
2	1	0.01	60	0	100

To account for these results, the hydrosilylation reaction in the presence of Wilkinson's catalyst was proposed to occur via a cis addition process (according to the Chalk and Harrod mechanism, cf. Sect. IV-A-1-a) with concomitant isomerization taking place, the catalyst retaining the olefinic product in its coordination sphere. Conversion of the more stable trans to cis product is proposed to be directed by steric interactions in an intermediate σ-alkylrhodium complex.

However, isomerization can hardly account for the formation of the less stable trans addition product (cis adduct), since conversion of the cis adduct to the more stable trans adduct was observed under the reaction conditions (197). It is more likely that cis and trans additions occur by competitive pathways as suggested for the hydrogermylation reaction for which the rate of the concurrent isomerization is slow compared with the rate of the addition reaction (23).

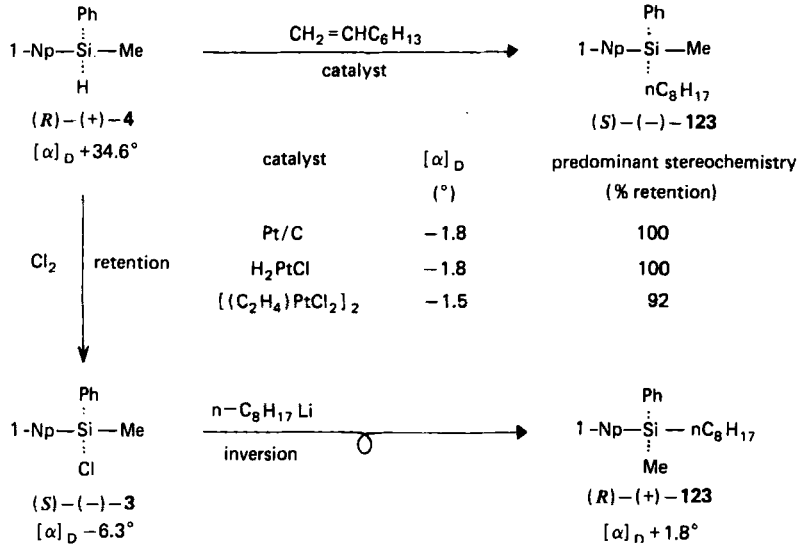

Scheme 46. Stereochemistry of the platinum-catalyzed addition of (*R*)-(+)-1-NpPhMeSiH.

From a synthetic point of view, a predominant trans addition pathway can be attained and the rhodium catalyzed hydrosilylation is an interesting route to *cis*-vinylsilanes (195).

Stereochemistry of Chiral Organosilane Addition Reactions. The addition reaction of optically active organosilicon hydrides to oct-1-ene has been reported to proceed with retention of configuration at silicon in the presence of platinum catalysts (199) (Scheme 46). The predominant stereochemistry and stereoselectivities were determined by a chemical correlation using pathways of known stereochemistry.

The same stereochemistry has been demonstrated in the platinum on charcoal catalyzed hydrosilylation of diphenylacetylene (191) (eq. [43]).

Retention of configuration was also observed in the analogous reaction of chiral germanes catalyzed by platinum and rhodium complexes (23). Of interest

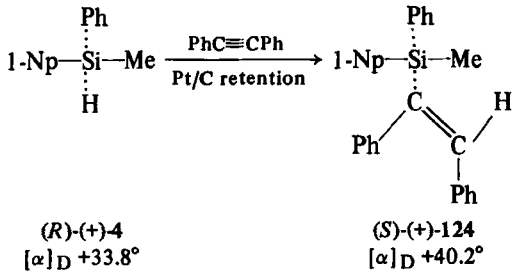

[43]

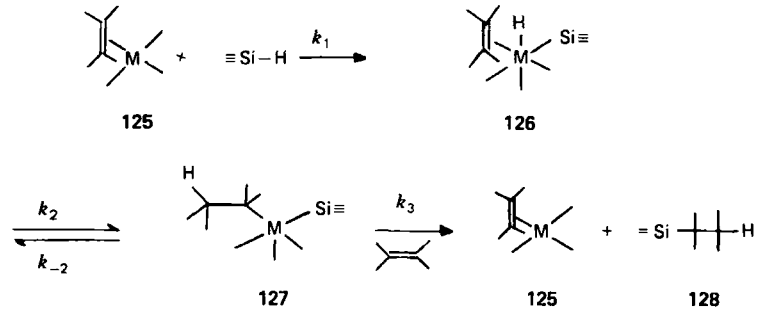

Scheme 47. Mechanism of the platinum-catalyzed hydrosilylation reaction.

also is the retention of configuration observed in the free-radical hydrogermylation which shows the optical stability of trialkylgermyl radicals. Brook, Sakurai and their colleagues have provided evidence for the stability of optically active silyl free radicals (17-19).

Mechanism of Homogeneously Catalyzed Hydrosilylation. A mechanism analogous to the homogeneous hydrogenation reaction has been proposed by Chalk and Harrod (200) (Scheme 47) for the platinum catalyzed hydrosilylation. In the first step, oxidative addition of the silane occurs and leads to an hexacoordinate intermediate complex **126**, in which both silane and olefin are cis oriented. Hydrogen migration produces a σ-alkyl complex **127** from which the hydrosilylation products **128** are obtained by reductive elimination.

Variations in the olefin isomerization that occur concurrently with hydrosilylation may be explained as follows: In the case where $k_3 > k_{-2}$, no isomerization would be expected, but if $k_{-2} > k_3$, isomerization will occur.

The Chalk and Harrod mechanism is consistent with the known stereochemical data and most steps now have known precedents. Cis addition is easily explained, since intramolecular hydrogen migration in complex **129** (eq. [44]) lead to a cis σ-vinyl complex **130**. Upon reductive elimination the cis addition product **131** is then obtained.

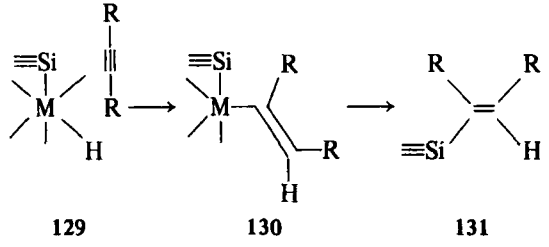

[44]

The proposed oxidative addition of the hydrosilane in the first step is now a well-known process in organosilicon chemistry (72, 201-209). Moreover, oxida-

tive addition of optically active organosilicon hydride on platinum complexes was shown to proceed with retention of configuration at silicon (210, 211) (eq. [45]).

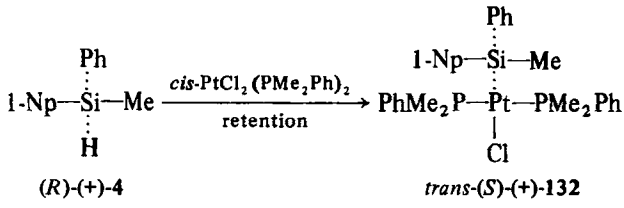

(*R*)-(+)-4 *trans*-(*S*)-(+)-132 [45]

The hydrogen migration in the second step will not change the configuration of the chiral silyl ligand.

The reductive elimination process that yields the hydrosilylation product has been recently observed in the decomposition of *cis*-alkyl(trimethylsilyl)iron carbonyl complexes **133** (212) (eq. [46]). To account for the overall retention of configuration at silicon the hydrosilylation process, the last step should occur with retention. Although not demonstrated, this is very likely, since reductive elimination of hydrosilanes in silyl hydride transition metal complexes occurs with retention of configuration (211, 213).

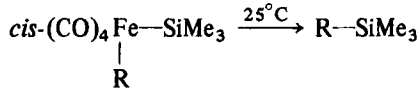

133 R = Me, $PhCH_2$ [46]

The dicobalt octacarbonyl catalyzed hydrosilylation was proposed to proceed via a somewhat different mechanism (214).

b. Hydrosilylation of Carbonyl Compounds. The hydrosilylation reaction of carbonyl compounds (eq. [47]) was first reported by Calas and coworkers (215). More recently, homogeneous transition metal catalysts of platinum, rhodium, and ruthenium were found to promote ketone hydrosilylation (70, 71, 216, 217). This reaction has been used for the reduction of carbonyl compounds (80).

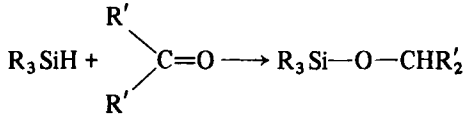

[47]

Optically active organosilanes were shown to add with retention of configuration at the silicon center (68) (eq. [48]).

A mechanism similar to that of olefin hydrosilylation has been proposed

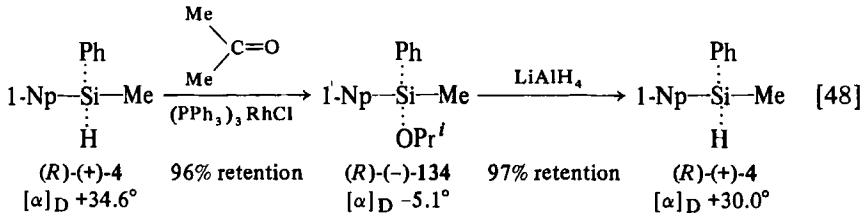

[48]

(Scheme 48). In the first step, oxidative addition of the hydrosilane leads to a pentacoordinated complex **136**. Such rhodium complexes have been isolated (72, 201, 202) and, as mentioned previously, the addition process occurs with retention of configuration at silicon. Hydrosilylation with observed overall retention suggests that the next step is coordination of the ketone onto the rhodium and formation of the hexacoordinated intermediate **137**. Results obtained in asymmetric synthesis at silicon (cf. Sect. II-D) strongly support a π-coordination of the ketone. Migration of the silyl ligand on the oxygen atom of the ketone gives the σ-alkyl-rhodium complex **138** from which the alkoxysilane is obtained by reductive elimination. Prior migration of the hydrogen on the ketone would lead to the same result. However initial migration of the silyl ligand is more likely owing to the stability of silicon-oxygen bonds and affinity of silicon towards oxygen. A recent observation of a related complex **140** in the reaction of (trimethylsilyl)manganese carbonyl **139** with benzaldehyde also supports the intervention of complex **138**, (218) (eq. [49]). Migration of the silyl ligand, within the coordination sphere of the catalyst, is likely to proceed with retention of configuration at silicon. Virtually complete retention at the chiral silicon center has been observed in intramolecular rearrangements of chiral silylated organic molecules (15).

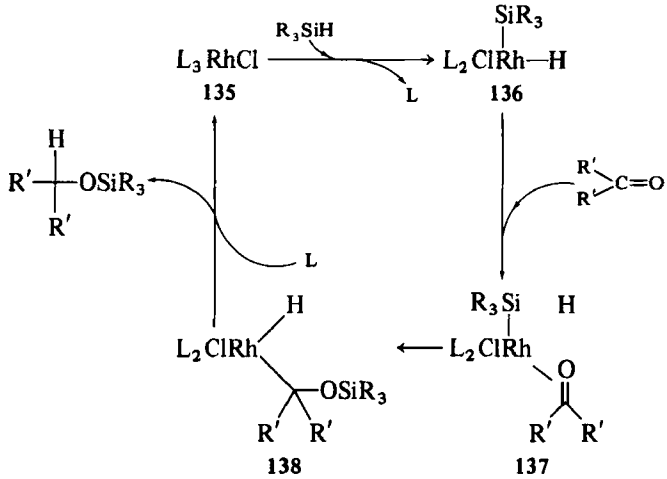

Scheme 48. Mechanism of the rhodium-catalyzed hydrosilylation of ketones.

$$\underset{\textbf{139}}{(CO)_5Mn{-}SiMe_3} + PhCH{=}O \longrightarrow \underset{\textbf{140}}{(CO)_5Mn{-}\overset{\displaystyle OSiMe_3}{\overset{|}{C}}H{-}Ph} \qquad [49]$$

2. *Dehydrogenative Silylation Reactions*

Proton donors have been shown to cleave the silicon-hydrogen bond of hydrosilanes in the presence of various catalysts (77, 219) (eq. [50]). The stereochemistry of this transition-metal-catalyzed reaction has been studied in the reaction of chiral hydrosilanes.

$$R_3SiH + XH \xrightarrow{\text{catalyst}} R_3SiX + H_2 \qquad [50]$$

$$XH = H_2O, ROH, R_2NH, RCOOH, RSH, H_2S, HCl, HF \ldots$$

Transition metal heterogeneous catalysts cause substitution of optically active 1-naphthylphenylmethylsilane with predominant inversion of configuration at the silicon center (220, 221) (eq. [51]). Some selected examples are given in Table 30. Palladium-catalyzed reactions are the most stereoselective. In order to account for the observed inversion at silicon, a mechanism has been proposed involving activation of the hydrosilane on the metal surface followed by backside attack of the nucleophile. However, the displacement of hydrogen by hydrogen chloride and hydrogen sulfide with retention of configuration has not been rationalized until now.

$$\underset{(R)\text{-}(+)\text{-}\mathbf{4}}{1\text{-}Np{-}\overset{\displaystyle Ph}{\overset{:}{\underset{\displaystyle H}{\underset{:}{Si}}}}{-}Me} + XH \xrightarrow[O]{\text{heterogeneous catalyst}} \underset{(S)\text{-}\mathbf{141}}{1\text{-}Np{-}\overset{\displaystyle Ph}{\overset{:}{\underset{\displaystyle Me}{\underset{:}{Si}}}}{-}X} + H_2 \qquad [51]$$

The stereochemistry of the homogeneous rhodium-catalyzed alcoholysis reaction has also been studied (77) (eq. [52]). The predominant stereochemistry was established through a Walden cycle, reduction of the alkoxysilane **142** occurring with almost complete retention at silicon. As shown in Table 31, the rhodium-catalyzed alcoholysis occurs with retention of configuration but low stereoselectivity. Moreover, when the alcohol was used as solvent, predominant inversion or racemization was observed. Predominant inversion was also found in alcoholysis of a substituted silacyclopentane (171), but concomitant epimerization yielding the equilibrium mixture of isomers was observed.

$$\underset{\textbf{4}}{1\text{-}NpPhMeSiH} \xrightarrow[(PPh_3)_3RhCl]{ROH} \underset{\textbf{142}}{1\text{-}NpPhMe\overset{*}{S}iOR} \xrightarrow[\substack{Et_2O\\ \text{retention}}]{LiAlH_4} \underset{\textbf{4}}{1\text{-}NpPhMe\overset{*}{S}iH} \qquad [52]$$

Table 30
Dehydrogenative Reactions of (*R*)-(+)-1-NpPhMeSiH with Proton Donors (XH) (eq. [51])

XH	Catalyst	Predominant Stereochemistry	Ref.
H_2O	10% Pd-C	81% Inversion	220
	Raney Ni	94% Inversion	220
MeOH	10% Pd-C	100% Inversion	220
	Raney Ni	100% Inversion	220
	5% Rh-C	58% Inversion	220
	5% Ru-C	59% Inversion	220
	H_2PtCl_6	Racemization	220
	Ag powder	Racemization	220
$C_6H_{11}OH$	10% Pd-C	99% Inversion	220
	Raney Ni	96% Inversion	220
PhOH	10% Pd-C	63% Inversion	220
	Raney Ni	92% Inversion	220
CH_3COOH	10% Pd-C	86% Inversion	220
	Raney Ni	90% Inversion	220
	5% Pd-Al_2O_3	100% Inversion	221
	10% Pd-C	Racemization	221
$MeNH_2$	5% Pd-Al_2O_3	69% Inversion	221
HF	5% Pd-Al_2O_3	83% Inversion	221
	10% Pd-C	77% Inversion	221
HCl	5% Pd-Al_2O_3	82% Retention	221
	10% Pd-C	68% Retention	221
H_2S	5% Pd-Al_2O_3	84% Retention	221

Table 31
$(PPh_3)_3RhCl$ Catalyzed Alcoholysis of Chiral 1-Naphthylphenylmethylsilane (eq. [52]) (ref. 77)

Alcohol	Solvent	Predominant Stereochemistry
MeOH	C_6H_6	54% Retention
MeOH (excess)	None	67% Inversion
i-PrOH	C_6H_6	72% Retention
i-PrOH (excess)	None	Racemization
cyclo-$C_6H_{11}OH$	C_6H_6	68% Retention
$PhCH_2OH$	C_6H_6	60% Retention
(-)-Menthol	C_6H_6	64% Retention

A more stereoselective reaction was seen in the ring closure of γ-silylthiol **70** (91) (eq. [53]). Since diisobutylaluminum hydride is known to cause reduction with complete retention at silicon (146), the intramolecular cyclization of (*S*)-(-)-**70** must occur with at least 90% retention of configuration.

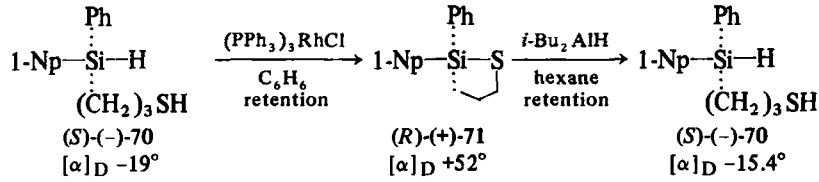

[53]

A proposed mechanism for the rhodium-catalyzed alcoholysis is represented in Scheme 49 (77). In the first step, activation of the hydrosilane occurs through oxidative addition. Formation of the alkoxysilane then takes place by nucleophilic attack of a noncoordinated alcohol molecule. The dihydro-rhodium complex **143** thus obtained liberates a hydrogen molecule upon reductive elimination. Nucleophilic cleavage of the silicon-rhodium bond, without prior coordination of the alcohol at the rhodium is supported by results obtained in asymmetric alcoholysis (cf. Sect. II-D). Optical yields were shown to be little dependent on the catalyst ligands (in marked contrast with the asymmetric hydrosilylation), indicating but weak interaction between alcohol and catalyst during the reaction. Moreover, inversion of configuration at silicon, which occurs in the particular case of methanol as solvent, is not likely to occur in a reaction between coordinated silane and alcohol.

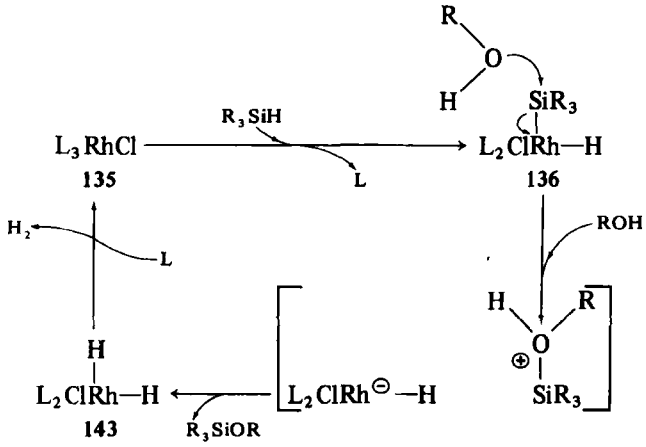

Scheme 49. Mechanism of the rhodium-catalyzed alcoholysis of hydrosilanes.

Variations of the predominant stereochemistry and variations in stereoselectivity appear characteristic of nucleophilic substitution at silicon and support the mechanism shown in Scheme 49. The stereochemistry depends on the nucleophile and the leaving group (cf. Sect. III). For example, the stereochemistry of rhodium catalyzed methanolysis (Table 31) parallels that reported for substitution by alcoholates (141) (eq. [54]). We recall that the alcoholate RO^- in benzene ("hard reagent") preferentially reacts with retention of configuration, whereas RO^- in the presence of ROH ("soft reagent," with the charge delocalized by hydrogen bonding) causes substitution with predominant inversion.

$$R_3SiX + RO^- \longrightarrow R_3SiOR + X^- \qquad [54]$$

$$X = OPh, SMe, F$$

3. *Protium-Deuterium Exchange Reactions*

Most hydrosilylation catalysts have also been found to catalyze the isotopic exchange reaction of hydro- and deuterosilanes (eq. [55]). Since protium-deuterium exchanges are rapid, hydrogen scrambling occurs during hydrosilylation reactions. Highly stereoselective reactions of chiral hydrosilanes thus imply that isotopic exchange occurs with complete retention of configuration at silicon. This was demonstrated in the reaction of optically active 1-NpPhMeSiH (**4**) with PhEtMeSiD (**144**) in the presence of heterogeneous and homogeneous catalysts (199) (eq. [56]). Selected examples are given in Table 32. Homogeneous catalysts gave complete retention at the silicon center. In the case of the rhodium catalysis, exchange of protium and deuterium is instantaneous (73) (eq. [57]). It implies a complete retention at silicon since rapid exchange with racemization or inversion is not compatible with the reported rhodium-catalyzed stereospecific reactions of chiral hydrosilanes. Rapid isotopic exchange was also reported between hydro- and deuterogermanes $R_3GeH(D)$ (222). Moreover the

Table 32
Transition Metal Catalyzed Protium–Deuterium Exchange Reactions of (*R*)-(+)-1-NpPhMeSiH (ref. 199) (eq. [56])

Catalyst	Reaction Time (min)	% Exchange	Predominant Stereochemistry % Retention
10% Pd-C	10	100	99
Raney Ni	10	100	98
5% Pt-C	30	67	98
H_2PtCl_6	180	100	100
$[(C_2H_4)PtCl_2]_2$	280	100	100
$Co_2(CO)_8$	1440	100	100
$IrCl(CO)(PPh_3)_2$	1020	100	100

room temperature NMR spectrum of n-Bu_3GeH, in the presence of 1.5% of $(PPh_3)_3RhCl$, exhibits a broad singlet for the Ge-*H* proton (absence of resolved H-C-Ge-H coupling), indicating a rapid intermolecular exchange on the NMR time scale.

$$R_3SiH + R'_3SiD \underset{}{\overset{\text{catalyst}}{\rightleftharpoons}} R_3SiD + R'_3SiH \qquad [55]$$

$$\underset{\text{(}R\text{)-(+)-4}}{\text{1-Np(Ph)(H)Si-Me}} + \underset{144}{\text{PhEtMeSiD}} \underset{\text{retention}}{\overset{\text{catalyst}}{\rightleftharpoons}} \underset{\text{(}R\text{)-(+)-145}}{\text{1-Np(Ph)(D)Si-Me}} + \underset{62}{\text{PhEtMeSiH}} \qquad [56]$$

$$Et_3SiH + Ph_3SiD \underset{C_6H_6\ 20°C}{\overset{(PPh_3)_3RhCl\ 0.5\%}{\rightleftharpoons}} Et_3SiD + Ph_3SiH \qquad [57]$$

The isotopic exchange between R_3SiD and H_2 also proceeds with complete retention at silicon **199** (eq. [58]). The mechanism of the isotopic exchange probably involves two molecules of catalyst. A kinetic study of the rhodium-catalyzed H_2-D_2 exchange revealed that the rate had second-order dependence on catalyst concentration (223). The intervention of a dinuclear intermediate complex is thus likely to occur. Complexes containing μ-hydrido ligands, as proposed for the hydrogermane $R_3GeH(D)$ isotopic exchange (222), could explain the rapid and stereospecific exchange. A possible mechanism is represented in Scheme 50. It involves stereospecific oxidative addition and reductive elimination of hydrosilanes and is consistent with complete retention of configuration at silicon. Exchange through the di-μ-hydrido dinuclear complex **148** is supported by the isolation and characterization of a related platinum complex **151** (224) (eq. [59]).

$$\underset{\text{(}R\text{)-(+)-145}}{\text{1-Np(Ph)(D)Si-Me}} + H_2 \underset{\text{10\% Pd/C, 5\% Pt/C, Raney Ni, 100\% retention}}{\overset{\text{catalyst}}{\rightleftharpoons}} \underset{\text{(}R\text{)-(+)-4}}{\text{1-Np(Ph)(H)Si-Me}} + HD \qquad [58]$$

An isotopic exchange by intermolecular reaction between a coordinated silane and free silane, involving transition state **152** (199) (Figure 14), may not be excluded, at least in the $Co_2(CO)_8$ catalyzed reaction.

Exchanges of silyl moieties in chiral silyl-cobalt complexes proceed with complete retention at silicon (eq. [60]). The chiral silyl-cobalt complex **13** has also been reported to catalyze the R_3SiH-(D) exchange with complete retention. Although a mechanism involving a cobalt III intermediate **153** (Figure 15) was proposed (183), a concerted process through transition state **152** is also conceivable.

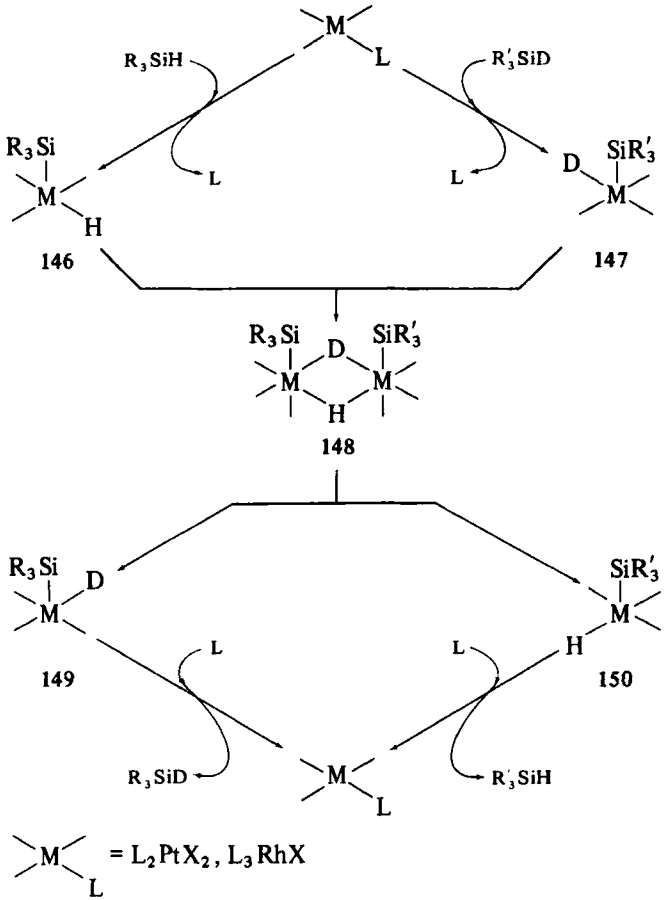

Scheme 50. Mechanism of the $R_3SiH(D)$ isotopic exchange catalyzed by rhodium and platinum complexes.

$$(C_6H_{11})_3PPt(C_2H_4)_2 + Et_3SiH \longrightarrow$$

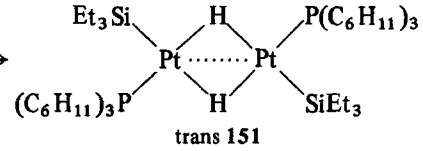

trans **151**

[59]

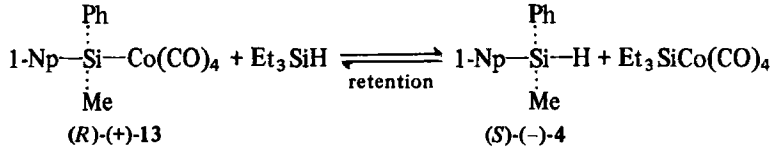

[60]

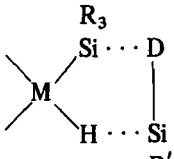

152

Figure 14. Possible transition state for the $R_3SiH(D)$ isotopic exchange.

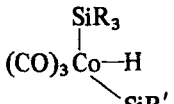

153

Figure 15. Possible intermediate for the cobalt-catalyzed $R_3SiH(D)$ isotopic exchange.

4. *Reactions of Activated Grignard Reagents*

New reactions of Grignard reagents in the presence of transition metal catalysts have been described. The synthetic and mechanistic aspects of the activation of Grignard reagents by transition metal compounds have been reviewed (225). In organosilicon chemistry, activated Grignard reagents permit novel substitution or reduction reactions. We discuss here the stereochemistry of these reactions.

a. Substitution Reactions. Organolithium reagents react with trisubstituted organosilicon hydrides; Grignard reagents do not. However, in the presence of catalytic amounts of $(PPh_3)_2NiCl_2$, nonreducing Grignard reagents react readily, leading to substitution of the hydrogen atom in good yields (226) (eq. [61]). These reactions are highly stereoselective. The optically active silane **45** undergoes substitution with more than 95% retention of configuration at silicon (eq. [62]). The same stereochemistry was observed in the substitution of optically active organogermanium hydrides (227).

$$R_3SiH + R'MgX \xrightarrow[Et_2O]{(PPh_3)_2NiCl_2} R_3SiR' \qquad [61]$$

The proposed mechanism (228) (Scheme 51) involves *in situ* generation of a zero-valent nickel catalyst and intervention of intermediates containing Ni-Mg bonds as proposed by Felkin and Swierczewski (225). Formation of the substituted silane arises from successive oxidative addition and reductive elimination, in agreement with the observed retention of configuration at silicon.

b. Reduction Reactions. No substitution reaction was observed upon reaction of reducing Grignard reagents with organosilicon hydrides. However, it has been shown that a deuteriosilane undergo a deuterium-hydrogen exchange reaction when treated with a reducing Grignard reagent in the presence of $(PPh_3)_2$-

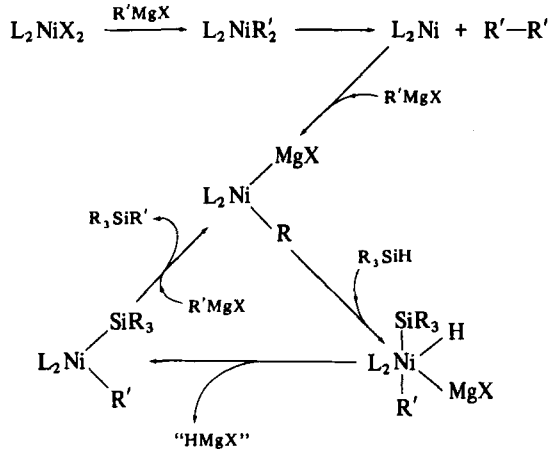

Scheme 51. Mechanism of the nickel catalyzed substitution by Grignard reagents.

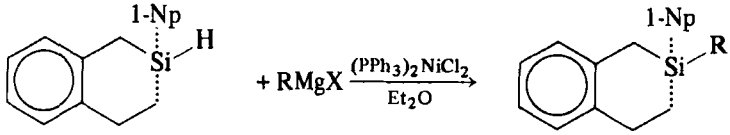

[62]

R-(+)-**45**

R	Predominant Stereochemistry (% Retention)
Me	95
Ph	95
CH_2=CH—	96
CH_2=CH—CH_2—	98
CH_3CH=CH—CH_2—	98
$PhCH_2$—	95

$NiCl_2$ (229) (eq. [63]). Deuterium-hydrogen exchange was shown to occur with retention of configuration at the silicon atom of the optically active deuteriosilane **154** (229) (eq. [64]).

$$R_3SiD + R'MgX \xrightarrow[Et_2O]{(PPh_3)_2NiCl_2} R_3SiH \qquad [63]$$

$$R' = Et, i\text{-}Pr, n\text{-}Bu, i\text{-}Bu$$

These results led to the development of a new reduction method for functional organosilanes R_3SiX (X = OR, Cl, F) (229-230). The results are presented in equation [65]. With the exception of chlorosilane, the reduction of optically active compounds occurs with retention of configuration at silicon.

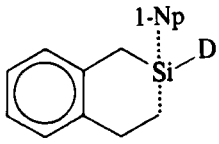

R-(+)-154

$$+ \text{RMgX} \xrightarrow[\text{Et}_2\text{O}]{(\text{PPh}_3)_2\text{NiCl}_2}$$

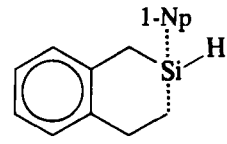

R-(+)-45 [64]

R	Predominant Stereochemistry % Retention
Et	100
n-Pr	98
i-Pr	100
n-Bu	96
i-Bu	98

$$1\text{-NpPhEt}\overset{*}{\text{Si}}\text{X} + \text{RMgBr} \xrightarrow[\text{Et}_2\text{O}]{\text{catalyst}} 1\text{-NpPhEt}\overset{*}{\text{Si}}\text{H} \qquad [65]$$

X	R	Catalyst	Predominant Stereochemistry
OMe	Et	$(PPh_3)_2NiCl_2$	94% Retention
OMe	*n*-Pr	$(PPh_3)_2NiCl_2$	98% Retention
OMe	*i*-Pr	$(PPh_3)_2NiCl_2$	94% Retention
OMe	*n*-Bu	$(PPh_3)_2NiCl_2$	99% Retention
OMe	*i*-Bu	$(PPh_3)_2NiCl_2$	93% Retention
F	*n*-Bu	$(PPh_3)_2NiCl_2$	90% Retention
Cl	*n*-Bu	$(PPh_3)_2NiCl_2$	98% Inversion
OMe	*i*-Pr	$(\eta\text{-}C_5H_5)_2TiCl_2$	100% Retention
F	*i*-Pr	$(\eta\text{-}C_5H_5)_2TiCl_2$	93% Retention
Cl	*i*-Pr	$(\eta\text{-}C_5H_5)_2TiCl_2$	99% Retention

The use of $(\eta\text{-}C_5H_5)_2TiCl_2$ as catalyst provides a more powerful reduction method similar to the use of $LiAlH_4$ (230). In this case, reduction of optically active functional silanes occurs with a high degree of retention of configuration (eq. [65]). The intervention of a transition-metal hydride catalyst is probably involved in these reductions.

The reactions of activated Grignard reagents for substitution and reduction in organosilicon chemistry have been used in new synthetic routes to chiral trisubstituted silanes (231).

B. Reactions of Silyl-Transition Metal Complexes

Stereochemical studies have brought new insights into catalytic reactions of organosilicon compounds. An approach to the mechanism of transition metal reactions has been made in the study of the stereochemistry of silyl-transition metal complexes. We review here the known chemistry of optically active com-

pounds and discuss two relevant points, displacement of silyl ligands and the interaction of hydrosilanes with transition metal complexes. As shown before, these two points are of importance in catalytic processes.

1. Chiral Silyl-Transition Metal Complexes

The chemistry of silicon, germanium, and tin transition metal compounds has been the subject of several reviews (12, 180). Optically active silyl ligands have been introduced in a transition metal complex by reaction of chiral functional organosilanes. However chiral silyl ligands containing complexes are limited to a few metal centers; we shall discuss in turn iron, cobalt, platinum, and manganese complexes.

a. Iron Complexes. The reaction of cyclopentadienyliron dicarbonyl anion was first used to prepare a trimethylsilyl-iron complex in 1956 (232). The reaction with the optically active chlorosilane **3** gave rise to an optically active iron complex **155** (233) (eq. [66]). After several crystallizations, compound **155** was isolated in 98% optical purity. On the basis of the known stereochemistry of nucleophilic displacement of chlorine atoms, the reaction was assumed to occur with inversion of configuration at silicon.

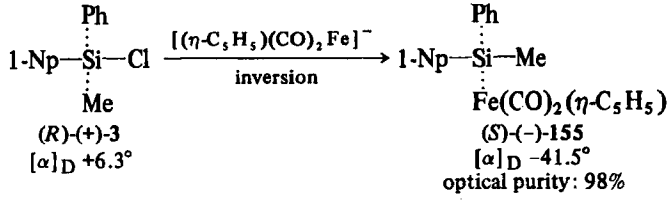

[66]

When submitted to UV irradiation in the presence of triphenylphosphine, compound **155** gave a 60/40 mixture of diastereomers, differing in their configuration about the iron atom (234, 235) (eq. [67]). Substitution of the diastereotopic carbonyl ligands occurred with different rates and a 10% asymmetric induction was thus observed in the phosphine reaction.

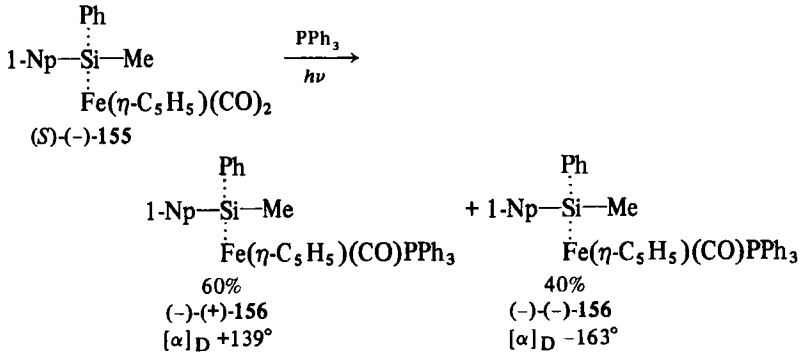

[67]

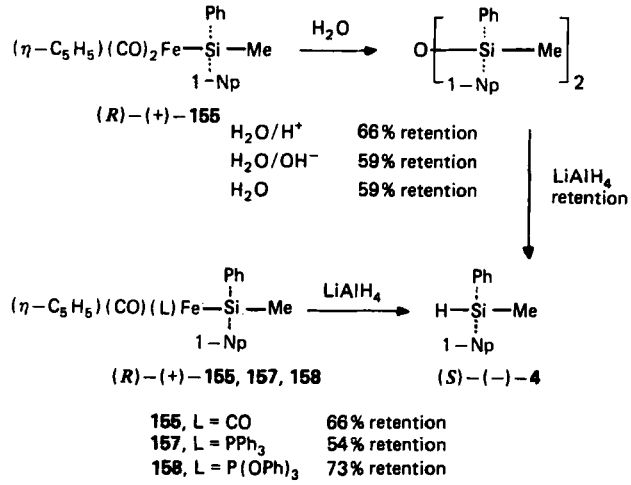

Scheme 52. Stereochemistry of the nucleophilic cleavage of Fe-Si bonds.

The iron-silicon bond in these complexes appeared to be very stable. Nucleophilic cleavage was observed only with water and with lithium aluminum hydride (Scheme 52). Although not specific, nucleophilic cleavage occurs with predominant retention of configuration at silicon.

The iron-silicon bond is more easily cleaved by electrophilic reagents. Results obtained in the chlorine or bromine cleavage reaction are given in equation [68].

Except in the case of the phosphite complex, the cleavage reaction occurs with low stereoselectivity. However, significant changes in the predominant ste-

$$(\eta\text{-}C_5H_5)(CO)(L)Fe{-}\overset{\overset{Ph}{|}}{\underset{\underset{1\text{-}Np}{|}}{Si}}{-}Me \xrightarrow{X_2} X{-}\overset{\overset{Ph}{|}}{\underset{\underset{1\text{-}Np}{|}}{Si}}{-}Me \quad \text{or} \quad Me{-}\overset{\overset{Ph}{|}}{\underset{\underset{1\text{-}Np}{|}}{Si}}{-}X \qquad [68]$$

L	X_2	Predominant Stereochemistry
CO	Cl_2	56% Retention
CO	$Cl_2/AlCl_3$	61% Retention
CO	$Cl_2/P(OEt)_3$	64% Inversion
CO	Br_2	53% Retention
PPh_3	Cl_2	63% Retention
PPh_3	$Cl_2/AlCl_3$	53% Retention
PPh_3	Cl_2/PPh_3	57% Inversion
$P(c\text{-}C_6H_{11})_3$	Cl_2	55% Retention
$P(c\text{-}C_6H_{11})_3$	$Cl_2/P(c\text{-}C_6H_{11})_3$	60% Inversion
$P(OEt)_3$	Cl_2	79% Inversion
$P(OEt)_3$	$Cl_2/AlCl_3$	91% Retention
$P(OEt)_3$	$Cl_2/P(OEt)_3$	73% Retention

reochemistry occur on changing the ligands in the silyl-iron complex or on changing the attacking electrophile.

The chlorine cleavage is clearly established to be an electrophilic attack of Cl^+ since no nucleophilic cleavage occurred by Cl^-. The reaction was explained as involving initial formation of cationic iron intermediates followed by a nucleophilic attack at silicon. Changes in ligands around the iron atom cause modifications in the electronic character of the leaving group and can thus modify the predominant stereochemistry.

Another interesting reaction of silyl-iron complexes is the protochemical formation of hydrosilanes upon reaction with phosphines (236) (eq. [69]). Optically active silyl-iron complexes led to the isolation of a chiral hydrosilane with complete retention of configuration at silicon. The iron moiety was recovered in some cases as a phospha-ferracycle **159**. A mechanism involving a cyclometallation reaction to a hydrido-iron complex was proposed.

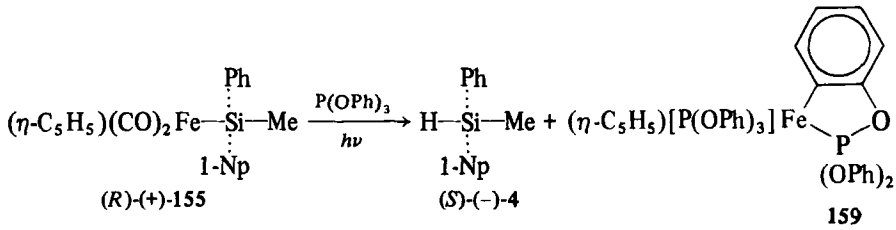

(*R*)-(+)-155 (*S*)-(−)-4 **159**

[69]

Formation of hydrosilanes then arises by a reductive elimination step, in agreement with the observed retention of configuration.

Formation of hydrosilanes has been extended to various phosphine reagents. Five-membered metallacycles are preferentially formed through abstraction of a hydrogen atom from an sp^2 carbon atom. The formation of a six-membered ring or abstraction of hydrogen from an sp^3 carbon atom is possible but requires higher energy. The use of 1-NpPhMeP as a reagent led to the formation of racemic mixtures of two diastereomeric phosphaferra-acenaphthenes **160** (Figure 16) which have been isolated by crystallization and identified by X-ray diffraction studies (237).

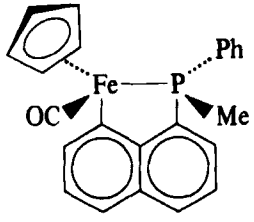

160 *Figure 16.* Cyclometalation product of 1-NpPhMeP.

b. Cobalt Complexes. Silyl–cobalt carbonyls have been obtained through the reaction of organosilicon hydrides with dicobalt octacarbonyl (238). From an optically active organosilicon hydride a chiral silylcobalt carbonyl was obtained (199) (eq. [70]). Phosphine-substituted cobalt complexes were similarly obtained by reaction of a chiral hydrosilane with $Co_2(CO)_6L_2$ ($L = PPh_3$, $P(OPh)_3$, $P(c\text{-}C_6H_{11})_3$) (239).

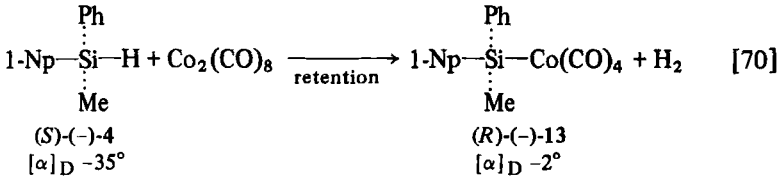

[70]

X-ray determination of the absolute configuration of complex **13** (240) allows one to assign retention of configuration at silicon in the reaction shown in equation [70].

Retention was also demonstrated in the analogous reaction of a chiral hydrogermane (241) on the basis of the configuration determined for the cobalt complex **161** (eq. [71]) (242).

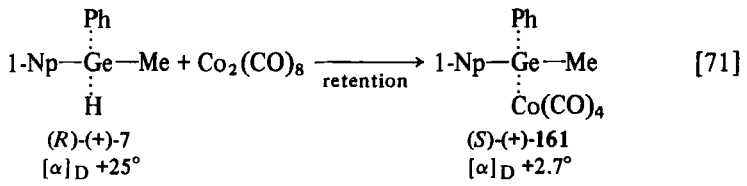

[71]

The reactions of silyl cobalt carbonyl **13** with electrophiles and nucleophiles have been examined (199, 241) and are shown in Scheme 53.

Electrophilic cleavages of the Si–Co bond occur with predominant retention of configuration at silicon. In contrast, nucleophilic cleavages take place with predominant inversion.

Interestingly, the reaction of carbon nucleophiles such as Grignard or lithium reagents have been shown to proceed differently (241, 243, 244). Several such reactions are summarized in Scheme 54.

Reactions of methyllithium or methyl Grignard reagents resulted in the formation of optically active silyl anions which were characterized after hydrolysis and reaction with allyl bromide (243). The observed overall predominant retention of configuration provides evidence for the optical stability of silyl anions. Their first preparation was reported by Sommer and Mason (245) and they appeared configurationally less stable than the chiral germyl anions (31).

In contrast with the above results, the reaction of phenyllithium led to the

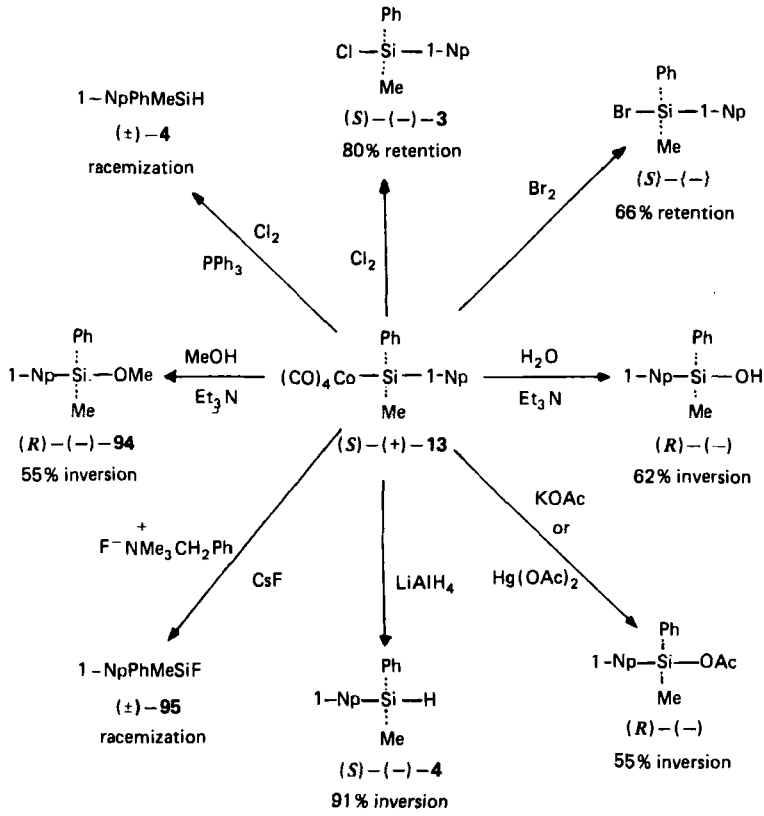

Scheme 53. Reactions of optically active 1-NpPhMeSi*-Co(CO)$_4$.

isolation of a benzoylsilane (244). Its formation proceeds with complete retention at silicon. It has been suggested to form via a benzoyl-silylcobalt carbonyl anion that was partially isolated from the reaction mixture. This is also supported by the preparation and X-ray characterization of trans di-apical germyl carbene complexes in the reaction of germylcobalt carbonyl analogs (246, 247) (eq. [72]).

$$(S)\text{-}(+)\text{-}(CO)_4CoGeR_3 \xrightarrow{n\text{-BuLi}} \xrightarrow{Et_3O^+} (S)\text{-}(-)\text{-}[n\text{-BuC(OEt)}](CO)_3CoGeR_3$$

$$R_3 = 1\text{-NpPhMe} \qquad [72]$$

c. **Platinum Complexes.** The importance of platinum-catalyzed reactions of organosilicon compounds prompted studies of silylplatinum complexes. This area was developed by Eaborn and co-workers.

Several optically active silylplatinum complexes have been obtained (211,

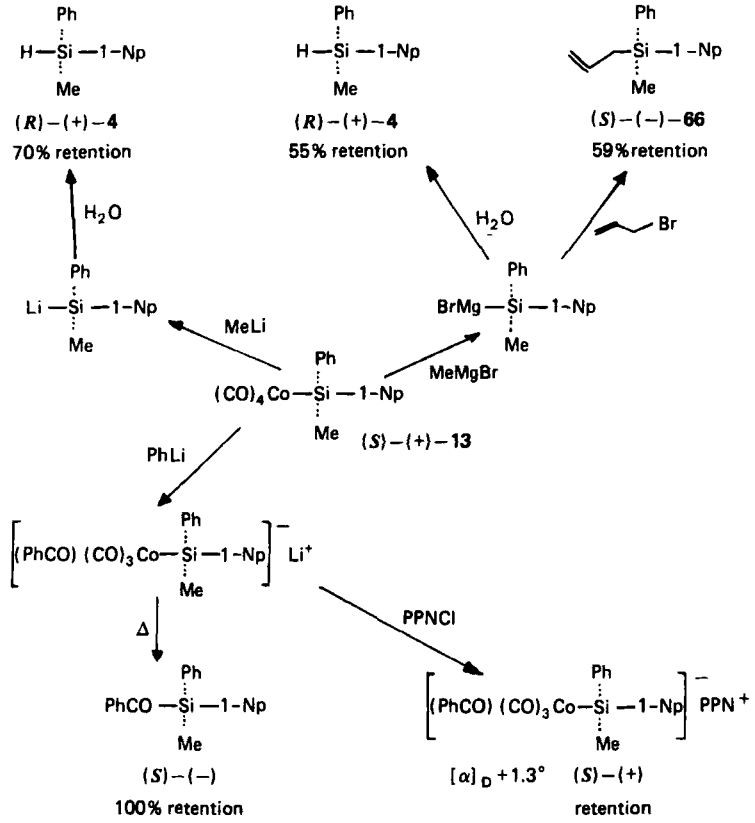

Scheme 54. Reactions of lithium and Grignard reagents with optically active 1-NpPhMeSi-$Co(CO)_4$.

248, 249). Their preparation always involves an initial oxidative addition of a chiral hydrosilane followed by ligand displacement. Complexes **132**, **162**, **163** were obtained according to equations [73]-[75] and have square planar geometry around the platinum atom. All these reactions were proposed to proceed with retention at the silicon atom. The X-ray structure determination of **132** (eq. [73]) confirmed the trans arrangement around platinum and the assigned retention at the silicon atom (210).

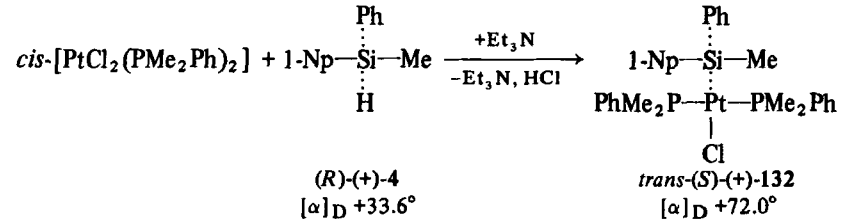

[73]

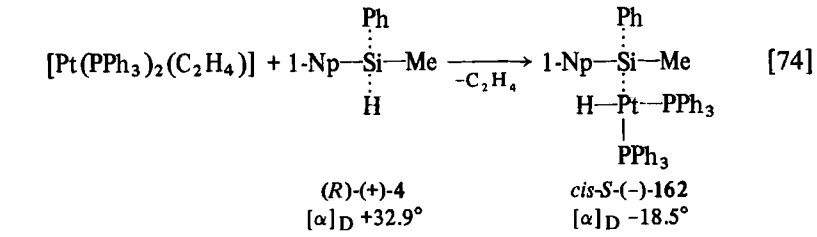

[74]

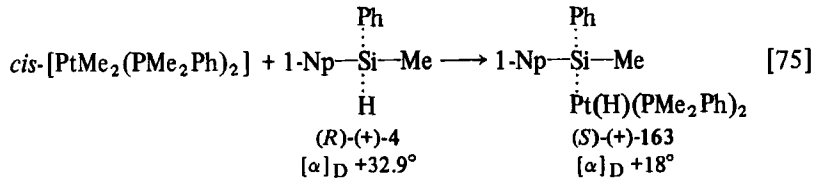

[75]

Complex **162** (eq. [74]) is less stable and dissociates in solution. An easy reductive-elimination process liberating the starting hydrosilane is consistent with the proposed structure in which the silyl and hydrido ligands are cis oriented.

The chemical reactivity of complexes **162** and **132** is depicted in Schemes 55 and 56.

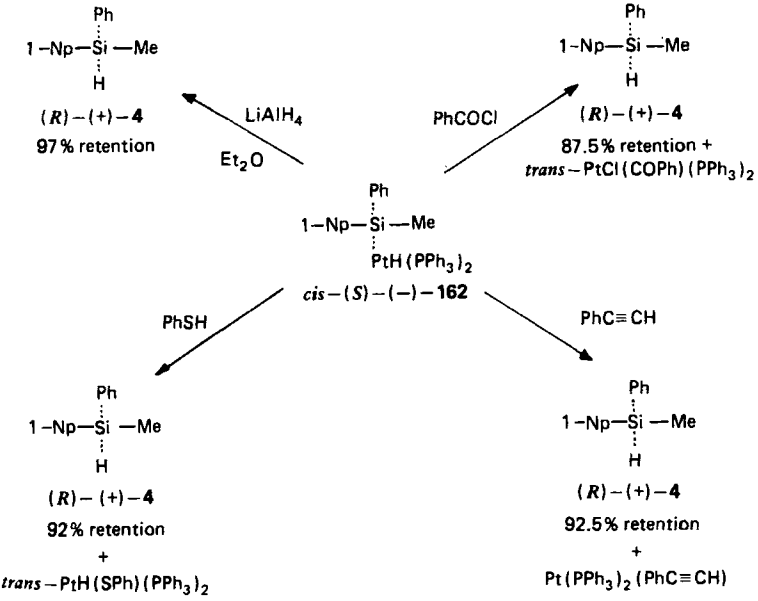

Scheme 55. Reactions of optically active platinum complex **162**.

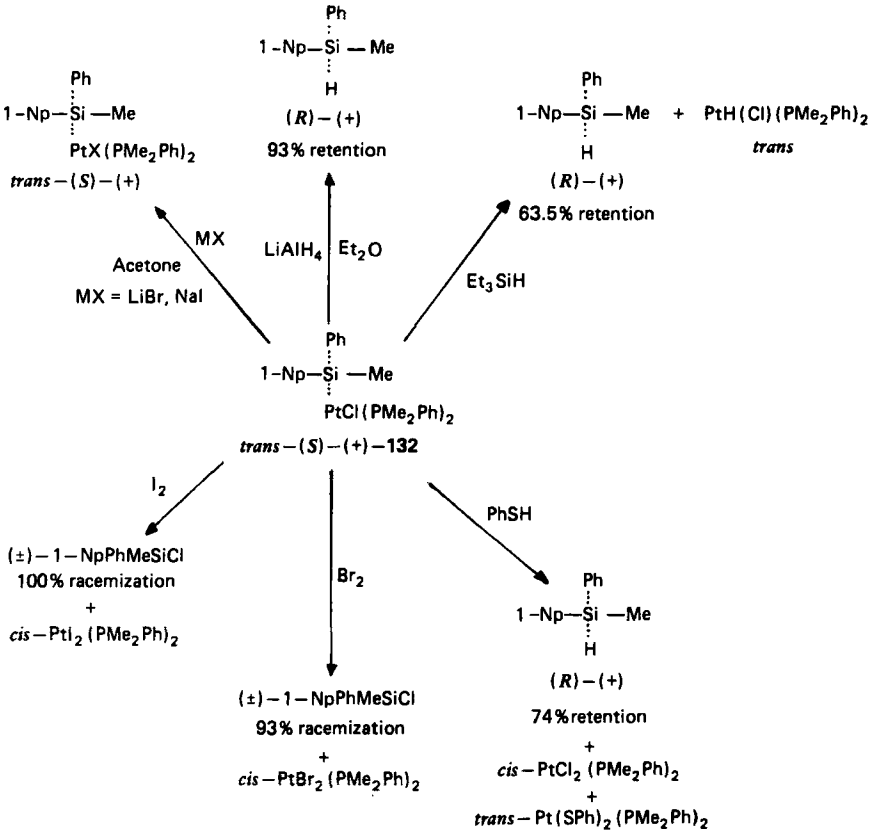

Scheme 56. Reactions of optically active platinum complex **132**.

Exchange of the chlorine ligand by bromine or iodine, without cleaving the silicon-platinum bond in complex **132**, has been achieved. Cleavage reactions with various reagents were shown to proceed with predominant retention of configuration at silicon. Only bromine and iodine cleavages occur with much racemization. No displacements of the silyl ligand with inversion were observed. Eaborn and co-workers suggested that the cleavage of the Si-Pt bonds involving reaction or formation of hydrosilanes may occur via oxidative-addition/reductive-elimination sequences. This is consistent with the complete or almost complete retention of configuration at silicon.

Although even in the $LiAlH_4$ cleavage of the Si-Pt bonds a reductive elimination process is likely to occur, since the configuration at silicon is almost completely retained, a nucleophilic displacement of the silyl ligand is still conceivable. Deuterium labeling experiments have unambiguously demonstrated this possibility in silyl-manganese complexes (213).

d. Manganese Complexes. Chiral silyl-manganese complexes have been obtained in two ways from optically active silicon hydrides. The reaction of metal carbonyl dimers with silicon hydrides (eqs. [76], [77]) leads to chiral complexes (239). The formation of the silyl-manganese complexes **164, 165** was presumed to proceed with retention of configuration at silicon.

The oxidative addition of silicon hydride to cyclopentadienyl manganese carbonyl also provide a convenient route to chiral complexes (213, 250) (eq. [78]).

Retention at the chiral silicon leading to complex **166** having the *S* configuration at silicon was proposed.

As shown in Scheme 57, complex **166** exhibits interesting reactivity. Different types of reagent were shown to react in two ways (213, 250): (i) Reagents giving substitution at silicon with cleavage of the Mn-Si bond; nucleophiles such as MeOH, H_2O, or $LiAlH_4$ fall into this category and cause inversion of configuration at silicon. (ii) Reagents leading to a reductive elimination of the organosilicon hydride. Surprisingly, both nucleophiles (MeLi, PPh_3) and electrophiles (Cl_2) may cause reductive elimination to take place. As expected for such a process, retention at silicon was observed.

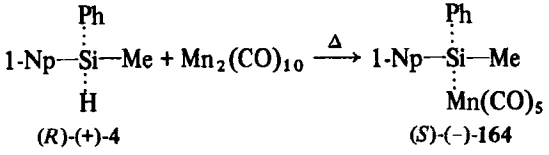

[76]

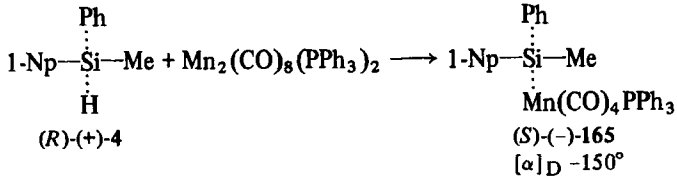

[77]

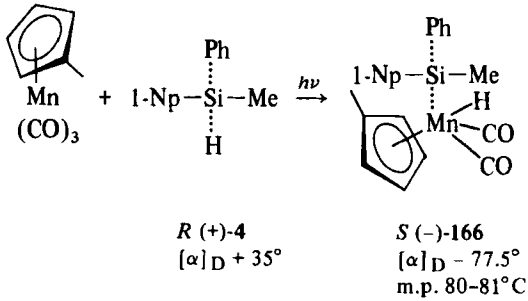

[78]

The easy reductive elimination process does not seem to arise from a particular lability of hydrosilane adduct **166**. Complex **166** is stable in solution. Moreover, functionalized silyl-manganese complexes were shown to undergo substitution at silicon without Si-Mn bond cleavage (251) (Scheme 58).

The particular chemical behavior of hydridosilyl-manganese complex **166**, which contrasts sharply with that of hydridosilyl-iron complexes (12, 252), has been interpreted in terms of a bonding interaction between hydrido and silyl ligands; this is detailed in Sect. IV-B-3 in connection with hydrosilylation processes.

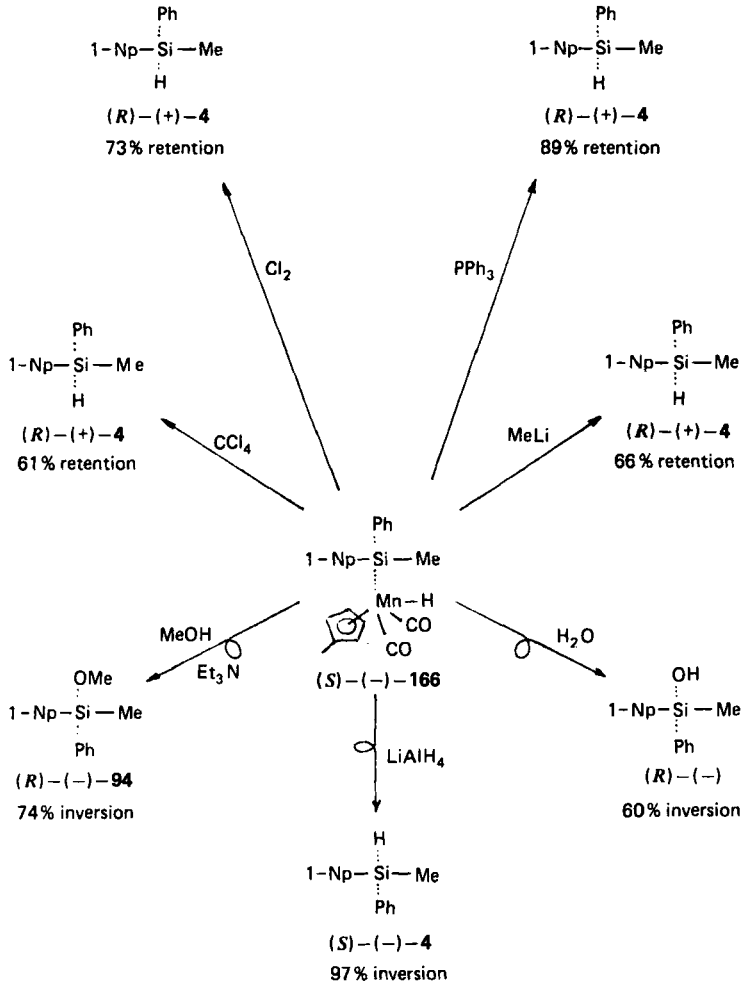

Scheme 57. Reactions of optically active manganese complex **166**.

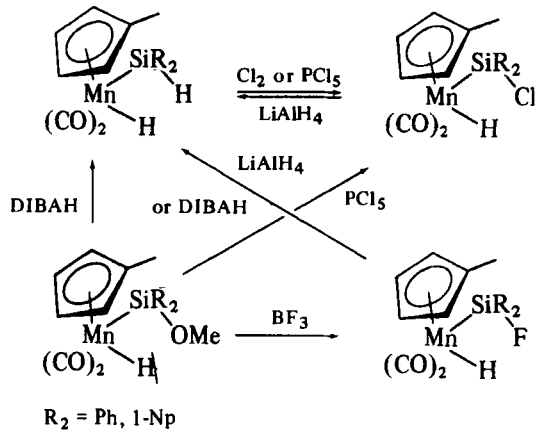

R_2 = Ph, 1-Np

Scheme 58. Substitution reactions at silicon in silylmanganese complexes.

2. *Displacement of Silyl Ligands*

A rationalization of the stereochemistry of the displacement of silyl ligands in silicon-transition metal compounds by various reagents may be difficult to come by. However the variety of experiments which have been performed makes some facts emerge and leads to a connection with the now well documented organic chemistry of silicon.

We must however keep in mind that some of the above reactions may not be simple reactions at the silicon atom, since transition metal complexes show multicenter reactivity (metal atom, ligands) as exemplified in the chemistry of triphenylgermyl-carbene complexes of cobalt carbonyl (253). Thus, displacements of a silyl ligand may result from a multistep process and a thorough examination of these reactions has to be made. An example can be drawn from molybdenum-germanium chemistry (247). As shown in Scheme 59, germanium is displaced from complex **167** by HCl with retention of configuration. Actually,

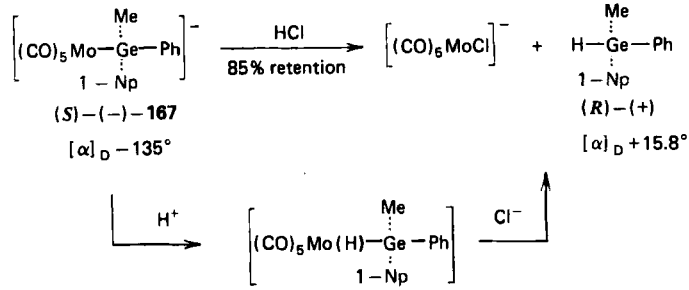

Scheme 59. Proposed pathway for the germyl ligand displacement in germylpentacarbonylmolybdenum anion.

this probably occurs in a two-step process through an intermediate germylmolybdenum hydride. The final hydrogermane results from a reductive elimination process in agreement with the observed retention.

The stereochemistry of displacement of chiral germyl ligand in germanium transition metal complexes [which has been reviewed elsewhere (12)] will also be discussed here, since silicon and germanium resemble each other and since complementary experiments have been undertaken.

a. **Electrophilic Displacement of Silyl Ligands.** Chlorine or bromine are reagents which displace the silyl ligand giving halogenosilanes and halides of transition metal complexes. As mentioned before, the electrophilic nature of these reagents seems established since no cleavage reaction was observed by chloride anion.

Results obtained in the chlorine cleavage of Si-Fe bonds (cf. Sect. IV-B-1a) are summarized in equation 79.

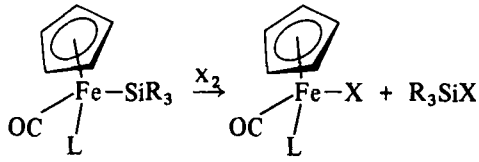

[79]

L	X_2	Predominant Stereochemistry at Si
CO or PR_3	Cl_2 or $Cl_2/AlCl_3$	Retention
CO or PR_3	Cl_2/PR_3	Inversion
$P(OEt)_3$	Cl_2	Inversion
$P(OEt)_3$	$Cl_2/AlCl_3$ or $Cl_2/P(OEt)_3$	Retention

Predominant retention or inversion at silicon was observed depending on the ligands attached to iron and on the nature of the reagent. By contrast the cleavage of Si-Co bonds (eq. [80]) was shown always to involve retention of configuration at silicon (239).

$$(CO)_3LCo—SiR_3 \xrightarrow{X_2} R_3SiX \qquad [80]$$

$L=CO, PPh_3, P(c\text{-}C_6H_{11})_3$ or $P(OPh)_3$ 75-84% retention

$X_2=Cl_2$ or $Cl_2/AlCl_3$

The results are of significance since stereoselectivities as high as 91% were obtained (though not in all cases) and since the products were shown to be optically stable under the reaction conditions.

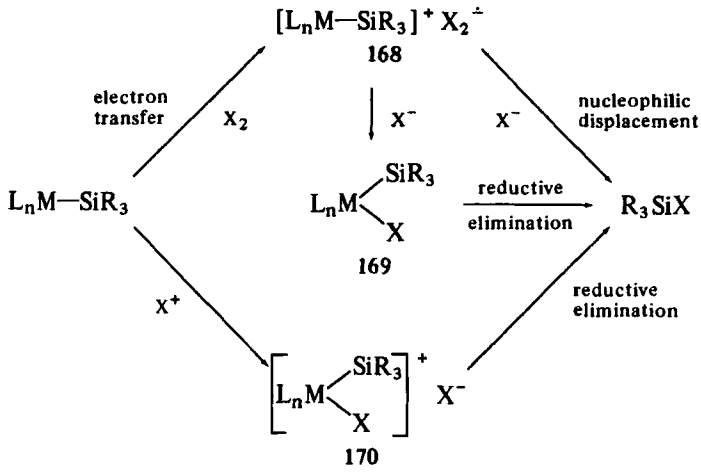

Scheme 60. Possible pathways for the electrophilic cleavage of silicon-transition metal bonds.

Reaction with Cl_2 or $Cl_2/AlCl_3$ probably involves initial attack of the electrophile Cl^+. However, in view of the oxidative properties of halogens, a mechanism involving electron transfer cannot be excluded. The exact mechanism of the reaction is difficult to determine. Possible pathways are represented on Scheme 60.

Electrophilic attack of X^+ will lead to a cationic intermediate **170** from which the product R_3SiX is formed upon reductive elimination. Such a pathway would be expected to involve retention at silicon.

An electron-transfer in the first step would give cationic intermediate **168**. Formation of R_3SiX may then arise via a direct nucleophilic displacement of the silyl ligand, or through the neutral intermediate **169** by a reductive-elimination process. Cleavage reaction may also occur by competitive pathways. In the present state of knowledge, since few experiments have been done, it is difficult to pinpoint definitive mechanisms.

b. Nucleophilic Displacement of Silyl Ligands. Nucleophilic substitution at silicon has been discussed in Section 2 and factors determining its stereochemical course have been pointed out. Nucleophilic displacement of silyl ligands in transition metal complexes may be considered similar, the transition metal moiety being the leaving group (eq. [81]). The stereochemistry of such nucleophilic reactions at silicon may be interpreted using the usual arguments (i.e., in terms of nature of the nucleophile, and electronic character of the leaving group). We will discuss here experiments which seem to fit with the current interpretations given for nucleophilic substitution at silicon.

$$L_nX_xM{-}SiR_3 \xrightarrow{Nu^-} L_nX_xM^- + Nu{-}SiR_3 \qquad [81]$$

The stereochemistry of the $LiAlH_4$ cleavage of Co-Si or Co-Ge bonds in $(CO)_3LCo\text{-}MR_3$ complexes has been shown to depend on the electronic environment of the transition metal center which is induced by the nature of the ligand (eq. [82]) (239, 254).

$$(CO)_3LCo{-}\overset{*}{M}R_3 \xrightarrow[Et_2O]{LiAlH_4} H{-}\overset{*}{M}R_3 \qquad [82]$$

L	Predominant Stereochemistry of Cleavage	
	M = Si	M = Ge
CO	91% Inversion	87% Inversion
$P(OPh)_3$	91% Inversion	87% Inversion
$P(OEt)_3$		65% Inversion
PPh_3	68% Inversion	60% Inversion
$P(t\text{-}Bu)_3$		63% Inversion
$P(c\text{-}C_6H_{11})_3$	58% Retention	Racemization
$P(n\text{-}Bu)_3$		58% Retention
$C(OEt)n\text{-}Bu$		55% Retention

The ligand L trans to the MR_3 group modifies the electronic character of the cobalt-silicon (germanium) bond. $(CO)_4Co^{\ominus}$ is a weak nucleophile and thus behaves as a good leaving group. Nucleophilic cleavage occurs with predominant inversion at silicon and with high stereoselectivity. Substitution of one carbonyl ligand by σ donor ligands (which are also less effective π-acceptors) results in increased electron density at the cobalt atom; $(CO)_3LCo^-$ thus becomes a poorer leaving group. This results in competing substitution with retention and thus in a decrease in stereoselectivity or even in inversion of the predominant stereochemistry. (i.e. 58% retention with $L = P(n\text{-}Bu)_3$).

In agreement with a nucleophilic substitution process at silicon, characteristic solvent effects have been observed. $LiAlH_4$ cleavages in dimethoxyethane always took place with inversion at silicon and with high stereoselectivity (239) (eq. [83]). Such behavior would be expected for a nucleophilic substitution at silicon in which increasing solvation of the nucleophile would cause the stereochemistry to be directed towards inversion of configuration. Cleavages with other nucleophiles (cf. Scheme 53) have also been observed to occur with predominant inversion (199, 241). For a given transition metal complex, nucleophilic displacements of silyl ligands occur with stereochemistry consistent with

the results observed in nucleophilic substitution at silicon and fitting with current mechanistic proposals.

$$(CO)_3LCo\text{—}\overset{*}{M}R_3 \xrightarrow[DME]{LiAlH_4} H\text{—}\overset{*}{M}R_3 \qquad [83]$$

L	Predominant Stereochemistry of Cleavage	
	M = Si	M = Ge
CO	94% Inversion	
$P(OPh)_3$		89% Inversion
$P(c\text{-}C_6H_{11})_3$	80% Inversion	81% Inversion
$P(n\text{-}Bu)_3$	82% Inversion	

A comparison of one transition metal with another seems more difficult. Predominant retention at silicon in the cleavage of the Si-Fe bond in complex **155** (cf. Scheme 52) is consistent with the above results with cobalt complexes, since $(\eta\text{-}C_5H_5)(CO)_2Fe^-$, a good nucleophile, is expected to be a bad leaving group. However the cleavage of the Si-Mn bond in a related manganese complex **166** (cf. Scheme 57) was observed to occur with inversion of configuration at silicon. This particular stereochemical behavior has been attributed to the existence of a bonding interaction between the Si and H atoms in this complex (cf. Sect. IV-B-3).

Interestingly, a new factor directing the predominant stereochemistry at silicon has been recently pointed out (255). The $LiAlH_4$ cleavages in hexacoordinated silyl-transition metal complexes were shown to proceed with predominant retention at silicon, whatever the ligands around the metal atom (eq. [84]). Stereoselectivity was low and no solvent effect was observed (similar results were obtained using DME). The octahedral geometry in these complexes seems to govern the stereochemical pathway. Other types of nucleophilic cleavage were shown to proceed similarly (255) (eq. [85]). A detailed interpretation of these results has not been given. However, nucleophilic substitution at silicon is currently accepted as a frontier orbital controlled process between the HOMO of the nucleophile and the σ^*Si-X antibonding orbital as LUMO. It may be considered that there are important differences in energy levels between octahedral and pentagonal complexes. Molecular orbital calculations might suggest a rationalization of these results.

3. Oxidative Addition and Reductive Elimination of Organosilicon Hydrides

As mentioned before, reactions of organosilicon hydrides with transition metal complexes represent a key step in catalytic hydrosilylation reactions. Cata-

$$(CO)_4LM_T-\overset{*}{M}R_3 \xrightarrow[Et_2O]{LiAlH_4} H-\overset{*}{M}R_3 \qquad [84]$$

L	M_T	M	Predominant Stereochemistry of Cleavage
CO	Mn	Si	68% Retention
PPh_3	Mn	Si	66% Retention
CO	Mn	Ge	57% Retention
C(OEt)Me	Mn	Ge	53% Retention
C(OEt)Me	Re	Ge	57% Retention
NO	W	Ge	67% Retention

$$(CO)_5Mn-\overset{*}{S}iR_3 \begin{cases} \xrightarrow{MeO^-/MeOH} MeO-\overset{*}{S}iR_3 & 53\% \text{ Retention} \\ \xrightarrow{MeOH} MeO-\overset{*}{S}iR_3 & 57\% \text{ Retention} \\ \xrightarrow{H_2O} HO-\overset{*}{S}iR_3 & 66\% \text{ Retention} \end{cases} \qquad [85]$$

lytic activation of silicon hydrides has been proposed to arise from an oxidative addition process to a transition metal center. Such a process has been shown to be reversible via a reductive elimination step (eq. [86]). The stereochemistry of addition to an iridium complex was shown to occur in a cis fashion (206) (eq. [87]).

$$R_3SiH + \diagup M \diagdown \rightleftharpoons \begin{matrix} R_3Si \\ | \\ \diagup M \diagdown \\ | \\ H \end{matrix} \qquad [86]$$

$$R_3SiH + \begin{matrix} H \\ | \\ Ph_3P \\ Ph_3P \end{matrix} \!\!\diagup\!\!\!\diagdown Ir-PPh_3 \; | \; CO \longrightarrow \begin{matrix} H \\ | \\ Ph_3P \\ Ph_3P \end{matrix} \!\!\diagup\!\!\!\diagdown Ir \begin{matrix} -H \\ -SiR_3 \\ | \\ CO \end{matrix} + PPh_3 \qquad [87]$$

A similar cis addition was established in the case of a rhodium complex (209).

As shown in Sect. IV-B-1, one of the main characteristics of oxidative addition as well as reductive elimination is that these processes occur with high stereoselectivity for optically active organosilicon hydride. Both processes involve retention of configuration about the silicon atom.

The detailed mechanism of oxidative addition is not known but it seems reasonable to assume that this is a simple one-step reaction. The above-mentioned stereochemical results allow one to reject a S_N2 type mechanism as was proposed for CH_3I oxidative addition reactions (256). Moreover, a nucleophilic at-

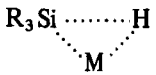

171 *Figure 17.* Three-center transition state for oxidative addition of R_3SiH.

tack of the transition metal center in the case of cationic complexes is hardly conceivable.

Cis addition and retention of configuration at silicon suggest that oxidative addition may occur through a three-center transition state **171** as in Figure 17.

An analogy with carbene insertion into Si-H bonds has been proposed by Eaborn and co-workers (211). Carbene insertions are supposed to involve a three-center mechanism and proceed with retention of configuration at silicon (257) (eq. [88]).

$$R_3\overset{*}{S}iH + CX_2 \longrightarrow \left[R_3Si\cdots\cdots H \quad CX_2\right] \longrightarrow R_3\overset{*}{S}iCX_2H \qquad [88]$$

A kinetic study by Harrod and Smith of oxidative addition to a square planar cationic iridium complex also supports the three-center mechanism (258). The rate law is first order in the iridium complex and first order in hydrosilane. Determination of the activation parameters indicated a moderate activation enthalpy ($\Delta H^{\ddagger} \simeq 5$-$6$ kcal/mol) and a large negative activation entropy ($\Delta S^{\ddagger} \simeq -47$ e.u.) No variations were observed on changing the solvent. Harrod and Smith concluded that oxidative addition proceeds via a concerted three-center transition state in which little bond-making or bond-breaking had occurred. The activation enthalpy was attributed to a deformation of the square planar complex on its approach to the transition state.

Interestingly, Harrod and co-workers (259) also compared the kinetics of triphenylphosphine and hydrosilane addition to a neutral iridium complex (eq. [89]). The kinetic parameters for the phosphine and silane reaction were almost identical: $\Delta H_p^{\ddagger} - \Delta H_{Si}^{\ddagger} = 0$ kcal/mol and $\Delta S_p^{\ddagger} - \Delta S_{Si}^{\ddagger} = 13$ e.u. This striking similarity is not necessarily proof that phosphine and silane addition are mechanistically analogous processes. However, this kinetic behavior is consistent with the above description of oxidative addition.

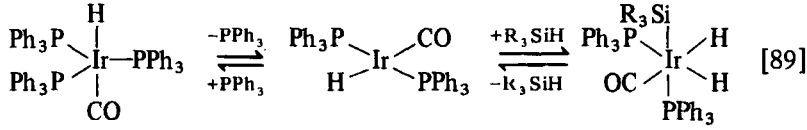

[89]

In connection with the similarity with simple coordination of two-electron ligands, it is of interest to discuss the oxidative addition of silicon hydride to

cyclopentadienylmanganese carbonyl and the nature of the bonding in the adduct. Hydrido silyl-manganese complexes **172** were first prepared by Jetz, Graham, and co-workers according to equation [90] (260). These complexes have been shown to undergo reductive elimination of R_3SiH readily upon reaction with various electrophilic or nucleophilic reagents (213, 261) (cf. Sect. IV-B-1-d).

$$R_3SiH + (\eta\text{-}C_5H_5)(CO)_3Mn \xrightarrow{h\nu} \underset{(CO)_2 \quad H}{\overset{SiR_3}{Mn}} + CO \qquad [90]$$

R = Cl, Ph — **172**

The hydrido ligand in these complexes exhibits weak acidic character. Abstraction of H^+ only occurs with strong bases (252) (eq. [91]). This chemical behavior contrasts sharply with that of a related hydrido silyl iron carbonyl **173** (12, 252) (eq. [92]). Complex **173** reacted with two-electron ligands without reductive elimination and appeared to be a stronger acid than HCl.

$$\text{no reaction} \xleftarrow{Et_3N} \underset{(CO)_2 \quad H}{\overset{SiR_3}{Mn}} \xrightarrow{HNa} \left[\underset{(CO)_2 \quad SiR_3}{Mn}\right]^- Na^+ \qquad [91]$$

$$(CO)_4Fe(H)(SiPh_3) \xrightarrow{L} L(CO)_3Fe(H)(SiPh_3) \qquad [92]$$

173

$$(CO)_4Fe(H)(SiPh_3) \xrightarrow{Et_4NCl \text{ or } Et_3N} [(CO)_4Fe{-}SiPh_3]^-$$

Of interest also is the intramolecular hydrogen-deuterium exchange invoked to explain the reactions depicted in equation [93] (262). Reactions of complexes **174** and **175** led to an equimolar mixture of complexes **176** and **177** indicating that these two compounds are in equilibrium. An intermolecular exchange has been rejected on the basis of the findings shown in equation [94]. The above exchange thus occurs within the coordination sphere of manganese and does not involve formation of free hydrosilane by a reductive elimination process. The

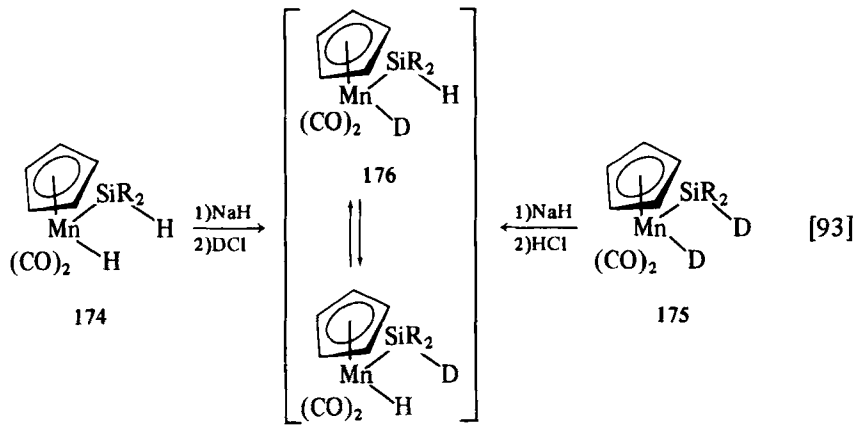

[93]

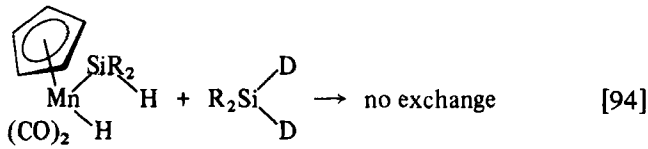

[94]

existence in the ^{1}HNMR spectra of compounds **174**, of two signals, Mn-*H* and Si-*H*, with a 4.5 Hz coupling constant, indicates that the exchange is slow on the NMR time scale.

The particular chemical behavior of hydrido silyl-manganese complexes has been related to their molecular structure determined by X-ray or neutron diffraction analysis. The hydrido and silyl ligands are cis oriented and the principal distances are given in Table 33. According to Jetz and Graham the hydrido ligand, while being located at a "normal" distance from the manganese atom, was close enough to silicon to imply some degree of bonding. The short Si-H dis-

Table 33

Principal Distances (Å) in 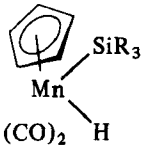

R_3	Ph_3	Cl_2Ph	FPh_2
Mn-Si	2.42	2.31	2.35
Mn-H	1.55	1.49	1.57
Si-H	1.76	1.79	1.80
Ref.	(261)	(261)	(263)

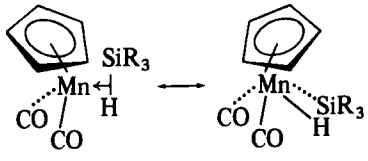

178 179

Figure 18. Representation of the structure of silyl-manganese complexes **172.**

tance in manganese complexes contrasts with the 2.73 Å found in iron complex **173.** Support for this idea comes from a ^{29}Si NMR study of complexes **172** (262). J(Si-H) coupling constants of 65 and 69 Hz were measured, representing higher values than expected for a ^{2}J(Si-Mn-H) coupling constant.

To explain their results, Hart-Davies and Graham proposed to depict manganese complexes **172** in terms of resonance hybrids between representations **178** and **179** (261) (Figure 18). However, the possibility that the close Si-H distance is due to steric constraints has been raised by Bennett and Simpson (264). Steric effects favor a cis orientation of silyl and hydrido ligands and thus facilitate reactions involving reductive elimination pathways.

The situation has also been discussed by Andrews, Kirtley, and Kaesz (265) and Harrod et al. (259) in terms of "incomplete" oxidative addition of R_3SiH to the manganese atom. Owing to steric crowding, the compound arising from an oxidative addition process is proposed to represent a case where the descent to the energy minimum is arrested at some point along the reaction coordinate, before complete separation of the Si-H bond.

In a more recent proposal from our group, a description of the bonding as a two-electron three-center Mn(μH)Si has been suggested (213, 251, 262) (Figure 19). Such a representation would account for the above-mentioned chemical and physical properties of these complexes. A similar suggestion has been put forward in the case of silyl-diplatinum complexes, where a Si-H distance of 1.72 Å was found (266).

Compounds of this type may be related to the heterogeneous transition metal catalyzed reaction of hydrosilane. They may represent a "nondissociative" activation process, and a possible parallelism can be drawn with heterogeneous activation of metal surface. Reactions of hydrosilanes with nucleophiles in the presence of heterogeneous catalysts were shown to occur with inversion at silicon (cf. Sect. IV-A-2). This was proposed to arise from an adsorption of the hydrosilane to the metal surface, followed by a back-side attack of the nucleophile. It

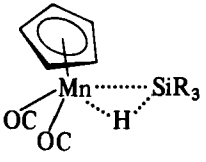

Figure 19. Representation of complexes **172** as a two-electron three-center Mn(μH)Si bond.

is noteworthy that manganese complexes **172** undergo nucleophilic displacement of the silyl ligand with inversion of configuration at the silicon atom (cf. Sect. IV-B-1-d) contrasting with related iron complexes (cf. Sect. IV-B-1-a).

V. HYPERVALENT SILICON SPECIES AS INTERMEDIATES IN THE REACTIONS OF ORGANOSILICON COMPOUNDS: DYNAMIC STEREOCHEMISTRY OF PENTACOORDINATE ORGANOSILICON

The ability of the silicon atom to increase its coordination number was recognized many years ago; penta- and hexacoordinate species have been isolated (267). However, it was more or less accepted that this expansion of coordination was implicated only when the silicon atom is surrounded by electronegative groups (267) and all attempts to access hypervalent silicon species were designed accordingly.

In the past few years, numerous experimental results have illustrated the fundamental importance of penta- and hexacoordinate silicon species in reactions at silicon. The implication of pentacoordinate intermediates in substitution reactions at silicon is now well accepted (10, 11); the nucleophilically induced racemization (13, 268) and hydrolysis (or alcoholysis) of halosilanes (268, 269), both controlled by entropy factors, take place through expansion of coordination at silicon. Pentacoordinate species with two or three carbon atoms attached to silicon have been isolated (129, 155); and finally, five-coordinate anions with five carbon atoms around silicon have been identified in the gas phase (107). This shows how much the expansion of coordination at silicon is an energetically favorable process.

At the same time, synthetic methods using the efficacy of nucleophilic agents in the activation of various silicon-element bonds, such as Si-H, Si-O, Si-N, and Si-C, were developed. The activation of these bonds was used as a tool for reduction of carbonyl compounds (271-273), Michael condensations (274, 275), and formation of heterodienes by cleavage of the Si-N bond (276). The activation of the Si-C bond has received particular attention, as illustrated by the cleavage of the Si-allyl bond (277) and the use of pentafluorosilicates as synthetic intermediates (278).

In this context, the existence of stable penta- and hexacoordinate silicon derivatives and their structure have elicited considerable interest. Isomerization processes of these compounds are also of importance, since penta- or hexacoordinate intermediates are implicated in the substitution and racemization of tetracoordinate silicon derivatives. For all these reasons, we include here (i) some available structural data for hypervalent silicon compounds (the review is not intended to be exhaustive), (ii) recent reports concerning the nucleophilically induced substitution and racemization reactions at silicon, and (ii) a criti-

cal discussion of recent studies of the dynamic stereochemistry of pentacoordinate organosilanes.

A. Penta- and Hexacoordinate Silicon Species

1. Pentacoordinate Silicon Species

Finely divided silica was first reported by Rosenheim et al. to react with catechol in the presence of various bases to yield crystalline salts (279). Frye (280) confirmed and extended this work, using alkoxysilanes as starting materials. A pentacoordinate anionic structure has been proposed. The X-ray structure was established for the bis(*o*-phenylenedioxy)phenyl siliconate (281); the geometry is a distorted trigonal bipyramid **180** (Figure 20). The axial Si-O bonds (1.794 Å) are about 5.5% longer than the equatorial ones (1.700 Å). The O-Si-O angles in the five-membered rings are 87.6°, while the angle formed by the two axial oxygens (167.7°) is bent from the 180° characteristic of an ideal trigonal bipyramid.

The presence of hypervalent silicon derivatives of aliphatic 1,2-diols in solution was inferred by Meerwein (282) and convincingly demonstrated by Müller and Heinrich (283). In more recent work, Frye describes the preparation of such stable, easily isolated, pentacoordinate silicon derivatives as **181** and **182** (284) (Figure 21). Silicon here appears to exhibit a maximum coordination number of five.

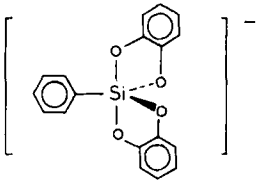

180

Figure 20.

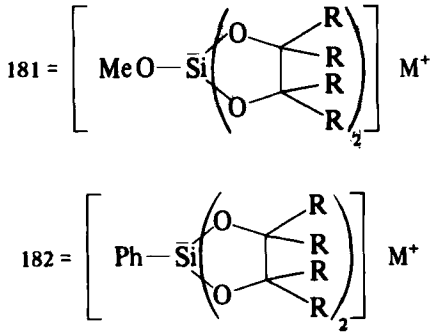

(M^+ = alkyl ammonium cation, R = H, Me, F)

Figure 21. **Preparation of stable, easily isolated, pentacoordinated silicon derivatives.**

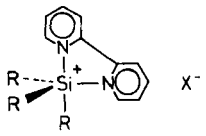

183 X = Br

184 X = I *Figure 22.*

Several other pentacoordinate silicon species have been described, including, for example, complexes of fluoride ion (285-287), amines (288-296), pyridine (297), and bipyridyl (298). The first formation of a pentafluorosilicate, SiF_5^-, was reported by Clark et al. (299). Since this initial work, detailed chemical and spectroscopic investigations (infrared, Raman, fluorine and proton NMR spectra) have been found to be consistent with trigonal bipyramidal geometry for this species (285, 300) (resembling that of PF_5^-). Alkyltetrafluoro- and dialkyltrifluorosilicates, $RSiF_4^-$ and $R_2SiF_3^-$, have also been reported (285). Triphenylbromo- or iodosilane and 2,2′-bipyridine in dichloromethane give the adducts triphenyl (bipyridyl) silicon iodide and bromide, which are completely dissociated in this solvent yielding the stable pentacoordinate ion $[Ph_3Si(bipy)]^\bullet$ (compounds **183** and **184**) (298) (Figure 22). Various 1 : 1 adducts of SiF_4 or $SiCl_4$ with amines or phosphines have been prepared (294); their infrared spectra are consistent with C_{3v} symmetry, implying trigonal bipyramidal 5-coordinate structures with amines or phosphines in the apical position. Other interesting examples of pentacoordinate silicon complexes of amines are illustrated by the crystal and molecular structures of the *N*-trifluorosilyltrimethylphosphinimine dimer **90** (132) and of 1,2,3,4-tetrahydro-1-(trifluorosilyl)-1,10-phenanthroline **91** (131) (Figure 23).

An interesting group of chelate compounds derived from triethanolamine, called silatranes, were first recognized by Frye et al. (301); major studies of these compounds were performed by Voronkov (302), and other Soviet chemists. Pertinent structures are shown in Figure 24. Considerable evidence has been amassed to indicate the presence of a dative bond between nitrogen and silicon, involving the lone electron pair of nitrogen and an empty orbital on silicon: a *d* orbital of silicon may be invoked (302, 307-310). X-ray diffraction studies provide direct evidence for the existence of this transannular Si ← N bond and show that the coordination at silicon in these structures is of a distorted trigonal bipyramidal type (305, 311-314). The Si-N bond distances between 2.023 and 2.344 Å, are considerably longer than the Si-N distances in silylamines [1.65 Å in $NMe_2(SiF_3)$ (315) to 1.767 Å in $N(PF_2)_2(SiH_3)$]. Structural studies of silatranes have also demonstrated the variable dependence of the Si-N bond length upon the substituents at silicon and the basicity of the nitrogen donor (312, 314, 316). A study of the ^1H, ^{13}C, and ^{29}Si NMR spectra show that Si ← N in-

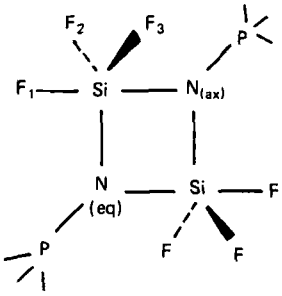

90

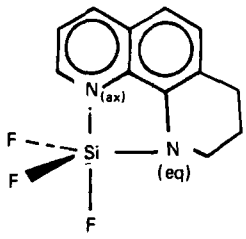

91

$F_1-Si-N_{eq} = 93.4°$ [4]

$N_{eq}-Si-N_{ax} = 79.4°$

$Si-N_{ax} = 1.857$ Å

$Si-N_{eq} = 1.736$ Å

$N_{ax}-Si-F_1 = 178.2°$

$N_{ax}-Si-N_{eq} = 83.9°$

$Si-N_{ax} = 1.969$ Å

$Si-N_{eq} = 1.732$ Å

Figure 23.

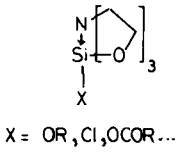

185

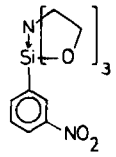

186

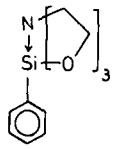

187

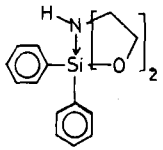

188

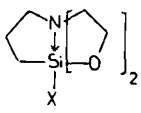

189

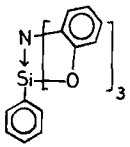

190

Figure 24.

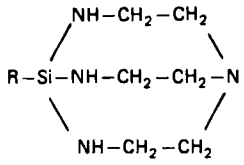

(R = H, CH_3, C_2H_5, CH_2=CH, C_6H_5)

191 *Figure 25.*

teraction in these compounds is strongly influenced by the electronic effects of the Si and N substituents and, in particular, by the steric effects of the latter (312, 314). Thus, ^{1}H, ^{13}C, and ^{29}Si spectra of 2,5,8,9-tetraaza-1-silatricyclo-(3.3.3.0)undecane **191** (Figure 25), which is formally a triaza analog of the silatranes, indicate that the transannular N → Si interaction in this compound is even stronger than in the corresponding silatranes (317).

An intramolecular coordination of a Lewis base atom affording pentacoordinate silicon similar to the situation in silatranes has been established for cyclobis(benzamidodimethyl)silane **192** (318) and, more recently, for a new class of organosilicon compounds (aroyloxymethyl)trifluorosilanes **193** (319) (Figure 26). The pentacoordinate character of silicon in compounds **192** and **193** has been confirmed by X-ray diffraction. In the latter case, the Si ← O bond length is 1.94 Å which is much less than the sum of van der Waals radii (3.4 Å) for silicon and oxygen. Similarly, the product of the reaction of bis-(trimethylsilyl)-

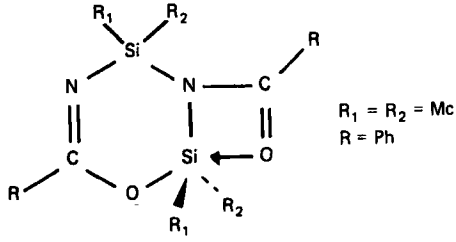

192

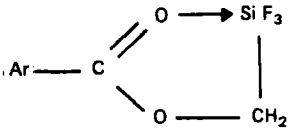

193 *Figure 26.*

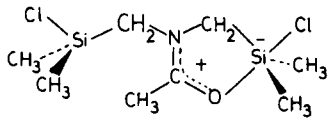

86

Figure 27.

acetamide with chlorosilane was found to have structure **86** with a pentacoordinate silicon, the carbonyl being coordinated to one of the silicon atoms in a planar five-membered ring; chlorine and oxygen occupy axial sites (129, 320) (Figure 27).

Although anionic, pentacoordinate silicon species have received attention, the isolation of siliconates **194**, **103**, **195**, **196** (Figure 28) by Perozzi, Martin and colleagues (155) has provided an opportunity to study in detail both structure and stereomutation of a pentacoordinate silicon compound (155, 321). This point will be discussed further in Sect. V-C. The crystal structure of **195** shows that the silicon is pentacoordinated with the fluorine and the two carbon atoms forming the equatorial plane of a somewhat distorted trigonal bipyramid (321). It is essentially the same as that proposed for similar siliconates on the basis of NMR data obtained in the solution phase (155).

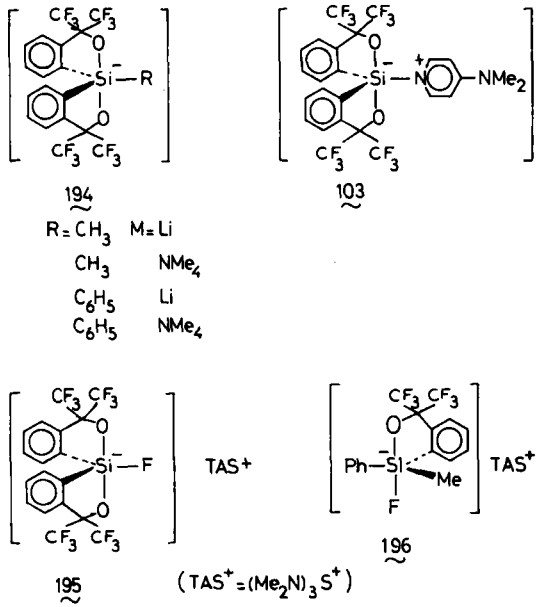

Figure 28.

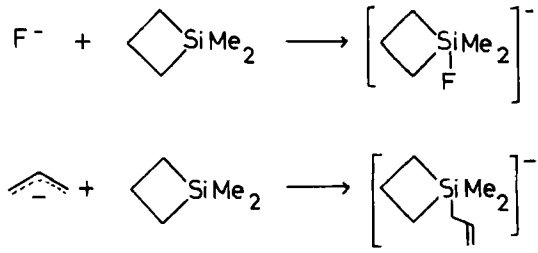

Scheme 61.

Finally, we wish to mention that a large number of organic pentacovalent silicon anions, including silicon anions with five carbon substituents, can be generated cleanly in the gas phase (107). Direct addition of F^- or of the allyl anion occurs leading to anions formulated as pentacoordinate silicon species (Scheme 61). The results suggest that the formation of pentavalent silicon anions is a general feature, extending even to cases where silicon anions bear five carbon substituents.

2. *Hexacoordinate Silicon Species*

Six-coordinate silicon compounds result only when the silicon atom is bonded to highly electronegative atoms like fluorine, chlorine, oxygen, or nitrogen. A well-known example of this is the fluorosilicate anion SiF_6^{2-}, in which the fluorines are located in an octahedral array about silicon (322). The existence of $(PhSiF_5)^{2-}$ in solution also has been confirmed by ^{19}F NMR spectroscopy (322).

The silicon catecholates **197** (Figure 29) are typical species in which silicon exhibits a coordination number of six (323). Characterization relies on elemental analysis and differences in IR, UV, and ^{29}Si NMR spectra compared with typical tetravalent silicon compounds (324, 325). The crystal structure of pyridinium tris(*o*-phenylenedioxy)siliconate, $[C_6H_5NH]_2^+$ $[(C_6H_4O_2)_3Si]^{2-}$ indicates hexacoordinate silicon dianions (326). A similar structure is assumed for **198** (325, 327) (Figure 30).

Cationic complexes are formed with 1,3-diketones, 2-hydroxypyridine *N*-oxide and tropolones (325). For example, tris(acetylacetonato)silicon (IV) chlo-

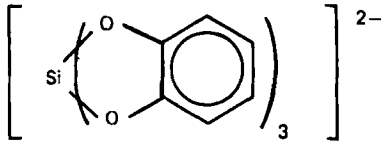

197 *Figure 29.*

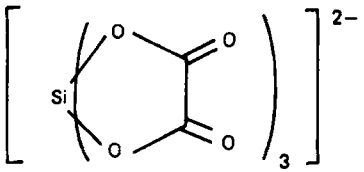

198

Figure 30.

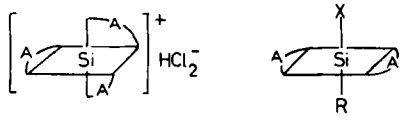

199 200

Figure 31.

ride hydrochloride was first prepared by Dilthey in 1903 (328). Since that time, a number of structurally related cationic hexacoordinate tris(1,3-dicarbonyl) and tropolonato chelates have been prepared and characterized by infrared analysis, partial resolution, and more recently by NMR spectroscopy (325, 329-332). Structures **199** and **200** (Figure 31) were proposed for the unsubstituted derivatives $SiA_3Cl \cdot HCl$ (A = 1,3-dicarbonyl ligand) and for monoalkyl compounds of the type $RSiA_2Cl$, respectively.

Tropolonato chelates, **201** (Figure 32) were first reported by Muetterties and Wright (332). All available spectroscopic data (infrared, ^1H, and ^{29}Si NMR) suggest a cationic octahedral structure around silicon. Analogous tropolonato chelates seem to have been isolated from plants and compared with the synthetic compounds (323).

Neutral complexes are also known in which silicon is hexacoordinate. Pike and Luongo found that tetracarboxysilanes undergo a general reaction with various 1,3-diketones to yield neutral silicon chelate derivatives **202** (330) (Figure 33). A hexacoordinate structure is assumed on the basis of IR and NMR spectral and chemical evidence (325, 330).

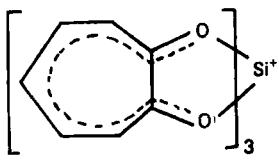

201

Figure 32.

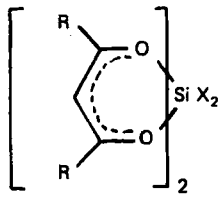

202

Figure 33.

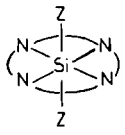

203

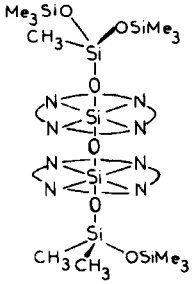

204

Figure 34.

Six-coordinate silicon atoms are also reported in complexes formed by tetradentate ligands, as in Si phorphyrins and Si phthalocyanines (333); their geometry is governed by the planar macrocycle and the free coordination positions are axial trans and may be occupied by F, $OSiR_3$, or $-(O)_2-$ (structures **203** and **204**, Figure 34). An interesting group of octahedral chelates was systematically and comprehensively studied by Kummer and co-workers. These studies led to the discovery of several 1,10-phenanthroline (**205**) and 2,2′-bipyridine (**206**) complexes of silicon (334). Some examples are summarized below (Figure 35). UV, IR, ESCA, ^1H, and ^{29}Si NMR spectra of these complexes were investigated in detail. The complexes are ionic, and structural investigations indicate *cis*-

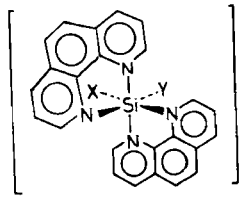

205

X	Y
Cl	Cl
CH_3	Cl
CH_3	CH_3
CH_3	OCH_3
OH	OH
OCH_3	OCH_3

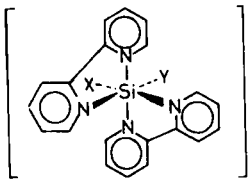

206

X	Y
Cl	Cl
Cl	CH_3
Cl	H
H	H
H	CH_3
CH_3	CH_3
C_6H_5	CH_3
OCH_3	CH_3
OCH_3	H

Figure 35.

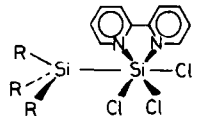

207

Figure 36.

octahedral silicon cations. The X-ray study of $[Si(OH)_2(bipy)_2]I_2, 2H_2O$ has confirmed the *cis*-octahedral geometry of the silicon cation (335). Such octahedral geometry had previously been reported for the tetrafluorobispyridinesilicon complex (336). Amine complexes of perhalodisilanes, Si_2F_6, Si_2Cl_6, and Si_2Br_6 are also known (337); 1 : 1 complexes are obtained exclusively. The structure of these complexes involves coordination of the base to the more acidic silicon and alignment of the Si-Si axis perpendicular to the plane of the bipyridyl ligand (structure **207**, Figure 36) (338). In the case of $Si_3Cl_8 \cdot$ bipy, spectroscopic and chemical evidence suggests bipy coordination to the center silicon (337). D. Kummer et al. have obtained, in high yield, $[Si(bipy)_3]^{4+}$ and $[Si(phen)_3]^{4+}$ complexes; spectroscopic investigations (IR, UV, and ^1H NMR) prove the presence of octahedral complex cations of charge +4 (339).

B. Penta- and Hexacoordinate Silicon Species as Intermediates in the Reactions of Organosilicon Compounds

1. Nucleophilically Induced Racemization at Silicon

Racemization of optically active halosilanes was first recognized by Sommer et al. (1-2). Methylphenyl-1-naphthylfluorosilane is racemized by hydroxylic reagents (H_2O, ROH) (1,340). (-)-Methylphenyl-1-naphthylchlorosilane $R_1R_2R_3Si^*$-Cl loses its optical activity in aprotic solvents such as CH_3NO_2, CH_3CN, CH_3COCH_3 (13); the ions Cl^-, Br^-, and I^- can also cause racemization of $R_1R_2R_3Si^*$-Cl (13). More recent data have been discussed in detail in a comprehensive review (13).

A second-order rate equation has been obtained for the racemization of various chloro- and bromosilanes induced by nucleophiles (HMPT, DMSO, DMF) (13, 268-269),

$$v_{rac}^{Si} = k_{rac}^{Si}[Nu]^2[R_3Si{-}Cl] \qquad [95]$$

Nu = HMPT, DMSO, or DMF

The efficiency of the racemizing reagents is HMPT > DMSO > DMF. The ability of the halosilanes to be racemized is Si-Br > Si-Cl >> Si-F. The process is controlled by entropic factors ($\Delta S^{\ddagger} \simeq -60$ e.u.), suggesting a highly organized tran-

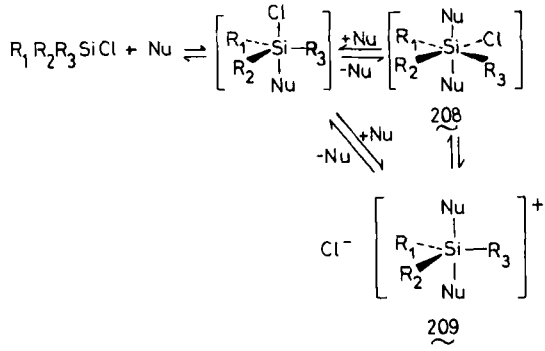

Scheme 62.

sition state; in contrast, the activation energy is very low ($\Delta H^{\ddagger} \simeq 3$ kcal/mol). Moreover, the solvent-induced racemization is a general process; triorganogermanium and tin chlorides behave similarly (268–269).

The data are interpreted by a reversible formation of a pentacoordinate silicon intermediate followed by attack of a second molecule of nucleophile in the rate-determining step, involving either a symmetrical octahedral intermediate **208** or a pentacoordinate siliconium ion **209** (Scheme 62). In either case, racemization takes place.

2. *Nucleophilic Activation at a Silicon Atom in Nucleophilic Substitution Reactions* ($SN_{NA}Si$)*

Hydroxylic solvents are able to promote heterolytic Si-X bond cleavage (X =F or Cl) (1, 268). The kinetics have been studied extensively and the activation of the reaction by an additional nucleophile has been observed (268, 269, 341, 342). A mechanism, involving an increase of the nucleophilicity of the alcohol by hydrogen bonding, has been proposed (Scheme 63) (103, 341). Alternatively, a pentacoordinate intermediate has been invoked (1, 342) (Scheme 64). Discrimination between the two above interpretations has recently been provided; good evidence for the nucleophilically induced process at silicon has been presented (268, 269, 343).

Under experimental conditions used for polarography, hydrolysis of halosilanes by residual water present in the solvents occurs (343). HCl is produced and a wave appears at -1.4 V (vs. SCE) increasing with time; this wave corresponds to the electroreduction of HCl (Scheme 65). When HMPA, DMF, or DMSO, that is, reagents which are known to be good coordinating species, are

*$SN_{NA}Si$ = Nucleophilic substitution at silicon activated by nucleophiles.

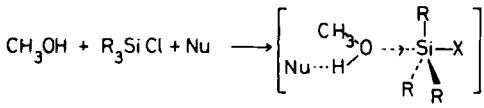

Scheme 63.

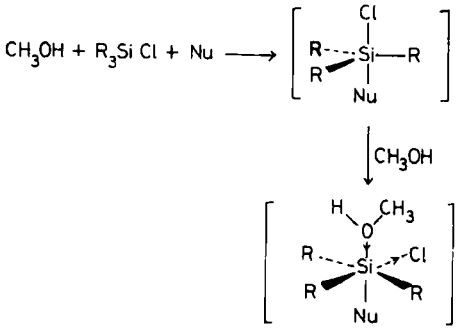

Scheme 64.

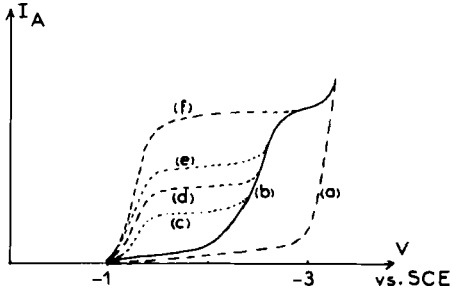

Scheme 65. Polarograms of (*a*) 0.1 M TBAP, DME solution; (*b*) with 7 Mm Ph_3SiCl; (*c*) after 30 mn; (*d*) after 60 mn; (*e*) after 90 mn; (*f*) with 7 mM Ph_3SiCl + 0.3 mM HMPT after 10 mn.

added, hydrolysis is quantitative and very fast; a 10^2-10^3 fold rate acceleration is observed for a 10^{-4} *M* concentration in HMPA*.

A detailed examination of the features concerning nucleophilically activated racemizations and hydrolysis (or alcoholysis) of chlorosilanes led to the following observations (268): (i) Kinetic data for racemization (eq. [96]) and for hydrolysis (eq. [97]) indicate very similar processes:

$$v_{rac}^{Si} = k_{rac}^{Si}[R_3SiCl]\ [Nu]^2 \qquad [96]$$

$$v_{H_2O}^{Si} = k'_{H_2O}{}^{Si}[R_3SiCl]\ [H_2O]\ [Nu] \qquad [97]$$

*These polarographic data–quantitative hydrolysis of halosilanes when a nucleophilic catalyst (HMPA) is present–give rise to a new method for the determination of water concentration in organic solvents (343) that is as sensitive as the Karl Fischer method.

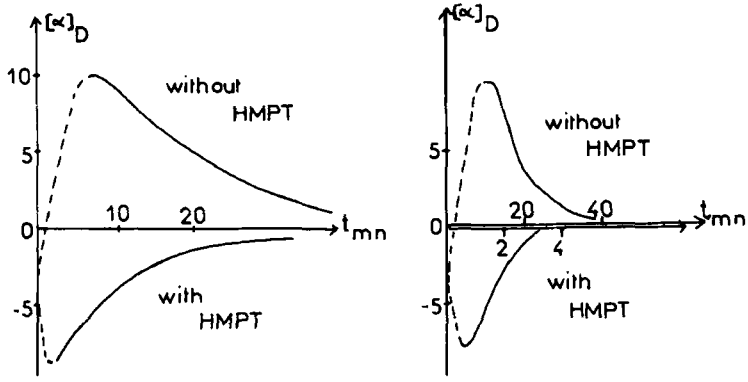

Figure 37. Tertiobutanolysis (left) and methanolysis (right) of (+)-1-NpPhMeSiCl.

(ii) The activation parameters, $\Delta H^{\ddagger} < 3$ kcal/mol and $-60 < \Delta S^{\ddagger} < -50$ e.u., indicate very similar processes, both controlled by entropic factors. In some cases, negative $\Delta H^{\ddagger}$'s have been observed; the rate increases when the temperature decreases (iii) The presence of a nucleophile such as HMPA changes the stereochemistry of hydrolysis or alcoholysis. Retention is observed (before subsequent racemization) instead of inversion, which normally takes place in the absence of nucleophilic catalysis (Figure 37). The observed racemization is only a second step, that is, it involves the reaction products (344). Alkoxysilanes are known to be racemized with an excess of alcohol in the presence of traces of HCl (Scheme 66) (13).

For explaining both the racemization scheme and the retention of configuration at silicon a common mechanism is proposed, involving reversible coordination of the nucleophilic agent opposite the halogen atom (Scheme 67), leading to the most stable trigonal bipyramidal intermediate **210** in a first step. This is followed by the attack of a second molecule of nucleophile (Nu or H_2O) in the rate-determining step. It is not possible to decide whether the displacement of the chloride ion is a concerted process via transition state **211** or whether it involves the hexacoordinate intermediate **212** (Figure 38). The second molecule (Nu or ROH) attacks the pentacoordinate intermediate with the same geometry, which must explain both racemization (Nu) and retention of configuration

$$
\begin{array}{ccc}
(-)\text{-}R_3Si\text{-}Cl + R'OH & \rightleftharpoons & (-)\text{-}R_3Si\text{-}OR' + HCl \\
 & & \Big\downarrow R'OH \\
(\pm)\text{-}R_3Si\text{-}Cl + R'OH & \rightleftharpoons & (\pm)\text{-}R_3Si\text{-}OR'
\end{array}
$$

Scheme 66.

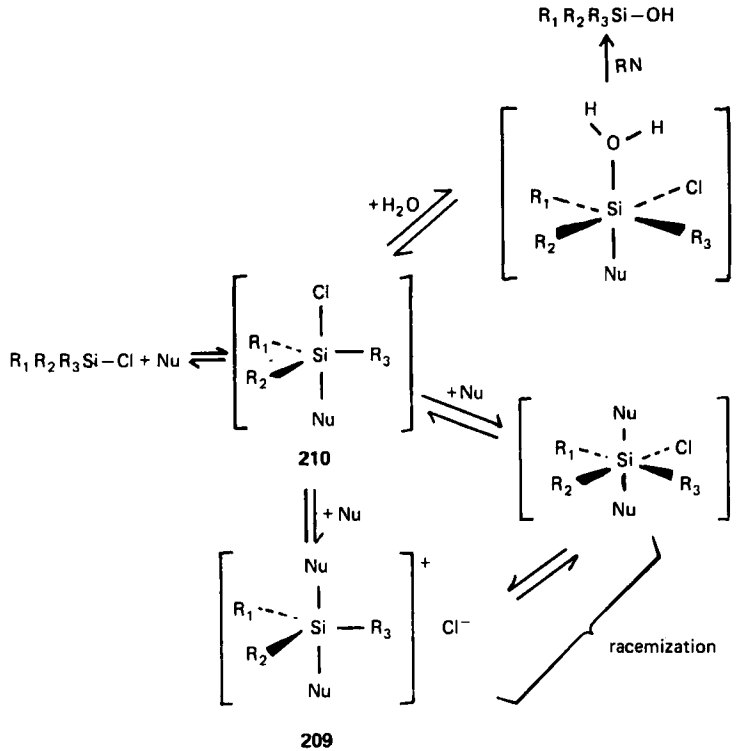

Scheme 67.

(ROH). The attack on one of the upper faces is the only way of explaining both results.

An ionic process could also be invoked to explain the experimental data. The formation of ionic adducts between Me_3Si-Br or Me_3Si-I (but not Me_3Si-Cl) and HMPT was reported (345) (eq. [98]).

$$(Me_2N)_3PO + Me_3Si\text{-}X \longrightarrow [(Me_2N)_3POSiMe_3]^+ X^- \qquad [98]$$

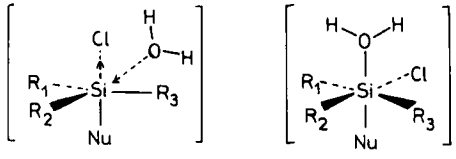

211 212

Figure 38.

The results led the authors to propose the mechanism shown in Scheme 68 for explaining the racemization and hydrolysis data observed for chlorosilanes. The retention of configuration at silicon observed in hydrolysis catalyzed by nucleophiles is explained in terms of two consecutive inversions. The HMPT-induced racemization of the halosilanes would involve nucleophilic attack of a second HMPT molecule at silicon in the phosphonium cation. However, such a mechanism fails to explain the following facts: (i) The high negative entropy of activation observed could be accounted for by ionic structures with ordered arrangements of the surrounding solvent molecules. However, this mechanism does not explain the low (or negative) value of the enthalpy of activation observed in both racemization and hydrolysis (269). (ii) It cannot account for the nucleophile-induced epimerization of chlorosilacyclobutanes. Retention of configuration is the exclusive stereochemical outcome observed with such a strained ring. Thus, two consecutive substitutions by HMPT could only give retention. (iii) It does not account for the racemization observed with other nucleophiles such as CH_3CN, $R\text{-}NO_2$, which are too weakly nucleophilic to bring about the replacement of Si-X bonds.

A reexamination of this problem by a systematic conductivity study of various triorganohalides of the main Group IV elements in the presence of nucleophiles known as racemization agents (HMPT, DMSO, DMF, Ph_3PO) led to the following observations:

1. The triorganohalogermanes and -stannanes, which are even more easily racemizable than triorganohalosilanes (14), do not give ionic adducts with HMPA or with nucleophiles. Thus the ease of racemization (especially in the case of tin compounds) does not seem connected with the existence of ionic 1:1 adducts. In contrast, polarographic studies confirm the existence in solution of 1:1 and 1:2 adducts of low conductiv-

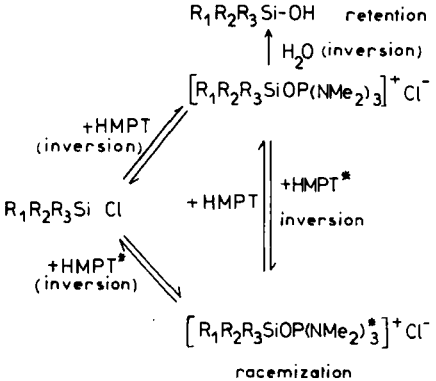

Scheme 68.

ity between tin compounds and nucleophiles; the measured values are always lower than those normally observed for HCl or HBr formed by hydrolysis between the halosilanes and the residual amount of water in the solvent. Moreover, tin compounds are known to give molecular pentavalent (41, 42) or hexavalent complexes (14, 346).

2. In hexane, triphenylchlorosilane gives a crystalline adduct with HMPT as does Me_3Si-Br, but this adduct is not ionic. A similar result is observed in the case of the 1:1 Ph_3PO/Me_3SiCl adduct. Thus the complexes between R_3Si-X and nucleophiles do not necessarily have ionic structures.
3. Nucleophiles such as DMF, which are effective in the racemization of optically active compounds, do not give 1:1 ionic adducts even with Me_3Si-Br or Ph_3Si-Br.

Consequently, the ionization process is a specific phenomenon caused by the lability of the Si-Br or Si-I bonds and the affinity of silicon for oxygen; not all racemization processes involve ionic 1:1 adducts. Moreover, the case of the tin compounds shows that the ability to undergo racemization is connected with the ability to increase coordination number. Thus, since silicon, germanium, and tin compounds show similar conductimetric and kinetic behavior, we may conclude that racemization and nucleophilic substitution are both activated by nucleophiles and involve a coordination extension process as shown in Scheme 67. However, existence of the siliconium ion **209** cannot be excluded in the case of bromosilanes.

The activation of reactions by an additional nucleophile is a general process. For example, it has been observed in phosphorus chemistry. Hydrolysis and racemization of chlorophosphorus compounds are catalyzed by nucleophiles (HMPA, DMSO, DMF). These reactions exhibit similar rate laws (347) (eqs. [99]-[102]):

$$v_{rac}^{Si} = k_{rac}^{Si}[Si{-}Cl]\,[Nu]^2 \qquad [99]$$

$$v_{rac}^{P} = k_{rac}^{P}[P{-}Cl]\,[Nu]^2 \qquad [100]$$

$$v_{H_2O}^{Si} = k_{H_2O}^{Si}[Si{-}Cl]\,[H_2O]\,[Nu] \qquad [101]$$

$$v_{H_2O}^{P} = k_{H_2O}^{P}[P{-}Cl]\,[H_2O]\,[Nu] \qquad [102]$$

$$P{-}Cl = Ph(MenO)\overset{\overset{O}{\|}}{P}{-}Cl \quad \text{or} \quad Ph(EtO)\overset{\overset{S}{\|}}{P}{-}Cl$$

Nucleophilic reactivity is in the same order: DMF < DMSO < HMPT. In both cases, the activation parameters are characterized by highly negative activation entropy factors ($\Delta S^{\ddagger} = -40$ to -65 e.u.). Only the enthalpy factors are markedly different for Si and P ($\Delta H^{\ddagger} \simeq 0$ and $\Delta H^{\ddagger} \simeq 7$ kcal/mol). As shown for silicon compounds, identical rate laws (eqs. [101] and [102]) and energy data are con-

sistent with a common mechanism for racemization and nucleophilically induced hydrolysis. A two-step process, involving rate-determining attack on a pentacoordinate complex is proposed to account for the kinetic and stereochemical data in the phosphorus compounds also.

C. Dynamic Stereochemistry of Pentacoordinate Organosilicon Compounds

Dynamic processes causing ligand permutation in pentacoordinate phosphorus compounds constitute a well-studied area (148). As illustrated in Sect. V-A, various authenticated penta- or hexacoordinate organosilanes have been reported. However studies of the isomerization processes of these compounds are limited. Such processes are of importance, since penta- or hexacoordinate intermediates are implicated in substitution reactions or in racemization of tetracoordinate silicon compounds. The stereochemical outcome of such reactions is therefore related to the configurational stability of penta- or hexacoordinate intermediates.

The stability of pentacoordinate phosphorus compounds has been discussed in terms of apicophilicity of the ligands. The isomerization of these compounds arises from intramolecular ligand permutation via Berry pseudo-rotation or turnstile rotation. It is of interest to know whether the concepts developed in the field of phosphorus chemistry are applicable or not to related organosilicon compounds. It is the aim of this Section to critically review recent studies of the dynamic stereochemistry of pentacoordinate organosilanes.

1. Pentacoordination Ability and Apicophilicity

Pentacoordinate organosilicon species formed by coordination of a neutral two-electron ligand to tetracoordinate organosilanes constitute an interesting class of compounds. These systems can serve as models for the study of nucleophilic substitution at tetracoordinate silicon.

In this respect, studies of compounds of the type *o*-$(Me_2NCH_2)C_6H_4SiXYZ$ **213** (Figure 39), in which the amino aryl ligand is known to provide intramolecular pentacoordination (41), have been reported recently by our group (133, 134, 348, 349).

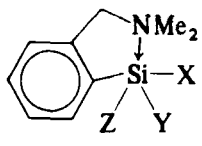

213

Figure 39. Intermolecular pentacoordination in *o*-$(Me_2NCH_2)C_6H_4SiXYZ$.

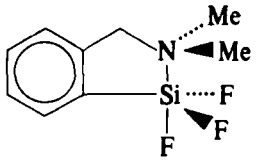

214 *Figure 40.* TBP geometry of *o*-$(Me_2NCH_2)C_6H_4SiF_3$.

A wide variety of functional organosilicon compounds with the same built-in ligand have been synthesized. A trigonal bipyramidal (TBP) structure for these compounds has been proposed on the basis of the similarity of their spectra with those of known pentacoordinate germanium (134) and tin (41) compounds. Furthermore the TBP structure follows from the low temperature ^{19}F NMR study (134) of *o*-$(Me_2NCH_2)C_6H_4SiF_3$ **214** (Figure 40), which exhibits a triplet and a doublet of relative intensities 1 and 2 consistent with two equatorial and one apical fluorine atoms.

The activation energy $\Delta G^{\ddagger}$ for silicon-nitrogen cleavage (eq. [103]) was determined from variable temperature ^1H NMR studies of derivatives of **231** (133).

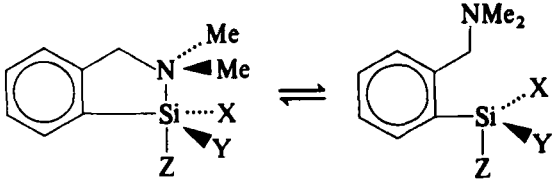

Closed form Open form [103]

At low temperature, the pentacoordinated form can be observed in the ^1H NMR spectrum, since the N-Me groups are diastereotopic. At elevated temperature, the cleavage of the silicon-nitrogen bond allows nitrogen inversion and a singlet is observed for the N-Me groups. The values of $\Delta G^{\ddagger}$ were calculated from the coalescence temperature T_c of the N-Me signals, and are given in Table 34. Whereas ^1H NMR is effective in proving the existence of the equilibrium shown in eq. [103], variable temperature ^{29}Si NMR data verify the presence of pentacoordination (348). As the temperature is lowered, the equilibrium (eq. [103]) shifts towards the closed form with a concomitant upfield shift of the ^{29}Si resonance. The ^{29}Si chemical shifts of ArSiXYZ [Ar = *o*-$(Me_2NCH_2)C_6H_4$] compared to those of PhSiXYZ are given in Table 35. The results may be summarized as follows: (i) No upfield shift of the resonance was observed in the case where X = OR or Me, down to -60°C, indicating that no coordination has occurred. (ii) When X = halogens, the ^{29}Si signal occurs in the region reported for pentacoordinate silicon centers over the entire temperature range and indicates

Table 34
Activation Energy for Silicon-Nitrogen Bond Cleavage (eq. [103])

	X	T_c (°C)	$\Delta G^{\ddagger}$ kcal/mol
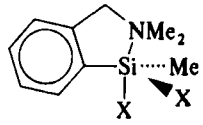	H	–	–
	OEt	–	–
	F	-105	8.3
	OAc	+20	15.8
	Cl	+30	15.6
	O-*t*-Bu	–	–
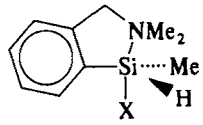	SEt	-65	10.8
	F	-52	11.5
	OAc	-46	11.7
	Cl	-40	12.3
	Br	-10	13.8
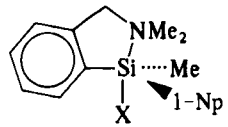	H	–	–
	OMe	–	–
	F	-65	10.3
	OAc	-35	12.3
	Cl	-35	12.2

that a high proportion of the closed form is present. (iii) For X = H, when the temperature is lowered, an upfield shift was observed which indicates that the concentration of the closed form increases with decreasing temperature.

The results obtained from ^{1}H and ^{29}Si NMR studies show that the nitrogen coordination is not a function of the electronegativity of X as in the case of phosphorus (148). The $\Delta G^{\ddagger}$ values for silicon-nitrogen bond breaking in **213** are lower when X = F than when X = Cl or Br. Nitrogen coordination is controlled by the ability of the Si-X bond to be stretched. It is well illustrated by the reported molecular structure of compound **86** (Figure 41) in which the $Si_{(1)}$-$Cl_{(1)}$ bond length (2.348 Å) is 15% longer than $Si_{(2)}$-$Cl_{(2)}$ (2.050 Å) at tetracoordinate silicon. Similar observations were also made in the hexacoordinate bipyridine complex of hexachlorodisilane (338).

In summary, the stability of the TBP geometry as a function of ligands at-

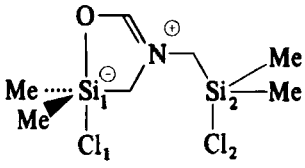

86

Figure 41. TBP geometry in *N,N*-bis(chlorodimethylsilylmethyl) acetamide **86**.

Table 35
^{29}Si NMR Chemical Shifts of Ar versus Ph Substituted Silanes (ppm)[a]

	60°C	30°C	0°C	-30°C	-60°C
$ArMeSiF_2$	-38.60	-40.82	-43.04	-46.22	-49.23
$PhMeSiF_2$	-12.27	-12.07	-11.90	-11.70	-11.40
ArMeSiHF	-33.98	-36.13	-38.30	-41.29	-43.96
PhMeSiHF	–	8.58	–	8.97	–
Ar_2SiF_2	-51.48	-52.95	-54.65	-57.02	-59.62
Ph_2SiF_2	-29.65	-29.57	-29.46	-29.33	-29.23
$ArSiF_3$	-101.47	-102.27	-103.21	-103.96	-104.86
$PhSiF_3$	-72.83	-72.86	-72.92	-72.97	-73.14
ArNpSiHCl	-55.01	-57.59	-60.61	-63.63	-66.29
PhNpSiHCl	-5.65	-5.56	-5.47	-5.38	-5.29
$ArNpSiH_2$	-46.39	-47.25	-48.18	-49.45	-50.77
$PhNpSiH_2$	-35.74	-35.63	-35.52	-35.40	-35.28
$ArSi(OMe)_3$	-54.28	-53.99	-53.79	-53.60	-53.45
$PhSi(OMe)_3$	–	-54.56	–	-53.85	–
$ArSi(OEt)_3$	-57.60	-57.17	-56.73	-56.30	-55.84
$PhSi(OEt)_3$	–	-57.76	–	-56.69	–
$ArMeSi(OEt)_2$	-18.40	-18.19	-18.00	-17.93	-17.86
$PhMeSi(OEt)_2$	–	-17.94	–	-17.20	–
$ArSiMe_3$	-4.85	-4.89	-4.92	-4.94	-4.96
$PhSiMe_3$	–	-4.11	–	-4.06	–

[a]All samples were approximately 10% in $CDCl_3$, with shifts reported relative to internal TMS. Ar = O-$(Me_2NCH_2)C_6H_4$.

tached to silicon is observed to follow the sequence R, RO < H < F, SR < OAc, Cl, Br.

^{19}F NMR studies of bifunctional fluorosilanes, *o*-$(Me_2NCH_2)C_6H_4SiMeFX$, confirmed the preceding observations and allows definition of a scale of apicophilicities for pentacoordinated silicon compounds. An examination of the ^{19}F NMR spectra of various fluorosilanes below the coalescence temperature permitted assignment of the fluorine ligands to apical or equatorial positions in the trigonal bipyramid (349). The observed TBP structure of **218** and **219** for various functional groups is shown in Figure 42.

The fluorine substituent is apical when X = H, OR, or NR_2 and equatorial when X = Cl. In the case where X = *p*-$YC_6H_4CO_2$, a mixture of two TBP isomers is observed. The dominant isomer contains an equatorial fluorine atom, however, the ratio of F_e/F_a depends on the nature of the para-substituent Y.

These results show that the major TBP isomer is not determined by the electronegativity of the F atom. The sequence of apicophilicities of X compared with the apicophilicity of F increases in the order:

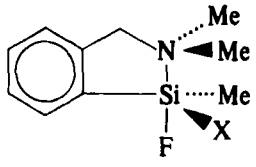

218

X = H, OR, NR_2

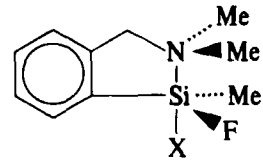

219

X = Cl; $OCOC_6H_4Y$ (Y = H, OMe, NO_2)

Y	$F_e:F_a$
NO_2	86:14
H	73:27
OMe	64:36

Figure 42. Observed TBP structures of bifunctional fluorosilanes.

$$H, OR, NR_2 < F < OCOC_6H_5Y, Cl$$

Interestingly, the apicophilicity sequence closely parallels the rate of racemization and the change of the stereochemical outcome in nucleophilic substitution from retention to inversion in reaction of tetracoordinated organosilanes:

$$H, OR < F, SR < AcO, Cl, Br$$

Increasing apicophilicity →

Increasing rate of racemization →

Shift of nucleophilic substitution mode.
Retention Inversion →

These factors taken together support the hypothesis that the ease of the stretching of the Si-X bond (tendency towards pentacoordination and apicophilicity) is the significant factor in directing the stereochemistry of substitution towards inversion of configuration. As an example, it was observed that nucleophilic displacement at 1-Np(Fc)SiFCl occurs only for the chloride, and with inversion (126). Similarly, in 1-Np(Fc)SiFOR only the fluoride is displaced, and with inversion (350). In each case the group displaced in the substitution reaction is the one that exhibits the greater apicophilicity.

2. *Isomerization Processes of Pentacoordinated Organosilanes*

a. Fluorosilicate Anions. NMR spectroscopy has proved to be a powerful tool for the investigation of dynamic processes at pentacoordinated organosi-

lanes. It was first employed by Muetterties who studied the isomerization of fluorosilicate anions. The study included the determination of ^{19}F and (where applicable) ^{1}H NMR spectra of the fluorosilicate anions: SiF_5^-, $RSiF_4^-$ and $R_2SiF_3^-$ as a function of temperature and solvent polarity (154). On the basis of a comparison with isoelectronic fluorophosphoranes, the fluorosilicate anions were proposed to have nearly trigonal bipyramidal geometry with the organic groups in equatorial positions (Figure 43). This was confirmed by a study of the disubstituted anion $Ph_2SiF_3^-$ **223**, which displays a ^{19}F NMR spectrum, at low temperature, consisting of two lines of relative intensities 2 and 1.

An examination of the NMR spectra of these anions provided evidence for rapid isomerization processes. The results may be summarized as follows:

1. The low-temperature ^{19}F NMR spectra of fluorosilicate anions **220**, **221**, and **222** show equivalent fluorine atoms; satellites due to ^{29}Si-^{19}F coupling are observed at -58°C.
2. When the temperature increases, the ^{19}F resonances gradually begin to broaden and the ^{29}Si-^{19}F coupling is apparently lost.
3. Addition of F^- or a protic solvent (water, alcohol) causes an upfield shift of the resonance accompanied by line broadening with concommitant loss the silicon-fluorine hyperfine structure.

Muetterties' experiments clearly demonstrate that two isomerization processes, which result in the equilibration of fluorine atom environments, are taking place: (i) At low temperature, spin-spin coupling of the silicon and fluorine nuclei is maintained, while at the same time the fluorine environments are averaged; therefore, the dominant exchange process does not involve silicon-fluorine bond breaking. Muetterties proposed as the probable mechanism an intramolecular rearrangement involving bending motions as first outlined by Berry (351) for PF_5. However the behavior of fluorosilicate anions for which ^{29}Si-^{19}F coupling vanishes above -50°C contrasts with that of PF_5 for which coupling is maintained over a very wide temperature range. (ii) In protic solvents or upon addition of fluoride ion, the disappearence of ^{29}Si-^{19}F coupling suggests that another dynamic process takes place that involves scission of the silicon-fluorine

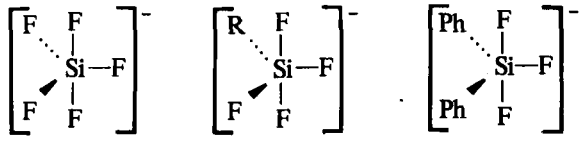

220 R = Me **221** R = Ph **222** **223**

Figure 43. Geometries of fluorosilicate anions.

bond. The exchange may be due to a bimolecular process, such as shown in equation [104].

$$RSiF_4^- + F^{*-} \rightleftharpoons RSiF_3F^{*-} + F^- \qquad [104]$$

Later, Janzen and co-workers emphasized the role of hydrolysis in fluorine exchange processes (352). As demonstrated by the collapse of the ^1H NMR doublet of Me_3SiF, a rapid fluorine exchange on the NMR time scale occurs upon addition of catalytic amounts of H_2O and Et_2NH. Exchange is due to the equilibrium nature of hydrolysis (eq. [105]).

$$Me_3SiF + H_2O \overset{Et_2NH}{\rightleftharpoons} Me_3SiOH + HF \xrightarrow{slow} 1/2(Me_3Si)_2O + 1/2\ H_2O \qquad [105]$$

Traces of moisture or HF, below the usual detection limit, could markedly influence the NMR spectra observed. This possibility was also raised by Klanberg and Muetterties (154) to account for the narrow temperature range in which the intramolecular fluorine exchange was observed.

Conclusive evidence that intermolecular fluorine exchange in SiF_5^- is due to hydrolysis has recently been provided (353). Removal of H_2O, by addition of hexamethyldisilazane (HMDS) to the NMR sample, resulted in the appearance of ^{29}Si-^{19}F coupling, indicating that intermolecular exchange has been slowed. Reintroduction of H_2O produced a loss of ^{29}Si-^{19}F coupling. These results are entirely consistent with hydrolysis as the mechanism for intermolecular exchange. The sensitivity to hydrolysis is probably also enhanced by the presence of a nucleophile such as F^-. Recent published work provided evidence for nucleophilically assisted hydrolysis of fluoro- and chlorosilanes (268, 341).

However, the existence of a single resonance for the five fluorine atoms in SiF_5^- at +38°C and -90°C with ^{29}Si-^{19}F coupling could be proof that a lower energy intramolecular mechanism of exchange is still equilibrating axial and equatorial fluorines. Ligands that permute by Berry pseudorotation (151, 351, 354) or turnstile rotation (152, 153) can account for such a low-energy process. However, another dynamic process cannot be eliminated. An intramolecular exchange of fluorine atoms resulting from a rapid interconversion between five- and six-coordinated geometries, as suggested by Janzen (353), also accounts for the NMR results (eq. [106]).

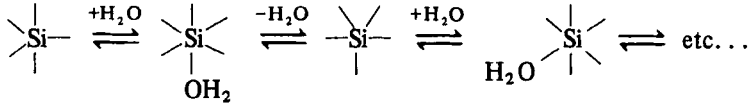

[106]

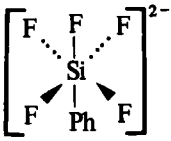

224 *Figure 44.* Hexacoordinate phenylfluorosilicate anion.

According to the rapid equilibria in eq. [106], the positions of the fluorine atoms are averaged but the coupling of the fluorine to the central atom is maintained.

The intervention of hexacoordinated intermediates in intramolecular ligand exchanges can be an alternative mechanism to pseudorotation. Hexacoordinated intermediates are involved in intermolecular ligand exchanges of pentacoordinated silicon compounds (286) and in the hexamethylphosphoric triamide (HMPA) catalyzed F-Cl exchange of tetracoordinated silanes (355).

The Lewis acid character of the fluorosilicate anion is well-illustrated by the isolation of phenylpentafluorosilicate anion **224** (322) (Figure 44). Moreover, the exchange mechanism outlined in eq. [106] is supported by NMR studies of hexacoordinate Lewis base adducts of SiF_5^- (353). The room-temperature ^{19}F NMR spectrum of $[Et_2NHSiF_5]^-$ exhibits a single resonance with ^{29}Si-^{19}F coupling, consistent with fluorine atoms that are rapidly averaged on the NMR time scale. Upon cooling to -60°C, the resonance is split into two components assigned to basal and apical fluorines, in agreement with a reduced rate of isomerization.

Berry pseudorotation as the mechanism of intramolecular exchange of ligands in pentacoordinate fluorosilicate anions represents a possible pathway. However, no definitive evidence has been presented for systems with monodentate ligands, and a pathway involving an intermediate hexacoordinated species can constitute an alternative mechanism.

b. Spirosiliconate Anions. A study of the isomerization of pentacoordinated spirosiliconate anions has recently been reported by Farnham and Harlow (321). The reaction of tris(dimethylamino)sulfonium trimethyldifluorosiliconate (TAS^+ $Me_3SiF_2^-$) with spirosilane **225** resulted in isolation of the spirosiliconate anion **195** (eq. [107]). An X-ray diffraction analysis of compound **195** has shown that the silicon atom is pentacoordinated with the fluorine and two carbon atoms forming the equatorial plane of a somewhat distorted trigonal bipyramid. This contrasts with the observed square pyramidal geometry of the related pentacoordinated spirogermanium compounds (356).

The isomerization of compound **195** has been followed by observing the changes in the signals of the diastereotopic CF_3 groups in the temperature-dependent ^{19}F spectra. The low-temperature (-15°C) spectrum of **195** exhibits

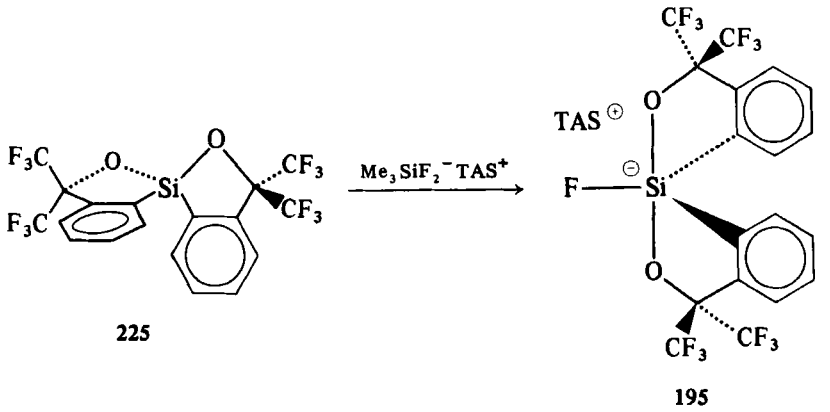

225 195

[107]

an $A_3A'_3B_3B'_3X$ pattern, and at 70°C an $A_{12}X$ pattern is observed, which is in agreement with a rapid interchange of diastereotopic trifluoromethyl groups on the NMR time scale. The activation parameters determined were $\Delta G^{\ddagger} = 16.6$ kcal/mol, $\Delta H^{\ddagger} = 14.1$ kcal/mol, $\Delta S^{\ddagger} = -8$ e.u. No dependence upon concentration or with solvents (acetonitrile, 1,2-dichloroethane) was observed. The exchange rate was unchanged by addition of HMDS or HMPA. The absence of a rapid intermolecular exchange of the silicon-bound fluorine atom was evidenced by the ^{29}Si NMR spectrum of **195** (−76.58 ppm, *d*, $J_{Si-F} = 227$ Hz).

The intervention of Berry pseudorotation processes was invoked to account for the intramolecular ligand permutation. The authors noted, however, that an isomerization by silicon-oxygen bond breaking cannot be strictly excluded. Indeed, it represents a plausible mechanism since a high activation energy is required (within the expected range for a bond cleavage in these anionic alkoxysilanes). To eliminate this possibility Farnham and Harlow prepared the spirosiliconate **196** (eq. [108]). Compound **196**, which contains an apical fluorine

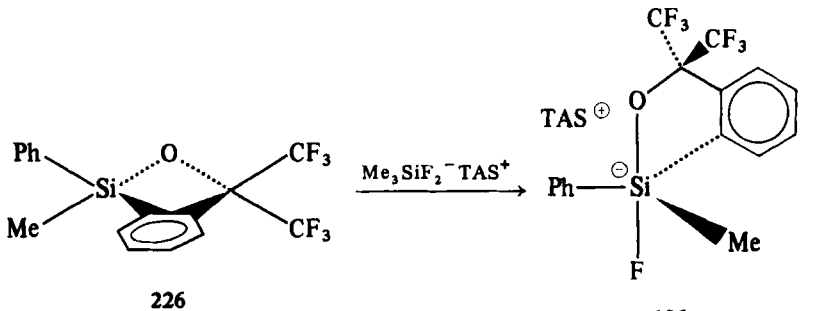

226 196

[108]

atom, exhibits different behavior from **195**. The low temperature ^{19}F NMR spectrum of **196**, even in the presence of HMDS, shows uncoupled signals for two CF_3 groups (A_3B_3) and the Si-F moiety. This clearly establishes that the fluorine ligand undergoes a very rapid intermolecular exchange in a process that does not permute the CF_3 groups. The exchange of the CF_3 groups occurs only at elevated temperature ($\Delta G^{\ddagger} = 17.0$ kcal/mol). In contrast to the behavior of the pentacoordinate compound **195**, it was found that the exchange of the CF_3 groups in **196** is solvent dependent; addition of HMDS reduced its rate and raised the activation energy to 19 kcal/mol.

Since the kinetics of isomerization of **195** and **196** are different, several mechanisms can be operating. Study of compound **196** when compared with **195** does not adduce any supplementary evidence for a pseudorotation mechanism. However, it confirms the multiplicity of exchange processes possible at silicon.

Interestingly, Martin and Stevenson recently reported a related study of the inversion at tetracoordinate silicon in nucleophilic media (357). The spirosilane **225** exhibits an A_3B_3 NMR spectrum in nonnucleophilic solvents. Addition of weak nucleophiles to the sample resulted in coalescence of the trifluoromethyl peaks. The averaged environment of the CF_3 substituents indicates that a rapid inversion of the silicon configuration occurs in solution on the NMR time scale.

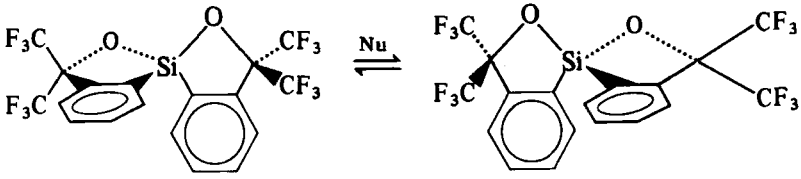

225

[109]

A kinetic study of the racemization equilibrium (eq. [109]) was carried out by a visual fit of observed and calculated ^{19}F NMR spectra. The rate constant so determined was shown to be first order with respect to the nucleophile for both tetrahydropyran and benzaldehyde. The activation parameters were $\Delta H^{\ddagger} = 6.9$ kcal/mol and $\Delta S^{\ddagger} = -27.9$ e.u.

The intervention of one mole of nucleophile in the inversion process contrasts with the results obtained for racemization of chlorosilane where two moles of nucleophiles are involved (13). To account for their results, Martin and Stevenson proposed that inversion at tetracoordinate silicon arises from an isomerization of a pentacoordinated intermediate via Berry pseudorotation steps. Several pathways were proposed, the most interesting being a nucleophilic attack at a carbon-oxygen edge of the tetrahedral silicon compound. In the resulting intermediate, a single Berry pseudorotation with the nucleophile as pivot and equatorial departure of the nucleophile causes an inversion at silicon (eq. [110]). *A*

priori one would expect attack of the nucleophile on the oxygen-oxygen edge to be the most probable, since it gives rise to a more stable trigonal bipyramid (eq. [111]). However, the necessary five pseudorotation steps (151, 354) needed to invert the chirality of the trigonal bipyramidal species in this case involve high energy intermediates (358) having two apical carbons or a diequatorial five-membered ring. Martin and Stevenson (357), therefore, suggest that a carbon-oxygen attack possibly represents a lower energy pathway for racemization.

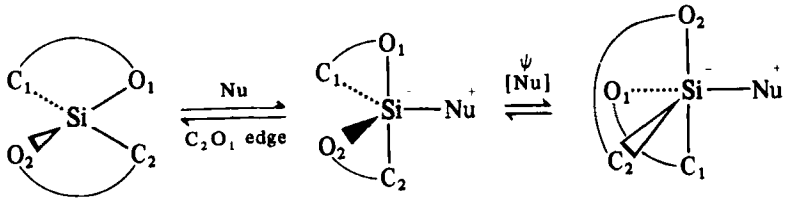

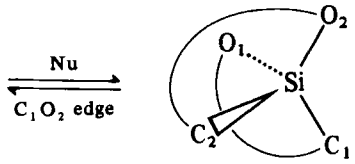

[110]

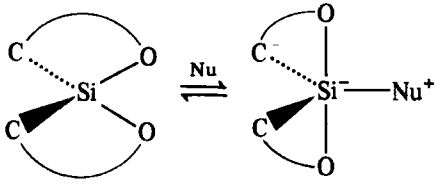

[111]

The kinetics of the inversion of spirosilane **225** appear consistent with the formation of a pentacoordinated intermediate in the rate-determining step ($\Delta G^{\ddagger}$ = 15.2 kcal/mol, $\Delta H^{\ddagger}$ = 6.9 kcal/mol, $\Delta S^{\ddagger}$ = -27.9 e.u.). The proposed isomerization via Berry pseudorotation is expected to contribute little to $\Delta S^{\ddagger}$. It is surprising that the observed activation energy ($\Delta G^{\ddagger}$ = 15.2 kcal/mol) for the overall inversion process (coordination of the nucleophile and isomerization) is slightly lower than the activation energy reported by Farnham for the isomerization of the isolated siliconate anion **195** ($\Delta G^{\ddagger}$ = 16.6 kcal/mol). Whereas isomerization involving pseudorotation represents an interesting possibility, other pathways cannot strictly be excluded. For instance, a mechanism involving silicon-oxygen bond cleavage and recombination steps at different sites may also account for inversion at silicon in compound **195** (eq. [112]).

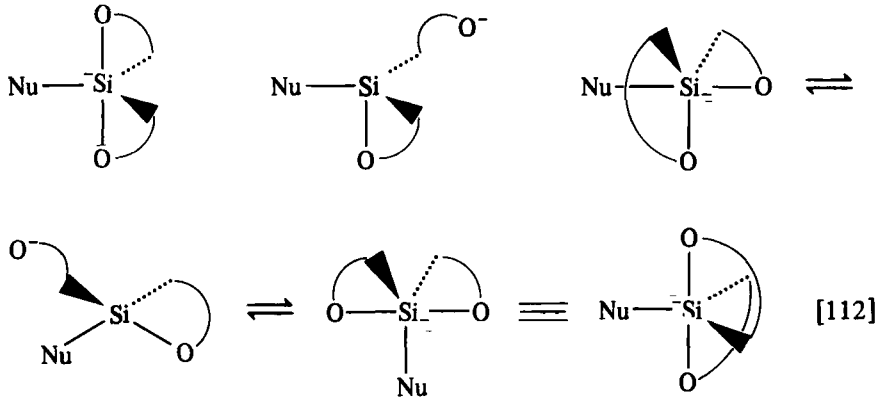

[112]

c. **[Ortho-(dimethylamino)methyl]phenyltrifluorosilane.** As mentioned previously (Sect. V-C-1), the low-temperature ^{19}F NMR spectrum of the amino-aryl trifluorosilane **214** established a trigonal bipyramidal structure with two fluorine atoms in equatorial positions (Figure 40). Above 0°C the environment of the three fluorine atoms is averaged into a single resonance. The persisting ^{29}Si-^{19}F coupling shows that no Si-F bond breaking occurs in this isomerization process. Moreover, the ^{29}Si NMR results show that compound **214** is essentially pentacoordinated over the -60°C to +60°C temperature range: $\Delta(\delta^{29}Si^{V} - \delta^{29}Si^{IV})_{60°C} = -29.6$ ppm, $\Delta(\delta^{29}Si^{V} - \delta^{29}Si^{IV})_{-60°C} = -31.7$ ppm (cf. Table 35). Therefore, the coalescence of the apical and equatorial fluorine atoms arises from an equilibrium between pentacoordinated species (eq. [113]). However, while the ^{29}Si resonance remains in the region for five-coordinate silanes, upon raising the temperature a downfield shift of the resonance, indicative of an increasing concentration of the tetracoordinate open form, is observed: $\Delta(\delta^{29}Si_{+60°C}{}^{V} - \delta^{29}Si_{-60°C}{}^{V}) = +3.4$ ppm.

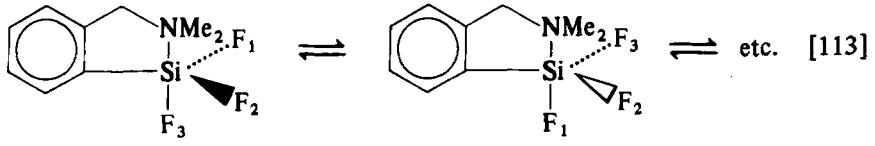

[113]

The observed averaging of the environment of the fluorine ligands thus results from rapid ring opening and closure on the NMR time scale. The activation energy determined was $\Delta G^{\ddagger} \cong 13$ kcal/mol. In this isomerization process, neither intermolecular fluorine exchange nor pseudorotation is involved. An equilibrium between open and closed forms represents the lowest energy pathway. It follows that if pseudorotation occurs, it involves an activation energy higher than 13

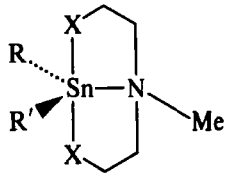

227
X = O, S

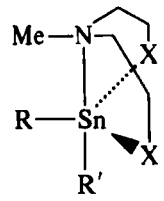

228

Figure 45. TBP geometries of diptychoxa- and -thia-azastannolidines.

kcal/mol. This value contrasts with that reported for five-membered cyclic trifluorophosphoranes for which a 7 kcal/mol energy barrier was calculated (148).

Based on these results, intervention of pseudorotation is not excluded but it represents a higher energy process. A similar conclusion was reached in the isomerization of related pentacoordinate tin compounds 227 and 228 (Figure 45) (359). The intramolecular mobility of these compounds was shown to involve a dissociation-inversion mechanism with a free energy of activation, $\Delta G^{\ddagger} \cong 15$ kcal/mol.

3. *Conclusions*

It appears that ligand exchange in pentacoordinate silicon species involves many pathways. Beside a possible intramolecular isomerization arising from Berry pseudorotation of a trigonal bipyramidal silane, several other processes may take place. The multiplicity of mechanisms comes from the possibility for pentacoordinate silanes to react by associative or dissociative pathways. Isomerization and exchange processes can involve a reduction of the coordination number to four or an expansion to six.

In dissociative ligand exchange, an equilibrium between four and five coordinate compounds is responsible for the rapid intermolecular fluorine exchange (without racemization at silicon) in compound **196** (p. 163) (321). A similar equilibrium between open and closed forms is also implicated in amino-arylsilanes **213** (p. 174) (133).

The intervention of four-coordinate compounds may account for the inversion of spirosiliconate **195** (p. 163) (321, 357), for which an opening-closing equilibrium occurring at different sites cannot be eliminated (cf. eq 112).

In associative ligand exchange, the intervention of hexacoordinated intermediates has been demonstrated in various intermolecular ligand exchange processes at five-coordinated silicon compounds (286, 355) (eq. [114]).

A rapid equilibrium between five- and six-coordinate molecules, as shown by Janzen and colleagues (353) (eq. [115]), can be responsible for the isomeriza-

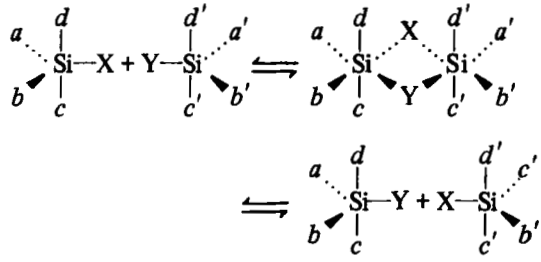

[114]

tion of five-coordinate fluorosilicate without Si-F bond breaking. A similar process may also account for the solvent-dependent inversion at silicon in spirosiliconate **196** (321).

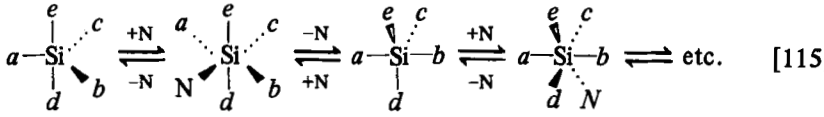

[115]

A related process is implicated in the nucleophilically induced racemization at tetracoordinate halogenosilanes (13), which has been shown to involve two molecules of nucleophilic agent. Racemization arises from an equilibrium between five- and six-coordinate intermediates (eq. [116]). This process is controlled by entropy. It is characterized by a highly negative activation entropy and a low or sometimes negative activation enthalpy.

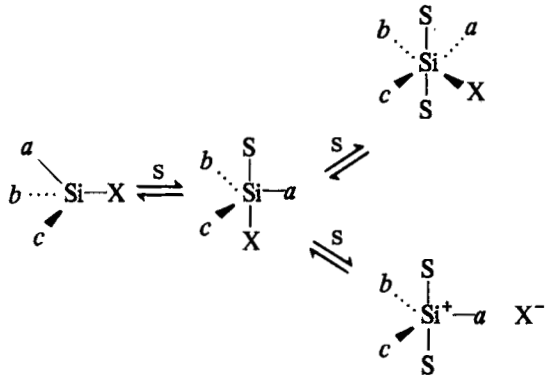

[116]

The question whether or not ligand permutations via Berry pseudorotation in five-coordinate silicon compounds occur is a very provocative one. With the present state of knowledge, no definitive evidence has been obtained for such a process to occur, even for SiF_5^-. It does, however, represent a possible isomerization pathway. From the results obtained, it appears to involve an activation

energy higher than expected from the results in phosphorus chemistry. Moreover, the apicophilicity of the ligands in five-coordinate silanes differs from that at five-coordinate phosphorus compounds. The ability of the apical bond to be stretched is a more important factor than the electronegativity of the apical ligand (349).

Among the multiplicity of processes taking place at silicon, pseudorotation has not yet been unambiguously established. It represents an exciting area for investigation, and we hope that further work will be stimulated.

ACKNOWLEDGMENTS

Collaboration with Professor Nguyen Trong Anh and Dr. C. Minot has been very fruitful. The stimulating interest of Drs. H. Felkin and J. Seyden-Penne is appreciated. The help of Dr. J. Jacques is gratefully acknowledged. In addition, Professor Corriu wishes to thank those co-workers whose names appear in the references.

Finally, we acknowledge support of the research cited herein by the CNRS.

REFERENCES

1. Sommer, L. H. "Stereochemistry, Mechanism and Silicon"; McGraw Hill: New York, 1965.
2. Sommer, L. H. *Intra-Science Chem. Rep.* **1973**, *7*, 1.
3. Kipping, F. S. *J. Chem. Soc.* **1907**, 209; *ibid.* **1908**, 457. Duff, B. D. W.; Kipping, F. S. *ibid.* **1908**, 2090. Challenger, F.; Kipping, F. S. *ibid.* **1910**, 755.
4. Eaborn, C.; Pitt, C. *Chem. Ind.* **1958**, 830.
5. Sommer, L. H.; Frye, C. L. *J. Am. Chem. Soc.* **1959**, *81*, 1013.
6. Eaborn, C.; Mahmoud, F. M. S. *J. Chem. Soc., Perkin II* **1981**, 1309, and references cited therein.
7. Brook, A. G.; Abdesaken, F.; Gutekunst, B.; Gutekunst, G.; Kallury, R. K. *J. Chem. Soc., Chem. Commun.* **1981**, 191.
8. West, R.; Fink, M. J.; Michl, J. *Science* **1981**, *214*, 1343.
9. Barton, T. J.; Banasiak, D. S. *J. Am. Chem. Soc.* **1977**, *99*, 5199.
10. Corriu, R. J. P.; Guérin, *C. J. Organometal. Chem.* **1980**, *198*, 231.
11. Corriu, R. J. P.; Guérin, C. *Adv. Organometal. Chem.* **1982**, *20*, 265.
12. Colomer, E.; Corriu, R. J. P. *Top. Curr. Chem.* **1981**, *96*, 79.
13. Corriu, R. J. P.; Henner, M. *J. Organometal. Chem.* **1974**, *74*, 1.
14. Gielen, M. *Top. Stereochem.* **1981**, *12*, 217.
15. Brook, A. G.; Bassindale, A. R. In "Rearrangement in Ground and Excited State," Vol. 2; Academic Press: New York, 1980, p. 149.
16. Dubac, J.; Mazerolles, P. *J. Organometal. Chem. Lib.* **1981**, *12*, 149.
17. Brook, A. G.; Duff, J. M. *J. Am. Chem. Soc.* **1969**, *91*, 2118.
18. Sakurai, H.; Murakami, M.; Kumada, M. *J. Am. Chem. Soc.* **1969**, *91*, 519.
19. Sakurai, H.; Murakami, M. *Chem. Lett.* **1972**, 7.
20. Bennett, S. W.; Eaborn, C.; Hudson, A.; Jackson, R. A.; Root, K. D. *J. Chem. Soc., A* **1969**, 348, and references cited therein.

21. Sakurai, H.; Mochida, K. *Chem. Commun.* **1971**, 1581.
22. Corriu, R. J. P.; Moreau, J. J. E. *Chem. Commun.* **1971**, 812.
23. Corriu, R. J. P.; Moreau, J. J. E. *J. Organometal. Chem.* **1972**, *40*, 73.
24. Sakurai, H.; to be published.
25. Gilman, H.; Winkler, H. J. S. In "Organometallic Chemistry"; Zeiss, H., Ed.; Reinhold: New York, 1960, p. 270.
26. Sommer, L. H.; Mason, R. *J. Am. Chem. Soc.* **1965**, *87*, 1619.
27. Colomer, E.; Corriu, R. J. P. *J. Chem. Soc., Chem. Commun.* **1976**, 177.
28. Colomer, E.; Corriu, R. J. P. *J. Organometal. Chem.* **1977**, *133*, 159.
29. Eaborn, C.; Jakson, R. A.; Tune, D. J.; Walton, D. R. M. *J. Organometal. Chem.* **1973**, *63*, 85.
30. Lambert, J. B.; Urdaneta-Perez, M.; Sun, Hs.-N. *J. Chem. Soc., Chem. Commun.* **1976**, 806.
31. Brook, A. G.; Peddle, G. J. D. *J. Am. Chem. Soc.* **1963**, *85*, 2338.
32. Eaborn, C.; Hill, R. E. E.; Simpson, P. *J. Organometal. Chem.* **1972**, *37*, 267.
33. Carré, F.; Corriu, R. J. P. *J. Organometal. Chem.* **1974**, *65*, 349.
34. Eaborn, C.; Hill, R. E. E.; Simpson, P. *J. Organometal. Chem.* **1972**, *37*, 275.
35. Colomer, E.; Corriu, R. J. P. *J. Chem. Soc., Chem. Commun.* **1978**, 435.
36. Carré, F.; Cerveau, G.; Colomer, E.; Corriu, R. J. P. *J. Organometal. Chem.* **1982**, *229*, 257.
37. Cerveau, G.; Colomer, E.; Corriu, R. J. P.; Vioux, A. *Organometallics* **1982**, *1*, 866.
38. Carré, F.; Corriu, R. J. P. *J. Organometal. Chem.* **1974**, *73*, C49.
39. Corriu, R. J. P.; Guérin, C., to be published.
40. Dhar, S. K.; Doron, V.; Kirschner, S. *J. Am. Chem. Soc.* **1958**, *80*, 753.
41. Van Koten, G.; Noltes, J. G. *J. Am. Chem. Soc.* **1976**, *98*, 5393.
42. Van Koten, G.; Jastrzebski, J. T. B. H.; Noltes, J. G.; Pontenagel, W. M. G. F.; Kroon, J.; Spek, A. L. *J. Am. Chem. Soc.* **1978**, *100*, 5021.
43. Wilen, S. H. In "Topics in Stereochemistry," Vol. 6; Allinger, N. L.; Eliel, E. L., Eds.; Wiley: New York, 1971, p. 107.
44. Sommer, L. H.; Frye, C. L.; Parker, G. A.; Michael, K. W. *J. Am. Chem. Soc.* **1964**, *86*, 3271.
45. Okaya, Y.; Ashida, T. *Acta Cryst.* **1966**, *20*, 461.
46. Davydova, S. L.; Yu; Purisson, A.; Lavrukhin, B. D.; Plate, N. A. *Izv. Akad. Nauk. SSSR*, Engl transl., **1965**, 387.
47. Corriu, R. J. P.; Royo, G. *J. Organometal. Chem.* **1968**, *14*, 291.
48. Corriu, R. J. P.; Lanneau, G.; Royo, G. *Bull. Soc. Chim. Fr.*, **1968**, 458.
49. Corriu, R. J. P.; Royo, G. *Tetrahedron* **1971**, *27*, 4289.
50. Sommer, L. H.; Rosborough, K. T. *J. Am. Chem. Soc.* **1969**, *91*, 7067.
51. Corriu, R. J. P.; Lanneau, G. F.; Ould-Kada, S. *J. Organometal. Chem.*, in press.
52. Corriu, R. J. P.; Lanneau, G. F.; Royo, G. L. *J. Organometal. Chem.* **1972**, *35*, 35.
53. Kanters, J. A.; Van Veen, A. M. *Cryst. Struct. Commun.* **1973**, *2*, 261.
54. Corriu, R. J. P.; Lanneau, G. F. *J. Organometal. Chem.* **1974**, *64*, 63.
55. Corriu, R. J. P.; Larcher, F.; Royo, G. *J. Organometal. Chem.* **1977**, *129*, 299.
56. Corriu, R. J. P.; Larcher, F.; Royo, G. *J. Organometal. Chem.* **1976**, *104*, 161.
57. Breliére, C.; Corriu, R. J. P.; De Saxcé, A.; Larcher, F.; Royo, G. *J. Organometal. Chem.* **1979**, *164*, 19.
58. Lanneau, G., Ph.D. Thesis, University of Montpellier, 1972.
59. Corriu, R. J. P.; Lanneau, G. F.; Leard, M. *J. Organometal. Chem.* **1974**, *64*, 79.
60. Brelière, C.; Corriu, R. J. P.; Royo, G. *J. Organometal. Chem.* **1978**, *107*, 148.
61. Corriu, R. J. P.; Massé, J. *Bull. Soc. Chim. Fr.* **1969**, 3491.
62. Vidal, J. P.; Falgueirettes, J. *Acta Cryst., B* **1973**, *29*, 2833.

63. Citron, J. D. *J. Organometal. Chem.* **1975**, *86*, 359.
64. Roark, D. N.; Sommer, L. H. *J. Am. Chem. Soc.* **1973**, *95*, 969.
65. Mathieu, J.; Weil-Raynal, J. *Bull. Soc. Chim. Fr.* **1968**, 1211. Morisson, J. D.; Mosher, H. S. "Asymmetric Organic Reactions"; Prentice Hall: Englewood Cliffs, N.J., 1971; American Chemical Society: Washington, D.C., 1976.
66. Holt, A.; Jarvie, A. W. P.; Jervis, G. J. *Tetrahedron Lett.*, **1968**, 4087; *ibid.*, *J. Chem. Soc., Perkin II* **1973**, 114.
67. Bertrand, G.; Dubac, J.; Mazerolles, P.; Ancelle, J. *J. Chem. Soc., Chem. Commun.* **1980**, 382.
68. Corriu, R. J. P.; Moreau, J. J. E. *J. Organometal. Chem.* **1974**, *64*, C51; *ibid.* **1975**, *85*, 19.
69. Klebe, J. F.; Finkbeiner, H. *J. Am. Chem. Soc.* **1966**, *88*, 4470; *ibid.* **1968**, *90*, 7255.
70. Corriu, R. J. P.; Moreau, J. J. E. *J. Chem. Soc., Chem. Commun.* **1973**, 38.
71. Ojima, I.; Nihonyanagi, M.; Nagai, Y. *Chem. Commun.* **1972**, 938.
72. Haszeldine, R. N.; Parish, R. V.; Parry, D. J. *J. Chem. Soc., A* **1969**, 683.
73. Corriu, R. J. P.; Moreau, J. J. E. *Tetrahedron Lett.* **1973**, 4469; *J. Organometal. Chem.* **1976**, *120*, 337.
74. Kagan, H. B.; Dang, T. P. *J. Am. Chem. Soc.* **1972**, *94*, 6429.
75. Morrison, J. D.; Masler, W. F. *J. Org. Chem.* **1974**, *39*, 270.
76. Fiaud, J. C.; Horeau, A. *Tetrahedron Lett.* **1972**, 2565.
77. Corriu, R. J. P.; Moreau, J. J. E. *J. Organometal. Chem.* **1976**, *114*, 135.
78. Corriu, R. J. P.; Moreau, J. J. E. *J. Organometal. Chem.* **1975**, *91*, C 27; *Nouv. J. Chim.* **1977**, *1*, 71.
79. Hayashi, T.; Yamamoto, K.; Kumada, M. *Tetrahedron Lett.* **1974**, 331.
80. Ojima, I.; Yamamoto, K.; Kumada, M. In "Aspects of Homogeneous Catalysis," Vol. 3; Ugo, R., Ed.; D. Reidel: Dordrecht, 1977, p. 185.
81. Dumont, W.; Poulin, J. C.; Dang, T. P.; Kagan, H. B. *J. Am. Chem. Soc.* **1973**, *95*, 8295.
82. Glaser, R. *Tetrahedron Lett.* **1975**, 2127.
83. Corriu, R. J. P.; Moreau, J. J. E. *Bull. Soc. Chim. Fr.* **1975**, 901.
84. Corriu, R. J. P.; Guérin, C. *J. Organometal. Chem.* **1980**, *195*, 261.
85. Corriu, R. J. P.; Henner, B. J. L. *J. Organometal. Chem.* **1976**, *105*, 303.
86. Richter, W. J. *J. Organometal. Chem.* **1979**, *169*, 9.
87. Sommer, L. H.; Michael, K. W.; Korte, K. W. *J. Am. Chem. Soc.* **1967**, *89*, 868.
88. Eaborn, C.; Steward, O. W. *Proc. Chem. Soc.* **1963**, 59.
89. Sommer, L. H.; Silverman, M. A. *J. Org. Chem.* **1973**, *38*, 636.
90. Corriu, R. J. P.; Guérin, C.; Massé, J. *J. Chem. Res.* (*S*) **1977**, 160; *ibid.* (*M*) **1977**, 1877.
91. Corriu, R. J. P.; Fernandez, J. M.; Guérin, C.; Kopton, A. *Bull. Soc. Chim. Belg.* **1980**, *89*, 783.
92. Eliel, E. L. "Stereochemistry of Carbon Compounds"; McGraw-Hill: New York, 1962.
93. Jacques, J.; Collet, A.; Willen, S. H. "Enantiomers, Racemates, and Resolutions"; Wiley: New York, 1981.
94. Fouquey, C.; Jacques, J. *Tetrahedron* **1967**, *23*, 4009.
95. Raban, M.; Mislow, K. *Top. Stereochem.* **1967**, *2*, 199.
96. Fredga, A. *Tetrahedron* **1960**, *8*, 126.
97. Sommer, L. H.; McLick, J. *J. Am. Chem. Soc.* **1969**, *91*, 2001.
98. Corriu, R. J. P.; Massé, J. *Tetrahedron* **1970**, *26*, 5123.
99. Anh, Nguyên Trong; Minot, C. *J. Am. Chem. Soc.* **1980**, *102*, 103.
100. Anh, Nguyên Trong, *Top. Curr. Chem.* **1980**, *88*, 145.

101. For instance: Berthell, D.; Gold, V. "Carbonium Ions: An Introduction"; Academic Press: London and New York, 1967, and references cited therein.
102. Allen, A. D.; Charlton, J. C.; Eaborn, C.; Modena, G. *J. Chem. Soc.* **1957**, 3668; Allen, A. D.; Modena, G. *ibid.*, **1957**, 3671.
103. Schott, G.; Bondybey, V. *Chem. Ber.* **1967**, *100*, 1773. Kaufmann, K. D.; Ruhlmann, K. *Z. Chem.* **1967**, *7*, 391. Schowen, R. L.; Latham, K. S. *J. Am. Chem. Soc.* **1967**, *89*, 4677.
104. Corriu, R. J. P.; Royo, G. *J. Organometal. Chem.* **1968**, *14*, 291; *ibid.*, *Bull. Soc. Chim. Fr.* **1972**, *4*, 1490.
105. Corriu, R. J. P.; Larcher, F.; Royo, G. *J. Organometal. Chem.* **1976**, *104*, 161.
106. Corriu, R. J. P.; Henner, B. *J. Chem. Soc., Chem. Comm.* **1973**, 116. Chauvière, G.; Corriu, R. J. P.; Henner, B. *J. Organometal. Chem.* **1975**, *86*, C1-C2. Corriu, R. J. P.; Henner, B.; *ibid.* **1975**, *102*, 407.
107. Sullivan, S. A.; De Puy, C. H.; Damrauer, R. *J. Am. Chem. Soc.* **1981**, *103*, 408.
108. Krusic, P. J.; Fagan, P. J.; San Filippo, J. *J. Am. Chem. Soc.* **1977**, *99*, 250. San Filippo, J.; Sibermann, J.; Fagan, P. J. *J. Am. Chem. Soc.* **1978**, *100*, 4834.
109. Felkin, H.; Knowles, P. J.; Meunier, B. *J. Organometal. Chem.* **1978**, *146*, 151.
110. Corriu, R. J. P.; Dabosi, G.; Martineau, M. *J. Chem. Soc., Chem. Comm.* **1979**, 457.
111. Mann, C. K.; Barnes, K. K. "Electrochemical Reactions in Nonaqueous Systems"; M. Dekker: New York, 1970. Baizer, M. M. "Organic Electrochemistry"; M. Dekker: New York, 1973. Rifi, M. R.; Covitz, F. H. "Introduction to Organic Electrochemistry"; M. Dekker: New York, 1974.
112. Sommer, L. H.; Korte, W. D. *J. Am. Chem. Soc.* **1967**, *89*, 5802.
113. Corriu, R. J. P.; Royo, G. *Tetrahedron* **1971**, *27*, 4289; *ibid.*, *Bull. Soc. Chim. Fr.* **1972**, 1497.
114. Sommer, L. H.; Korte, W. D.; Rodewald, P. G. *J. Am. Chem. Soc.* **1967**, *89*, 862.
115. Sommer, L. H.; McLick, J. *J. Am. Chem. Soc.* **1966**, *88*, 5359; *ibid.*, **1967**, *89*, 5806.
116. Corriu, R. J. P.; Fernandez, J. M.; Guérin, C. *J. Organometal. Chem.* **1978**, *152*, 25.
117. Corriu, R. J. P.; Royo, G. *J. Organometal. Chem.* **1972**, *40*, 229.
118. Sommer, L. H.; Frye, C. L.; Parker, G. A.; Michael, K. W. *J. Am. Chem. Soc.* **1964**, *86*, 3271.
119. Reference 1, Chapter 4.
120. Sommer, L. H.; Parker, G. A.; Lloyd, N. C.; Frye, C. L.; Michael, K. W. *J. Am. Chem. Soc.* **1967**, *89*, 857.
121. Sommer, L. H.; Frye, C. L.; Musolf, M. C.; Parker, G. A.; Rodewald, P. G.; Michael, K. W.; Okaya, Y.; Popinski, R. *J. Am. Chem. Soc.* **1961**, *83*, 2210.
122. Reference 1, Chapter 6.
123. Sommer, L. H.; Frye, C. L.; Parker, G. A. *J. Am. Chem. Soc.* **1964**, *86*, 3276.
124. Brelière, C.; Corriu, R. J. P.; Royo, G. *J. Chem. Soc., Chem. Comm.* **1976**, 906.
125. Brelière, C.; Corriu, R. J. P.; De Saxcé, A.; Royo, G. *J. Organometal. Chem.* **1979**, *166*, 153. Corriu, R. J. P.; Lanneau, G. *Bull. Soc. Chim. Fr.* **1973**, 3102. Corriu, R. J. P.; Lanneau, G.; Léard, M. *J. Organometal Chem.* **1974**, *64*, 79.
126. Corriu, R. J. P.; Larcher, F.; Royo, G. *J. Organometal. Chem.* **1975**, *102*, C25. Brelière, C.; Corriu, R. J. P.; Royo, G. *ibid.* **1978**, *148*, 107.
127. Sommer, L. H.; Parker, G. A.; Frye, C. L. *J. Am. Chem. Soc.* **1964**, *86*, 3280.
128. Brewster, J. H. *J. Am. Chem. Soc.* **1959**, *81*, 5475.
129. Onan, K. D.; McPhail, A. T.; Yoder, C. H.; Hillyard, R. W. *J. Chem. Soc., Chem. Comm.* **1978**, 209.
130. Ebsworth, E. A. V. "Volatile Silicon Compounds"; Pergamon: Oxford, 1963, p. 54.
131. Hensen, K.; Klebe, G., private communication.

132. Sheldrick, W. S.; Wolfsberger, W. *Z. Naturforsch B; Anorg. Chem. Org. Chem.* **1977**, *32b*, 22.
133. Corriu, R. J. P.; Royo, G.; De Saxcé, A. *J. Chem. Soc., Chem. Comm.* **1980**, 893.
134. Brelière, C.; Carré, F.; Corriu, R. J. P.; De Saxcé, A.; Poirier, M.; Royo, G. *J. Organometal. Chem.* **1981**, *206*, C1.
135. Corriu, R. J. P.; Dutheil, J. P.; Lanneau, G.; Ould-Kada, S. *Tetrahedron* **1979**, *35*, 1889.
136. Corriu, R. J. P.; Massé, J. *J. Chem. Soc., Chem. Comm.* **1968**, 1373; *ibid., J. Organometal. Chem.* **1972**, *35*, 51.
137. Corriu, R. J. P.; Guérin, C. *J. Organometal. Chem.* **1982**, *225*, 141.
138. Corriu, R. J. P.; Massé, J. *Tetrahedron Lett.* **1968**, 5197; *ibid., J. Organometal. Chem.* **1972**, *34*, 221.
139. Eisenstein, O.; Lefour, J. M.; Minot, C.; Anh, Nguyên Trong; Soussan, G. *C. R. Hebd. Sceances Acad. Sci., Ser. C.* **1972**, *274*, 1310.
140. Corriu, R. J. P.; Massé, J.; Royo, G. *J. Chem. Soc., Chem. Comm.* **1971**, 252.
141. Sommer, L. H.; Fujimoto, H. *J. Am. Chem. Soc.* **1968**, *90*, 982.
142. Corriu, R. J. P.; Henner, B. *J. Organometal. Chem.* **1974**, *71* 393.
143. Corriu, R. J. P.; Fernandez, J. M.; Guérin, C. *J. Organometal. Chem.* **1978**, *152*, 21; *ibid., Tetrahedron* **1981**, *37*, 2467.
144. Lehn, J. M. *Acc. Chem. Res.* **1978**, *11*, 49.
145. Corriu, R. J. P.; Guérin, C. *J. Chem. Soc., Chem. Comm.* **1977**, 74; *ibid., J. Organometal. Chem.* **1978**, *144*, 165.
146. Sommer, L. H.; McLick, J.; Golino, C. J. *Am. Chem. Soc.* **1972**, *94*, 669.
147. Corriu, R. J. P.; Fernandez, J. M.; Guérin, C. *Tetrahedron Lett.* **1978**, 3391.
148. Luckenbach, R. "Dynamic Stereochemistry of Pentacoordinated Phosphorus and Related Elements"; Georg Thieme: Stutgart, 1973.
149. McEwen, W. E.; Berlin, K. D., Eds.; "Organophosphorus Stereochemistry," Parts I and II; Bench Mark Papers (Vol. 3), Dowden, Hutchinson and Ross: Stroudsburg, PA, 1975.
150. Westheimer, F. H. *Acc. Chem. Res.* **1968**, *1*, 70.
151. Mislow, K. *ibid.* **1970**, *3*, 321.
152. Gillespie, P.; Hoffman, P.; Keusacek, H.; Marquarding, D.; Pfohl, S.; Ramirez, F.; Tsolis, E. A.; Ugi, I. *Angew. Chem. Int. Ed.* **1971**, *10*, 687.
153. Gillespie, P.; Ramirez, F.; Ugi, I.; Marquarding, D. *ibid.* **1978**, *12*, 91.
154. Klanberg, F.; Muetterties, E. L. *Inorg. Chem.* **1968**, *7*, 155.
155. Perozzi, E. F.; Martin, J. C. *J. Am. Chem. Soc.* **1979**, *101*, 1591. Perozzi, E. F.; Michalak, R. S.; Figuly, G. D.; Stevenson, W. H.; Dess, D. B.; Ross, M. R.; Martin, J. C. *J. Org. Chem.* **1981**, *46*, 1049.
156. Boudreau, J. A.; Brown, C.; Hudson, R. F. *J. Chem. Soc., Chem. Comm.* **1975**, 679.
157. Salem, L. *Chem. Br.* **1969**, *5*, 449.
158. Gray, R. W.; Chapleo, C. B.; Vergnani, T.; Dreiding, A. S.; Liesner, M.; Seebach, D. *Helv. Chim. Acta*, **1975**, *58*, 1524.
159. Pearson, R. G. *J. Chem. Educ.* **1975**, *45*, 581.
160. Minot, C.; Anh, Nguyên Trong *Tetrahedron Lett.* **1975**, 3905.
161. Berson, J. A.; Salem, L. *J. Am. Chem. Soc.* **1972**, *94*, 8917. David, S.; Eisenstein, O.; Hehre, W. J.; Salem, L.; Hoffmann, R. *ibid.* **1973**, *95*, 3806.
162. Kermister, G.; Pross, A.; Radom, L.; Taft, R. *J. Org. Chem.* **1980**, *45*, 1056.
163. Clark, F.; Jemmis, E. D.; Schleyer, P. J. R. *J. Organometal. Chem.* **1978**, *150*, 1.
164. Jean, A.; Lequan, M. *Tetrahedron Lett.* **1970**, 1517.
165. Gerteis, R. L.; Dickerson, R. E.; Brown, T. I. *Inorg. Chem.* **1964**, *3*, 872.
166. Wolfrum, R.; Sauermunn, G.; Weiss, E. *J. Organometal. Chem.* **1969**, *18*, 27.

167. Vilkov, L. S.; Mastrivukov, B. S.; Baowrover, J. V.; Vdovin, V. M.; Trinberg, L. *Dokl. Akad. Nauk.* SSSR **1967**, *117*, 1084.
168. Dubac, J.; Mazerolles, P.; Seves, B. *Tetrahedron Lett.* **1972**, 529; *ibid.* **1972**, 3495; *ibid.*, *Tetrahedron* **1974**, *30*, 749; *ibid.* **1974**, *30*, 759.
169. McKinnie, B. G.; Bhacca, N. S.; Cartledge, F. K.; Fayssous, J. *J. Am. Chem. Soc.* **1974**, *96*, 2637; *ibid.*, *J. Org. Chem.* **1976**, *41*, 1534.
170. Carledge, F. K.; Wolcott, J. W.; Dubac, J.; Mazerolles, P.; Fagoaga, P. *Tetrahedron Lett.* **1975**, 3593. Wolcott, J. M.; Cartledge, F. K. *J. Organometal. Chem.* **1976**, 111, C35. Cartledge, F. K.; Wolcott, J. M.; Dubac, J.; Mazerolles, P.; Joly, M. *ibid.* **1978**, *154*, 187.
171. Dubac, J.; Mazerrolles, P.; Joly, M.; Cartledge, F. K.; Wolcott, J. M. *ibid.* **1978**, *154*, 203.
172. Dzhaparidze, K. G. *Soobshch. Akad. Nauk Gruz. SSR* **1962**, *29*, 401; *Chem. Abstr.* **1963**, *58*, 9703b; Durig, J. R.; Willes, J. N., Jr. *J. Mol. Spectrosc.* **1969**, *32*, 320. Durig, J. R.; Lafferty, W. J.; Kalinsky, W. F. *J. Phys. Chem.* **1976**, *80*, 1199.
173. Vidal, J. P.; Lapasset, J.; Falgueirettes, J. *Acta Crystallogr., Sec. B*, **1972**, *28*, 3137.
174. Sommer, L. H.; Bennet, O. F. *J. Am. Chem. Soc.* **1957**, *79*, 1008; *ibid.* **1959**, *81*, 251. Homer, G. D.; Sommer, L. H. *ibid.* **1973**, *95*, 7700; Boudjouk, P.; Kapfer, C. A.; Cunico, R. F. results to be published.
175. Hilderbrandt, R. L.; Homer, G. D.; Boudjouk, P. J. *J. Am. Chem. Soc.* **1976**, *98*, 7476.
176. Schei, S. H.; Shen, Quang; Cunico, R. F.; Hilderbrandt, R. L. *J. Molec. Struc.* **1980**, *63*, 59.
177. Shen, Quang; Kapfer, C. A.; Boudjouk, P.; Hilderbrandt, R. L. *J. Organometal. Chem.* **1979**, *169*, 147.
178. Shen, Quang; Hilderbrandt, R. L.; Turns, G. T.; Barton, T. J.; *J. Organometal. Chem.* **1980**, *195*, 39.
179. Lukevits, E. Y.; Voronkov, M. G. "Organic Insertion Reactions of Group IV Elements"; Consultants Bureau: New York, 1966. Eaborn, C.; Bott, R. W. In "Organometallic Compounds of the Group IV Elements," Vol. 1, Part I; A. G. McDiarmid, Ed.; Marcel Dekker: New York, 1968.
180. Brooks, E. H.; Cross, R. J. *J. Organometal. Chem. Rev., A* **1971**, *6*, 227. Ang, H. G.; Lau, P. T.; *ibid.* **1972**, *8*, 235. Hofler, F. *Top. Curr. Chem.* **1974**, *50*, 129.
181. Corriu, R. J. P.; Moreau, J. J. E. *J. Chem. Soc., Chem. Commun.* **1980**, 278. Corriu, R. J. P.; Moreau, J. J. E.; Pataud-Sat, M. *J. Org. Chem.* **1981**, *46*, 3372.
182. Johnson, D. L.; Gladysz, J. A. *J. Am. Chem. Soc.* **1979**, *101*, 6433. Blakeney, A. J.; Gladysz, J. A. *J. Organometal. Chem.* **1981**, *210*, 303.
183. Chalk, A. J.; Harrod, J. F. *J. Am. Chem. Soc.* **1967**, *89*, 1640.
184. Murai, S.; Sonoda, N. *Angew Chem. Int. Ed. Engl.* **1979**, *18*, 837.
185. Meals, R. N. *Pure Appl. Chem.* **1966**, *13*, 141.
186. Speier, J. L. In "Advances in Organometallic Chemistry," Vol. 17; Stone, F. G. A.; West, R. Eds.; Academic Press. New York, 1979, p. 407.
187. Ojima, I.; Kogure, T. *Rev. Silicon Germanium Tin. Lead Compd.* **1981**, *7*, 5.
188. Sommer, L. H.; Pieturza, E. W.; Whitmore, F. C. *J. Am. Chem. Soc.* **1947**, *188*, 69.
189. Speier, J. L.; Webster, J. A.; Barnes, G. H. *J. Am. Chem. Soc.* **1957**, *79*, 974.
190. Benkeser, R. A.; Cunico, R. F.; Dunny, S.; Jones, P. R.; Nerlekar, P. G. *J. Org. Chem.* **1967**, *32*, 2634.
191. Brook, A. G.; Pannell, K. H.; Anderson, D. G. *J. Am. Chem. Soc.* **1968**, *90*, 4374.
192. Green, M.; Spencer, J. L.; Stone, F. G. A.; Tsipis, C. A. *J. Chem. Soc. Dalton* **1977**, 1525. Tsipis, C. A. *J. Organometal. Chem.* **1980**, *187*, 427.
193. Benkeser, R. A. *Pure Appl. Chem.* **1966**, *13*, 133.

194. Van Der Kerk, G. J. M.; Noltes, J. G. *J. Appl. Chem.* **1959**, *9*, 106. Leusink, A. J.; Marsman, J. W.; Budding, H. A.; *Rec. Trav. Chim. Pays-Bas* **1965**, *84*, 689.
195. Ojima, I.; Kumagai, M.; Nagai, Y. *J. Organometal. Chem.* **1974**, *66*, C 14.
196. Hill, J. E.; Nile, T. A. *J. Organometal. Chem.* **1977**, *137*, 293.
197. Watanabe, H.; Kitahara, T.; Motegi, T.; Nagai, Y. *J. Organometal. Chem.* **1977**, *139*, 215.
198. Dickers, H. M.; Haszeldine, R. N.; Mather, A. P.; Parish, R. V. *J. Organometal. Chem.* **1978**, *161*, 91.
199. Sommer, L. H.; Lyons, J. E.; Fujimoto, H. *J. Am. Chem. Soc.* **1969**, *91*, 7051.
200. Chalk, A. J.; Harrod, J. F. *J. Am. Chem. Soc.* **1965**, *87*, 16.
201. De Charentenay, F.; Osborn, J. A.; Wilkinson, G. *J. Chem. Soc., A*, **1968**, 787.
202. Ojima, I.; Nihonyanagi, N.; Kogure, T.; Kumagai, M.; Horiuchi, S.; Nakatsugawa, K.; Nagai, Y. *J. Organometal. Chem.* **1975**, *94*, 449.
203. Baird, M. C. *J. Inorg. Nucl. Chem.* **1967**, *29*, 367.
204. Bentham, J. E., Cradock, S.; Ebsworth, E. A. V. *J. Chem. Soc., A* **1971**, 587.
205. Chatt, J.; Eaborn, C.; Kapoor, P. N. *J. Chem. Soc., A* **1970**, 881.
206. Harrod, J. F.; Gibson, D. F. R.; Charles, R. *Can. J. Chem.* **1969**, *47*, 2205.
207. Jetz, W.; Graham, W. A. G. *J. Am. Chem. Soc.* **1969**, *91*, 3375.
208. Oliver, A. J.; Graham, W. A. G. *Inorg. Chem.* **1971**, *10*, 1.
209. Muir, K. W.; Ibers, J. A. *Inorg. Chem.* **1970**, *9*, 440.
210. Eaborn, C.; Hitchcok, P. B.; Tune, D. J.; Walton, D. R. M. *J. Organometal. Chem.* **1973**, *54*, C 1.
211. Eaborn, C.; Tune, D. J.; Walton, D. R. M. *J. Chem. Soc. Dalton* **1973**, 2255.
212. Blakeney, A. J.; Gladysz, J. A. *Inorg. Chim. Acta Lett.* **1981**, *53*, L 25.
213. Colomer, E.; Corriu, R. J. P.; Vioux, A. *J. Chem. Res., (S)* **1977**, *168 (M)* 1939.
214. Harrod, J. F.; Chalk, A. J. *J. Am. Chem. Soc.* **1965**, *87*, 1133.
215. Calas, R.; Duffaut, N. *C. R. Acad. Sci.* **1957**, *245*, 906. Calas, R.; Duffaut, N.; Menard, M. *Rev. Franç. Corps Gras* **1959**, *2*, 1; *Chem. Abstr.* **1959**, *53*, 11281i.
216. Yamamoto, K.; Hayashi, T.; Kumada, M. *J. Organometal. Chem.* **1972**, *46*, C 65. Hayashi, T.; Yamamoto, K.; Kumada, M. *ibid.* **1973**, *54*, C 45.
217. Eaborn, C.; Odell, K.; Pidcock, A. *J. Organometal. Chem.* **1973**, *63*, 93.
218. Johnson, D. L.; Gladysz, J. A. *Inorg. Chem.* **1981**, *20*, 2508.
219. Boyer, J.; Corriu, R. J. P.; Reyé, C.; Perz, R. *J. Organometal. Chem.* **1978**, *157*, 153, and references cited therein.
220. Sommer, L. H.; Lyons, J. E. *J. Am. Chem. Soc.* **1969**, *91*, 7061.
221. Sommer, L. H.; Citron, J. D. *J. Org. Chem.* **1967**, *32*, 2470.
222. Corriu, R. J. P.; Moreau, J. J. E. *J. Organometal. Chem.* **1972**, *40*, 55.
223. Osborn, J. A.; Jardine, F. H.; Young, J. F.; Wilkinson, G. *J. Chem. Soc., A* **1966**, 1711.
224. Green, M.; Howard, J. A.; Proud, J.; Spencer, J. L.; Stone, F. G. A.; Tsipis, C. A. *J. Chem. Soc., Chem. Commun.* **1976**, 671.
225. Felkin, H.; Swierczewski, G. *Tetrahedron* **1975**, *31*, 2735.
226. Corriu, R. J. P.; Massé, J. *Chem. Commun.* **1970**, 213. Corriu, R. J. P.; Massé, J.; Meunier, B. *J. Organometal. Chem.* **1973**, *55*, 73.
227. Carré, F. H.; Corriu, R. J. P. *J. Organometal. Chem.* **1974**, *74*, 49.
228. Colomer, E.; Corriu, R. J. P.; Meunier, B. *J. Organometal. Chem.* **1974**, *71*, 197.
229. Corriu, R. J. P.; Meunier, B. *J. Chem. Soc., Chem. Commun.* **1973**, 164. Corriu, R. J. P.; Meunier, B. *J. Organometal. Chem.* **1973**, *60*, 31.
230. Corriu, R. J. P.; Meunier, B. *J. Organometal. Chem.* **1974**, *65*, 187.
231. Corriu, R. J. P.; Meunier, B. *J. Organometal. Chem.* **1975**, *93*, 81.

232. Piper, T. S.; Lemal, D.; Wilkinson, G. *Naturwiss.* **1956**, *43*, 129.
233. Corriu, R. J. P.; Douglas, W. E. *J. Organometal. Chem.* **1973**, *51*, C 3.
234. Cerveau, G.; Colomer, E.; Corriu, R. J. P.; Douglas, W. E. *J. Chem. Soc., Chem. Commun.* **1975**, 410.
235. Cerveau, G.; Colomer, E.; Corriu, R. J. P.; Douglas, W. E. *J. Organometal. Chem.* **1977**, *135*, 373.
236. Cerveau, G.; Chauvière, G.; Colomer, E.; Corriu, R. J. P. *J. Organometal. Chem.* **1981**, *210*, 343.
237. Carré, F. H. *Cryst. Struct. Commun.*, in press.
238. Hagen, A. P.; Mac Diarmid, A. G. *Inorg. Chem.* **1966**, *6*, 686. Aylett, B. J.; Campbell, J. M. *Chem. Commun.* **1967**, 159.
239. Cerveau, G.; Colomer, E.; Corriu, R. J. P. *J. Organometal. Chem.* **1982**, *236*, 33.
240. Manassero, H., personnal communication.
241. Corriu, R. J. P.; Colomer, E. *J. Organometal. Chem.* **1977**, *133*, 159.
242. Dahan, F.; Jeannin, Y. *J. Organometal. Chem.* **1977**, *136*, 251.
243. Colomer, E.; Corriu, R. J. P. *J. Chem. Soc., Chem. Commun.* **1976**, 176.
244. Colomer, E.; Corriu, R. J. P.; Young, J. C. *J. Chem. Soc., Chem. Commun.* **1977**, 73.
245. Sommer, L. H.; Mason, R. *J. Am. Chem. Soc.* **1975**, *87*, 1619.
246. Carré, F.; Cerveau, G.; Colomer, E.; Corriu, R. J. P.; Young, J. C.; Ricard, L.; Weiss, R. *J. Organometal. Chem.* **1979**, *179*, 215.
247. Carré, F. H.; Cerveau, G.; Colomer, E.; Corriu, R. J. P. *J. Organometal. Chem.* **1982**, *229*, 257.
248. Eaborn, C.; Kapoor, P. N., Tune, D. T.; Turpin, C. L.; Walton, D. R. M. *J. Organometal. Chem.* **1972**, *34*, 153.
249. Eaborn, C.; Tune, D. J.; Walton, D. R. M. *J. Chem. Soc., Chem. Commun.* **1972**, 1233.
250. Colomer, E.; Corriu, R. J. P.; Vioux, A. *J. Chem. Soc., Chem. Commun.* **1976**, 175.
251. Colomer, E.; Corriu, R. J. P.; Vioux, A. *Inorg. Chem.* **1979**, *18*, 695.
252. Colomer, E.; Corriu, R. J. P.; Vioux, A., to be published.
253. Cerveau, G.; Colomer, E.; Corriu, R. J. P.; Young, J. C. *J. Organometal. Chem.* **1981**, *205*, 31.
254. Cerveau, G.; Colomer, E.; Corriu, R. J. P. *Angew. Chem. Int. Ed. Engl.* **1981**, *20*, 478.
255. Cerveau, G., Colomer, E.; Corriu, R. J. P. *Organometallics*, **1982**, *1*, 867.
256. Chock, P. B.; Halpern, J. *J. Am. Chem. Soc.* **1966**, *88*, 3511.
257. Sommer, L. H., Ulland, L. A.; Parker, G. A. *J. Am. Chem. Soc.* **1972**, *94*, 3469.
258. Harrod, J. F.; Smith, C. A. *J. Am. Chem. Soc.* **1970**, *92*, 2699.
259. Harrod, J. F.; Smith, C. A.; Than, K. A. *J. Am. Chem. Soc.* **1972**, *94*, 8321.
260. Jetz, W.; Graham, W. A. G. *Inorg. Chem.* **1971**, *10*, 4.
261. Hart-Davis, A. J.; Graham, W. A. G. *J. Am. Chem. Soc.* **1971**, *93*, 4388, and references cited therein.
262. Colomer, E.; Corriu, R. J. P.; Marzin, C.; Vioux, A. *Inorg. Chem.* **1982**, *21*, 368.
263. Schubert, U., personnal communication.
264. Bennett, M. J.; Simpson, K. A. *J. Am. Chem. Soc.* **1971**, *93*, 7156.
265. Andrews, M. A.; Kirtley, E. W.; Kaesz, M. D. *Adv. Chem. Ser.* **1978**, *176*, 215.
266. Auburn, M.; Ciriano, M.; Howard, J. A. K.; Murray, M.; Pugh, N. J.; Spencer, J. L.; Stone, F. G. A.; Woodward, P. *J. Chem. Soc. Dalton* **1980**, 659.
267. Bürger, H.; *Angew. Chem. Int. Ed.* **1973**, *12*, 475.
268. Corriu, R. J. P.; Dabosi, G.; Martineau, M. *J. Organometal. Chem.* **1978**, *150*, 27; *ibid.* **1978**, *154*, 33.

269. Corriu, R. J. P.; Dabosi, G.; Martineau, M. *ibid.* **1980**, *186*, 25.
270. Colvin, E.; "Silicon in Organic Synthesis"; Butterworths Monographs in Chemistry and Chemical Engineering, Butterworths: London, 1981, p. 178.
271. Boyer, J.; Corriu, R. J. P.; Perz, R.; Reyé, C. *J. Organometal. Chem.* **1978**, *148*, C 1; *ibid.* **1978**, *157*, 153; *ibid.* **1979**, *172*, 143; *ibid.* **1980**, *184*, 157.
272. Boyer, J.; Corriu, R. J. P.; Perz, R.; Poirier, M.; Reyé, C. *Synthesis* **1981**, 559.
273. Boyer, J.; Corriu, R. J. P.; Perz, R.; Reyé, C. *Tetrahedron* **1981**, *37*, 2165.
274. Boyer, J.; Corriu, R. J. P.; Perz, R.; Reyé, C. *Tetrahedron* **1983**, *39*, 117.
275. Ostaszinski, A.; Wielgat, J.; Urbanski, T. *Tetrahedron* **1969**, *25*, 1929.
276. Corriu, R. J. P.; Huynh, V.; Moreau, J.; Pataud-Sat, M. *Tetrahedron Lett.* **1982**, *23*, 3257.
277. Hosomi, A.; Shirata, A.; Sakurai, H. *Tetrahedron Lett.* **1978**, 3043. Sarkar, T. K.; Andersen, N. H. *Tetrahedron Lett.* **1978**, 3513. Trost, B. M.; Vincent, J. E. *J. Am. Chem. Soc.* **1980**, *102*, 5680.
278. Yoshida, J.; Tamao, K.; Yamamoto, H.; Kakui, T.; Uchida, T.; Kumada, M. *Organometallics* **1982**, *1*, 543, and references cited therein.
279. Rosenheim, A.; Raibmann, B.; Schendel, G. *Z. Anorg. Allg. Chem.* **1931**, *196*, 160.
280. Frye, C. L. *J. Am. Chem. Soc.* **1964**, *86*, 3170.
281. Boer, F. P.; Flynn, J. J.; Turley, J. W. *J. Am. Chem. Soc.* **1968**, *90*, 6973.
282. (a) Meerwein, H. *Justus Liebigs Ann. Chem.* **1929**, *476*, 113. (b) Meerwein, H. *Angew Chem.* **1951**, *63*, 489.
283. Müller, R.; Heinrich, L. *Chem. Ber.* **1961**, *94*, 1943.
284. Frye, C. L. *J. Am. Chem. Soc.* **1970**, *92*, 1205.
285. Clark, H. C.; Dixon, R. K.; Nicolam, J. G. *ibid.* **1969**, *8*, 450.
286. Marat, R. K.; Janzen, A. F. *Can. J. Chem.* **1977**, *55*, 1167; *ibid.* **1977**, *55*, 3845.
287. Murphy, M. K.; Beauchamp, J. L. *J. Am. Chem. Soc.* **1977**, *99*, 4992.
288. Wilkins, C. J.; Grant, D. K. J. *J. Chem. Soc.* **1953**, 927.
289. Burg, A. B. J. *J. Am. Chem. Soc.* **1954**, *76*, 2674.
290. Fergusson, J. E.; Grant, D.; Hickford, R. H.; Wilkins, C. J. J. *J. Chem. Soc.* **1959**, 99.
291. Beattie, I. R.; Gilson, T. *ibid.* **1965**, 6595.
292. Campbell-Ferguson, H. J.; Ebsworth, E. A. J. *J. Chem. Soc., A.* **1966**, 1508.
293. Cook, D. I.; Green, M.; Hazeldine, R. N.; Iles, B. R.; Jones, A.; Newlands, M. J. *ibid.* **1966**, 887.
294. Beattie, I. R.; Ozin, G. A. *ibid.* **1970**, 370.
295. Boal, D.; Ozin, G. A. *Can. J. Chem.* **1973**, *51*, 609.
296. Graddon, D. P.; Rana, B. A. *J. Organometal. Chem.* **1977**, *136*, 315; *ibid.* **1977**, *140*, 21.
297. Beattie, I. R.; Leigh, G. L. *J. Chem. Soc.* **1961**, 4249.
298. Corey, J. Y.; West, R. *J. Am. Chem. Soc.* **1963**, *85*, 4034.
299. Clark, H. C.; Corfield, P. W. R.; Dixon, K. R.; Ibers, J. A. *J. Am. Chem. Soc.* **1967**, *89*, 3360.
300. Ault, Bruce S. *Inorg. Chem.* **1979**, *18*, 3339.
301. (a) Frye, C. L.; Vogel, G. E.; Hall, J. A. *J. Am. Chem. Soc.* **1961**, *83*, 996. (b) Frye, C. L.; Vincent, G. A.; Finzel, W. A. *ibid.* **1971**, *93*, 6805.
302. Voronkov, M. G. *Pure Appl. Chem.* **1966**, *13*, 35. Frye, C. L.; Vincent, G. A.; Hauschildt, G. L. *J. Am. Chem. Soc.* **1966**, *88*, 2727.
303. Turley, J. W.; Boer, F. P. *J. Am. Chem. Soc.* **1969**, *91*, 4129.
304. Frye, C. L.; Vincent, G. A.; Hauschildt, G. L. *J. Am. Chem. Soc.* **1966**, *88*, 2727.
305. Daly, J. J.; Sanz, F. *J. Chem. Soc. Dalton* **1974**, 2051.
306. Morehouse, E. L. U.S. Patent 3,032,576 (1962); *Chem. Abstr.* **1962**, *57*, 9981h.

307. Pestunovich, V. A.; Voronkov, M. G.; Zelchan, G. I.; Lukevics, E. J.; Libert, L.; Egorochkin, A. N.; Burov, A. N. *Khim. Geterotsikl. Soedin. Sb.* **1970**, *2*, 339.
308. Gray, R.; Hercules, D. M. *Inorg. Chem.* **1977**, *16*, 1426.
309. Harris, R. K.; Jones, J.; Soon, N. G. *J. Magn. Resonance* **1978**, *30*, 521.
310. Pestunovich, V. A.; Tandura, S. N.; Voronkov, M. G.; Baryshok, V. P.; Zelchan, G. I.; Glükhikh, V. J. *Spectrosc. Lett.* **1978**, *11*, 339.
311. (a) Turley, J. W.; Boer, F. P. *J. Am. Chem. Soc.* **1968**, *90*, 4026. (b) Boer, F. P.; Turley, J. W.; Flynn, J. J. *ibid.* **1968**, *90*, 5102. (c) Turley, J. W.; Boer, F. P. *ibid.* **1969**, *91*, 4129; *ibid.* **1969**, *91*, 4134. (d) Kemme, A.; Bleidelis, J.; Solomennifova, I.; Zelchan, G.; Lukevics, E. *J. Chem. Soc., Chem. Commun.* **1976**, 1041.
312. Parkanyi, L.; Nagy, J.; Simon, K. *J. Organometal. Chem.* **1975**, *101*, 11, and references cited therein.
313. Kemme, A.; Bleidelis, J.; Zelcans, G.; Urtane, I.; Lukevics, E. *Zh. Strukt. Khim.* **1977**, *18*, 343; *Chem. Abstr. 87*, 068,452.
314. Kemme, A.; Bleidelis, J.; Urtane, I.; Zelchan, G.; Lukevics, E. *J. Organometal. Chem.* **1980**, *202*, 115, and references cited therein.
315. Laurenson, G. S.; Rankin, D. W. H. *J. Chem. Soc. Dalton* **1981**, 425; Ebsworth, E. A. V.; Murray, E. K.; Rankin, D. W. H.; Robertson, H. E. *ibid.* **1981**, 1501.
316. Parkanyi, L. H.; Hencsei, P.; Bihatsi, L. *J. Organometal. Chem.* **1982**, *232*, 315.
317. Lukevics, E.; Zelchan, G. I.; Solomennikova, I.; Liepin'sh, E. E.; Yankovska, I. S.; Mazheika, I. B. *Zh. Obshch. Khim.* **1977**, *47*, 109. Tandura, S. N.; Pestunovich, V. A.; Voronkov, M.; Zelchan, G.; Solomennikova, I. I.; Lukevics, E. *Khim. Geterotsikl. Soedin.* **1977**, 1063; *Chem. Abstr. 88*, 005,715.
318. Boer, F. P.; Van Remoortere, F. P. *J. Am. Chem. Soc.* **1970**, *92*, 801.
319. Voronkov, M.; Frolov, Yu. L.; D'Yakov, V. M.; Chipanina, N. N.; Gubanova, L. I.; Gavrilova, G. A.; Klyba, L. V.; Aksamentova, T. N. *J. Organometal. Chem.* **1980**, *201*, 165.
320. Hillyard, R. W.; Ryan, C. M.; Yoder, C. H. *J. Organometal. Chem.* **1978**, *153*, 369. Yoder, C. Y.; Ryan, C. M.; Martin, C. F.; Ho, P. S. *ibid.* **1980**, *190*, 1.
321. Farnham, W. B.; Harlow, R. L. *J. Am. Chem. Soc.* **1981**, *103*, 4608.
322. For a hexacoordinated silicon atom having fluorine ligands, see: Marat, R. K.; Janzen, A. F. *J. Chem. Soc., Chem. Commun.* **1977**, 671.
323. Weiss, A.; Herzog, A., In "Biochemistry of Silicon and Related Problems"; Bendz, G.; Lindqvist, I., Eds.; Plenum Press: New York, 1977, p. 109.
324. Schraml, J.; Bellama, J. M. In "Determination of Organic Structure by Physical Methods," Vol. 6; Nachod, F. D.; Zuckerman, J. J.; Randall, E. W.; Eds., Academic Press: New York, 1976, Chapter 4. Williams, E. A.; Cargioli, J. D. In "Annual Reports on n.m.r. Spectroscopy," Vol. 9, Webb, G. A., Ed.; Academic Press, New York, 1979.
325. Cella, J. A.; Cargioli, J. D.; Williams, E. A. *J. Organometal. Chem.* **1980**, *186*, 13.
326. Flynn, J. J.; Boer, F. P. *J. Am. Chem. Soc.* **1969**, *91*, 5756.
327. Marsmann, H. C.; Lower, R. *Chem. Ztg.* **1973**, *97*, 660.
328. Dilthey, W.; *Berichte* **1903**, *36*, 923. Dilthey, W. *Annalen* **1906**, *344*, 300.
329. West, R. *J. Am. Chem. Soc.* **1958**, *80*, 3246. Dahr, S. K.; Doron, V.; Kirschner, S. *J. Am. Chem. Soc.* **1958**, *80*, 753.
330. Pike, R.; Luengo, R. R. *J. Am. Chem. Soc.* **1965**, *87*, 1403; *ibid.* **1966**, *88*, 2972.
331. Herter, R. E. *Chem. Ind. (London)* **1963**, 1397.
332. Muetterties, E. L.; Wright, C. M. *J. Am. Chem. Soc.* **1964**, *86*, 5132; *ibid.* **1965**, *87*, 21; *ibid.* **1965**, *87*, 4706.
333. Kroenke, W. J.; Sutton, L. E.; Joyner, R. D.; Kenney, H. E. *Inorg. Chem.* **1963**, *2*, 1064. Doylan, D. B.; Calvin, M. *J. Am. Chem. Soc.* **1967**, *89*, 5472. Kane, A. R.;

Sullivan, J. F.; Kenny, D. K.; Kenney, E. *Inorg. Chem.* **1970**, *9*, 1445. Sayer, P.; Gouterman, M.; Connel, C. R. *Acc. Chem. Res.* **1982**, *15*, 73; Hush, N. S.; Cheung, A. S. *Chem. Phys. Lett.* **1977**, *47*, 1.

334. Kummer, D.; Köster, H. *Z. Anorg. Allg. Chem.* **1973**, *398*, 279. Kummer, D.; Seshadri, T. *Angew. Chem.* **1975**, *87*, 742; *Angew. Chem. Int. Ed. Engl.* **1975**, *14*, 699. Kummer, D.; Seshadri, T. *ibid.* **1977**, *428*, 129. Kummer, D.; Gaisser, K. E.; Seshadri, T. *Chem. Ber.* **1977**, *110*, 1950. Kummer, D.; Seshadri, T. *ibid.* **1977**, *110*, 2355.
335. Sawitzki, G.; Von Schnering, H.; Kummer, D.; Seshadri, T. *Chem. Ber.* **1978**, *111*, 3705.
336. Barn, V. A.; Killean, R. C. G.; Webster, M. *Acta Cryst.* **1969**, *B 25*, 156.
337. Kummer, D.; Köster, H.; Speck, M. *Angew. Chem. Int. Ed. Engl.* **1969**, *8*, 599; *ibid.* **1969**, *8*, 878. Kummer, D.; Balkir, A.; Köster, H. *J. Organometal. Chem.* **1979**, *178*, 29.
338. Sawitzki, G.; Von Schnering, H. G. *Chem. Ber.* **1976**, *109*, 3728.
339. Kummer, D.; Gaisser, K. E.; Serfert, J.; Wagner, R. *Z. Anorg. Allg. Chem.* **1979**, *459*, 145.
340. Sommer, L. H.; Bauma, D. L. *J. Am. Chem. Soc.* **1969**, *91*, 7045.
341. Gibson, J. A.; Janzen, A. F. *Can. J. Chem.* **1972**, *50*, 3087, and references cited therein.
342. Vasylishen, R. E.; Biroli, G. S.; Janzen, A. F. *Inorg. Chem.* **1976**, *15*, 3054. Swain, C. G.; Esteve, R. M.; Jones, R. H. *J. Am. Chem. Soc.* **1949**, *71*, 965.
343. Corriu, R. J. P.; Dabosi, G.; Martineau, M. *J. Organometal. Chem.* **1981**, *222*, 195.
344. Corriu, R. J. P.; Leard, M. *J. Organometal. Chem.* **1968**, *15*, 25.
345. Chojnowski, J.; Cypryk, M.; Michalski, J. *J. Organometal. Chem.* **1978**, *161*, C 31.
346. Bos, K. D.; Bulten, E. J.; Noltes, J. G. *J. Organometal. Chem.* **1975**, *99*, 379; *ibid.* **1976**, *120*, 211.
347. Corriu, R. J. P.; Lanneau, G.; Leclercq, D. *Tetrahedron* **1980**, *36*, 1617.
348. Helmer, B. J.; West, R.; Corriu, R. J. P.; Poirier, M.; Royo, G. **1983**, *251*, 295.
349. Corriu, R. J. P.; Poirier, M.; Royo, G. *J. Organometal. Chem.* **1982**, *233*, 165.
350. Brelière, C.; Corriu, R. J. P.; De Saxcé, A.; Royo, G. *J. Organometal. Chem.* **1979**, *164*, 19.
351. Berry, S. *J. Chem. Phys.* **1960**, *32*, 933.
352. Janzen, A. F.; Gibson, J. A.; Ibott, D. G. *Inorg. Chem.* **1972**, *11*, 2853.
353. Gibson, J. A.; Ibott, D. G.; Janzen, A. F. *Can. J. Chem.* **1973**, *51*, 3203.
354. Schmutzler, R. *Angew. Chem. Int. Ed. Engl.* **1965**, *4*, 496. Holmes, R. R.; *Acc. Chem. Res.* **1972**, *5*, 296 and references cited therein.
355. Corriu, R. J. P.; Larcher, F.; Royo, G. *J. Organometal. Chem.* **1977**, *129*, 299.
356. Sau, A. C.; Day, R. O.; Holmes, R. R. *J. Am. Chem. Soc.* **1980**, *102*, 7972.
357. Stevenson, W. H.; Martin, J. C. *J. Am. Chem. Soc.* **1982**, *104*, 309.
358. Tripett, S. *Pure Appl. Chem.* **1974**, *40*, 595.
359. Jurkschat, K.; Mügge, C.; Tzschach, A.; Zschunke, A.; Larin, M. F.; Pestunovich, V. A.; Vornnkov, M. G. *J. Organometal. Chem.* **1977**, *139*, 279. Mügge, C.; Jurkschat, K.; Tzschach, A.; Zschunke, A. *J. Organometal. Chem.* **1979**, *164*, 135.

The Synthesis and Stereochemistry of Chiral Organic Molecules with High Symmetry

MASAO NAKAZAKI

Department of Chemistry
Faculty of Engineering Science
Osaka University
Toyonaka, Osaka, Japan

I. INTRODUCTION

In 1856, the Royal Society of London awarded the Rumford medal to Louis Pasteur for his then recent outstanding accomplishment in the study of "Dissymétrie Moléculaire." The citation (1) afforded an explanation of the word "dissymmetry" that must have sounded strange at that time: "[two hemihedral forms] were dissymmetric, that is, could not be superposed on each other, but each could be superposed on the image of the other in a mirror."

Unfortunately, Pasteur's "dissymmetry" became confused with "asymmetry," as can be seen in the Alembic Club's translation of his lecture "Recherches sur la *Dissymétrie* Moléculaire des Produits Organiques Naturels" (2), delivered before the Chemical Society of Paris four years later (1860). The title of the English version (3, 4) is "Researches on the Molecular *Asymmetry* of Natural Organic Products." This confusion seems to have arisen partly because of the organic chemist's indifference to symmetry concepts, apparently accelerated by the overwhelming success of van't Hoff's "*asymmetric* carbon atom theory" (5) (my italics).

Asymmetry (lack of all elements of symmetry, except for C_1 axes, which are always present) is a necessary but insufficient criterion for an object to have a nonsuperposable enantiomer. This can be seen in Figure 1, which illustrates enantiomeric four-bladed windmills. Having nonsuperposable mirror images, these geometrical figures are dissymmetric, but they are not asymmetric because of their fourfold axes of symmetry (C_4 axes).

Fortunately, revival of Kelvin's "chirality" (6) and its introduction into stereochemistry (7) has served to prevent further misuse of the term asymmetry

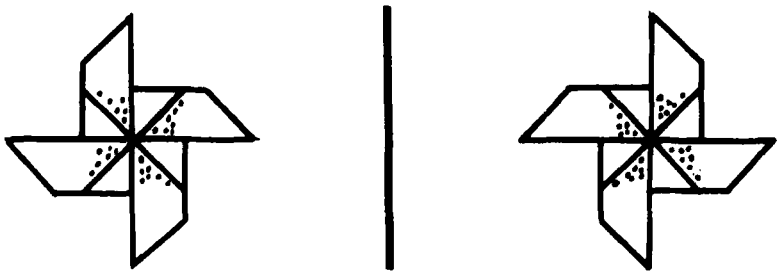

Figure 1. Enantiomeric four-bladed paper windmills (dissymmetric but not asymmetric).

Table 1.
Classification of Molecular Symmetry

archiral (nondissymmetric)	
chiral (dissymmetric)	asymmetric
	"high-symmetry chiral" (chiral but not asymmetric)

in place of dissymmetry, which had stubbornly persisted despite repeated cautions (8, 9). Unfortunately, however, stereochemistry has newly become contaminated by a misuse of the word "dissymmetry" itself; there has emerged a trend to call a chiral *but not* asymmetric object "dissymmetric" (10, 11, 12).

To circumvent this situation, an unambiguous and separate word to define "chiral but not asymmetric" is needed, and in this article the term "high-symmetry chiral" is proposed (13) (Table 1).

II. SYMMETRY CRITERIA IN MOLECULAR CHIRALITY

Related to the distinction between chiral and achiral objects, symmetry elements can be conveniently classified into two categories: simple axes of symmetry (C_n), and alternating (or mirror) axes of symmetry (S_n) (15).

An example of a twofold simple axis of symmetry (C_2 axis) can be seen in planar (*S*,*S*)-1,2-dimethylcyclopentane (**1**) (Figure 2), which can be brought to an indistinguishable position by a 180° rotation around this axis. As the *R*-*S* notation attached to the two asymmetric carbon atoms indicates, these centers have the same chirality; in general a C_n axis may have *n* identical asymmetric (*AS*) units disposed $2\pi/n$ apart around this axis.

The spiro compound (**2**) provides an example of a fourfold alternating axis (S_4 axis), and this molecule (or more precisely, molecular model) can be brought

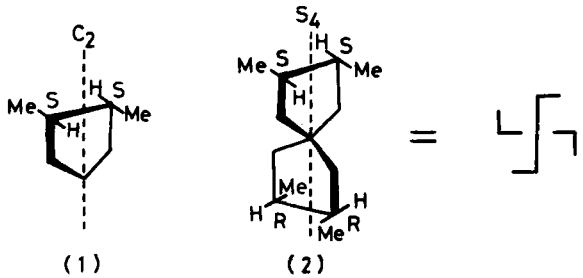

Figure 2. C_2 Simple axis of symmetry and S_4 alternating axis of symmetry.

Table 2.
Classification of Chiral Point Groups

chiral	asymmetric	$\mathbf{C_1}$		
	"high-symmetry chiral"	$\mathbf{C_n}$	$(n \geqslant 2)$	
		$\mathbf{D_n}$	$(n \geqslant 2)$	(dihedral symmetry)
		$\mathbf{T}$, $\mathbf{O}$, $\mathbf{I}$		(polyhedral symmetry)

to an indistinguishable position by a 90° rotation around the axis followed by a mirror reflection through the plane perpendicular to this same axis. The *R*-*S* notations attached to the four asymmetric centers imply that this molecule consists of two identical enantiomeric pairs of *AS* units disposed $2\pi/4$ apart around the axis with alternating opposite chiralities. Despite the lack of a plane of symmetry or center of symmetry, the customary criteria for chirality, **2** is achiral, emphasizing that the true criterion for chirality is the nonexistence of any S_n axis that comprises, as special cases, both the plane of symmetry (S_1) and the center of symmetry (S_2).

Combinations of C_n axes and S_n axes afford the symmetries for all finite geometrical figures, which are conveniently described by the point group notation.

Since any C_n axis in a $\mathbf{C_n}$ or $\mathbf{D_n}$ point group has *n AS* units with the same chirality oriented around itself, geometrical figures whose symmetry elements consist solely of this type of axis are chiral, the opposite is true for the figures having an S_n axis.

Table 2 gives the classification of chiral point groups, manifesting that "high-symmetry chiral" point groups include all chiral point groups except for the asymmetric one ($\mathbf{C_1}$). Any figures belonging to $\mathbf{C_n}$ point groups possess only C_n axes as their symmetry elements (except for the ubiquitous C_1 axis) and are composed of *n AS* units of the same chirality. This number *n* in $\mathbf{C_n}$ point groups is also equal to the symmetry number, which refers to the number of indistinguishable spatial orientations that a molecule can occupy as a result of simple rotation.

When a figure has one C_n axis and *n* C_2 axes (dihedral axes) perpendicular to it, it is said to belong to the $\mathbf{D_n}$ point group whose symmetry number is $2n$, indicating that this figure is composed of $2n$ *AS* units with same chirality. The remaining three point groups, **T**, **O**, and **I**, are customarily referred to as the chiral polyhedral symmetry point groups because of their relationship to the Platonic regular polyhedra: $\mathbf{T_d}$ (tetrahedron), $\mathbf{O_h}$ (octahedron), and $\mathbf{I_h}$ (icosahedron). Their respective symmetry elements are $(4C_3 + 3C_2)$, $(3C_4 + 4C_3 + 6C_2)$, and $(6C_5 + 10C_3 + 15C_2)$ with symmetry numbers 12, 24, and 60, respectively.

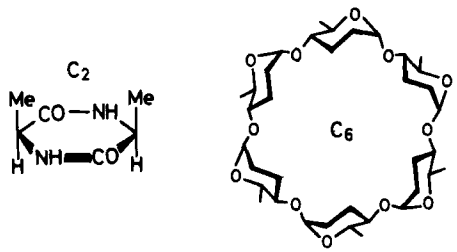

(3) (4)

Figure 3. Generation of C_2 and C_6 symmetry by arranging natural asymmetric units.

III. GENERATION OF HIGH-SYMMETRY CHIRAL MOLECULES BY ARRANGING ASYMMETRIC UNITS

Analysis of the nature of C_n axes suggests that one can create high-symmetry chiral figures by proper arrangement of n *AS* units with the same chirality around appropriate axes. A simple example of this procedure can be found in the planar diketopiperazine (**3**) (Figure 3) of C_2 symmetry, which is constructed by combining two *AS* units of the same chirality, that is, two molecular fragments of (+)-(*S*)-alanine.

Condensation of six molecules of D-(+)-glucose yields α-cyclodextrin (**4**), whose conformation of highest symmetry belongs to the C_6 point group and whose symmetry number 6 corresponds to the total number of its submolecular *AS* units.

IV. GENERATION OF HIGH-SYMMETRY CHIRAL MOLECULES BY DESYMMETRIZATION OF AN ACHIRAL MOLECULAR FRAMEWORK

Another way to generate high-symmetry chiral figures is by systematic desymmetrization of an achiral figure which, as a matter of principle, must have at least one S_n axis. The nature of an S_n axis demands the pairwise arrangement of enantiomeric *AS* units (*A* and *A**) around this axis, and the exchange of all *AS* units of the same chirality (say, *A**) with another *AS* unit (say, *B*) generates high-symmetry chiral shapes. Figure 4 illustrates an application of this principle, "Curie's principle" (16), to a figure of C_{2v} symmetry that is intrinsically constituted of two pairs of enantiomeric *AS* units (*A* and *A**).

While the exchange $A^* \rightarrow B$ destroys two planes of symmetry inherent in the original C_{2v} symmetry, it keeps the C_2 axis intact, creating a figure of C_2 symmetry. Another, mirror-image mode of desymmetrization $A \rightarrow B^*$ affords the enantiomeric figure of C_2 symmetry. In ethylene oxide (C_{2v} symmetry) (Figure

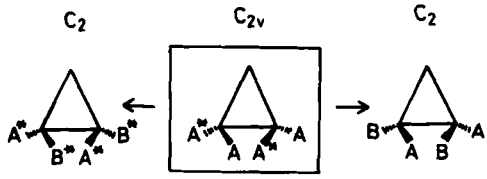

Figure 4. Generation of enantiomers of C_2 symmetry by desymmetrization of C_{2v} symmetry.

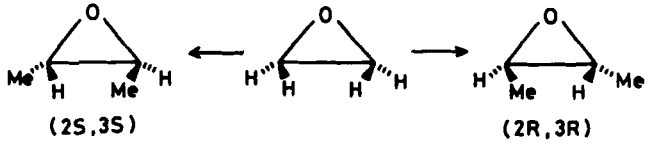

Figure 5. Desymmetrization of C_{2v} symmetry by pair-wise substitution of enantiotopic ligands.

5), one can distinguish two pairs of homotopic hydrogen atoms (17) which in turn are enantiotopic to each other. Substitution of one pair of homotopic hydrogen atoms by methyl groups affords one enantiomer of the *trans*-2,3-dimethyl derivative, whereas substitution of the other pair of hydrogen atoms provides the other enantiomer.

Another illustrative example of this principle can be found in McCasland's classic paper (18), in which he reported the synthesis of one of the very rare compounds with S_4 symmetry (Figure 6). His esterification of pentaerythritol with optically active menthoxyacetic acid may be regarded as the desymmetrization of the T_d symmetry inherent in the methane molecule to generate tetraesters of either D_2 or S_4 symmetry.

Farina (19) has provided a number of examples of the application of "Curie's principle" in his review entitled "High Symmetry Chiral Molecules," and Prelog (20) has extended the same principle to his "simplex" in relation to his studies of generalized pseudoasymmetry.

The desymmetrization of an achiral figure to transform it into a high-symmetry chiral one can also be achieved by a twist deformation around the C_n axis, and the direction of the twist determines the chirality of the figures generated

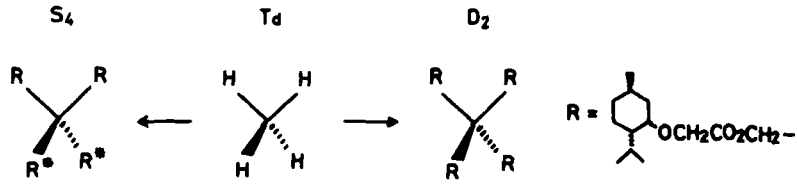

Figure 6. Generation of D_2 and S_4 symmetry by desymmetrization of T_d symmetry.

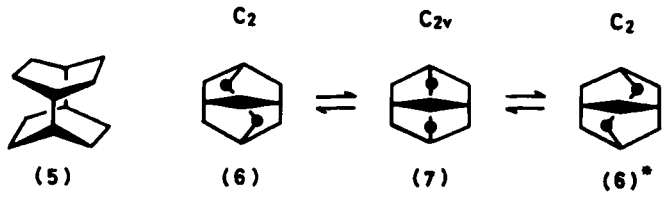

(Figure 7). Osawa's recent force-field calculation study (21) of cage-shaped molecules with ethano bridges affords an excellent demonstration of this twist deformation at the molecular level. In six achiral cage-shaped molecules so far studied, his calculations showed that each molecule assumed a twisted, chiral conformation to minimize torsional and nonbonding strain. Tricyclo[4.2.2.2.^{2,5}]dodecane (**5**) was shown to be 1.1 kcal/mol more stable in a twisted D_2 than in the eclipsed D_{2h} conformation, and his calculation also suggests that perhydrotriquinacene and C_{16}-hexaquinane should assume C_3 rather than C_{3v} conformations, contrary to naive pictures obtained by a casual observation of molecular models.

The situation is more complicated in homoadamantane (**7**) where a casual study of the molecular model would suggest that the molecule ought to assume two strain-free enantiomeric C_2 conformations (**6** and **6***). Schleyer's force-field calculation (22) has predicted, however, that the achiral C_{2v} conformer (**7**) will be more stable than the twisted conformers, and this has been borne out by a dynamic NMR study (23), as well as by CD spectral analyses of its mono- and C_2 diketone derivatives (24).

Another striking example is the **T** symmetry of tetrakis[trimethylsilyl]silane (25), the discussion of which is deferred to the last section, dealing with high-symmetry chiral polyhedral symmetry. An interesting conformational deformation in a crystal lattice has been analyzed by X-ray crystallography coupled with force-field calculations (26).

As the Table of Contents for this chapter indicates, the sections to follow describe the synthesis and stereochemistry of high-symmetry chiral compounds classified according to their main structural characteristics. It seems pertinent here to give a few criteria applied in the selection of the material covered in this review. Since Farina's article (19) covered the literature up to the beginning of

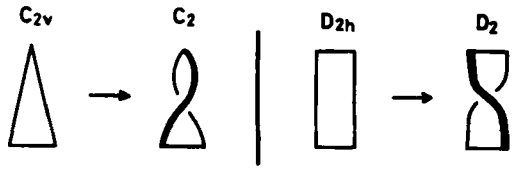

Figure 7. Generation of chiral shapes of C_2 or D_2 symmetry by twisting achiral frameworks.

1973, this chapter mainly concentrates on the information published from then until the end of 1980, although almost all of Farina's examples are discussed again from a somewhat different angle.

The enormous number of compounds with C_2 symmetry has forced the reviewer to abandon the attempt to include them in this review, except for those that happen to be closely related to compounds of higher symmetry (symmetry number $\geqslant 3$), which are described in detail. Also excluded from this review are conformational aspects of relatively simple compounds whose high-symmetry chiral conformations exhibit energy barriers between them so low as to prevent their successful isolation.

Pertinent to these fascinating subjects, quite a number of excellent articles have appeared in *Topics in Stereochemistry* and elsewhere (27-30); this may justify the exclusion of these topics from the present review.

Another policy adopted here is that priority is always given to the discussion of optically active forms of pertinent structures. Information on earlier work with the corresponding racemic modifications should be sought in the references cited in the articles concerned with the optically active substances.

As implicitly understood in earlier discussions (Figures 3 and 6), the symmetry of flexible molecules discussed here refers, unless stated otherwise, to their highest available symmetry, for example, [8][8]paracyclophane (**100**) is said here to have D_2 symmetry, notwithstanding our ignorance of the precise conformation assumed by the two octamethylene bridges spanning the benzene ring.

V. HIGH-SYMMETRY CHIRAL MOLECULES DIRECTLY RELATED TO NATURAL PRODUCTS

The abundance in nature of amino acids and carbohydrates in optically pure modifications, together with their polyfunctionality, recommends them as candidates for convenient *AS* units for constructing high-symmetry chiral molecules

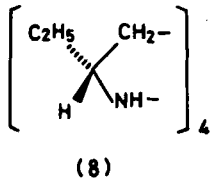

(8)

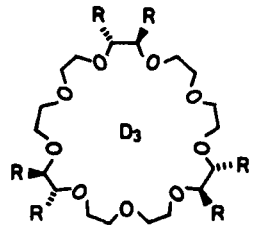

R=CONMe2 (9)

R= CH2OH / OH / H (10)

such as α-cyclodextrin (**4**), which, in its potassium acetate complex, was shown to assume a conformation of slightly distorted C_6 symmetry (31, 32).

Cyclo[tri-L-prolyl] offers another example of a high-symmetry chiral cyclic peptide, whose conformation of C_3 symmetry in the crystal lattice has been revealed by an X-ray study (33). The C_4 symmetry of the cyclic tetramer of chiral aziridine **8** was also confirmed by X-ray analysis (34).

Because of the easy accessibility of (+)-tartaric acid and D-mannitol, it is not surprising to find that many efforts (35) have been made for the preparation of various high-symmetry chiral crown ethers having these natural products as the *AS* units.

Among numerous compounds of this class so far reported, two crown ethers of D_3 symmetry, **9** and **10**, are shown here by way of examples having (+)-tartaric acid (36) and D-mannitol (37) as the chiral modifiers.

VI. HIGH-SYMMETRY CHIRAL MOLECULES OF SPIRO STRUCTURES

The meso-(2*S*, 3*S*, 7*R*, 8*R*)-tetramethyl derivative (**2**) of S_4 symmetry discussed in Figure 2 is one of seven possible stereoisomers generated by desymmetrization of the original D_{2d} symmetry inherent in the parent spiro[4.4]nonane framework, as shown by the projection formula in Figure 8.

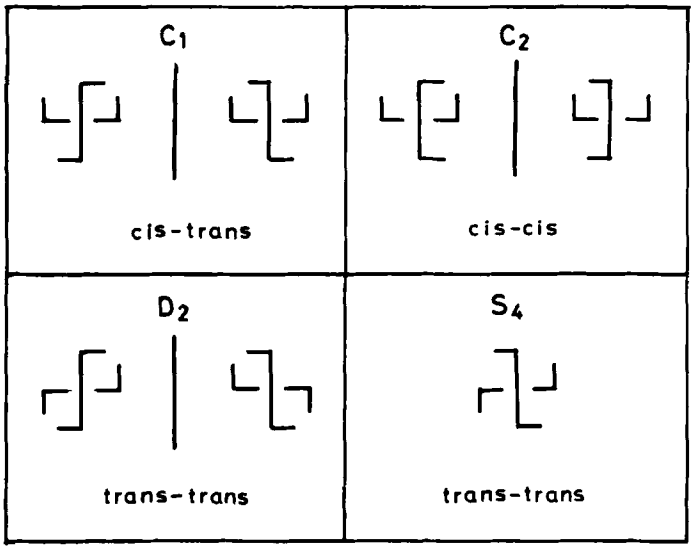

Figure 8. Desymmetrization of spiro[4.4]nonane by 2,3,7,8-tetramethyl substitution.

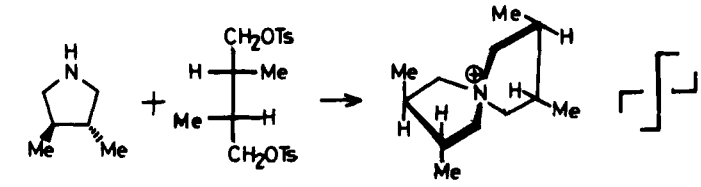

(+)-(3R,4R) (11) (-)-(2R,3R) (12) $[\alpha]_D$ +19.9° (13)

In his classical synthetic study of a meso spiro compound of S_4 symmetry, McCasland (38) reported the preparation of dextrorotatory quaternary spiro ammonium compound (**13**) (D_2) by combining (+)-(3*R*,4*R*)-3,4-dimethylpyrrolidine (**11**) and (-)-(2*R*,3*R*)-ditosylate (**12**), whereas combination of (+)-**11** and (+)-(2*S*,3*S*)-ditosylate (the enantiomer of **12**) afforded the first synthetic organic molecule of S_4 symmetry.

While McCasland was also successful in preparing the optically active C_1 cis,trans isomer with known absolute configuration, the optical resolution and elucidation of the absolute configuration of the C_2 cis,cis isomer remained to be accomplished.

A mixture of stereoisomers of the allene **14** was reported (39) to form in a gas phase reaction of *trans*-2-butene and "triatomic carbon." The stereochemical aspects in **14** are, in principle, identical with those of the spiro compounds depicted in Figure 8, and isolation of two isomers (1 : 1 ratio), presumably of D_2 and S_4 symmetry, was reported without identification of the individual structures.

Another interesting example of desymmetrization of the D_{2d} spiro framework to D_2 symmetry has been demonstrated in the double bridging of spirobifluorene. In their synthetic work on the class of "vespirenes" whose generic name was derived from a combination of the German name of their common symmetry (D_2 = Viererpunktsymmetrie) and the name of their parent spirobifluorene, Prelog and co-workers (40) treated the optically active dicarboxylic acid **15** with polyphosphoric acid to give (-)-[6.6]vespirone (**16**). Removal of

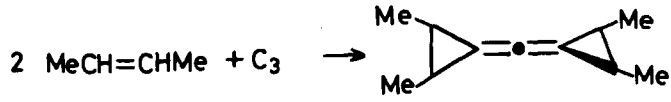

(14)

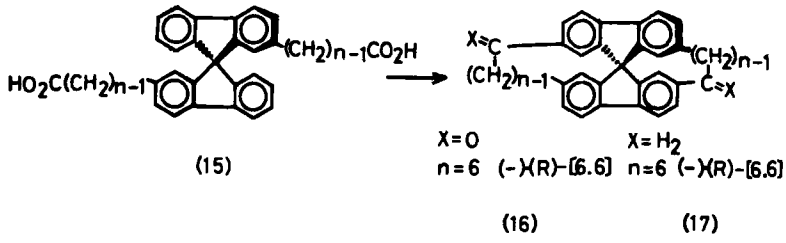

(15) (16) (17)

the carbonyl groups yielded (-)-[6.6]vespirene (**17**). The [7.7] and [8.8] homologs were prepared by a similar sequence. CD spectral analysis of the intermediate diketone **16** led to assignment of the absolute configurations.

Before ending this section, some mention of a recent synthetic study (41) of the first "primary helical molecule" of cumulative spiro structure seems pertinent.

Reaction of cyclopentanone and α-lithio-α-methoxyallene provided **18**, which was converted into the spiroketone **19**, and repetition of the same sequence of conversions for four times eventually afforded cyclopentyl[5]helixane (**20**), m.p. 195-197°C, whose uniformly helical structure is secured by steric hindrance from the neighboring spiro ring.

Removal of the cyclopentane moiety at one end and the carbonyl group at the other would furnish a homogeneous helical structure whose symmetry, despite its beautiful appearance, belongs to the C_1 point group because of the polarity induced by the presence of oxygen atoms. A similar situation is true for the α-helix of peptides, the helical structure of nucleic acids (42), and bacterial flagellae (43), even though these are built from identical *AS* units having the same chirality (e.g., (+)-(*S*)-alanine).

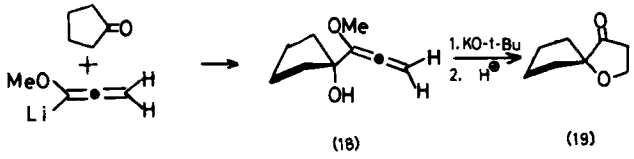

(18) (19)

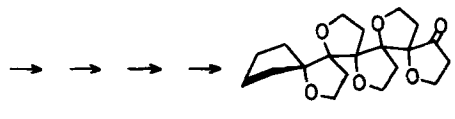

(20)

In this connection, it is interesting to note that fascinating enantiomeric helical aggregates have been observed in electron microscopic photographs of lithium 12-hydroxystearate (44); the D-(−)-acid salt exhibits a helix of *P* helicity while the enantiomer gave one of opposite (*M*) helicity.

VII. HIGH-SYMMETRY CHIRAL TWISTED π-ELECTRON SYSTEMS 1: CYCLOALKENES AND CYCLOALKYNES

A. Monocyclic Dienes and Triynes

Cope's classical papers (45, 46) on the successful optical resolution of *trans*-cyclooctene (**21**) (Figure 9) demonstrate a way to desymmetrize the $\mathbf{D_{2h}}$ symmetry of ethylene by trans bridging. In this molecule, the -$(CH_2)_6$- bridge is short enough to prevent interconversion between the enantiomeric $\mathbf{C_2}$ conformers **21** ⇌ **23** through the "loop-jumping" mechanism.

In an interesting contrast to the observed optical lability of *trans*-cyclodecene, successful resolution (47) has been recently reported for 1,2-dimethyl-*trans*-cyclodecene (**22**) and the higher homolog, 1,2-dimethyl-*trans*-cycloundecene.

Cope and co-workers (48) obtained unstable *trans,trans*-1,5-cyclooctadiene (**24**) by photolysis of bis[chloro(*cis,cis*-cyclooctadiene)copper(I)], and Allinger's force-field calculation (49) suggested that the $\mathbf{D_2}$ cross-form conformation (**24**) is 5.35 kcal/mol more stable than a chair conformation of $\mathbf{C_{2h}}$ symmetry.

An X-ray crystallographic study (50) revealed a $\mathbf{D_3}$ conformation for *trans, trans,trans*-1,5,9-cyclododecatriene (**25**) in the crystal lattice. A dynamic NMR study was carried out, and gave the free energy of activation as 8.6 kcal/mol for the interconversion between the enantiomeric $\mathbf{D_3}$ conformers, while a force-field calculation (51) gave 9.5 kcal/mol for this energy barrier.

A stable pseudo-chair conformation of $\mathbf{D_3}$ symmetry was also indicated for 1,5,9-cyclododecatriyne (**26**) by means of an *ab initio* STO-3G calculation, as well as by photoelectron spectral analysis (52).

A brief survey of a few medium-sized heterocyclic compounds (53) showing interesting conformational aspects ends this section. The cis,cis (**27**) and trans,

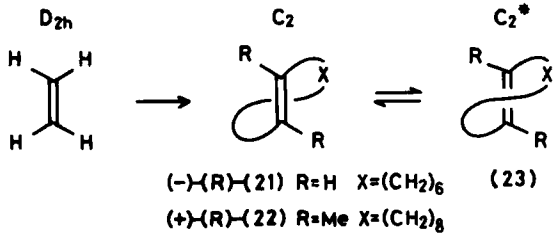

Figure 9. Desymmetrization of $\mathbf{D_{2h}}$ symmetry of ethene by trans bridging.

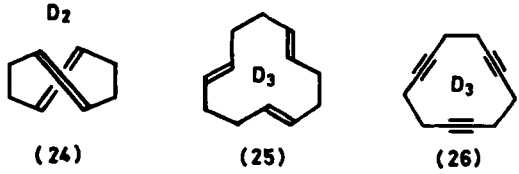

(24) (25) (26)

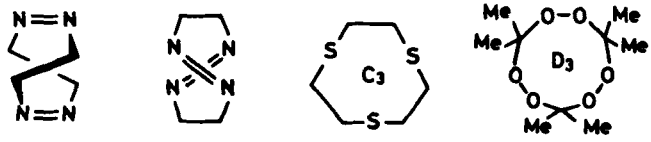

(27) (28) (29) (30)

trans(28) stereoisomers of 1,2,5,6,-tetraaza-1,5-cyclooctadiene have been shown to exhibit an interesting contrast; while a force-field calculation (54) showed that for the trans,trans isomer the D_2 conformation (28) is the most stable, the same calculation indicates the D_2 conformation of the cis,cis-isomer (27) to be intermediate in stability between chair and boat conformations.

Another striking contrast has been found in cyclononane and its 1,4,7-trithia derivative (29); whereas the former's most stable conformer has D_3 symmetry (55), the most stable conformation of the latter displays C_3 symmetry (56). A D_3 conformation has been assigned to trimeric acetone peroxide (30) by X-ray crystallography (57).

B. Monocyclic Diallenes

The D_{2d} symmetry of allene **31** allows its 1,3-disubstitution with the same achiral substituents to generate an enantiomeric pair of stereoisomers of C_2 symmetry (Figure 10), making an interesting contrast to ethylene (Figure 9) where

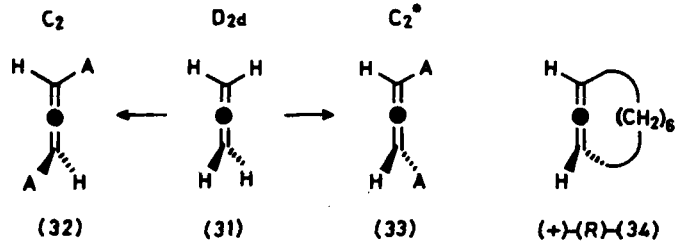

(32) (31) (33) (+)-(R)-(34)

Figure 10. Desymmetrization of D_{2d} symmetry of allene.

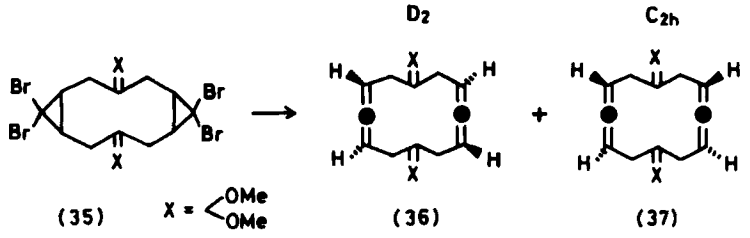

similar desymmetrization of its intrinsic D_{2h} symmetry by 1,2-disubstitution merely gives rise to cis,trans isomerism. And this difference between the symmetry in ethylene and allene is reflected in that 1,3-bridging in allene automatically generates an enantiomeric pair of C_2 symmetry, the first example of which (+)-(*R*)-1,2-cyclononadiene (**34**) of known absolute configuration, was synthesized by Cope and co-workers (58).

It may be remarked in passing that the 1,3-bridged allene **34** possesses axial chirality of a configurational nature, and the "loop-jumping" conformational change (see above) does not affect its chirality, while the chirality of a 1,2-*trans*-bridged ethylene such as **21** should be classified as planar and its conformational nature is revealed by the chirality inversion accompanying a "loop-jumping" internal rotation.

Conceptually, 1,2,7,8-cyclododecatetraene (**36**) may be regarded to be constructed by combining two units of 1,3-disubstituted allene **32** and this structural feature suggests that combination of two units of the same chirality yields an enantiomeric pair of D_2 symmetry, while combination of two units of opposite chirality yields a meso compound of C_{2h} symmetry.

The first synthesis of this class of monocyclic diallenes has been reported by Sondheimer and co-workers (59, 60). They treated the dibromocarbene adduct **35** with (-)-sparteine-CH_3Li complex at -10°C to obtain **36** (D_2 symmetry), m.p. 113-116°C, $[\alpha]_D$ + 24.4°, together with the optically inactive meso **37** (C_{2h} symmetry) m.p. 86-87.5°C. X-ray crystallographic data (61) have become available which show that the only isolable isomer of 1,2,6,7-cyclodecatetraene, m.p. 36°C (62), a lower homolog of **37** ($X=H_2$), has a center of symmetry, indicating that this is a meso compound with C_{2h} symmetry.

C. Doubly Bridged Allenes

The doubly bridged allene **38** of D_2 symmetry was first cited by Cahn, Ingold, and Prelog in their classic paper "Specification of Molecular Chirality" (7) to illustrate the procedure for specifying the axial chirality of a molecule with this unusually high symmetry. Our group reported the synthesis of the optically

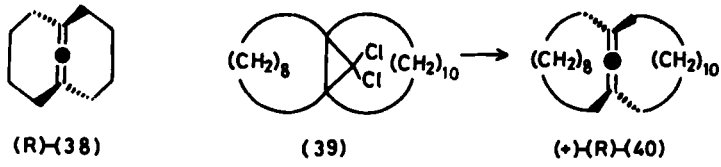

(R)-(38) (39) (+)-(R)-(40)

active higher homolog **40** (C_2 symmetry) with two different polymethylene bridges (63, 64); we treated the dichlorocarbene adduct **39** with (-)-sparteine-*n*-BuLi complex, and isolated (+)-bicyclo[10.8.1]heneicosa-1(21),12(21)-diene (**40**), m.p. 60-64°C (9% yield). The observed (+)(220 nm)- and (-)(231 nm)-Cotton effects led to assigning it the *R* configuration (65).

D. Trans Doubly Bridged Ethylenes

The number of the *sp* carbon atoms sandwiched between the terminal sp^2 carbon atoms determines the symmetry of homologous cumulenes (66); an odd number ($2p + 1$) generates a series of $\mathbf{D_{2d}}$ cumulenes, and an even number ($2p$) generates a series of $\mathbf{D_{2h}}$ cumulenes. As mentioned earlier, a double bridge connecting the terminal sp^2 centers desymmetrizes these parent cumulenes (Figure 11); the [8.10] doubly bridged allene (**40**) described in the preceding section may be regarded as a specific case of such doubly bridged $\mathbf{D_{2d}}$ cumulenes (**41**) with $p = 0$, $m = 8$, and $n = 10$.

In the $\mathbf{D_{2h}}$ cumulenes, chirality is generated only by trans double bridging. The doubly bridged ethylene **43** ("bis(*trans*-polymethylene)ethylene") cited first in Cahn, Ingold, Prelog's paper (7) is the simplest example of a trans doubly bridged $\mathbf{D_{2h}}$ cumulene (**42**) where $p = 0$ and $m = n = 6$.

Actual syntheses of trans doubly bridged ethylenes have been accomplished almost simultaneously by our group at Osaka University (67, 68) and by Marshall's group at Northwestern University (69). Because of its straightforwardness and extremely simple procedure, our photochemical method (Figure 12) has, since its publication, become virtually the sole method used for synthesizing various members of this series of compounds.

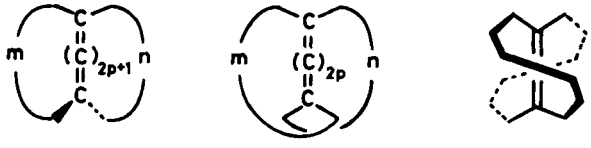

(41) (42) (43)

Figure 11. Desymmetrization of $\mathbf{D_{2d}}$ and $\mathbf{D_{2h}}$ cumulenes by double bridging.

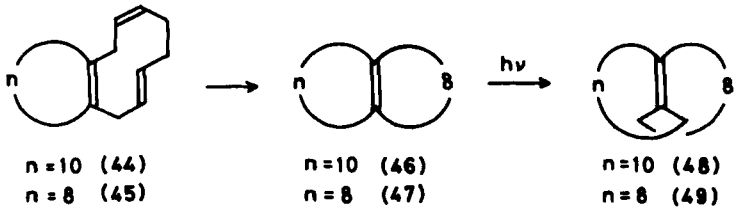

Figure 12. Syntheses of [8.10] and [8.8] doubly bridged ethylenes (Osaka University).

The starting material in our synthesis was cyclododecyne whose oligomerization with two moles of butadiene gave the bicyclic triene **44**, which in turn was converted into the cis doubly bridged ethylene **46** by partial catalytic hydrogenation with Raney nickel. Irradiation of **46** with a low-pressure mercury lamp in cyclohexane led to a 1 : 2 cis-trans mixture, from which the trans isomer **48**, m.p. 37-38°C, was isolated after removal of the unchanged cis isomer as a dichlorocarbene adduct.

Similar irradiation of the lower homolog **47** afforded a much lower conversion ratio (cis : trans = 9 : 1); the isolated **49** of D_2 symmetry boiled at 125-127°C/0.1 mmHg.

As expected from the buried nature of the unsaturated center sandwiched between two polymethylene bridges, the trans isomers were found to be inert toward dichlorocarbene attack and were recovered after 32 hr of attempted catalytic hydrogenation in acetic acid ethyl acetate solution (PtO_2, at 60-65°C).

While the corresponding cis isomer gave a wine-red color reaction with tetracyanoethylene, no color reaction was observed with trans doubly bridged ethylenes. This, together with their lack of reactivity to oxidation by peracids also revealed the inert nature of the central double bonds in these isomers.

Interestingly, irradiation of the trans isomers was found to yield almost the same mixture of cis-trans isomers as that obtained starting from the cis precursors.

The synthesis of [10.10]-betweenanene (**55**) at Northwestern University was rather involved, so only part of it is reproduced in Figure 13. The starting material is 1,2-cyclododecanedione (**50**), which was converted into a 1 : 1.5 mixture of cis-trans isomers of the diepoxides (**51**). After separation from the cis isomer, the trans isomer was transformed into the diester **54** via **52** and **53** through eight steps. Acyloin condensation of **54** followed by modification of the remaining functional groups completed the synthesis of **55**, m.p. 64-65°C.

Although in a recent paper (70) it was reported that the procedure has been improved to provide **55** in a yield as high as 2.6% starting from cyclododecanone through 12 steps, the claim of a novel synthesis of **55** involving acidic rearrangement of the cis precursors (71a) has proved to be erroneous (71b).

Nickon and Zurer (72) have reported a convenient synthetic route to the cis-[11.11] precursor involving an acidic rearrangement. Topological aspects

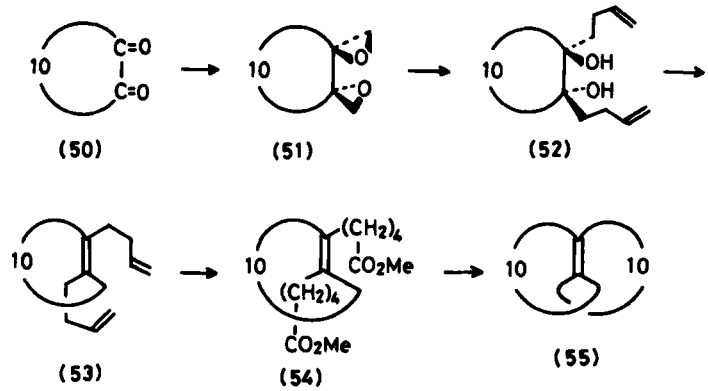

Figure 13. Synthesis of [10.10] doubly bridged olefins (Northwestern University).

of conformational isomerism (68) (Figure 14) in the trans doubly bridged ethylenes have been discussed in relation to those of the [m][n]paracyclophanes (73). Unlike trans singly bridged ethylenes, such as *trans*-cyclooctene (**21**) whose conformational transformation via "halfway (180°) loop-jumping" leads to chirality inversion, the same conformational change in the [m.m]-trans doubly bridged ethylenes generates anti and syn diastereomers of D_2 and C_2 symmetry, respectively. The situation becomes more complicated in the [m][n]-isomers where there arise two syn conformers of C_2 symmetry, depending upon the relative spatial orientation of the two bridges with regard to the planar unsaturated center.

In his recent review of "betweenanenes," Marshall (74) reported the synthesis of the [22.10]-compound, which was found to be inert toward complex formation with tetracyanoethylene, and toward hydroboration with isopinocampheylborane, suggesting that the [22]-bridge is not long enough to let the [10]-bridge pass through it.

Preparation of the first optically active specimen of a trans doubly bridged ethylene was achieved by our group (75); we treated the cis-[8.8] precursor with *N*-bromosuccinimide to obtain the bromide **56**, which in turn was trans-

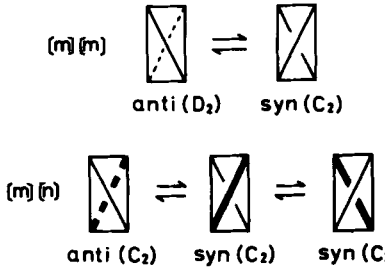

Figure 14. Chemical topology in [m.m] and [m.n] trans doubly bridged ethylenes.

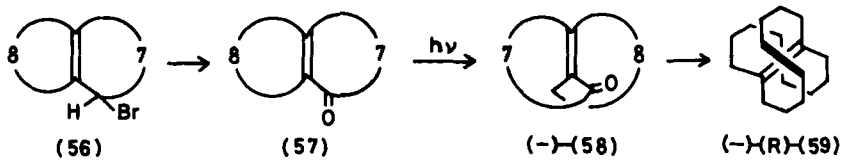

(56) (57) (−)-(58) (−)-(R)-(59)

formed to the α,β-unsaturated ketone **57**. Irradiation of **57** in hexane with a medium-pressure mercury lamp yielded a 1:5.5 mixture of the cis precursor **57** and the trans isomer **58**. When carried out in diethyl (+)-(*R*)-tartrate, the same photoconversion afforded levorotatory **58**, $[\alpha]_D$ $-13°$, which after removal of the functional group provided the (−)-enantiomer (**59**), $[\alpha]_D$ $-2.3°$, $[\theta]_{222.5\,nm}$ -1.8×10^3. The *R* configuration and optical purity of 0.5–1.0% were assigned to this levorotatory specimen on the basis of CD spectral comparison with optically active *trans*-cyclooctene (**21**).

The announcement of this result was followed by Marshall and Black's paper (76) reporting their successful preparation of (−)-[26.10]-, $[\alpha]_D$ $-24.7°$ (6.6% e.e.) and (−)-[24.10]-betweenanenes, $[\alpha]_D$ $-32.4°$ (7.6% e.e.). This was accomplished via asymmetric oxidation [with (+)-monoperoxycamphoric acid] of the racemic [26.10]- and [24.10]betweenanenes secured by photoisomerization of their cis precursors.

Two reviews (74, 77) covering the same subjects discussed in this section have appeared, with somewhat different emphasis.

VIII. HIGH-SYMMETRY CHIRAL TWISTED π-ELECTRON SYSTEMS 2: AROMATICS

A. Biaryls

Asymmetric Meerwein-Ponndorf disproportionation (78) with (+)-(*S*)-2-octanol led to assignment of the *R* configuration to the doubly bridged biphenyldiketone (**60**). This was further confirmed by stereochemical correlation based on X-ray diffraction data (79). These correlations have been extended to

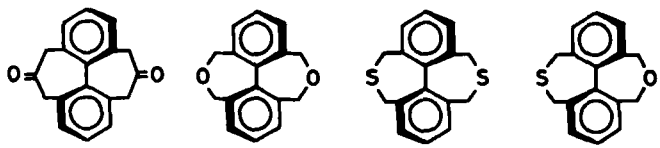

(+)-(R)-(60) (+)-(R)-(61) (+)-(R)-(62) (+)-(R)-(63)

assigning the *R* configurations to the closely related biphenyl derivatives **61** and **62**, both with D_2 symmetry, and **63** with C_2 symmetry. Their optical stability was reported to depend on the nature of the central atoms in the bridges giving the order $S > CO > O \gg CH_2$; in fact, the trimethylene doubly bridged biphenyl has been shown to be too labile for optical resolution.

It might be mentioned in passing that a recent study (80) on microbial reduction of (±)-**60** with *Rhodotorula rubra* offered a convenient method for its optical resolution in that the microbe preferentially reduced the (-)-(*S*)-enantiomer and left (+)-(*R*)-ketone intact with 58% optical purity.

In connection with their synthetic approach to the study of axial pseudo-asymmetry, Prelog and co-workers (81) systematically desymmetrized the D_{2d} symmetry inherent in biphenyl-2,2′,6,6′-tetracarboxylic acid (Figure 15) by converting the four functional groups to proper *AS* units. In principle this is identical with the desymmetrization of spiro[4.4]nonane (Figure 8), which was shown to afford four symmetries: D_2, S_4, C_2, and C_1. The desymmetrization (81) was achieved by amidation with optically active α-phenylethylamine. It should be noted that the interesting compound (-)-**64**, m.p. 140°C of D_2 symmetry, which was prepared simply by amidation with the (-)-(*S*)-amine, possesses no axial chirality.

While **67** of C_1 symmetry has been obtained only in a racemic modification, **66** of C_2 symmetry was prepared in a levorotatory modification whose axial *S* configuration was established by correlating an intermediate in its synthesis to (-)-2,2′-dimethylbiphenyl-6,6′-dicarboxylic acid of known *R* configuration.

Among numerous optically active crown ethers so far synthesized to test their chiral recognition aptitudes, there may be found quite a number of molecules with D_2 and D_3 symmetry. Typical examples are (-)-**69** (D_2 symmetry)

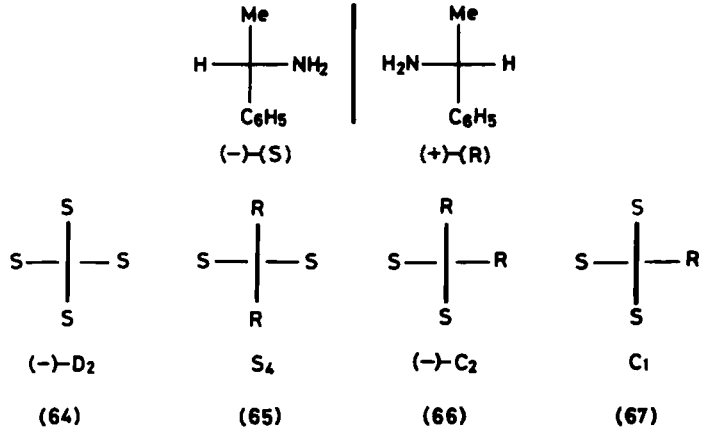

Figure 15. Schematic representation of the diastereomers generated by desymmetrization of biphenyl-2,2′,6,6′-tetracarboxylic acid with enantiomeric α-phenylethylamines.

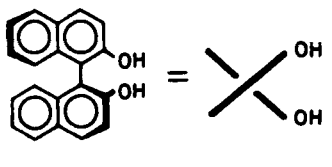

(−)-(S)-(68)

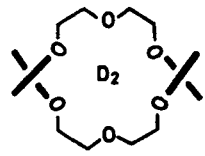

(−)-(69)

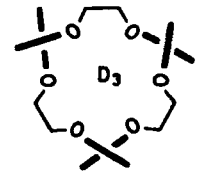

(−)-(70)

(82) and (−)-**70** (D_3 symmetry) (83), which possess two and three units of (−)-(*S*)-bi-α-naphthol (**68**) as their fundamental structural feature. A series of crown ethers of D_2 symmetry having C_2 9,9′-spirobifluorenedicarboxylic acid (cf. **15**) as *AS* units has been prepared (84).

B. Multilayered Paracyclophanes (85)

The unsaturated [4.4]paracyclophane **71**, m.p. 136-137°C, was prepared (86) by dehydrobromination of the corresponding tetrabromide and was said (19) to be the first paracyclophane of D_2 symmetry. Inspection of the molecular model suggests that this molecule assumes a rigid conformation with a rather high activation energy of racemization, although no attempt has been made to resolve it.

Two interesting compounds, **72** (87) and **73** (88), were prepared, and suggestions were made that these molecules should be most stable in their twisted conformations of D_3 symmetry.

To study bridgehead reactivity, our group (89) prepared a cyclophane of C_3 symmetry **74**; a comparison with triphenylmethyl chloride indicated that the bridgehead chloride of **74** is conspicuous in its striking lack of reactivity in S_N1 displacement reactions and in free radical formation.

Dynamic NMR spectral analysis of the deuterio derivative of **74** provided $E_a = 15.5$ kcal/mol for the interconversion between two enantiomeric C_3 conformations.

Structurally, the [2.2]paracyclophane **75** (D_2 symmetry) can be envisaged to

(71)

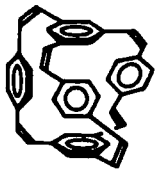

(72)

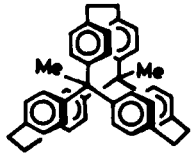

(73)

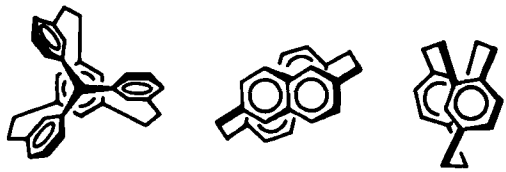

(74) (75) (76)

be constructed by combining two 2,6-disubstituted naphthalenes (C_{2h} symmetry) with their enantiotopic molecular planes of the same chirality face-to-face. Syntheses of **75** (90) and the analogous [2.2]paracyclophane (D_2) possessing 1,5-disubstituted naphthalene moieties (91) have been reported, and a successful partial resolution of **75** by SiO_2-(-)-TAPA column chromatography was carried out to support the chiral nature of **75**.

Another interesting cyclophane of an unusually twisted structure is the recently prepared [2.2.2](1,2,4)(1,2,5)cyclophane (**76**) (92). Its C_2 symmetry reflects its unique structural feature in that this molecule is built up by combining two 1,2,4-trisubstituted benzene moieties (C_s symmetry) with their enantiotopic faces of the same chirality face-to-face, as discussed for **75**.

Cram and co-workers (93) once called [2.2]paracyclophane (**77**) "one of the rigid cyclophanes that illustrate stereochemical principles," and they demonstrated various ways to desymmetrize its intrinsic D_{2h} symmetry by substitution.

The tetramethyl derivative **78** (94) of D_2 symmetry was the first in this class of compounds to have been optically resolved, followed by the tetramethoxy derivative **79** (95); the former through (-)-TAPA complexing, the latter through SiO_2-(-)-TAPA column chromatography.

An interesting class of optically active crown ethers of D_2 symmetry having tetrahydroxy[2.2]paracyclophane moieties corresponding to **79** has been reported (96).

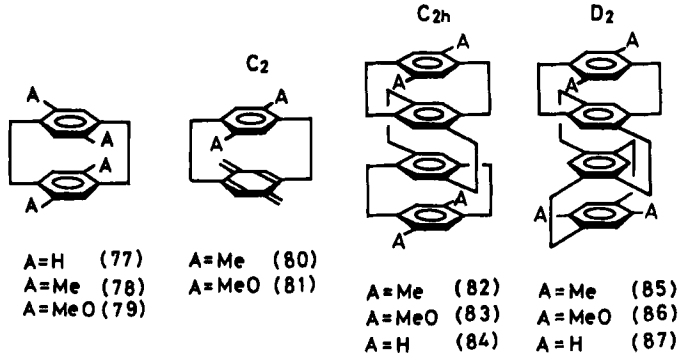

In their pioneering work in multilayered cyclophane chemistry, Longone and Chow (97) prepared a mixture of four-layered [2.2]paracyclophanes **82** and **85** by making use of the elegant procedure of Cram, which involves coupling of the *p*-xylylene intermediate **80** derived by a 1,6-Hofmann elimination of the corresponding quaternary ammonium base. There are available two alternatives for coupling the racemic **80** of C_2 symmetry; either between enantiomers of opposite chirality or between enantiomers of same chirality. The former should provide *meso*-**82** of C_{2h} symmetry, whereas the latter should yield **85** of D_2 symmetry.

Although they were unsuccessful in cleanly separating **82** and **85**, Staab and Zapf (98) reported chromatographic separation of **83** and **86** from a 1:2 reaction product mixture. They confirmed the meso structure of **83** by X-ray diffraction, which indicated the presence of a center of symmetry.

In the course of an extensive exploration of the syntheses and absolute configurations of optically active multilayered [2.2]paracyclophanes, our group has proposed (99) the name [n]chochin for the whole family of layered cyclophanes constructed from the [2.2] paracyclophane moiety. "Chochin" is the Japanese name for an old-fashioned, cylindrically shaped lantern having helical chirality, and *n* stands for the number of benzene rings in the molecule–for example, both **84** and **87** are called [4]chochin. This proposal also incorporates the way to specify the intrinsic stereochemistry of the 1,2,4,5-tetrasubstituted benzene rings sandwiched between the two terminal benzene rings as illustrated in Figure 16. The *meso*-**84** of C_{2h} symmetry and **87** of D_2 symmetry are to be named (*R*,*S*)-[4]chochin and (*S*,*S*)-[4]chochin respectively.

In carrying out our syntheses of a homologous family of optically active [n]chochins of D_2 symmetry, ($n = 3$, 4, 5, and 6), our group (99) started from (-)-(*R*)-[2.2]paracyclophanecarboxylic acid (**88**) (100), which was converted to the (-)-quaternary ammonium compound **90** via **89**. Coupling of (-)-**90** and **91** mediated by AgOH afforded (-)-(*R*)-[3]chochin (**92**) and (-)-(*R*,*R*)-[4]chochin (**93**) with yields of 5% and 4% respectively.

As an extension of this method to higher homologs, they coupled (-)-**90** with (-)-[3]chochin quaternary ammonium base **94** to obtain (-)-(*R*,*R*)-[4]chochin (**93**) [6% yield, by self-coupling of (-)-**90**], (-)-(*R*,*R*,*R*)-[5]chochin (**95**) [3% yield, by cross-coupling between (-)-**90** and (-)-**94**], and (-)-(*R*,*R*,*R*,*R*)-[6]chochin (**96**) [1.4% yield, by self-coupling of the three-layered (-)-**94**]. CD spectral analysis showed that this class of [n]chochins of D_2 symmetry all ex-

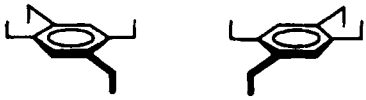

Figure 16. Specification of planar chirality of the inner benzene rings in [n]chochins.

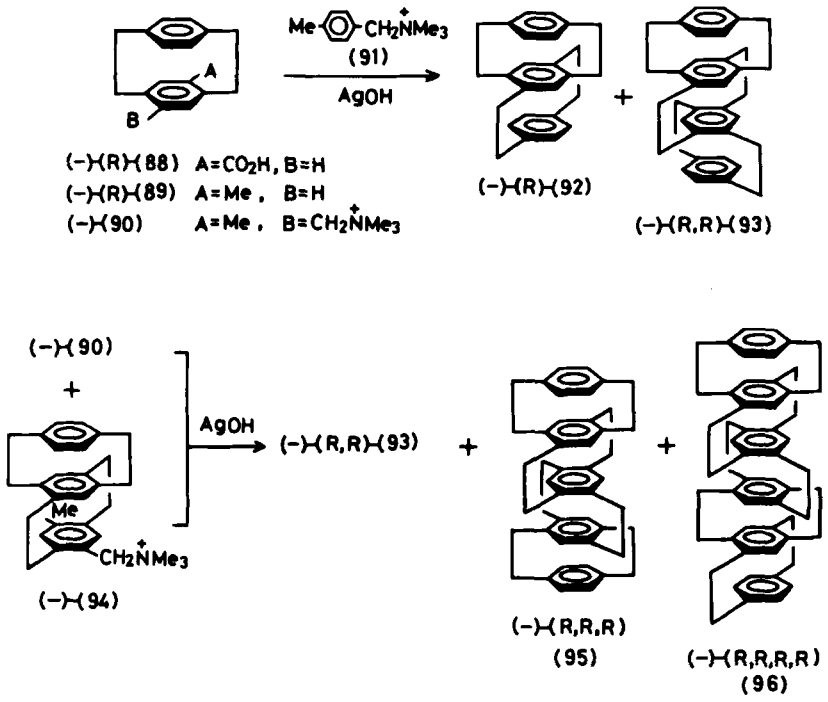

hibit complex (-)-Cotton effect curves in the 240-360 nm region. Table 3 records the formulas for the enumeration of stereoisomers in [n]chochins, and it is particularly interesting to note (a) the progressive increase in the number of possible stereoisomers with n, which is quite impressive, giving 131,328 isomers for [20]chochin, and (b) the symmetry, $\mathbf{C_2}$, $\mathbf{C_{2h}}$, or $\mathbf{D_2}$, for each member of the family.

Table 3.
Stereoisomer Enumeration in [n]Chochin

	n = odd ($n \geqslant 3$)	n = even ($n \geqslant 4$)	$n = 6$	$n = 20$
$\mathbf{D_2}$	$2^{(n-1)/2}$	$2^{(n-2)/2}$	4	512
$\mathbf{C_2}$	$2^{n-3} - 2^{(n-3)/2}$	$2^{n-3} - 2^{(n-2)/2}$	4	130560
$\mathbf{C_{2h}}$ (meso)		$2^{(n-4)/2}$	2	256
Total	$2^{n-3} + 2^{(n-3)/2}$	$2^{n-3} + 2^{(n-4)/2}$	10	131328

C. [m][n]Paracyclophanes

Although the name [m][n]paracyclophane was proposed for the family of paracyclophanes possessing two *p*-polymethylene bridges spanning the 1-4 and 2-5 positions of a benzene ring (199), no member of this class of compounds had been reported at that time (1964). This prompted our group (101) to undertake a synthetic study of optically active [8][8]- and [8][10]-paracyclophanes.

After correlating the absolute configuration of (+)-carboxylic acid **97** with (+)-(*S*)-[2.2]paracyclophanecarboxylic acid (**88**) of established configuration via the liaison compound (+)-**101**, we converted (+)-**97** into the (-)-quaternary ammonium base **98**, which in turn was transformed into the furanophane **99** by Cram's method. Cleavage of the furan ring followed by removal of the functional groups finally provided (+)-(*S*)-[8][8]paracyclophane (**100**) of $\mathbf{D_2}$ symmetry, which exhibits a (+)-Cotton effect in the 220-300 nm region. The (-)-(*R*)-[8][10]paracyclophane ($\mathbf{C_2}$ symmetry) was prepared via a similar sequence of reactions and was shown to exhibit an enantiomeric (-)-Cotton effect in the same wavelength region.

It is interesting to note that a common feature of the optically active [n]cochins of $\mathbf{D_2}$ symmetry and the [m][n]paracyclophanes so far synthesized is that the ones containing a *R* unit of a 1,2,4,5-tetrasubstituted benzene (Figure 16) are all, without exception, levorotatory at the D line.

A brief comment on the chemical topology of [m][n]paracyclophanes seems to be pertinent here. This is entirely parallel to that already discussed for the [m][n]trans doubly bridged ethylenes (Figure 14), in that there arises anti- and syn-diastereomerism when one of bridges becomes long enough to let the other "loop-jump" through it.

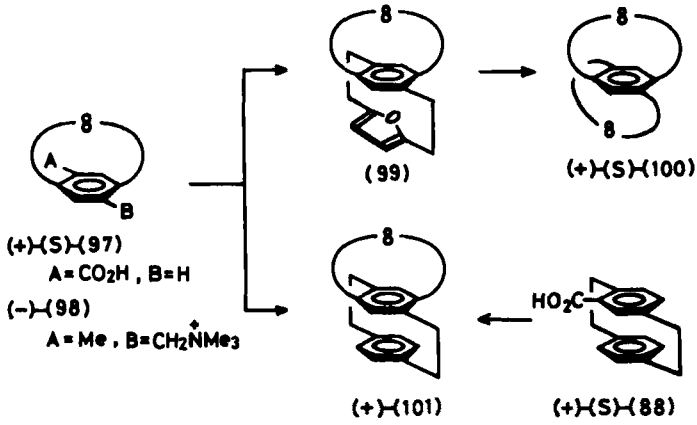

(102)

(103)

[m][n][p]Paracyclophane (**102**) may be classified as a type of "superphane" (102) which has C_2 symmetry even when $m = n = p$. A conspicuous stereochemical feature of **102** is that this molecule cannot be conceptually flattened to a non-crossing-over two-dimensional figure by any topological disfiguration.

This interesting characteristic is shared with a D_3 trefoil knot (**103**); a study of molecular models has suggested that a polymethylene ring as large as $C_{45}H_{90}$ will be required to allow the molecule to assume this configuration (103).

D. Helicenes (104) and Propellicenes

The successful synthesis of [13]helicene (105) may be regarded as a token of the tremendous progress made in recent helicene chemistry. From the standpoint of symmetry, however, this exquisite three-layered molecule shares the same C_2 symmetry with [6]helicene, the simplest among this class of compounds. Fusing two C_2 [n]helicenes (**104**) will generate "double" helicenes either of C_i symmetry **105** or of C_2 symmetry **106**, depending on the way of combination of the enantiomers. The preparation of several "double" helicenes of C_i and C_2 symmetry has been reported (106).

Fusion of both ends of **106** will generate a "closed" (palindromic) helicene **107** of D_2 symmetry; a preliminary report describes an unsuccessful synthetic approach to a "closed" [13]helicene by photochemical ring closure of **108** (107). Synthesis of an interesting class of compounds called "propellicenes" of D_2 symmetry, which is closely related to the "closed" helicene, has been reported (108); both **109** and **110** were prepared in 65-70% yield from their pre-

(104)

(105)

(106)

(107)

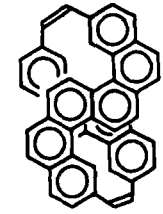

(108)

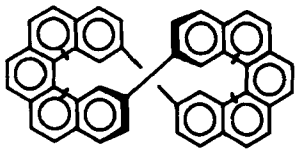

(109)

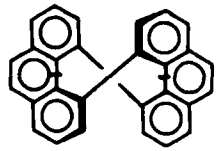

(110)

cursors by photochemical ring closure (the wavy lines in the structural formula indicate the positions of the ring closure). Kauffmann and Lexy (109) have reported a preparation of a heterocyclic compound of $\mathbf{D_2}$ symmetry with a similar structure.

E. *o*-Hexaphenylenes

On oxidation of the chromium complex **111** with $CuCl_2$, Wittig and Rümpler (110) obtained a mixture of two rigid conformers **112** and **113** of *o*-hexaphenylene (3% yield). The $\mathbf{D_2}$ symmetry of **113**, m.p. 345–346°C, was demonstrated by its spontaneous optical resolution (up to $[\alpha]_D \pm 11°$) as well as by chromatographic resolution employing SiO_2-(−)-TAPA columns (up to $[\alpha]_{365}$ +110°). The chiral nature of **113** was further confirmed by X-ray crystallography.

F. Tribenzo- and Tetrabenzocyclododecane Derivatives

Tri-*o*-thymotide (**114**), a trioxa derivative of tribenzocyclododecane, has been one of the most quoted representatives of optically labile compounds. Since a number of reviews (19, 111) have extensively described the fascinating aspects of this compound, including its spontaneous optical resolution and inclusion complexing, we shall here focus attention on more recent work in this and related fields.

Variable temperature NMR studies of **114** (112) have elucidated a fairly detailed picture of conformational transformations. A three-bladed propeller-like

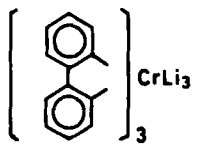

(111)

(112)

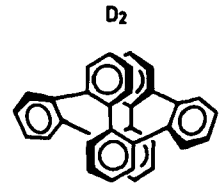

(113)

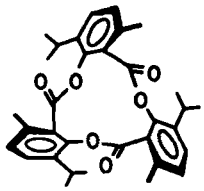

(-)-(M)-(114)

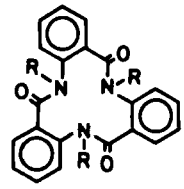

R=Me (115)
R=$CH_2C_6H_5$ (116)

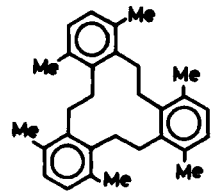

(117)

conformation of C_3 symmetry is first converted into a C_1 conformation, then to the C_1^* conformation enantiomeric to C_1, and finally to the C_3^* conformation that is the enantiomer of the starting C_3 conformation.

The original assignment of *M* helicity to (+)-tri-*o*-thymotide based on CD spectral analysis (113) was corrected by an X-ray crystallographic study (114), which provided evidence that the (-)-enantiomer has the C_3 symmetry of a three-bladed propeller with *M* helicity. Facile deformation from C_3 symmetry in the crystal lattice has been suggested to explain this molecule's striking ability to form a vast number of inclusion complexes with a variety of molecular species (115).

The trimethyl derivative **115** of trianthranilide was shown to assume a C_1 conformation in the crystal lattice, and only 5.5% of the C_3 conformer was detected in $CDCl_3$ solution at room temperature (116). By means of silica gel chromatography performed at +5°C, Ollis and co-workers (117) succeeded in separating two conformers of the tribenzyl derivatives **116**; a kinetically controlled product of C_1 symmetry melting at 134-136°C, and a thermodynamically controlled product of C_3 propeller symmetry, m.p. 260-263°C. NMR study showed that an equilibrated $CDCl_3$ solution contains a 41:59 mixture of the C_1 and C_3 conformers at ambient temperature, and that raising the temperature of the solution shifts the equilibrium towards the C_1 conformer until the peaks characteristic to the C_3 conformer become unobservable. A variable temperature NMR study gave $\Delta G^{\ddagger} = 26.2$ kcal/mol for the $C_3 \rightleftharpoons C_3^*$ interconversion, which may be compared with $\Delta G^{\ddagger} = 17.1$ kcal/mol for the conformational racemization process ($D_3 \rightleftharpoons D_3^*$) in the related hydrocarbon **117** (118).

Another X-ray study (119) has disclosed interesting helical structures of the dimethyl- and dibenzyl-trianthranilides in the crystal lattice. Two recent reviews have concisely surveyed the multistep conformational interconversions in medium rings of lower symmetry related to **117** (27, 120).

The tetrabenzocyclododecane **120** (121) of D_2 symmetry, conspicuous in having two acetylene bonds only 2 Å apart (122), was prepared in a 7.8% yield

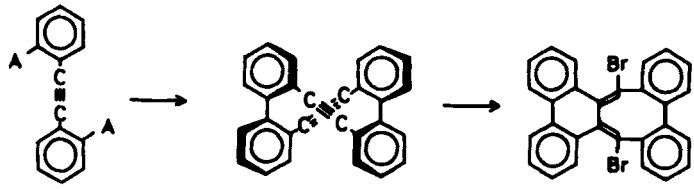

A = Br (118)
A = Li (119)

(120)

(121)

by oxidative coupling ($CuCl_2$) of the dilithio derivative **119** derived from the dibromide **118**. Hydrogenation to the octahydro compound and transannular bromination to **121** confirms the chiral structure of **120**, although attempted optical resolutions were fruitless.

Recent X-ray diffraction studies now seem to have brought some order into the stereochemistry of the tetrabenzo[a,c,q,i]cyclodecane isomers (123) prepared from **122** through the Stevens rearrangement, followed by dehydration of the resulting glycol. Inspection of molecular models indicates that three stereoisomers of $\mathbf{C_{2h}}$, $\mathbf{C_2}$, and $\mathbf{D_2}$ **(123)** symmetry are possible for the cis-cis combination, but so far only two isomers have been reported, one of $\mathbf{C_{2h}}$ symmetry (m.p. 306.5°C) (124), and the other of $\mathbf{C_2}$ symmetry (m.p. 253°C).

X-ray analysis (125, 126) of a *trans-trans* isomer m.p. 301-301.5°C, indicated that the molecule assumes the conformation **124** with slightly deformed $\mathbf{D_2}$ symmetry.

Lüttringhaus and Peters (127) confirmed the expected rigid $\mathbf{C_{3v}}$ conformation inherent to cyclotriveratrylene by their successful partial optical resolution of its monobenzyl derivative through cellulose $2\frac{1}{2}$-acetate chromatography. This stimulating study has been followed up by a group at the Collège de France (128, 129), who succeeded in preparing an enantiomeric pair of this class of compound of $\mathbf{C_3}$ symmetry. Acidic trimerization of the (+)-(*R*)-monomer **125** yielded a mixture of diastereomers **126** and **129**, both of $\mathbf{C_3}$ symmetry. After separation through SiO_2 chromatography, **126** and **129** were separately hydro-

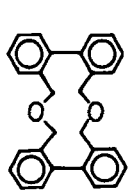

(122)

cis-cis

(123)

trans-trans

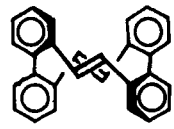

(124)

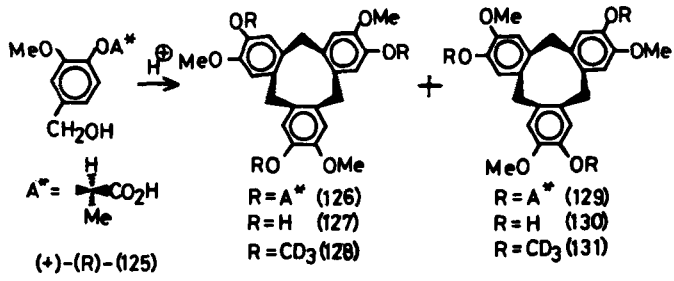

lyzed to the enantiomeric **127** and **130**, which in turn were converted into the enantiomeric deuterio compounds **128** and **131**. The reported optical rotation of $[\alpha]_D$ ±3° for the final products is claimed to be among the highest yet reported for chirality due to isotopic substitution, and polarimetric observation gave a half-life of 36 days for racemization of this deuterio compound. CD spectral analysis utilizing coupled oscillator theory enabled the French authors to assign *M* helicity **127** to the dextrorotatory enantiomer, and this has been confirmed further by X-ray crystallographic data.

IX. HIGH-SYMMETRY CHIRAL CAGE-SHAPED MOLECULES

A. Cage-shaped Molecules with a D_3 Twisted Bicyclo[2.2.2]octane Core: Triblattanes (130)

The X-ray diffraction method has been applied to elucidate a twisted conformation with D_3 symmetry (dihedral angle 5°) for bicyclo[2.2.2]octane (**132**) (Figure 17) in the crystal lattice (131), and this was also confirmed in the isolated molecule by a force-field calculation (132), which showed that the D_3 conformation is 0.1 kcal/mol more stable than the eclipsed D_{3h} conformation. Diagonal bridging between the 2-8, 5-7, and 3-6 positions in this molecule with a single bond, a CH_2 or a CH_2CH_2 group gives rise to a group of cage-shaped compounds of rigid conformation (Figure 17) whose common structural feature is a twisted bicyclo[2.2.2]octane moiety of D_3 symmetry. Since cubane (O_h symmetry) (**145**) may be regarded as being composed of two enantiomeric D_3 bicyclo[2.2.2]octane molecular frameworks, the pentacyclic species **138–144** may also be envisaged to be derived by dissymmetric homologation of cubane with CH_2 and/or CH_2CH_2 bridges.

A generic name "triblattane," from the German *Blatt*, meaning leaf, is proposed for this group of cage-shaped saturated hydrocarbons (Table 4); the nature of the above-defined diagonal bridging is indicated in the parentheses preceding

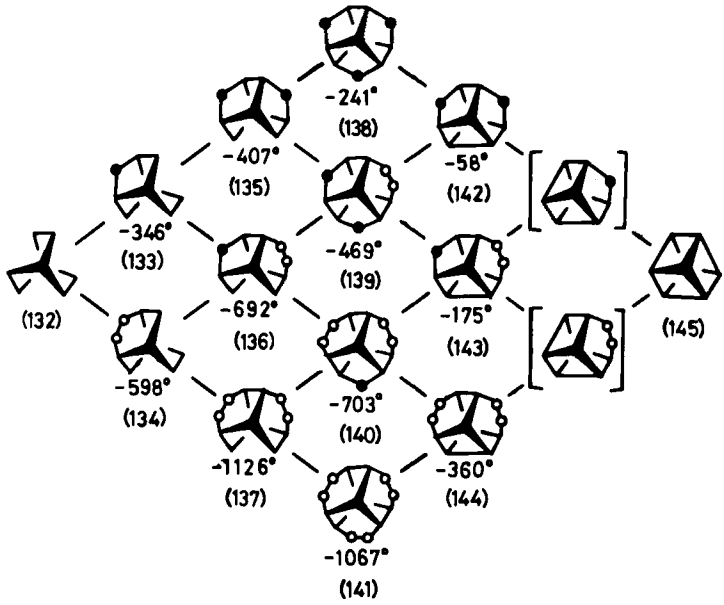

Figure 17. Absolute configurations and molecular rotations of the levorotatory triblattanes having D_3-twisted bicyclo[2.2.2]octane moiety with *M* helicity.

the name: tri-, tetra-, and pentacyclic species are now to be called [n]-, [m.n]-, and [m.n.p] triblattanes where *m*, *n*, and *p* may be 0, 1, and 2, corresponding to a single bond, CH_2 or CH_2CH_2 bridge, respectively.

Demonstrating the convenience of this nomenclature, D_2 twistane (**134**), C_2 ditwistane (**137**), D_3 trishomocubane (**138**) and C_1 homobasketane (**143**) are now simply called [2]-, [2.2]-, [1.1.1]-, and [2.1.0]triblattanes respectively. It might be noted that only twistane (D_2), trishomocubane (D_3), and tritwistane (D_3) (**141**) have high-symmetry chiral molecular frameworks with symmetry numbers higher than 2.

1. Twistane and Twistbrendane

Twistane (**134**), first synthesized in racemic form by Whitlock (133) as early as 1962, is composed of four twist-boat cyclohexane moieties with the same chirality, corresponding to a symmetry number of 4, which is inherent in its D_2 symmetry. Our group (134) synthesized this interesting compound in an optically active modification. We started from (-)-bicyclo[2.2.2]octanecarboxylic acid **146** (Figure 18), which was converted to (+)-twistane (**134**) via the ketone **147**, but our application of Djerassi-Klyne's empirical rule (135) to this intermediate ketone **147** led us to an erroneous conclusion as to abolute configuration.

Table 4.
Trivial and IUPAC Names of the Levorotatory Triblattanes

Trivial Name	IUPAC Name	Absolute Configuration
Twistbrendane (133)	Tricyclo[4.3.0.$0^{3,8}$]nonane	(1*R*, 3*S*, 6*S*, 8*R*)
Twistane (134)	Tricyclo[4.4.0.$0^{3,8}$]decane	(1*R*, 3*R*, 6*R*, 8*R*)
Ditwistbrendane (135)	Tetracyclo[5.2.1.$0^{2,6}$.$0^{4,8}$]decane	(1*R*, 2*R*, 4*R*, 6*R*, 7*R*, 8*R*)
C_1-Methanotwistane (136)	Tetracyclo[6.2.1.$0^{2,7}$.$0^{4,9}$]undecane	(1*R*, 2*R*, 4*S*, 7*R*, 8*S*, 9*R*)
C_2-Ditwistane (137)	Tetracyclo[6.2.2.$0^{2,7}$.$0^{4,9}$]dodecane	(1*S*, 2*S*, 4*S*, 7*R*, 8*R*, 9*S*)
D_3-Trishomocubane (138)	Pentacyclo[6.3.0.$0^{2,6}$.$0^{3,10}$.$0^{5,9}$]undecane	(1*S*, 3*S*, 5*S*, 6*S*, 8*S*, 10*S*)
C_2-Bismethanotwistane (139)	Pentacyclo[7.3.0.$0^{2,7}$.$0^{3,11}$.$0^{6,10}$]dodecane	(1*S*, 2*R*, 3*S*, 6*S*, 7*S*, 9*S*, 10*R*, 11*S*)
C_2-Methanoditwistane (140)	Pentacyclo[7.4.0.$0^{2,6}$.$0^{3,11}$.$0^{5,10}$]tridecane	(1*S*, 2*S*, 3*S*, 5*S*, 6*S*, 9*S*, 10*S*, 11*S*)
D_3-Tritwistane (141)	Pentacyclo[8.4.0.$0^{2,7}$.$0^{3,12}$.$0^{6,11}$]tetradecane	(1*S*, 3*S*, 6*S*, 7*S*, 10*S*, 12*S*)
C_2-Bishomocubane (142)	Pentacyclo[5.3.0.$0^{2,5}$.$0^{3,9}$.$0^{4,8}$]decane	(1*S*, 2*S*, 3*S*, 4*S*, 5*R*, 7*R*, 8*S*, 9*R*)
C_1-Homobasketane (143)	Pentacyclo[5.4.0.$0^{2,6}$.$0^{3,9}$.$0^{4,8}$]undecane	(1*R*, 2*R*, 3*S*, 5*R*, 6*S*, 7*S*, 8*S*, 9*S*)
C_2-3,10-Dehydroditwistane (144)	Pentacyclo[6.4.0.$0^{2,7}$.$0^{3,10}$.$0^{6,9}$]dodecane	(1*R*, 2*S*, 3*S*, 6*R*, 7*S*, 8*S*, 9*S*, 10*S*)

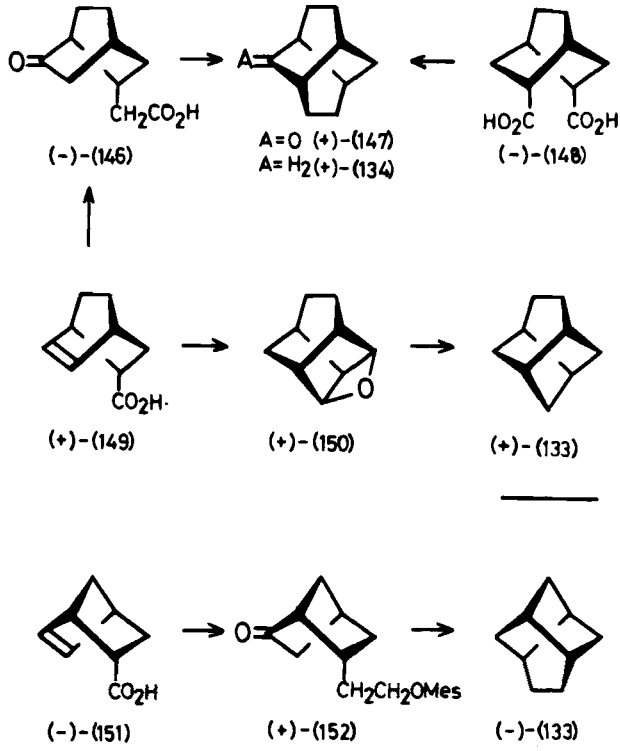

Figure 18. Stereochemical correlation between optically active twistane and twistbrendane.

The next year, Tichý and Sicher (136) reported another synthetic approach to (+)-twistane, starting from the (-)-dicarboxylic acid **148**, and they were also led to the same erroneous configurational assignment, which was later corrected by both groups (137, 138). Figure 18 illustrates the configurational correlation between (+)-twistane (**134**) and (+)-twistbrendane (**133**), carried out by our group who had prepared the enantiomeric (-)-twistbrendane from the levorotatory unsaturated carboxylic acid (-)-**151** of known configuration (139).

The absolute configuration of (-)-bissecocubane **160** (C_2), the lowest homolog of the triblattanes, which may also be called 9-nortwistbrendane or, more conveniently, [0]triblattane, was correlated to (-)-twistbrendane (**133**) as illustrated in Figure 19 (140). Double Favorskii rearrangement of (-)-dibromodiketone **153** afforded the (-)-dicarboxylic acid **158**, which was then converted to (-)-3,6-dimethylbissecocubane **159** (C_2). Comparison of the CD spectrum of the (-)-diketone **154** derived from the (-)-dibromodiketone **153** with that of homologous (-)-diketone **156** (whose configuration had been established (141) by converting its precursor **155** into (-)-twistbrendane (**133**) via the dicarboxylic acid **157**) gave the 1*S*,3*R* configuration for (-)-diketone

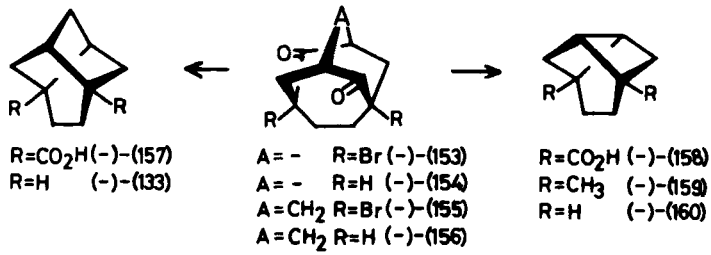

Figure 19. Stereochemical correlation between optically active twistbrendane and C_2 bissecocubane.

154, eventually permitting assignment of the 1*R*,3*S* configuration to the levorotatory dimethyl derviative (-)-**159**.

This, coupled with other evidence, led us to conclude (140) that the levorotatory C_2 bissecocubane (**160**) should share the same skeletal chirality with the (-)-(1*R*,3*S*)-3,6-dimethyl derivative **159**. Almost simultaneously, Paquette et al. (142) reported a preparation of the parent (+)-bissecocubane **160** (C_2) by pyrolytic denitrogenation of (+)-diazatwistane; application of the chiroptical regularity found by us (vide infra) in the family of triblattanes enabled them to assign the same absolute configuration.

Like C_2 bissecocubane (**160**) mentioned above, bisnoradamantane (**164**) (D_{2d}) (Figure 20) is the next lower homolog of twistbrendane, and is specially interesting in that its D_{2d} symmetry has the origin in the intrinsic tricyclic system conceptually composed of two enantiomeric D_2 twisted cyclohexanes interlocked together.

Introduction of a carbonyl group desymmetrizes the D_{2d} symmetry of **164** to give bisnoradamantanone **163** of C_2 symmetry. Figure 20 shows its preparation in optically active form, as well as the established stereochemical correlation with the bicyclic carboxylic acid (-)-**151** (143). Optical resolution of the racemic carboxylic acid **161**, employing (+)-2-(1-aminoethyl)naphthalene as the resolving agent, furnished (-)-**161**, which was transformed into (-)-bisnoradamantanone **163** via the unsaturated intermediate (-)-**162**. Information concerning the absolute configuration of (-)-**163** was obtained from comparison of its negative Cotton effect centered at 300 nm with that of the dextrorotatory isopropyl derivative (+)-**167**.

Photocyclization of isopropyl ketone (-)-**165**, prepared from (-)-**151** of known configuration, gave the oxetane **166**, whose reductive cleavage followed by Jones oxidation afforded (+)-**167**. Contrary to their opposite optical rotations at the D line, both (-)-**163** and (+)-**167** exhibit similar negative Cotton effects in the 300 nm region, unambiguously correlating their skeletal absolute configurations.

Included also in Figure 20 is an outline of the preparation of (+)-brexane

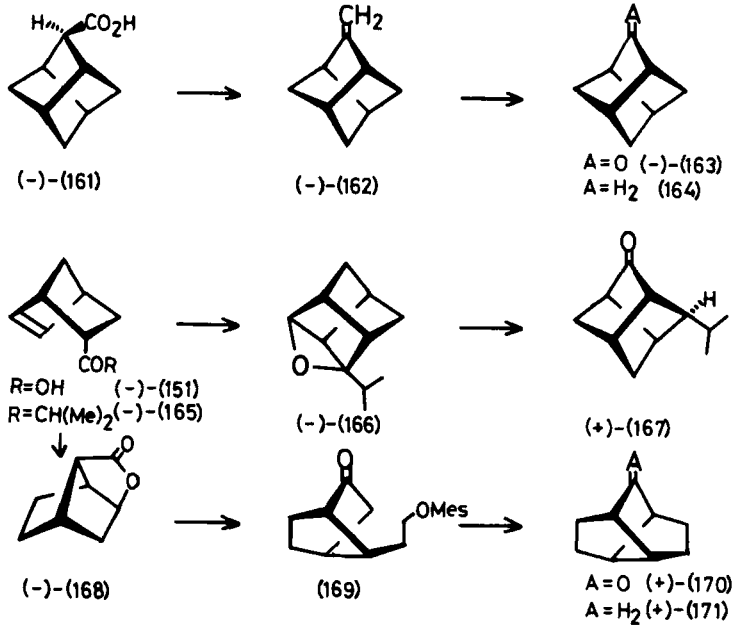

Figure 20. Stereochemical correlation between D_{2d} bisnoradamantanone and brexane.

(**171**) (C_2 symmetry), a high-symmetry chiral cage-shaped tricyclic hydrocarbon closely related to D_2 twistane. Wagner-Meerwein rearrangement (144) of the unsaturated carboxylic acid (-)-**151** provided the lactone (-)-**168**, which in turn was converted into the ketone (+)-**170** via a series of intermediates, including the mesylate **169** whose intramolecular alkylation was a crucial step in this approach. Removal of the carbonyl group by Wolff-Kishner reduction completed the synthesis of (+)-brexane (**171**) (145).

2. *Bishomocubane* (C_2), *Ditwistbrendane, Dehydroditwistane, and Ditwistane*

Besides the obvious D_3 twisted bicyclo[2.2.2]octane framework, another characteristic of pentacyclic [m.n.o]triblattanes is the presence of a strained bicyclo[2.2.0]hexane moiety whose facile reductive cleavage of the central single bond correlates this class of triblattanes to the corresponding tetracyclic [m.n]triblattanes. Figure 21 illustrates the configurational correlation between these two classes of triblattanes; the key liaison compound is the (+)-α,β-unsaturated ketone **172**, whose absolute configuration had been related to that of the levorotatory carboxylic acid (-)-**151** via (+)-methyl 3-(*endo*-2-norbornyl) propionate (**179**) (146).

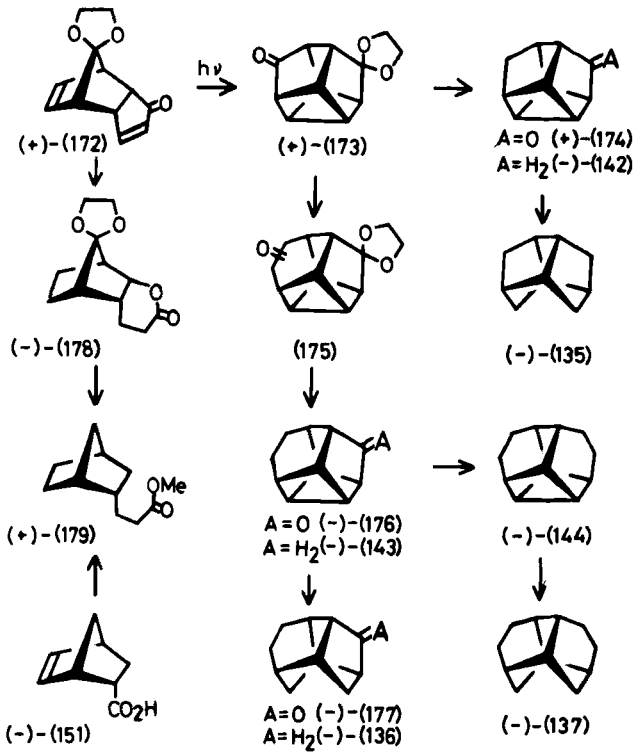

Figure 21. Stereochemical correlation between C_2 bishomocubane, ditwistbrendane, dehydroditwistane, and ditwistane.

The $[\pi^2 + \pi^2]$ photocyclization of (+)-**172** yielded (+)-**173**, which in turn was transformed into (-)-bishomocubane (C_2) (**142**) via the ketone (+)-**174** (147). Catalytic hydrogenation (5% Pd/C) of (-)-**142** furnished (-)-ditwistbrendane (**135**) (148).

Diazomethane ring expansion of [1.1.0]triblattane provided the pathways to [2.1.0] and [2.2.0]triblattanes, which could then be converted to [2.1]- and [2.2]triblattanes by catalytic hydrogenolytic opening of the strained central single bond.

The diazomethane ring expansion, when applied to (+)-**173**, led to the formation of **175**, which was converted via ketone (-)-**176** into (-)-homobasketane (**143**) (C_1). A similar sequence of conversions, including a second diazomethane ring expansion, transformed (-)-**176** to (-)-3,10-dehydroditwistane (C_2) (**144**). Catalytic hydrogenolysis cleaved the strained central bonds of (-)-**143** and (-)-**144** furnishing (-)-methanotwistane (**136**) (C_1) and (-)-ditwistane (**137**), (C_2) respectively (149).

Barrettane (**181**) (C_2 symmetry) corresponds to a dehydroditwistbrendane,

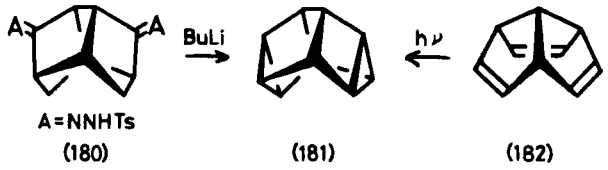

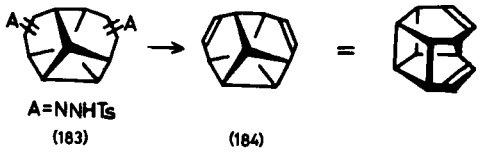

and was synthesized by de Meijere (150) either from the ditosylhydrazone **180** by intramolecular carbene insertion, or from triquinacene (**182**) by ultraviolet irradiation. As expected, its facile hydrogenolysis to ditwistbrendane (**135**) has been observed.

Another interesting molecule related to [2.2.0]triblattane is ansaradine (**184**) (C_2) (151), a bis-vinylog of cubane and a sort of benzene dimer. This highly strained cage-shaped chiral molecule was synthesized from the ditosylhydrazone **183**, and in fact was found to be quite unstable. It was quantitatively split into two benzene molecules upon refluxing in hexachlorobutadiene for 2 hr.

3. *Trishomocubane* (D_3) *and Bismethanotwistane* (C_2)

Among the eight theoretically possible trishomo homologs of cubane, four are chiral, comprising two of C_1, one of C_2, and one of D_3 symmetry. Inspection of a molecular model of D_3 trishomocubane (**138**) reveals that this beautiful rigid cage-shaped molecule is composed of six twisted cyclopentane moieties with the same chirality, as the symmetry number 6 inherent in this symmetry demands.

The first synthesis of this exquisite molecule in racemic modification was reported by Underwood and Ramamoorthy (152) as early as 1970. In our preparation of trishomocubane (D_3) in an optically active modification (148), we followed Barborak's elegant procedure (153) and started from the easily accessible diene adduct **185**. A $[\pi^2 + \pi^2]$ photocyclization followed by hydride reduction converted **185** into the glycol **186**, whose acidic rearrangement gave the pentacyclic diol **187** with the trishomocubane D_3 framework. Removal of one of the functional groups from diol **187** provided **188**, and optical resolu-

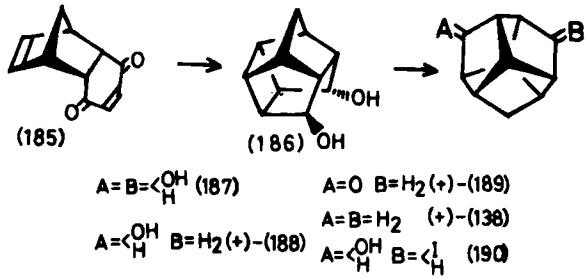

tion via the phthalate was carried out at this stage. The resolved dextrorotatory alcohol (+)-**188** was transformed to ketone (+)-**189**, whose carbonyl group was removed by Wolff-Kishner reduction to yield the desired dextrorotatory hydrocarbon (+)-**138** of D_3 symmetry.

A CD spectral analysis of the positive Cotton effect exhibited by the intermediate ketone (+)-**189** allowed assignment of the *R* configuration to (+)-trishomocubane (**138**); this is in agreement with Helmchen's result (154), obtained from X-ray study on the (−)-camphanate of the iodoalcohol **190**. Eaton and Leipzig (155) reported a convenient optical resolution of **189** employing (−)-ephedrine as the resolving agent.

Diazomethane ring expansion of (+)-trishomocubanone (**189**) followed by removal of the carbonyl group yielded (+)-bismethanotwistane (**139**) of C_2 symmetry, thus correlating the absolute configurations of these species (156).

4. *Tritwistane* (D_3) *and Methanoditwistane* (C_2)

Tritwistane (**141**) of D_3 symmetry is one of the most interesting compounds in the family of triblattanes. As D_3 trishomocubane (**138**) can be seen to be composed of three interlocked C_2 twistbrendanes of same chirality, three D_2 twistane moieties of same chirality interlock together to form tritwistane, reflecting its D_3 symmetry.

In our preparation of optically active **141**, (157), we started from the next higher homolog of **185** having a CH_2CH_2 instead of a CH_2 bridge, and a similar sequence of conversions as was outlined for D_3 trishomocubane provided the diacetate **191**. Transformations involving diazomethane ring expansion of one of the ketone rings yielded (±)-methanoditwistanone **192** (C_2), the optical resolution of which was accomplished by microbial stereodifferentiating reduction. Incubation of racemic ketone **192** with *Rhodotorula rubra* gave a metabolite mixture from which the levorotatory ketone (−)-**192** was recovered. Application of the "microbial C_2 ketone rule" (vide infra) indicated that this enantiomer should be the one with *M* helicity, which was supported by the observed posi-

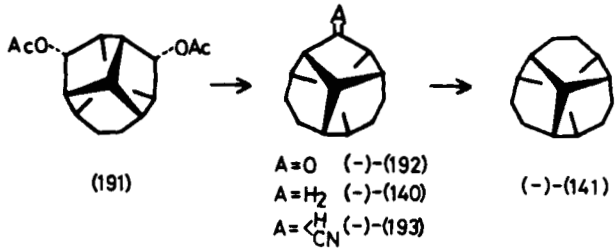

(191) (-)-(141)

tive Cotton effect centered at 291 nm. While the Wolff-Kishner reduction of ketone (-)-**192** gave (-)-methanoditwistane **140** ($\mathbf{C_2}$), a further sequence of steps involving conversion into the levorotatory nitrile followed by Demjanov type ring expansion finally provided (-)-tritwistane (**141**) of the *S* configuration and $\mathbf{D_3}$ symmetry.

5. *Topology and Chiroptical Properties of Triblattanes*

Adamantane was shown to be the "stabilomer" (158) among a family of $C_{10}H_{16}$ hydrocarbons, and this has been nicely demonstrated by smooth conversion of tricyclic twistane **134**, an inhabitant of "Adamantland," into adamantane with an $AlBr_3$ catalyst (159).

Schleyer et al. (160) also showed that $\mathbf{D_3}$ trishomocubane (**138**) is the stabilomer among pentacyclic $C_{11}H_{14}$ hydrocarbons. This stability of the trishomocubane molecular framework seems to be nicely demonstrated in a facile rearrangement (BF_3, -20°C, 5 min) of the triepoxide **194** into 3,7,10-trioxatrishomocubane (**195**) ($\mathbf{D_3}$) (161), whose attempted optical resolution has been reported (162).

In an interesting contrast to the chair form of cyclohexane ($\mathbf{D_{3d}}$ symmetry) as the fundamental structural unit of adamantane, which is the prototype of the regular diamond (F_{d3m} space group, cubic system), the $\mathbf{D_2}$ twist-boat form of cyclohexane may be regarded as the fundamental unit of twistane (**134**), $\mathbf{C_2}$ ditwistane (**137**), $\mathbf{D_3}$ tritwistane (**141**), and of a "twist diamond" ($P6_3$ space group, hexagonal system).

(194) (195) (196)

As the ready conversion of twistane into adamantane suggests, the latter group of molecular species is more stable than the former. This has also been demonstrated by a smooth rearrangement of D_3 tritwistane (**141**), which gave diamantane (congressane) (**196**) in quantitative yield on standing in a CS_2 solution with $AlBr_3$ catalyst at room temperature (157).

Rigid conformations together with the high symmetry characteristics of triblattanes obviously make this family of compounds a testing ground for various theories of optical activity, and Brewster (163) was the first to apply his "helical model" to correct the erroneous absolute configuration previously assigned to twistane (**134**) (134, 136); his calculated $[M]_D$ 484° for **134** was found to be close to the now known maximum rotation of 598°.

A casual inspection of Figure 17 will show a regularlity in $[M]_D$ values for the triblattanes. First of all, the most conspicuous feature is the levorotation exhibited by every member of the triblattane family having a bicyclo[2.2.2]-octane moiety of *M* helicity as its central molecular core.

Figure 17 also shows a systematic increase in $[M]_D$ on going toward the bottom of the figure; this marked regularity can be more clearly seen within the same series of high-symmetry molecules; (**144**)→(**140**)→(**141**) in [2.2.n] triblattanes, (**142**)→(**138**)→(**139**) in [1.1.n] triblattanes, and (**160**) ($[M]_D$ - 107°) (**157**)→(**133**)→(**134**) in [n] triblattanes.

Examination of Figure 17 also provides a rough estimate of the increment of $[M]_D$ corresponding to the change in bridge span: single bond→CH_2, Δ = +250° and CH_2→CH_2CH_2, Δ = +250°.

Significant increases in $[M]_D$ have also been observed accompanying the single bond rupture in going from [m.n.o] to [m.n] triblattanes, for example, (**142**)→(**135**) and (**143**)→(**136**). This is most dramatically shown by the $[M]_D$ increase of 766° observed in the hydrogenolysis of 3,10-dehydroditwistane (**144**) to ditwistane (**137**) (both of C_2 symmetry).

A brief discussion of the preparation and chiroptical properties of hetero-triblattanes may appropriately end this section.

As a part of their extensive study of hetero cage-shaped compounds, Ganter et al. (164) treated the (-)-*endo*-alcohol **197** with $Hg(OAc)_2$ followed by KI/I_2 solution to obtain the iodide **198**, which was then converted into (-)-2,7-dioxatwistane (**200**) via the tosylate **199**. Their elegant correlation of absolute configuration between the starting material **197** and (-)-(*S*)-malic acid leads to the (1*R*,3*R*,6*R*,8*R*)-configuration for (-)-**200**. Their subsequent success in preparing a series of unsaturated compounds closely related to twistane and its oxa analog, for example (+)-**201** (165) and (+)-**202** (166), enabled them to conclude: (a) CH_2→O exchange does not affect the sign of rotations, (b) a decrease in $[M]_D$ accompanies this structural modification, and (c) the unsaturated compounds invariably have larger $[M]_D$ values than do the corresponding saturated ones. The effect of unsaturation has also been observed in 4-twistene (136); to support

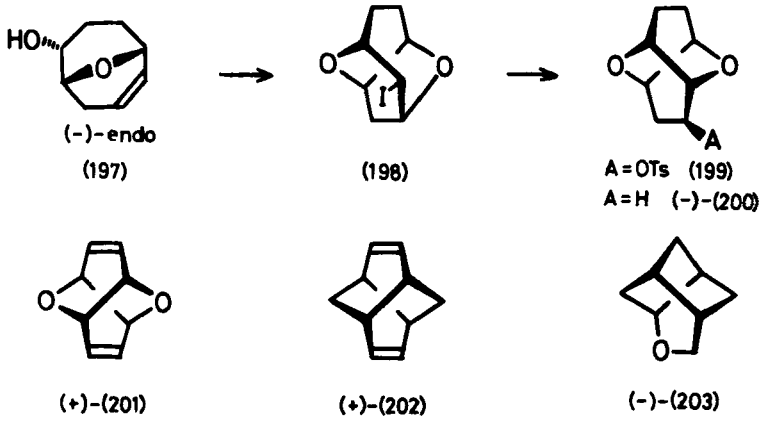

the first and second conclusions, the $[M]_D$ (absolute value) decrease observed in going from (-)-twistbrendane (**133**) ($[M]_D$ -346°) to (-)-2-oxatwistbrendane (**203**) ($[M]_D$ -229°) (167) will be cited.

An extension of these generalizations seems to suggest that not-yet-resolved 3,7,10-trioxatrishomocubane (**195**), which has a D_3 twisted bicyclo[2.2.2]-octane core of *M* helicity, should be levorotatory with $[M]_D$ ca. -170°.

6. *Biological Transformation of Cage-Shaped* C_2 *Ketones*

The carbonyl derivatives of triblattanes are ideal candidates for mapping the stereochemistry around the active site of alcohol dehydrogenases because of the compactness in their molecular shapes and their well-established configurations. These merits, combined with a fairly large accumulation of various carbonyl compounds related to triblattane in our laboratory, motivated us (168) to study biological stereodifferentiating reduction of the carbonyl derivatives in this class of compounds. We classified the type of ketones according to their symmetry: C_s ketones belong to the C_s point group and have a plane of symmetry coincident with the carbonyl plane; C_2 ketones belong to the C_2 point group and have a C_2 axis coincident with the carbonyl axis; C_1 ketones have no symmetry element passing through the carbonyl group.

When incubated with these racemic cage-shaped C_2 ketones–such as 9-twistbrendanone (**204**), 2-brexanone (**170**), D_{2d} bisnoradamantanone (**163**), D_3 trishomocubanone (**189**), or C_2 4-methanoditwistanone (**192**)–both *Curvularia lunata* and *Rhodotorula rubra* preferentially reduce the enantiomers (*P* C_2 ketones) whose common stereochemical feature is that they have larger parts of molecule in upper-right and lower-left quadrants in their quadrant pro-

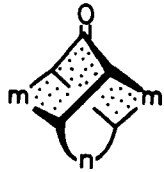

m=1 n=2 (204)
m=2 n=0 (170)
m=n=1 (163)
m=2 n=1 (147)

m=1 (189)
m=2 (192)

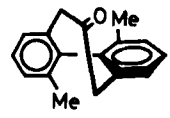

(-)-(205)

jections (Figure 22) (169). This same enantiomer differentiation—and with a strikingly high selectivity—has also been demonstrated in a C_2 ketone of fairly different molecular structure: incubation of the racemic bridged biphenyl-ketone (**205**) with *R. rubra* afforded a mixture of metabolites consisting of (+)-(*S*)-alcohol and the recovered (+)-(*R*)-ketone (*M* C_2 ketone) with respective optical purities of 94% and 100%.

2-Twistanone (**147**) was found peculiar in its outstanding inertness toward these microbial reductions, and this reluctance was also found in D_{2d} bisnor-adamantanone (**163**), though to a lesser extent. This has been attributed to the presence of the protruding methylene group opposite the carbonyl function across the twist-boat cyclohexane ring.

The opposite enantiomer selectivity towards these cage-shaped C_2 ketones was demonstrated in oxidation-reduction mediated by horse liver alcohol dehydrogenase (HLADH) (170). Incubation of racemic C_2 ketones with HLADH in a phosphate buffer (pH 7.0) containing coenzyme NADH afforded a mixture of the alcohols corresponding to the *M* C_2 ketone and the recovered *P* C_2 ketones, both with much higher optical purities than that found in the microbial reduction. In the oxidative direction (with NAD^+ coenzyme), HLADH was found to preferentially catalyze oxidation of the alcohols corresponding to the *M* C_2 ketone with excellent selectivity.

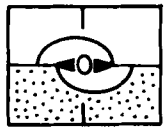

M-C_2-ketone

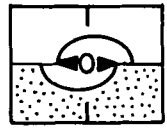

P-C_2-ketone

Figure 22. Two quadrant orientations for the enantiomers of C_2 ketones with *M* and *P* helicity.

X=CO_2H (206)
X=Cl (207)
X=$\oplus$ (208)

X=CO_2H (209)
X=Cl (210)
X=$\oplus$ (211)

A=$NH^{\oplus}$ (212)
A=$C^{\oplus}$ (213)
A=CH (214)

Chart 35.

B. Trishomobarrelyl and Trishomobullvalyl Cations

Optical resolution of 1-trishomobarrelenecarboxylic acid (**206**) with (+)-α-phenylethylamine was carried out by Spielmann and de Meijere (171), who converted the resulting (+)-acid (**206**) into the chloride (**207**) of C_3 symmetry, $[\alpha]_D$ +159°. A dramatic change of optical rotation was observed when the chloride (+)-**207** was dissolved in SbF_3/CH_2Cl_2 solution to be converted into trishomobarrelyl cation (**208**), $[\alpha]_D$ -1516°. Similar inversion of rotation occurred when (+)-1-trishomobullvalyl chloride (**210**), $[\alpha]_D$ +273°, prepared from acid (+)-**209**, was converted into the cation **211** $[\alpha]_D$ -2473°.

Application of Brewster's helical model (172) enabled Spielmann and de Meijere to assign the all-*S* configuration to the carboxylic acids (+)-**206** and (+)-**209**. A kinetic study (173) also indicated that S_NI reactivity of **207** is less than that of **210**, which, in turn, is 1.6×10^5 times more reactive than *tert*-butyl chloride. Notwithstanding their conformational mobility, a brief comment on manxane derivatives closely related to the trishomobarrelyl cation (**208**) seems pertinent here. X-ray crystallography of 1-azamanxane hydrochloride (**212**) (174) confirmed its approximate C_3 symmetry in the crystal lattice (175). Schleyer's force-field calculation (176) concluded that in going from 1-chlorobicyclo-[3.3.3]undecane to the corresponding cation (**213**), 6.8 kcal/mol is released, accounting for the facile S_N1 displacement, which is 10^4 times faster than in *tert*-butyl chloride. This release of strain also explains the remarkable reactivity of manxane (**214**) at its bridgehead position, for example, facile autoxidation, and ready chlorination with *tert*-BuOCl.

C. Perhydrotriphenylene and Perhydrotriptycene (D_3)

High pressure catalytic hydrogenation of dodecahydrotriphenylene (Pd/C, 150-250 atm, 300°C, 48 hr) affords a mixture of perhydrotriphenylene stereoisomers which theoretically should comprise four meso forms plus three pairs of enantiomers. An isomer melting at 124°C isolated by Farina (177) was shown to be the thermodynamically controlled product. Its *trans-transoid-trans-transoid-trans* structure (**215**) with D_3 symmetry was established by NMR study and con-

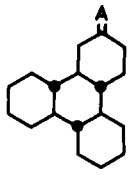

A = H_2 (+)-(S)-(215)

A =  (+)-(216)

A = O (+)-(217)

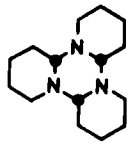

(218)

(219)

firmed by X-ray crystallography. In their chiroptical study of **215**, Farina et al. (178) first converted this racemic hydrocarbon to the racemic carboxylic acid (**216**), the optical resolution of which yielded (+)-**216**. A routine sequence of conversions removed the carboxyl functional group to afford the (+)-ketone (**217**), and the CD spectrum of which eventually permitted assignment of the all-(*S*) configuration to (+)-perhydrotriphenylene (**215**) ($\mathbf{D_3}$). As part of their important contributions to the study of inclusion compounds of **215** (179), Farina et al. irradiated 1,3-pentadiene in the presence of (−)-(*R*)-**215** ($[\alpha]_D$ − 9.3°) and obtained isotactic *trans*-1,4-polypentadiene with $[\alpha]_D + 2.5 \pm 0.3°$ (180). A ^{13}C NMR study of the α-isomer of tripiperidine (**218**) (closely related to $\mathbf{D_3}$ perhydrotriphenylene (**215**)) showed that this molecule assumes the asymmetric ($\mathbf{C_1}$) conformation (**219**) because of repulsion between nitrogen lone pairs, and a 1.1 kcal/mol enthalpy difference was estimated between the $\mathbf{C_1}$ and $\mathbf{C_3}$ conformations (181). A "stereo-rational synthesis" was reported for the interesting triketone (**220**) of $\mathbf{D_3}$ symmetry, but no optical resolution or absolute configuration study appears to have been reported (182) so far.

Another compound of unique structure related both to the triblattanes and to $\mathbf{D_3}$ perhydrotriphenylene mentioned above is the perhydrotriphenylene (**221**), m.p. 195°C, isolated by Farina et al. (183) from a mixture of stereoisomers obtained by medium-pressure catalytic hydrogenation (10% Pd/C, 60 atms., 150°C) of triptycene. Simple patterns observed in the ^{13}C NMR and ^1H NMR spectra of this isomer suggested its $\mathbf{D_3}$ symmetry, which was confirmed by X-ray analysis.

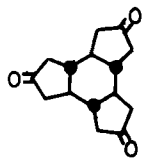

(220)

(221)

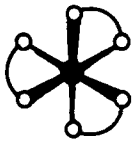

(P)-(222)

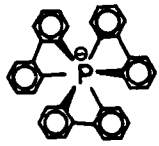

(M)-(223)

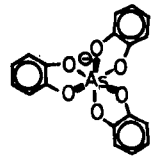

(P)-(224)

X. HIGH SYMMETRY CHIRAL MOLECULES WITH HEXA- AND OCTADENTATE CENTRAL ATOMS

In their pioneering X-ray diffraction study of $(+)_{589}$-$[Co(en)_3]^{3+}$ (which constituted the first investigation to disclose the absolute configuration of a chelate complex) Saito, Kuroya and their co-workers (184) established its $\mathbf{D_3}$ symmetry with *P* helicity (222). Since there have appeared in *Topics in Stereochemistry* two excellent articles (185, 186) dealing with this fascinating field, a brief comment on "more organic looking" high symmetry chiral molecules with central hexadentate and octadentate atoms will complete this section.

M helicity of the (-)-tris-2,2′-biphenylenephosphorus (V) ion (223) was assigned by CD spectral analysis (187), and *P* helicity of the closely related (-)-triscatechylarsenate (V) ion (224) was assigned, both by CD analysis and by X-ray study (188).

The very rare $\mathbf{D_4}$ symmetry has been revealed in an octaligate niobium (IV) complex, Nb[*tert*-BuCOCHCO-*tert*-Bu]$_4$, by X-ray crystallography (189).

XI. CHIRAL MOLECULES OF POLYHEDRAL SYMMETRY

The first experimental proof of the existance of a molecule with conformational T symmetry was given by Bartell and co-workers (190) in 1970. Their electron diffraction study of tetrakis[trimethylsilyl]silane, $Si[Si(CH_3)_3]_4$, unambiguously showed that this molecule assumes a conformation of T symmetry in the gas phase as a result of nonbonded interactions between the methyl groups which undergo a cooperative torsional displacement of about 14° from the staggered $\mathbf{T_d}$ symmetry.

Iroff and Mislow (25) carried out empirical force-field calculations on this molecule and confirmed that the expected nonbonded interaction forces the molecule to undergo a coordinated twist motion ("gear effect"). Their calculations also indicated that the molecule exists, not only in this ground state conformation with T symmetry, but also in a higher energy conformer with achiral $\mathbf{S_4}$ symmetry. The energy gap, ΔE_T, between the T and $\mathbf{S_4}$ forms was found to

be 4.08 kcal/mol. Extension of their calculations to $C[Si(CH_3)_3]_4$ and the unknown $C[C(CH_3)_3]_4$ enabled them to show that these molecules have, respectively, 9.64 and 16 kcal/mol for their ΔE_T values, and a calculation based on the parameters formulated by Allinger (1971) disclosed the existence of another conformer of C_2 symmetry for $C[C(CH_3)_3]_4$.

Their expectation of a similar coordinated "gear effect" in the newly synthesized tetra-*tert*-butyltetrahedrane (191) was fulfilled in their finding that this molecule again has ground state T symmetry (192). Interestingly, a calculation using Allinger's parameters (1971) alone predicted a S_4 conformer corresponding to the second energy minimum.

For all these molecules, however, facile racemization is expected since T_d conformers–potential achiral transition states–were shown to lie only 2 to 5 kcal/mol above the ground states of T symmetry.

In their classical paper on molecular chirality, Cahn, Ingold, and Prelog (7) proposed a hypothetical molecule **225** of T symmetry which can be constructed by bridging four tetrahedral atoms situated at the vertices of a tetrahedron with six submolecular units of intrinsic C_2 symmetry and of the same chirality (e.g., *trans*-olefins) (193).

By way of potentially more accessible models, Farina (19) proposed **226** and **227**, where the ^+R substituents are asymmetric submolecular units of the same chirality, while the moieties $^+C_3$ are symmetric submolecular units of local C_3 symmetry and of the same chirality.

In our attempted synthesis of the first organic molecule of T symmetry with known absolute configuration, we (194) utilized the D_3 trishomocubane moiety (**228**) of *M* helicity as the "$^+C_3$ submolecular unit" in **227**. Mislow (195), however, negated the alleged T symmetry of (-)-1,3,5,7-tetrakis[[(2-trishomocubanyl)acetoxy]methyl]adamantane because of asymmetry introduced by the CH_2OCOCH_2 groups connecting the T_d adamantane core and surrounding $^+C_3$ symmetric trishomocubane frameworks, and this has prompted our group to focus attention on the preparation of an example of **227** that has the subunit **229** (n = 0, 1, or 2) as a possible C_3 symmetry modifier to the T_d symmetry inherent in the adamantane framework. Recently, we have reported the successful synthesis (196) of (+)-1,3,5,7-tetrakis[[2-(1*S*,3*S*,5*R*,6*R*,8*R*,10*R*)-trisho-

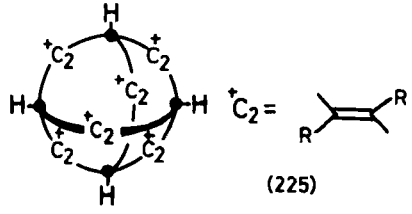

(225)

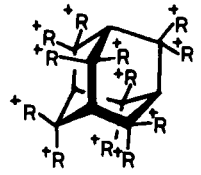

(226)

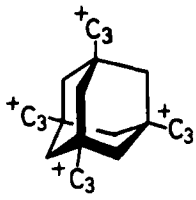

(227)

R=CH_2OCOCH_2 (228)

R=$(C{\equiv}C)_n$ (229)

mocubanyl]-1,3-butadiynyl]adamantane, m.p. > 350°C, $[\alpha]_D$ +65.3° ($CHCl_3$), which possesses cylindrically symmetric C≡C—C≡C groups between the central adamantane core (T_d) and the trishomocubane components (C_3). This type of desymmetrization might possibly be extended to cubane (O_h) (197) and dodecahedrane (I_h) (198) for preparing molecules of known absolute configuration having **O** and **I**, respectively as their highest attainable static symmetry.

ACKNOWLEDGMENT

I am grateful to Drs. Koichiro Naemura and Koji Yamamoto for their excellent draftsmanship in preparing the structural formulas for this article.

REFERENCES

1. *Proc. Roy. Soc. London*, 1857, *8*, 254.
2. Pasteur, L; Recherches sur la Dissymétrie Moléculaire des Produits Organiques Naturels. In Vallery-Radot, Pasteur, Ed.; "Dissymétrie Moléculaire" (Œuvres de Pasteur, Vol. 1); Masson: Paris, 1922, p. 314.
3. Pasteur, L.; "Researches on the Molecular Asymmetry of Natural Organic Products"; Alembic Club Reprints, No. 14: Edinburgh, 1948.
4. The dissymmetry-asymmetry misunderstanding also appears in the German translation. L. Pasteur, "Über die Asymmetrie bei Natürlich vorkommenden Organischen Verbindungen"; Ostwald Klassiker No. 28; Engelmann: Leipzig, 1891.
5. S. F. Mason. In "Topics in Stereochemistry," Vol. 9, Allinger, N. L.; Eliel, E. L., Eds.; Wiley-Interscience: New York, 1976, p. 1.
6. "I call any geometrical figure, or group of points, *chiral* and say that it has *chirality*, if its mirror image in a plane mirror, ideally realized, cannot be brought to coincide with itself." Quoted by L. L. Whyte, *Nature*, 1957, *180*, 513; *Ibid.* 1958, *182*, 198.
7. Cahn, R. S.; Ingold, C. K.; Prelog, V. *Angew, Chem. Int. Ed. Engl.* 1966, *5*, 385.
8. Wheland, G. W. "Advanced Organic Chemistry," 3rd ed.; Wiley: New York, 1960, p. 216.
9. Eliel, E. L. "Stereochemistry of Carbon Compounds"; McGraw-Hill: New York, 1962, p. 12.

10. Hawkins, C. J. "Absolute Configuration of Metallic Complexes"; Wiley-Interscience: New York, 1971, p. 7.
11. Rossi, R.; Diversi, P. *Synthesis* **1973**, 25.
12. D. Gutsche and D. J. Pasto, "Fundamentals of Organic Chemistry"; Prentice-Hall: Englewood Cliffs, N.J., 1975, p. 498.
13. Nakazaki, M.; Naemura, K.; Yoshihara, H. *Bull. Chem. Soc. Jpn.* **1975**, *48*, 3278. The term originally proposed was "gyrochiral" (14), but it has not been generally accepted.
14. For perplexed Alice, Humpty Dumpty interpreted a line of the poem called "Jabberwocky": "To *gyro* is to go round and round like a gyroscope," Gardner, M. "The Annotated Alice"; New American Library: New York, 1960, p. 272.
15. Mislow, K. "Introduction to Stereochemistry"; W. A. Benjamin: New York, 1965, p. 23. Jaffé, H. H.; Orchin, M. "Symmetry in Chemistry"; Wiley: New York, 1965.
16. Curie, P. *J. Phys. (Paris)* 1894, *3*, 393.
17. Mislow, K.; Raban, M. In "Topics in Stereochemistry," Vol. 1; Allinger, N.L.; Eliel, E. L. Eds.; Wiley-Interscience: New York, 1967, p. 1.
18. McCasland, G. E.; Horvat, R.; Roth, M. R. *J. Am. Chem. Soc.* **1959**, *81*, 2399.
19. Farina, M.; Morandi, C. *Tetrahedron* **1974**, *30*, 1819.
20. Prelog, V.; *Chem. Br.* **1968**, *4*, 382; *Science* **1976**, *193*, 17. Prelog, V; Helmchen, G. *Helv. Chim. Acta* **1972**, *55*, 2581.
21. Osawa, E. *J. Am. Chem. Soc.* **1979**, *101*, 5523.
22. Gleicher, G. J.; Schleyer, P. v. R. *J. Am. Chem. Soc.* **1967**, *89*, 582.
23. Liggero, S. H.; Schleyer, P. v. R.; Ramey, K. C. *Spectrosc. Lett.* **1969**, *2*, 197.
24. Nakazaki, M.; Naemura, K. *J. Org. Chem.* **1977**, *42*, 4108.
25. Iroff, L. D.; Mislow, K. *J. Am. Chem. Soc.* **1978**, *100*, 2121.
26. Bernstein, J.; Hagler, A. T. *J. Am. Chem. Soc.* **1978**, *100*, 673.
27. Dale, J. In "Topics in Stereochemistry," Vol. 9; Allinger, N.L.; Eliel, E.L., Eds.; Wiley-Interscience: New York, 1976, p. 199.
28. J. Sicher. In "Progress in Stereochemistry, Vol. 3; de la Mare, P. B. D.; Klyne, W., Eds.; Butterworths: London, 1962, p. 210.
29. Wilson, E. B.; *Chem. Soc. Rev.* **1972**, *1*, 293.
30. Mislow, K.; *Top. Curr. Chem.* **1974**, *47*, 1. Mislow, K.; *Acc. Chem. Res.* **1976**, *9*, 26.
31. Hybl, A.; Rundle, R. E.; Williams, D. E. *J. Am. Chem. Soc.* **1965**, *87*, 2779.
32. Noltemeyer, M.; Saenger, W. *J. Am. Chem. Soc.* **1980**, *102*, 2710.
33. Druyan, M. E.; Coulter, C. L.; Walter, R.; Kartha, G.; Ambady, G. K. *J. Am. Chem. Soc.* **1976**, *98*, 5496.
34. Tsuboyama, K.; Tsuboyama, S.; Uzawa, J.; Kobayashi, K.; Sakurai, T. *Tetrahedron Lett.* **1977**, 4603.
35. Synthesis: Gokel, G. W.; Durst, H. D.; *Synthesis 1976*, 168. Bradshaw, J. S.; Scott, P. E. *Tetrahedron*, **1980**, *36*, 461. Guest-host design: Cram, D. J.; Cram, J. M. *Acc. Chem. Res.* **1978**, *11*, 8; MacNicol, D. D.; McKendrick, J. J.; Wilson, D. R. *Chem. Soc. Rev.* **1978**, *7*, 65; Cram, D. J.; In "Applications of Biochemical Systems in Organic Chemistry" (Techniques of Chemistry, Vol. 10), Part 2; Jones, J. B.; Sih, C. J.; Perlman, D. Eds.; Wiley-Interscience: New York, 1976, p. 815.
36. Girodeau, J. M.; Lehn, J. M.; Sauvage, J. P. *Angew. Chem. Int. Ed. Engl.* **1975**, *14*, 764. Behr, J.-P; Lehn, J.-M.; Vierling, P. *Chem. Commun.* **1976**, 621. Lehn, J.-M.; Sirlin, C.; *ibid.* **1978**, 949. Lehn. J.-M.; Vierling, P.; Hayward, R. C. *Chem. Commun.* **1979**, 296.
37. Curtis, W. D.; Laidler, D. A.; Stoddart, J. F.; Jones, G. H.; *J. Chem. Soc., Perkin I* **1977**, 1756. Stoddart, J. F.; *Chem. Soc. Rev.* **1979**, *8*, 85.

38. McCasland, G. E.; Proskow, S. *J. Am. Chem. Soc.* **1955**, *77*, 4688; *ibid.* **1956**, *78*, 5646.
39. Skell, P. S.; Wescott, L. D., Jr.; Golstein, J.-P.; Engle, R. R. *J. Am. Chem. Soc.* **1965**, *87*, 2829.
40. Haas, G.; Prelog, V. *Helv. Chim. Acta* **1969**, *52*, 1202. Haas, G.; Hulbert, P. B.; Klyne, W.; Prelog, V.; Snatzke, G. *ibid.* **1971**, *54*, 491. Sagiv, J.; Yogev, A.; Mazur, Y. *J. Am. Chem. Soc.* **1977**, *99*, 6861.
41. Gange, D.; Magnus, P.; Bass, L.; Arnold, E. V.; Clardy, J. *J. Am. Chem. Soc.* **1980**, *102*, 2134.
42. Poland, D.; Scheraga, H. A. "Theory of Helix-Coil Transition in Biopolymers"; Academic Press: New York, 1970. Flory, P.J.; Miller, W. G. *J. Mol. Biol.* **1966**, *15*, 284.
43. Bode, W. *Angew. Chem. Int. Ed. Engl.* **1973**, *12*, 683.
44. Tachibana, T.; Kambara, H. *Bull. Chem. Soc. Jpn.* **1969**, *42*, 3422. Tachibana, T.; Kitazawa, S.; Takeno, H. *ibid* **1970**, *43*, 2418. Tachibana, T.; Kayama, K.; Takeno, H. *ibid.* **1972**, *45*, 415.
45. Cope, A. C.; Ganellin, C. R.; Johnson, H. W., Jr. *J. Am. Chem. Soc.* **1962**, *84*, 3191.
46. Cope, A. C.; Mehta, A. S.; *J. Am. Chem. Soc.* **1964**, *86*, 1268. Manor, P. C.; Shoemaker, D. P.; Parkes, A. S. *ibid* **1970**, *92*, 5260.
47. Marshall, J.A.; Konicek, T. R.; Flynn, K. E. *J. Am. Chem. Soc.* **1980**, *102*, 3287.
48. Whitesides, G. M.; Goe, G. L.; Cope, A. C. *J. Am. Chem. Soc.* **1967**, *89*, 7136.
49. Allinger, N. L.; Sprague, J. T. *J. Am. Chem. Soc.* **1972**, *94*, 5734.
50. Bogdanovic, B.; Heimbach, P.; Kröner, M.; Wilke, G. *Justus Liebigs Ann. Chem.* **1969**, *727*, 143.
51. Anet, F. A. L.; Rawdah, T. N. *J. Am. Chem. Soc.* **1978**, *100*, 5003.
52. Houk, K. N.; Strozier, R. W.; Santiago, C.; Gandour, R. W.; Vollhardt, K. P. C. *J. Am. Chem. Soc.* **1979**, *101*, 5183.
53. Romers, C.; Altona, C.; Buys, H. R.; Havinga, E. In "Topics in Stereochemistry," Vol. 4; Eliel, E. L.; Allinger, N. L., Eds.; Wiley-Interscience: New York, 1969, p. 39.
54. Kao, J.; Huang, T.-N. *J. Am. Chem. Soc.* **1979**, *101*, 5546.
55. Anet, F. A. L; Wagner, J. J. *J. Am. Chem. Soc.* **1971**, *93*, 5266.
56. Glass, R. S.; Wilson, G. S.; Setzer, W. N. *J. Am. Chem. Soc.* **1980**, *102*, 5068.
57. Groth, P. *Acta Chem. Scand.* **1969**, *23*, 1311.
58. Cope, A. C.; Moore, W. R.; Bach, R. D.; Winkler, H. J. S. *J. Am. Chem. Soc.* **1970**, *92*, 1243. Rauk, A.; Drake, A. F.; Mason, S. F. *J. Am. Chem. Soc.* **1979**, *101*, 2284.
59. Garratt, P. J.; Nicolaou, K. C.; Sondheimer, F. *Chem. Commun.* **1970**, *1219*.
60. Garratt, P. J.; Nicolaou, K. C.; Sondheimer, F. *J. Am. Chem. Soc.* **1973**, *95*, 4582. For their approach to monocyclic dicumulenes, see: Garratt, P. J.; Nicolaou, K. C.; Sondheimer, F. *J. Org. Chem.* **1973**, *38*, 2715.
61. Irngartinger, H.; Jäger, H.-U. *Tetrahedron Lett.* **1976**, 3595. For the force-field calculation, see: Anet, F. A. L.; Yavari, K. *J. Am. Chem. Soc.* **1977**, *99*, 7640.
62. Skattebøl, L. *Acta Chem. Scand.* **1963**, *17*, 1683.
63. A preliminary account has appeared in: Nakazaki, M.; Yamamoto, K.; Miura, H. 34th Annual Meeting of the Chemical Society of Japan, Tokyo; April 1976; Abstracts Vol. 2, p. 503.
64. Nakazaki, M.; Yamamoto, K.; Maeda, M. *Chem. Lett.* **1981**, 1035. Nakazaki, M.; Yamamoto, K.; Maeda, M.; Sato, O.; Tsutusi, T. *J. Org. Chem.* **1982**, *47*, 1435.
65. Crabbé, P.; Verlarde, E.; Anderson, H. W.; Clark, S. D.; Moore, W. R.; Drake, A. F.; Mason, S. F. *Chem. Commun.* **1971**, 1261. Rauk, A.; Drake, A. F.; Mason, S. F. *J. Am. Chem. Soc.* **1979**, *101*, 2284.
66. van't Hoff, J.; "La Chimie dans l'Espace"; P. M.Bazendijk: Rotterdam, 1875, p. 29.

67. Nakazaki, M.; Yamamoto, K.; Yanagi, J. *Chem. Commun.* 1977, 346.
68. Nakazaki, M.; Yamamoto, K.; Yanagi, J. *J. Am. Chem. Soc.* 1979, *101*, 147.
69. Marshall, J. A.; Lewellyn, M. *J. Am. Chem. Soc.* 1977, *99*, 3508.
70. Marshall, J. A.; Chung, K.-H. *J. Org. Chem.* 1979, *44*, 1566.
71. (a) Marshall, J. A.; Bierenbaum, R. E.; Chung, K.-H. *Tetrahedron Lett.* 1979, 2081. (b) Marshall, J. A.; Black, T. H.; Shone, R. L. *ibid.* 1979, 4737.
72. Nickon, A.; Zurer, P. St. J. *Tetrahedron Lett* 1980, 3527. Synthesis of a sulfur analog has been reported: Ceré, V.; Paolucci, C.; Pollicino, S.; Sandri, E.; Fava, A. *Chem. Commun* 1980, 755. *J. Org. Chem.* 1981, *46*, 486.
73. Nakazaki, M.; Yamamoto, K.; Tanaka, S. *J. Org. Chem.* 1976, *41*, 4081.
74. Marshall, J. A. *Acc. Chem. Res.* 1980, *13*, 213.
75. Nakazaki, M.; Yamamoto, K.; Maeda, M. *Chem. Commun.* 1980, 294; *J. Org. Chem.* 1980, *45*, 3229.
76. Marshall, J. A.; Black, T. H. *J. Am. Chem. Soc.* 1980, *102*, 7581.
77. Nakazaki, M.; Yamamoto, K. *J. Synth. Org. Chem. Soc. (Yuki Gosei Kagaku Kyokai Shi)* 1981, *39*, 624.
78. Mislow, K. *Angew. Chem.* 1958, *70*, 683.
79. Akimoto, H.; Shioiri, T.; Iitaka, Y.; Yamada, S. *Tetrahedron Lett.* 1968, *97*.
80. Nakazaki, M.; Chikamatsu, H.; Nishino, M.; Murakami, H. *J. Org. Chem.* 1981, *46*, 1151.
81. Helmchen, G.; Haas, G.; Prelog, V. *Helv. Chim. Acta* 1973, *56*, 2255.
82. Kyba, E. P.; Koga, K.; Sousa, L. R.; Siegel, M. G.; Cram, D. J. *J. Am. Chem. Soc.* 1973, *95*, 2692.
83. Kyba, E. P.; Gokel, G. W.; de Jong, F.; Koga, K.; Sousa, L. R.; Siegel, M. G.; Kaplan, K.; Sogah, G. D. Y.; Cram. D. J. *J. Org. Chem.* 1977, *42*, 4173.
84. Prelog, V.; Bedeković, D. *Helv. Chim. Acta* 1979, *62*, 2285.
85. Review: Cram, D. J.; Cram, J. M. *Acc. Chem. Res.* 1971, *4*, 204. Vögtle, F.; Neumann, P. *Angew. Chem. Int. Ed. Engl.* 1972, *11*, 73. Misumi, S.; Otsubo, T.; *Acc. Chem. Res.* 1978, *11*, 251.
86. Cram, D. J.; Dewhirst, K. C. *J. Am. Chem. Soc.* 1959, *81*, 5963.
87. Högberg, H.-E.; Thulin, B.; Wennerström, O. *Tetrahedron Lett.* 1977, 931.
88. Hohner, G.; Vögtle, F. *Chem. Ber.* 1977, *110*, 3052.
89. Nakazaki, M.; Yamamoto, K.; Toya, T. *J. Org. Chem.* 1980, *45*, 2553.
90. Haenel, M.; Staab, H. A. *Tetrahedron Lett.* 1970, 3585; *Chem. Ber.* 1973, *106*, 2203.
91. Haenel, M. W. *Tetrahedron Lett.* 1974, 3053; *Chem. Ber.* 1978, *111*, 1789.
92. Nakazaki, M.; Yamamoto, K.; Miura, Y. *Chem. Commun.* 1977, 206; *J. Org. Chem.* 1978, *43*, 1041.
93. Cram, D. J.; Hornby, R. B.; Truesdale, E. A.; Reich, H. J.; Delton, M. H.; Cram, J. M. *Tetrahedron* 1974, *30*, 1757.
94. Longone, D. T.; Reetz, M. T. *Chem. Commun.* 1967, 46.
95. Rebafka, W.; Staab, H. A. *Angew. Chem. Int. Ed. Engl.* 1973, *12*, 776.
96. Helgeson, R. C.; Timko, J. M.; Cram, D. J. *J. Am. Chem. Soc.* 1974, *96*, 7380.
97. Longone, D. T.; Chow, H. S. *J. Am. Chem. Soc.* 1964, *86*, 3898; *ibid.* 1970, *92*, 994.
98. Staab, H. A.; Zapf, U. *Angew. Chem. Int. Ed. Engl.* 1978, *17*, 757.
99. Nakazaki, M.; Yamamoto, K.; Tanaka, S. *Chem. Commun.* 1972, 433. Nakazaki, M.; Yamamoto, K.; Tanaka, S.; Kametani, H. *J. Org. Chem.* 1977, *42*, 287.
100. Falk. H.; Schlögl, K. *Angew. Chem. Int. Ed. Engl.* 1968, *7*, 383. Falk. H.; Reich-Rohrwig, P.; Schlögl, K. *Tetrahedron* 1970, *26*, 511. Guest, A.; Hoffman, P. H.; Nugent, M. J. *J. Am. Chem. Soc.* 1972, *94*, 4241. For a recent correlation with

(–)-hexahelicene see: Nakazaki, M.; Yamamoto, K.; Maeda, M. *Chem. Lett.* **1980**, 1533; *J. Org. Chem.* **1981**, *46*, 1985.

101. Racemic modification: Nakazaki, M.; Yamamoto, K.; Tanaka, S.; *Tetrahedron Lett.* **1971**, 341; ref. 73. Optically active modification: Nakazaki, M.; Yamamoto, K.; Ito, M. *Chem. Commun.* **1972**, 433. Absolute configuration: Nakazaki, M.; Yamamoto, K. *Chem. Lett.* **1974**, 1051. Nakazaki, M.; Yamamoto, K.; Ito, M.; Tanaka, S. *J. Org. Chem.* **1977**, *42*, 3468.
102. Boekelheide, V.; *Acc. Chem. Res.* **1980**, *13*, 65.
103. Schill, G. "Catenanes, Rotaxanes, and Knots"; Academic Press: New York, 1971. Boeckmann, J.; Schill, G. *Tetrahedron* **1974**, *30*, 1945.
104. Wynberg, H. *Acc. Chem. Res.* **1971**, *4*, 65. Martin, R. H.; *Angew. Chem. Int. Ed. Engl.* **1974**, *13*, 649.
105. Martin, R. H.; Morren, G.; Schurter, J. J. *Tetrahedron Lett.* **1969**, 3683.
106. Laarhoven, W. H.; Cuppen, Th. J. H. M. *Tetrahedron Lett.* **1971**, 163; *Rec. Trav. Chim. Pay-Bas* **1973**, *92*, 553. Martin, R. H.; Eyndels, Ch.; Defay, N. *Tetrahedron Lett.* **1972**, 2731; *Tetrahedron* **1974**, *30*, 3339.
107. Nakazaki, M.; Yamamoto, K.; Shiota, J. 43rd Annual Meeting of the Chemical Society of Japan, Tokyo; April 1981; Abstracts Vol. 2, p. 1034.
108. Thulin, B.; Wennerström, O. *Acta Chem. Scand., B* **1976**, *30*, 688; *Tetrahedron Lett.* **1977**, 929. Leach. D. N.; Reiss, J. A. *J. Org. Chem.* **1978**, *43*, 2484.
109. Kauffmann, T.; Lexy, H. *Angew. Chem. Int. Ed. Engl.* **1978**, *17*, 755.
110. Wittig, G.; Rümpler, K.-D. *Justus Liebigs Ann. Chem.* **1971**, *751*, 1. Wittig, G. *Acc. Chem. Res.* **1974**, *7*, 6.
111. Harris. M. M. In "Progress in Stereochemistry," Vol. 2; Klyne, W.; de la Mare, P. B. D., Eds.; Butterworths: London, 1958, p. 157.
112. Ollis, W. D.; Sutherland, I. O. *Chem. Commun.* **1966**, 402. Downing, A. P.; Ollis, W. D.; Sutherland, I. O. *J. Chem. Soc., B* **1970**, 24.
113. Downing, A. P.; Ollis, W. D.; Sutherland, I. O.; Mason, J.; Mason, S. F. *Chem. Commun.* **1968**, 329.
114. Gerdil, R.; Allemand, J. *Tetrahedron Lett.* **1979**, 3499.
115. Williams, D. J.; Lawton, D. *Tetrahedron Lett.* **1975**, 111.
116. Ollis, W. D.; Price, J. A.; Stephanatou, J. S.; Stoddart, J. F. *Angew. Chem. Int. Ed. Engl.* **1975**, *14*, 169.
117. Ollis, W. D.; Stephanatou, J. S.; Stoddart, J. F.; Ferrige, A. G. *Angew. Chem. Int. Ed. Engl.* **1976**, *15*, 223.
118. Brickwood, D. J.; Ollis, W. D.; Stoddart, J. F. *Chem Commun.* **1973**, 638. Brickwood, D. J.; Ollis, W. D.; Stephanatou, J. S.; Stoddart, J. F. *J. Chem. Soc., Perkin I* **1978**, 1398. For the corresponding thia analogs, see: Ollis, W. D.; Stoddart, J. F.; Nógrádi, M. *Angew. Chem. Int. Ed. Engl.* **1975**, *14*, 168. Ollis, W. D.; Stephanatou, J. S.; Stoddart, J. F.; Nógrádi, M. *J. Chem. Soc., Perkin I* **1978**, 1421.
119. Williams, D. J. *Chem. Commun.* **1977**, 170.
120. Ollis, W. D.; Stoddart, J. F.; Sutherland, I. O. *Tetrahedron* **1974**, *30*, 1903.
121. Staab, H. A.; Wehinger, E. *Angew. Chem. Int. Ed. Engl.* **1968**, *7*, 225. Staab, H. A.; Wehinger, E.; Thorwart, W. *Chem. Ber.* **1972**, *105*, 2290. For the corresponding C_2 dibenzo derivatives, see: Staab, H. A.; Mack, H.; Nissen, A. *Chem. Ber.* **1972**, *105*, 2310. Irngartinger, H. *ibid,* **1973**, *106*, 751.
122. Irngartinger, H. *Chem. Ber.* **1973**, *106*, 761.
123. Wittig, G.; Koenig, G.; Clausz, K. *Justus Liebigs Ann. Chem.* **1955**, *593*, 127; Wittig G.; Skipka, G. *ibid,* **1973**, 59. Bestmann, H. J.; Schaper, W., *Tetrahedron Lett.* **1975**, 3511.
124. Irngartinger, H. *Chem. Ber.* **1973**, *106*, 2786.

125. Irngartinger, H. *Chem. Ber.* 1973, *106*, 2796.
126. A trans-trans isomer (mp 312°C) prepared by Wittig's ylide coupling (Agranat, I.; Kraus, M. A.; Bergmann, E. D.; Roberts, P. J.; Kennard, O. *Tetrahedron Lett.* 1973, 1265) was shown to have D_2 symmetry: Roberts, P. J.; Kennard, O. *J. Chem. Soc., Perkin II* 1973, 1984.
127. Lüttringhaus, A.; Peters, K. C. *Angew. Chem. Int. Ed. Engl.* 1966, *5*, 593.
128. Collet, A.; Jacques, J. *Tetrahedron Lett.* 1978, 1265.
129. Collet, A.; Gabard, J. *J. Org. Chem.* 1980, *45*, 5400. Collet, A.; Gottarelli, G. *J. Am. Chem. Soc.* 1981, *103*, 204.
130. Review: Nakazaki, M.; Naemura, K.; *J. Synth. Org. Chem. Soc. (Yuki Gosei Kagaku Kyokai Shi)* 1974, *32*, 905; *ibid.* 1977, *35*, 883; *ibid.* 1982, *40*, 1128.
131. Cameron, A. F.; Ferguson, G.; Morris, D. G. *J. Chem. Soc., B* 1968, 1249.
132. Engler, E. M.; Chang, L.; Schleyer, P. v. R. *Tetrahedron Lett.* 1972, 2525. Ermer, O.; Dunitz, J. D. *Helv. Chem. Acta* 1969, *52*, 1861.
133. Whitlock, H. W., Jr. *J. Am. Chem. Soc.* 1962, *84*, 3412.
134. Adachi, K.; Naemura, K.; Nakazaki, M. *Tetrahedron Lett.* 1968, 5467.
135. Djerassi, C.; Klyne, W. *Proc. Natl. Acad. Sci. USA* 1962, *48*, 1093.
136. Tichý, M.; Sicher, J. *Tetrahedron Lett.* 1969, 4609.
137. Tichý, M. *Tetrahedron Lett.* 1972, 2001. Tichý M.; Sicher, J. *Collect. Czech. Chem. Commun.* 1972, *37*, 3106.
138. Nakazaki, M.; Naemura, K.; Harita, S. *Bull. Chem. Soc. Jpn.* 1975, *48*, 1907.
139. Naemura, K.; Nakazaki, M. *Bull. Chem. Soc. Jpn.* 1973, *46*, 888.
140. Nakazaki, M.; Naemura, K.; Sugano, Y.; Kataoka, Y. *J. Org. Chem.* 1980, *45*, 3232.
141. Carried out with the enantiomers, ref. 24.
142. Jenkins, J. A.; Doehner, R. W., Jr.; Paquette, L. A. *J. Am. Chem. Soc.* 1980, *102*, 2131.
143. Nakazaki, M.; Naemura, K.; Arashiba, N. *Chem. Commun.* 1976, 678; *J. Org. Chem.* 1978, *43*, 888.
144. Nakazaki, M.; Naemura, K.; Kadowaki, H. *J. Org. Chem.* 1978, *43*, 4947.
145. Carried out with the enantiomers: Nakazaki, M.; Naemura, K.; Kadowaki, H. *J. Org. Chem.* 1976, *41*, 3725.
146. Nakazaki, M.; Naemura, K.; Nakahara, S. *J. Org. Chem.* 1978, *43*, 4745.
147. Nakazaki, M.; Naemura, K. *J. Org. Chem.* 1977, *42*, 2985.
148. Nakazaki, M.; Naemura, K.; Arashiba, N. *J. Org. Chem.* 1978, *43*, 689.
149. Nakazaki, M.; Naemura, K.; Kondo, Y.; Nakahara, S.; Hashimoto, M. *J. Org. Chem.* 1980, *45*, 4440.
150. Bosse, D.; de Meijere, A. *Tetrahedron Lett.* 1977, 1155.
151. Martin, H.-D.; Pföhler, P. *Angew. Chem. Int. Ed. Engl.* 1978, *17*, 847.
152. Underwood, G. R.; Ramamoorthy, B. *Tetrahedron Lett.* 1970, 4125.
153. Smith, E. C.; Barborak, J. C. *J. Org. Chem.* 1976, *41*, 1433.
154. Their final product was (–)-trishomocubane (D_3). Helmchen G.; Staiger, G. *Angew. Chem. Int. Ed. Engl.* 1977, *16*, 116. For the X-ray crystallography of (±)-diiodotrishomocubane, see: Marchand, A. P.; Chou, T.-C.; Ekstrand, J. D.; van der Helm, D. *J. Org. Chem.* 1975, *41*, 1438.
155. Eaton, P. E.; Leipzig, B. *J. Org. Chem.* 1978, *43*, 2483.
156. Carried out with the enantiomers: Nakazaki, M.; Naemura, K.; Arashiba, N.; Iwasaki, M. *J. Org. Chem.* 1979, *44*, 2433.
157. Nakazaki, M.; Naemura, K.; Chikamatsu, H.; Iwasaki, M.; Hashimoto, M. *Chem. Lett.* 1980, 1571; *J. Org. Chem.* 1981, *46*, 2300. For preparation of the racemic modification, see: Hirao, K.; Yonemitsu, O. *Chem. Commun.* 1980, 423.

158. Engler, E. M.; Farcasiu, M.; Sevin, A.; Cense, J. M.; Schleyer, P. v. R. *J. Am. Chem. Soc.* 1973, *95*, 5769. Review: McKervey, M. A. *Chem. Soc. Rev.* 1974, *3*, 479.
159. Whitlock, H. W., Jr.; Siefken, M. W. *J. Am. Chem. Soc.* 1968, *90*, 4929.
160. Kent, G. J.; Godleski, S. A.; Osawa, E.; Schleyer, P. v. R. *J. Org. Chem.* 1977, *42*, 3852.
161. Weitemeyer, C.; de Meijere, A. *Angew. Chem. Int. Ed. Engl.* 1976, *15*, 686.
162. Spielmann, W.; Weitemeyer, C.; Huang, T.-N.; de Meijere, A.; Snatzke, F.; Snatzke, G. *Israel J. Chem.* 1976-77, *15*, 99.
163. Brewster, J. H. *Tetrahedron Lett.* 1972, 4355. Review: Brewster, J. H. *Top. Curr. Chem.* 1974, *47*, 29. Brewster, J. H. In "Topics in Stereochemistry," Vol. 2; Allinger, N. L.; Eliel, E. L., Eds.; Wiley-Interscience: New York, 1967, p. 1.
164. Ackermann, P.; Tobler, H.; Ganter, C. *Helv. Chim. Acta.* 1972, *55*, 2731.
165. Ackermann, P.; Ganter, C. *Helv. Chim. Acta* 1976, *59*, 2531.
166. Capraro, H.-G.; Ganter, C. *Helv. Chim. Acta* 1980, *63*, 1347.
167. Nakazaki, M.; Naemura, K.; Kondo, Y. *J. Org. Chem.* 1976, *41*, 1229. For (−)-4-azatwistan-5-one, see: Tichý, M.; Dušková, E.; Bláha, K. *Tetrahedron Lett.* 1974, 237.
168. Review: Nakazaki, M.; Chikamatsu, H. *Kagaku no Ryoiki* 1977, *31*, 819; Nakazaki, M. *Chemistry Today* (*Gendai Kagaku*) 1982, *134*, 38. For the related microbial "C_1 ketone rule," see: Nakazaki, M.; Chikamatsu, H.; Naemura, K.; Hirose, Y.; Shimizu, I.; Asao, M. *Chem. Commun.* 1978, 668. Nakazaki, M.; Chikamatsu, H.; Naemura, K.; Asao, M. *J. Org. Chem.* 1980, *45*, 4432.
169. Nakazaki, M.; Chikamatsu, H.; Naemura, K.; Nishino, M.; Murakami, H.; Asao, M. *Chem. Commun.* 1978, 667. *J. Org. Chem.* 1979, *44*, 4588.
170. Nakazaki, M.; Chikamatsu, H.; Naemura, K.; Sasaki, Y.; Fujii, T. *Chem. Commun.* 1980, 626; Nakazaki, M.; Chikamatsu, H.; Naemura, K.; Suzuki, T.; Iwasaki, M.; Sasaki, Y.; Fujii, T. *J. Org. Chem.* 1981, *46*, 2726.
171. Spielmann, W.; de Meijere, A. *Angew. Chem. Int. Ed. Engl.* 1976, *15*, 429.
172. Brewster, J. H. *J. Am. Chem. Soc.* 1959, *81*, 5475, 5493; *Tetrahedron* 1961, *13*, 106.
173. Andersen, B.; Schallner, O.; de Meijere, A. *J. Am. Chem. Soc.* 1975, *97*, 3521. de Meijere, A.; Weitemeyer, C.; Schallner, O. *Chem. Ber.* 1977, *110*, 1504, de Meijere, A. *Angew. Chem. Int. Ed. Engl.* 1979, *18*, 809.
174. Coll, J. C.; Crist, D. R.; Barrio, M. d. C. G.; Leonard, N. J. *J. Am. Chem. Soc.* 1972, *94*, 7092.
175. Leonard, N. J.; Coll, J. C.; Wang, A. H.-J.; Missavage, R. J.; Paul, I. C. *J. Am. Chem. Soc.* 1971, *93*, 4628. Wang, A. H.-J.; Missavage, R. J.; Byrn, S. R.; Paul, I. C. *ibid.* 1972, *94*, 7100.
176. Parker, W.; Tranter, R. L.; Watt, C. I. F.; Chang, L. W. K.; Schleyer, P. v. R. *J. Am. Chem. Soc.* 1974, *96*, 7121.
177. Farina, M. *Tetrahedron Lett.* 1963, 2097. Farina, M.; Audisio, G. *Tetrahedron* 1970, *26*, 1827.
178. Farina, M.; Audisio, G. *Tetrahedron Lett.* 1967, 1285; *Tetrahedron* 1970, *26*, 1839.
179. Allegra, G.; Farina, M.; Colombo, A.; Casagrande-Tettamanti, G.; Rossi, U.; Natta, G. *J. Chem. Soc., B* 1967, 1028.
180. Farina, M.; Audisio, G.; Natta, G. *J. Am. Chem. Soc.* 1967, *89*, 5071.
181. Binsch, G.; Kessler, H. *Angew. Chem. Int. Ed. Engl.* 1980, *19*, 411.
182. Hill, R. K.; Ladner, D. W., *Tetrahedron Lett.* 1975, 989.
183. Morandi, C.; Mantica, E.; Botta, D.; Gramegna, M. T.; Farina, M. *Tetrahedron Lett.* 1973, 1141. Farina, M.; Morandi, C.; Mantica, E.; Botta, D. *J. Org. Chem.* 1977, *42*,

2399. For the conformational analysis and X-ray crystallography, see: Brückner, S.; Allegra, G.; Albinati, A.; Farina, M.; *J. Chem. Soc., Perkin II* **1980**, 523.
184. Saito, Y.; Nakatsu, K.; Shiro, M.; Kuroya, H. *Acta Crystallogr.* **1955**, *8*, 729; *Bull. Chem. Soc. Jpn.* **1957**, *30*, 795.
185. Saito, Y. In "Topics in Stereochemistry," Vol. 10; Eliel, E. L.; Allinger, N. L., Eds.; Wiley-Interscience: New York, 1978, p. 95. Saito, Y. "Inorganic Molecular Dissymmetry"; Springer: New York, 1979.
186. Buckingham, D. A.; Sargeson, A. M. In "Topics in Stereochemistry," Vol. 6; Allinger, N. L.; Eliel, E. L., Eds.; Wiley-Interscience: New York, 1971, p. 219.
187. Hellwinkel, D.; Mason, S. F. *J. Chem. Soc., B* **1970**, 640.
188. Ito, T.; Kobayashi, A.; Marumo, F.; Saito, Y. *Inorg. Nuclear Chem. Lett.* **1971**, *7*, 1097.
189. Pinnavaia, T. J.; Podolsky, G.; Codding, P. W. *Chem. Commun.* **1973**, 242.
190. Bartell, L. S.; Clippard, F. B., Jr.; Boates, T. L. *Inorg. Chem.* **1970**, *9*, 2436.
191. Maier, G.; Pfriem, S.; Schäfer, U.; Matusch, R. *Angew. Chem. Int. Ed. Engl.* **1978**, *17*, 520.
192. Hounshell, W. D.; Mislow, K. *Tetrahedron Lett.* **1979**, 1205.
193. An imaginary osmium complex having O symmetry was suggested in: Cadwell, D. J.; Eyring, H. "The Theory of Optical Activity"; Wiley-Interscience: New York, 1971, p. 157.
194. Nakazaki, M.; Naemura, K. *Chem. Commun.* **1980**, 911; *J. Org. Chem.* **1981**, *46*, 106.
195. Mislow, K. *Chem. Commun.* **1981**, 234.
196. Nakazaki, M.; Naemura, K.; Hokura, Y. *Chem. Commun.* **1982**, 1245.
197. Eaton, P. E.; Cole, T. W., Jr. *J. Am. Chem. Soc.* **1964**, *86*, 3157.
198. Ternansky, R. J.; Balogh, D. W.; Paquette, L. A. *J. Am. Chem. Soc.* **1982**, *104*, 4503.
199. Smith, B. H., "Bridged Aromatic Compounds"; Academic Press: New York, 1964, Chap. 1.

Stereochemistry of Biological Reactions at Proprochiral Centers

HEINZ G. FLOSS*

Department of Medicinal Chemistry and Pharmacognosy
Purdue University
West Lafayette, Indiana

MING-DAW TSAI

Department of Chemistry
The Ohio State University
Columbus, Ohio

RONALD W. WOODARD

College of Pharmacy
University of Michigan
Ann Arbor, Michigan

*Present address: Department of Chemistry, The Ohio State University, Columbus, Ohio.

ABBREVIATIONS USED

9-BBN, 9-borabicyclo[3.3.1]nonane; PGA, 3-phosphoglyceric acid; PEP, phosphoenolpyruvate; ADH, alcohol dehydrogenase; CoA, coenzyme A; NAD, adenine nicotinamide dinucleotide; LDH, lactate dehydrogenase; TDP, thymine diphosphate; SAM, *S*-adenosylmethionine; COMT, catechol-*O*-methyltransferase; P_i, inorganic phosphate; Ps_i, inorganic thiophosphate; AMP, adenosine 5′-monophosphate; ADP, adenosine 5′-diphosphate; ATP, adenosine 5′-triphosphate; AMPS, adenosine 5′-thiophosphate; ADPαS, adenosine 5′-(1-thiodiphosphate); ADPβS, adenosine 5′-(2-thiodiphosphate); ATPαS, adenosine 5′-(1-thiotriphosphate); ATPβS, adenosine 5′-(2-thiotriphosphate); ATPγS, adenosine 5′-(3-thiotriphosphate); tRNA, transfer ribonucleic acid; TpNP, thymidine 3′-[(4-nitrophenyl)phosphate]; TMP, thymine monophosphate; U > pS, uridine 2′,3′-cyclic phosphorothioate; UMPS, uridine 5′-thiophosphate; DPPE, dipalmitoylphosphatidylethanolamine; DPPC, dipalmitoylphosphatidylcholine; EDTA, ethylenediaminetetraacetate.

I. INTRODUCTION

Enzymes have a remarkable ability to recognize the stereochemical properties of chiral or prochiral substrates and to catalyze chemical transformations with a high degree of stereospecificity. This stereospecificity is exerted not only in cases where it may serve a utilitarian purpose, that is, in situations in which there is a functional advantage to operating with only one enantiomer, as in the distinction between D and L amino acids. It is also seen in instances where there

seems to be no particular advantage to carrying out a reaction stereospecifically, for example, in many reactions involving discrimination between two heterotopic* ligands at a prochiral center, such as the dehydrogenation of a primary alcohol to an aldehyde. This, of course, is because enzymes, in order to achieve high substrate specificity and significant reaction-rate enhancements, must orient substrates rigorously in their macromolecular matrix. Since the matrix is chiral, the reactions catalyzed are almost inescapably stereospecific.

The steric course of a reaction, for example, a substitution at an sp^3 carbon atom, can only be observed if the reaction leads from a chiral center to another chiral center. The majority of biochemical reactions, however, take place at centers that are not chiral, hence their steric course is not evident from an inspection of the substrates and products. Such reactions have been called "stereochemically cryptic" (1); to unravel their steric course requires labeling of the center with either isotopes or heteroatoms to convert it into a chiral center of observable stereochemical behavior. In the isotopic labeling approach a chiral center is generated by replacing stereoheterotopic or homotopic groups with groups containing or consisting of a different isotope of the same element, such as replacing ^1H with ^2H or ^3H, ^{12}C with ^{13}C, or ^{16}O with ^{17}O or ^{18}O. Since the size differences between the isotopes are very small, even in the extreme case of replacement of protium with tritium, the isotopically chiral species will bind to the enzyme in the same way as the nonlabeled version, and except for rate changes due to isotope effects, it will react in the same way. In the heteroatom labeling approach, one introduces chirality by replacing stereoheterotopic or homotopic groups with different elements, such as replacing hydrogen by CH_3, as in a study of the stereochemistry of the pyruvate kinase reaction (2), or replacing oxygen by sulfur, as in many of the studies on the stereochemistry of reactions at phosphorus. The advantage of this approach is that it requires, in general, less elaborate analytical methodology. Unlike the isotopic substitution, such a heteroatomic replacement in a substrate may, of course, be recognized by the enzyme, potentially resulting in a different orientation, binding of only one of the stereoisomers, or simply nonacceptance or nonreactivity of the substrate analog. For the latter reason, the utility of this approach is limited by the usu-

*The following terminology is used: **Homomorphic** groups are groups that are identical when detached from their environment. They can be **homotopic**, that is, occupy equivalent positions in space, or **heterotopic**, occupy nonequivalent positions. **Stereoheterotopic** groups occupy stereochemically nonequivalent positions in space; they may be **enantiotopic** if replacement of either one or the other (but not both) by a different achiral ligand gives rise to a pair of enantiomers, or they may be **diastereotopic** if their separate replacement gives rise to a pair of diastereomers. In general, stereoheterotopic groups in a molecule will be enantiotopic if the molecule itself is achiral and contains no chiral centers; they will be diastereotopic if the molecule is chiral or contains chiral centers. (For a more detailed discussion, see: E. L. Eliel, "Prostereoisomerism (Prochirality)," *Topics in Current Chemistry*, Vol. 105, Springer Verlag, Heidelberg, 1982.)

ally high substrate specificity of enzymes. It has, however, served extremely well in studies on biological reactions at phosphorus, where chiral phosphorothioates have been very useful tools. Because of the potential problem that heteroatomic substitution can be recognized by the enzyme and can result in different binding and reactivity, the results obtained by this approach are, strictly speaking, not as rigorous as those obtained by the isotopic substitution approach. Nevertheless, for example, in all the studies on enzymatic reactions at phosphorus there is no case in which the two approaches have given different stereochemical results.

Ever since the appearance of Ogston's pioneering article in 1948 (3), which pointed out the ability of an enzyme to distinguish what we now call enantiotopic groups in a substrate, the stereochemistry of many reactions at prochiral centers has been determined (for reviews, see refs. 1, 4-18). However, the stereospecificity of enzyme reactions, as pointed out before, is not limited to chiral and prochiral systems. This was first demonstrated experimentally in 1969, when the groups associated with Cornforth and Eggerer (19) and Arigoni and Rétey (20) synthesized (*R*)- and (*S*)-[2-D,T]acetic acid and used this chiral variety of an achiral center of the *Xaaab* type to determine the steric course of the reaction catalyzed by the enzyme malate synthase. Subsequently, chiral versions of another biologically important center of the *Xaaab* type, a phosphate monoester, were synthesized and used for stereochemical studies (21-23). Two other stereochemically interesting and biologically important achiral systems are malonic acid (substitution type *Xaabb*) and inorganic phosphate (*Xaaaa*). While no synthesis of chiral malonic acid has been reported as yet, two groups have recently prepared a chiral version of inorganic phosphate (24, 25). In general the conceptual difficulty in developing methods for studying the steric course of reactions at centers of the *Xaaab* and *Xaaaa* type resided not so much in the synthesis of chiral versions of such centers as in the design of analytical methodology to determine the chirality of samples of unknown configuration. This is due to the different properties of these systems compared with prochiral centers. However, in the malonic acid example of the *Xaabb* substitution type, even the synthesis is a formidable problem because the chiral integrity of this system is jeopardized by the exchangeability of the α-hydrogens.

The term "prochiral" was coined in 1966 by Hanson (26) to describe elements (centers, planes, axes) in a molecule giving rise to a pair of features (ligands, faces) that can be distinguished only by reference to an external or internal chiral environment. The term originates from the fact that one substitution step is required to transform a prochiral center *Xaabc* into a chiral center *Xabcd*; hence studies on the stereochemistry of reactions at prochiral centers require one isotopic or heteroatomic substitution. A prochiral center *Xaabc* has certain properties, in particular the attribute that the two stereoheterotopic groups *a* are distinct because they are seen, and behave, differently in a chiral environment. Hence an enzyme can differentiate between the two groups *a* by

virtue of the fact that the protein represents a chiral matrix. This is not true with systems of the *Xaaab* or *Xaabb* type. In these systems the homomorphic ligands are intrinsically identical, because even in a chiral environment they can be superimposed by internal or external rotations. The systems *Xaaab* and *Xaabb* are one substitution step removed from a prochiral center and two substitution steps removed from a chiral center. Therefore, two isotopic or heteroatomic substitutions are required to study the steric course of reactions at such centers. Based on this formalism we call the systems *Xaaab* and *Xaabb* proprochiral centers. This provides a convenient classification of the status of these relative to other achiral systems, although it must be recognized that proprochirality is not an observable property. In an enzyme reaction at a proprochiral center the replacement of a homotopic ligand will occur at random; apart from rate differences due to isotope effects this will be true also for the isotopically chiral species. However, a proprochiral center labeled with one heteroatom will assume the properties of a prochiral center–the remaining two homomorphic ligands are now stereoheterotopic and therefore distinguishable by the usual methods.

In a system *Xaaaa* the *a* groups are, of course, also homotopic and thus indistinguishable. By the same formalism used above such a center can be called *pro*proprochiral, because it is *three* substitution steps removed from a chiral center. Hence, three isotopic and/or heteroatomic replacements are required in order to study the steric course of reactions at such a center. The only chiral version of a proproprochiral center synthesized to date is an inorganic phosphate molecule carrying one heteroatomic and two isotopic replacements, (*R*)- and (*S*)-[^{16}O,^{17}O,^{18}O]phosphorothioate. The presence of the sulfur heteroatom, of course, gives this chirally labeled species the properties of a proprochiral center with the concomitant simplification in the analytical methodology required to distinguish an *R* from an *S* isomer.

In the following sections we discuss the methods that have been developed to study the steric course of reactions at proprochiral and proproprochiral centers on carbon and phosphorus, and some of the biochemical applications of these methods. Specifically, we consider chiral methyl groups, chiral malonic acid, chiral phosphate monoesters, and chiral inorganic phosphate.

II. CHIRAL METHYL GROUPS

A. General

The existence of enantiomers of a chiral methyl group C(R,H,D,T) was predicted as early as 1962 by Levy, Talalay, and Vennesland (27). The authors stated, "It is certain that two enantiomorphs of this molecule will exist, although no satisfactory methods are as yet available for their separation." While the

separation of the two enantiomers of such a molecule is indeed for all practical purposes impossible, their separate syntheses present no particular problem. However, the development of methods to distinguish a methyl group of *R* configuration from its *S* enantiomer required conceptually new approaches. With such methodology at hand it became possible to examine the steric course of reactions in which methyl groups are generated from methylene groups ($R—CH_2—X \rightarrow R—CH_3$) or are converted into methylene groups ($R—CH_3 \rightarrow R—CH_2—X$) and of processes in which methyl groups are transferred from one ligand to another ($R—CH_3 \rightarrow R'—CH_3$). This methodology and its application have been reviewed before (28-30).

B. Synthesis of Chiral Methyl Groups

Most of the syntheses of chiral methyl groups reported to date involve the use of purely chemical methods, purely enzymic methods, or various combinations of the two. Most of these routes produce acetic acid, pyruvic acid, or lactic acid, which can then be converted into more complex molecules.

1. Chemical Methods

The synthesis reported by Cornforth et al. (31) is one of the original syntheses of chiral acetate and the first entirely chemical approach. The original method, which relied on the introduction of tritium with $[^3H]LiAlH_4$, proved unsatisfactory and was subsequently modified (32) to introduce the tritium via $[^3H]H_2O$ as shown in Scheme 1. The *trans*-2-tritio-1-phenylethylene was epoxidized in a stereospecific syn reaction to give only one racemic diastereomer. The mixture of epoxides was subjected to stereospecific reductive ring opening with $LiAl^2H_4$, a process known to proceed with inversion of configuration. The (1*S*,2*S*)- and (1*R*,2*R*)-2-deuterio-2-tritio-1-phenylethanol mixture thus obtained was then resolved into the enantiomers using classical resolution techniques since the benzylic carbon is a normal chiral center. The enantiomers, once resolved, contained methyl groups which had opposite configurations. The remainder of the synthesis involved the conversion of the phenylethanol isomers to acetate with retention of the configuration of the chiral methyl center. The analysis of the products revealed them to be of high chiral purity [(*R*)-acetate 93% e.e. (enantiomer excess), and (*S*)-acetate 86% e.e.]. This modified procedure allowed the synthesis of ~3 mCi of chiral acetate in an overall yield of 7.7% based on the starting styrene.

Clearly the most elegant chemical synthesis of chiral acetate is the route reported by Townsend et al. (33). The method, outlined in Scheme 2, has the advantage that tritium is introduced at a late stage in the synthesis, and both of the remaining steps, pyrolysis and Kuhn-Roth oxidation, proceed in high

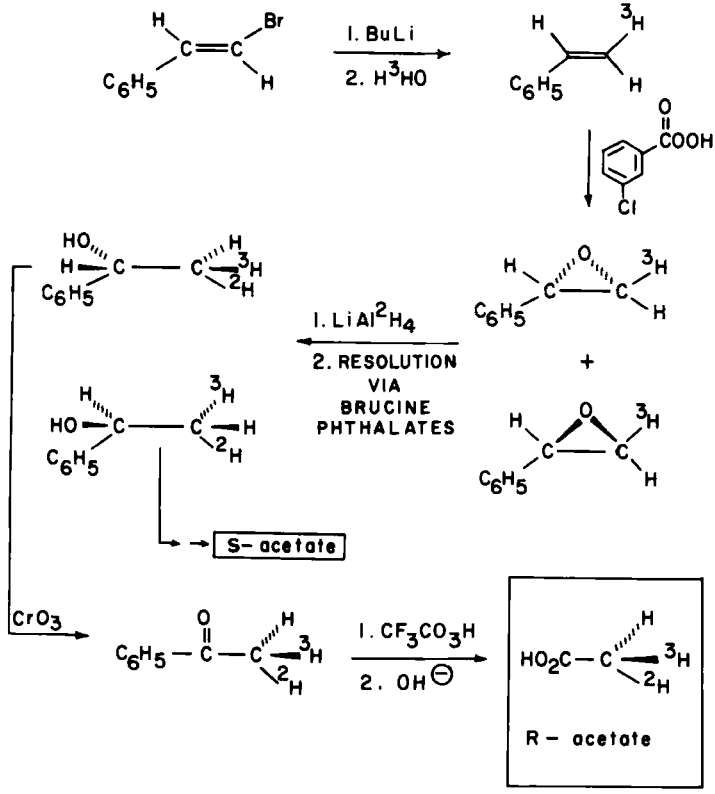

Scheme 1

chemical yield. The pyrolysis of the deuterated ether brings together the three different isotopes of hydrogen in succession from three different positions in the molecule in a two-step process. The first reaction is an "ene" reaction in which the geometry of the system dictates syn addition to the triple bond. In the reductive elimination of methyl formate, the geometry of the addition of deuterium to the double bond is controlled by the stereochemistry of the alcohol function. The (*R*)-acetate was obtained from the ether of the (*R*)-alcohol in high chiral purity (93% e.e.) and the (*S*)-ether gave the corresponding (*S*)-acetate in equally high chiral purity.

More recently, Bosnich and co-workers (34) have published a method for the synthesis of (*S*)-lactic acid containing a chiral methyl group using asymmetric catalytic hydrogenation. The (*Z*)-ethyl 2-acetoxy-3-bromoacrylate shown in Scheme 3 was converted into the isomerically pure (*Z*)-ethyl 2-acetoxy-3-tritio-acrylate by cleavage of the $Pd(PPh_3)_4$ adduct with $CF_3CO_2{}^3H$. The olefin was then hydrogenated with deuterium gas in the presence of [Rh(R-prophos)]$^+$ to

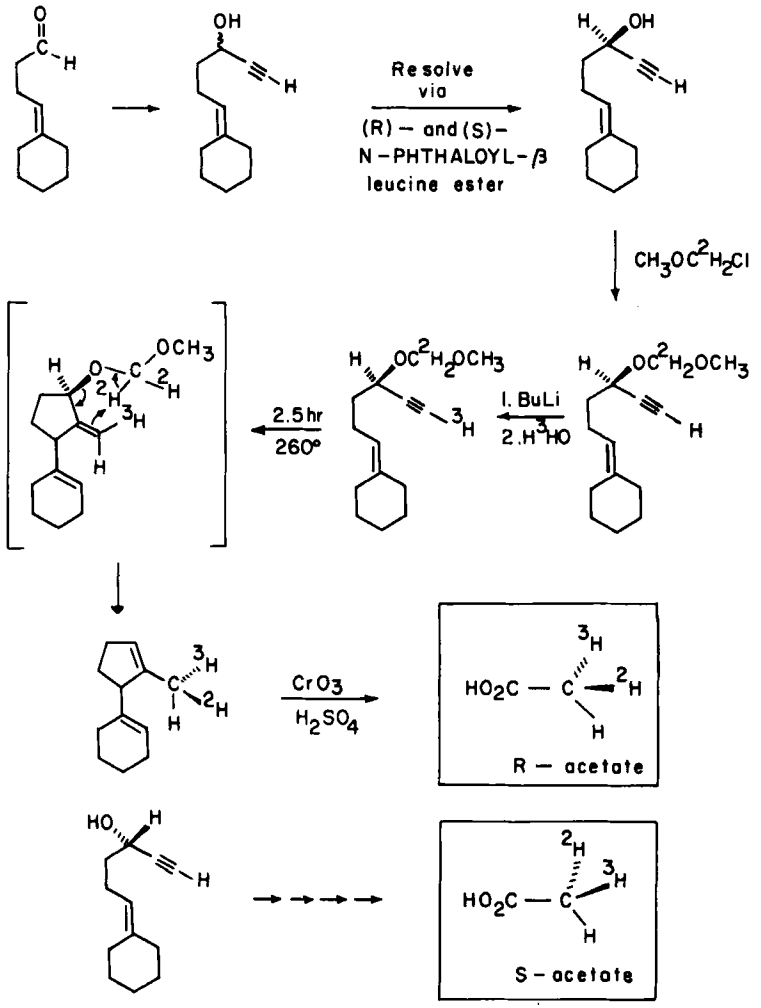

Scheme 2

give the lactic acid shown. However, the validity of this method has not been verified by chirality analysis of the methyl group.

Two other purely chemical routes to chiral acetic acid have been pursued in our laboratory. In one of these, outlined in Scheme 4, stereospecifically α-deuterated or -tritiated 3,5-dimethoxybenzyl alcohol is prepared by reduction of the aldehyde with Midland's reagent (*B*-3-pinanyl-9-borabicyclo[3.3.1]-nonane, α-pinanyl-9-BBN) (35), followed by conversion to the tosylate and reductive displacement with lithium aluminum hydride or superhydride (lithium

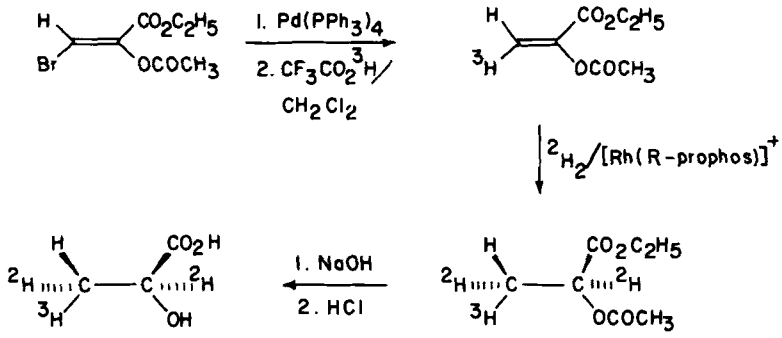

Scheme 3

triethylborohydride) (36). Various combinations of deuterated and tritiated reagents and substrates can be used to introduce the three hydrogen isotopes in the desired configuration. For example, deuterated aldehyde, prepared via the the 1,3-dithiane derivative, was reduced with unlabeled (+)- and (-)-α-pinanyl-9-BBN followed by displacement of the tosylate with [^{3}H]$LiAlH_4$ or, in better yield, [^{3}H]superhydride. The latter can be readily prepared from [^{3}H]LiH and triethylborane (37). The critical step in the overall sequence is the oxidation of the 3,5-dimethoxytoluene to acetic acid. Kuhn-Roth oxidation produced material of low chiral purity (~25-35% e.e.), but ozonolysis followed by afteroxidation with $HgSO_4$ gives consistently good yields (80-85%) of acetic acid of high chiral purity (>90% e.e.). Under these conditions the limiting factor for the chiral purity of the acetic acid is the optical purity of the α-pinene used. Another version of this synthesis involved reducing the unlabeled aldehyde with [^{3}H]$NaBH_4$, one of the cheapest sources of tritium, reoxidation to the tritiated aldehyde, followed by reduction with unlabeled (+)- and (-)-pinanyl-9-BBN and displacement of the tosylate with superdeuteride. Additional permuta-

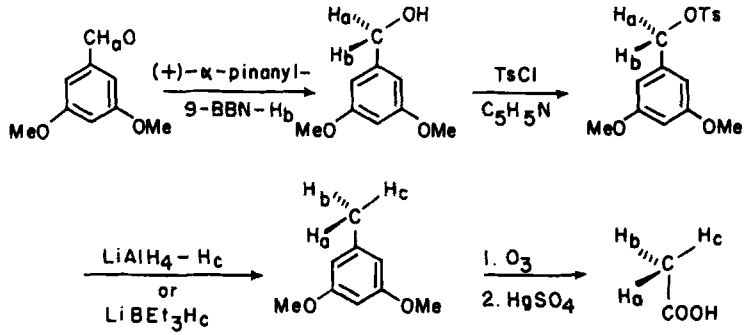

Scheme 4

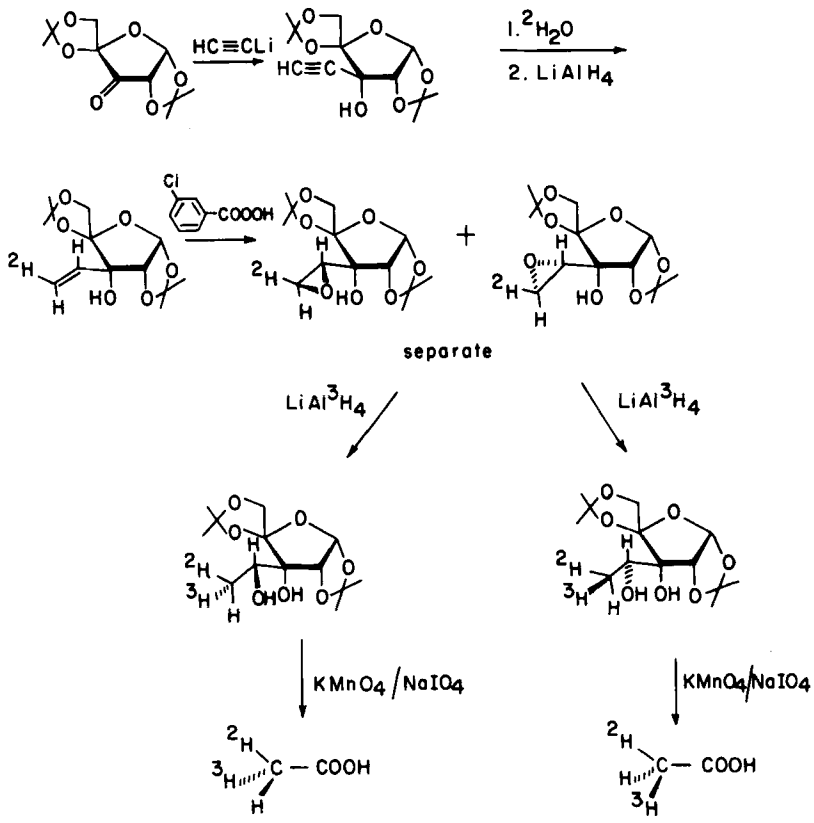

Scheme 5

tions are obvious; which one is most suitable for a given laboratory depends on the relative availability of different reagents and facilities.

Another chemical route is based on the work of Kakinuma et al. (38), who synthesized the two chiral, deuterated epoxides shown in Scheme 5. Separation of the two diastereomers and reductive epoxide ring opening with tritiated $LiAlH_4$ followed by permanganate/periodate oxidation gave acetic acid which within the limits of detection was chirally pure (100 ± 7% e.e.) (39).

2. *Enzymatic Methods*

One of the most efficient methods relying on enzymatic reactions is that reported by our laboratory (40, 41), a modification of the original procedure published by Rose (42) for the synthesis of chiral pyruvate and acetate. The route, as shown in Scheme 6, utilizes the commercially available purified glycolytic

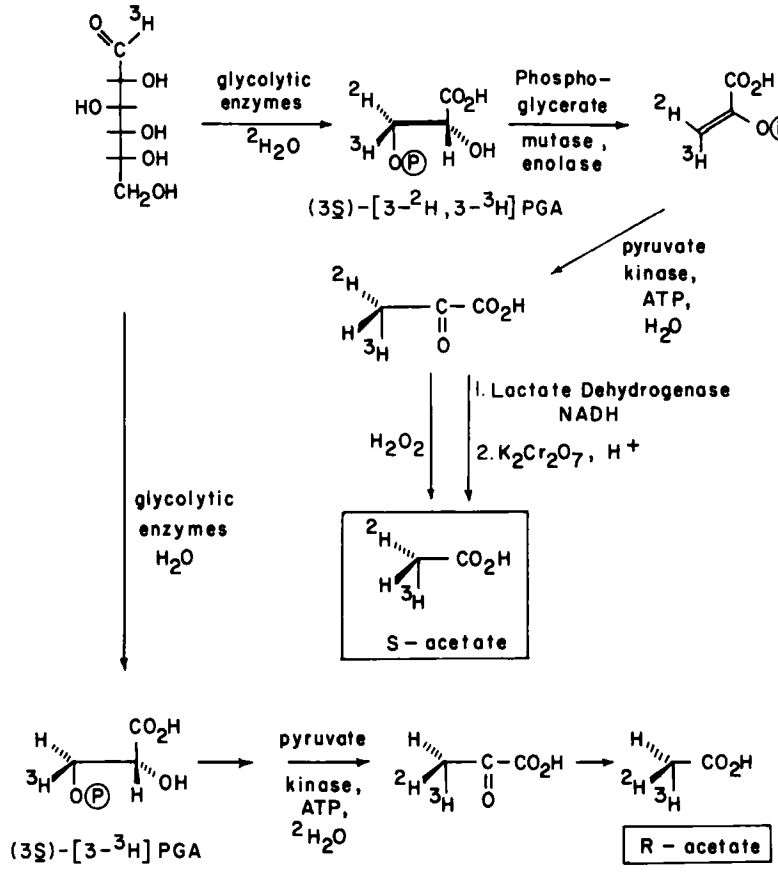

Scheme 6

enzymes to convert [1-^{3}H]glucose to (3*S*)-[3-^{3}H]phosphoglyceric acid (PGA) in one single incubation. The (3*S*)-[3-^{3}H]PGA was converted to (3*R*)-lactate in a second incubation by a series of enzymatic reactions carried out in deuterated water, the key step being the pyruvate kinase reaction (43) which stereospecifically protonates phosphoenolpyruvate from the *Si* face to give pyruvate. The chiral lactate was oxidized with dichromate to give (*R*)-acetate of 72% e.e. The lactate of opposite configuration was obtained by converting [1-^{3}H]glucose to (3*S*)-[3-^{2}H,3-^{3}H]PGA with the same enzymes previously described but in ^2H_2O instead of H_2O. The incubation with pyruvate kinase, in H_2O, gave (3*S*)-lactate, which upon oxidation produced (*S*)-acetate of 65% e.e. The overall yield based on [1-^{3}H]glucose was 20%. The low chiral purity of the acetate samples is due to the known slow deprotonation of pyruvate by pyruvate kinase before its release from the enzyme's active site (44).

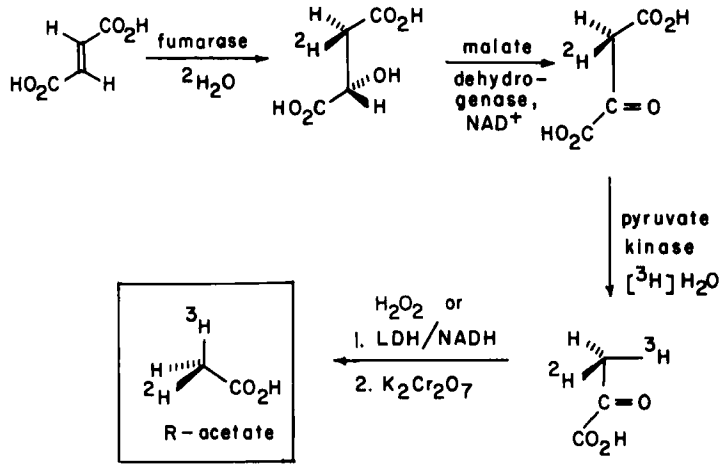

Scheme 7

Creighton and Rose (45) have explored the route shown in Scheme 7 to synthesize chiral pyruvate. The method takes advantage of the fact that pyruvate kinase decarboxylates oxalacetate with retention of configuration. The requisite labeled oxalacetates were prepared as shown from the appropriately labeled L-malates, available from equilibration with fumarase in either deuterated or tritiated water. This method is convenient for the preparation of small amounts of chiral acetate but suffers from the low oxalacetate decarboxylase activity of pyruvate kinase.

Simon and co-workers (46) reported the quantitative conversion of (3*R*)-L-[3-^{2}H]malate to (3*S*)-[3-^{2}H,3-^{3}H] lactate by the organism *Leuconostoc mesenteroides* in tritiated water. The (3*R*)-lactate was obtained by fermentation of the tritiated malate in ^2H_2O; however, the chiral purity of both acetates, obtained by oxidation of the lactate samples with dichromate in dilute H_2SO_4, was lower than expected (34-52% e.e.). The specific activity of the acetates was somewhat lower than that of the starting lactates indicating possible racemization during oxidation. However, in our laboratory this oxidation of lactate has usually produced acetate without loss of chiral purity.

The Stickland reaction (47) has received much attention as a possible route to chiral acetate due to the availability of chiral glycine (48). In the Stickland reaction two moles of glycine and one mole of D-alanine are converted quantitatively into three moles of acetate, three moles of ammonia, and one mole of CO_2 by the organism *Clostridium sticklandii*. The presence of amino acid transaminase in the intact organisms leads to extensive hydrogen exchange although in the purified enzyme the replacement of NH_2 by H occurs stereospecifically with inversion (49, 50). Unfortunately, the rates of conversion with the purified enzyme are too low to be synthetically useful.

3. *Combinations of Chemical and Enzymatic Methods*

The second original route for the synthesis of chiral acetate as reported (20) by the Zürich group, outlined in Scheme 8, involved a combination of enzymatic and chemical reactions. [2-^{3}H]Glyoxylic acid was produced from oxalic acid and tritiated water and was reduced to (*S*)-[2-^{3}H]glycolic acid by lactate dehydrogenase (51) and to (*R*)-[2-^{3}H]glycolic acid with glyoxylate reductase from spinach leaves (52). The acids were converted to the methyl esters, which were reduced to ethylene glycol. The latter were converted to their monobrosylates and

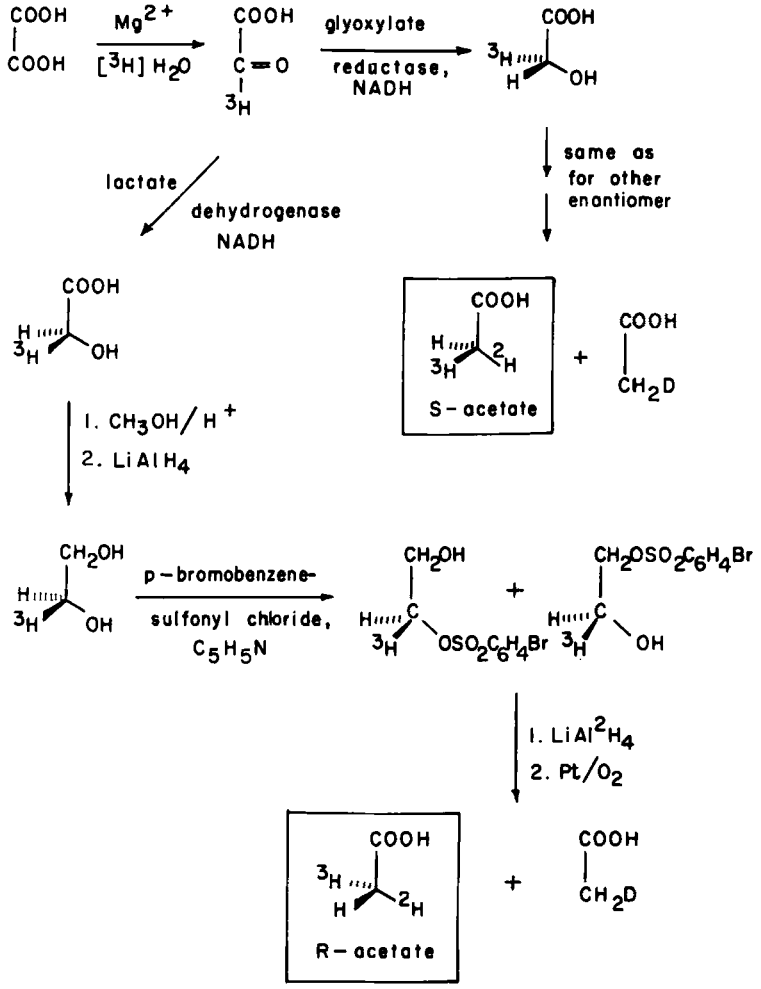

Scheme 8

displaced with $LiAl^2H_4$, a reaction known to occur with inversion of configuration, to give the corresponding chiral-methyl ethanols, which were then oxidized with O_2 in the presence of Pt to their respective acetates. One of the problems with this approach is the generation of the symmetrical intermediate ethylene glycol. Half the tritiated molecules are converted to $CH_2{}^2H\text{-}CO_2H$, thereby lowering the specific activity by half. The overall yield is 2% based on oxalic acid.

Kajiwara et al. (53) reported a synthesis of chiral acetic acid based on the successive conversion of (*R*)-[2-^{2}H]glycine into bromoacetic acid and then, with tritiated $LiAlH_4$, into ethanol, which was oxidized with chromic acid to chiral acetic acid of *R* configuration (92% e.e.). The chiral glycine in their work was prepared from benzaldehyde in a seven-step sequence; however, it can also be obtained in other ways, such as enzymatic exchange of glycine with alanine transaminase (54). A simplified version of this synthesis, worked out in our laboratory, is outlined in Scheme 9. Chiral [2-^{2}H,2-^{3}H]glycine is generated by enzymatic exchange and the reductive displacement of the bromine in bromoacetic acid is carried out with superhydride to give directly acetic acid (55).

Caspi and co-workers (56) have reported the synthesis of *n*-octane containing a chiral methyl group by the displacement of the mesylate of (*R*)- and (*S*)-1-[1-^{3}H]octanol with superdeuteride. A unique feature of their approach (56, 57) was the chemical conversion of the more readily available tritiated 1*S* alcohol, obtained from the reduction of [1-^{3}H]octanal by horse liver alcohol dehydrogenase, to the more difficult-to-obtain 1*R* alcohol by the Mitsunobu reaction. Using the conditions shown in Scheme 10, the (1*S*)-alcohol was converted to the (1*R*)-benzoate which gave the (1*R*)-alcohol by reductive cleavage with $LiAlH_4$.

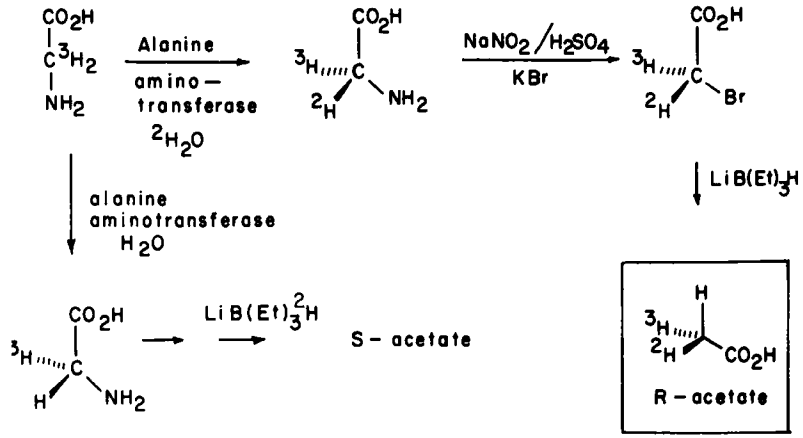

Scheme 9

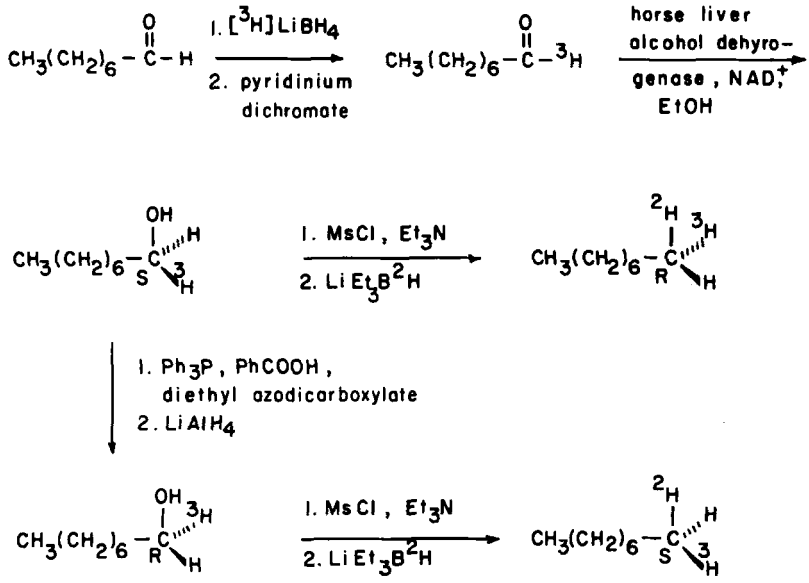

Scheme 10

This interconversion was carried out in 88% yield with complete inversion of configuration as judged, for example, by incubation with yeast alcohol dehydrogenase. A similar general route, reductive displacement of a sulfonate ester, was used to prepare chiral-methyl labeled decane (58). In neither case was the chiral purity of the product determined by analysis, but further work by Caspi's group (56, 59) indicated that their material must have had good chiral purity.

4. *Generation of Chiral Methyl Groups in More Complex Molecules*

In most of the examples discussed so far the synthetic target was chiral-methyl acetic acid either used per se as substrate or serving as starting material for the synthesis of more complex molecules, for example, (*3'R*)- and (*3'S*)-[3'-^{2}H,^{3}H]mevalonolactone (60) or (*methyl-R*)- and (*methyl-S*)-[methyl-^{2}H,^{3}H]methionine (40, 41, 61). In a number of other instances, chiral methyl groups were generated directly in more complex molecules required for a particular experiment. Chiral-methyl octane and decane, mentioned above, are examples, as is the synthesis of squalene carrying a chiral methyl group at carbon 6, which was published by Altman and his group (62). Two recent papers deal with the synthesis of compounds in which a chiral methyl group is part of an isopropyl group: systems containing two chiral centers which both owe their chirality only to isotopic substitution. In a synthesis by Aberhart and Tann (63), reduction of (*Z*)- and (*E*)-[3-^{2}H]methacrylate with tritium gas over chlorotris-

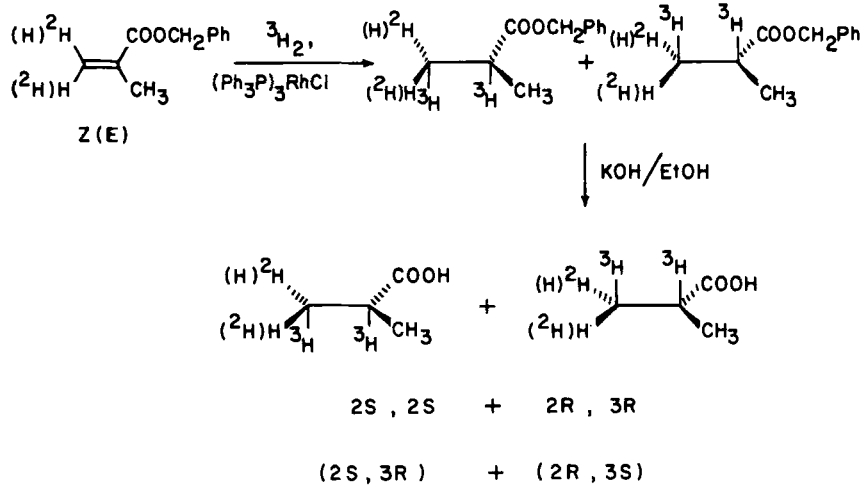

Scheme 11

(triphenylphosphine)rhodium catalyst gave isobutyrate as the 2*S*,3*R* + 2*R*,3*R* and the 2*S*,3*R* + 2*R*,3*S* racemic mixtures, respectively (Scheme 11). The problem of controlling the stereochemistry at the two isotopically chiral centers separately was addressed in a synthesis by Townsend and co-workers (64) of valine carrying a chiral methyl group in the pro-*R* position at C-3 (Scheme 12). The synthesis starts with (*S*)-α-methyldihydrocinnamic acid, predetermining the correct absolute configuration of the chiral center which is to become C-3 of valine. The chiral center which is to become the chiral methyl group is built up by alcohol dehydrogenase reduction of a deuterated aldehyde. Inversion of the configuration of the resulting (*S*)-alcohol by the Mitsunobu reaction allows independent elaboration of the methyl group in both configurations while keeping the configuration of the other chiral center fixed.

III. ANALYSIS OF CHIRAL METHYL GROUPS

The standard method of distinguishing enantiomers by their ability to rotate the plane of polarized light is not applicable in the case of chiral methyl groups. Compounds of the type $R_1CH^2HR_2$ have specific rotations on the order of 1 to 2° (65), rarely greater than 5°, which are one or two orders of magnitude smaller than those of the corresponding $R_2CHR_2R_3$ type compounds. It would be expected that replacement of another "large" (R_1 or R_2) group by ^3H would again lower the specific rotation one or two orders of magnitude. However, unlike deuterium, tritium is present only at tracer levels, and therefore only a small

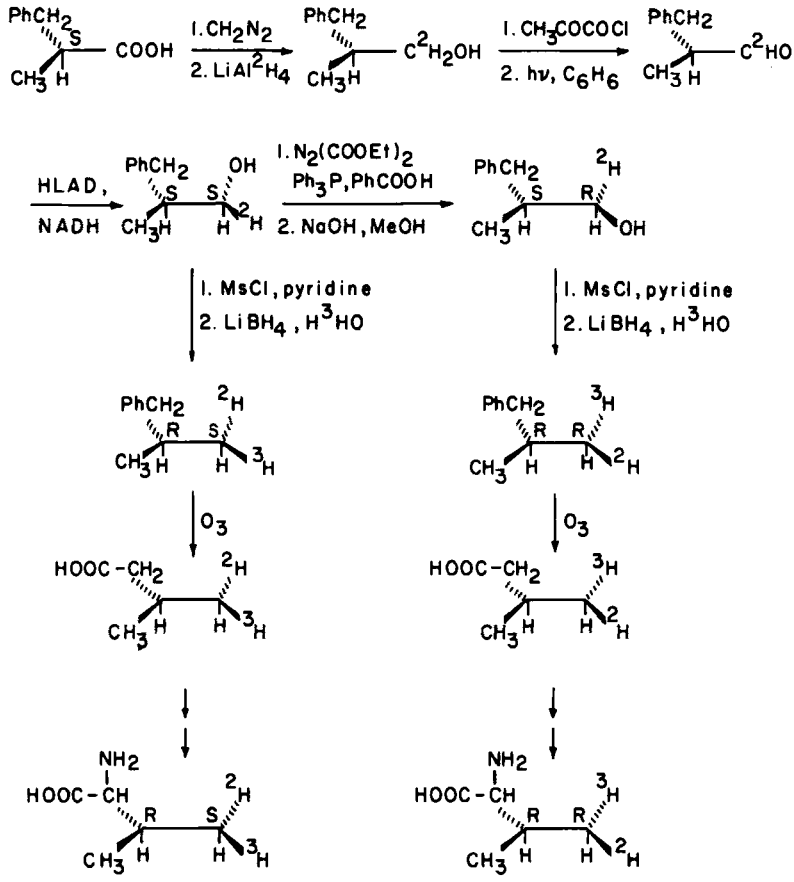

Scheme 12

number of methyl groups actually contain all three isotopes of hydrogen and are thus chiral. The majority of methyl groups contain one deuterium and two hydrogens and are prochiral. Since only about one in 10^7 molecules contain tritium, at the levels of specific radioactivities handled in most laboratories, the specific rotation would be well below detectable levels. If any spectroscopic method has the potential to distinguish a chiral methyl group of *S* configuration from its *R* isomers, tritium NMR spectroscopy (66) is probably the best candidate. This would require several experimental conditions to be met; one is slowing the rotation of the methyl group down to below the NMR time scale of resolution in a chiral environment, and another is the availability of relatively large amounts of tritiated sample (0.1 to 1.0 mCi per analysis). The feasibility of this approach has yet to be established.

All practical methods of analysis are based on carrying out a reaction in which one of the methyl hydrogens is replaced in a stereospecific, irreversible reaction by some other ligand, thereby generating a chiral methylene group. Each enantiomer of the methyl group gives rise to a set of three products. This process is illustrated in Scheme 13 for a process in which a methyl hydrogen of acetic acid is replaced with inversion by a group X ($X \neq -CO_2H$). This replacement leaves the remaining two hydrogens stereoheterotopic and thus distinguishable. The product set **a**, **b**, **c**, arising from the *R* isomer (**1**, **2**, **3**), is clearly different from set **d**, **e**, **f**, produced by the *S* isomer (**4**, **5**, **6**); the two product sets are mirror images of each other. Since tritium is present only in tracer amounts, products (**c**) and (**f**) are useless for analysis because they are formed mostly from the carrier species $CH_2{}^2H\text{-}CO_2H$. Therefore, the analysis requires a distinction between the sets (**a**) + (**b**) and (**d**) + (**e**). This can be done, for example, by determining whether the species tritiated at H_A (see bottom of Scheme 13) has arisen from the replacement of a normal hydrogen or from the replacement of deuterium. This determination may be made by converting **1**, **2**, **3** into **a**, **b**, **c** and **4**, **5**, **6** into **d**, **e**, **f** by a reaction that exhibits a significant primary kinetic

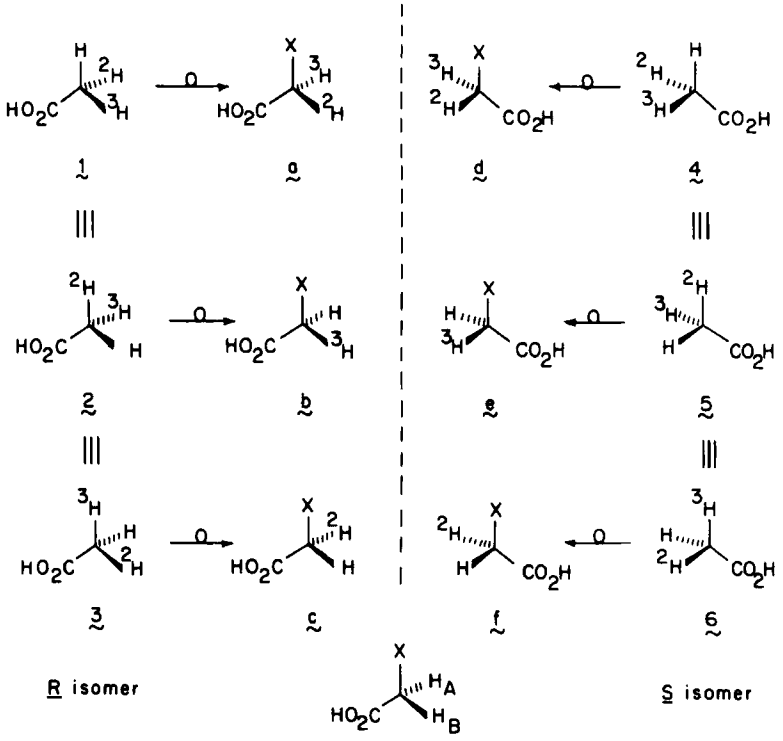

Scheme 13

isotope effect in the carbon-hydrogen bond cleavage. If the isotope effect were infinitely high, rotamer (**1**) would react infinitely faster than (**2**) or (**3**) and thus only (**a**) (all tritium located in the H_A position) would be produced, whereas in the absence of an isotope effect equal amounts of (**a**) and (**b**) (tritium equally distributed between the H_A and H_B position) would be formed. By the same logic the opposite enantiomer would give rise to only (**d**), where all the tritium is located in the H_B position, if the isotope effect were infinitely large. It is therefore possible to distinguish between set (**a, b, c**) and set (**d, e, f**) by generating them in a reaction which exhibits a primary kinetic isotope effect and determining the tritium distribution between H_A and H_B. Four factors control the ratio of tritium in H_A to tritium in H_B: (i) the chiral purity of the methyl group; (ii) the configuration of the methyl group; (iii) the sign and magnitude of the isotope effect; (iv) the steric course of the reaction. Since the steric course and the isotope effect k_H/k_D are constant for a given enzyme, once the system has been calibrated with chiral methyl samples of known absolute configuration and chiral purity, the analysis of the configuration and chiral purity of unknown samples can be accomplished. The first (19, 20) and most widely employed method for chiral methyl group analysis, the malate synthase/fumarase assay, makes use of this principle. Scheme 14 summarizes the essential features of this method. The chiral acetic acid is mixed with a known amount of [^{14}C]acetic acid to bring the $^3H/^{14}C$ ratio to approximately 4 and is converted into the coenzyme A ester either enzymatically (31) or chemically via the anhydride (50, 67). The acetyl CoA is then condensed with glyoxylate using malate synthase (68) from yeast to give malate. The malate synthase reaction is known to involve condensation on the *Si* face of the glyoxylate aldehyde carbon to form (*S*)-malate. The purified malate is incubated with fumarase. In the reversible anti dehydration-hydration of (*S*)-malate and fumarate, respectively, catalyzed by fumarase, the *pro*-3*R* hydrogen of malate is stereospecifically removed or equilibrated with solvent protons. Therefore, an equilibrium mixture of malate and fumarate is formed in which tritium from the pro-3*S* position of the original malate remains carbon bound whereas tritium from the pro-3*R* position is released into the water. After lyophilization to remove the water, the $^3H/^{14}C$ ratio of the residue is measured and compared with that of the starting malate in order to establish the tritium distribution between the two diastereotopic hydrogen positions of malate. The tritium content of the water is also routinely analyzed. The percentage tritium retention in the fumarase reaction observed in the chiral acetate assay is referred to as the F value (61) where F = $^3H/^{14}C$ ratio of the residue of the fumarase reaction $\times$ 100 $\div$ $^3H/^{14}C$ ratio of the malate. Based on the primary kinetic deuterium isotope effect in the malate synthase reaction (k_H/k_D = 3.7-3.8) and the steric course of the reaction (inversion) established in the development of the assay (19, 20), a sample of chirally pure (*R*)-[$^2H_1$,$^3H_1$]acetate gives an F value of 79. Conversely, a chirally pure *S*-acetate

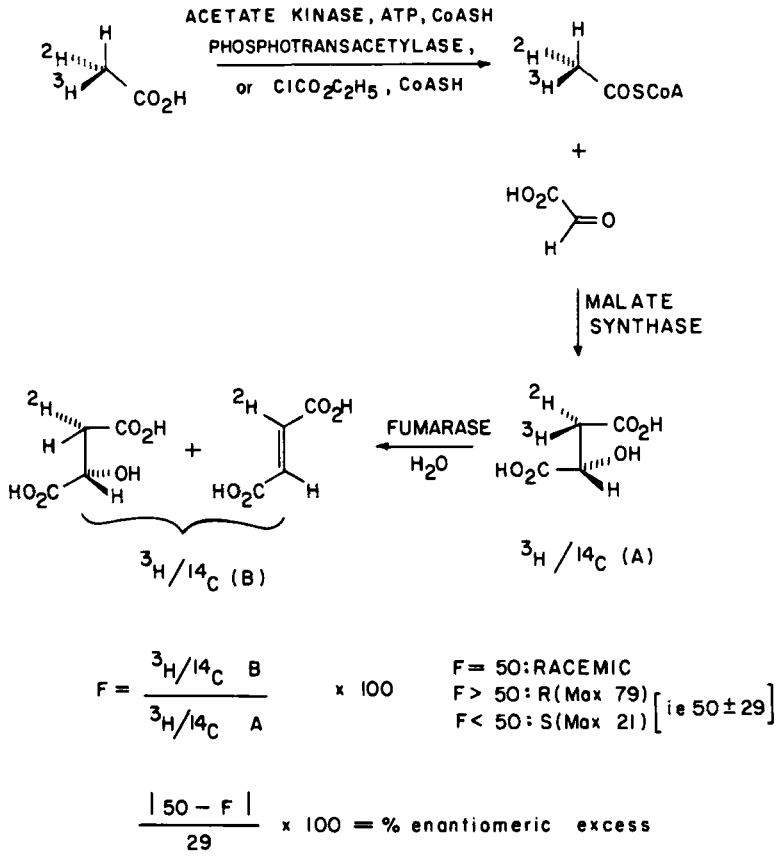

Scheme 14

will give an F value of 21. These numbers for chirally pure samples are based on the work of Eggerer and co-workers (69, 70) who have shown that the amplitude of the configurational assay with the malate synthase/fumarase system is 50 ± 29. The reproducibility of the assay depends somewhat on the amount of radioactivity available; the F values are usually accurate to about ±1-2 unless only very small amounts of radioactivity (<5000 dpm ^3H) are available. The experimental details for the procedure have been described (29-31, 50).

Other enzymes that exhibit a primary kinetic isotope effect in the irreversible removal of one methyl hydrogen can also be used in the chirality analysis of methyl groups. Based on the work of Rose (42), pyruvate carrying a chiral methyl group was incubated by Walsh and Cheung (71) with CO_2 and pyruvate carboxylase in the presence of malate dehydrogenase to give malate. The malate was then incubated with fumarase as previously described to determine the distribution of tritium between the heterotopic hydrogens at C-4.

The two sets of products (**a**, **b**, **c**) and (**d**, **e**, **f**) of Scheme 13 can be distinguished based on a second principle. This involves determining whether the methylene species carrying tritium in the H_A position contains a normal hydrogen as in (**e**) or a deuterium as in (**a**) in the H_B position and conversely whether ^2H or H is present in the H_A position of the H_B-tritiated species. This distinction can be made by tritium NMR spectroscopy. Separate signals for the methylene hydrogens may be observed in the tritium NMR spectrum if they are diastereotopic or are analyzed in the presence of a chiral shift reagent. Analysis of the two coupling constants would immediately indicate which of the tritium atoms is coupled to deuterium and which is coupled to ^1H. This approach allows discrimination between the two enantiomeric starting materials (**1**, **2**, **3**) and (**4**, **5**, **6**) even if the conversion CH_3CO_2H to XCH_2CO_2H does not involve an isotope effect. This type of approach was used by Altman (62) to study cycloartenol biosynthesis in which the C-6α chiral methyl group is converted to the methylene carbon of a cyclopropane. The steric course of the reaction was determined by tritium NMR to be retention of configuration. More recently Aberhart and Tann have applied this methodology to study the dehydrogenation of isobutyryl-CoA by *Pseudomonas putida* (63).

Rétey et al. (72) used this same principle in their work on the stereochemistry of citrate formation from chiral acetyl-CoA with *Si*-citrate synthase (Scheme 15). The chiral methyl group was converted into one of the methylene groups of succinate and the distinction between sets (**1**, **2**, **3**) and (**4**, **5**, **6**) was then based on the known different isotope effects for the removal of pro-*R* (k_H/k_D = 5.3 $\approx k_H/k_T$ = 12) vs. pro-*S* (k_H/k_D = 1.35 $\approx k_H/k_T$ = 1.5) hydrogens of succinate in the succinate dehydrogenase reaction (73). However, the malate synthase/fumarase procedure is clearly the most commonly used method to analyze the configuration and chiral purity of chiral methyl groups.

D. Biochemical Applications of Chiral Methyl Groups

Chiral methyl group methodology has been used to analyze about 70 different stereochemical questions, which can be categorized into three groups according to the type of conversion examined: (i) conversion of a methylene into a methyl group; (ii) conversion of a methyl into a methylene group; (iii) transfer of a methyl group. A detailed discussion of each of these applications is beyond the scope of this chapter. (For comprehensive reviews, see refs. 5, 29, 30.) However, a few examples within each class will be presented to demonstrate the principle involved in that type of conversion.

1. Conversion of a Methylene into a Methyl Group

Almost two-thirds of the reported uses of the chiral methyl group methodology fall into this category. The chiral methyl group may be formed from either

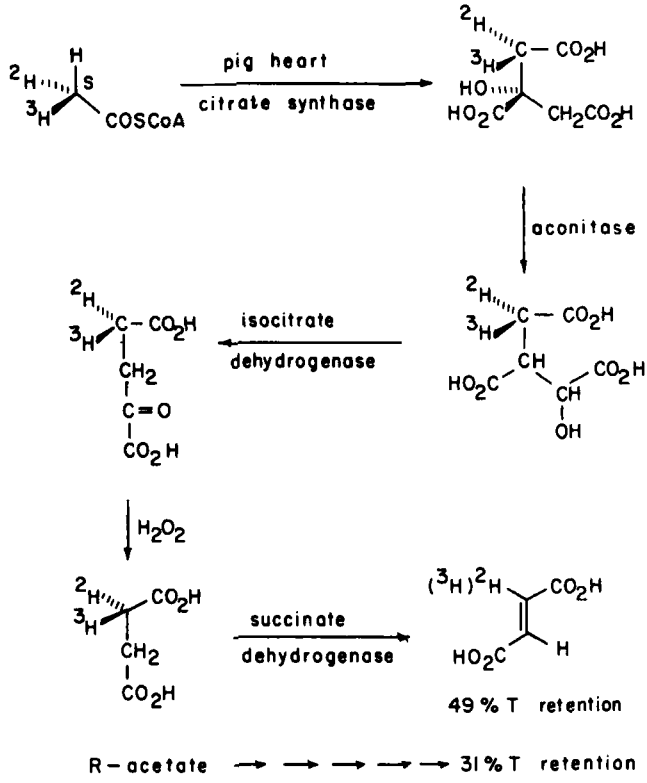

Scheme 15

a saturated methylene (sp^3) group in such reactions as retro-Claisen condensations, decarboxylations, pyridoxal phosphate-catalyzed eliminations (both α, β, and β, γ) and others, or an unsaturated (sp^2) group in such reactions as those catalyzed by kinases and double-bond reductases. In order to analyze these reactions and the reactions of the type $CH_3 \rightarrow CH_2$, it is essential that the formation of the methyl or methylene group either be irreversible or be made irreversible by trapping the product, since repeated back reaction would lead to racemization.

If the steric course of the reaction that converts a methylene to a methyl group is known, then the analysis of the chiral methyl group could be used to determine the initial configuration at a stereospecifically labeled methylene group. This approach has been used in our laboratory to analyze the configuration of the methylene group of a stereospecifically tritiated tryptophan (74). The method outlined in Scheme 16 involved conversion of the tryptophan into lactate by incubation with tryptophanase/lactate dehydrogenase in D_2O. This methodology has been applied by Arigoni et al. (see 29) to determine the configuration of a mevalonate-C-5-derived methylene group in linalool.

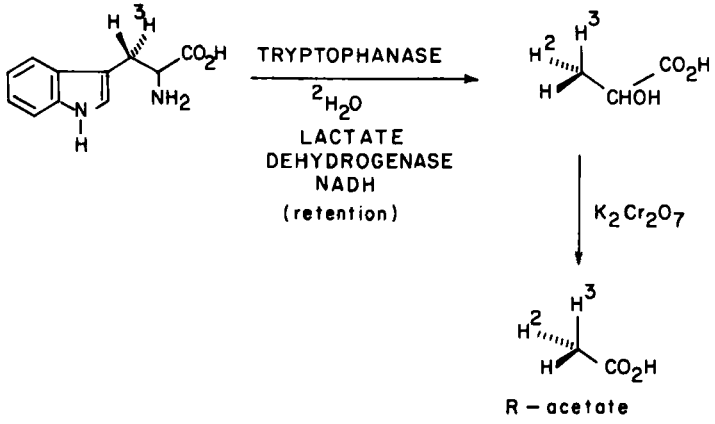

Scheme 16

Willadsen and Eggerer (75) have studied the stereochemistry of the enzyme acetyl CoA acetyltransferase, a key enzyme in both the terminal step in C-3 oxidation of fatty acids and the initial step in the biosynthesis of terpenes and steroids. The enzyme, when incubated separately with (2*S*)-[2-$^2H_1$,2-$^3H_1$]acetoacetyl CoA and the (2*R*) isomer gave two moles of acetyl CoA as depicted in Scheme 17. Eggerer et al. (76) utilized the enzyme enoyl CoA hydratase to convert properly labeled crotonyl CoA, via syn addition, to the doubly isotopically labeled 3-hydroxyacyl CoA derivatives needed in this study. A discussion of this unique type of hydration has been presented by Rose (9). The labeled

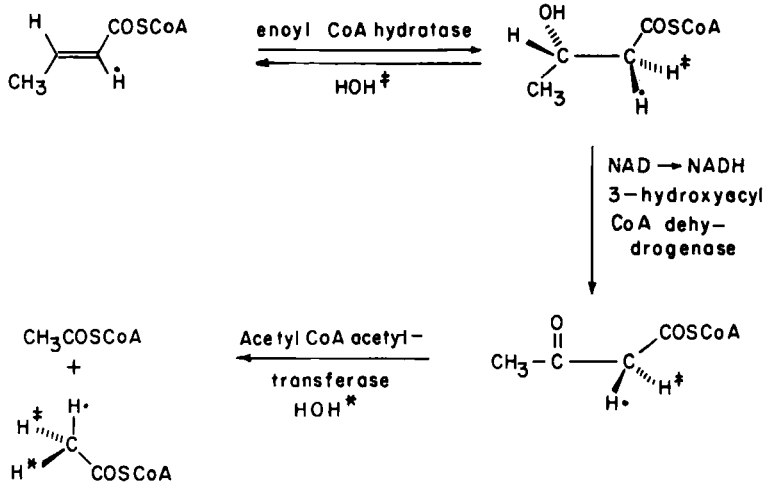

Scheme 17

3-hydroxyacyl CoA samples were oxidized to the 3-keto acyl derivatives with NAD and 3-hydroxyacyl CoA dehydrogenase. The acetyl CoA samples obtained in the reverse Claisen condensation were then subjected to chirality analysis. This reaction occurs with inversion of configuration as do all the other Claisen reactions thus far studied.

The stereochemistry of the malic enzyme from chicken liver (77), which catalyzes the conversion of malate to pyruvate (Scheme 18) has been studied by Cornforth's group. The two malic acids needed for the study were obtained

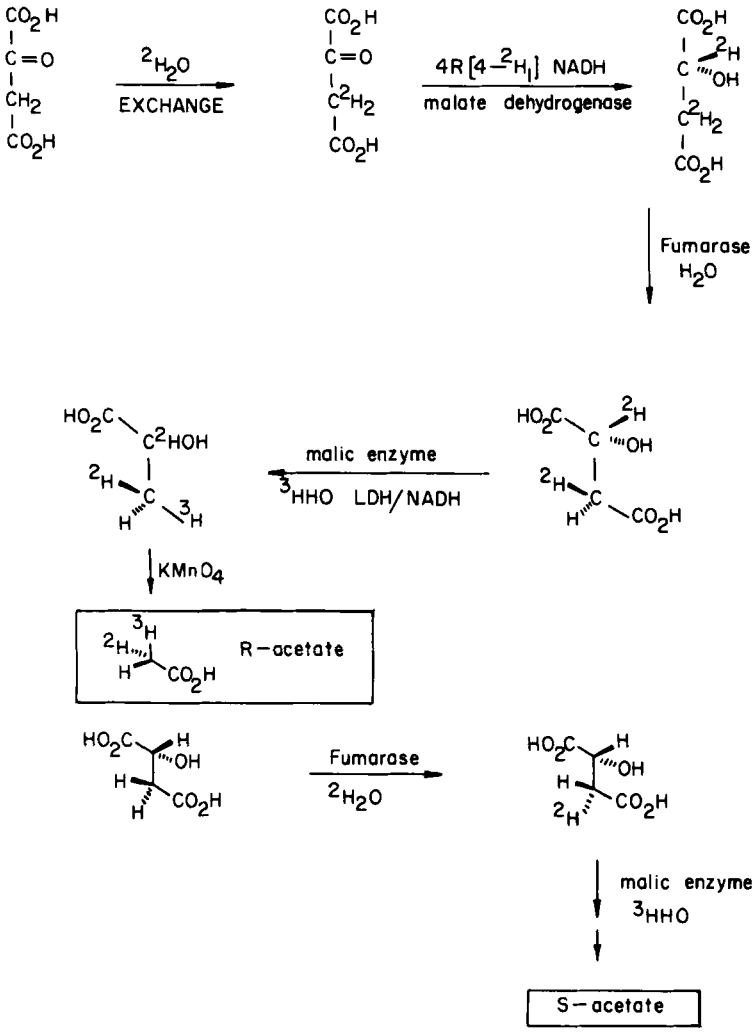

Scheme 18

by (i) incubation of fumaric acid in ^2H_2O with fumarase to give (2*S*,3*R*)-[3-$^2H_1$]malic acid, and (ii) by incubation of (2*S*)-[2,3,3-$^2H_3$]malic acid, available by reduction of dideuterated oxaloacetate with malate dehydrogenase and (4*R*)-[4-$^2H_1$]NADH, in H_2O with fumarase, to give (2*S*,3*S*)-[2,3-$^2H_1$]malic acid. The malic acids were incubated in separate experiments with the malic enzyme in ^3HHO and the pyruvate formed captured as lactate by LDH and NADH. The lactate samples were converted by oxidation with $KMnO_4$ to acetate for chirality analysis. The acetate samples (F values 70.5% and 43%) were slightly racemized but the results indicated a net retention of configuration in the decarboxylation reaction, which is in agreement with the finding of Rose on the enzymes from both *E. coli* and pigeon liver (42).

Our laboratory has studied the stereochemistry of methyl group formation in a number of α, β elimination reactions of amino acids catalyzed by pyridoxal phosphate enzymes. The reactions include the conversions of L-serine to pyruvate with tryptophan synthase β_2 protein (78) and tryptophanase (79), of L-serine and L-tyrosine with tyrosine phenol-lyase (80), and L-cystine with *S*-alkylcysteine lyase (81). In the latter study, the stereospecific isotopically labeled L-cystines were obtained enzymatically by incubation of L-serines appropriately labeled in the 3-position with the enzyme *O*-acetyl serine sulfhydrase (82). The serines tritiated in the 3-position were prepared enzymatically starting from [1-^{3}H]glucose and [1-^{3}H]mannose by a sequence of reactions of known stereochemistry (81). The cysteines were then incubated with *S*-alkylcysteine lyase in ^2H_2O as outlined in Scheme 19. The pyruvate was trapped as lactate, which was oxidized with $K_2Cr_2O_7$ to acetate for analysis. Similarly, Cheung and Walsh (71) examined the conversion of D-serine to pyruvate with

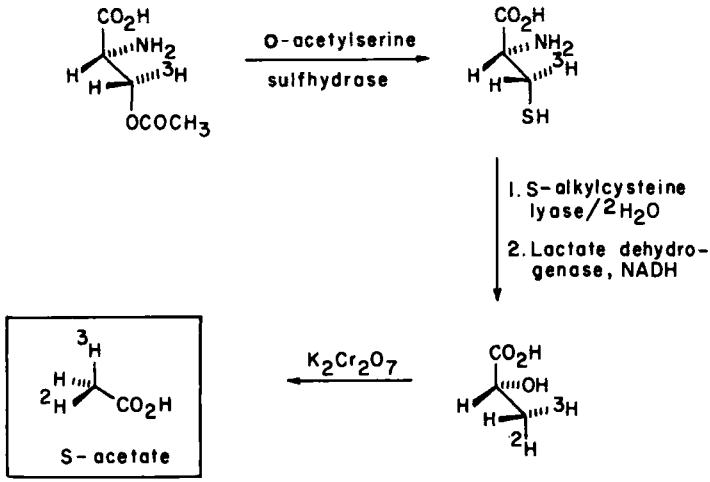

Scheme 19

D-serine dehydratase. This reaction as well as the other α,β elimination reactions of this type studied to date occur with retention of configuration.

Walsh and Chang (83) have investigated the stereochemistry of methyl group formation in β, γ elimination reactions of amino acids catalyzed by pyridoxal phosphate enzymes. They have solved the stereochemistry for both the γ replacement mode (vinylglycine or *O*-succinylhomoserine to cystathionine) and γ elimination mode (vinylglycine or *O*-succinylhomoserine to α-ketobutyrate) of the reaction catalyzed by the bacterial enzyme cystathionine γ-synthase. By using (*Z*)-D,L-[4-^{2}H]vinylglycine and (*E*)-D,L-[4-^{2}H]vinylglycine, one enters the reaction sequence at the halfway point and can solve the stereochemistry of the second half-reactions (either for the elimination mode or the replacement mode). If the reaction is carried out in ^{3}HHO in the absence of L-cysteine, α-ketobutyric acid is formed, which can be converted into acetate for chirality analysis. Likewise, the incubation of either (4*R*)- or (4*S*)-*O*-succinyl-L-[4-^{2}H]homoserines with cystathionine γ-synthase in the absence of cysteine in ^{3}HHO, gives α-ketobutyric acid chiral at C-4. Analysis of the chirality of this methyl group gives the overall stereochemistry of both the elimination and replacement reaction. Therefore, the steric course of the elimination half-reaction may be deduced. The results are shown in Scheme 20, (*Z*)- and (*E*)-[4-^{2}H]vinylglycine are converted to (4*S*)- and (4*R*)-[4-^{2}H,^{3}H]-2-ketobutyrate, respectively, while (4*R*)-*O*-succinyl-L-[4-^{2}H]homoserine yields (4*R*)-[4-^{2}H]cystathionine. The overall γ replacement reaction occurs with retention of configuration at C_4, the γ carbon undergoing substitution.

In situations where the third hydrogen required to convert a methylene into a methyl group comes from the same substrate, it is possible to determine by the chiral methyl group methodology whether this hydrogen is transferred inter-

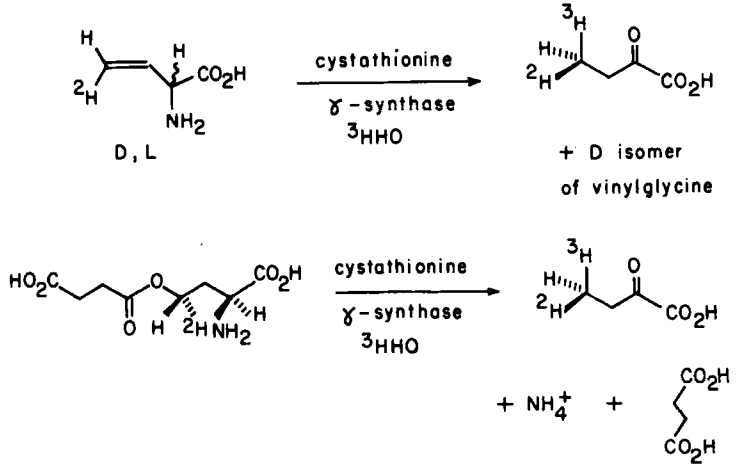

Scheme 20

or intramolecularly. This is based on the fact that a methyl group is chiral only if ^{1}H, ^{2}H, and ^{3}H are present in the same molecule. We used this approach in a study on the steric course of the α,β-elimination of L-serine catalyzed by tryptophan synthase B_2 protein (78) and in some work on the stereochemistry of the enzyme TDP-glucose oxidoreductase. In the latter case (Scheme 21) conversion of (6*S*)- and (6*R*)-TDP-[4-^{2}H,6-^{3}H]glucose into TDP-4-keto-6-deoxyglucose in the presence of a 100-fold excess of unlabeled substrate gave product containing an *R* and an *S* methyl group, respectively, of high chiral purity (84), proving that the hydrogen transfer from C-4 to C-6 is strictly intramolecular. Had it been intermolecular, 99% of the tritiated methyl groups formed would have contained two normal hydrogens and would, hence, have been achiral.

In some recent work Markler and Rétey (85) established the steric course of the phosphoketolase reaction in which carbon atoms 1 and 2 of fructose-6-phosphate are converted to acetyl phosphate. The hydroxy group at C-1 of the sugar is replaced by a solvent hydrogen with inversion of configuration. Two groups have examined the decarboxylation of the acetic acid residues of uroporphyrinogen-III to the methyl groups of coproporphyrinogen-III, one in chicken erythrocytes as part of the heme biosynthetic pathway (86) and the other in *Rhodopseudomonas spheroides* in the formation of bacteriochlorophyll a (87). The latter work also examined the steric course of formation of the ethyl groups from propionic acid residues. All these reactions were found to occur with retention. Several reactions have been found in which a racemic or achiral methyl group is formed. For example, ethanol-amine ammonia-lyase (88) and propanediol dehydrase (89) convert (*R*)- and (*S*)-[2-^{2}H,^{3}H]ethanolamine and (*R*)- and

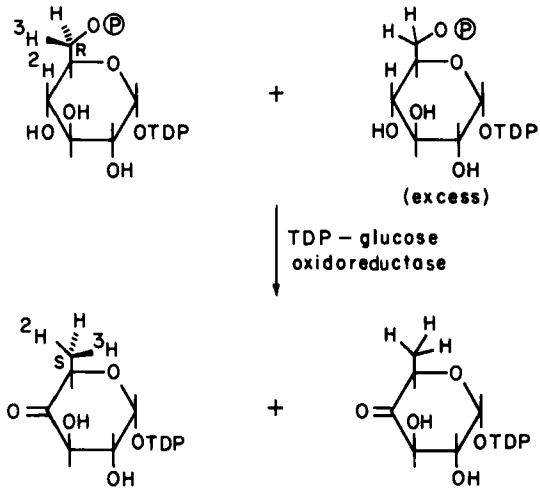

Scheme 21

(*S*)-[1-^{2}H,^{3}H]ethylene glycol, respectively, to racemic acetaldehyde. Racemic acetaldehyde is also formed in the cleavage of 2-deoxyribose 5-phosphate by a specific aldolase (90), and the incubation of stereospecifically labeled dihydroxyacetone phosphate with methylglyoxal synthetase gives racemic methylglyoxal (pyruvic aldehyde) (91).

2. *Conversions of Methyl into Methylene Groups*

The first efforts to utilize the chiral methyl group methodology were studies of the conversion of methyl groups to methylene groups in Claisen-type condensations, such as the conversions of acetate into malate or citrate. The stereochemical composition of the resulting labeled methylene group is then analyzed based on the principles discussed in Sect. II-C, Analysis of Chiral Methyl Groups. In the simplest case, when the conversion involves a substantial primary kinetic deuterium isotope effect, this requires only that one hydrogen of the methylene group is removed or replaced stereospecifically. Numerous studies have made use of this approach; these include several enzymatic Claisen and aldol condensations and carboxylation reactions (see 29, 30). All the Claisen condensations studied proceed with inversion, whereas all the aldol condensations and carboxylations proceed with retention of configuration. In some recent work the same analytical approach was employed by Caspi and co-workers (56, 59) to establish the steric course of hydroxylations at the chiral methyl group of octane. Analysis of the resulting 1-octanol for the configuration at C-1 by oxidation with horse liver alcohol dehydrogenase was complicated by further oxidation of the octanal formed to octanoic acid with a large isotope effect. The authors therefore developed an alternative procedure based on the differential exchange of the (1-pro-*R*)- and the (1-pro-*S*)-hydrogen of 1-octanol with horse liver ADH and diaphorase (92).

In cases where the abstraction of a hydrogen from the methyl group is not accompanied by a substantial isotope effect one has to rely on methods, like tritium NMR, that can determine whether tritium in a given heterotopic position has deuterium or protium as a neighbor. The studies of Altman and coworkers (62) on cycloartenol formation and by Aberhart and Tann (63) on the dehydrogenation of isobutyryl coenzyme A are pertinent examples. Alternatively, one can convert the chiral methylene group back into a methyl group by a reaction or series of reactions of known steric course, followed by the normal configurational assay of this methyl group. The methylene group will contain two tritiated species, corresponding to (**a** + **b**) or (**d** + **e**) in Scheme 13. Reconversion into a methyl group, for example, by stereospecific replacement of X by ^{1}H, will generate a chiral methyl group from **a** and from **d**, mixed with an achiral $CH_2{}^3H$ group formed from **b** or **e**. Barring an isotope effect in the $CH_3 \rightarrow CH_2$ conversion, the regenerated methyl group will have half the chiral purity of the starting methyl group and either the same or opposite configura-

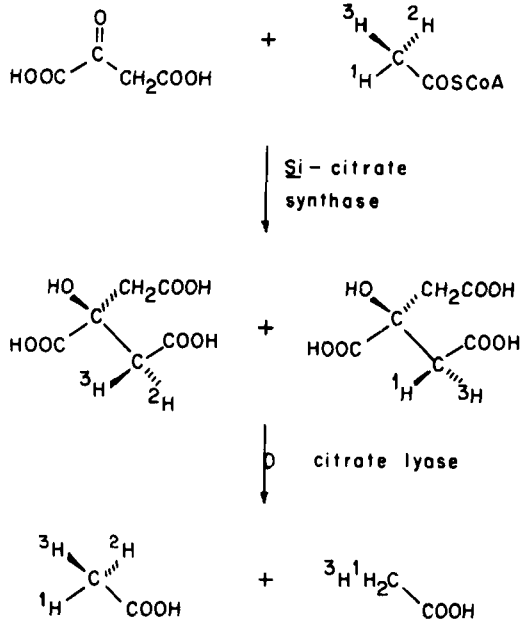

Scheme 22

tion, depending on whether the two reactions occurred with the same or opposite stereochemistry. Hence, if one knows the stereochemistry of one reaction that of the other can be determined. Cornforth, Eggerer, and their colleagues (32) first used this principle in their analysis of the stereochemistry of the *Si*-citrate synthase reaction (Scheme 22). The analytical reaction, catalyzed by citrate lyase, had been shown to proceed with inversion (93), and since the configuration of the chiral acetate eventually obtained was the same as that of the original starting material, the *Si*-citrate synthase reaction involves inversion also.

3. Transfer of Methyl Groups

Applications of this type are more recent. Elucidation of the steric course of methyl group transfers requires the incorporation of a chiral methyl group of known configuration into the transferring species. Once the methyl group has been transferred to the acceptor species, it is then necessary to convert the chiral methyl group into an analyzable form such as acetate or pyruvate in a series of reactions of known stereochemical consequences. It should be appreciated that both the activation of the chiral methyl group into a transferable moiety and the conversion of the transferred chiral methyl group into acetate or pyruvate frequently require manipulations at the chiral center that may lead to racemization.

The first account of the transfer of an intact methyl group was reported by Phillips and Clifford (60). Their study determined the steric course of the methyl group rearrangement from C-14 to C-13 in lanosterol biosynthesis. This enzymatic carbonium ion rearrangement occurred with retention of configuration of the migrating chiral methyl group.

Both our laboratory and that of Arigoni have studied a variety of reactions in which the methyl group of *S*-adenosylmethionine (SAM) is transferred to nucleophilic substrates by methyltransferases. The requisite samples of methionine carrying a chiral methyl group were synthesized as shown in Scheme 23 (41, 61). The last step, alkylation of the *S*-anion of homocysteine by methyl-*N*, *N*-ditosylimine, proceeds with inversion at the methyl group, as we deduced indirectly and Arigoni's group demonstrated directly (61).

Our laboratory has utilized these chiral methionine samples to study both the *C*-methylation and *N*-methylation involved in the biosynthesis of the antibiotic indolmycin (41). They were fed to cultures of *Streptomyces griseus* and the isolated indolmycin was degraded as shown in Scheme 24, which shows the steric course of all the reactions involved. We have also examined the stereochemistry of the catechol-*O*-methyltransferase (COMT) reaction (94). For this study, the chiral methionine samples were enzymatically activated to the corresponding *S*-adenosylmethionines, which were then incubated with liver COMT and epinephrine or 3,4-dihydroxybenzoic acid as the acceptor substrate. These reactions as well as the degradation route of the methylated catechols are shown in Scheme 25 (p. 284). All three reactions as well as a fourth studied in our laboratory, the methylation of the carboxyl groups of polygalacturonic acid in pectin formation (95), were found to proceed with inversion of configuration of the methyl group. The same stereochemical result has been obtained for all the methyl transferases studied in Arigoni's laboratory (61), which catalyze methylations as diverse as those of homocysteine, loganic acid, and the corrin ring system of vitamin B_{12}. These stereochemical results, together with evidence from isotope effect studies (96), suggest that in all these cases the methyl group under-

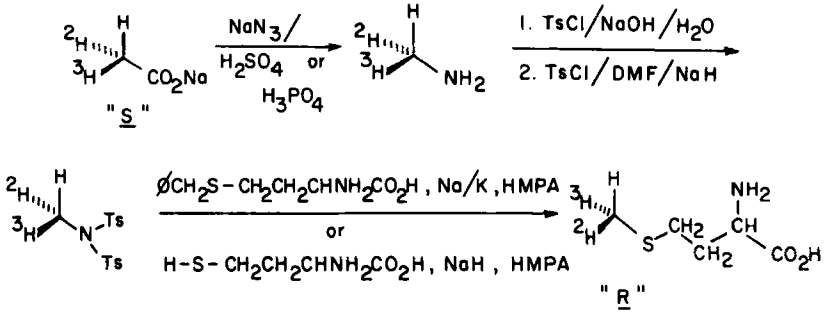

Scheme 23

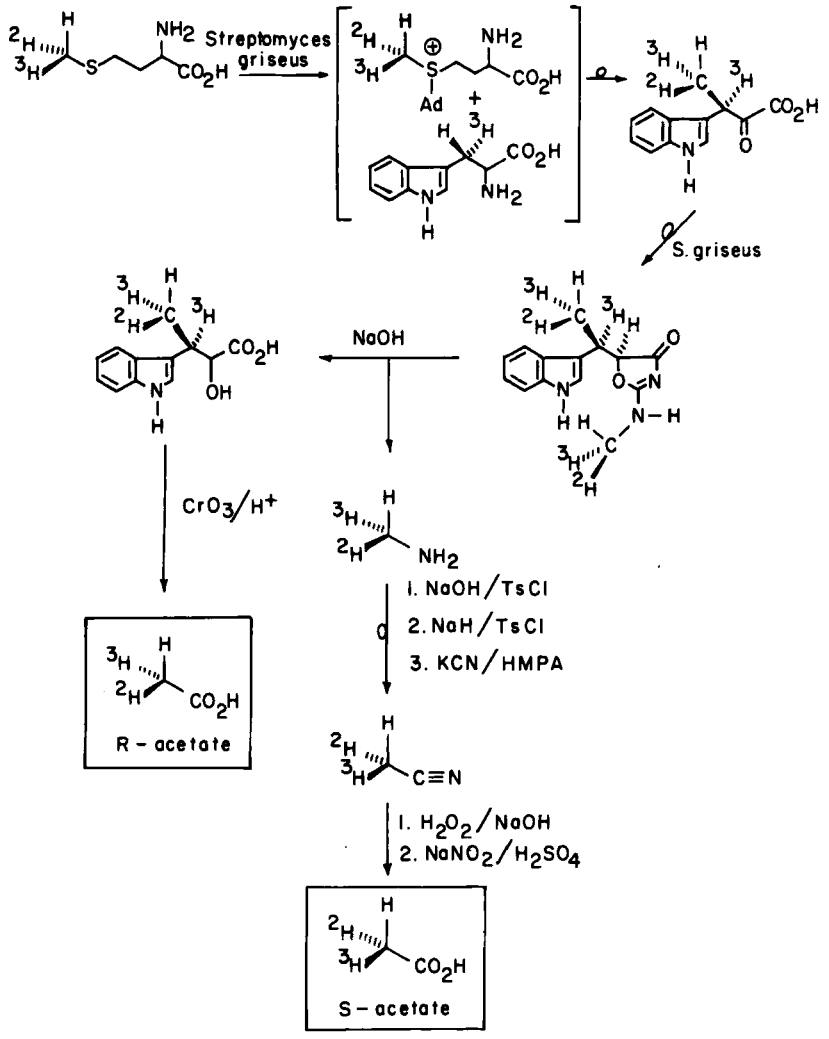

Scheme 24

goes a single S_N2 type of transfer directly from the sulfur atom of SAM to the nucleophilic acceptor site in the second substrate.

A significantly more complicated situation exists in the case of the side-chain methylation leading to ergosterol, where the initial transfer of the methyl group is followed by a hydride shift from the acceptor carbon and proton loss from the methyl group to give a methylene intermediate (I), which is then reduced stereospecifically. The stereochemistry of each of these reaction steps has been determined by Arigoni and co-workers (61, 97), with the outcome summarized in Scheme 26 (p. 285).

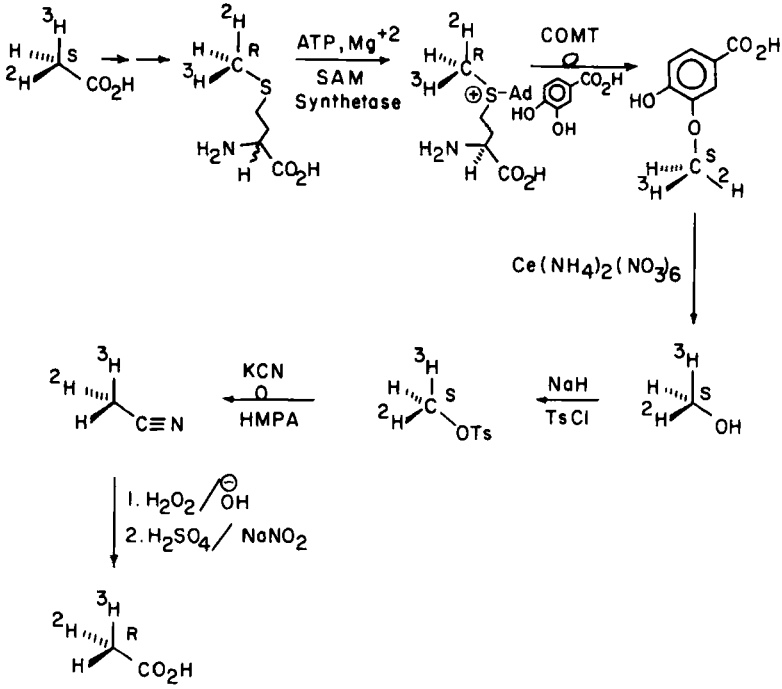

Scheme 25

III. CHIRAL MALONATE

As mentioned earlier, no synthesis of chiral malonic acid, one of the simplest and biologically most relevant Caabb systems, has yet been reported. However, Sedgwick et al. (98) have executed a synthesis of (2*R*)- and (2*S*)-[2-^{3}H]malonyl-coenzyme A, the biological activation product of malonate, as shown in Scheme 27. The major obstacle in the preparation and use of this compound is the readily occurring hydrogen exchange at the methylene group which, of course, leads to racemization. Malonic acid itself in D_2O at 35°C shows a $t_{1/2}$ for exchange of the methylene hydrogens of about 90 min; thioesters of malonic acid exchange substantially faster (98). The conditions for the synthesis therefore had to be chosen very carefully. Under the conditions used, only the final transesterification step seems to involve some tritium exchange with the solvent.

The chiral samples of malonyl-CoA were then used to probe the steric course of fatty acid biosynthesis. Again, the experiment was complicated by tritium exchange during the incubation, both before and after the Claisen condensation step, resulting in 51% tritium retention from the *S* isomer and 23% tritium retention from the *R* isomer. Fatty acid biosynthesis involves Claisen condensation of malonyl-CoA with an acyl-CoA ester of $2n$ carbon chain length to

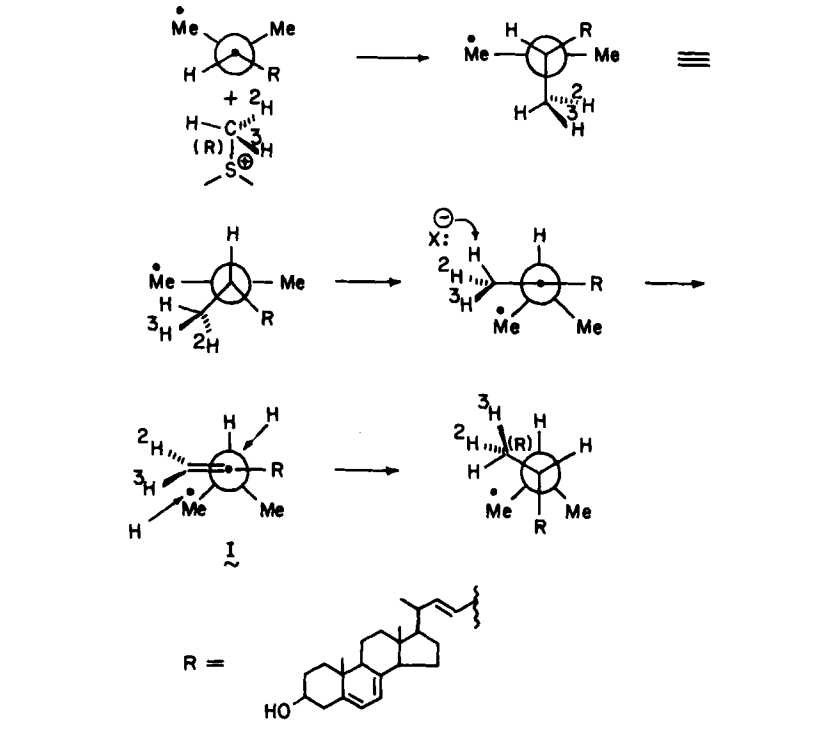

Scheme 26

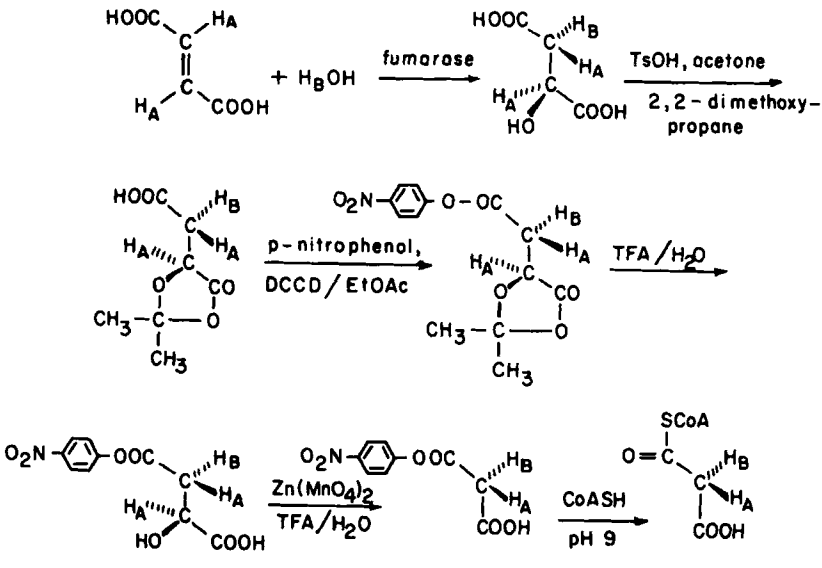

Scheme 27

give a 3-ketoacyl-CoA ester of chain length $2(n+1)$, which is reduced to a β-hydroxyacyl-CoA ester of 3-*R* configuration. Syn elimination of water (99) followed by reduction of the resulting *E* double bond completes the reaction cycle. Since the elimination of water involves removal of H_R from C-2, it follows that the 3-ketoacyl-CoA from (2*S*)-[2-^{3}H]malonyl-CoA carried tritium predominantly in the pro-*S* position, and that from the 2*R* isomer was tritiated predominantly in the pro-*R* position. These results allowed the conclusion that the Claisen condensation constituting the chain elongation step occurs with net inversion at the methylene group of the malonate unit (Scheme 28).

As a result of this work the necessary stereochemical information is now at hand to determine whether a chirally labeled malonic acid sample of unknown configuration ($HO_2C^{\bullet}CHH^{*}CO_2H$) represents the *R* or the *S* enantiomer. There remains, however, the problem of a suitable choice of isotopic labels and of analytical methodology to deduce the stereochemical identity of a given chiral malonate sample from its fate in a metabolic reaction sequence. One approach, outlined by one of us some time ago (100), is shown in Scheme 29. The malonic acid would be chirally labeled by carrying ^{13}C in one carboxyl group and deuterium in one methylene hydrogen. Activation to the coenzyme A ester would occur with equal probability at the labeled and the unlabeled carboxyl group, producing a mixture of two species of malonyl-CoA, which are epimeric at C-2 and which, in addition, differ in the location of the ^{13}C. Conversion of these malonyl-CoA species into fatty acids with yeast fatty acid synthase would ultimately produce from the (*R*)-malonate a fatty acid in which each chain extension unit carries one isotopic label, half being ^{13}C and the other half deuterium. The (*S*)-malonate, on the other hand, would produce fatty acids in which half

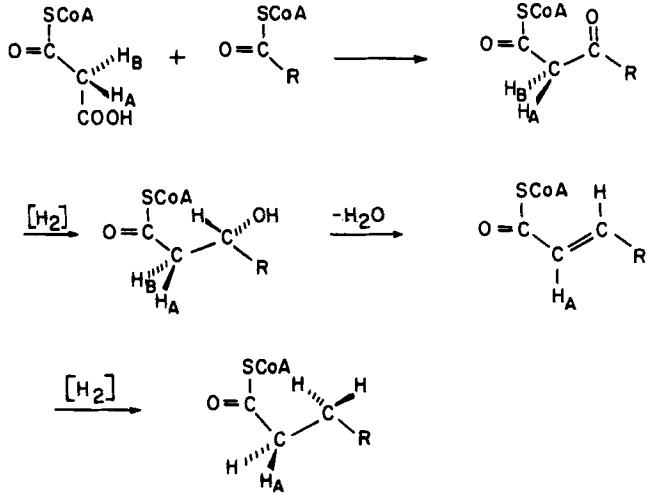

Scheme 28

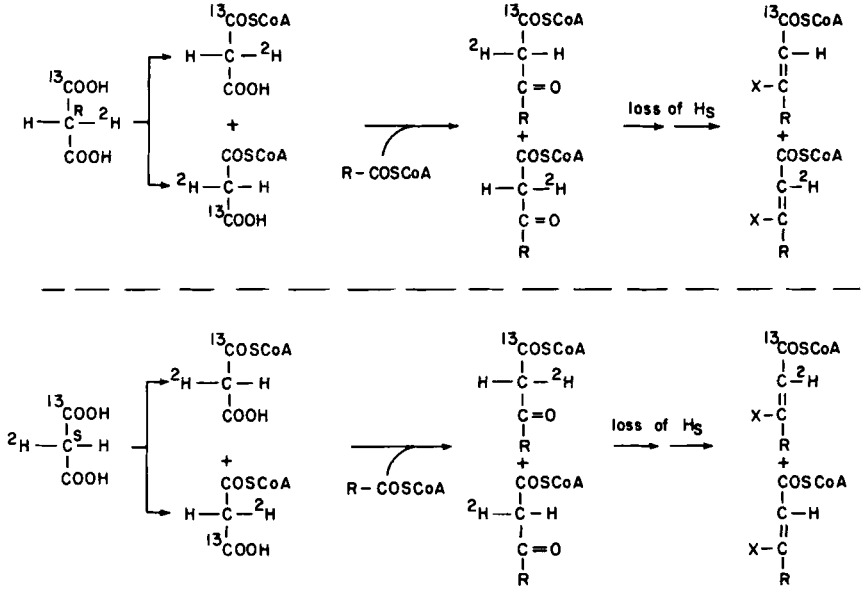

Scheme 29

the chain extension units contain two labels, ^{13}C and deuterium, and the other half are devoid of label. These two sets of products can be distinguished by mass spectrometry or by NMR spectroscopy. Of course, if the configuration of the starting malonates is known, this approach can be used to elucidate the steric course of other biochemical processes utilizing malonate, for example, the biosynthesis of polyketides. The experimental feasibility of this general approach is under investigation.

IV. CHIRAL PHOSPHATE

A. Biological Reactions Involving a Proprochiral Phosphorus Center

1. Types of Reaction

The enzyme-catalyzed reactions involving a proprochiral phosphorus center can be categorized into the following types based on the stereochemistry involved:

(a) $ROPO_2\text{-}OR'$ (prochiral) $\rightleftarrows$ $ROPO_3$ (proprochiral)*

(b) $RO\text{-}PO_3$ (proprochiral) $\rightleftarrows$ $R'O\text{-}PO_3$ (proprochiral)*

(c) $RO\text{-}PO_3$ (proprochiral) $\rightleftarrows$ PO_4 (proproprochiral)*

*Here and in several of the schemes the negative charge (or delocalized charges) on phosphate is omitted.

The recent development in the stereochemical study of these reactions has already been covered by several reviews (16, 17, 101-108). The aim of this survey is to provide a general view of the synthesis and configurational analysis of chiral phosphates, and of the significance of stereochemical results in enzyme mechanisms.

Enzymes which catalyze the reaction type (a) include phosphodiesterases, phospholipases (C and D), nucleotidyl transferases, nucleases, and pyrophosphokinases. The type (b) reaction involves mainly phosphokinases and phosphomutases. The hydrolysis of phosphomonoesters (reaction type c) is catalyzed by phosphatases, nucleotidases, ATPases, and so on. Most phosphatases also catalyze the phosphoryl transfer reaction, type (b), if an alcohol is used as an acceptor.

2. *General Approaches to the Elucidation of Reaction Stereochemistry*

The general approach in elucidating the stereochemical course of an enzyme-catalyzed reaction involves the following steps: (i) synthesis of substrates chirally labeled (with ^{17}O, ^{18}O, or S) at phosphorus; (ii) use of chirally labeled substrates to perform the reaction and isolate the product; and (iii) determination of the absolute or relative configuration of the substrate and the product.

A phosphodiester $ROPO_2OR'$ can be made chiral by substituting an oxygen with S (**1**), ^{17}O (**2**), or ^{18}O (**3**). A phosphomonoester $ROPO_3$ can be made chiral by labeling with ^{17}O and S (**4**), ^{18}O and S (**5**), or ^{17}O and ^{18}O (**6**). The inorganic phosphate P_i can be made chiral by labeling with ^{17}O, ^{18}O and S (**7**). (^{18}O is commonly represented by ● and ^{17}O by Ø).

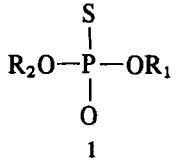

1

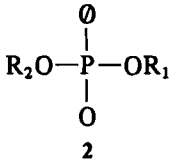

2

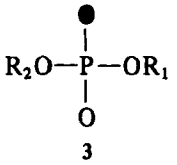

3

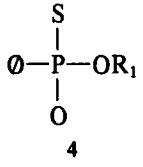

4

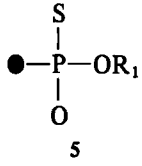

5

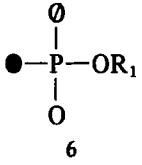

6

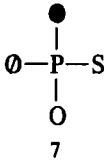

7

The sulfur atom, of course, representing a heteroatomic substitution, is considerably different from oxygen in chemical and physical properties. However, the stereochemical study of biological reactions at phosphorus began with the use of phosphorothioates (21). For the reactions involving a proproprochiral phosphorus center (i.e., inorganic phosphate, P_i), the use of sulfur is unavoidable since there are only three oxygen isotopes ^{16}O, ^{17}O and ^{18}O available (other isotopes of oxygen have very short lifetimes). For other reactions, both

chiral phosphates and chiral phosphorothioates have been employed for stereochemical study. In general, the use of chiral phosphates requires more sophisticated synthetic and analytical procedures, and gives more authentic results. Use of chiral phosphorothioates results in a decrease in reaction rates to $\lesssim$10% (in many cases $\lesssim$1%). Although it has been questioned whether the stereochemical course elucidated with phosphorothioates reflects the real mechanism of a particular enzyme, for all the enzymes that have been investigated by both chiral phosphates and chiral phosphorothioates (see tables in later sections), the stereochemical outcome is the same without exception. In addition, the use of phosphorothioates offers some advantages. It reduces a prochiral center to a chiral center, thus generating two separable diastereomers for most biphosphates. It also reduces a proprochiral center to a prochiral center and thus allows stereospecific phosphorylations at one of the two heterotopic oxygens. These stereoisomers of phosphorothioates are useful as stereochemical probes for the mechanism of enzyme catalysis.

B. Synthesis of Chiral Phosphates

Description of the synthesis of phosphodiesters (prochiral phosphorus center) is beyond the scope of this chapter. Only the chemical synthesis of chiral phosphomonoesters (**4–6**) and chiral inorganic phosphates (**7**) are discussed. The chiral phosphates or chiral phosphorothioates obtained from enzyme reactions are not described in this section.

1. Synthesis of Chiral [^{16}O,^{17}O,^{18}O]Phosphomonoesters

Two general synthetic procedures for chiral [^{16}O,^{17}O,^{18}O]phosphomonoesters have been reported, one by Knowles' group (22, 109) and the other by Lowe's group (23, 110).

The Knowles procedure is outlined in Scheme 30. Reaction of $P^{17}OCl_3$ with (-)-ephedrine yielded two diastereomeric chloro adducts **8** and **9** (approximately 9/1), which were then converted to **10** and **11** by reaction with 2-benzyl-(*S*)-propane-1,2-diol. The alcoholysis is known to proceed with retention of configuration (111). Chromatographic separation gave separate diastereomers **10** and **11** in 65% and 7% yields, respectively. Acid-catalyzed ring opening of **10** ($H_2{}^{18}O/CF_3COOH$) gave **12**. Hydrogenolysis of **12** yielded [^{16}O,^{17}O,^{18}O]phospho-(*S*)-propane-1,2-diol (**13**) in 72% yield from **10**. On the basis of the work of Inch and co-workers (111), **13** should have the *R* configuration at phosphorus, and this has been unequivocally established by the stereochemical analysis discussed in Sect. IV-C. By inverting the order in which ^{17}O and ^{18}O are introduced, the opposite isomer, [1(*S*)-^{16}O,^{17}O,^{18}O]phospho-(*S*)-propane-1,2-diol can be synthesized. In addition, phenyl [^{16}O,^{17}O,^{18}O]phosphate (**14**) (112) and 2-[^{16}O,^{17}O,^{18}O]phospho-D-glycerate (**15**) (113) have been synthesized by this

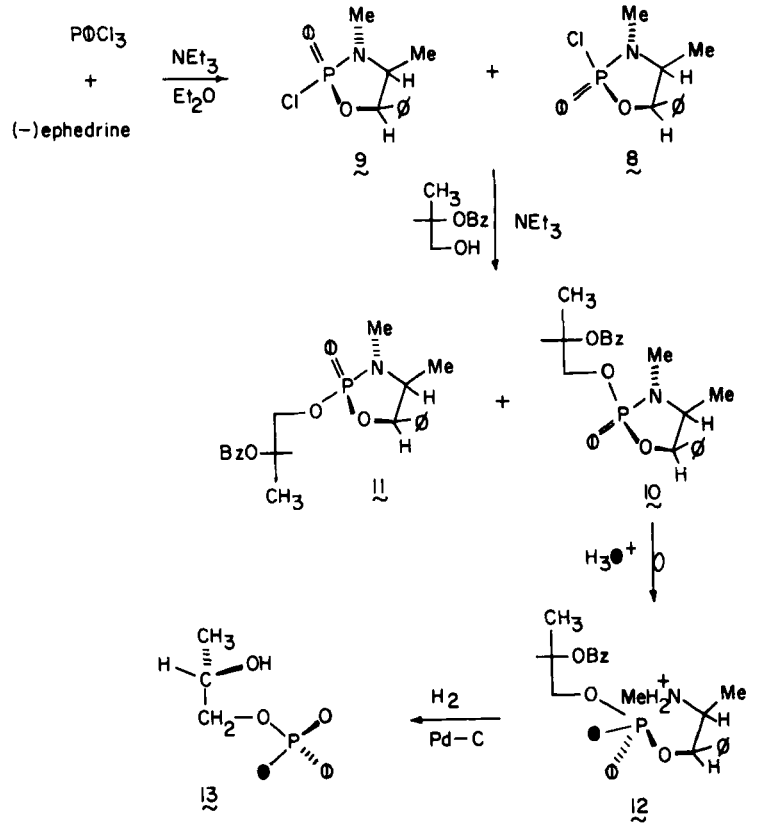

Scheme 30

route, and adenosine [γ-^{16}O,^{17}O,^{18}O]triphosphate (**16**) has been synthesized by a slight modification of Scheme 30 (114).

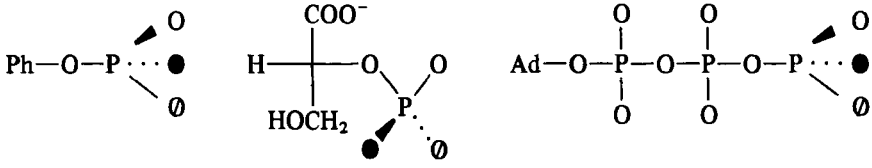

14 **15** **16**

The procedure of Lowe (110) is outlined in Scheme 31. Reaction of (*S*)-mandelic acid (**17**) with phenyllithium yielded (*S*)-benzoin (**18**). Acid-catalyzed ketalization of **18** with ethylene glycol gave **19**, which was converted back to [(*S*)-^{18}O]benzoin (**20**) by acidic hydrolysis in $H_2{}^{18}O$. Reduction of **20** with $LiAlH_4$ at 0°C (115) gave exclusively (1*R*,2*S*)-1,2-[1-^{18}O]dihydroxy-1,2-diphenylethane (**21**), according to Cram's (chelate) Rule. Treatment with

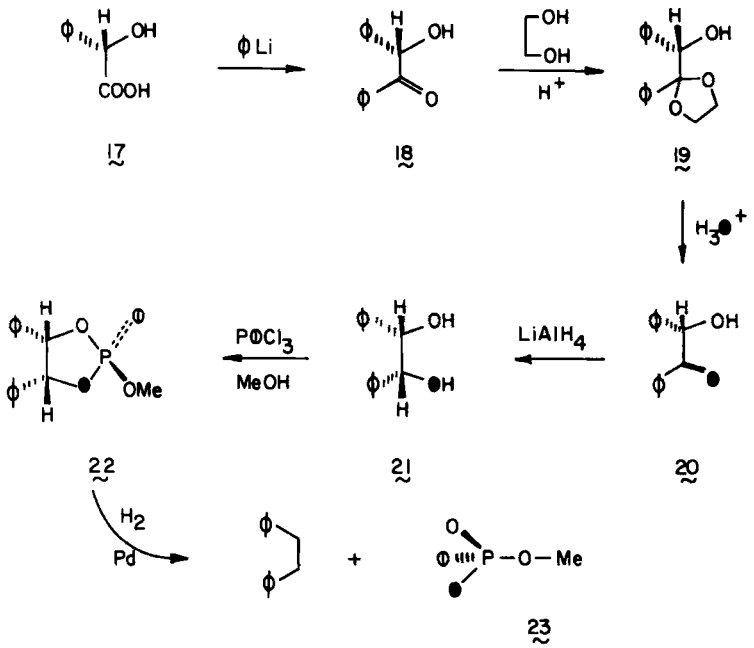

Scheme 31

$P^{17}OCl_3$ followed by methanolysis in pyridine gave **22** as a single crystalline isomer. Catalytic hydrogenolysis of **22** gave methyl [(*S*)-^{16}O,^{17}O,^{18}O]phosphate (**23**). By use of other alcohols to replace methanol, the following chiral [^{16}O, ^{17}O,^{18}O]phosphate monoesters have also been synthesized (110): inorganic [^{16}O,^{17}O,^{18}O]pyrophosphate (**24**), glucose 6-[^{16}O,^{17}O,^{18}O]phosphate (**25**), adenosine 5′-[^{16}O,^{17}O,^{18}O]phosphate (**26**), adenosine 5′-[γ-^{16}O,^{17}O,^{18}O]triphosphate (**16**), *sn*-glycerol-3-[^{16}O,^{17}O,^{18}O]phosphate (**27**), and 2-[^{16}O,^{17}O, ^{18}O]phospho-(*R*)-glycerate (**15**). The isomers of opposite configuration at phosphorus can be obtained by inverting the order in which ^{17}O and ^{18}O are introduced.

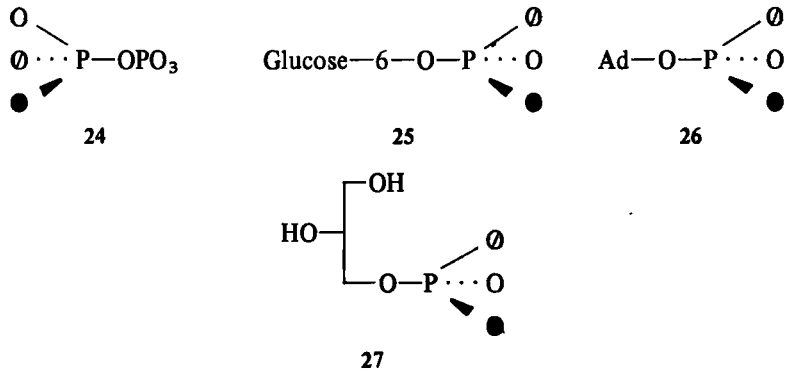

In the preliminary report of the synthesis (23) **22** was erroneously assigned the opposite configuration at phosphorus, which resulted in the assignment of *R* configuration to **23** and other chiral phosphomonoesters. The authors have corrected the assignment recently (116), and the configurations reported in the full paper (110) and in Scheme 31 are the correct ones.

2. *Synthesis of Chiral Phosphorothioates*

A number of chiral [^{18}O]phosphorothioate monoesters (compound **5**) have been synthesized, and these syntheses have been described in detail in several reviews (102, 103, 108). In this section only the most commonly used compounds, chiral [α-^{18}O]AMPS (**28**), chiral [β-^{18}O]ADPβS (**29**), and chiral [γ-^{18}O]ATPγS (**30**) are discussed.

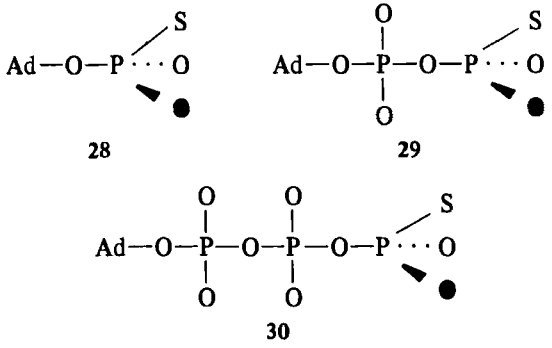

(*R*)- and (*S*)-[α-^{18}O]AMPS have been prepared by Lowe's group by a chemical synthetic procedure analogous to that shown in Scheme 31 (117). However, two simpler procedures based on a combination of chemical and biochemical reactions have been reported by Frey and co-workers (118) (Scheme 32) and by Tsai (25, 119) (Scheme 33). In Scheme 32, [α-$^{18}O_2$]AMPS (**31**), prepared from adenosine, $PSCl_3$, and $H_2{}^{18}O$ (120), was condensed with AMP by the procedure of Michelson (121) to give the two diastereomeric dinucleotides **32** and **33**, which were separated by chromatography. Hydrolysis of **32** and **33** by *C. adamanteus* nucleotide pyrophosphatase gave the two isomers of [α-^{18}O]AMPS **34** and **35**, respectively. The configuration of **34** and **35** at Pα can be determined by procedures to be discussed in Sect. IV-C. In an alternative synthesis (Scheme 33) (25, 119), [α-$^{18}O_2$]**31** was chemically phosphorylated to give a diastereomeric mixture of [α-^{18}O]ADPαS (**36**). Incubation of **36** with pyruvate kinase followed by chromatographic separation (122) gave (*S*)-[α-^{18}O]ATPαS (**37**) and unreacted (*R*)-[α-^{18}O]ADPαS (**38**). Hydrolysis of **37** and **38** with calf intestine alkaline phosphatase produced (*S*)-[α-^{18}O]AMPS (**39**) and (*R*)-[α-^{18}O]AMPS (**40**), respectively, with known configuration at phosphorus. The hydrolysis was easily

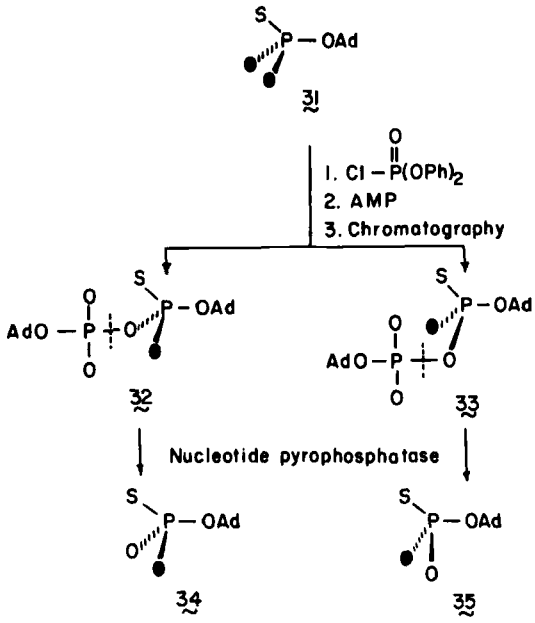

Scheme 32

arrested at the AMPS stage since most phosphorothioate monoesters are poor substrates for alkaline phosphatase.

(*R*)- and (*S*)-[β-^{18}O]ADPβS were synthesized by Richard et al. (123) according to Scheme 34. Condensation of [α-$^{18}O_2$]AMPS (**31**) with 2′,3′-methoxymethylidene-AMP (**41**) by the Michelson procedure gave two separable diastereomeric dinucleotides **42** and **43**. The configurations at the chiral phosphorus centers of **42** and **43** were assigned by chemically degrading each isomer to the corresponding [α-^{18}O]ADPαS and determining its Pα configuration by ^{31}P NMR. The diastereomers **42** and **43** of known configuration were then converted to (*R*)-[β-^{18}O]ADPβS (**44**) and (*S*)-[β-^{18}O]ADPβS (**45**), respectively, by chemical removal of the unblocked adenosyl group and deblocking of the protected nucleoside.

Chiral [γ-^{18}O]ATPγS was first synthesized by Richard and Frey (124) as shown in Scheme 35. The (*S*)-[α-^{18}O,$\alpha\beta$-^{18}O]ADPαS* (**46**), prepared from enzyme-catalyzed stereospecific phosphorylation of **31**, was condensed with 2′,3′-methoxymethylidene-AMP (**41**) to give the dinucleotide **47**. Chemical re-

*Oxygen atoms bonded to only one phosphorus atom, i.e., nonbridged oxygens, are indicated by the Greek letter identifying the phosphorus atom to which they are attached. Similarly, bridged oxygens are designated by the two Greek letters identifying the attached phosphorus atoms.

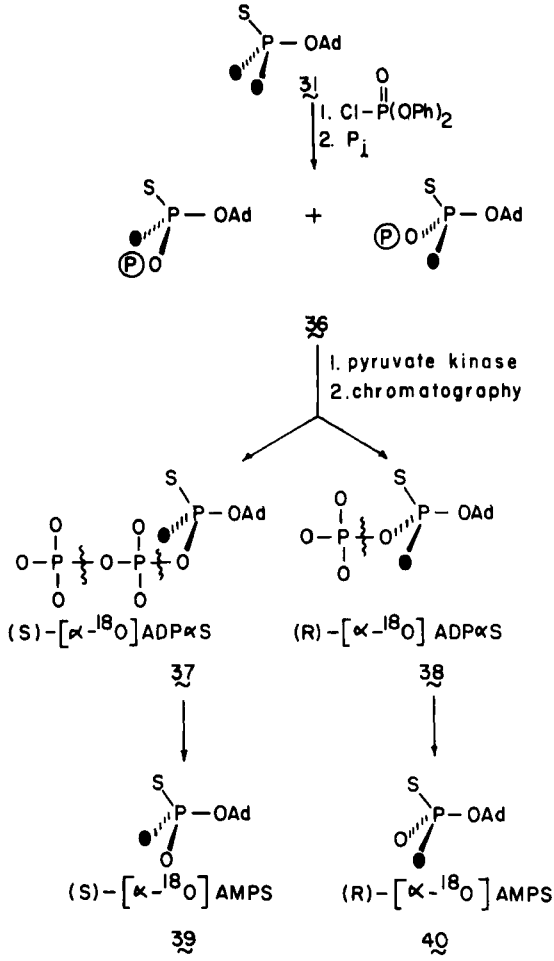

Scheme 33

moval of the unblocked adenosyl group and the methoxymethylidene group gave (*R*)-[γ-^{18}O,$\beta\gamma$-^{18}O]ATPγS (**48**).

Synthesis of chiral inorganic [^{16}O,^{17}O,^{18}O]phosphorothioates (Ps_i) of known configuration was first reported by Webb and Trentham (24) according to Scheme 36. The two intermediates **49** and **50** were obtained analogously to **37** and **38**, respectively, in Scheme 33, except that ^{17}O-labeled P_i was used. After transferring its γ-phosphoryl group to glucose (catalyzed by hexokinase), **49** was treated with IO_4^- followed by OH^- to give the pyrophosphate **51**. The same treatment of **50** gave the enantiomer **52**. Hydrolysis of **51** and **52** by inor-

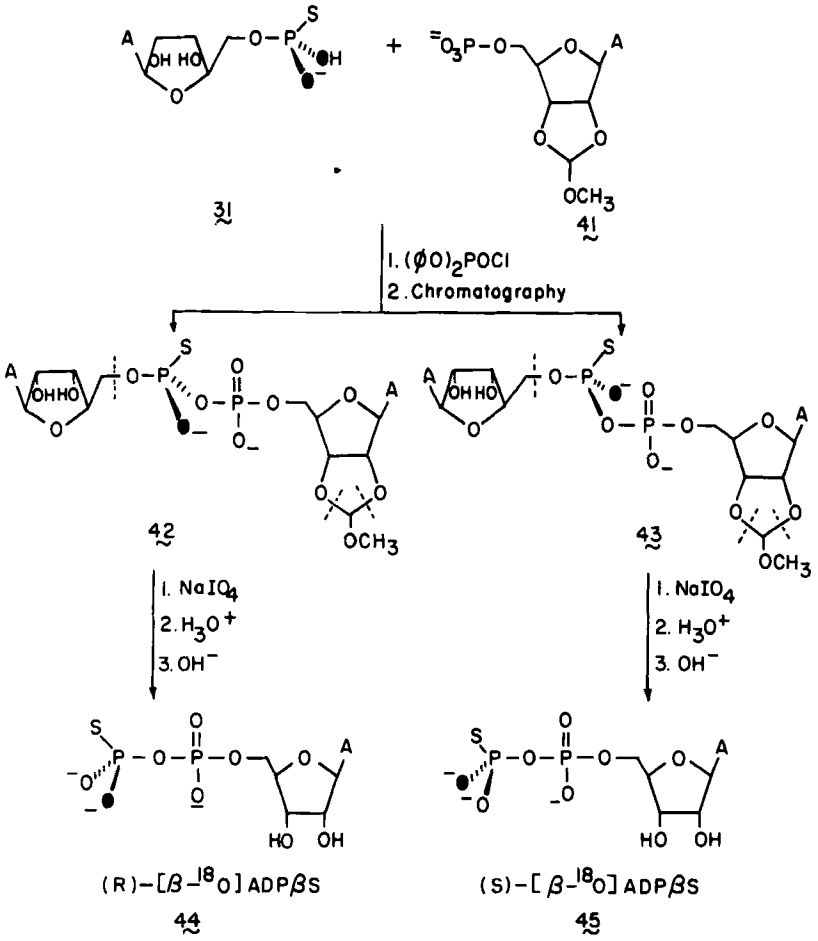

Scheme 34

ganic pyrophosphatase gave (*S*)-[^{16}O,^{17}O,^{18}O]Ps$_i$ (**53**) and (*R*)-[^{16}O,^{17}O,^{18}O]-Ps$_i$ (**54**), respectively.

C. Configurational Analysis of Chiral Phosphates

1. ^{18}O Isotope Shift and ^{17}O Quadrupolar Effect in ^{31}P NMR

While the configurational analysis of chiral methyl groups is based on the radioactivity of ^{3}H and the kinetic isotope effect k_H/k_D, neither factor is applicable to a chiral phosphoryl group. Both ^{17}O and ^{18}O are stable isotopes, and

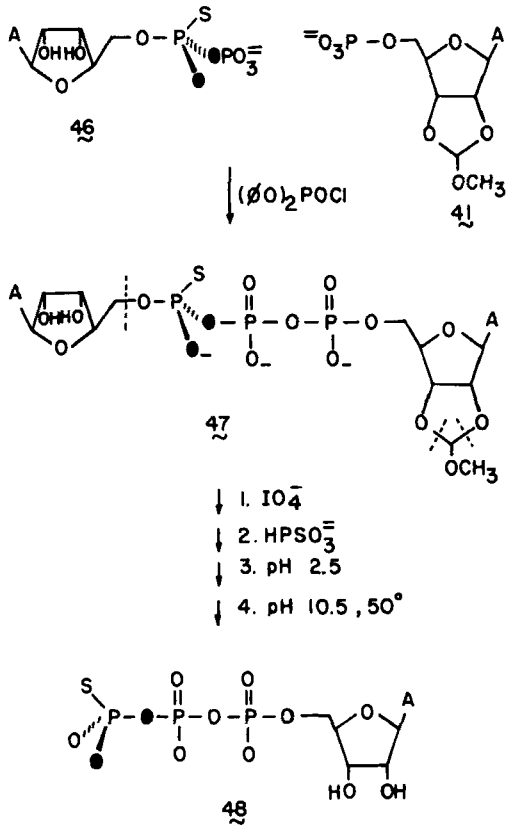

Scheme 35

the kinetic isotope effect is much smaller than 5%. In the early stages (ca. before 1979), the main tool in the configurational analysis of chiral phosphate was mass spectrometry, which requires relatively elaborate derivatization and degradation of the compound. Fortunately, ^{31}P NMR methods based on the ^{18}O isotope effect (125) and the ^{17}O quadrupolar effect (126) have been developed, which have now largely, if not completely, replaced the mass spectral method.

The ^{18}O isotope shift and the ^{17}O quadrupolar effect in ^{31}P NMR and their application in phosphorus stereochemistry have been reviewed recently by Cohn (106) and Tsai (105, 127). Figure 1 shows the ^{31}P NMR spectrum of $H_3P^{17}O_4$ (40 atom % ^{17}O). The spectrum consists of a "broad" signal due to the $^{31}P—^{17}O$ species and a "sharp" signal due to the residual non-^{17}O-labeled species. Since the ^{17}O-enriched water always contains some ^{18}O ($^{18}O/^{17}O = 0.67$ in this case), the "sharp" signal contains both ^{16}O and ^{18}O species, as shown by the expanded

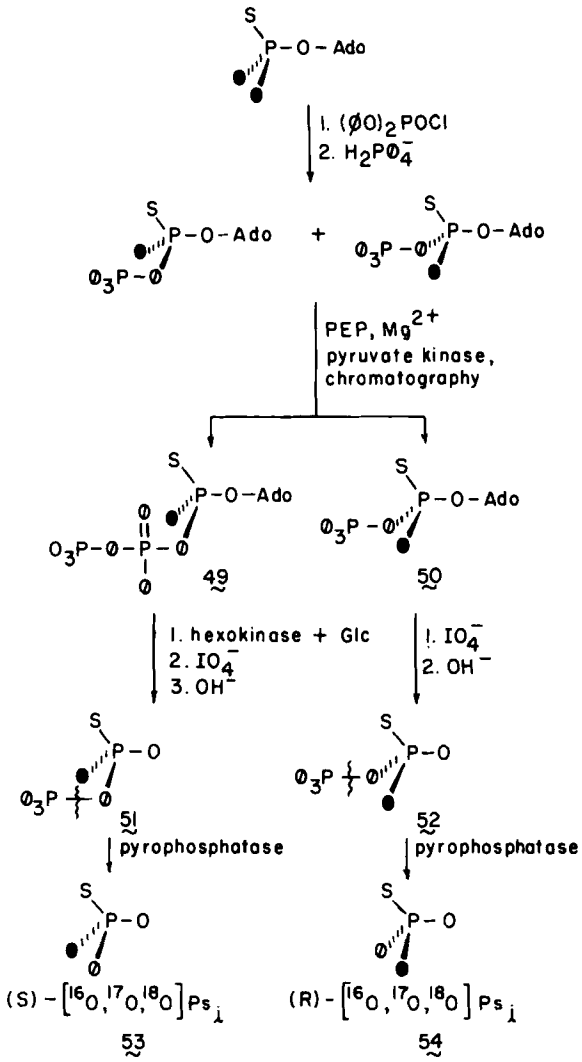

Scheme 36

spectrum in the inset. In this compound, the ^{31}P NMR signal of the ^{18}O-labeled species is shifted upfield by 0.020 ppm per ^{18}O atom. The magnitude of the ^{18}O isotope shift in ^{31}P NMR is defined as the "S" value (127). The S value for a P=O double bond is 0.038-0.044 ppm, whereas that for a P—O single bond is 0.015-0.025 ppm. Bonds with a partial double bond character have S values between these two extremes. The correlation between the S value and the bond

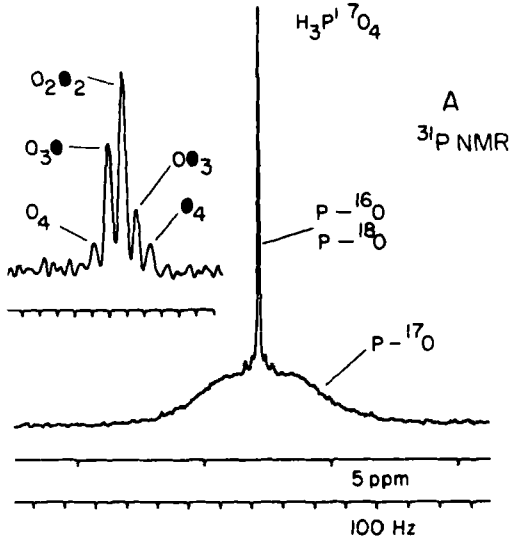

Figure 1. (A) ^{31}P NMR spectrum of 50 mM $H_3P^{17}O_4$ (40 atom % ^{17}O) in D_2O, pD = 1.8, at 81.0 MHz. Spectral parameters: Acquisition time 4.1 sec, delay time 1.0 sec, spectral width 2 KHz, 70° pulse, line broadening 2.0 Hz, 1600 scans. The insets show the expanded spectrum of the sharp peak, processed with Gaussian multiplication (LB = −2, GB = 0.2). Chemical shift: 0.09 ppm downfield from 1 *M* H_3PO_4.

order provides a convenient way to distinguish P—O—X (X = P, C, Si, etc.) bridging ^{18}O from a P=O (or P ⋯ O) nonbridging ^{18}O.

The "broadening" of the ^{31}P NMR signal by directly bonded ^{17}O nuclei is due to "scalar relaxation of the second kind," as termed by Abragam (128). Although the ^{31}P—^{17}O interaction depends greatly upon the quadrupolar relaxation time of ^{17}O (105, 127), it has been shown that the "line broadening effect" is present for most small biophosphate molecules in solution (129). The "broad signal" due to ^{31}P—^{17}O species is not always observable. However, the bonding of ^{31}P to ^{17}O can always be detected by a decrease in the apparent intensity of the "sharp" ^{31}P NMR signal (which represents the residual non-^{17}O species). In other words, the net effect of ^{17}O is that it "quenches" the ^{31}P NMR signal of all ^{31}P—^{17}O species, an important property upon which the configuration analysis of chiral phosphates is based.

2. *Configurational Analysis of Chiral Phosphates and Phosphorothioates*

Since most biophosphate compounds contain other chiral centers, the stereoisomers of type **1** (p. 288) can be distinguished simply based on ^{31}P chemical shifts.

The configurational analysis of compounds **2** to **5** involves determining whether the labeled oxygen (^{17}O in **2** and **4**, ^{18}O in **3** and **5**) occupies the pro-*R* or pro-*S* position. In most cases, the compound is first stereoselectively derivatized at one of the two oxygens. The position of ^{17}O or ^{18}O is then determined by one of three methods: (i) stereoselective derivatization and degradation followed by mass spectral analysis; (ii) isotope shift effect in ^{31}P NMR; or (iii) ^{17}O quadrupolar effect in ^{31}P NMR. Since these methods are straightforward, no further discussion is provided here. Specific examples will be presented in Section IV, E.

The chiral [^{16}O,^{17}O,^{18}O]phosphomonoester **6** and the chiral [^{16}O,^{17}O, ^{18}O]Ps_i **7** both have a chiral phosphorus center due to three oxygen isotopes. Three techniques have been used to characterize the configuration at phosphorus: circular dichroism (CD) (23), mass spectrometry (109), and ^{31}P NMR (24, 25, 130).

Unlike a chiral methyl group, in which the tritium is isotopically dilute, a chiral phosphoryl group can be obtained with >50% purity ("purity" is defined as the percentage of the chirally labeled species, i.e., the M + 3 species) and with >95% chirality ("chirality" is defined as the optical purity of the chirally labeled species) (119). Therefore it is not impractical to ask whether the chiroptical properties of a chiral phosphoryl group can be observed. Cullis and Lowe (23) have reported a CD curve of methyl [(*S*)-^{16}O,^{17}O,^{18}O]phosphate with a maximum at 208 nm ($\Delta\epsilon = 2.7 \times 10^{-3}$). Although this is a direct way to measure the chirality of a phosphoryl group, it would be useful only in compounds which do not contain any other chiral centers. Furthermore, the CD curve of only one enantiomer of the above compound has been reported. Results based on CD should be evaluated with reservation until they can be confirmed with the opposite isomer.

Knowles and co-workers first developed a mass spectral analysis to determine the configuration of a chiral [^{16}O,^{17}O,^{18}O]phosphomonoester (22, 101, 109). As shown in Scheme 37, [1(*R*)-^{16}O,^{17}O,^{18}O]phospho-(*S*)-propane-1, 2-diol (**55**) is first "cyclized", with inversion of configuration, to the 1,2-cyclic phosphate, which consists of an equimolar mixture of three isotopically different species **56a**, **56b**, and **56c**. Methylation of the cyclic phosphate **56** occurs on either of the exocyclic oxygens and gives two sets ("syn" and "anti") of diastereomeric phosphotriesters **57** and **58**, respectively. **57** and **58** are then separated chromatographically and analyzed by metastable ion mass spectrometry. Since this method is not now generally used in configurational analysis, it is not discussed in detail here. Interested readers are referred to the full description of the method by Buchwald et al. (101). In summary, the two sets of syn isomers (**57**, and the corresponding set from the opposite isomer of **55**) are differentiated based on the relationships between individual daughter ions and their parents.

As the $^{31}P(^{18}O)$ and $^{31}P(^{17}O)$ NMR techniques became available later, it was

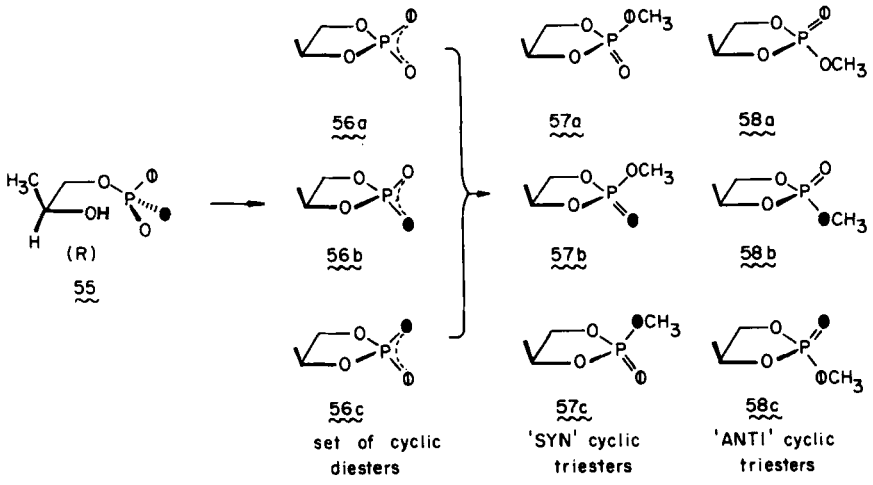

Scheme 37

obvious to a number of researchers that the two sets of triesters **57** and **58** can be distinguished by ^{31}P NMR. Each set of isomers consists of two species bearing a ^{17}O and a third species which contains only ^{16}O and ^{18}O. Since ^{17}O is expected to "quench" the ^{31}P NMR signal, only the species without ^{17}O (**57b** and **58b**) will show sharp ^{31}P NMR signals. In the syn isomer **57b**, the ^{18}O is nonbridging ($P{=}^{18}O$), thus causes a larger isotope shift (S = 0.043 ppm). In the anti isomer **58b**, the ^{18}O is located at the P—O—C bridging position, thus causes a smaller isotope shift (S = 0.018 ppm). An opposite pattern should be observed for the opposite isomer of **55**. In addition, the two diastereomers **57** and **58** show different chemical shifts, which allows a direct analysis of the mixture **57** and **58** without chromatographic separation. In reporting the ^{31}P NMR analysis of the configuration of **55** (130), the authors stated that the NMR method is "simpler both conceptually and practically".

The ^{31}P NMR method has now become a standard method of configurational analysis of chiral phosphomonoesters including [^{16}O,^{17}O,^{18}O]phospho(*S*)-propane-1,2-diol (**55**), adenosine 5′-[^{16}O,^{17}O,^{18}O]phosphate (AMP) (131), 3′-deoxyadenosine 5′-[^{16}O,^{17}O,^{18}O]phosphate (dAMP) (132), thymidine 3′-[^{16}O,^{17}O,^{18}O]phosphate (3′-TMP) (133), glucose 6-[^{16}O,^{17}O,^{18}O]phosphate (**25**) (134), dipalmitoyl [^{16}O,^{17}O,^{18}O]phosphatidic acid (135), and [^{16}O,^{17}O,^{18}O]-thiophosphate (Ps_i) (24, 25, 129). The general approach for the ^{31}P NMR analysis of a chiral phosphoryl group is illustrated in Scheme 38. The first required step is the displacement of one of the three oxygen isotopes by a process of known stereochemistry. Starting with **59**, (in which X = OR or S, with *R* configuration), and assuming the displacement by RO^- proceeds with inversion, a mixture of three inseparable, isotopically different species (**60a**, **60b**, **60c**) is

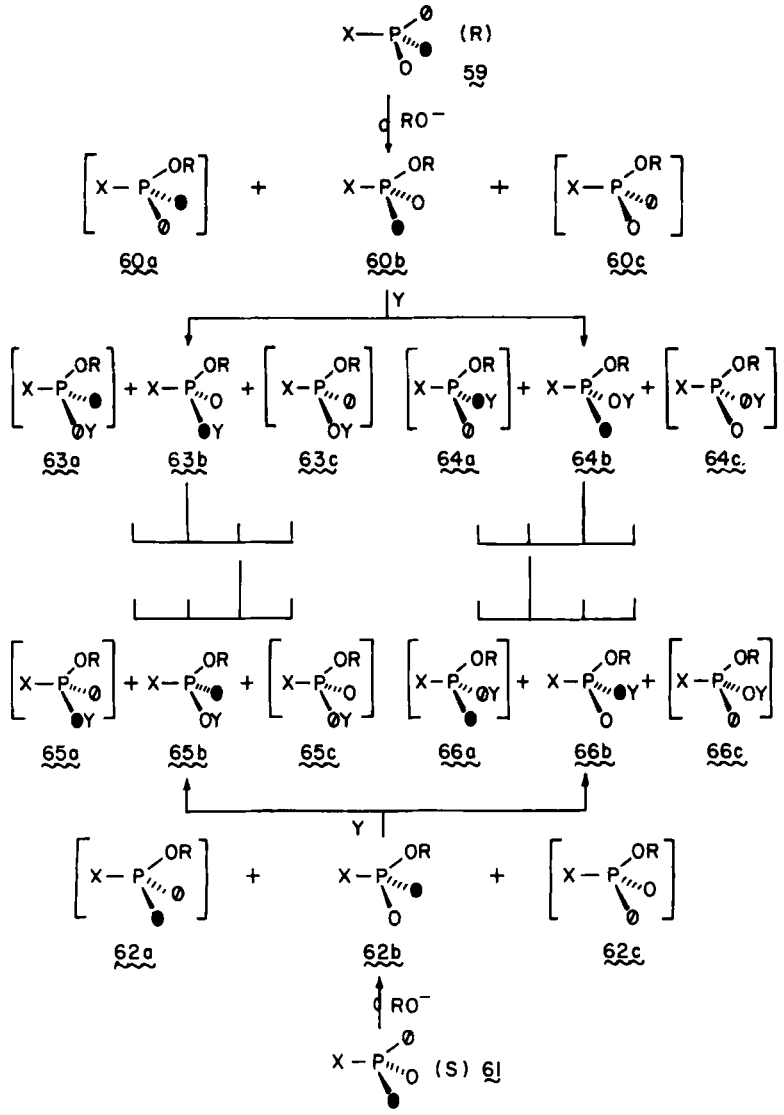

Scheme 38

obtained. Among them, two (those shown in brackets) contain a ^{17}O isotope, which should quench the corresponding ^{31}P NMR signals. Only **60b**, which contains ^{16}O and ^{18}O, with ^{18}O at the pro-*R* position, should give a sharp, unquenched ^{31}P NMR signal. Analogously, the *S* isomer **61** should produce a non-^{17}O-containing species **62b** in which ^{18}O is located at the pro-*S* position (assuming X has highest sequence rule priority).

Thus, determination of whether ^{18}O is located at the pro-*R* and pro-*S* position would reveal the configuration of chiral Ps_i or chiral phosphate monoesters. A general way to achieve this is to derivatize the pro-*R* or pro-*S* oxygen stereospecifically. However, a nonstereospecific derivatization (by a group Y) is sufficient if a chiral center is present in either X or R. Under these conditions two sets of diastereomers **63** and **64** will be generated from **60**. Since diastereomers **63** and **64** most likely will have different ^{31}P chemical shifts, they can be analyzed directly without separation. Among the three species of **63**, only **63b** contains no ^{17}O and is observable by ^{31}P NMR. Since the ^{18}O isotope in **63b** is located at the P—O—Y bridging position, it is expected to cause a smaller isotope shift (0.015-0.025 ppm). On the other hand, the ^{18}O isotope in **64b** is located at the P=O nonbridging position, which should cause a larger isotope shift (0.038-0.044 ppm), as shown in the bar graphs of the expected spectra. In real experiments, however, a chiral phosphoryl group is not 100% pure. The observed spectra generally consist of 4 peaks for **63** and 4 peaks for **64**, due to unlabeled species, species with a bridging ^{18}O, species with a nonbridging ^{18}O, and species with both bridging and nonbridging ^{18}O. The opposite ^{31}P NMR pattern should be observed for the opposite isomer **61**.

Scheme 39 shows the procedures of chemical derivatization of the chiral phosphomonoesters analyzed by the ^{31}P NMR method. The procedures for phosphopropane-1,2-diol (**55**), 5′-AMP (**67**), 5′-dAMP (**70**), 3′-TMP (**73**), and glucose-6-phosphate (**76**) all involve a cyclization step (with inversion of configuration at phosphorus), followed by methylation or ethylation. The dipalmitoylphosphatidic acid (**79**) was first converted to dipalmitoylphosphatidylethanolamine (135), which was then silylated and analyzed by ^{31}P NMR (136).

For the chiral Ps_i, the two main steps required were already available separately in the literature (123, 124, 137), as shown in Scheme 40. The stereochemical course of each step in Scheme 40 had been elucidated earlier (123, 124), except that of phosphoglycerate kinase, which was established by Webb and Trentham by use of synthetic chiral Ps_i of known configuration (24) on the basis of the same NMR analysis discussed below.

According to Scheme 40, the *R*-chiral Ps_i should give ATPαS(B) (isomer B has *R* configuration at P_β) with ^{18}O located specifically at the β-nonbridging position. The *S* enantiomer should give ATPβS(B) with ^{18}O at the $\beta\gamma$-bridging position. It must be noted that Scheme 40 only shows the species which will give an unquenched ^{31}P NMR signal. In reality, each chiral Ps_i species should give a mixture of three ATPβS(B) species (I/1, I/2 and I/3 in Scheme 41). In addition, it is impossible to have a chiral Ps_i of 100% purity. A chiral Ps_i sample actually contains up to six isotopic species, as shown in the left column of Scheme 41 (two of them, III and V, are identical species), each of them, reacting with net retention as shown in Scheme 40, gives three ATPβS(B) species. Fortunately, a careful examination of Scheme 41 reveals that there are only four different

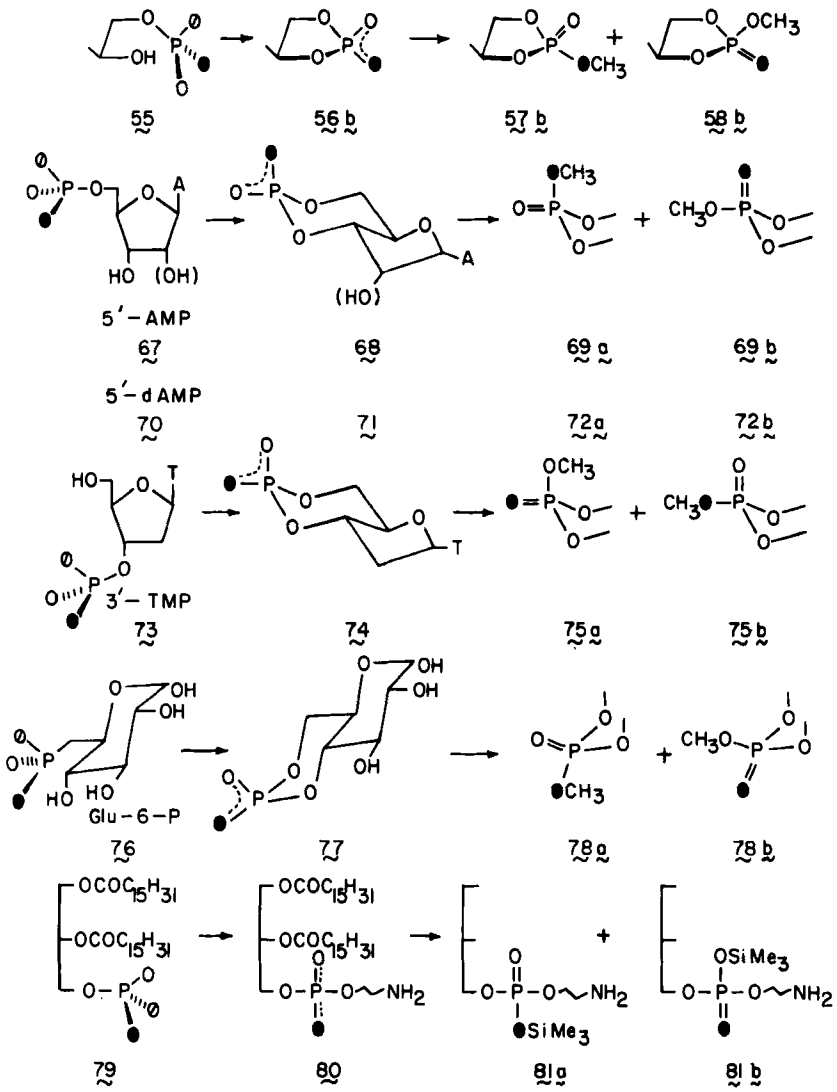

Scheme 39

non-^{17}O-containing species, **a**, **b**, **c** and **d**, and that all the non-chirally labeled Ps_i species contribute **equally** to species **b** and **c**. Only the [^{16}O,^{17}O,^{18}O]Ps_i species gives rise specifically to **b** or **c**, depending on whether the configuration is *S* or *R*, respectively. The amounts of species **a** and **d** depend only on isotopic enrichments but not on configuration.

Figure 2 shows the P_β signal of the ATPβS(B) obtained from $PS^{18}O_3^{3-}$

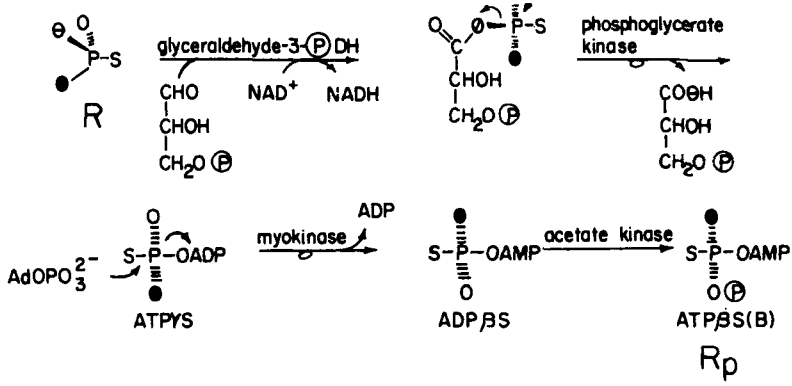

Scheme 40

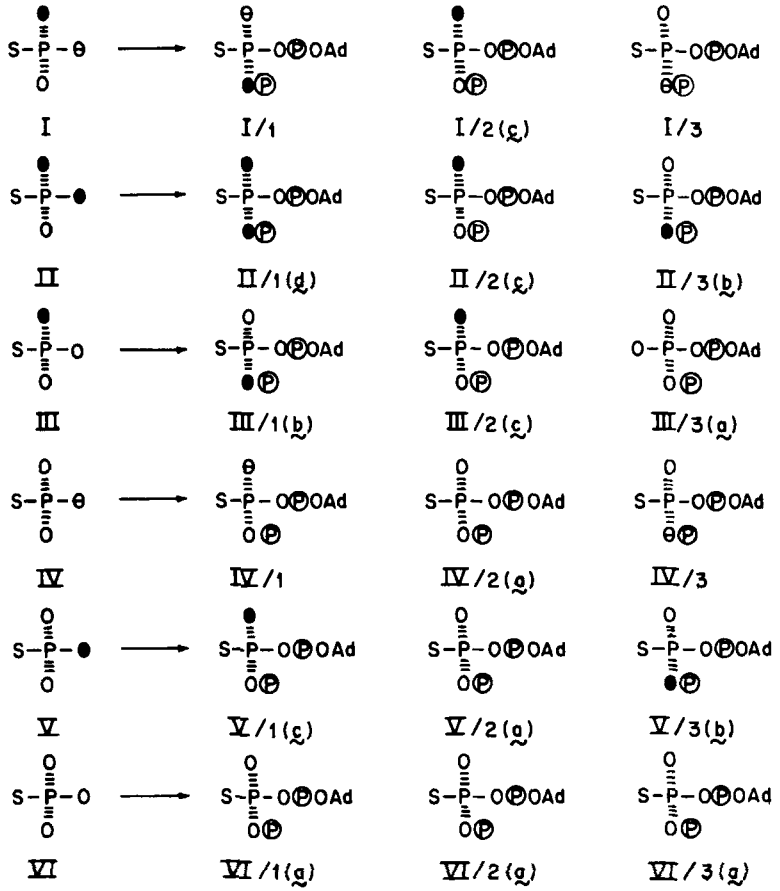

Scheme 41

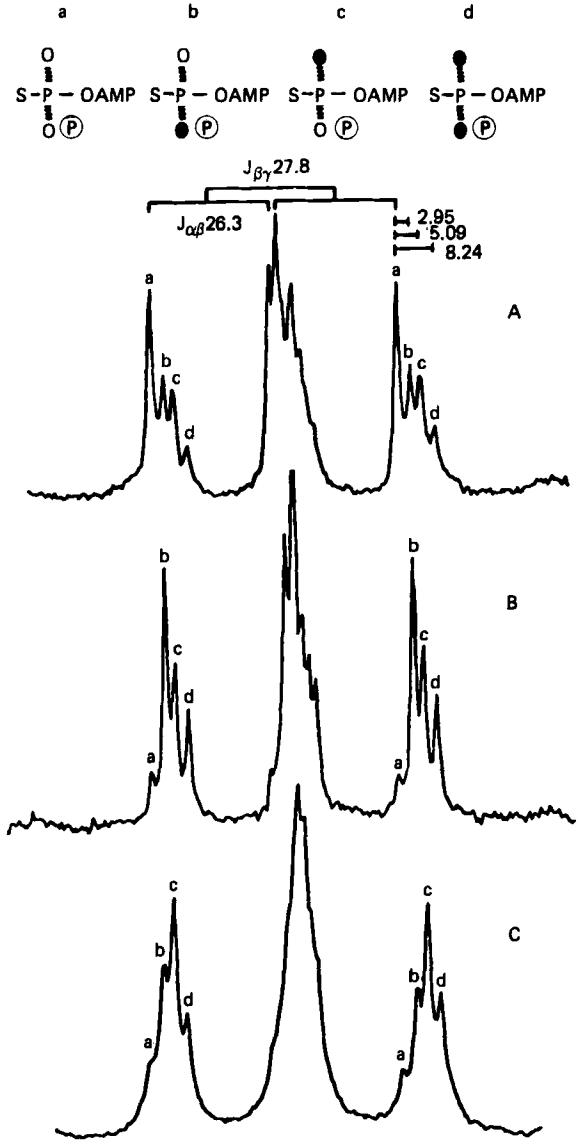

Figure 2. The P_β signals of the ^{31}P NMR spectra of the ATPβS(B) obtained from [$^{18}O_3$]-P_{si}(A) and from the two chiral P_{si}(B, C). The sample (30 μmol) was dissolved in 2.5 mL of D_2O containing 10 mM EDTA and the spectra were recorded at 145.7 MHz at ambient temperature. The coupling constants and isotope shifts are expressed in Hertz. The chemical shift of the P_β signal is 29.8 ppm downfield from H_3PO_4. From M.-D. Tsai (119).

and the two chiral Ps_i enantiomers. The signal contains two overlapping doublets due to $^{31}P—^{31}P$ coupling. Each half of a doublet (cf. the outer peaks) contains four lines due to the four species. The results are summarized in Table 1, where the "F" value is defined as the ratio **b/c**.

An issue remaining to be addressed is a unified way to represent the "chirality" of a chiral phosphoryl group. It is obvious from Scheme 41 that a pure *R* isomer of chiral Ps_i (Species I) should give exclusively species **c** (and a pure *S* iomer should give exclusively species **b**). It is the contaminating ^{16}O in the ^{18}O position and the contaminating ^{16}O and ^{18}O in the ^{17}O position (a typical commercial $H_2{}^{17}O$ contains ca. 50-55% ^{17}O and 30-40% ^{18}O) that give rise to other species. Tsai (119) has suggested separating "purity" from "chirality" in defining the quality of a chiral phosphoryl group. The highest possible purity of a chiral phosphoryl group is ca. 55% due to the limit in ^{17}O enrichment. A chiral phosphoryl group may have lower purity if there is further isotopic dilution during synthesis, but it could have a 100% "chirality" if all steps involved are 100% stereospecific. The "purity" of a chiral phosphoryl group can be determined from the isotopic enrichments at both the ^{17}O and the ^{18}O positions. The theoretical F values can then be calculated based on the known purity, assuming 100% chirality. If the observed F values deviate from the theoretical F values, it suggests that the chirality is <100%. Different values of chirality can then be assumed to calculate the F values until they fit the experimentally observed ones.

In a simplified representation, Knowles and co-workers (101) have suggested use of the Quality Index, Q, as a measure of the quality of both the experimental design and its execution. Assuming the ^{18}O enrichment in the "^{18}O-position" is very close to 100%, the maximum ratio of peak intensities **b/c** in Fig. 2B (and **c/b** in Fig. 2C) is 1/x, where x = fractional ^{16}O and ^{18}O contents of the ^{17}O used. They define Q_{max} as 1-x, the fractional ^{17}O content of the ^{17}O used. The experimental results provide Q_{obs}, which is the fractional difference

Table 1
^{31}P NMR Analysis of the ATPβS(B) Derived from Chiral Ps_i

Ps_i Samples	Intensity[a] (%) a	b	c	d	F Value	Configuration
A	41.3 ± 1.2	24.6 ± 0.1	22.1 ± 0.0	11.8 ± 1.2	1.11	racemic
B	8.8 ± 0.5	42.8 ± 0.6	28.1 ± 0.5	20.3 ± 0.5	1.52	*S*
C	12.2 ± 0.5	26.5 ± 1.6	38.8 ± 0.1	22.4 ± 2.0	0.68	*R*

[a]Obtained from peak height measurements for the P_β signal of ATPβS. The errors represent deviations between the two nonoverlapping halves of the two doublets.

between peaks **b** and **c**. A comparison of Q_{obs} with Q_{max} provides a measure of the overall quality of the experimental procedures and the stereochemical integrity of the transformation. A comparison between the Q_{obs} of the substrate and that of the product in a biochemical transformation gives the extent of stereospecificity in the reaction. The best quality experiment reported is in the determination of the stereochemistry of cyclic phosphodiesterase (132), in which the Q_{max} was 0.51 and the Q_{obs} was 0.49 and 0.52.

D. Mechanistic Significance of Stereochemistry

The initial interest in the field has been in trying to unravel the mechanism of enzyme catalysis: by which route they proceed among the four mechanistic extremes depicted by physical organic chemists (Scheme 42) (17, 138, 139). The dissociative pathway (mechanism A) involves the formation of the highly reactive metaphosphate intermediate, which is then captured by the acceptor group. If this species is free and symmetrically solvated, *racemization* at phosphorus can be predicted. Pathway B is analogous to a S_N2 reaction at carbon, and thus predicts *inversion* of configuration. Mechanism C is similar to B, except that it involves a stable pentacovalent intermediate which may undergo pseudorotation.

A. Dissociative (via monomeric metaphosphate):

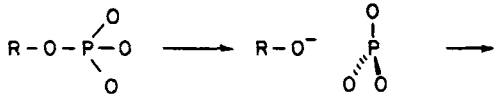

B. In-line associative (via a pentacoordinate transition state):

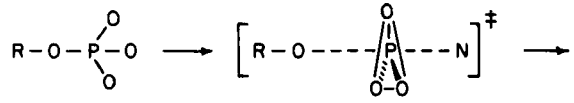

C. In-line associative (via a pentacoordinate intermedinat):

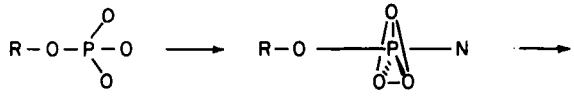

D. Adjacent associative (via a pentacoordinate intermediate and pseudorotation):

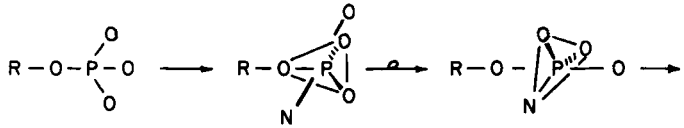

Scheme 42

In the "adjacent associative" pathway (mechanism D), a pseudorotation is *required* in order for the leaving group to leave from an apical position; it thus predicts *retention* of configuration. There is enough physical organic evidence to support the existence of these four pathways under different conditions (137, 138, 140–142).

However, the stereochemical results on enzymatic reactions have not led to identifying one of the four possibilities as the general mechanism in enzyme catalysis. First, formation of a metaphosphate intermediate (mechanism A) may not necessarily result in racemization since in the enzyme active site it may not be free to rotate before it is trapped by the acceptor. Racemization did not even occur in the chemical methanolysis of some phosphomonoesters under dissociative conditions (143). Therefore an observed inversion does not rule out pathway A. Second, the two in-line associative pathways B and C may not be distinguishable in enzyme catalysis and may both proceed with inversion. Lastly, stereochemical results can not differentiate between mechanism D and a double displacement mechanism in which each displacement occurs with inversion.

For all the enzymes investigated to date, *inversion* of configuration has always been observed for reactions known to be single-step processes. For reactions known to involve two steps (via the formation of a covalent enzyme-substrate intermediate), the stereochemical result is always *retention*. These results suggest that the general mechanism of enzyme-catalyzed phosphoryl transfer reactions always involves inversion, which rules out the adjacent pathway D but does not differentiate the dissociative pathway and the in-line associative pathway.

Although other approaches have been used to determine whether the dissociative mechanism or the in-line associative mechanism is the preferred mechanism in enzyme catalysis, the stereochemical results are now generally used to differentiate a double-displacement mechanism from a single-displacement mechanism. The stereochemical approach becomes especially powerful and valuable when there is an ambiguity in the mechanism proposed based on kinetic studies. However, caution in the interpretation of stereochemical results for 1,2-phosphoryl group migrations is advisable. Since mechanism D has been demonstrated in a chemical 1,2-phosphoryl migration (142), the observed retention in the reaction catalyzed by phosphoglycerate mutase (113) does not distinguish between a double-displacement mechanism and a single displacement via pathway D.

E. Stereochemistry of Specific Enzymes

1. Prochiral Substrate ⇄ Proprochiral Product

The stereochemical results on enzymes catalyzing type (a) reactions are summarized in Table 2. There are two main approaches: use of sulfur and an oxygen isotope, and use of oxygen isotopes only. The substrate was in most cases syn-

Table 2
Summary of Stereochemical Results for Type a Reactions: $ROPO_2—OR' \rightleftarrows ROPO_3$

Enzyme	Substrate	Product	Final Derivative	Analytical Method	Result	Ref.
Acetyl CoA synthetase	(*R*)-ATPαS (α-^{17}O)	AMPS (α-^{17}O)	(*S*)-ATPαS (α-^{17}O)	$^{31}P(^{17}O)$	Inv.	126
Aminoacyl tRNA synthetases	ATPαS (α-^{18}O)	AMPS (α-^{18}O)	ATPαS (α-^{18}O)	$^{31}P(^{18}O)$	Inv.	149, 150
cAMP phosphodiesterase	cyclic dAMP (^{17}O,^{18}O)	dAMP (α-^{16}O,^{17}O,^{18}O)	71	$^{31}P(^{17}O,^{18}O)$	Inv.	132
Exonuclease (bovine spleen)	TpNP (^{17}O,^{18}O)	3′-TMP (^{16}O,^{17}O,^{18}O)	74	$^{31}P(^{17}O,^{18}O)$	Ret.	133
Nucleotide pyrophosphatase	ATP (γ-CNEt) (α-^{17}O,^{18}O)	AMP (α-^{16}O,^{17}O,^{18}O)	Cyclization + ethylation	$^{31}P(^{17}O,^{18}O)$	Ret.	151
Nonspecific phosphohydrolase	*endo*-U > pS (^{18}O)	UMPS (^{18}O)	*exo*-U > pS (^{18}O)	$^{31}P(^{18}O)$	Inv.	152
Phosphodiesterase (snake venom)	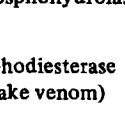	AMPS (α-^{18}O)	(*S*)-ATPαS (α-^{18}O)	MS	Ret.	153
Phosphodiesterase (snake venom)	(*R*)-ATPαS	AMPS (α-^{18}O)	(*S*)-ATPαS (α-^{18}O)	MS	Ret.	154
Phosphodiesterase (snake venom)	ATP (α-^{16}O,^{17}O,^{18}O)	AMP (α-^{16}O,^{17}O,^{18}O)	68	$^{31}P(^{17}O,^{18}O)$	Ret.	131
Nuclease (*Staphylococcal*)	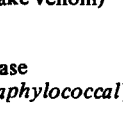	ArO-P(^{16}O,^{17}O,^{18}O)	57 + 58	$^{31}P(^{17}O,^{18}O)$	Inv.	155
Ribonuclease A, T_1, T_2	(Two-step reaction)				Inv. Inv.	21, 156-158
Phospholipase D (cabbage)	DPPC (^{18}O)	79	81	$^{31}P(^{17}O,^{18}O)$	Ret.	135

thesized with known configuration. The product was often derivatized and analyzed by the mass spectral method or by ^{31}P NMR methods based on ^{17}O or ^{18}O effects or both. An example from Tsai's laboratory (126) is described in detail as follows. Acetyl-CoA synthetase catalyzes the following reaction:

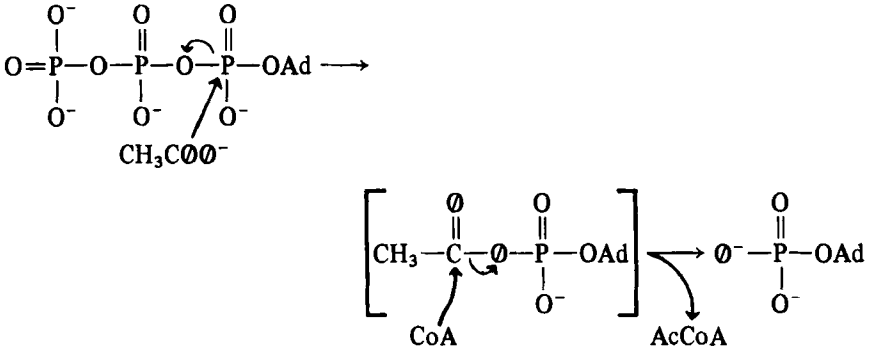

It was found that the enzyme is specific for (*R*)-ATPαS but does not react with (*S*)-ATPαS. As shown in Scheme 43, when (*R*)-ATPαS and ^{17}O-acetate are used as substrates, the ^{17}O from acetate will be incorporated into the pro-*S* position of AMPS if the reaction proceeds with retention of configuration or into the pro-*R* position if inversion occurs. To determine the configuration of the ^{17}O-labeled AMPS (compound type **4**), it is converted to (*S*)-ATPαS by stereospecific phosphorylation at the pro-*R* oxygen catalyzed by adenylate kinase, followed by a second phosphorylation catalyzed by pyruvate kinase (144, 145). By such a conversion, ^{17}O should be incorporated into the nonbridging position of (*S*)-ATPαS if the step of acetate activation proceeds with retention of configuration. On the other hand, ^{17}O should be located at the P—O—P bridging

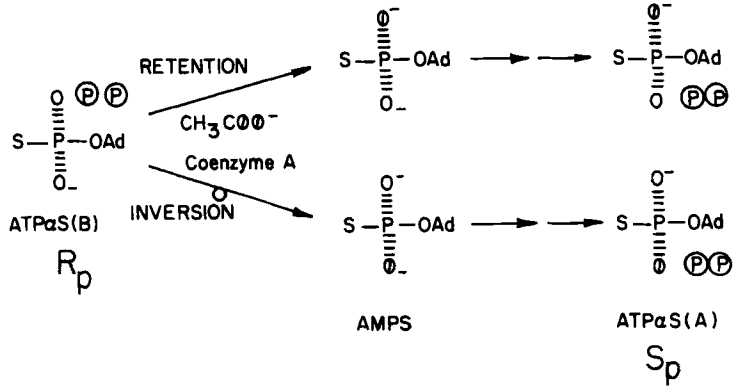

Scheme 43

position if inversion occurs. A nonbridging ^{17}O at P_α should cause the P_α signal in the ^{31}P NMR to broaden and decrease, whereas a bridging ^{17}O should quench both the P_α and P_β signals.

Figure 3 shows ^{31}P NMR spectra of unlabeled (*S*)-ATPαS (A), the synthetic (*S*)-[α-^{17}O,αβ-^{17}O] ATPαS (B), and the (*S*)-ATPαS obtained from the enzyme reaction (C). The ^{17}O isotope used was 20% enriched and the enrichment of ^{17}O-acetate was determined as 19%. In Figure 3B, the P_α signal decreases to 67 ± 1% and the P_β signal to 83 ± 4%. In Figure 3C, the P_α signal decreases to 80 ± 4% and the P_β signal to 82 ± 5%. Since the signals for both P_α and P_β have decreased in Figure 3C, the results indicate that ^{17}O must be located at the bridging position, and the reaction catalyzed by acetyl-CoA synthetase must proceed with inversion of configuration (126).

The example presented above is a typical approach to a typical problem. However, there are several alternative analytical methods in differentiating a bridging oxygen from a nonbridging oxygen. The ^{17}O NMR signal of a bridging ^{17}O in adenine nucleotides was not observed at a low magnetic field (129). However, it has been observed, and shown to be distinguishable from the signal of a nonbridging ^{17}O, at higher magnetic field and higher temperature (105, 146, 147). If ^{18}O instead of ^{17}O is used, the position of ^{18}O can be located by the mass spectral method developed by Frey and co-workers (123, 124) or by the ^{31}P NMR method based on the magnitude of ^{18}O isotope shift. Midelfort and Sarton-Miller (148) have independently elucidated the steric course of acetyl-CoA synthetase by converting the product [^{18}O]AMPS to (*S*)-ATPαS as shown in Scheme 43, followed by degrading the (*S*)-[$^{18}O_1$]ATPαS with lysyl-tRNA synthetase and analyzing the resulting AMPS and PP_i by mass spectrometry.

2. *Proprochiral Substrate ⇄ Pro-prochiral Product*

The stereochemical studies in this category, the transfer of a phosphoryl group between two phosphomonoesters, are summarized in Table 3 for those using a thiophosphoryl group and in Table 4 for those using a [^{16}O,^{17}O,^{18}O]-phosphoryl group.

The approach by use of a thiophosphoryl group was mainly developed in Frey's and Knowles' laboratories. Various biophosphates carrying an [^{18}O]-thiophosphoryl group were synthesized and subjected to enzymatic reactions. The products were derivatized and analyzed mainly by the mass spectral method, since most work was done earlier, before the widespread use of ^{31}P NMR methods.

The use of a chiral [^{16}O,^{17}O,^{18}O]phosphoryl group to study the steric course of phosphoryl transfer reactions was developed mainly in two laboratories, initially in Knowles' group and more recently in Lowe's group. The key step in Knowles' approach is the reaction catalyzed by *E. coli* alkaline phosphatase. This

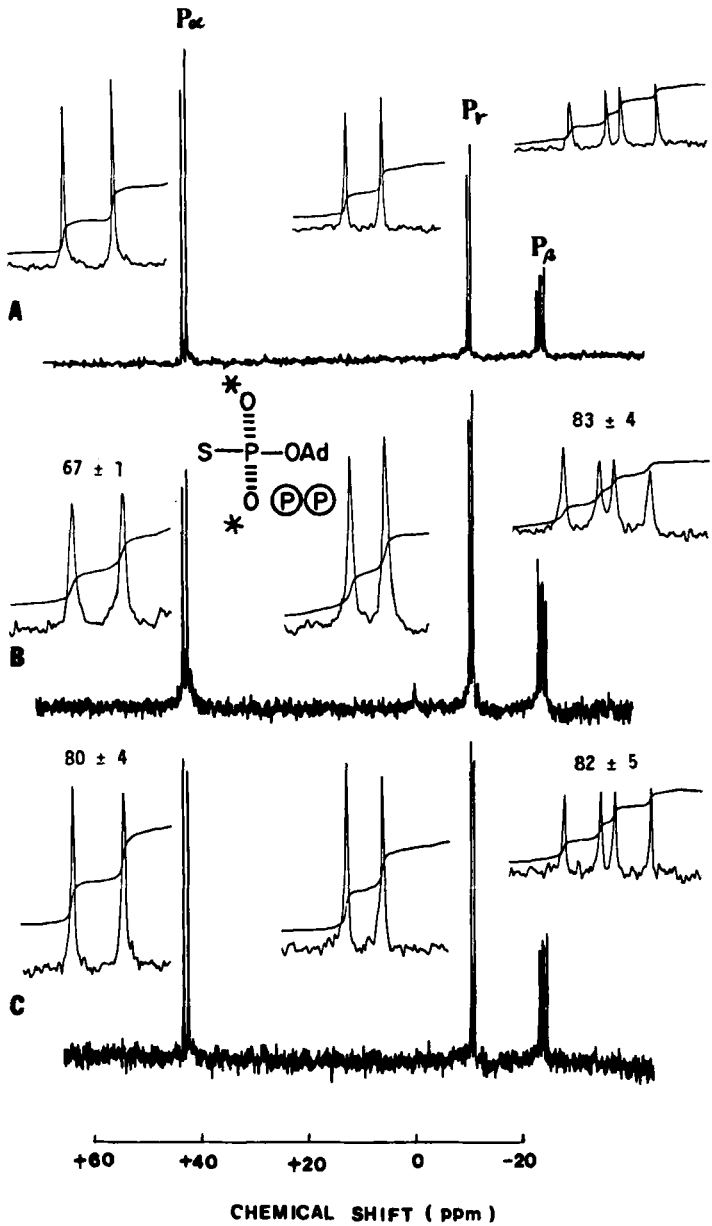

Figure 3. ^{31}P NMR spectra (at 32.2 MHz) showing the results on acetyl CoA synthetase. (A). Unlabeled (*S*)-ATPαS; (B). Synthesized (*S*)-[α-^{17}O,-αβ^{17}O] ATPαS; (C). The (*S*)-ATPαS from [$^{17}O_2$] acetate. The insets represent the integrations of the corresponding signals. From M.-D. Tsai (126).

Table 3
Summary of Stereochemical Results for Phosphoryl Transfer Reactions (Type b) by Use of a Thiophosphoryl Group

Enzyme	Substrate	Product	Final Derivative	Analytical Method	Result	Ref.
Phosphoglycerate kinase	Glycerate-1,3-diP (1-^{17}O,^{18}O,S)	ATPγS (γ-^{17}O,^{18}O)	(*S*)-ATPβS	$^{31}P(^{17}O,^{18}O)$	Inv.	24
Adenylate kinase	ATPγS (γ-^{18}O)	ADPβS (β-^{18}O)	ATPβS	MS	Inv.	124
Glycerol kinase	ATPγS (γ-^{18}O)	Glycerol-3-P (^{18}O,S)	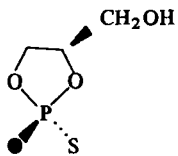	MS X-ray	Inv.	159, 160
Pyruvate kinase	Phosphoenol-pyruvate (S,^{18}O)	ATPγS (γ-^{18}O)	Same as above		Inv.	159, 160
Hexokinase	ATPγS (γ-^{18}O)	Glucose-6-P (^{18}O,S)	Same as above		Inv.	159, 160
Adenosine kinase	ATPγS (γ-^{18}O)	AMPS (α-^{18}O)	(*S*)-ATPαS	MS	Inv.	161
Nucleoside phosphotransferase	AMPS (α-^{18}O)	AMPS (α-^{18}O)	(*S*)-ATPαS	MS	Ret.	122
Nucleoside diphosphate kinase	ATPγS (γ-^{18}O)	ATPγS (γ-^{18}O)	(*R*)-ATPβS	MS	Ret.	162
Polynucleotide kinase	ATPγS (γ-^{18}O)	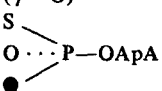	(*S*)-ATPαS	MS	Inv.	163

Table 4
Summary of Stereochemical Results for Phosphoryl Transfer Reactions (Type b) by Use of a Chiral [^{16}O,^{17}O,^{18}O] Phosphoryl Group

Enzyme	Substrate	Product	Final Derivative	Analytical Method	Result	Ref.
Alkaline phosphatase (*E. coli*)	Phenyl-P (^{16}O,^{17}O,^{18}O)	**55**	**57 + 58**	MS	Ret.	112
Glycerol kinase	ATP (γ-^{16}O,^{17}O,^{18}O)	Glycerol-P (^{16}O,^{17}O,^{18}O)	**57 + 58**	MS	Inv.	164
Acetate kinase	ATP (γ-^{16}O,^{17}O,^{18}O)	Acetate-P (^{16}O,^{17}O,^{18}O)	**57 + 58**	MS	Inv.	164
Phosphoglycerate mutase (rabbit muscle and wheat germ)	Glycerate-2-P	Glycerate-3-P	**57 + 58**	MS	Ret.	113
Creatine kinase	ATP (γ-^{16}O,^{17}O,^{18}O)	Creatine-P (^{16}O,^{17}O,^{18}O)	**57 + 58**	$^{31}P(^{17}O,^{18}O)$	Inv.	165
Acid phosphatase	Phenyl-P (^{16}O,^{17}O,^{18}O)	**55**	**57 + 58**	$^{31}P(^{17}O,^{18}O)$	Ret.	166
Hexokinase	ATP (γ-^{16}O,^{17}O,^{18}O)	Glucose-6-P (^{16}O,^{17}O,^{18}O)	**78**	$^{31}P(^{17}O,^{18}O)$	Inv.	167
Pyruvate kinase	Phosphoenolpyruvate (^{16}O,^{17}O,^{18}O)	ATP (γ-^{16}O,^{17}O,^{18}O)	**78**	$^{31}P(^{17}O,^{18}O)$	Inv.	168
Phosphofructokinase	Fructose-1,6-diP (1-^{16}O,^{17}O,^{18}O)	ATP (γ-^{16}O,^{17}O,^{18}O)	**78**	$^{31}P(^{17}O,^{18}O)$	Inv.	169
Phosphoglucomutase	Glucose-1-P (^{16}O,^{17}O,^{18}O)	Glucose-6-P (^{16}O,^{17}O,^{18}O)	**78**	$^{31}P(^{17}O,^{18}O)$	Ret.	170
Polynucleotide kinase	ATP (γ-^{16}O,^{17}O,^{18}O)	3′,5′-ADP (5′-^{16}O,^{17}O,^{18}O)	**78**	$^{31}P(^{17}O,^{18}O)$	Inv.	171

alkaline phosphatase is a nonspecific phosphate monoesterase which also catalyzes the transfer of phosphoryl groups to acceptors other than water, such as alcohols. By use of phenyl[(*R*)-^{16}O,^{17}O,^{18}O]phosphate as a substrate and (*S*)-propane-1,2-diol as an acceptor, the chiral phosphoryl group was transferred by alkaline phosphatase to form 1-[^{16}O,^{17}O,^{18}O]phosphopropane-1,2-diol, and its configuration was then analyzed as described in Scheme 37. The results indicate *retention* of configuration (112). Since alkaline phosphatase has a low substrate specificity, other phosphomonoesters can be analyzed by transferring their chiral phosphoryl group to (*S*)-propane-1,2-diol followed by configurational analysis.

The key compound in Lowe's approach is glucose 6-[^{16}O,^{17}O,^{18}O]phosphate (**25**), which was synthesized with known configuration according to Scheme 31 (p. 291). The configuration can be characterized by ^{31}P NMR analysis after cyclization of **25** followed by methylation (134). The steric course of hexokinase and phosphoglucomutase can be readily elucidated since glucose-6-phosphate is the product in these reactions. The steric course of other kinases can be determined by converting [γ-^{16}O,^{17}O,^{18}O]ATP (as a product) to glucose-6-[^{16}O,^{17}O,^{18}O]phosphate with hexokinase.

3. *Proprochiral Substrate ⇄ Proproprochiral Product*

The enzymes in this category inlcude phosphatases, nucleotidases, ATPases, and so on. Except for the phosphatases, which also catalyse the "transfer" reaction in addition to the "hydrolysis" reaction (112, 166), the stereochemistry has to be studied by use of a chiral inorganic phosphate (P_i, a proproprochiral center). To make a P_i chiral, it is necessary to use ^{16}O,^{17}O,^{18}O and sulfur. The synthesis and configurational analysis of chiral [^{16}O,^{17}O,^{18}O]thiophosphate (Ps_i) have been described in previous sections; the first application of chiral [^{16}O,^{17}O,^{18}O]Ps_i in the reaction type c is the elucidation of the stereochemistry

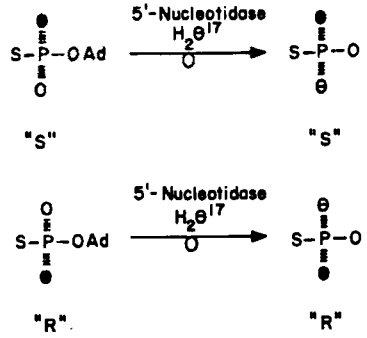

Scheme 44

Table 5
Summary of Stereochemical Results for Type c Reactions: $RO—PO_3 \rightleftarrows PO_4$

Enzyme	Substrate	Product	Final Derivative	Analytical Method	Result	Ref.
5′-Nucleotidase	AMPS (α-^{18}O)	Psi (^{16}O,^{17}O,^{18}O)	(*R*)-ATPβS	$^{31}P(^{17}O,^{18}O)$	Inv.	25, 119
Myosin ATPase	ATPγS (γ-^{18}O)	Psi (^{16}O,^{17}O,^{18}O)	(*S*)-ATPβS	$^{31}P(^{17}O,^{18}O)$	Inv.	172
Mitochondrial ATPase	ATPγS (γ-^{18}O)	Psi (^{16}O,^{17}O,^{18}O)	(*S*)-ATPβS	$^{31}P(^{17}O,^{18}O)$	Inv.	173
Sarcoplasmic reticulum ATPase	ATPγS (γ-^{17}O,^{18}O)	Psi (^{16}O,^{17}O,^{18}O)	(*S*)-ATPβS	$^{31}P(^{17}O,^{18}O)$	Ret.	174
Ribosome-dependent GTPase	GTPγS (γ-^{17}O,^{18}O)	Psi (^{16}O,^{17}O,^{18}O)	(*S*)-ATPβS	$^{31}P(^{17}O,^{18}O)$	Inv.	175

of hydrolysis of AMP to adenosine and P_i catalyzed by 5′-nucleotidase. As shown in Scheme 44, hydrolysis of (*R*)- and (*S*)-[α-$^{18}O_1$]AMPS in $H_2{}^{17}O$ gave (*R*)- and (*S*)-[^{16}O,^{17}O,^{18}O]Ps_i, respectively, indicating an "inversion" of configuration (25, 119). Webb and co-workers (172-175) have elucidated the steric course of several ATPases and GTPases. The results are summarized in Table 5.

REFERENCES

1. Hanson, K. R.; Rose, I. A. *Accts. Chem. Res.* **1975**, *8*, 1-10.
2. Bondinell, W. E.; Sprinson, D. B. *Biochem. Biophys. Res. Comm.* **1970**, *40*, 1464-1467.
3. Ogston, A. G. *Nature* **1948**, *162*, 963-964.
4. Arigoni, D.; Eliel, E. *Top. Stereochem.* **1969**, *4*, 127-243.
5. Cornforth, J. W. *Quart. Rev. Chem. Soc. (London)* **1969**, *23*, 125-140.
6. Bentley, R. "Molecular Asymmetry in Biology"; Academic Press: New York, Vol. 1, 1969, Vol. 2, 1970.
7. Floss, H. G. *Naturwissenschaften* **1970**, *57*, 435-442.
8. Alworth, W. L. "Stereochemistry and Its Application in Biochemistry"; Wiley-Interscience: New York, 1972.
9. Rose, I. A. *Crit. Rev. Biochem.* **1972**, *1*, 33-57.
10. Hanson, K. R. *Ann. Rev. Plant Physiol.* **1972**, *23*, 335-366.
11. Goodwin, T. W. *Essays Biochem.* **1973**, *9*, 103-160.
12. Vennesland, B. *Fortschr. Chem. Forschg.* **1974**, *48*, 39-65.
13. Battersby, A. R.; Staunton, J. *Tetrahedron* **1974**, *30*, 1707-1715.
14. Hanson, K. R. *Ann. Rev. Biochem.* **1976**, *45*, 307-330.
15. Simon, H.; Kraus, A. In "Isotopes in Organic Chemistry," Vol. 2; Buncel, E.; Lee, C. C., Eds.; Elsevier: Amsterdam, 1976, p. 153-229.
16. Eckstein, F. *Accts. Chem. Res.* **1979**, *12*, 204-210.
17. Knowles, J. R. *Ann. Rev. Biochem.* **1980**, *49*, 877-919.
18. Neuberger, A.; van Deenen, L. L. M., Gen. Eds.; "New Comprehensive Biochemistry," Vol. 3: "Stereochemistry", Tamm, Ch., Ed., Elsevier Biomedical Press: Amsterdam, 1982.
19. Cornforth, J. W.; Redmond, J. W.; Eggerer, H.; Buckel, W.; Gutschow, C. *Nature* **1969**, *221*, 1212-1213.
20. Lüthy, J.; Rétey, J.; Arigoni, D. *Nature* **1969**, *221*, 1213-1215.
21. Usher, D. A.; Richardson, D. I., Jr.; Eckstein, F. *Nature* **1970**, *228*, 663-665.
22. Abbott, S. J.; Jones, S. R.; Weinman, S. A.; Knowles, J. R. *J. Am. Chem. Soc.* **1978**, *100*, 2558-2560.
23. Cullis, P. M.; Lowe, G. *J.C.S. Chem. Comm.* **1978**, 512-514.
24. Webb, M. R.; Trentham, D. R. *J. Biol. Chem.* **1980**, *255*, 1775-1779.
25. Tsai, M.-D.; Chang, T. T. *J. Am. Chem. Soc.* **1980**, *102*, 5416-5418.
26. Hanson, K. R. *J. Am. Chem. Soc.* **1966**, *88*, 2731-2742.
27. Levy, H. R.; Talalay, P.; Vennesland, B. *Prog. Stereochem.* **1962**, *3*, 299-349.
28. Cornforth, J. W. *Chemistry in Britain* **1970**, 431-436.
29. Floss, H. G.; Tsai, M.-D. *Adv. Enzymol.* **1979**, *50*, 243-302.
30. Floss, H. G. *Methods Enzymol.* **1982**, *87*, 126-159.
31. Cornforth, J. W.; Redmond, J. W.; Eggerer, H.; Buckel, W.; Gutschow, C. *Eur. J. Biochem.* **1970**, *14*, 1-13.

32. Lenz, H.; Buckel, W.; Wunderwald, P.; Biedermann, G.; Buschmeier, V.; Eggerer, H.; Cornforth, J. W.; Redmond, J. W.; Mallaby, R. *Eur. J. Biochem.* **1971**, *24*, 207–215.
33. Townsend, C. A.; Scholl, T.; Arigoni, D. *J.C.S. Chem. Comm.* **1975**, 921–922.
34. Fryzuk, M. D.; Bosnich, B. *J. Am. Chem. Soc.* **1979**, *101*, 3043–3049.
35. Midland, M. M.; Greer, S.; Tramontano, A.; Zderic, S. A. *J. Am. Chem. Soc.* **1979**, *101*, 2352–2355.
36. Kobayashi, K.; Jadhav, P. K.; Floss, H. G., unpublished results.
37. Pearce, Z.; Coates, R. M., personal communication. We thank Drs. Pearce and Coates for providing [^{3}H]superhydride and the use of their facilities for these reductions.
38. Kakinuma, K.; Imamura, N.; Saba, Y. *Tetrahedron Lett.* **1982**, *23*, 1697–1700.
39. Kobayashi, K.; Kakinuma, K.; Floss, H. G., unpublished results.
40. Mascaro, L., Jr.; Hörhammer, R.; Eisenstein, S.; Sellers, L.K.; Mascaro, K.; Floss, H. G. *J. Am. Chem. Soc.* **1977**, *99*, 273–274.
41. Woodard, R.W.; Mascaro, L., Jr.; Hörhammer, R.; Eisenstein, S.; Floss, H. G. *J. Am. Chem. Soc.* **1980**, *102*, 6314–6318.
42. Rose, I. A. *J. Biol. Chem.* **1970**, *245*, 6052–6056.
43. Cohn, M.; Pearson, J. E.; O'Connell, E. L.; Rose, I. A. *J. Am. Chem. Soc.* **1970**, *92*, 4095–4098.
44. Robinson, J. L.; Rose, I. A. *J. Biol. Chem.* **1972**, *247*, 1096–1105, and references cited therein.
45. Creighton, D. J.; Rose, I. A. *J. Biol. Chem.* **1976**, *251*, 61–68.
46. Kraus, A.; Dessau, W.; Simon, H. *Hoppe Seyler's Z. Physiol. Chem.* **1976**, *357*, 1209–1214.
47. Stickland, L. H. *Biochem. J.* **1935**, *29*, 889–898.
48. Armarego, W. L. F.; Milloy, B. A.; Pendergast, W. *J. Chem. Soc., Perkin Trans. I* **1976**, 2229–2237, and references cited therein.
49. Barnard, G. F.; Akhtar, M. *J. Chem. Soc., Chem. Comm.* **1975**, 980–982.
50. Lüthy, J., Ph.D. Dissertation No. 4764, ETH, Zürich, 1972.
51. Johnson, C. K.; Gabe, E. J.; Taylor, M. R.; Rose, I. A. *J. Am. Chem. Soc.* **1965**, *87*, 1802–1804.
52. Krakow, G.; Vennesland, B. *Biochem. Z.* **1963**, *338*, 31–35.
53. Kajiwara, M.; Lee, S.-F; Scott, A. I.; Akhtar, M.; Jones, C. R.; Jordan, P. M. *J. Chem. Soc., Chem. Comm.* **1978**, 967–968.
54. Besmer, P.; Arigoni, D. *Chimia*, **1968**, *22*, 494. P. Besmer, Ph.D. Dissertation No. 4435, ETH, Zürich, 1970.
55. Houck, D.; Woodard, R. W.; Floss, H. G., unpublished work; see ref. 30.
56. Caspi, E.; Shapiro, S.; Piper, J. *Tetrahedron* **1981**, *37*, 3535–3543.
57. Caspi, E.; Eck, C. R. *J. Org. Chem.* **1977**, *42*, 767–768.
58. Golding, B. T.; Ioannou, P. V.; Eckhard, I. F. *J. Chem. Soc., Perkin Trans. I* **1978**, 774–780.
59. Shapiro, S.; Piper, J. U.; Caspi, E. *J. Am. Chem. Soc.* **1982**, *104*, 2301–2305.
60. Phillips, G. T.; Clifford, K. H. *Eur. J. Biochem.* **1976**, *61*, 271–286.
61. Arigoni, D. *Ciba Found. Symp.* (new series) **1978**, *60*, 243–261.
62. Altman, L. J.; Han, C. Y.; Bertolino, A.; Handy, G.; Laungani, D.; Muller, W.; Schwartz, S.; Shanker, D.; de Wolf, W. H.; Yang, F. *J. Am. Chem. Soc.* **1978**, *100*, 3235–3237.
63. Aberhart, D. J.; Tann, C.-H. *J. Am. Chem. Soc.* **1980**, *102*, 6377–6380.
64. Townsend, C. A.; Neese, A. S.; Theis, A. B. *J. Chem. Soc., Chem. Comm.* **1982**, 116–118.

65. Verbit, L. *Progr. Phys. Org. Chem.* **1970**, *7*, 51-127.
66. Bloxsidge, J. P.; Elvidge, J. A.; Jones, J. R.; Mane, R. B.; Evans, E. A. *J. Chem. Res. (S)* 1977, 258-259, and references cited therein.
67. Wieland, T.; Rueff, L. *Angew. Chem.* **1953**, *65*, 186.
68. Durchschlag, H.; Biedermann, G.; Eggerer, H. *Eur. J. Biochem.* **1981**, *114*, 255-262.
69. Lenz, H.; Wunderwald, P.; Buschmeier, V.; Eggerer, H. *Hoppe Seyler's Z. Physiol. Chem.* **1971**, *352*, 517-519.
70. Lenz, H.; Eggerer, H. *Eur. J. Biochem.* **1976**, *65*, 237-246.
71. Cheung, Y.-F.; Walsh, C. *J. Am. Chem. Soc.* **1976**, *98*, 3397-3398.
72. Rétey, J.; Lüthy, J.; Arigoni, D. *Nature* **1970**, *226*, 519-521.
73. Tchen, T. T.; van Milligan, H. *J. Am. Chem. Soc.* **1960**, *82*, 4115-4116.
74. Tsai, M.-D.; Floss, H. G.; Rosenfeld, H. J.; Roberts, J. *J. Biol. Chem.* **1979**, *254*, 6437-6443.
75. Willadsen, P.; Eggerer, H. *Eur. J. Biochem.* **1975**, *54*, 253-258.
76. Eggerer, H.; Willadsen, P. *Eur. J. Biochem.* **1975**, *54*, 247-252.
77. Clifford, K. H.; Cornforth, J. W.; Donninger, C.; Mallaby, R. *Eur. J. Biochem.* **1972**, *26*, 401-406.
78. Tsai, M.-D.; Schleicher, E.; Potts, R.; Skye, G. E.; Floss, H. G. *J. Biol. Chem.* **1978**, *253*, 5344-5349.
79. Vederas, J. C.; Schleicher, E.; Tsai, M.-D.; Floss, H. G. *J. Biol. Chem.* **1978**, *253*, 5350-5354.
80. Kumagai, H.; Yamada, H.; Sawada, S.; Schleicher, E.; Mascaro, K.; Floss, H. G. *J.C.S. Chem. Comm.* **1977**, 85-86.
81. Tsai, M.-D.; Weaver, J.; Floss, H. G.; Conn, E. E.; Creveling, R. K.; Mazelis, M. *Arch. Biochem. Biophys.* **1978**, *190*, 553-559.
82. Floss, H. G.; Schleicher, E.; Potts, R. *J. Biol. Chem.* **1976**, *251*, 5478-5482.
83. Walsh, C. T.; Chang, M. N. T. *J. Am. Chem. Soc.* **1981**, *103*, 4921-4927.
84. Snipes, C. E.; Brillinger, G.-U.; Sellers, L.; Mascaro, L.; Floss, H. G. *J. Biol. Chem.* **1977**, *252*, 8113-8117.
85. Merkler, I.; Rétey, J. *Eur. J. Biochem.* **1981**, *120*, 593-597.
86. Barnard, G. F.; Akhtar, M. *J. Chem. Soc., Perkin Trans. I* **1979**, 2354-2360.
87. Battersby, A. R.; Gutman, A. L.; Fookes, C. J. R.; Günther, H.; Simon, H. *J. Chem. Soc., Chem. Comm.* **1981**, 645-647.
88. Rétey, J.; Suckling, C. J.; Arigoni, D.; Babior, B. M. *J. Biol. Chem.* **1974**, *249*, 6359-6360.
89. Bonetti, V., Ph.D. Dissertation No. 5366, ETH Zürich, 1974.
90. Corina, D. L.; Wilton, D. C. *Biochem. J.* **1976**, *157*, 573-576.
91. Summers, M. C.; Rose, I. A. *J. Am. Chem. Soc.* **1977**, *99*, 4475-4478.
92. Shapiro, S.; Piper, J. U.; Caspi, E. *Anal. Biochem.* **1981**, *117*, 113-120.
93. Buckel, W.; Lenz, H.; Wunderwald, P.; Buschmeier, V.; Eggerer, H.; Gottschalk, G. *Eur. J. Biochem.* **1971**, *24*, 201-206.
94. Woodard, R. W.; Tsai, M.-D.; Floss, H. G.; Crooks, P. A.; Coward, J. K. *J. Biol. Chem.* **1980**, *255*, 9124-9127.
95. Woodard, R. W.; Weaver, J.; Floss, H. G. *Arch. Biochem. Biophys.* **1981**, *207*, 51-54.
96. Hegazi, M. F.; Borchardt, R. T.; Schowen, R. L. *J. Am. Chem. Soc.* **1979**, *101*, 4359-4365.
97. Arigoni, D., lecture presented at the 184th Meeting of the American Chemical Society, Kansas City, September, 1982.
98. Sedgwick, B.; Cornforth, J. W.; French, S. J.; Gray, R. T.; Kelstrup, E.; Willadsen, P. *Eur. J. Biochem.* **1977**, 481-495.

99. Sedgwick, B.; Morris, C.; French, S. J. *J. Chem. Soc., Chem. Comm.* **1978,** 193-194.
100. Floss, H. G., lecture series presented at USDA Northern Regional Research Laboratories, Peoria, Ill., May, 1969.
101. Buchwald, S. L.; Hansen, D. E.; Hassett, A.; Knowles, J. R. *Meth. Enzymol.* **1982,** *87*, 279-301.
102. Frey, P. A.; Richard, J. P.; Ho, H.-T.; Brody, R. S.; Sammons, R. D.; Sheu, K.-F. *Meth. Enzymol.* **1982,** *87*, 213-235.
103. Frey, P. A. in ref. 18, pp. 201-248.
104. Frey, P. A. *Tetrahedron* **1982,** *38*, 1541-1568.
105. Tsai, M.-D. *Meth. Enzymol.* **1982,** *87*, 235-279.
106. Cohn, M. *Ann. Rev. Biophys. Bioeng.* **1982,** *11*, 23-42.
107. Webb, M. R. *Meth. Enzymol.* **1982,** *87*, 301-316.
108. Eckstein, F.; Romaniuk, P. J.; Connolly, B. A. *Meth. Enzymol.* **1982,** *87*, 197-212.
109. Abbott, S. J.; Jones, S. R.; Weinman, S. A.; Bockoff, F. M.; McLafferty, F. W.; Knowles, J. R. *J. Am. Chem. Soc.* **1979,** *101*, 4323-4332.
110. Cullis, P. M.; Lowe, G. *J. Chem. Soc., Perkin Trans. I* **1981,** 2317-2321.
111. Cooper, D. B.; Hall, C. R.; Harrison, J. M.; Inch, T. D. *J. Chem. Soc., Perkin Trans. I* **1977,** 1969-1980.
112. Jones, S. R.; Kindman, L. A.; Knowles, J. R. *Nature (London)* **1978,** *275*, 564-565.
113. Blättler, W. A.; Knowles, J. R. *Biochemistry* **1980,** *19*, 738-743.
114. Blättler, W. A.; Knowles, J. R. *J. Am. Chem. Soc.* **1979,** *101*, 510-511.
115. Pohoryles, L. A.; Sarel, S.; Ben-Shoshan, R. *J. Org. Chem.* **1959,** *24*, 1878-1881.
116. Cullis, P. M.; Jarvest, R. L.; Lowe, G.; Potter, B. V. L. *J. Chem. Soc., Chem. Comm.* **1981,** 245-246.
117. Jarvest, R. L.; Lowe, G. *J. Chem. Soc., Chem. Comm.* **1979,** 364-366.
118. Richard, J. P.; Prasher, D. C.; Ives, D. H.; Frey, P. A. *J. Biol. Chem.* **1979,** *254*, 4339-4341.
119. Tsai, M.-D. *Biochemistry* **1980,** *19*, 5310-5316.
120. Murray, W. A.; Atkinsons, M. R. *Biochemistry* **1968,** *7*, 4023-4029.
121. Michelson, A. M. *Biochim. Biophys. Acta* **1964,** *91*, 1-13.
122. Eckstein, F.; Goody, R. S. *Biochemistry* **1976,** *15*, 1685-1691.
123. Richard, J. P.; Ho, H. T.; Frey, P. A. *J. Am. Chem. Soc.* **1978,** *100*, 7756-7757.
124. Richard, J. P.; Frey, P. A. *J. Am. Chem. Soc.* **1978,** *100*, 7757-7758.
125. Cohn, M.; Hu, A. *Proc. Natl. Acad. Sci. USA* **1978,** *75*, 200-203.
126. Tsai, M.-D. *Biochemistry* **1979,** *18*, 1468-1472.
127. Tsai, M.-D.; Bruzik, K. "Biological Magnetic Resonance," Vol. 5; Berliner, L. J.; Reuben, J., Eds.; Plenum Press: New York, 1983, pp. 129-181.
128. Abragam, A. "Principles of Nuclear Magnetism"; Oxford University Press, London and New York, 1961.
129. Tsai, M.-D.; Huang, S. L.; Kozlowski, J. F.; Chang, C. C. *Biochemistry* **1980,** *19*, 3531-3536.
130. Buchwald, S. L.; Knowles, J. R. *J. Am. Chem. Soc.* **1980,** *102*, 6601-6602.
131. Jarvest, R. L.; Lowe, G. *Biochem. J.* **1981,** *199*, 447-451.
132. Coderre, J. A.; Mehdi, S.; Gerlt, J. A. *J. Am. Chem. Soc.* **1981,** *103*, 1872-1875.
133. Mehdi, S.; Gerlt, J. A. *J. Am. Chem. Soc.* **1981,** *103*, 7018-7020.
134. Jarvest, R. L.; Lowe, G.; Potter, B. V. L. *J.C.S. Chem. Comm.* **1980,** 1142-1145; *J. Chem. Soc., Perkin Trans. I* **1981,** 3186-3195.
135. Bruzik, K.; Tsai, M.-D, unpublished results.
136. Bruzik, K.; Tsai, M.-D. *J. Am. Chem. Soc.* **1982,** *104*, 863-865.
137. Eckstein, F. *Biochim. Biophys. Acta* **1977,** *483*, 1-5.

138. Benkovic, S. J.; Schray, J. J. "The Enzymes," Vol. 8; P. D. Boyer, Ed.; Academic Press: New York, 1973, p. 201.
139. Benkovic, S. J.; Schray, K. J. In "Transition States of Biochemical Processes"; Gandour, R. D.; Schowen, R. L., Eds.; Plenum Press: New York, 1978, p. 493.
140. Westheimer, F. H. *Acc. Chem. Res.* **1968,** *1*, 70–78.
141. Westheimer, F. H. *Chem. Rev.* **1981,** *81*, 313–326.
142. Buchwald, S. L.; Pliura, D. H.; Knowles, J. R. *J. Am. Chem. Soc.* **1982,** *104*, 845–847.
143. Buchwald, S. L.; Knowles, J. R. *J. Am. Chem. Soc.* **1982,** *104*, 1438–1440.
144. Sheu, K. F. R.; Frey, P. A. *J. Biol. Chem.* **1977,** *252*, 4445–4448.
145. Jaffe, E. K.; Cohn, M. *Biochemistry* **1978,** *17*, 652–657.
146. Gerlt, J. A.; Demou, P. C.; Mehdi, S. *J. Am. Chem. Soc.* **1982,** *104*, 2848–2856.
147. Gerothanassis, I. P.; Sheppard, N. *J. Magn. Reson.* **1982,** *46*, 423.
148. Midelfort, C. F.; Sarton-Miller, I. *J. Biol. Chem.* **1978,** *253*, 7127–7129.
149. Jaffe, E. K.; Cohn, M. *J. Biol. Chem.* **1979,** *254*, 10,839–10,845.
150. Langdon, S. P.; Lowe, G. *Nature* **1979,** *281*, 320–321.
151. Sammons, D.; Frey, P. A., **1983,** submitted for publication.
152. Gerlt, J. A.; Wan, W. H. Y. *Biochemistry* **1979,** *18*, 4630–4638.
153. Burgers, P. M. J.; Eckstein, F.; Hunneman, D. H. *J. Biol. Chem.* **1979,** *254*, 7476–7478.
154. Bryant, E. R.; Benkovic, S. J. *Biochemistry* **1979,** *18*, 2825–2828.
155. Mehdi, S.; Gerlt, J. A. *J. Am. Chem. Soc.* **1982,** *104*, 3223–3225.
156. Usher, D. A.; Erenrich, E. S.; Eckstein, F. *Proc. Natl. Acad. Sci. USA* **1972,** *69*, 115–118.
157. Eckstein, F.; Schulz, H. H.; Rüterjans, H.; Haar, W.; Maurer, W. *Biochemistry* **1982,** *11*, 3507–3512.
158. Burgers, P. M. J.; Eckstein, F. *Biochemistry* **1979,** *18*, 592–596.
159. Orr, G. A.; Simon, J.; Jones, S. R.; Chin, G. J.; Knowles, J. R. *Proc. Natl. Acad. Sci. USA* **1978,** *75*, 2230–2233.
160. Pliura, D. H.; Schomburg, D.; Richard, J. P.; Frey, P. A.; Knowles, J. R. *Biochemistry* **1980,** *19*, 325–329.
161. Richard, J. P.; Carr, M. C.; Ives, D. H.; Frey, P. A. *Biochem. Biophys. Res. Comm.* **1980,** *94*, 1052–1056.
162. Sheu, K. F. R.; Richard, J. P.; Frey, P. A. *Biochemistry* **1979,** *18*, 5548–5556.
163. Bryant, R.; Sammons, R. D.; Frey, P. A.; Benkovic, S. J. *J. Biol. Chem.* **1981,** *256*, 5965–5966.
164. Blätteer, W. A.; Knowles, J. R. *Biochemistry* **1979,** *18*, 3927–3933.
165. Hansen, D. E.; Knowles, J. R. *J. Biol. Chem.* **1981,** *256*, 5967–5969.
166. Saini, M. S.; Buchwald, S. L.; VanEtten, R. L.; Knowles, J. R. *J. Biol. Chem.* **1981,** *256*, 10,453–10,455.
167. Lowe, G.; Potter, B. V. L. *Biochem. J.* **1981,** *199*, 227–233.
168. Lowe, G.; Cullis, P. M.; Jarvest, R. L.; Potter, B. V. L.; Sproat, B. S. *Phil. Trans. R. Soc. Lond., B.* **1981,** *293*, 75–92.
169. Jarvest, R. L.; Lowe, G.; Potter, B. V. L. *Biochem. J.* **1981,** *199*, 427–432.
170. Lowe, G.; Potter, B. V. L. *Biochem. J.* **1981,** *199*, 693–698.
171. Jarvest, R. L.; Lowe, G. *Biochem. J.* **1981,** *199*, 273–276.
172. Webb, M. R.; Trentham, D. R. *J. Biol. Chem.* **1980,** *255*, 8629–8632.
173. Webb, M. R.; Grubmeyer, C.; Penefsky, H. S.; Trentham, D. R. *J. Biol. Chem.* **1980,** *255*, 11,637–11,639.
174. Webb, M. R.; Trentham, D. R. *J. Biol. Chem.* **1981,** *256*, 4884–4887.
175. Webb, M. R.; Eccleston, J. F. *J. Biol. Chem.* **1981,** *256*, 7734–7737.

SUBJECT INDEX

CUMULATIVE INDEX, VOLUMES 1-15